# The Geology of the Lower Pohangina Valley, Manawatu, New Zealand

A thesis presented in partial fulfilment of the requirements for the degree of

Master of Science in Earth Science

at Massey University, Palmerston North, New Zealand.

MASSEY UNIVERSITY

Callum Rees

2015

*Cross bedded tuff unit within the Css Member, Takapari Formation, Antler Stream, Broadlands Station, Pohangina Valley.*

# Acknowledgments

Firstly, I wish to thank Dr Alan Palmer for always having his door open, and teaching me how to read and understand the landscape. I think your past students would understand when I say that since keeping up with you in the field, I have become incredibly fit and will now endeavour to join the Olympic speed walking team.

Special thanks also to Julie Palmer for her infectious enthusiasm and useful discussions regarding sedimentology. I have now gained a wondrous appreciation for what the majority of people refer to as 'dirt'. My initial apprehension at studying sedimentology has been replaced with a growing excitement at finding new exposures with amazing sedimentary structures.

I acknowledge Matt Erwin for all his help with GIS, and the many applications to which it can be used during the construction of geological maps. You are indispensible to all students wishing to use a Massey computer.

Thanks Anja Mobis for your enthusiasm with tephra work and the way you willingly give up your time for so many students. Your help in the lab with sample preparation and grain size analysis has been a great help. I have become acutely aware and very appreciative of the methodical German lab etiquette, which it has brought to my attention many of us kiwis severely lack.

Many thanks to Alan Beu from GNS science for your help with macro-fossil identification and useful discussions regarding the interpretation of various fossil assemblages. Julie and I both found our tour around the National Paleontological Collection invigorating, invoking a renewed determination to add to our own personal collections.

A special thanks to Ian Schipper, the microprobe technician at Victoria Universtiy, your deep understanding and passion for volcanology was of enormous value and greatly appreciated.

Cheers to Hugh and Judy Akers from Broadlands Station; you patiently put up with me for many months without so much as a complaint, both during the busy shearing and weaning season of summer (2013-2014), and lingering on through the winter of 2014. Your patience with me as well as your keen interest in the land has made the field work portion of this project very worthwhile for me. I will carry fond memories of the beautiful valley sides and ridge tops of Broadlands Station with me for as long as I live, along with a keen respect for the ferocity of the local weather systems.

Thank you to all the famers and lifestyle block owners, who permitted me access to their properties in the lower Pohangina Valley, including:

James Moar
Shane Robinson
Graeme and Julie Harding

James Taylor
Marton Telford
Craig Knight
Craig Deadman

I hope you all find your copies of the geological map interesting and informative. Sincere apologies for running large fault lines through your properties, there was no way round it.

This work was supported financially though a Massey University Masterate Scholarship, the Hastie Award and Hornibrook Award from the Geoscience Society of New Zealand, the Helen E. Akers Postgraduate Scholarship, the William Hudson Scholarship, the TrustPower Tararua Wind Farm Research Bursary, and the C V Fife Memorial Scholarship.

Lastly, thank you to all my friends and family who have had to suffer my geological ramblings over the last two years (and in some cases substantially longer). Moments spent with you not discussing the various interpretations of flow velocity from a hyper concentrated homo-pycnal flow deposit, has kept me vaguely sane.

# Abstract

The geology of the lower Pohangina Valley has been mapped at a scale of 1:30,000. This has involved the reclassification of formations described by Carter (1972) in northern Pohangina and correlation of stratigraphy and stratigraphic nomeclamenture to both the Whanganui and Dannevirke subdivisions (Fleming, 1953; Lillie, 1953).

Pohangina geology has been linked to the cyclostratigraphy preserved within the Whanganui Basin (Naish, *et al*, 1998; e.t.c.) via tephrochronology and biostratigraphy, allowing basin wide correlation. The Kaimatira Pumice Sand Formation (Fleming, 1953) is recognised within the study area by the identification of the Potaka Tephra, allowing an upper boundary to be placed upon the Takapari Formation of Carter (1972). Kai Iwi Group sediments are mapped near the axis of the Pohangina Fauted Monocline allowing correlation to the Beehive Creek, Cullings Gully and Finnis Road sections to the west of the study area (Brackley,1999; Townsend, 1993; Seward, 1976; Manning, 1988; and MacPherson, 1985).

Balanced geological cross sections have been constructed and used as aids in structural interpretation. The Pohangina Faulted Monocline (Marden, 1984), a major regional structure, is controlled at depth by a shallow reverse fault. This underlying reverse fault is correlated to the Raukawa Fault of Rich (1959), which outcrops at the western end of the Manawatu Gorge. The Pohangina Faulted Monocline is tentatively correlated with another monoclinal flexure to the south of the Manawatu Gorge, also interpreted to be related to and controlled by the Ruakawa Fault (Rich, 1959). When the eastward dipping Ruakawa Fault is at greater depth, westward dipping normal faults are found and are interpreted as antithetic faults splaying off from the underlying thrust fault.

The Pohangina Fault is mapped as an active normal fault, displacing an Ohakean terrace on the western side of the Pohangina River. The potentially active Whareroa Fault (Ower, 1943) is inferred to cross the Manawatu Saddle area trending SE – NW as a contact fault between Torlesse greywacke and Plio-Pleistocene sediments.

The thrust faulting in the area has resulted in the intense deformation and uplift of Torlesse bedrock contemporaneous with drag-tilting and folding of the Plio-Pleistocene sediments. Erosion within the study area has exposed Takapari Formation beds dipping at up to 70° to the west. Steep dips are traced SW-NE across the landscape, interpreted as representing the axis of the Pohangina Faulted Monocline and also allowing links to be made between areas of exposed faulting mapped by Rich (1959), Ower (1943) and in this study.

Lignite and tephra beds within the Takapari Formation are associated with deposition in an estuarine environment on a coastal plain bordering the Whanganui Basin, during Early Castlecliffian time. Geochemical analyses are used to identify eight tephras, which are used for both stratigraphic control and paleogeographic interpretation.

During Early Nukumaruan time an influx of gravel within the south eastern Whanganui Basin is associated with the formation of a prograding Gilbert-type fan delta within the Cg Member of the Konewa Formation. The gravels are interpreted as being derived from exposed greywacke in the vicinity of the present day northern Ruahine Ranges, 40 to 70 km north of Pohangina. Distance from source is calculated from clast size within the conglomerate and together with mineralogy provide evidence of provenance. Biostratigraphic and lithostratigraphic changes are used as evidence to support wider interpretations involving paleogeography and the geological history of the lower North Island.

Depositional environments are interpreted using facies analysis, tephrochronology, grain size analysis, and biostratigraphy. Detailed stratigraphic logs are compiled and interpreted in terms of depositional history and sequence stratigraphy. Marker horizons and bio-events allow correlation of stratigraphy to the Whanganui Basin cyclostratigraphy and marine oxygen isotope record. This information is then used to build an overall regional geological history of the area, including understanding basin development, paleogeography, provenance and depositional history.

# Table of Contents

Frontispiece ..... ii
Acknowledgements ..... iii
Abstract ..... v
Table of contents ..... vii
Appendices ..... ix
List of figures ..... x
List of tables ..... xv

1. Introduction ..... 1
    1.1 Outline of the study ..... 1
    1.2 Location of study area ..... 2
    1.3 Geological setting ..... 4
        1.3.1 Plate tectonic setting ..... 4
        1.3.2 Basement rock ..... 6
        1.3.3 The Whanganui Basin ..... 8
    1.4 Physiography ..... 9
        1.4.1 Overview ..... 9
        1.4.2 River Terraces ..... 12

2. Review of previous research in the Whanganui Basin ..... 16
        2.1 Whanganui Basin ..... 16
        2.2 Biostratigraphy ..... 17
        2.3 Tephrochronology ..... 17
        2.4 Magnetostratigraphy ..... 19
        2.5 Sequence stratigraphic model ..... 19
        2.6 Application of the sequence stratigraphic model to the Whanganui Basin ..... 21
        2.7 Geology of the Pohangina area ..... 23

3. Regional Structure ..... 27
    3.1 Overview ..... 27
    3.2 Folds ..... 27
    3.3 Faults ..... 28

4. Introduction to Stratigraphy and Sedimentology ..... 44

5. Komako Formation ..... 46
    5.1 Coarse flaggy grit Member ..... 47

5.1.1 Facies analysis of Cf Member, Stratigraphic log 5.1 ..... 49
5.1.2 Grain size analysis ..... 51
5.2 Fossiliferous mudstone Member ..... 52
5.2.1 Grain size analysis ..... 55
5.2.2 Shelf processes ..... 56
5.2.3 Bioturbation and sedimentation rates ..... 58
5.2.4 Modern analogue ..... 58
5.3 Fossiliferous sandstone Member ..... 59
5.3.1 Facies analysis of Fss Member, Stratigraphic log 5.2 ..... 60
5.3.2 Regional correlations ..... 68

6. Konewa Formation ..... 71
6.1 Conglomerate Member ..... 72
6.1.1 Facies and Facies Associations ..... 78
6.1.2 Fan delta clast analysis ..... 85
6.1.3 Fan delta foreset analyses ..... 90
6.2 Sandy blue grey mudstone Member ..... 96
6.2.1 Grain size analysis ..... 97
6.2.2 Modern analogue ..... 99
6.3 Red cross bedded sandstone Member ..... 101
6.3.1 Facies analysis of Rss Member, Stratigraphic log 6.2 ..... 104
6.4 Marine sandstone Member ..... 109
6.4.1 Ichnofossils ..... 111
6.4.2 Facies analysis of Kss Member, Stratigraphic log 6.3 ..... 112
6.5 Coquina limestone Member ..... 115

7. Takapari Formation ..... 119
7.1 Blue grey sandy mudstone Member ..... 120
7.1.1 Grain size analysis ..... 123
7.2 Cross bedded sandstone Member ..... 124
7.2.1 Grain size comparison ..... 125
7.2.2 Stratigraphy ..... 126
7.2.3 Estuary depositional environments ..... 133
7.2.4 Cyclostratigraphy ..... 135
7.2.5 Volcaniclastic facies ..... 137
7.3 Tephrochronology ..... 141
7.3.1 New Zealand rhyolitic volcanism during the Quaternary ..... 141
7.3.2 Geochemistry ..... 142
7.3.3 Scrimmys Tephra (New Tephra) ..... 143

7.3.4 Rewa Pumice ..... 145
7.3.5 Mangapipi Tephra ..... 146
7.3.6 Ridge Tephra ..... 147
7.3.7 Pakihikura Tephra ..... 148
7.3.8 Tephra grain size analysis ..... 150
7.3.9 Paleoenvironmental reconstruction ..... 152

8. Kaimatira Pumice Sand Formation ..... 153
8.1 Cross bedded sandstone Member ..... 153
8.2 Tephrochronology ..... 154
8.2.1 Potaka Pumice ..... 154
8.2.2 Paleoenvironmental reconstruction ..... 156

9. Kai-iwi Group ..... 158

9.1 Red conglomerate Member ..... 159
9.1.1 Rc Member, Kai Iwi Group, Fig 9.3 ..... 161
9.1.2 Rc Member, Kai Iwi Group, Fig 9.6 ..... 166
9.1.3 Kaukatea Tephra ..... 171
9.2 Sandstone Member ..... 172
9.2.1 Facies Analysis of eQk Member, Stratigraphic log 9.3 ..... 173

10. Geological History ..... 178

References ..... 198

Appendices: ..... 217
Appendix 1: Tephra geochemical and grain size data ..... 217
Appendix 2: Grain size data ..... 261
Appendix 3: Clast analysis data ..... 283
Appendix 4: Fossil data ..... 290
Appendix 5: Paleomagentic analysis data ..... 296

Fold out Sheet I: Geological Map of the Lower Pohangina Valley

Fold out Sheet II: Stratigraphy of the Lower Pohangina Valley correlated to the Whanganui Basin cyclostratigraphy and marine oxygen isotope records

# List of Figures


1.1 Location map of study area near Ashhurst township and general distribution of basement, Late Cenozoic & Quaternary cover rocks.
1.2 Tectonic setting of the lower North Island, New Zealand
1.3 The basement terranes of New Zealand.
1.4 Location map and west-east cross section showing the location of the Whanganui Basin, study area and regional tectonic structures.
1.5 Map of the main tributaries within the study area
1.6 The Ohakean and Ratan Terraces Whareroa Stream, Pohangina.
1.7 Horizontal Ohakean gravels forming angular unconformity with underlying eQk Member, Kai-iwi Group dipping 15°@280 (NW).Maungatukurangi Stream, Broadlands Station.
1.8 Kawakawa tephra preserved within Ohakean loess on the Ratan terrace.

2.1 The sequence stratigraphic model, showing the highstand (HST) transgressive (TST), lowstand (LST), and Regressive systems tracts (RST).
2.2 The seven major cyclothemic (sequence) motifs recognised within the Whanganui Basin.

3.1 Fold axes of the Manawatu anticlines overlaid on an Enhanced Thematic Mapper satellite image of the Whanganui Basin.
3.2 Geological map of the lower Pohangina Valley, showing cross section lines.
3.3 Top: Geological Cross section west to east, A to A-. Bottom: restored section.
3.4 Top: Geological cross section west to east, B to B-. Bottom: restored section.
3.5 Top: Geological cross section west to east, C to C-. Bottom: restored section.
3.6 Top: Geological cross section west to east, D to D-. Bottom: restored section.
3.7 Antithetic fault plane dipping 75°W, south branch of Whareroa Stream, Broadlands Station, Pohangina Valley.
3.8 Exposure of a normal antithetic fault in Scrimmys Stream, interpreted to be connected to the Raukawa Fault at depth, Broadlands Station, Pohangina Valley.
3.9 Contact between Torlesse greywacke and Cf Member Komako Formation, note highly sheared and shattered greywacke, Antler Stream, Pohangina.
3.10 Offset Ohakean Terrace crossed by the Pohangina Fault, Pohangina Valley.

5.1 A fossil assemblage of Cf Member, Komako Formation; *Zeacolpus vittatus* and *Maoricolpus* roseus. Collected from Stallion Stream, Broadlands Station, Pohangina Valley.
5.2 Stratigraphic log of Cf Member, Komako Formation, Stallion Stream, Broadlands Station, Pohangina.

5.3 Mollusc species found within the sediments of Pohangina Valley and their associated time spans through the Mangapanian Stage.
5.4 Depth ranges of selected mollusc taxa present within Fms Member.
5.5 Thick beds of *Crassostrea ingens* form an oyster reef within Fss Member, Komako Formation. Saddle stream, Pohangina Valley.
5.6 Fossils from Fss Member, Komako Formation: 1: *Ruditapes largillierti*, 2: *Polinices waipipiensis*, 3: *Aulacomya maoriana*, 4: *Perna canaliculus*, 5: *Talabrica senecta*, 6: *Purpurocardia purpurata*. Collected from Stallion Stream, Broadlands Station, Pohangina Valley.
5.7 Juvenile specimens of *Phialopecten triphooki*, Stallion Stream, Broadlands Station, Pohangina.
5.8 Stratigraphic log of Fss Member, Komako Formation, Stallion Stream, Broadlands Station, Pohangina.
5.9 The depth range of *Notorotalia zealadica* on the New Zealand shelf

6.1 Depth ranges of selected mollusc taxa present within Cg Member.
6.2 A fossil assemblage from Cg Member, Konewa Formation.
6.3 Stratigraphic log of Cg Member, Konewa Formation, Scrimmys Stream, Broadlands Station, Pohangina Valley.
6.4 Correlation of Konewa Formation (Cg Member) to cycle 6 in the Wanganui Basin cyclothem record, and marine isotope stages (MIS) 90 and 91.
6.5 Shoreline profile showing different subenvironments, facies and processes.
6.6 Cross section of a Gilbert-type fan delta.
6.7 Zingg diagram showing clast shape from 50 clasts of facies LDS (bed 5) and facies Gmu (bed 6).
6.8 Line graph showing decrease in clast size with distance from source.
6.9 A comparison of fan-deltas, braid deltas, and fine-grained deltas based on distributary-channel patterns and stability, sediment load and size, stream gradient, flow velocity, steadiness of discharge and distance of shoreline from source.
6.10 Gilbert-type fan delta cross section.
6.11 Schematic model illustrating the depositional setting of a fan-delta.
6.12 Paleogeographic map showing the lower North Island during Nukumaruan time, Early Pliocene time (2.4 Ma) Map depicts a interglacial period.
6.13 Cg Member forming a ridge, high angle dip plaes formed by movement along the Whareroa Fault located in the far right of this image.
6.14 Classic dome shaped hills formed by Cg Member, Konewa Formation, Broadlands Station, Pohangina.
6.15 The genereralised distribution of sediments within the modern Whanganui Basin and Cook Strait area with contours of percent sand in the non-gravel fraction. Solid arrows indicate present sediment transport paths and broken arrows indicate transport during the last glacial.

6.16 Depth ranges of selected mollusc taxa present within Rss Member.
6.17 *Struthiolaria papulosa* from Rss Member, Konewa Formation, Stallion Stream, Broadlands Station, Pohangina Valley
6.18 Rss Member above Kst Member, Konewa Formation, Scrimmys Stream, Broadlands Station, Pohangina Valley.
6.19 Stratigraphic log of Rss Member, Konewa Formation, Scrimmys Stream, Broadlands Station, Pohangina Valley.
6.20 Depth ranges of selected mollusc taxa present within Kss Member.
6.21 Bioturbation, Kss Member, Konewa Formation, Scrimmys Stream, Broadlands Station, Pohangina Valley.
6.22 Stratigraphic log of Kss Member, Konewa Formation, Scrimmys Stream, Broadlands Station, Pohangina Valley.
6.23 Top: Cq Member in Scrimmys Stream. Bottom: close up of the Cq Member showing the fossils *Talochlamys gemmulata, Pleuromeris hectori*, and *Ostrea chilensis*. Broadlands Station, Pohangina Valley.
6.24 Environments of deposition within the northwestern Manawatu Strait (eastern Whanganui Basin) during Late Nukumauan time.

7.1 Depth ranges of selected mollusc taxa present within Bms Member
7.2 A fossil assemblage from Bms Member, Takapari Formation; 1: *Austrovenus stutchburyi*, 2: *Talochlamys gemmulata* and *Stiracolpus symmetricus*, 3: *Amalda (Baryspira) mucronata*.
7.3 Grain size distributions of Takapari Formation and Kaimatira Pumice Sand Formation.
7.4 Stratigraphic log of Css Member, Takapari Formation, and Kaimatira Pumice Sand Formation, Scrimmys Stream, Broadlands Station, Pohangina Valley.
7.5 Diagram showing location of facies within a wave dominated estuary system.
7.6 Correlation of Takapari and Kaimatira Pumice Sand formations to the MIS and Whanganui cyclothem records.
7.7 Tuff unit (Potaka Pumice) within Kaimatira Pumice Sand Formation, pumice clast 150mm in diameter seen near spade handle, Broadlands Station, Pohangina.
7.8 Water escape structures caused by sediment loading within tuff unit (Potaka Pumice), Kaimatira Pumice Sand Formation, entrance to Antler Stream, Broadlands Station, Pohangina.
7.9 Css Member showing dewatering structures, Maungatukurangi Stream, Broadlands Station, Pohangina Valley.
7.10 CaO versus FeO (wt %) composition of volcanic glass shards from Kaukatea Tephra, Potaka Pumice, Scrimmys, Rewa, and Pakihikura Tephras sampled in various locations around Broadlands Station, Pohangina Valley.
7.11 Location of the Scrimmys Tephra type locality on hair pin

corner of Awahou South Rd, entrance to Scrimmys Stream, Broadlands Station, Pohangina Valley
7.12 Mangapipi Tephra enclosed by lignite beds within Takapari Formation, Antler Stream, Broadlands Station, Pohangina.
7.13 Ternary diagram displaying FeO: 1/3 $K_2O$: CaO Wt % data for tephras collected from Takapari Formation, Kai Iwi Group and Kaimatira Pumice Sand Formation.
7.14 Grain size distribution curve of the fluvially deposited Potaka Pumice compared with grain size distributions of aerially deposited Tephras.

8.1 Map of the North Island, New Zealand, showing the minimum inferred original extent (black outline) of the Kidnappers ignimbrite.

9.1 Rc Member, Kai Iwi Group, Broadlands Station
9.2 Base of Rc Sub-Member showing Facies Fsf deposited by fluvial scour and fill processes, Telfords Farm, Pohangina.
9.3 Stratigraphic log of Rc Member, Kai Iwi Group, entrance to Whareroa Stream, Telfords Farm, Pohangina Valley.
9.4 Zingg diagram of facies Fc from the Rc Member Kai Iwi Group, Telfords Farm, Pohangina.
9.5 Rc Member unconformably overlying Kaimatira Pumice Sand Formation, forming a ridge at Broadlands Station, Pohangina Valley
9.6 Stratigraphic log of Rc Member, Kai Iwi Group, Maungatukurangi Stream, Broadlands Station, Pohangina.
9.7 Rc Member, Kai Iwi Group, Maungatukurangi Stream, Broadlands Station, Pohangina
9.8 eQk Member, Kai Iwi group, planar laminations and lenticular bedding, Maungatukurangi Stream, Broadlands Station, Pohangina.
9.9 Stratigraphic log of eQk Member, Kai Iwi Group, Maungatukurangi Stream, Broadlands Station, Pohangina.

10.1 Paleogeographic map showing the lower North Island during Opoitian time, Early Pliocene time (4 Ma).
10.2 Paleogeographic map showing the lower North Island during Waipipian time, Early Pliocene time (3.35 Ma) Map depicts an interglacial stage
10.3 Paleogeographic map showing the lower North Island during Mangapanian time, Early Pliocene time (2.7 Ma) Map depicts a interglacial period
10.4 Composite stratigraphic log showing stratigraphy of the Lower Pohangina Valley.
10.5 Box diagrams displaying depositional environments on the northwestern side of the Manawatu Strait from Early Mangapanian to Early Castlecliffian time.
10.6 Paleogeographic map showing the lower North Island during Nukumaruan time, Early Pliocene time (2.4 Ma) Map depicts a interglacial period
10.7 The Ruahine Range showing faults and location of the Ohara Depression.

10.8 Southern North Island showing Wairarapa region, Manawatu Gorge and location of the Pahiatua Basin, the Wellington Fault, West Wairarapa Fault, and Palliser-Kaiwhata Fault.
10.9 Paleogeographic map showing the lower North Island during Castlecliffian time, Early Pliocene time (1 Ma) Map depicts a interglacial period
10.10 Box diagram displaying depositional environments on the northwestern side of the Manawatu Saddle during Mid Castlecliffian time

# List of Tables


1.1 Major aggradational alluvial terraces in the Rangitikei Valley .

2.1 Ages for tuff and tephra horizons in Whanganui Basin.

4.1 Stratigraphic nomenclature used in Whanganui Basin, East Coast Basin, and Pohangina lithostratigraphy.

5.1 Fossil assemblages from Cf Member, Komako Formation.
5.2 Lithofacies of Cf Member, Komako Formation, Fig 5.2.
5.3 Fossil assemblages from Fms Member, Komako Formation.
5.4 Fossil assemblages from Fss Member, Komako Formation.
5.5 Lithofacies of Fss Member, Komako Formation from stratigraphic log 5.2.

6.1 Fossil assemblages from Cg Member, Konewa Formation.
6.2 Lithofacies of Cg Member, Konewa Formation, Fig 6.3, Scrimmys Stream, Pohangina.
6.3 Fossil assemblage from Kst Member, Konewa Formation.
6.4 Fossil assemblage from Rss Member, Konewa Formation
6.5 Lithofacies of Rss Member, Konewa Formation, Fig 6.19.
6.6 Fossil assemblages from Kss Member, Konewa Formation.
6.7 Lithofacies of Kss Member, Konewa Formation, Fig 6.22.
6.8 Fossil assemblage from Cq Member, Konewa Formation.

7.1 Fossil assemblages from Bms Member, Takapari Formation.
7.2 Lithofacies of Css Member, Fig 7.4, Takapari Formation.
7.3 List of tephras identified in Pohangina Valley.
7.4 Scrimmys Tephra normalised data.
7.5 Grain size distribution statistics for Kawakawa Tephra, Potaka Pumice, Mangapipi Tephra and Pakihikura Tephra.

9.1 Formations of Kai Iwi Group.
9.2 Lithofacies of Rc Member, Fig 9.3, Kai Iwi Group.
9.3 Lithofacies of Rc Member, Fig 9.6, Kai Iwi Group.
9.4 Lithofacies of eQk Member, Fig 9.9, Kai Iwi Group.

# Chapter 1
# Introduction

## 1.1 Outline of the study

The geology of the Pohangina Valley was investigated and described by the author over the summer of 2013-2014. During this field work particular effort was put into finding the most continuous outcrops and linking members within these outcrops across the landscape, enabling both a structural and stratigraphic interpretation of the area to be made. Aggradational river terraces were mapped and any offsets were used to determine recent fault movements.

This research has been undertaken with several main objectives in mind. One of the key goals is to map the geology of the lower Pohangina Valley at a scale of 1:30,000. This has involved an extensive stratigraphic study of the Plio-Pleistocene cover beds, using formations set out by Carter (1972), Fleming (1953), and Lillie, (1953). Formations have been further subdivided into members, through the application of tephrochronology, biostratigraphy and sedimentology. The application of these geological techniques has allowed the depositional history of the area to be interpreted and related to changes in eustatic sea level, tectonics, accommodation space, and the paleogeography.

Sequence stratigraphic models based on the work by the EXXON Production Research Group (Wilgus, *et al,* 1988) have been applied to cyclothemic sedimentary sequences farther west within the Whanganui Basin (Naish & Kamp, 1995; Abbott & Carter, 1994; Naish *et al*, 1996). A part of this research is to investigate the application of sequence stratigraphy in Pohangina and the correlation of Pohangina geology to the well documented Whanganui Basin cyclostratigaphy (Naish *et al*, 1998) and marine oxygen isotope record.

Several techniques were used to construct a chronostratigraphic framework, both to date members and to correlate members across the landscape. Because sediments within the Whanganui Basin are geologically young, they contain fossil fauna and sedimentary facies which are similar to well-described modern counterparts around New Zealand (Carter & Naish, 1998). Therefore biostratigraphy is a very important tool in the Whanganui Basin, providing age constraints, insights into environments of deposition, and evidence of lateral facies changes within members, as first shown by Fleming (1953).

Tephra, derived from the Taupo Volcanic Zone (TVZ), was sampled and analysed using electron microprobe analysis (EMPA). These tephras occur within the Kaimatira Pumice Sand Formation (Castlecliffian) and Takapari Formation (Late Nukumaruan to Early Castlecliffian). They provide excellent chronohorizons for correlating sedimentary sequences

both within the Whanganui Basin and between the western and eastern sides of the main axial ranges.

Clastic sediments were analysed in terms of lithology, grain size, clast shape, and sorting to investigate changes in depositional environments and paleogeography. These characteristics are controlled by changes in sea level, tectonic subsidence/ uplift, accommodation space, and paleogeography. The orientation of bedding was measured to provide information on the direction of paleocurrents.

This thesis is structured to reflect the natural progression of techniques applied during the development of the research. Firstly the study area is described in detail focusing on location, geological setting and physiography of the area. Then an extensive review of previous research into the Whanganui Basin is provided. This is particularly important as it sets the scene for the most important aspect of this study, which is to incorporate local stratigraphic studies based in Pohanigna, within the more regional stratigraphic studies of the Whanganui Basin. Chapter three looks at the regional structure, drawing from previous work and incorporating new data to provide a more comprehensive interpretation of Pohangina's structural geology. The formations are then described from oldest to youngest, introducing new stratigraphic members, nomenclature and definitions. This is followed by a chapter drawing from the body of the work to interpret the geological history of the area. The chapters are arranged in this way to fully describe the stratigraphy from youngest through to oldest, followed by more regional interpretations and inferences gained from research and new data collected during this study.

## 1.2 Location of the study area

The study area (Fig 1) is located 20 km NE of Palmerston North, near the Manawatu township of Ashhurst. The mapping area, approximately 11.5 by 5 km, trending NE – SW from the Manawatu Gorge north to just past the Ruamai Bridge (WGS84 40°12'27.62"S, 175°47'21.63"E), extends from the Pohangina River 5 km into the Ruahine Ranges to where the contact between the Torlesse greywacke and the Plio-Pleistocene cover beds occurs. Access to the study area can be gained via the Saddle Road Bridge just out of Ashhurst and the Ruamai Bridge farther to the north. The majority of the study area is private land and may only be accessed with the express permission of the landowners.

The Manawatu Gorge forms the southern boundary of the study area, as well as forming the geographical boundary between the Tararua Range to the south and the Ruahine Range to the north. The Ruamai Bridge marks approximately the northern boundary of the study area 11 km north of the Manawatu Gorge. The majority of the study area is located on the Manawatu Saddle and the strip of foothills bordering the western side of the Ruahine Range, north of the Manawatu Gorge. The elevation of the study area reaches a maximum of 450 m asl while the peaks of the Ruahine Ranges continue up to an elevation of 1643 m

**Fig 1.1:** Location map of study area near Ashhurst township and general distribution of basement, Late Cenozoic & Quaternary cover rocks (adapted from Abbott, 2000).

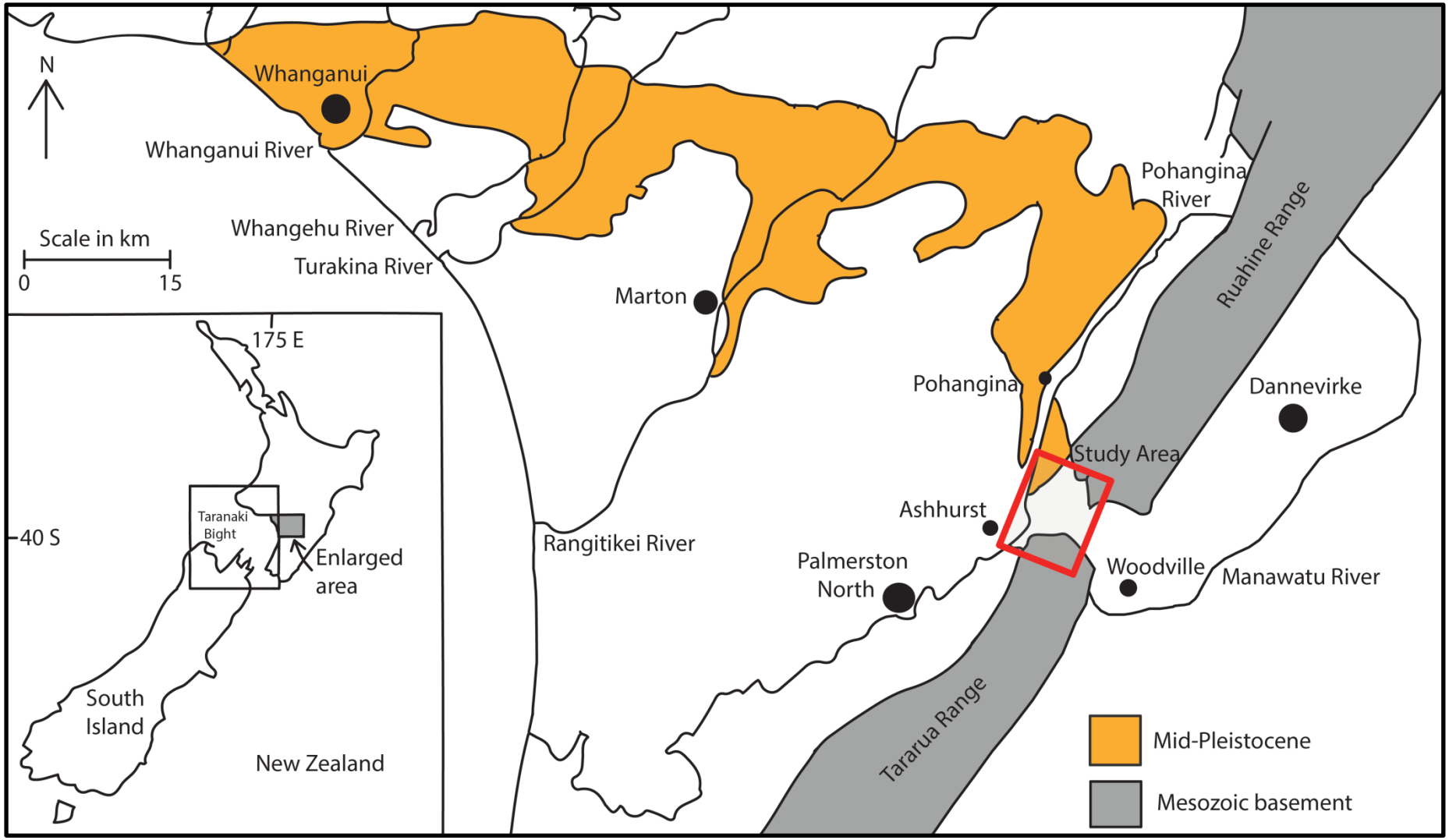

asl (LINZ, 2015). Land use in the study area includes residential (Ashhurst), plantation forestry, and pastoral farming.

# 1.3 Geological setting

## 1.3.1 Plate tectonic setting

Continental New Zealand has evolved along the boundary between the largely continental Australian plate and the oceanic Pacific plate (Fig 2). This boundary is referred to as the Kermadec-Hikurangi subduction system and is a continuation of the Tonga-Kermadec arc system (Cole & Lewis, 1981). East of North Island, oblique subduction of the Pacific plate is taking place; this obliquity increases southward to the northern South Island (Stern *et al*, 2006). The North Island is being obliquely underthrust from the east by the subducting Pacific Plate at a rate of 40-50 mm $yr^{-1}$ (Begg & Johnston, 2000). Intermediate earthquakes and active volcanism within the North Island result from the subduction along this plate margin. Strain generated by the convergence is transferred onto the leading edge of the Australian Plate resulting in crustal shortening and deformation (Cole & Lewis, 1981). The geometry of the plate boundary has produced thrusting and transcurrent faulting in the fore-arc area on the east coast of the North Island (Cole & Lewis, 1981).

To the south, in the Puysegur Trench the Australian plate is being thrust beneath the Pacific Plate (Christoffel, 1971). The Australian-Pacific plate boundary crosses the continental crust of the South Island as a zone of deformation up to 200 km wide (Walcott, 1978a). The principal focus of displacement between the two plates in the South Island is the Alpine Fault, a major strike-slip fault with 480 km of right-lateral slip (Wellman, 1953). A majority of the movement along the Alpine Fault has occurred since Miocene time (23 Ma). Relative plate motion is manifest by strike-slip movement, however, at different times throughout the Cenozoic considerable tension and compression have occurred (Sporli, 1980). A change from dominantly strike-slip tectonics to oblique convergence, crustal shortening and mountain building occurred around 6 – 8 Ma (Batt, *et al*, 2004).

The initiation of subduction in New Zealand began at 27 Ma; associated North Island volcanism began in the Miocene around 23 Ma (Begg & Johnston, 2000). The dip on the subducting plate is at a relatively low angle (15°), adjacent to the shallow Hikurangi Trough, and the dip increases towards the east coast of the North Island where it reaches an angle of 50° (Reyners, 1980). This steep section of the subducting plate is represented at the surface by the axis of a 100 mGal gravity anomaly which runs parallel to the east coast of the North Island (Stern *et al*, 2006). This gravity anomaly coincides with the East Coast Basin (Stratford & Stern, 2004).

**Fig 1.2**: Tectonic setting of the lower North Island, New Zealand. Displaying selected fault lines of the North Island Dextral Fault Belt (NIDFB), and locations of the subduction front, Whanganui Basin and study area. The outline of the Whanganui Basin has been drawn overlapping the current day main axial ranges. This is based on evidence of marine seaways which connected the Whanganui and Wairarapa shelves from Kapitean to Late Nukumaruan time (Browne, 2004; adapted from Clement, 2011).

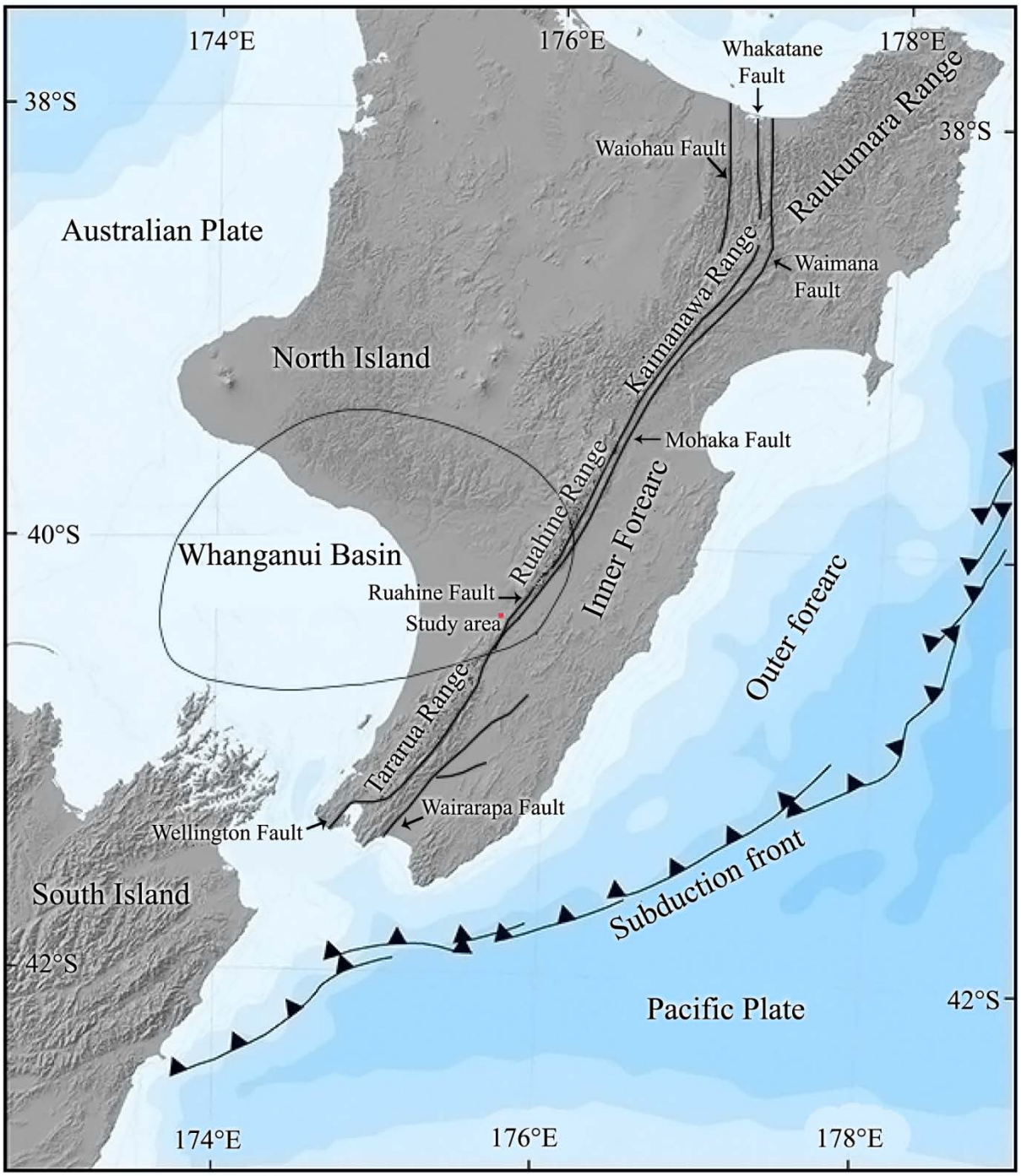

During the Neogene and Quaternary, the North Island was subjected to a complex pattern of arc volcanism, regional compression, extension and transcurrent displacements, collectively referred to as the Kaikoura Orogeny (Suggate, 1978). Arc volcanism began in the Northland volcanic belt in the Early Miocene (23-16 Ma) with calc-alkaline andesitic, basaltic, dacitic and rhyolitic volcanism (Schellart, 2007). The Northland Volcanic Arc is a precursor to the modern Tonga-Kermadec-New Zealand Arc (Hayward *et al*, 2001). Volcanic activity in the Taupo Volcanic Zone (TVZ) began around 1.6 Ma, with andesitic and rhyolitic activity (and some minor basaltic and dacitic activity) (Wilson *et al*, 1995). The Tongariro volcanic centre including the active Mt Ruapehu and Mt Ngauruhoe mark the south-western end of the volcanic front in the North Island (Reyners, 1980).

### 1.3.2 Basement rock

The Ruahine Ranges are composed of indurated quartzofeldspathic and lithic sandstone (greywacke) and mudstone (argillite) basement rocks (Marden, 1984). These basement rocks are part of the Torlesse Terrane (Fig 1.3). The basement rock of the southern Ruahine Range is Jurassic (Adams *et al,* 2009). The Torlesse rocks were deposited into a deep marine trench located off the eastern margin of Gondwana. The alternating sequences of sandstone and argillite formed from turbidites, which transported sediments eroded off the Gondwana super-continent into an ocean basin environment. The few fossils preserved within the greywacke give the Torlesse an age range from Permian to Late Jurassic (Begg *et al*, 2005).

The Torlesse greywacke was uplifted during the Rangitata Orogeny (200 - 110 Ma) (Veevers, 2000). The following period of relative tectonic quiescence during the Early Tertiary (65 - 23 Ma) eroded the New Zealand landscape forming an extensive erosion surface visible today on the main axial ranges (Kingma, 1958; Wellman, 1948). The Kaikoura Orogeny began in Miocene time (approximately 23 Ma) when initiation of convergence between the Australian and Pacific Plates began, resulting in compression of the New Zealand continental crust causing the Torlesse terrane to become folded, faulted and uplifted forming the axial ranges of the North and South Islands (Marden, 1984).

**Fig 1.3:** The basement terranes of New Zealand (Campbell *et al*, 2012; Mortimer, 2004).

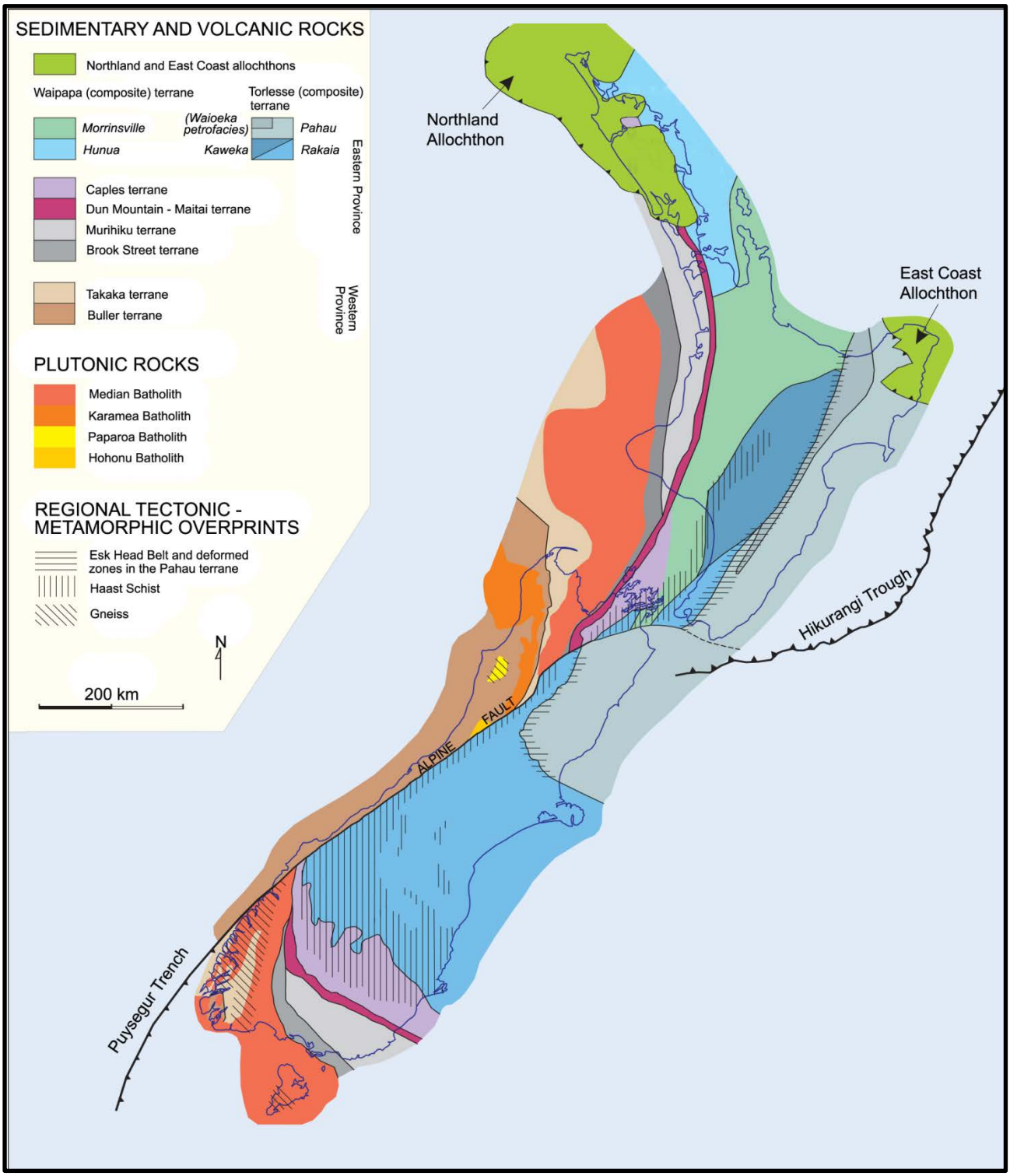

## 1.3.3 The Whanganui Basin

The study area is located in the eastern Whanganui Basin. The Whanganui Basin contains one of the most complete Quaternary stratigraphic records in the world (Pillans, 1994). Up to 4 km of Pliocene-Pleistocene sediments have accumulated over greywacke basement within the Whanganui Basin. The basin formed due to downwarping of the crust caused by frictional shear between the westward dipping subducted Pacific Plate and the over-riding Australian Plate (Fig 1.4) (Stern et al, 1993). Marginal uplift on the north flank of

**Fig 1.4:** Location map and west-east cross section showing the location of the Whanganui Basin, study area and regional tectonic structures (adapted from Shane, 1991; Naish & Kamp, 1995).

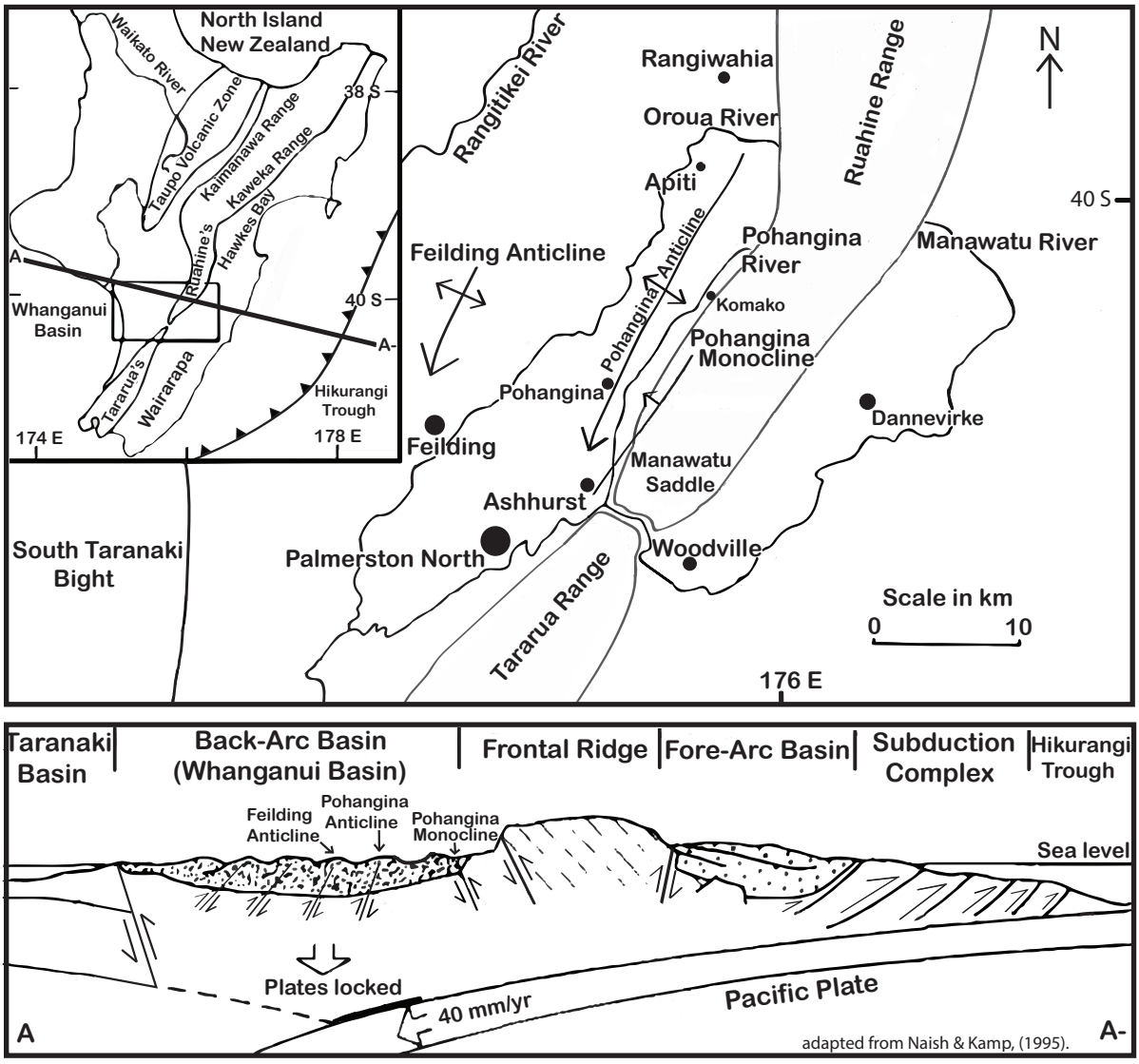

the basin has exposed sections of Plio-Pleistocene sediments and led to the development of marine and river terraces (Pillans, 1994). Back-arc volcanism within the Taupo Volcanic Zone through the Quaternary has provided a source of sediment to the basin, creating a number of rhyolitic tephra horizons which have been dated and allow basin wide correlations to be made (Shane, 1994).

The sediments in the Whanganui Basin are mainly of Pliocene and Pleistocene age whereas the King Country Basin contains an Oligocene-late Miocene sequence. This pattern of older strata towards the north is associated with a southward migration of the Whanganui Basin's depocentre through the Plio-Pleistocene (Anderton, 1981). Contemporaneous with the shift of the depocentre to the southeast, was off-lap and emergence in the north caused by tectonic uplift. By the early Pleistocene the basin was confined within the limits of the present basin, and by late Pleistocene time the depocentre was located at its present position off the Manawatu coast (Anderton, 1981). Anderton suggests that the southward propagation of the Whanganui Basin depocentre is consistent with the southward propagation of the subduction zone beneath northern New Zealand proposed by Walcott (1978).

Anderton (1981) suggests that during the early Pliocene, marine connections existed across the trend of the main axial ranges between the South Whanganui Basin and the Hawkes Bay and Wairarapa Basins to the east. This seaway is referred to in the literature as the 'Manawatu Strait'. The marine connection between the east and west coast basins became progressively limited as the axial ranges emerged during the Plio-Pleistocene. Eventually in the Early Pleistocene this connection became cut off completely.

# 1.4 Physiography

## 1.4.1 Overview

The physiography of the study area is closely connected to the stratigraphic and tectonic history of the Ruahine Ranges. Uplift rates of 3 mm/yr and high erosion rates occur within the Ruahine Range (Whitehouse & Pearce, 1992). The study area is located on the western side of the Ruahine Range where Plio-Plesitocene sediments of the Whanganui Basin unconformably overlie Torlesse greywacke. The Ruahine Range has been interpreted by Lillie (1953) as a simple anticlinal flexure with a southward plunge. The Tararua Range to the south is interpreted as an anticlinal fold which plunges to the north (Adkin, 1930). The two sets of ranges are separated by a physiographic depression called the 'Manawatu Saddle' across which the Manawatu Gorge is incised (Marden, 1984).

The Ruahine Range is flanked by a series of en-echelon faults along its steep eastern side. Marden (1984) described the range as a “high, outstanding, tilted bedrock block” which has a steep eastern side and a more gently sloping western side, making it markedly asymmetrical. The Ruahine Range exposes the erosion suface which was carved into the Torlesse greywacke during the Early Tertiary (Wellman, 1948). This surface is prominent at approximately 1000-1100 m altitude near the Manawatu Gorge/Saddle Road area where it is exposed at the northern end of the Tararua Range and southern end of the Ruahine Range. Within the Manawatu Saddle a well-defined erosion surface is overlain by fossiliferous marine sediments of Mangapanian to Nukumaruan age.

The physiographic boundary between the Ruahine Range and adjacent steep-land of the Pohangina Valley corresponds to the boundary between the semi-consolidated sediments of the Whanganui Basin with the indurated Torlesse greywacke bedrock lithologies.

Streams draining the range generally flow perpendicular to its axis. The streams draining the western flank of the Ruahine Range have longer channels and more gentle profiles than those draining the east which are generally shorter and steeper. A weak radial drainage pattern has formed on the peneplained bedrock surface at the southern end of the Ruahine Range. Stream dissection in this area is minimal and the interfluve areas are broad and smooth in relief. Streams draining the western front of the range carry less bedload than those on the eastern front, and when they emerge from the range they can be incised to depths of 150 m (Marden, 1984).

The stream channels of Pohangina Valley are often confined within narrow steep walled canyons which extend from the western flank of the Ruahine Range to the Pohangina River. The Pohangina River drains southwards approximately parallel to the western front of the Ruahine Range, towards its confluence with the Manawatu River near Ashhurst township. The Manawatu River then continues to meander across the Manawatu Plains to its mouth at Foxton where it enters the Tasman Sea.

**Fig 1.5:** The main tributaries within the study area (several unnamed streams have been given informal names for reference and are shown in italics below) (NZ Topo Map 250, 2014).

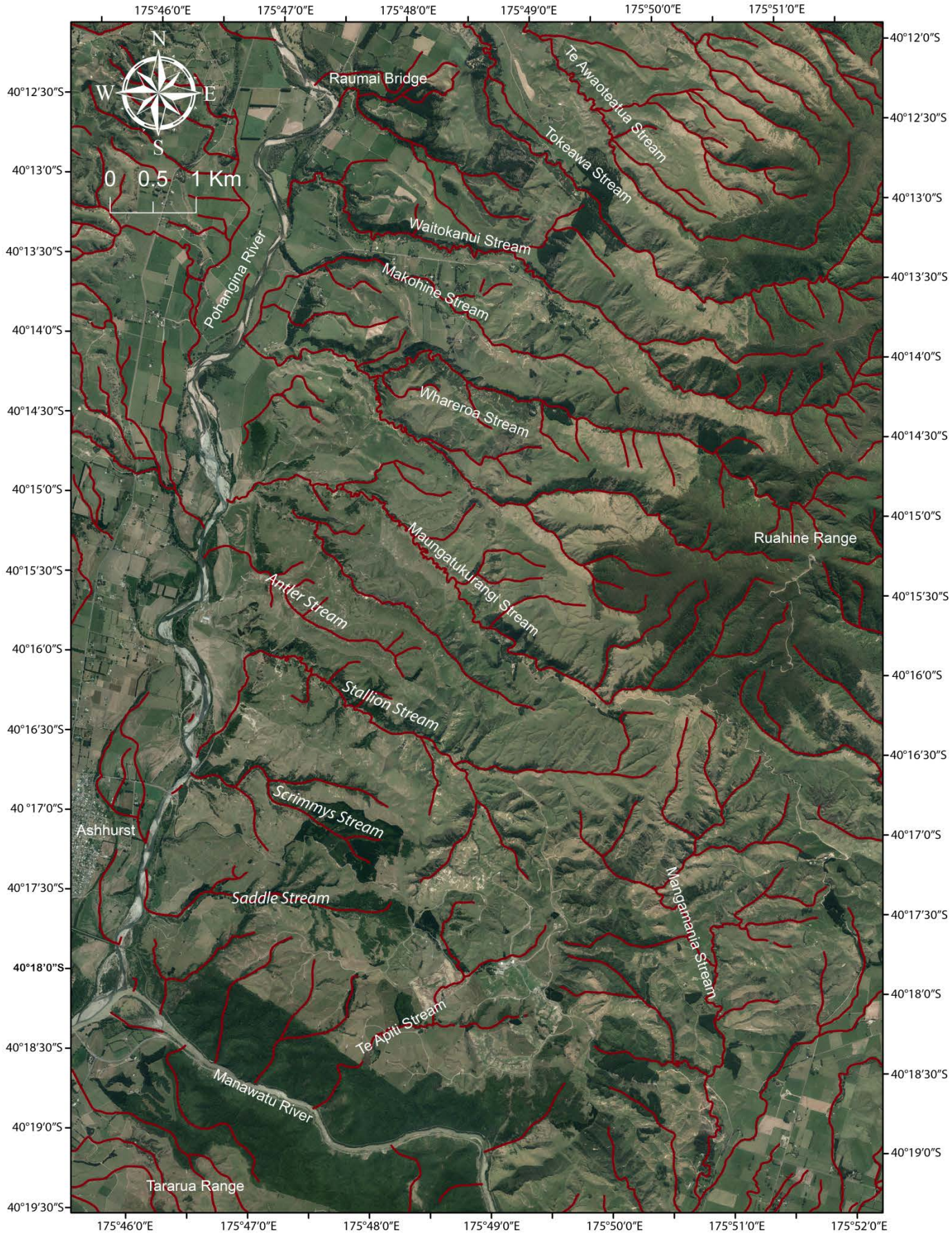

### 1.4.2 River terraces

The steep-land and foot hills of the study area display aggradation surfaces. These surfaces are remnants of aggradational floodplains formed by streams and rivers draining the Ruahine Range over the last 1 Ma. Aggradation surfaces represent cool climate episodes (stadials) during the Quaternary when increased erosion rates during glacials lead to river aggradation. Subsequent fluvial incision during intervening warm periods (interglacials or interstadials) resulted in the creation of a new flood plain surfaces set lower in the landscape. The continuing uplift within the eastern Whanganui Basin has resulted in the preservation of these surfaces as flights of river terraces, each one representing a different stadial period (Pillans, 1994). Most of the work in the Whanganui Basin focusing on fluvial terraces has been carried out in the Rangitikei River valley (Te Punga, 1952; Milne, 1973a; Cowie & Milne, 1973) and the lower Manawatu River valley (Fair, 1968).

Rhyolitic volcanisim from the TVZ over the last 1.6 Ma has produced extensive tephra deposits which are used as valuble marker horizons, to date river terraces. The Kawakawa Tephra, formerly the Aokautere Ash (Cowie, 1964a), has a calibrated age of 25.3 ka (Vandergoes *et al,* 2013). It was originally identified and described by Cowie (1964a) in the Manawatu District. Cowie (1964b) was able to show that the Kawakawa Tephra occurs in the coverbeds on the terraces.

Loess began accumulating while rivers were aggrading during the Otiran (last) Glacial. In glacial periods the tree line lowers in upland areas. This results in increased erosion within river catchments and as a result rivers become choked with debris and aggrade. The increased winds during glacial periods transport silt from the exposed river flood plain depositing it as loess over the surrounding landscape. A modern analogue to this process is occurring on the Canterbury Plains today, where silt is blown from the wide gravel beds of the Rakaia River to become deposited as loess on the adjacent landscape. In warm interglacial and interstadials periods erosion rates become lower due to greater vegetation cover and rivers begin to cut down into their beds. Inter-glacials are associated with more stable, soil forming conditions.

Table 1.1 Major aggradational alluvial terraces in the Rangitikei Valley (Pillans, 1994).

| Terrace | Age |
|---|---|
| Ohakean | 15-30 ka |
| Ratan | 30-50 ka |
| Porewan | 70-80 ka |
| Cliff | 90-100 ka |
| Greatford | 110-120 ka |
| Marton | 140-170 ka |
| Burnard | 240-280 ka |
| Aldworth | 340-350 ka |
| Waituna | 360-370 ka |

Fig 1.6: The Ohakean and Ratan Terraces Whareroa Stream, Pohangina (WGS84 40°14'18.32"S, 175°48'06.21"E, elev 175 m.

Loess continued to be deposited until shortly after the end of the Otiran Glacial and the formation of the Ohakean Terrace (Te Punga, 1952; Milne, 1973a, 1973b). Subsequently during the Holocene, interglacial conditions have prevailed resulting in river incision. Ohakean loess was deposited from 30 – 15 ka during the Otiran Glacial and contains the Kawakawa Tephra; the Ohakean loess is preserved on all terrace surfaces older than Ohakean (Cowie & Milne, 1973).

Milne (1973a) subdivided the river terraces into aggradational and degradational terraces. Nine aggradational terraces have formed over the last 370 ka (Table 1.1). Degradational terraces have formed over the Holocene (last 10 ka) due to fluvial incision.

The Pohangina River and its tributaries display suites of terraces formed by oscillations in climate coupled with regional uplift during the Late Quaternary. The terraces are not as well preserved as in the Rangitikei River Valley. Two of the nine major aggradational terraces of Milne (1973a) are recognised within the lower Pohangina Valley. The Ohakean Terrace (Fig 1.6) is the most widespread aggradational terrace found in the study area, with small remnants of the Ratan terrace also preserved in certain areas.

Fig 1.7: Horizontal Ohakean gravels forming angular unconformity with underlying eQk Member, Kai-iwi Group dipping 15°@280 (NW). Maungatukurangi Stream, Broadlands Station, Pohangina Valley (WGS84 40°15'00.75"S, 175°47'46.95"E, elev 133 m).

The Ohakean Terrace is well represented in the landscape forming a major flat terrace surface upon which Ashhurst township is built; the road from Ashhurst to Pohangina runs across the Ohakean Terrace. The Ohakean Terrace is easily recognised as it forms large flat surfaces near the Pohangina River and its tributaries. In outcrop the Ohakean gravels are commonly several meters thick with clasts up to 600 mm in size, they occur as an angular unconformity above the tilted beds of Plio-Pleistocene sediments (Fig 1.7)

The Ratan Terrace is far less common in the landscape as it has been largely eroded due to the high rates of erosion in this area. Ratan Terraces are observed as flat surfaces 5 to 10 m higher in the landscape from the Ohakean Terrace. In outcrop they contain a thick Ohakean loess sequence (up to 4 m) with the Kawakawa Tephra (300mm) preserved approximately 2 m down section (Fig 1.8). The Kawakawa tephra was erupted from Taupo during the Last Glaical Maximum (LGM) and is dated to 25,358 ± 162 cal. yr BP (Vandergoes *et al,* 2013; Lowe *et al*, 2013). This eruptive event was one of the largest in Late Quaternary time, making it a very widespread and therefore a valuable chronohorizon.

Fig 1.8: Kawakawa tephra preserved within Ohakean loess on the Ratan terrace adjacent to Pohangina River, Broadlands Station, Pohangina Valley (WGS84 40°15'00.79"S, 175°47'46.91"E, elev 92 m).

# Chapter 2
# Review of previous research in the Whanganui Basin

## 2.1 Whanganui Basin

The well-preserved fossil faunas from the Whanganui Basin have attracted the attention of palaeontologists around the world from as early as the middle 19th century, e.g. Hutton (1873). Pioneer geologists in New Zealand began to study the stratigraphy of the Whanganui Basin and particularly the fossils preserved within the sediments (Hochstetter, 1864; Buchanan, 1870; Hutton, 1886). Thomson (1917) and Finlay & Marwick (1940, 1947) set up biostratigraphic stages based on assemblages of fossils, which would aid correlation. The Waitotaran, Nukumaruan and Castlecliffian stages and their substages were based on type localites in the Whanganui region (Fleming, 1953; Carter & Naish, 1998). More recently a Haweran stage has been added for sediments younger than 0.35 Ma. Magnetostratigraphy and tephrochronology have now been implemented in defining stages (Carter & Naish, 1998).

One of the first extensive studies of the stratigraphy within the Whanganui Basin was conducted by the Superior Oil Company (Feldmeyer *et al*, 1943) who produced a report on 'the Geology of the Palmerston-Wanganui Basin'. This mapping field work was based on sections in the Whanganui, Turakina, Mangawhero and Rangitikei Rivers. Foraminifera were sampled and used to establish faunal zones and to correlate the sections to the standard New Zealand stages. Te Punga (1952) provided the first description of the stratigraphy in the Rangitikei Valley. He incorporated biostratigraphy and tephrochronology allowing correlation with other study areas such as Turakina and the Whanganui coastal sections. Later, Fleming (1953) mapped the sediments of the Whanganui Basin. Fleming's work was supported by detailed biostratigraphy and provided a full description of the sediments preserved in the coastal sections of the Whanganui Basin. Fleming's work has been used as the basis for all subsequent studies in the area.

A number of different methods have been used to study the structure of the Whanganui Basin, enabling a better understanding of the basin's history. Anderton (1981) interpreted CRP (common reflection point) seismic profiles in order to determine the structure and evolution of the South Whanganui Basin. Seismic data showed that the South Whanganui Basin is a broad half graben trending north-northeast, bordered to the south east by a complex zone of block faulting. The western boundary is marked by broad north-south trending basement uplifts, the D'Urville and Patea Highs which lie en echelon with a narrow graben between.

## 2.2 Biostratigraphy

One of the most important methods of relative dating in the Whanganui Basin is biostratigraphy. Fleming (1957) developed the use of the macrofossil *Pecten* and its subspecies as a way of dating and correlating beds. *Pecten* are now of global importance and is recognized as an index fossil. *Pecten* are not found in deposits older than Castlecliffian (Mid-Pliestocene). The first appearance datum (FAD) is found within the Kaikokopu Shell Grit in the Whanganui coastal sequence and coincides with the Bruhnes/Matuyama boundary (0.78 Ma). Fossil assemblages can provide important information on environments of depositon, paleoecology and paleogeography.

## 2.3 Tephrochronology

Widespread, reworked pumice horizons (tuffs) and tephra beds are commonly found within the Whanganui Basin sediments. These tuff and tephra beds are the distal correlatives of ignimbrite sheets erupted from the Taupo Volcanic Zone (TVZ) during the last 1.6 Ma. Tephrochronology can be very useful in understanding the depositional history of a sedimentary basin. The position of the Whanganui Basin adjacent to the TVZ has allowed scientists to establish a firm and reliable chronostratigraphic framework around which detailed sedimentological studies can be based (Alloway *et al,* 1993).

Fundamental work on the tephras and tuff units of the Whanganui Basin was carried out by Seward (1974a, 1974b). The tephras and tuffs were dated using the fission track method and found to be mainly Middle Pleistocene in age. Seward described the units, their mineral assemblages, and other characteristics. This has allowed the tuffs and tephras to provide both intrabasinal and interbasinal correlation.

An important new development arose when Froggatt (1983) demonstrated the usefulness of the electron microprobe in the development of a comprehensive volcanic stratigraphy for the upper Quaternary in New Zealand (Brackley, 1999). Recent dates of Whanganui Basin tephras and tuffs are included in Table 2.1. It was shown by Froggatt (1983) that tephras and tuffs can be identified in many different environments with the electron microprobe technique. This allows correlation of the tephra or tuff with a distal ignimbrite sheet. The use of electron microprobe analysis on glass shards has allowed a more accurate chronology of accumulation rates, and timing of tectonic events in the Whanganui Basin to be constructed. This technique allows the intergration of stratigraphic studies on river terraces, marine terraces, and palynological studies.

Alloway *et al,* (1993) revised the marine chronology of the Whanganui Basin which was based on some key fission track dates from Seward (1974a, 1974b). In this work Alloway highlights the problems associated with fission track dating of glass shards. Fission track

dating is more accurate when applied to the zircon grains in a tephra or tuff bed. However, due to low abundance of zircons, fine grain size and presence of detrital grains, it is often not possible to date tephra or tuff beds unless glass shards are used (Alloway, *et al*, 1993). Fission track dating of glass shards gives less reliable ages than zircons due to partial fading of fission tracks in the glass. This has resulted in many fission track ages being younger than the true sample age (Seward, 1979).

Westgate (1988, 1989) combined two methods of correcting for partial annealing of zircon fission tracks into a method termed isothermal plateau fission track (ITPFT) dating. Alloway *et al*, (1993) applied this new technique to zircons from tephras and tuffs in the Whanganui Basin. The Rangitawa tephra yielded ages that were in agreement with previously determined zircon fission-track age estimates of 0.35 Ma (Kohn *et al*, 1992). The previously determined ages for the Potaka pumice and the Pakihikura pumice were found to be underestimated.

Table 2.1: Ages for tuff and tephra horizons in Whanganui Basin (Pillans *et al,* 2005).

| Tuff | Published ages (Ma) |
|---|---|
| Rangitawa | 0.35 (z) |
| Kupe | 0.63 ± 0.08 (z) |
| Kaukatea | 0.86 ± 0.08 (z) |
| Potaka | 1.00 ± 0.03 (z) |
| Rewa | 1.20 ± 0.14 (z) |
| Mangapipi | 1.51 ± 0.16 (z) |
| Ridge | 1.56 (a) |
| Pakihikura | 1.58 ± 0.08 (z) |
| Birdgrove | 1.60 (a) |
| Mangahou | 1.63 (a) |
| Maranoa | 1.64 (a) |
| Ototoka | 1.72 ± 0.32 (z) |
| Table Flat | 1.71 ± 0.12 (z) |
| Vinegar Hill | 1.75 ± 0.20 (z) |
| Waipuru | 1.79 ± 0.15 (z) |

z = Isothermal plateau fission track date
a = Astronomical age

New ITPFT ages of 1.05 ±0.05 and 1.63 ±0.15 Ma for the Potaka and Pakihikura pumice respectively are consistent with new magnetostratigraphic data; placing the Potaka within the Jaramillo Subchron and the Pakihikura within the Matuyama Chron (Alloway *et al,* 1993). Generally, the original glass fission track ages of Seward (1976) are considered to be minimum ages for the Whanganui Basin tephras (Alloway *et al*, 1993).

## 2.4 Magnetostratigraphy

Magnetostratigraphy has proved to be a useful tool in the Whanganui Basin, not only in helping to construct a chronostratigraphic framework for the sedimentary sequences but also for correlating them to the oxygen isotope timescale. The blue-grey (mostly highstand) siltstones which occur cyclically throughout the Whanganui succession yield excellent palaeomagnetic signatures (Carter & Naish, 1998). Turner & Kamp (1990) described and revised the magnetostratigraphy for the lower part of the Castlecliff section in the Whanganui Basin, presenting the first published data on the occurrence of the Matuyama/Bruhnes boundary.

Pillans *et al,* (1994) extended the work of Turner and Kamp (1990) and presented magnetostratigraphic, lithostratigraphic and tephrostratigraphic results from four successions of early to middle Pleistocene age. The Matuyama to Jaramillo transition at 0.98 Ma (Berggren *et al*, 1985) is contained in the unconformity between the Upper Maxwell Formation and the Butlers Shell Conglomerate. The Jaramillo to Matuyama transition at 0.91 Ma lies within the unconformity between the Okehu Shell Grit and the Lower Okehu Silt-stone. The Matuyama-Brunhes transition is recorded almost completely within the Kaikokopu Shell Grit and the lower part of the Upper Westmere Siltstone (Kamp & Turner, 1990). Key paleomagnetic tiepoints which are used for calibrating sections to the isotope record include; the Gauss/Matuyama boundary (2.58 Ma), the Olduvai Subchron (1.94–1.76 Ma), the Cobb Mountain Subchron (1.19 Ma), the Jaramillo Subchron (1.07–0.99 Ma), and the Matuyama/Brunhes boundary (0.78 Ma) (Carter & Naish, 1998).

## 2.5 The sequence stratigraphic model

The sequence stratigraphic model and its predecessor seismic stratigraphy were developed by the Exxon group in the 1970's and 1980's. Their model, published in the 1988 Special Publication 42 of SEPM (Wilgus *et al*, 1988) defines a depositional sequence as one that is bounded by sub-aerial unconformities on the basin margin and their correlative surfaces farther basinward (Embry, 2009).

The depositional sequence can be divided into four component units termed systems tracts. The lower unit, the lowstand systems tract (LST) consists of a basal unit of turbidites overlain by a progradational wedge which on-laps the upper slope portion of the sequence

bounding unconformity. Progradational sedimentation is where sediments build out in a basinward direction, while retrogradation is where sediments begin to onlap in a landward direction.

The LST is bounded by the sequence boundary below and the transgressive systems tract (TST) above. It is deposited during a slow relative rise in sea level immediately following a relative fall in sea level. The LST is only preserved in the seaward portion of the basin, given the majority of the continental shelf is exposed to erosion during eustatic sea level fall, forming a widespread unconformity.

The TST contains retrogradational sediments that overstep the LST (Fig 2.1). The transgressive surface is the bottom of the TST; this surface represents the change from progradational to retrogradational sedimentation. The TST is bounded by the transgressive surface and the maximum flooding surface (MFS). The MFS has been defined as the surface that marks the change from retrogradational sedimentation below to progradational

Fig 2.1: The sequence stratigraphic model, showing the highstand (HST) transgressive (TST), lowstand (LST), and Regressive systems tracts (RST) (adapted from Holland, 2013).

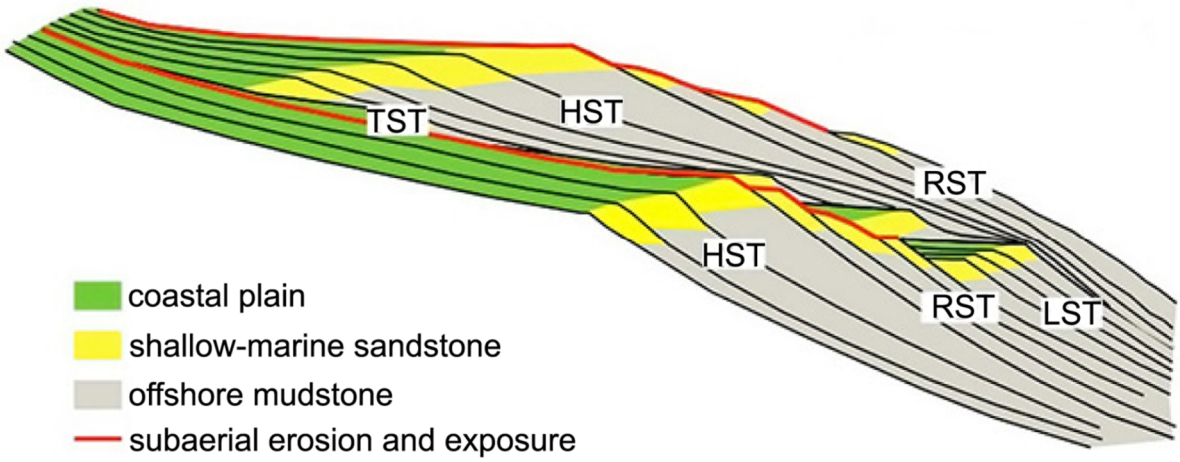


sedimentation above (Wilgus *et al*, 1988). This systems tract forms during a relative rise in sea level that is rapid enough to outpace the rate of sediment accumulation. A mid cycle condensed *in situ* shell bed often occurs between the TST and the HST (Type B shellbed). A mid cycle condensed shell bed is where crushed up shell material is concentrated within a nearshore environment during eustatic sea level rise (Type A shellbed).

The highstand systems tract (HST) comprises progradational sediments capped by a sub-aerial unconformity. The HST forms during the waning stage of eustatic sea level rise and the early portion of eustatic sea level fall (Wilgus *et al*, 1988). This is where the rate of sea level rise drops below the sedimentation rate, allowing progradational sedimentation to occur.

The regressive systems tract (RST) follows the HST, forming as the rate of eustatic sea level fall exceeds the rate of subsidence, leading to a relative fall in sea level. This causes a forced regression during which the coast is forced to build seaward. The erosional surface which marks the beginning of the RST is known as the surface of forced regression. The RST may contain several surfaces of forced regression and does not usually contain cycles bounded by unconformities.

## 2.6 Application of the sequence stratigraphic model to the Whanganui Basin

Many studies have focused on the Whanganui Basin and applying sequence stratigraphic models to its sedimentary succession. A model has been developed for the western Whanganui Basin, where sedimentation kept pace with subsidence throughout much of the basin history (Carter & Naish, 1998). A majority of the sedimentation occurred in a shallow marine shelf environment with a maximum water depth of around 75 m (Brackley, 1999).

The sedimentary sequences preserved at the Whanganui coastal section represent the TST, HST and part of the RST during interglacial periods; while the LST during glacial periods are represented by unconformities due to exposure of the shelf to erosion as a result of eustatic sea level fall. Sedimentation during TST characteristically occurred in terrestrial, beach or shoreline environments, while sedimentation during HST occurred on the mid to outer shelf environments.

Abbott and Carter (1994) described ten superposed cyclothems from the coastal Castlecliff section of Whanganui Basin and correlated them with interglacial parts of oxygen isotope stages 31–11 (0.95– 0.35 Ma). The Castlecliff motif recognised by Abbott and Carter (1994) comprises a lower interval of shallow marine sands and transported shellbeds (TST), an in-situ or near-situ mid-cycle condensed unit (shellbed), and an upper interval of shelf siltstone (HST).

Naish and Kamp (1995, 1997a) described twenty superposed cyclothems from the Late Pliocene–Early Pleistocene succession which occur in Rangitikei River. The Rangitikei motif described by these authors, comprises a lower fossiliferous unit (combined TST/mid-cycle condensed unit), followed by a middle aggradational interval of siltstone (HST) which grades up into a progradational shoreline facies assemblage (RST). Carter *et al*, (1997) and Saul *et al*, (1998) have summarised the complete fill of the Whanganui Basin, recognising seven major sedimentary motifs (Fig. 2.2) which occur as variations of the 47 vertically stacked cyclothems.

Fig 2.2: The seven major cyclothemic (sequence) motifs recognised within the Whanganui Basin (Carter & Naish, 1998).

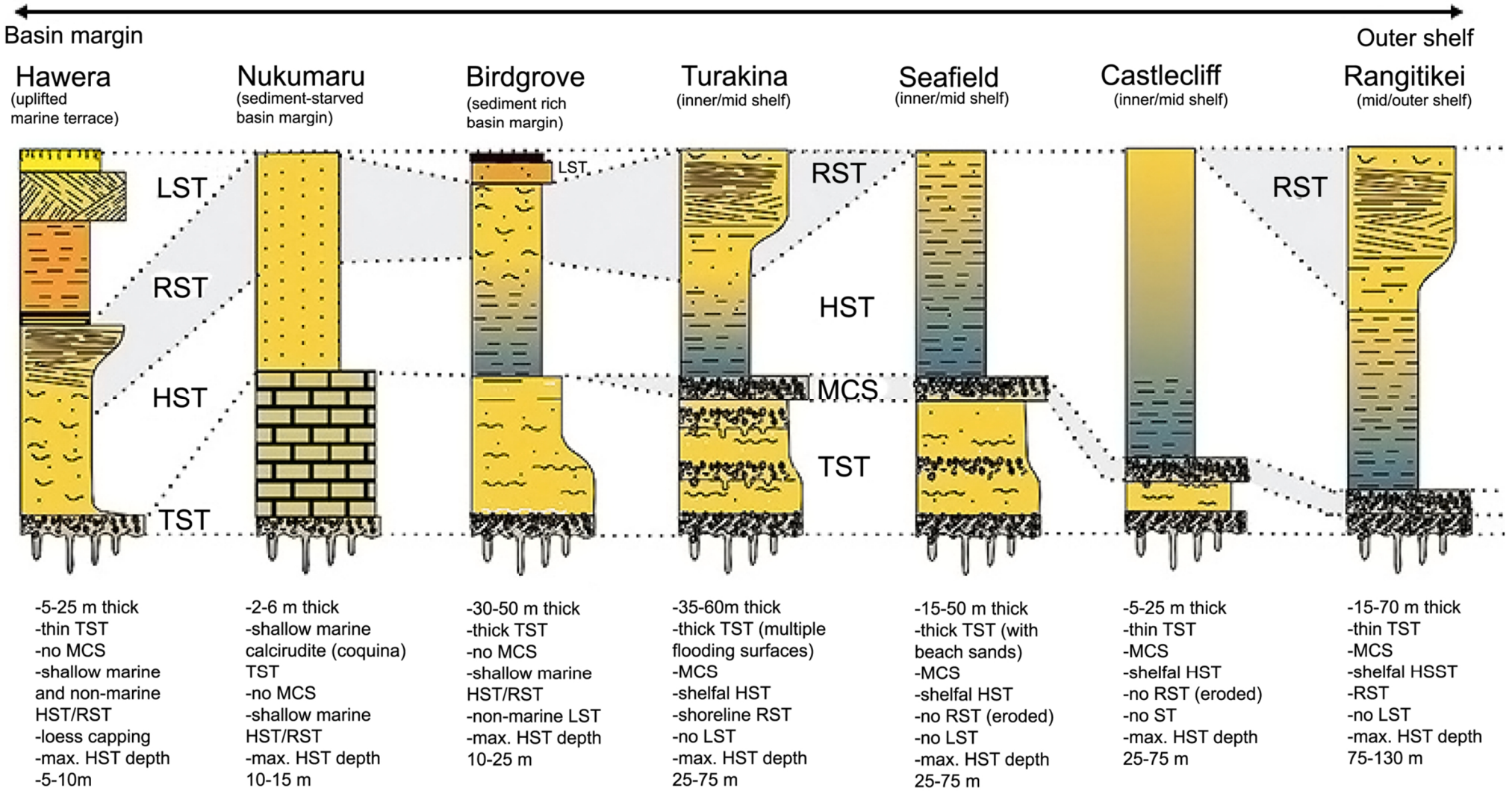

Shellbeds are associated with the transgressive surface of erosion, a local flooding surface, the downlap surface and marine flooding surfaces (Naish, *et al*, 2004). Abbott & Carter (1994) distinguished type A shellbeds within the TST from type B shell beds which occur between the transgressive and highstand systems tract (mid-cycle shellbed). Type A shellbeds often show cross-bedding and contain reworked shallow water species. Type B shellbeds include offshore shelf species which are preserved in or near situ. The interpretation of sedimentary cyclicity in the Whanganui Basin depends on the identification of sediment bounding surfaces within each sequence (Abbott & Carter, 1994). Accurate identification of these surfaces and interpretation of the sequences is aided by an understanding of the shellbed types present and the habitat of the faunas within these beds (Naish *et al*, 2004).

## 2.7 The geology of the Pohangina area

Two of the earliest and most detailed studies on the Cenozoic stratigraphy of the Pohangina area were conducted by the Superior Oil Company (Ower, 1943; Feldmeyer *et al,* 1943). Ower (1943) investigated the Pohangina area for The Superior Oil Company Ltd and identified several 'ash beds'. A fault line, Pohangina Fault, was interpreted to run through the lower part of the Pohangina Valley. To the west of the Pohangina Fault, the Pohangina Anticline was identified.

Te Punga (1952), Lillie (1953) and Kingma (1957a, 1957b, 1958, 1959) included parts of the Pohangina area in their mapping and stratigraphic descriptions, although their studies largely focused on different areas. The mapping included the Rangitikei (Te Punga, 1952), Dannevirke (Lillie, 1953) and the Ruahine Range (Kingma, 1957a, 1957b, and 1959).

Rich (1959) mapped the lower Manawatu Valley on the western side of the Tararua Ranges. His mapping area extended right to the Manawatu Gorge, where he mapped several fault lines as being present. Rich identified a reverse fault he named the 'Raukawa Fault' trending north-northeast across the Manawatu River, near the confluence of the Manawatu and Pohangina Rivers. This fault is exposed in the bank of the Manawatu River, however, to the south west the fault plane is covered by recent deposits. Steeply dipping beds on the trend of the fault suggest it passes into a monoclinal flexure to the southwest. North of the Manawatu River the fault swings slightly northwards and continues along the left bank of the Pohangina River where it has been mapped by Lillie (1953) and (Ower, 1943) as the "Lower Pohangina fault".

Kingma (1962) mapped most of the Pohangina Anticline strata as Castlecliffian gravels, sands and silts with or without pumice bands, either in marine sequences or in highly dissected river terraces.

Carter (1972) published a field study in the Komako district of the Pohangina Valley. He subdivides the late Plio-Pleistocene sedimentary succession into three formations: the Takapari, Konewa, and Komako Formations. These formations were dated using biostratigraphy and found to be Mangapanian to Castlecliffian in age. The upper Pohangina Fault of the Superior Oil Company geologists (Ower, 1943; Feldmeyer *et al,* 1943) was re-interpreted by Carter as a monocline structure.

Detailed palynological work was undertaken by Mildenhall (1975) on the carbonaceous beds identified by Carter (1972) within the Takapari Formation. Mildenhall infers a coastal environment largely consisting of swamp sedges with scrub and grassland species. Tree pollen was found to be rare and the trees interpreted to be restricted to high country to the east. The paleo-climate is interpreted as being cool to mild during Nukumaruan-Okehuan time. He also describes the palynomorph of the extinct *Acacia* type pollen.

Seward (1974a, 1974b) studied the sedimentary sequences preserved at Finnis Road, Pohangina. The Upper Finnis Road and Lower Finnis Road ashes were included in her study of Pleistocene tephras preserved in the Whanganui Basin. Seward used fission track dating to date the tephras preserved within the sediments. The fission track method has since been found to underestimate the ages of tephras and isothermal plateau fission track (ITPFT) dating has now been used to more accurately date the tephras (Alloway *et al*, 1993).

MacPherson (1985) provided a detailed investigation of the stratigraphy and tephras preserved at Finnis Road. Eleven tephras were correlated from around Finnis Road to known tephras of the North Island. The tephras were identified as being correlatives of the Kawakawa Tephra, Kaingaroa Ignimbrite, Matahina Ignimbrite, Mount Curl Tephra, Omokoroa Tephra, and the Lower Kakariki Tephra. The provenance of the sediments at Finnis Road was interpreted to be largely from the Central North Island Volcanic Zone. The sediments were interpreted to have been deposited in shallow marine environments from 420 to 180 ka. Since this time the tephras preserved at Finnis Road have been re-dated and the sedimentary sequence has been re-interpreted (Brackley, 1999).

Marden (1984) mapped the Torlesse greywacke of the southern Ruahine Ranges extending to the Manawatu Saddle and Manawatu Gorge area. The study mapped the greywacke at a scale of 1:25,000 focusing on the Mesozoic greywacke and subdividing the bedrock into separate lithologies. The geological structures of this area were studied in detail, including folding, deformation, and style and timing of faulting. A detailed geological history of the area is provided. Fault lines mapped by Rich (1959) and Ower (1943) were included in the map along with a detailed investigation of the eastern side of the Ruahine Ranges including the Wellington and Ruahine Faults.

Manning (1988) described the stratigraphy and interpreted paleoenvironment of deposition of Mid-Quaternary sediments in Cullings Gully, north east of Finnis Road. Manning correlated the upper tuff unit (Tephra A) with the Lower Finnis Road Ash of Seward (1974). He interpreted that the major source of the sediments preserved at Culling's Gully was the main axial greywacke ranges and the central North Island volcanic region. Manning interpreted planar laminated sands as being deposited into a high energy, shallow marine environment. The environment of deposition was interpreted as a wave influenced shallow marine delta, just seaward of an estuary.

Jackson, *et al,* (1988) examined the drainage systems on the Marton, Feilding, Mt Stewart Halcombe and Pohangina anticlines. These anticlines have been interpreted to be located above buried west dipping reverse faults in the basement (Melhuish *et al,* 1996). Using a 0.3 Ma marine horizon, it was calculated that the anticlines have vertical uplift rates of <1mm per year, and their drainage patterns have evolved in response to the regional tilting (Jackson *et al*, 1988). It was identified that the four anticlines are asymmetric, with gently sloping western limbs and steeply dipping eastern limbs, which was interpreted as reflecting the westward dip of the underlying reverse faults.

Townsend (1993) conducted a study on the sedimentary sequences preserved at Beehive Creek, approximately 2 km northeast of Pohangina township. Townsend interpreted the provenance of the sediments as being the greywacke axial ranges to the east and the Central Volcanic Plateau to the north. Large trough cross beds were interpreted as being deposited within a fluvial system, while planar laminated sands and cross beds were interpreted as representing a shallow marine environment. Lignite beds within the sequence were interpreted as representing an estuarine environment. The environment of deposition was interpreted as being a river dominated delta, with a shallow marine component just seaward of an estuary. Townsend (1993) sampled and probed four tephras from Beehive Creek. T3 was the only sample which could be correlated to a sample of known age, that being the Rangitawa Pumice. Since this study the Beehive Creek section has been re-interpreted and tephra beds contained within the sequence have been correlated to substantially older tephras (Brackley, 1999).

Alloway *et al*, (1993) revised the marine chronology of the Whanganui Basin which had up until this point had been based on fission track dating of tephras. Alloway *et al*, (1993) used isothermal plateau fission track dating to gain more accurate dates for the tephras preserved within the Whanganui Basin. The Upper Finnis Road tephra is correlated with the Middle Griffins Road Tephra and the Lower Finnis Road tephra is correlated with the Kakariki tephra of Bussell (1984). More recently the tephras at Finnis Road have been correlated with the Rewa and Potaka Tephras (Brackley 1999).

Pillans (1994) worked on the Finnis Road sedimentary sequence. He found radiolarian preserved within assemblages lacked *Stylatractus universus*, known to become extinct around 420 ka (Morley & Shackleton, 1978). Pillans (1994) concluded that the Lower Finnis Road tephra was younger than 340 ka as it also contained occasional reworked Rangitawa Pumice glass shards.

Brackley (1999) investigated Nukumaruan/Castlecliffian sedimentary sequences in the Pohangina region. The study area included Beehive Creek, Finnis Road, and Cullings Gully over an area of approximately 133 km between the Oroua and Pohangina Rivers. Age control of the sequences was provided by several coarse pumiceous tuffs. The tuffs were correlated through microprobe analysis. The tuffs included the Rewa pumice (1.29 ±0.12 Ma), the Potaka pumice (1.05 ±0.05 Ma), the Kaukatea pumice (0.87 ±0.05 Ma) and the Kupe pumice (0.63 ± 0.08 Ma). Rates of deformation of 7 degrees per 100 ka were calculated by using the absolutely dated tuff horizons. The environment of deposition was interpreted to be a shallow marine environment until around the eruption of the Potaka Tephra, above which the sediments are dominantly fluvial including lignites, overbank deposits and channel gravels deposited in a lower coastal plain setting. Through the use of sequence stratigraphy and tephrochronology Brackley (1999) correlated the Pohangina sections to age equivalent sections in Castlecliff, Turakina and Rangitikei River sections. Cyclothems 33 -40 were found to be present in the Pohangina sections.

# Chapter 3
# Regional structure

## 3.1 Overview

Continental shortening across the Whanganui Basin as a result of convergent plate tectonics has formed a number of northeast to north-northeast striking active faults (Anderton, 1981). Seismic reflection profile studies indicate these are reverse faults, dipping westward (Melhuish *et al,* 1996). Many of the faults are buried by late Quaternary and Holocene sediments and therefore fail to penetrate the surface. These major reverse faults are relatively long lived and are believed to have been active since the early Pleistocene (Begg *et al*, 2005).

The structure of the Whanganui Basin has been determined via onshore geological mapping by Fleming, (1953); Te Punga, (1957); Feldmeyer *et al*, (1943); Lensen, (1977); and Jackli, (1957). Later, seismic reflection profiles show sediments have low angle regional dips towards a depocentre located to the south of Whanganui City (Anderton, 1981). Emergence of the northern Whanganui Basin has been associated with offlap and a southward migration of the basin depocentre through the Quaternary.

## 3.2 Folds

Towards the eastern margin of the Whanganui Basin gentle anticlines, including the Pohangina, Feilding, Marton, Mt Stewart-Halcombe, and Oroua anticlines, are found (Fig 3.1). These large scale active structures run parallel to the Ruahine Range and were first identified by Te Punga (1957). The anticlines are related to faulting of the basement at depth (Anderton, 1981). Both Feldmeyer *et al*, (1943) and Te Punga (1957) inferred that ridges of basement rock form the core of these anticlines. The controlling faults were moving during deposition and some of these faults are still growing (Jackli, 1957; Te Punga, 1957; Lensen, 1977). Active dextral reverse faults of the North Island Dextral Fault Belt (NIDFB) including the Wellington–Mohaka and Ruahine Faults border the eastern side of the ranges (Kingma, 1967; Lensen, 1977).

The Pohangina Anticline west of the Pohangina River is the eastern most of the anticlines; although this structure is not within the mapping area it plays an important role in the local geology. The Pohangina Anticline has a gentle western slope dipping, 2 – 4°, and a steep eastern limb with dips of up to 70 °. The anticline divides the drainage pattern of the Pohangina valley. This is visible from aerial/satellite photography (Fig 3.1). The divide occurs close to the eastern limb, representing the anticline axis which plunges southwards.

## Pohangina Faulted Monocline

The Pohangina faulted monocline is located between the Ruahine Ranges and the Pohangina River (Fig 1.5). The monocline becomes evident as the strata begin to dip at angles of up to 70° towards the west near the true left bank of the Pohangina River. The geological structure of the Pohangina Valley between the Ruahine Ranges and the Pohangina Anticline has been interpreted in several different ways over the past 60 years.

A survey of the Pohangina area by Greenall *et al*, (1951) and later mapping of the geology of the Manawatu Valley by Rich (1959), both interpreted the structure as being a syncline. These two studies identified strata dipping sharply eastwards near the Pohangina River, forming the limb of a syncline. Rich (1959) suggests the Pohangina syncline is occupied by the Pohangina River farther to the north of his study area (which ends at the Manawatu Gorge). Mapping by Te Punga (1957) and Kingma (1962) interpret the structure as a fault. Kingma (1962) mapped the fault as being active in recent times. Carter (1972) found there were no offsets of river terraces in the Komako District even where they are crossed by the 'faulted monocline'. This led Carter to reject Kingma's interpretation of the Pohangina monocline being an active fault.

Carter interprets the Pohangina monocline as being controlled by a fault in the greywacke basement at very shallow depth. No evidence for Late Quaternary fault displacement along the Pohangina Monocline has been found. It is therefore considered to have been inactive during Late Quaternary times. However, evidence for recent faulting has been found during this study, along the Pohangina River west of the monocline. Offset strata, offset of the Ohakean Terrace and changing dip directions all provide evidence for a fault along the path of the Pohangina River. This fault is informally named the Pohangina Fault. However, the Pohangina Fault runs to the west of the Pohangina Faulted Monocline and is not related to its formation which likely predates any rupture along the Pohangina Fault.

Thrust faulting has resulted in the growth of the Ruahine Ranges as greywacke basement is thrust up along contact faults, which separate greywacke basement from the overlying Plio-Pleistocene sediments (e.g. Whareroa Fault, Fig 3.5). Thrust faulting has also resulted in the deformation of the Plio-Pleistocene sediments as the underlying greywacke basement is thrust up, and faults begin to propagate up through the overlying sedimentary units. The Pohangina Faulted Monocline is a feature that has developed in response to the basement faulting. The thrust faults are evident in Fig 3.5, cross section C to C-.

The Pohangina Faulted Monocline can be traced across the study area by interpreting dip data and the distribution of lithologies. The monoclinal structure does not form a discrete surface trace, although its presence is clear in outcrop. Continued convergence along the Pacific Australian Plate boundary is driving movement along fault lines uplifting the Ruahine

Range. The ongoing convergence could in the future result in fault rupture along the Pohangina Faulted Monocline; therefore this structure is classified as a potentially active fault.

During the geological mapping of the Lower Pohangina Valley particular effort was made at tracing the Pohangina Faulted Monocline and fault lines across the landscape. Cross sections (Figs 3.3 – 3.6) were constructed and balanced across the valley at regular intervals to accurately document geological structures. The geological map of the Lower Pohangina Valley (Fig 3.2) is included in this section to show the local geology and the location of cross section lines.

Fig 3.1: Fold axes of the Manawatu anticlines overlaid on an Enhanced Thematic Mapper satellite image of the Whanganui Basin (after Jackson *et al*, 1998; Clement, 2011)

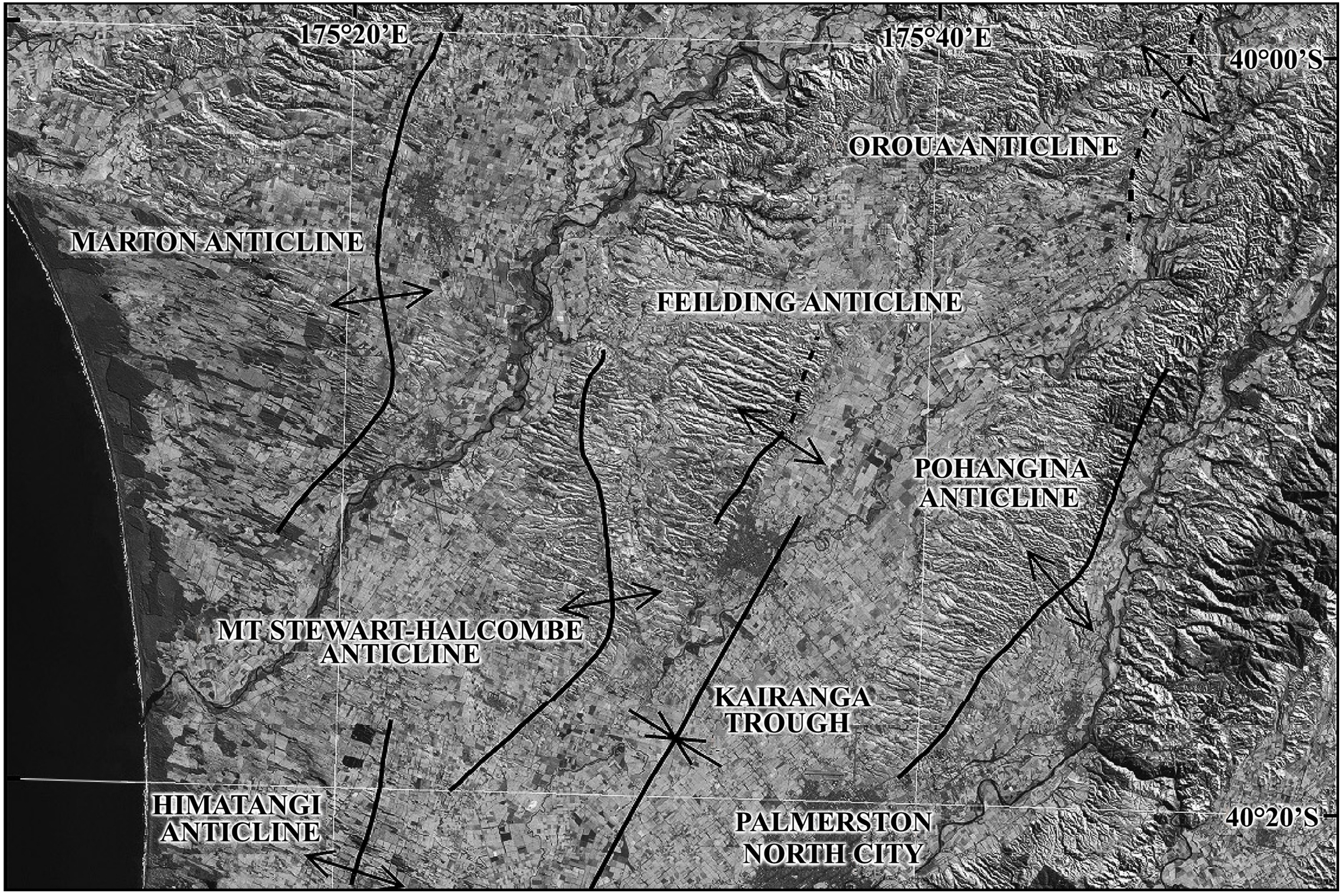

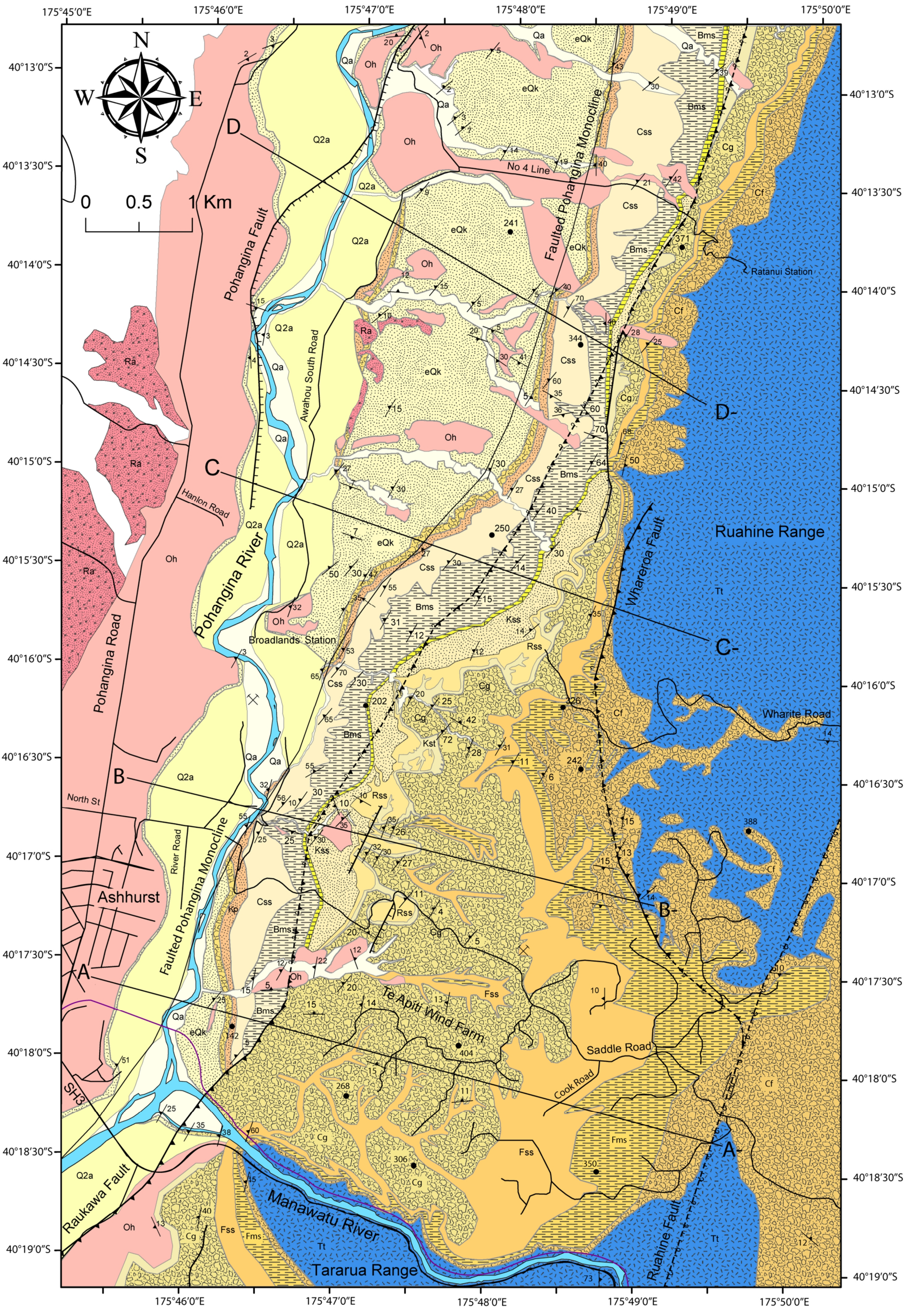


Drawn on Transverse Mercator Projection
Origin of projection: 175°45’0’’E Long, 40°13’0’’S Lat.
Grid line labels are in terms of the WGS84 Datum
Base complied from data supplied by Land Information New Zealand

Fig 3.2: Geological map of the lower Pohangina Valley, showing location of cross sections.

| LEGEND | | | | | | |
|---|---|---|---|---|---|---|
| Symbol | Member | Formation | Zone | Stage | Series | Epoch |
| Qa | Alluvium | Recent | Not applicable | Haweran | | Holocene |
| Qa2 | Degradational Terraces | | | | | |
| Oh | Ohakean Terrace | Ohakean | | | | |
| Ra | Ratan Terrace | Ratan | | | | |
| Unconformity | | | | | | |
| eQk | Sandstone Member | Kai Iwi Group | Not applicable | Castlecliffian | Whanganui | Pleistocene |
| Rc | Red conglomerate Member | | | | | |
| Kp | Kaimatira Pumice Sand Formation | | | | | |
| Css | Crossbedded sandstone Member | Takapari Formation | | | | |
| Bms | Blue grey sandy mudstone Member | | | | | |
| Cq | Coquina limestone Member | Konewa Formation | *Struthiolaria (Pelicaria) convexa* | Nukumaruan | | |
| Kss | Marine sandstone Member | | | | | |
| Rss | Red cross bedded sandstone Member | | | | | |
| Kst | Sandy blue grey mudstone Member | | | | | |
| Cg | Conglomerate Member | | | | | |
| Fss | Fossiliferous sandstone Member | Komako Formation | *Chlamys (Phialopecten) triphooki* | Mangapanian | | |
| Fms | Fossiliferous mudstone Member | | | | | Pliocene |
| Cf | Flaggy grit Member | | | | | |
| Unconformity | | | | | | |
| TJ | Greywacke | Torlesse Supergroup | | | | Jurassic |

## GEOLOGICAL SYMBOLS

- Transform fault
- Dip and dip direction
- Inferred normal fault (ticks on downthrown side)
- Inferred reverse fault (teeth on overthrust side)
- Normal fault (ticks on downthrown side)
- Reverse fault (teeth on overthrust side)
- Monocline

## TOPOGRAPHICAL REFERENCE

- Elevation in metres
- Quarry
- Railway
- Roads
- River

**Fig 3.3:** Top: Geological cross section running west to east, A to A-. Bottom: restored section

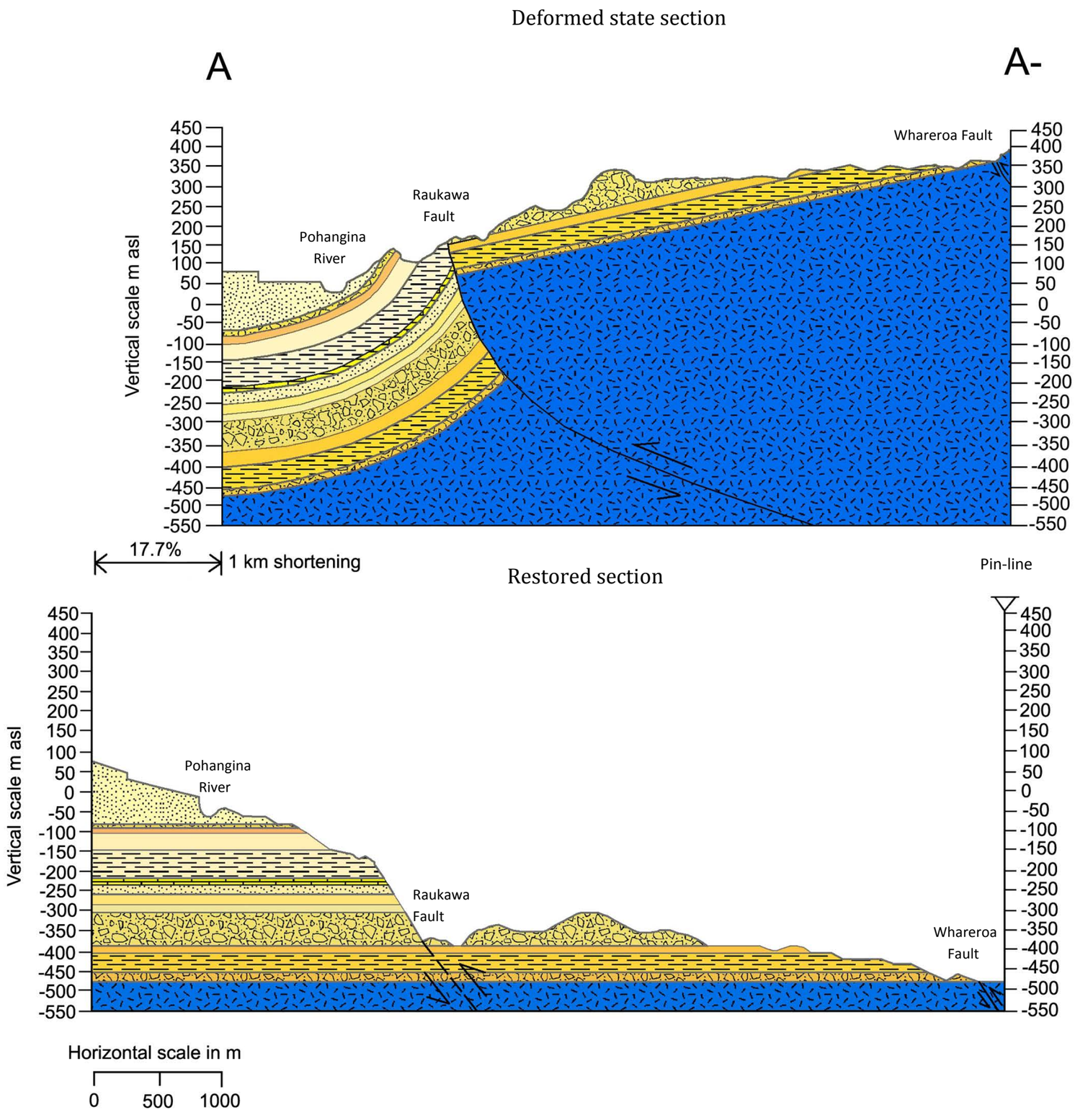

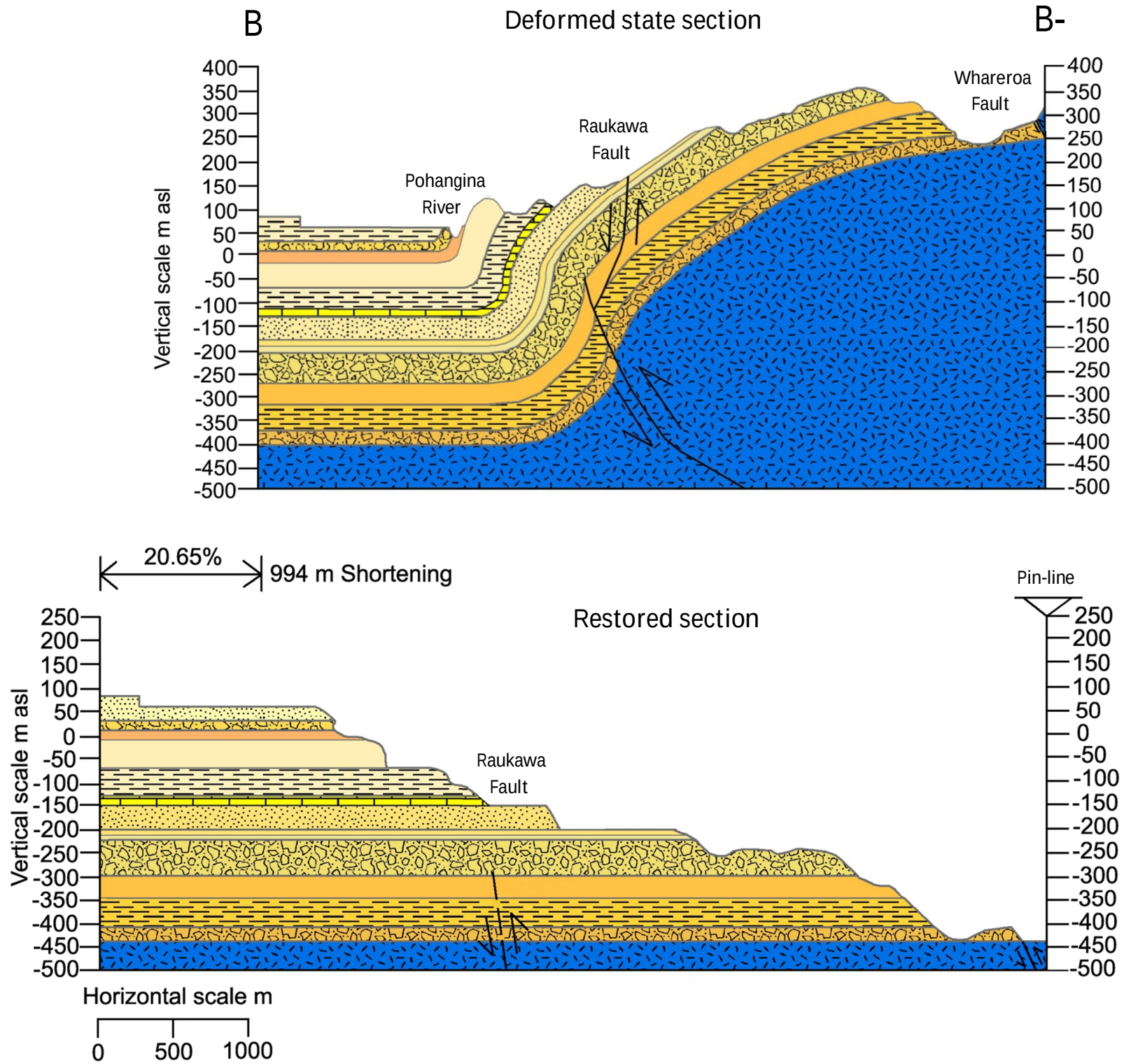


Fig 3.4: Top: Geological cross section running west to east, B to B-. Bottom: restored section

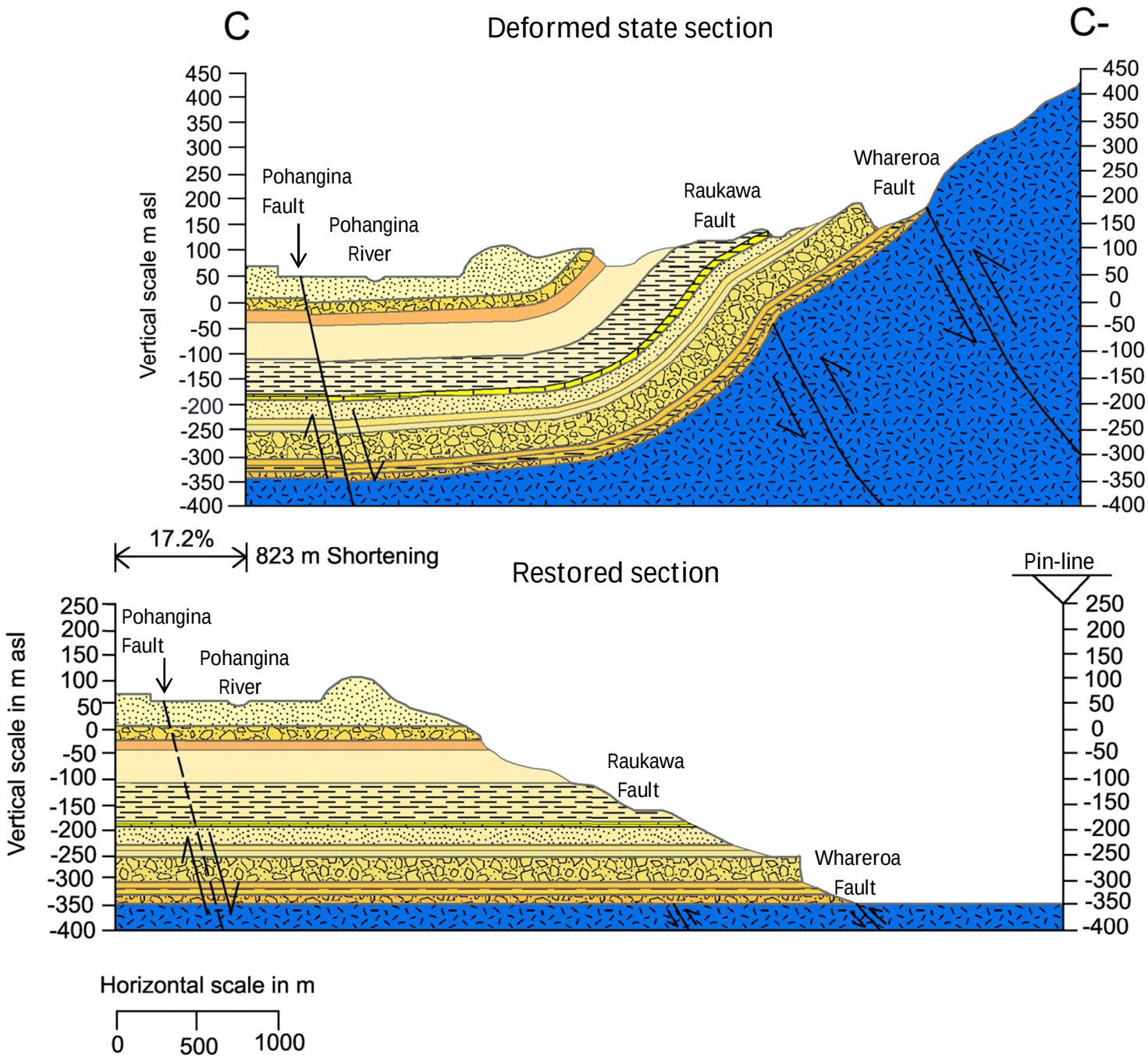


Fig 3.5: Top: Geological cross section running west to east, C to C-. Bottom: restored section

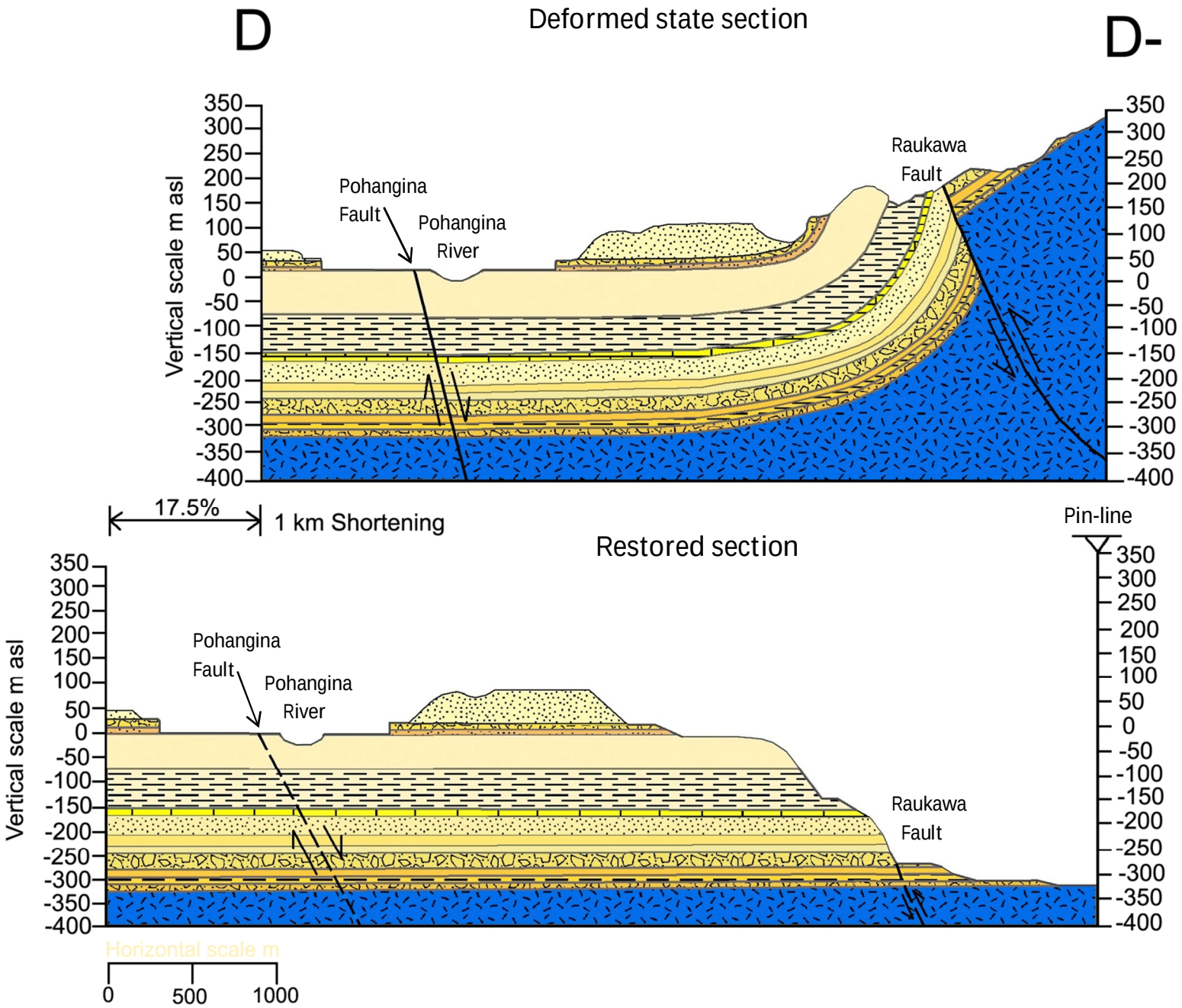


Fig 3.6: Top: Geological cross section running west to east, D to D-. Bottom: restored section

## 3.2. Faults

### Ruakawa Fault

One of the most conspicuous fault lines in the lower Pohangina area is the Raukawa Fault (Figs 3.2 and 3.3). It has been traced along the true left side of the Manawatu River valley by Rich (1959). The Raukawa Fault is a high angle reverse fault trending NE-SW. Rich (1959) noted an outcrop of the fault plane in the Manawatu River near the site of the former Raukawa Pa. Here the fault plane strikes 30° E and dips 80° SE. Rich (1959) traces the Raukawa Fault from the confluence of the Pohangina and Manawatu Rivers 4.8 km to the southwest. Rich (1959) interprets the Ruakawa Fault as passing into a monoclinal flexture to the southwest of the Manawatu Gorge. Evidence for this is seen in the steeply dipping beds on the trend of the Raukawa Fault in an area with low regional dips.

In this study the Ruakawa Fault is traced a further 705 m NE from where it no longer has surface exposure and is interpreted to the NE. The outcrop of the Ruakawa Fault at the far western end of the Manawatu Gorge is suggested to be a result of the high rates of down cutting of the Manawatu River in the area, which has stripped away the majority of the Plio-Pleistocene cover rocks, exposing the fault plane. Farther to the NE the fault does not propagate to the surface due to a greater thickness of overlying sediments. In this area the fault is considered to be present at shallow depth and is responsible for the tilting of the overlying strata into a monoclinal flexure.

Evidence for offset on the Ruakawa Fault is also provided by unconformable stratigraphy in the Manawatu Gorge area, where strata of the Konewa Formation have been thrust up over both Takapari Formation and Kai-Iwi Group sediments. In cross section A to A- (Fig 3.3) up to 300 m of displacement is present on the Raukawa Fault; this displacement represents the maximum displacement in an area where the underlying thrust fault has propagated to the surface. Farther NE the displacement is less, as the fault becomes a shallow reverse fault which only displaces the underlying Torlesse greywacke and Komako Formation (Cross sections B to B-, Fig 3.4; C to C-, Fig 3.5; and D to D-, Fig 3.6).

Marden (1984) suggests that the Pohangina Monocline is similar and possibly connected to the monoclinal structure to the south of the Manawatu Gorge that was mapped by Rich (1959). In this study it is suggested that these two monoclines are in fact connected and are both controlled at depth by the Raukawa Fault. Evidence for a link between the two folds is provided by Rich's observation of the Raukawa Fault becoming a monoclinal flexure south of the Manawatu Gorge. A similar observation has been noted north of the Manawatu Gorge in this study. The underlying thrust fault and the two monoclinal flexures are likely part of the same structure which has formed on the western margin of the main axial range, due to ongoing convergence.

The Raukawa Fault is inferred to continue in a NE direction from its exposure in the Manawatu River to Whareroa stream where it once again crops out. The fault exposure in Whareroa Stream is a normal fault dipping 75°W, this fault is interpreted to be the result of thrusting at shallow depth. Due to the stress generated by thrust faulting, the overlying strata have become offset by a normal antithetic fault (Fig 3.4, cross section B to B-).

Two unnamed normal faults with offsets in the order of 2 to 5 m are mapped on the Saddle Road and in Scrimmys Stream (Fig 3.2). These faults, too, are considered to be antithetic faults. Rupture is believed to have been caused by the build up of stress generated by thrust movement along the Raukawa Fault.

No offsets of river terraces are noted, therefore the Raukawa Fault is not considered to have been active recently. The Ruakawa Fault has been classifed as potentially active by Marden (1984), due to its close proximity and association with the rising main axial ranges.

## Whareroa Fault

The Whareroa Fault is a steep reverse fault which extends from the northern end of the Manawatu Saddle ending near the southern branch of Whareroa Stream. It has been mapped by Marden (1984) as a 1.5 km long, steep northwest- striking scarp separating Torlesse bedrock to the east from gently dipping Plio-Pleistocene marine deposits to the west. Ower (1943) observed the fault plane dipping at 80°E in the south branch of Whareroa Stream. In this study no east dipping fault planes were observed in Whareroa Stream, however, a fault dipping 75°W was observed in the true left fork of Whareroa Stream (Fig 3.7). This fault has been interpreted as an antithetic normal fault which joins the underlying thrust (Ruakawa Fault) at shallow depth (Cross section B to B-, Fig 3.4).

In this study the Whareroa Fault is interpreted as a 5 km long contact fault separating Torlesse greywacke from Plio-Pleistocene sediments. The Whareroa Fault is inferred to splay off from the Ruahine Fault half way between the Whariti and Saddle Roads (Fig 3.2). Dip data taken in this area show opposing directions, the up thrown eastern side dipping W to NW and the downthrown western side dipping S. The fault trace has been inferred to trend NW-SE along pockets of Torlesse greywacke, which display a very sheared and shattered nature (Fig 3.9). The fault veers sharply towards the NE at Whariti Road and begins to trend NE-SW, parallel with the Ruahine Range.

The fault trace does not outcrop at the surface in the Manawatu Saddle area. This is considered to be a result of the thrust fault not propagating to the surface and the fault plane being covered by Late Quaternary deposits. Fault gouge and breccia composed of angular, greywacke clasts are present along the Torlesse greywacke contact near Maungatukurangi Stream. The greywacke in this area is highly shattered and folded.

Fig 3.7: Antithetic fault plane dipping 75°W, south branch of Whareroa Stream, Broadlands Station, Pohangina Valley, Manawatu (WGS84 40°14'53.57"S 175°48'40.18"E elev 221m).

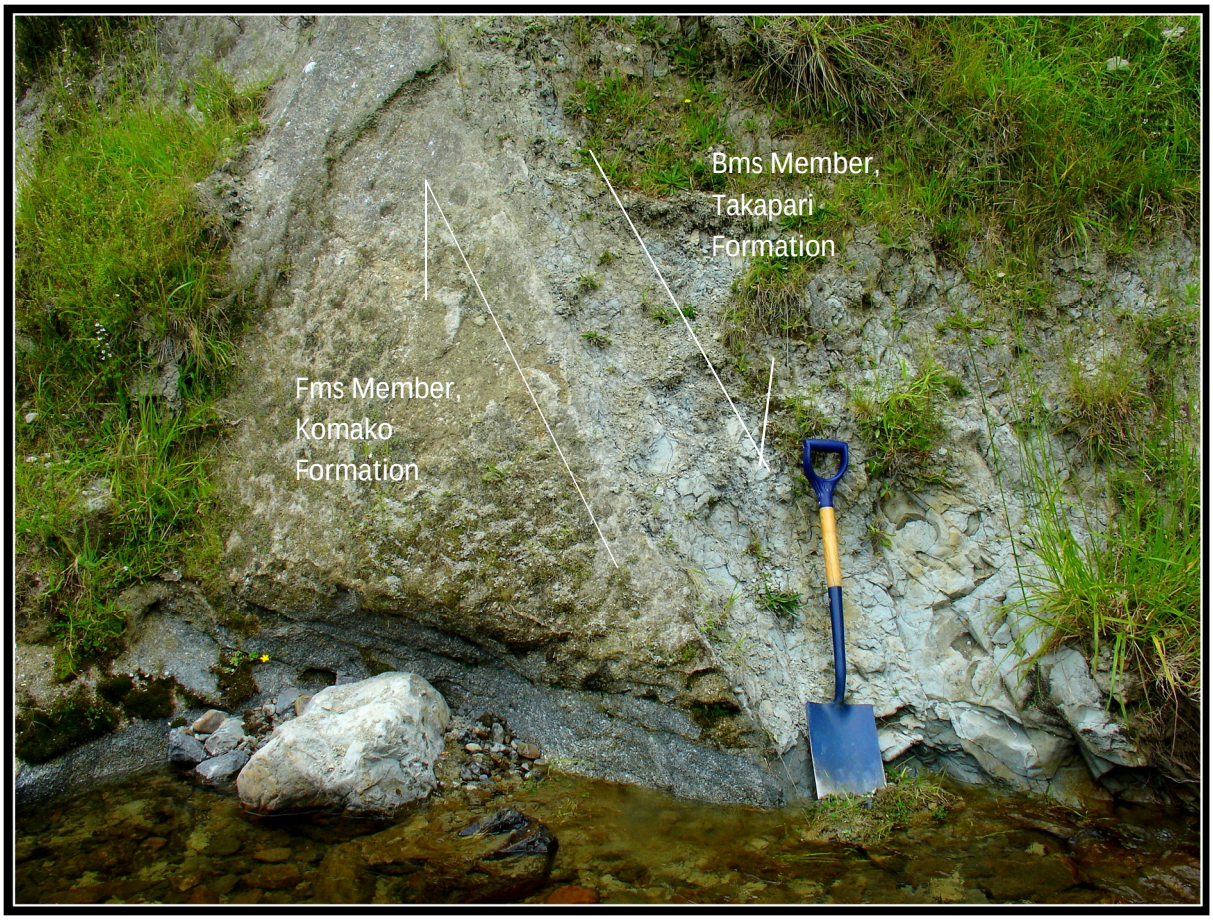

Fig 3.8: Exposure of a normal antithetic fault in Scrimmys Stream, interpreted to be connected to the Raukawa Fault at depth, Broadlands Station, Pohangina Valley (WGS84 40 °16'50.47"S, 175 °46'46.25"E, elev 98 m).

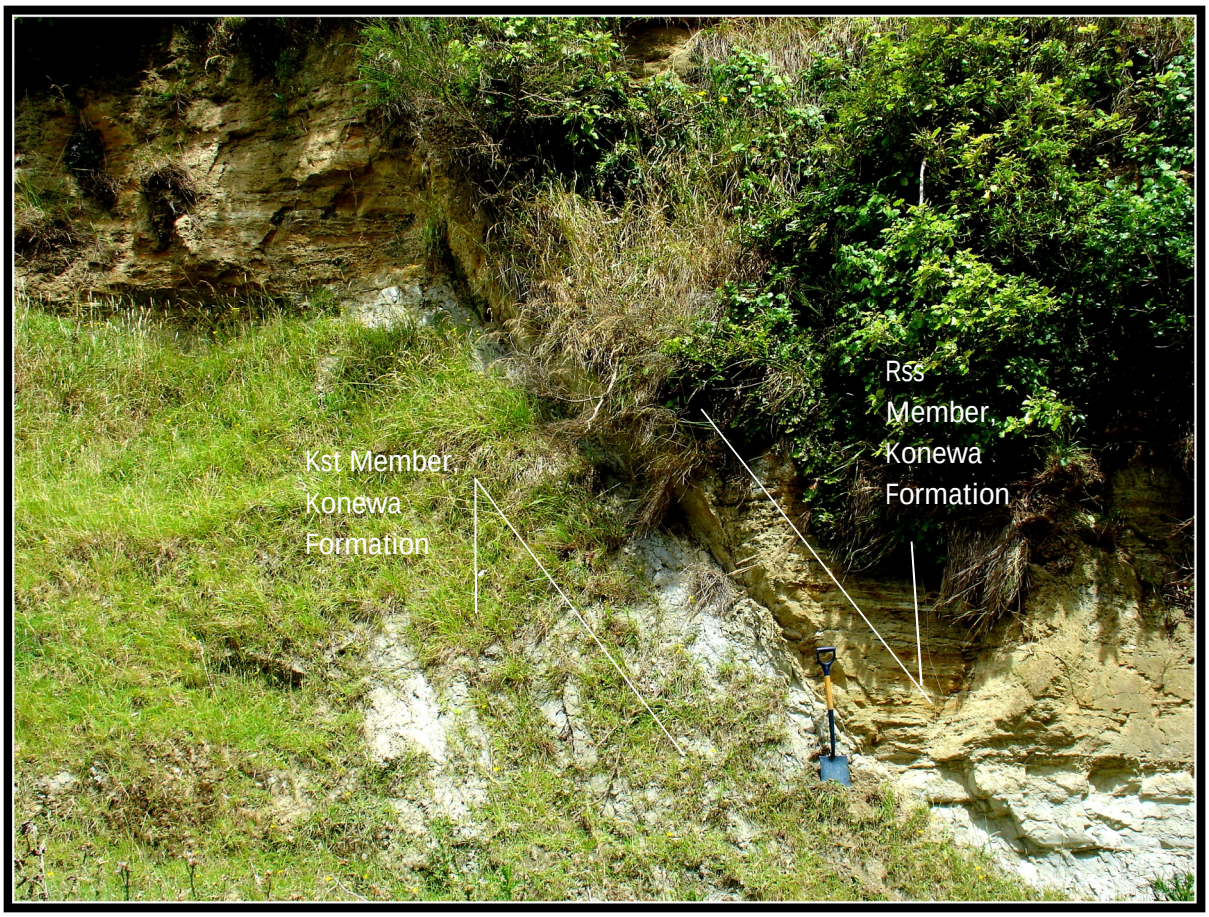


Ower (1943) observed the fault plane dipping at 80°E in the south branch of Whareroa Stream. The Plio-Pleistocene sediments to the west and south of Whareroa Fault have been dragged into moderate to steep attitudes as a result of uplift along the fault. Dips rapidly decrease over short distances west of the Whareroa Fault. No geomorphic features suggest recent fault displacement and no river terraces were found to be displaced where crossed by the fault. This suggests no movement has occurred along the Whareroa Fault over the past 50,000 years. Marden (1984) considered the similar strike and physiographic expression between the active and contact faults in the lower Ruahine Range to provide evidence that all contact faults in this area are potentially active.

Fig 3.9: Contact between Torlesse greywacke and Cf Member Komako Formation, note the highly sheared and shattered greywacke, Antler Stream, Pohangina (WGS84 40°17'31.12"S, 175°49'19.90"E, elev 327 m).

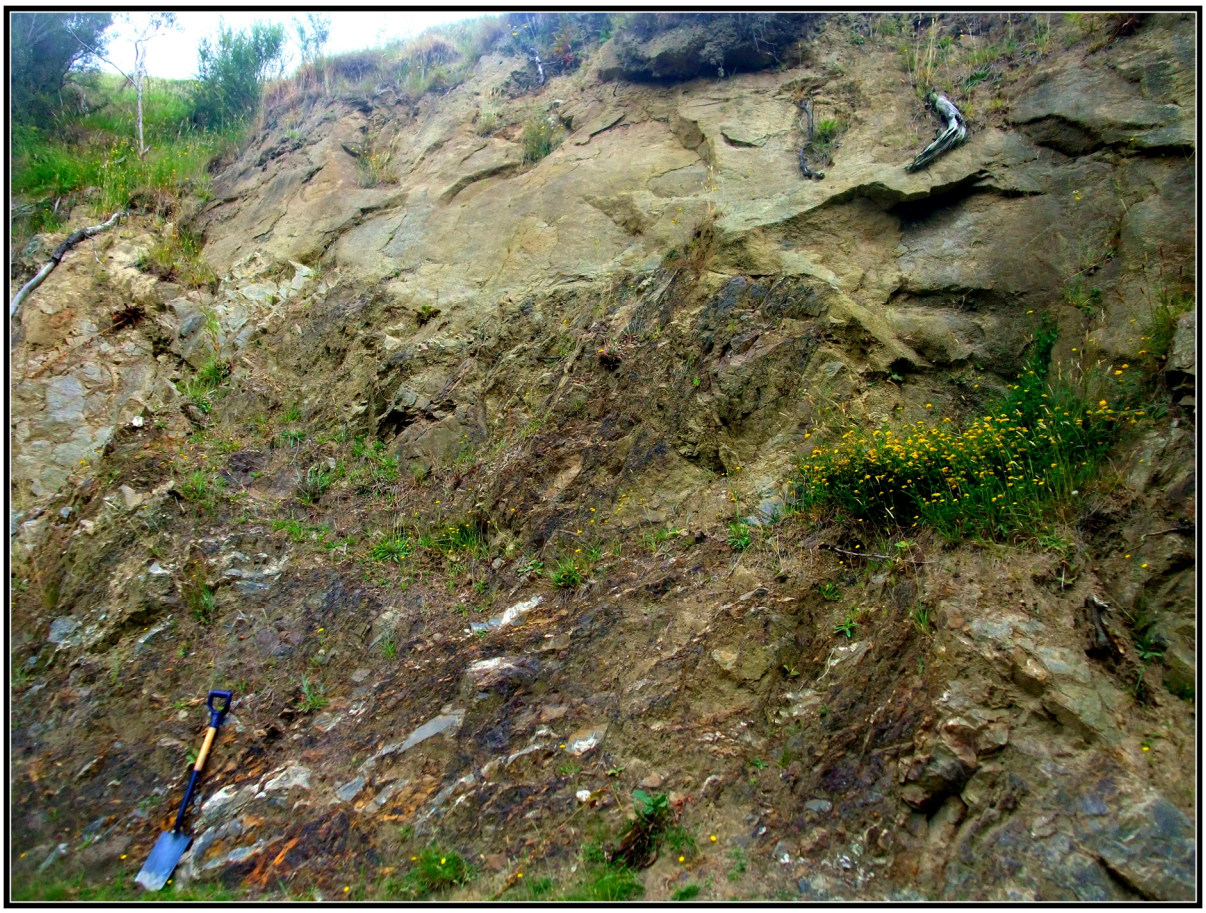

## Pohangina Fault

The Pohangina Fault is a high angle normal fault, downthrown to the east. The fault crops out at two localities in the study area. The first outcrop occurs on the true right bank of the Pohangina River 4.7 km north of Ashhurst, where the fault displaces both the Ohakean Terrace (Fig 3.10) and Kai-Iwi Group sediments by approximately 3 m. The fault plane dips 80° E, sediments on the downthrown side dip 15° SW while those on the upthrown side dip at 2-4° towards the W to NW. Dips of 2 - 4° are considered part of the regional dip as this area is located on the lower limb of the Faulted Pohangina Monocline where dips even out to around 5° towards the Pohangina River. This enables sudden increases in dip and opposing dip directions within the sediments to be used as evidence for faulting. The Pohangina Fault is interpreted to trend N - NW for a further 3.7 km toward the northern boundary of mapping.

The second outcrop occurs 300 m downstream of the Ruamai Bridge where the fault can be seen displacing strata on the true left side of the Pohangina River. The attitudes of beds at the second outcrop are similar to those found at the first outcrop, however, due to inaccessibility no offsets could be measured on the outcrop. The offset of the Ohakean Terrace provides evidence that movement along this fault has occurred within the last 15,000 years. The Pohangina Fault is therefore classified as an active fault line.

Fig 3.10: Offset Ohakean Terrace crossed by the Pohangina Fault, Pohangina Valley, (WGS84 40°14'11.20"S, 175°46'16.00"E, elev 102 m) (GoogleEarth, 2014).

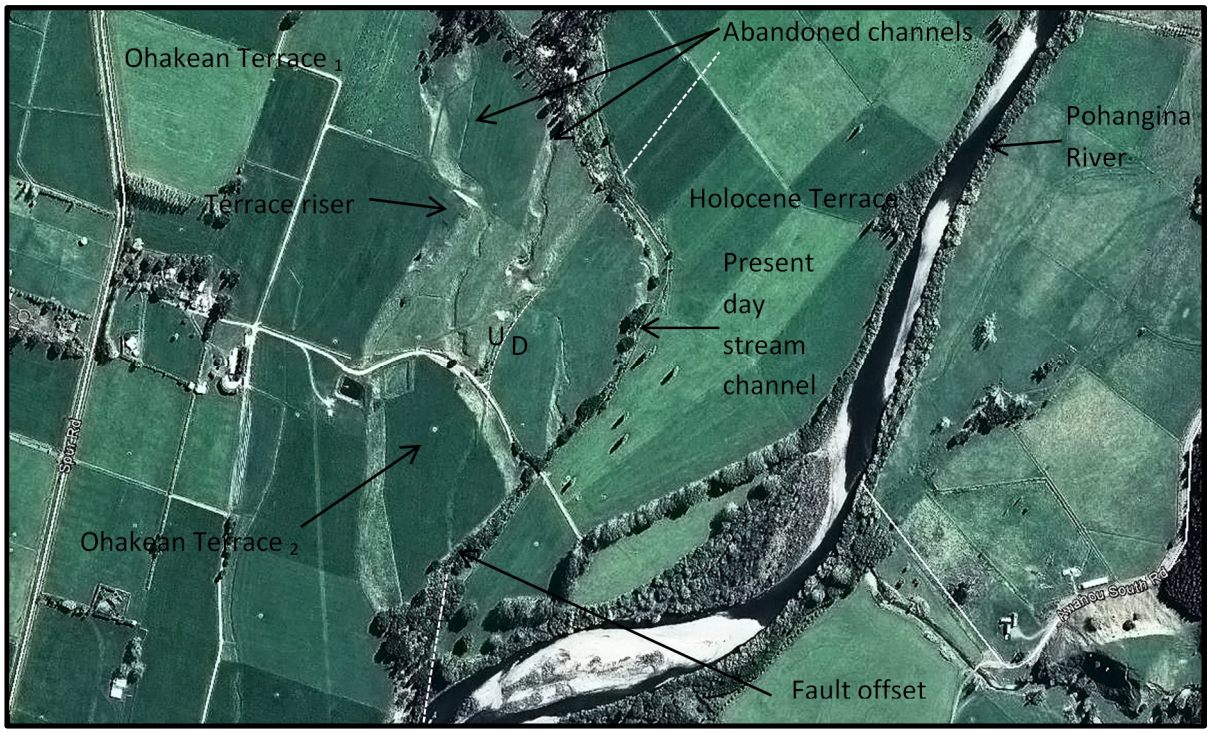


A small ephemeral stream running along the base of the terrace riser (Holocene Terrace up to Ohakean $_2$ Terrace) has changed course twice; abandoned stream channels can be seen in the surrounding landscape. These abandoned channels could be related to changes in drainage resulting from offset along the Pohangina Fault.

## Ruahine Fault

The Ruahine Fault is a dextral fault which is part of the North Island dextral fault belt (Beanland, 1995). The fault trace is poorly preserved due to severe erosion within the Ruahine Range which erodes away evidence of fault displacement in the landscape. The location of the fault trace is mainly based on locations of fault gouge in the Torlesse greywacke (Marden, 1984).

Hanson (1998) classifies the Ruahine Fault as active, with at least 9 fault movements within the last 12,000 years. Approximately three of these faulting events have occurred since the deposition of the Taupo Tephra (1850 yrs B.P.) (Hanson, 1998). The absence of a surface expression of the Ruahine Fault across the Manawatu Saddle is interpreted as being a result of both extensive erosion and the thick covering of Plio-Pleistocene rocks.

The Ruahine Fault has been traced south along the Tararua Range by a zone of fault gouge and brecciated Torlesse greywacke, a marked topographical disruption in the landscape and the presence of fault guided streams (Marden, 1984). However, due to the lack of evidence for the location of the fault across the Manawatu Saddle, interpretations of its location in the study area differs greatly between authors. One of the most common interpretations is that the Ruahine Fault crosses the Manawatu Saddle as a contact fault separating a series of isolated greywacke outcrops to the west from Plio-Pleistocene deposits to the east. However, Marden (1984) provides evidence for a second interpretation in which the trace of the Ruahine Fault occurs farther west down the Manawatu Gorge and into Te Apiti Stream where it then heads north east across the Manawatu Saddle. Evidence includes a zone of fault gouge and shattered greywacke in Te Apiti Stream.

Beanland (1995) suggests the Ruahine Fault has a sinistral, compressional side-step splinter fault in the Manawatu Gorge, due to the strike of the fault trace north and south of the Manawatu Gorge, and in consideration of the evidence provided by Marden (1984). Beanland (1995) picks up the trace of the Ruahine Fault 200 m south of the Saddle Road as a linear patch of swamp where the fault cuts through Plio-Pleistocene rocks. The fault trace is then detected north of the Saddle Road for 150 m in a steep ravine before becoming inconspicuous across the eroded Plio-Pleistocene rocks of the Manawatu Saddle (Lillie, 1953). Marden (1984) documents the Ruahine Fault trace again from Mangamanaia Stream (Fig 1.5) where it separates Torlesse greywacke to the west from Plio-Pleistocene rocks to the east. From Wharite Road the Ruahine Fault trace continues in a NE direction. This trace is marked by a series of fault breccia zones. Marden (1984) suggests that the Ruahine Fault trace is one of a swarm of traces within a more extensive Ruahine Fault zone.

The total amount of tilting of the Plio-Pleistocene sediments in Pohangina Valley solely from fault movement is uncertain. This is because the sediments which overlie Torlesse greywacke have been affected by drag tilting during tectonic uplift of the Ruahine Range (Lillie, 1953). Non-faulted contacts between the Torlesse greywacke and Komako Formation generally show a dip of 20 to 25°. This dip is due to tectonic uplift in the region resulting in both the uplift of the Ruahine Ranges and the contemporaneous drag tilting of the overlying Plio-Pleistocene sediments. Basement contacts with dips greater than 25° are considered to be a result of more localised faulting. Basement contacts with steep dips are associated with highly shattered and sheared Torlesse greywacke.

The amount of vertical displacement on active and potentially active faults in the southern Ruahine Range has not been uniform along individual fault lines. The displacement measured across the length of an individual fault trace is also seen to be unevenly distributed (e.g. Ruakawa Fault, see Fig 18 – 21). Greatest fault uplift has occurred along the Wellington Fault (Marden, 1984). Vertical displacements are greatest along the eastern margin of the main axial ranges and least within the vicinity of the Manawatu Saddle. Most of the Late Quaternary faulting took place before Ohakean time (>30 ka) as evidenced by the lack of offsets on the Ohakean Terraces.

# Chapter 4
# Introduction to Stratigraphy and Sedimentology

Pohangina Valley contains a Plio-Pleistocene sequence, extending from Mangapanian through to mid Castlecliffian, unconformably overlying Torlesse greywacke. Carter (1972) mapped the Plio-Pleistocene sequence in the Komako District, dividing the strata into three formations: Komako Formation, Konewa Formation and Takapari Formation. These formations are specific to the Pohangina area, given their deposition in the eastern Whanganui Basin adjacent to the proto-Ruahine Range. The tectonic regime of the North Island main axial range has strongly controlled the pattern of sedimentation within the eastern Whanganui Basin.

Carter's (1972) formations are retained and extended into the study area (Table 4.1). Formations are further subdivided into members based on major lithological changes, biostratigraphy and tephrochronology.

The upper contact of the Takapari Formation is set at the first occurrence of Potaka Pumice within the sedimentary record. This tephra allows correlation between Pohangina and the well documented Whanganui Basin stratigraphy. Using Potaka Pumice and Kaukatea Tephra as chronohorizons, Kai Iwi Group strata are recognised and correlated to the Pohangina Valley stratigraphy. This allows the stratigraphic nomenclature used in Pohangina to be preserved, whilst relating it with the more widely recognised Whanganui Basin stratigraphy (Pillans *et al*, 2005; Naish *et al*, 2005), allowing basin wide correlations to be made.
A thick Plio-Pleistocene sedimentary sequence occurs in the Manawatu Saddle area. This sequence has been mapped by several authors (Lillie, 1953; Beanland, 1995; Kingma, 1962), resulting in the inclusion of the Manawatu Saddle stratigraphy into both Whanganui Basin and East Coast Basin stratigraphic nomenclature and creating inconsistencies in the literature.

During the Plio-Pleistocene the Whanganui and Wairarapa continental shelves were connected via sea ways across areas which are now part of the Norh Island main axial range. These connections between the lower North Island's western and eastern sedimentary basins have created close relationships between the sequences preserved on both sides of the present day main axial ranges. The Whanganui and Wairarapa shelves acted as a single shelf at times during the Early Quaternary.

Table 4.1: Stratigraphic nomenclature used in Whanganui Basin, Dannevirke, and local Pohangina lithostratigraphy

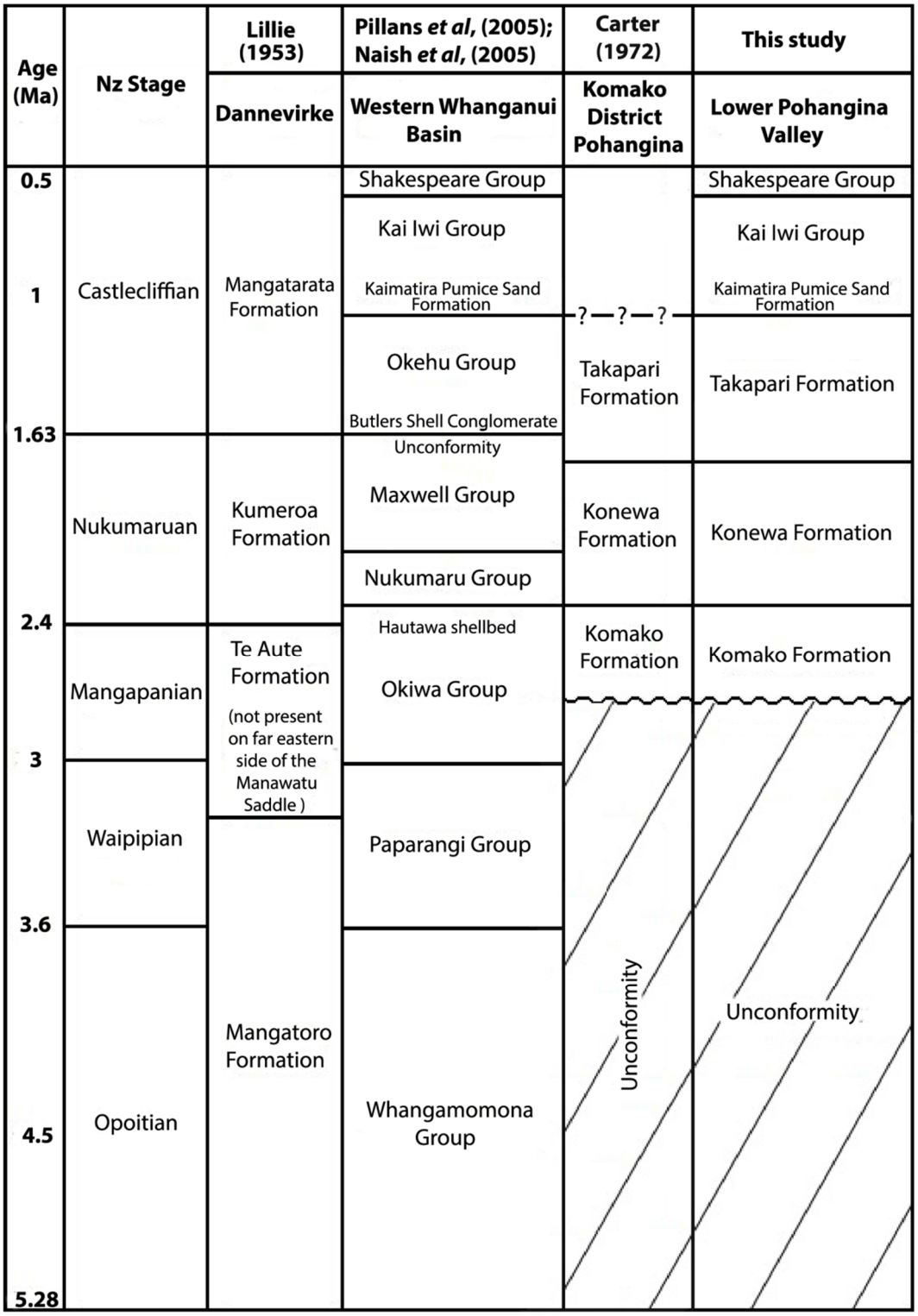

# Chapter 5
# Komako Formation

The Komako Formation was defined by Carter (1972) as the group of greywacke conglomerate, grits unfossiliferous brown sands, and sparsely fossiliferous blue-grey silts, which unconformably overlie Ruahine greywacke. The type section is at Te Ekaou Creek in the Komako District, Pohangina Valley. The name was taken from a farm owned by Mr and Mrs H. D. Rutherford, which was mapped during Carter's (1972) work.

The formation reaches its maximum thickness of 292 m in the Manawatu Saddle area, and thins out rapidly northwards to 162 m in the middle of the mapping area. The Komako Formation continues to thin out towards the northeast boundary of the mapping area, and is inferred to continue to thin to the north, based on work by Ower (1943).

In this study the Komako Formation is separated into three members; Fossiliferous Sandstone Member (Fss Member), Fossiliferous Mudstone Member (Fms Member), and Flaggy Grit Member (CF Member). These members are distinguished on changes in lithology.

Molluscan faunas preserved within the Komako Formation indicate an age of Late Mangapanian to Earliest Nukumaruan, falling within the *Chlamys delicatula* zone. While the type section of the Komako Formation is at the Te Ekaou Creek locality in the Komako District, given the greater thickness of Mangapanian to Early Nukumaruan sediments preserved at the Manawatu Saddle a second key locality is located in the upper reaches of Stallion Stream (WGS84 40 °17'20.16"S, 175 °48'52.10"E, elev 317 m). This locality can be accessed by walking east up Stallion Stream from where the stream crosses Awhaou South Road.

Mangapanian to Early Nukumaruan deposition is identified using the macro fauna in this study and Carter (1972). Micropalentological work by Finnlayson (1980) is also used to help constrain the timing of deposition. The chronostratigraphic boundary between the Mangapanian and Nukumaruan stages is placed at the unconformable contact between the Komako and Konewa Formations, located 1.5 km SE up Stallion Stream, Broadlands Station, Pohangina (WGS84 40°16'10.43"S, 175°47'44.48"E) . Age determinations of Komako Fomation are based upon biostratigraphy and stratigraphic correlation.

## 5.1 Coarse Flaggy Grit Member

### Lithological description

Code: Cf

Rock type: Fine to granular sandstone, grit; clast supported grit.

Colour: Yellow (2.5Y 7/8) to very dark grey (2.5Y 3/0). (All rock description colour determinations in this thesis have been made using a Munsell colour chart).

Hardness: Well consolidated, lime cemented, moderately hard.

Weathering: Highly weathered, displaying karst weathering features such as karren.

Grain size: Fine to coarse sand matrix with fine granular grit, grains 1 -2 mm in diameter.

Texture: Coarse gritty texture.

Crystals/minerals: Quartz, feldspar, calcite.

Thickness: Measured thickness of 91 m at the Manawatu Saddle thinning rapidly to 35 m north of the Manawatu Saddle, inferred to continue to thin farther north based on mapping by Ower, (1943).

Type section: Antler Stream, Hardings Farm, Pohangina (WGS84 40 °16'40.41"S, 175 °49'21.04"E, elev 319 m). Access via Saddle Road with express permission of the land holders.

Fossils:

Table 5.1: Fossil assemblages from Cf Member, Komako Formation

| Family/species | Sample no | |
|---|---|---|
| | FS18 | FS19 |
| *Zeacolpus vittatus* (Hutton, 1873). | X | |
| *Maoricolpus* roseus (Quoy & Gaimard, 1834). | X | |
| *Phialopecten thomsoni* (Marwick, 1965) | | X |

### Biostratigraphy

The presence of *Phialopecten thomsoni* indicates a Mangapanian age for this formation. *Phialopecten thomsoni* is restricted to the Mangapanian stage and only ever rarely found within Early Nukumaruan facies (Beu, 1995). Further evidence for a Mangapanian age is

provided by the occurrence of the microfossils *Hyalinea cf. balthica*, *Notorotalia inornata* and *Notorotalia zelandica mangaoaria* within Komako Formation sediments analysed by Finlayson (1980).

Carter (1972) notes the presence of *Janthina typica* (Bronn, 1861), *Lamprodomina neozelanica* (Hutton, 1885), *Glycymeris waipipiensis (*Marwick 1923), *Phialopecten thomsoni* (Marwick 1965), and *Arca cottoni* (Waghorn, 1926) within basal Komako sediments. This assemblage too is indicative of Mangapanian deposition.

The presence of *Zeacolpus vittatus* (Hutton, 1873) and *Maoricolpus roseus* (Quoy & Gaimard, 1834) are indicative of deposition within a shallow water soft bottom environment. *Phialopecten* species are relatively common within shell bed facies of shallow marine environments (Beu, 1995).

Fig 5.1: A fossil assemblage of Cf Member, Komako Formation; 1: *Zeacolpus vittatus* and *Maoricolpus roseus*. Collected from Stallion Stream, Broadlands Station, Pohangina Valley.

### 5.1.1 Facies analysis of Cf Member, Komako Formation

Cf Member unconformably overlies Torlesse greywacke. The unconformity is an erosional surface formed during sub-aerial exposure of the Torlesse greywacke during sea level low stands. A widespread Miocene erosional unconformity exists in the Whanganui Basin. Overlying this erosional surface a sequence of Plio-Pleistocene sediments upto 4 km in thickness has been preserved. However, within the Pohangina region periodic sub-aerial exposure of the Torlesse greywacke basement during the Early Pliocene has formed an erosional unconformity upon which Mangapanian sediments have been deposited (Komako Formation).

Cf Member is overlain by Fms Member representing a change from coarse calcareous grit to fossiliferous fine sands and muds. Both the upper and lower contacts of Cf Member are sharp and erosional. A 24 m section at the type locality in Stallion Stream was selected for detailed facies analysis. This section contains the contact between Torlesse greywacke and overlying Cf Member, Komako Formation. The sequence examined is characterised by coarse grained mixed calcareous and quartzofeldspathic sedimentation. The sequence is highly calcareous displaying karst like features such as flaggy weathering. Fossils occur throughout Cf Member, the majority are *Phialopecten sp*.

Facies Gh: Well sorted clast supported conglomerate/ grit
The Gh facies is composed of well sorted grits with sporadic pebbles, often with *Phialopecten* fossils preserved. The calcareous grit is clast supported; the matrix is composed of fine to medium grained sand. A majority of the clasts range in size from 1–2 mm, this falls within the grit classification as 30% of clasts are less than 2 mm in diameter. Beds display karst like features such as flaggy weathering. Beds are around 2 - 6 m thick.

*Interpretation:*
Facies Gh is interpreted as a high energy shoreface environment, where continued wave action has sorted and shaped the clasts. The calcium carbonate cement and concentration of fine bioclastic material is interpreted to represent high productivity within the marine environment, and also strong wave action where shells and other bioclastic material are ground up, producing a fine sand matrix. The small size of the quartzofeldspathic clasts is interpreted as either a long distance from siliciclastic source, or substantial reworking of clasts within the shallow marine shoreface environment where clasts are further abraded and sorted by wave action.

| Table 5.2 Lithofacies of Cf Member, Komako Formation, (Stratigraphic log of Cf Member, Fig 5.2); facies codes are modified from Horton & Schmitt (1996). | | | |
|---|---|---|---|
| Facies code | Description | Depositional processes | Environment |
| Gh | Moderately sorted granule conglomerate, clast supported, no grading, horizontal stratification | Sheetfloods; wave driven traction | Shallow marine shoreface |

Fig 5.2: Straigraphic log of Cf Member, Komako Formation, Stallion Stream, Broadlands Station, Pohangina (WGS84 40 °16'39.27"S, 175 °49'12.39"E, elev 285 m).

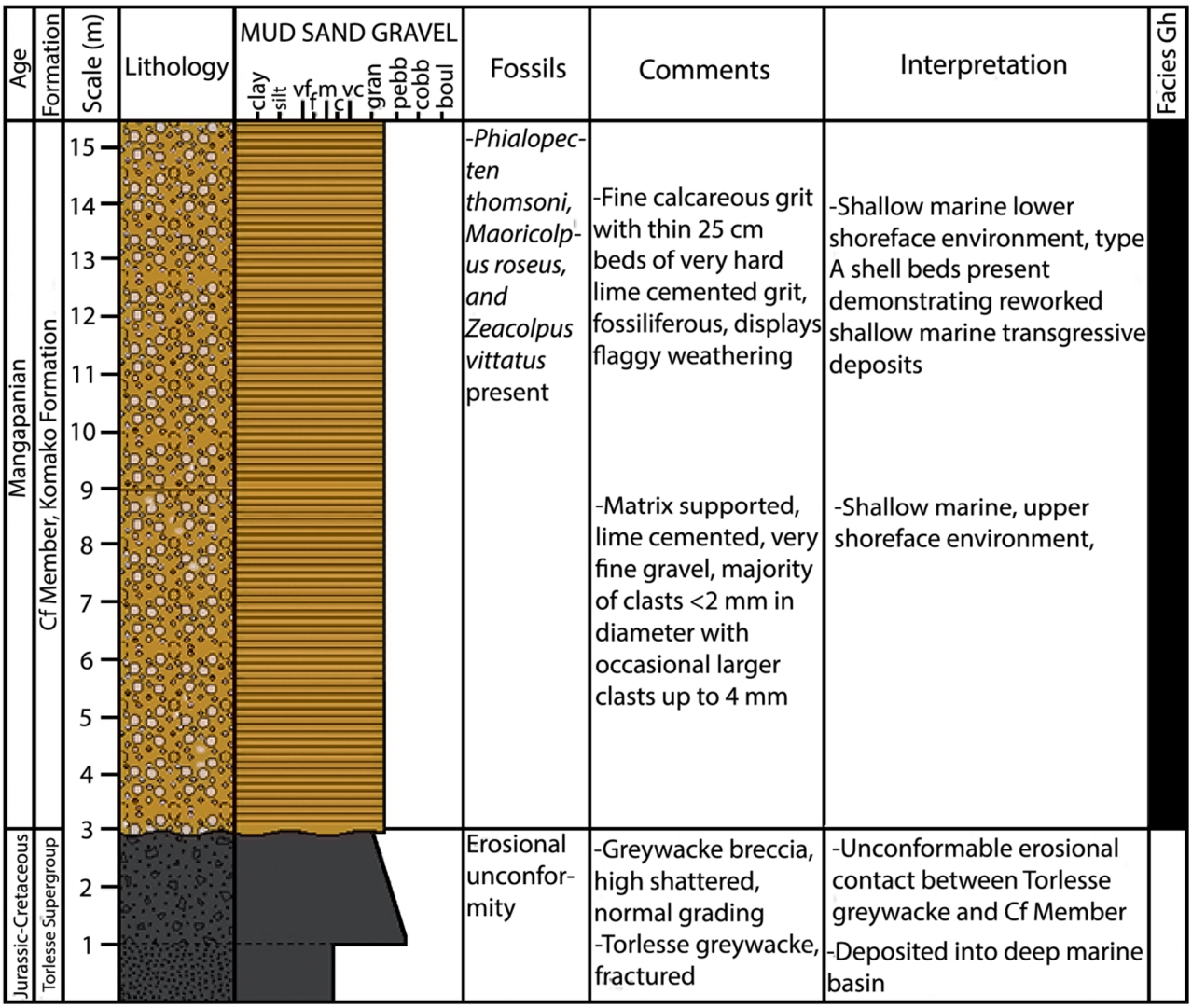

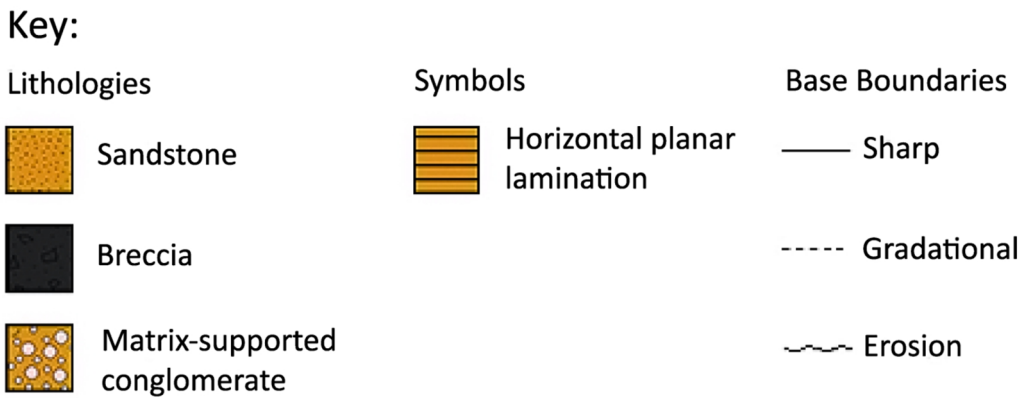


### 5.1.2 Grain size analysis

Grain size is the most fundamental property of sedimentary particles, affecting their entrainment, transportation and deposition. Grain size analysis therefore provides important clues to sediment provenance, transportation history and depositional conditions (e.g. Folk & Ward, 1957; Friedman, 1979; Bui *et al*, 1990).

Grain size data from Cf Member (Appendix 2.9) show a bimodal distribution. These two modes represent the coarse granular grit and the finer sand matrix in between the grit. This member is defined as a coarse grit. It is not technically a conglomerate as 30% of the clasts are not over 2 mm in size. Most of the clasts are less than 2 mm most falling around 1 – 2 mm in size. The matrix is composed of fine sand (2 to 4 phi range) (Folk, 1954) with a calcareous cement.

### Interpretation

It is interpreted that the bioclastic content composes much of the matrix while the grit is composed of small quartzo feldspathic greywacke clasts. The deposit is poorly sorted and fine skewed. The two modes are sufficiently distinct to have separate sources; the matrix having an autochthonous bioclastic source and the clasts having an allocthonous quartzofeldspathic source. The quartzofeldspathic clasts have been delivered to the shallow marine environment via a paleo-river system which has transported the sediment from a distal source of elevated basement.

Cf Member unconformably overlies Torlesse greywacke and underlies Fms Member, of Konewa Formation. The basal contact is often observed as a faulted contact with extensively brecciated greywacke forming sheared zones with folding, foliation, and fracturing present. Some greywacke breccia zones are heavily iron stained, interpreted to be a result of ground water reaching the surface through the permeable breccia zone (Marden, 1984).

Dip planes on Konewa and Komako Formation within faulted areas reach 30 – 50° due to tilting of the Plio-Pleistocene sediments, caused by thrust faulting. Dips recorded at non-faulted Torlesse greywacke – Plio-Pleistocene contacts are relatively low at around 15-25°. This is interpreted to be due to localised tectonic uplift of the ranges which has dragged up the overlying Plio-Pleistocene sediments. Drag tiliting of the Plio-Pleistocene sediments has occurred mainly over the last 1 Ma (Marden, 1984). Although the main axial ranges have been uplifted over the last 1 Ma the sedimentary record is far from continuous over the Plio-Pleistocene. Sub-aerial exposure of the continental shelf during sea level low stands has created a series of unconformities which separate periods of sediment infilling and preservation.

## 5.2 Fossiliferous Mudstone Member

### Lithological description

Code: Fms

Rock type: Sandy mudstone.

Colour: Light grey (5Y 7/1) to grey (5Y 5/1).

Hardness: Moderately consolidated sandy mudstone.

Weathering: Moderately weathered many fractures present, secondary iron oxides present, reducing conditions present in the mudstone beds.

Grain size: Fine sandy muds and sands.

Texture: Silty mud texture.

Crystals/minerals: Quartz, feldspar, calcite, biotite, hornblende.

Thickness: Approximately 89 m at the Manawatu Saddle thinning rapidly to 63 m to the north, inferred to continue to thin farther north based on mapping by Ower, (1943).

Type section: Stallion Stream, Broadlands Station, Pohangina (WGS84 40 °17’20.16”S, 175 °48’52.10”E, elev 317 m). Access via Saddle Rd with express permission of the land holders.

Fossils:

Table 5.3: Fossil assemblages from Fms Member, Komako Formation

| Family/species | Sample no | |
|---|---|---|
| | FS16 | FS17 |
| *Phialopecten triphooki (Beu & Maxwell, 1990)*. | x | |

| | | |
|---|---|---|
| *Phialopecten thomsoni* (Marwick, 1965). | x | |
| *Alcithoe brevis* (Marwick, 1926). | x | |
| *Zeacolpus vittatus* (Hutton, 1873). | | x |
| *Ruditapes largillierti* (Philippi, 1844). | | x |
| *Talabrica senecta* (Powell, 1931). | x | |
| *Polinices waipipiensis* (Marwick, 1924). | | x |
| *Aulacomya maoriana* (Iredale, 1915). | | x |
| *Perna canaliculus* (Gmelin, 1791). | | x |
| *Purpurocardia purpurata* (Deshayes, 1854). | | x |
| *Tawera subsulcata* (Suter, 1905). | | x |
| *Glycymerita tohunga (King, 1933).* | | x |

## Biostratigraphy

The overlap of the Nukumaruan restricted mollusc *Phialopecten triphooki* and the Mangapanian restricted mollusc *Phialopecten thomsoni* is interpreted to be indicative of Late Mangapanian deposition.

Fig 5.3: Mollusc species found within the sediments of Pohangina Valley and their associated time spans through the Mangapanian Stage (Beu & Maxwell, 1990, McIntyre, 2002).

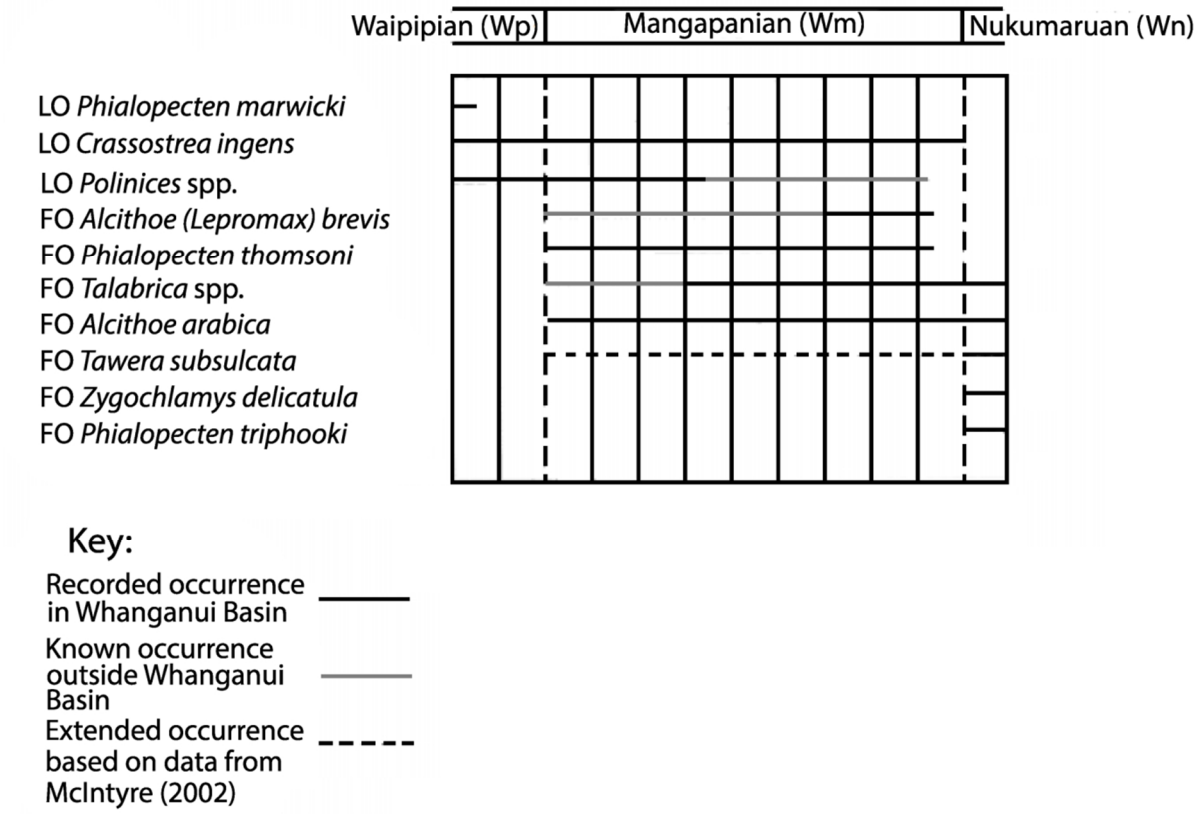

*Alcithoe brevis* (Fig 5.3) is not known to be older than Mangapanian in age. The occurrence of *Glycymerita tohunga* and *Polinices waipipiensis* indicates that Fms Member is not younger than Mangapanian in age. Given this assemblage of macro fossils it is interpreted that Fms Member was deposited in Late Mangapanian time.

Depth ranges have been collated from Powell (1979), Morley, & Hayward (1999), Beu & Maxwell (1990), McIntyre (2002), and Morley & Hayward (2007). Extant species have been assigned depth ranges using both living and dead speicmens. Extinct species have been assigned depth ranges by using taxonomically similar extant species of the same genus as a guide e.g. *Tawera spissa* for *Tawera subsulcata*. Some error is expected for the depth ranges given the effects of downslope reworking, wave action, and ocean currents. These ranges are regarded as broad estimates, which nevertheless allow important environmental interpretations to be made.

The depth ranges of mollusc species found within Fms Member are presented in Fig 5.4. The minimum water depth is estimated at 15 m given the presence of *Ruditapes larillierti, Aulacomya maoriana* and *Perna canaliculus.* These species inhabit very shallow water environments and are most common between 5 – 20 m depth (Beu & Maxwell 1990). These very shallow water species are found in combination with *Tawera subsulcata* and *Purpurocardia purpurata* which are also indicative of shallow water environments, although have wider depth ranges extending to over 100 m. Given this assemblage of species a maximum water depth of 50 m is estimated for Fms Member.

*Ruditapes larillierti* is indicative of a protected oceanic setting which has slightly lower salinity than the open ocean. The occurrence of this species within Fms Member is interpreted to indicate the presence of sheltered bay environments present within areas of the Manawatu Strait, where greywacke headlands have protected shallow marine envrionments from open ocean conditions.

Fig 5.4: Depth ranges of selected mollusc taxa present within Fms Member (Powell, 1979; Morley, & Hayward, 1999; Beu & Maxwell, 1990; McIntyre, 2002; Morley & Hayward, 2007).

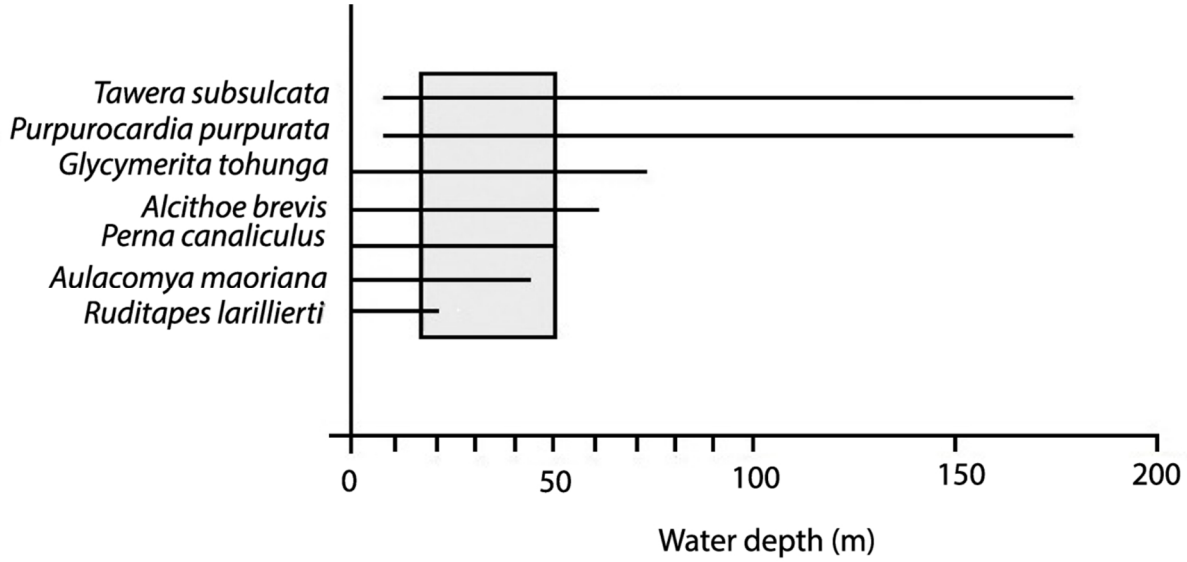

### 5.2.1 Grain size analysis

Grain size distribution data for Fms Member (Appendix 2.8) show a unimodal distribution, with a mean grain size falling within the coarse silt fraction. Overall the grain size distribution is fine skewed and poorly sorted; the fine skewed nature of the sediment is interpreted to be a result of the influence of river systems delivering large quantites of fine grained sediments into the marine environment. This strong fluvial influence has resulted in the fine skewed and poorly sorted nature of the sediments.

### Interpretation

Fms Member is interpreted as being deposited within muddy, inner shelf to nearshore environments of the Manawatu Strait. Shallow marine conditions prevailed during the deposition of Fms Member, with extensive bioturbation leading to the destruction of primary sedimentary strutures. The main modes of sediment transport were suspension fall out and traction currents (rolling, sliding and saltation) (Appendix 2.8, cumulative frequency graph).

Suspension fall out deposits are interpreted as allocthonous material brought into the marine environment via a paleo-river system flowing north to south discharging into the eastern Whanganui Basin. At this outlet large plumes of fine grained sediments entered the ocean, where they were then carried farther out onto the shelf eventually settling out from suspension. Traction currents generated by storm activity moved larger sand sized particles via saltation and rolling along the floor of the ocean.

Fms Member is characteristically massive with no visible bedding. This is interpreted to be a result of bioturbation occurring on the sandy mud bottom of shallow marine inner shelf environment. Burrowing increases the rate of weathering and destroys primary sedimentary structures such as parallel laminations (Friedman & Sanders, 1978).

Extensive thin (<300 mm) shell beds are found throughout this member containing species such as *Glycymerita tohunga (King, 1933)*, *Tawera subsulcata* (Suter, 1905), *Purpurocardia purpurata* (Deshayes, 1854), *Polinices waipipiensis* (Marwick, 1924), *Ruditapes largillierti* (Philippi, 1844). These shell beds along with elongated (up to 400 mm) concretions, are the only features from which dips can be obtained. Otherwise Fms Member lacks bedding or sedimentary structures. Areas which are more fossiliferous show signs of bioturbation such as crawling tracks, and burrows.

The fossil assemblages from samples FS16 and FS17 contain shallow marine fauna such as *Aulacomya maoriana*, *Glycymerita tohunga*, *Polinices waipipiensis*, *Zeacolpus vittatus*, and

*Alcithoe brevis.* These fossils are interpreted to represent shallow innermost shelf to nearshore environments within the Manawatu Strait during Late Mangapanian time.

The absence of *Zygochlamys delicatula* (Hutton, 1873) within the fossil assemblages of Komako Formation can be interpreted in two ways. Firstly *Zygochlamys delicatula* is an index fossil for Early Nukumaruan deposition. Its absence therefore is indicative of pre-Nukumaruan deposition. Secondly *Zygochlamys delicatula* is found within moderately deep water of the outer shelf, and is only found in open oceanic settings. The shallow marine Manawatu Strait was sheltered by headlands and likely did not provide suitable habitat for this open ocean dwelling species.

The occurrence of *Zygochlamys delicatula* in the basal conglomerate units mapped by Carter (1972) in the Komako District highlights a difference in the depositional setting between the upper and lower Pohangina Valley. It is likely the basal conglomerate in the Komako District represents a cold climate episode in which the cold water migrant fauna became incorporated in a conglomeratic deposit formed at a cliffed shoreline during Late Mangapanian to Early Nukumaruan time. Deeper oceanic settings prevailed in the area of present day Komako, whislt shallow water, high energy conditions prevailed in the Manawatu Strait.

### 5.2.2 Shelf processes

Mudstones and shales are the most abundant sedimentary rock on earth (Boggs, 2011). Mudstones form under certain environmental conditions, requiring an abundance of fine sediments and low water energy, which allows suspended fine silt and clay to settle. Generally when siliciclastic rocks are weathered the fine grained fraction exceeds the coarse fraction. Therefore fine grained sediments are often abundant within depositional environments. Due to the abundance of fine sediments within sedimentary systems, they can be deposited within a wide range of quiet water environments.

Sedimentation patterns on storm-dominanted continental shelves (e.g. modern Taranaki Bight) can be complex, depending on the extent of relict and modern sediments which mantle the shelf (Boggs, 2011). Shelf processes important in transporting sediments are storm waves, wind forced currents, and tidal currents. In the storm dominated shelf off Whanganui, storm waves and wind driven currents play a more important role in sediment transport than tidal currents (Abbott, 1998). Longshore drift also plays an important role in sediment transportation and is responsible for the distribution of titanomagnetite sands SE down the Whanganui coast.

The amount of sediment supplied to the shelf is often a limiting factor to a sedimentary system (Galloway & Hobday, 1996). Shelf sediments are either allocthonous i.e. derived from a contemporaneous depositional system (external source), or autochthonous i.e. have an internal source. Autochthonous sediments are derived by erosion of the sea floor due to wave action, erosion of the shoreface during a marine transgression, and *in situ* biogenic or chemical precipitation (Thorne & Swift, 1991).

Allocthonous sediments are delivered to the shelf via tidal flows, delta front bypass, coastal defection plumes, and storm generated flows (Galloway & Hobday, 1996). Fms Member is interpreted to be composed of a combination of allocthonous and autochthonous material. The allocthonous material has been delivered to the depositional environment via paleo-river systems running into the eastern Whanganui Basin. Allocthonous sediments make up the bulk of Fms Member forming the quartzofeldspathic fraction.

Autochthonous material is also present in the form of calcium carbonate which has been precipitated *in situ* by marine organisms living in a marine shelf environment. Calcium carbonate forms a smaller yet still substantial fraction of the sediment. The calcium carbonate was deposited along with the siliciclastic material; however, it has undergone secondary alteration during diagenesis. Diagenesis has resulted in the concentration of calcium carbonate into fine grained areas where it acts as cement.

Sediments which are delivered to the coast via rivers may be carried out onto the shelf either as buoyant plumes or underflows (Galloway & Hobday, 1996). Buoyant (hypopycnal) plumes arise where low salinity water from a river or estuary flows out on top of the denser saline sea water. Generally these buoyant plumes reach to the inner to middle shelf before being carried parallel to the coast due to the Coriolis force (Nittrouer & Wright, 1994). During a buoyant plume, the coarse sediment is deposited near the river mouth while the finer sediments can be transported farther out into the marine environment until they settle onto the sea floor.

Underflows (hyperpycnal flows) occur where rivers with very high suspended sediment loads enter the ocean. The river water in this instance is denser than the sea water and therefore flows beneath it. Generally these underflows deposit their sediment near the river mouth; however, they may flow out onto the inner part of the shelf (Seymour, 1990). It is likely a combination of buoyant plumes and underflows have occurred during the deposition of Fms Member. Underflows likely occurred during storms, when rivers have higher amounts of suspended sediment due to increased rates of rain fall and erosion. Buoyant plumes occuring during fair weather periods when the amount of suspended sediment within paleo-river systems was lower.

### 5.2.3 Bioturbation and sedimentation rates

Mudstone facies are usually distinguished by differences in sedimentary features, which are indicative of depositional energy and the degree of mixing (Galloway & Hobday, 1996). Bioturbated muds which lack well stratified sedimentary structures, such as Fms Member, indicate well mixed bottom water and moderate to low rates of deposition. Organisms living on the sea floor rework the sediment by crawling, burrowing and ingesting activities (Galloway & Hobday, 1996). These activites can often lead to the destruction of primary sedimentary structures e.g. planar lamination, leaving a variety of traces in their place such as burrows, tracks, and trails.

Generally bioturbation is more prevalent in areas with slow sedimentation rates and fine grain size. These areas are more characteristic of deep water environments, although they can be found in shallow shelf environments where the amount of terrigenous sedimentation is limited due to the type of sediment transportation processes operating. For example, terrigenous sedimentation rates near a river outlet will be substantially higher than on the continental shelf. This is due to large amounts of terrigenous sediment being delivered to areas surrounding the river outlet, while farther out on the shelf the amount of terrigenous sedimentation is drastically reduced.

### 5.2.4 Modern analogue

Fms Member is interpreted to have formed within the shallow shelf setting of the Manawatu Strait. This area would have had a strong wind and ocean driven current flowing across it similar to Cook Strait today. The modern analogy of Cook Strait can be used to understand processes likely to have been in operation within the Manawatu Strait during Mangapanian time.

The modern Cook Strait occurs within the southern hemisphere's strong westerly wind currents; the 'roaring forties'. At the northwestern approach the prevailing westerly winds are funnelled through the strait, and are associated with strong wind forced oceanographic conditions (Lewis *et al*, 1994). The strait is also subject to semi-diurnal tides. The diurnal tides occur as a tidal wave propagates anticlockwise around New Zealand over one tide cycle, resulting in a phase difference of 140 degrees on either end of the strait (Bye & Heath, 1975). This phase difference means that when one end of the strait is at high tide the other end of the strait is nearly at low tide. Hence very strong flows are created through the strait with peak tidal flows of 1.53 m/s (Carter *et al*, 1991).

Sedimentation rates within the shelfal parts of the Manawatu Strait were moderately low, due to both a moderate terrigenous sediment supply, and sediment bypass occurring through the Manawatu Strait. Resulting in areas of the shelf becoming isolated from the

main sediment transportation pathways and essentially lowering the rate of terrigenous sedimentation. Further evidence for this moderate terrigenous sedimentation rate is seen in the formation of large 400 mm concretions, which demonstrate the high concentration of calcerous material within the fine sediments of Fms Member. A high concentration of bioclastic calcium carbonate suggests that dilution via terrigenous sedimentation was relatively low at this time.

The sediments on the modern Whanganui shelf are accumulating in a broadly similar depositional setting to the Plio-Pleistocene sediments of the Whanganui Basin. The modern shelf off the coast from Whanganui has a low gradient seabed (<1°), which extends offshore for approximately 100 km reaching a depth of around 110 m depth (Gillespie *et al*, 1998). Currently the Taranaki Bight and continental shelf off Whanganui are classified as storm-dominated. It is likely that the same storm dominated oceanographic setting exisited during the deposition of Fms Member during the Early to Mid Nukumaruan.

The modern Whanganui wave environment comprises a dominant southwesterly background swell from the Southern Ocean and locally generated southwesterly to westerly sea waves (Pickrill & Mitchell, 1979; Harris, 1990). A south-easterly directed longshore littoral dift system is present off Whanganui, created by the interaction of the dominant wave approach direction along with the arcuate coastline between Taranaki and Wellington (Abbott, 1998). As in the Pleistocene, the modern Taranaki Bight faces the prevailing westerly weather patterns. Tidal flow is relatively sluggish over the Whanganui shelf, therefore storm generated waves and currents are the main sediment transport mechanisms (Proctor & Carter, 1989). The oblique to acute orientation of the Whanganui Coastline to the prevailing westerly weather favours the development of strong coast-parallel (NW to SE) longshore littorial drift (Lewis, 1979).

## 5.3 Fossiliferous Sandstone Member

### Lithological description

Code: Fss

Rock type: Fine sparsely fossiliferous sandstone with intercalated mudstone beds. Massive bedding. Condensed shell beds up to 400mm thick present.

Colour: Pale olive (5Y 6/3) to olive grey (5Y 4/2).

Hardness: Weakly consolidated soft sandstone to moderately consolidated mudstone.

Weathering: Highly weathered, secondary iron oxides present, reduced conditions present in mudstone beds.

Grain size: Fine sand with occasional beds of mudstone.

Texture: Gritty sand texture.

Crystals/minerals: Quartz, feldspar, calcite.

Thickness: Approximately 112 m at the Manawatu Saddle thinning rapidly to 56 m north of the Manawatu Saddle, inferred to continue to thin farther north based on mapping by Ower, (1943).

Type section: Stallion Stream, Broadlands Station, Pohangina (WGS84 40 °17'20.16"S, 175 °48'52.10"E, elev 317 m). Access via Saddle Rd with express permission of the land holders.

Fossils:

Table 5.4: Fossil assemblages from Fss Member, Komako Formation

| Family/species | Sample no | | |
|---|---|---|---|
| | FS13 | FS14 | FS15 |
| *Glycymerita tohunga (King, 1933).* | | x | |
| *Perna canaliculus* (Gmelin, 1791). | | x | |
| *Tawera subsulcata* (Suter, 1905). | | x | |
| *Purpurocardia purpurata* (Deshayes, 1854). | | x | |
| *Aulacomya maoriana* (Iredale, 1915). | | x | |
| *Polinices waipipiensis* (Marwick, 1924). | | x | |
| *Ruditapes largillierti* (Philippi, 1844). | | x | |
| *Talabrica senecta* (Powell, 1931). | x | | |
| *Alcithoe brevis* (Marwick, 1926). | x | | |
| *Phialopecten triphooki (Beu & Maxwell, 1990)*. | x | | |
| *Cassostrea ingens,* (Zittel, 1864). | | | x |

## Biostratigraphy

Fss Member represents a phase of Late Mangapanian deposition. An unconformable contact between Fss Member, Komako Formation and Cg Member, Konewa Formation represents the change from Late Mangapanian to Early Nukumaruan deposition. The presence of *Phialopecten triphooki, Glycymerita tohunga*, and *Polinices waipipiensis*, indicates that Fss Member is not younger than Mangapanian in age. In addition, *Talabrica senecta, Tawera subsulcata* and *Alcithoe brevis* are not known to be older than Mangapanian in age. This

macro-fossil assemblage is interpreted to indicate a Late Manapanian age for Fss Member. Further conclusive evidence is provided by the occurrence of the microfossils *Hyalinea cf. balthica*, *Notorotalia inornata* and *Notorotalia zelandica mangaoaria* within Komako Formation sediments analysed by Finlayson (1980).

Occurrences of *Tawera subsulcata*, *Purpurocardia purpurata*, *Glycymerita tohunga, Aulacomya maoriana*, and *Polinices waipipiensis* indicate a shallow-water, near-shore, soft-bottom environment. While *Alcithoe brevis* and *Talabrica senecta* indicate a shallow water inner most shelf environment. Therefore it is suggested that the fossil assemblage within sample FS13 represents a shallow, inner most shelf environment, while the assemblage of sample FS14 is characteristic of a near-shore depositional environment.

The occurrence of *Ruditapes largillierti* suggests that the western end of the Manawatu Strait comprised an enclosed shelf environment bordered by elevated basement both to the north and south. During Manapanian time elevated basement extended from the far eastern edge of the Marlborough Sounds area northwards to the southern boundary of the Manawatu Strait (Trewick & Bland, 2012). An island of elevated basement also extended south from the Kuripapango area to the northern boundary of the Manawatu Strait. Between these two headlands exisited a shallow marine seaway, connecting a shallow shelf environment over the present day Whanganui and Wairarapa regions. Sheltered areas of the Manawatu Strait likely had slightly lower salinitiy and warmer temperatures than the open ocean, which occurred further to the east.

The giant oyster *Crassostrea ingens* (Fig 5.5) became extinct between the end of the Mangapanian Stage and the beginning of the Nukumaruan Stage. Thick beds of lime cemented sand, containing abundant *Crassostrea ingens* are present near the contact between Fss Member, Komako Formation and Cg Member, Konewa Formation in Saddle Stream. The thick oyster beds are only present in the southwestern end of the Manawatu Saddle area near the Manawatu Gorge.

These oyster beds represent the last occurrence of *Crassostrea ingens* within the Plio-Pleistocene sediments of the Pohangina Valley. Carter (1972) notes the occurrence of *Crassostrea ingens* within the basal conglomerate and grit of Te Ekaou Creek (Komako Formation). The presence of *Crassostrea ingens* within the Komako Formation in Te Ekaou Creek correlates well with the macrofossil data gathered within this study. The thick oyster beds found in the Saddle Stream represent a lateral facies change within Fss Member.

The reef formed where the oysters colonised a shallow, rocky, intertidal area of the western Manawatu Strait. The oysters filled an ecological niche in which conditions suitable for habitation prevailed. Oysters are tolerant organisms, able to withstand variations in the amount of suspended sediment within the water column and changes in temperature. The

oyster reef would have provided suitable habitat for other organisms, creating a unique ecological zone of diverse fauna and flora.

Fig 5.5: Thick beds of *Crassostrea ingens* form an oyster reef within Fss Member, Komako Formation. Saddle stream, Pohangina Valley (WGS84 40°17'33.75"S, 175°40'52.88"E, elev 152m).

Farther offshore from the rocky, shallow, nearshore environment inhabited by *Perna canaliculus*, *Aulacomya maoriana* and *Crassostrea ingens* other species such as *Alcithoe Arabica*, *Talabrica senecta*, *Amalda mucronata*, *Pelicaria convexa* and *Tanea zelandica* thrived. These species prefer slightly deeper water, inhabiting a soft ground area of the sea floor more suited to their ecological traits. Here the fine to medium grained sand provided a suitable substrate for burrowing and feeding activities.

### 5.3.1 Facies analysis of Fss Member, Komako Formation

Fss Member overlies Fms Member and underlies Cg Member, Konewa Formation. The upper contact of the Fss Member is a sharp, unconformable contact. The lower contact between the Fms and Fss members of the Komako Formation is a gradational boundary defined by a change in grain size from coarse silt (mean grain size of 5.8 φ) to very fine sand (mean grain size of 3.9 φ) respectively (Appendix 2.8 and 2.7).

Fig 5.6: Fossils from Fss Member, Komako Formation: 1: *Ruditapes largillierti* (Philippi, 1844), 2: *Polinices waipipiensis* (Marwick, 1924), 3: *Aulacomya maoriana* (Iredale, 1915), 4: *Perna canaliculus* (Gmelin, 1791), 5: *Talabrica senecta* (Powell, 1931), 6: *Purpurocardia purpurata* (Deshayes, 1854). Collected from Stallion Stream, Broadlands Station, Pohangina Valley.


A 41.5 m section at the type locality in Stallion Stream was selected for detailed facies analysis. This section contains the contact between the Komako and overlying Konewa Formations (Fss Member and Cg Member). The sequence examined is characterised by fine grained sand followed by matrix supported to clast supported conglomerate, with clasts ranging from pebbles to boulders. The contact is an erosive surface, representing an unconformity which exisits between the Komako and Konewa Formations.

Facies Sh; Fine to medium grained sandstone, massive to laminated bedding, fossiliferous with large concretions.

The Facies Sh is characterised by fine to medium grained sandstone; massive bedded to finely laminated. This facies contains sporadic disseminated fossils including *Polinices waipipiensis*, *Ruditapes largillierti*, *Tawera subsulcata*, *Glycymerita tohunga*, and *Perna canaliculus*. Large 400 mm concretions present within this facies are generally of an elongated spheroid shape, aligned parallel to the pressumed bedding plane. Beds are

approximately 3 m thick. Concretions contain fragmented fossil remains of *Perna canaliculus.*

Fig 5.7: Juvenile specimens of *Phialopecten triphooki* (Beu & Maxwell, 1990), Stallion Stream, Broadlands Station, Pohangina.

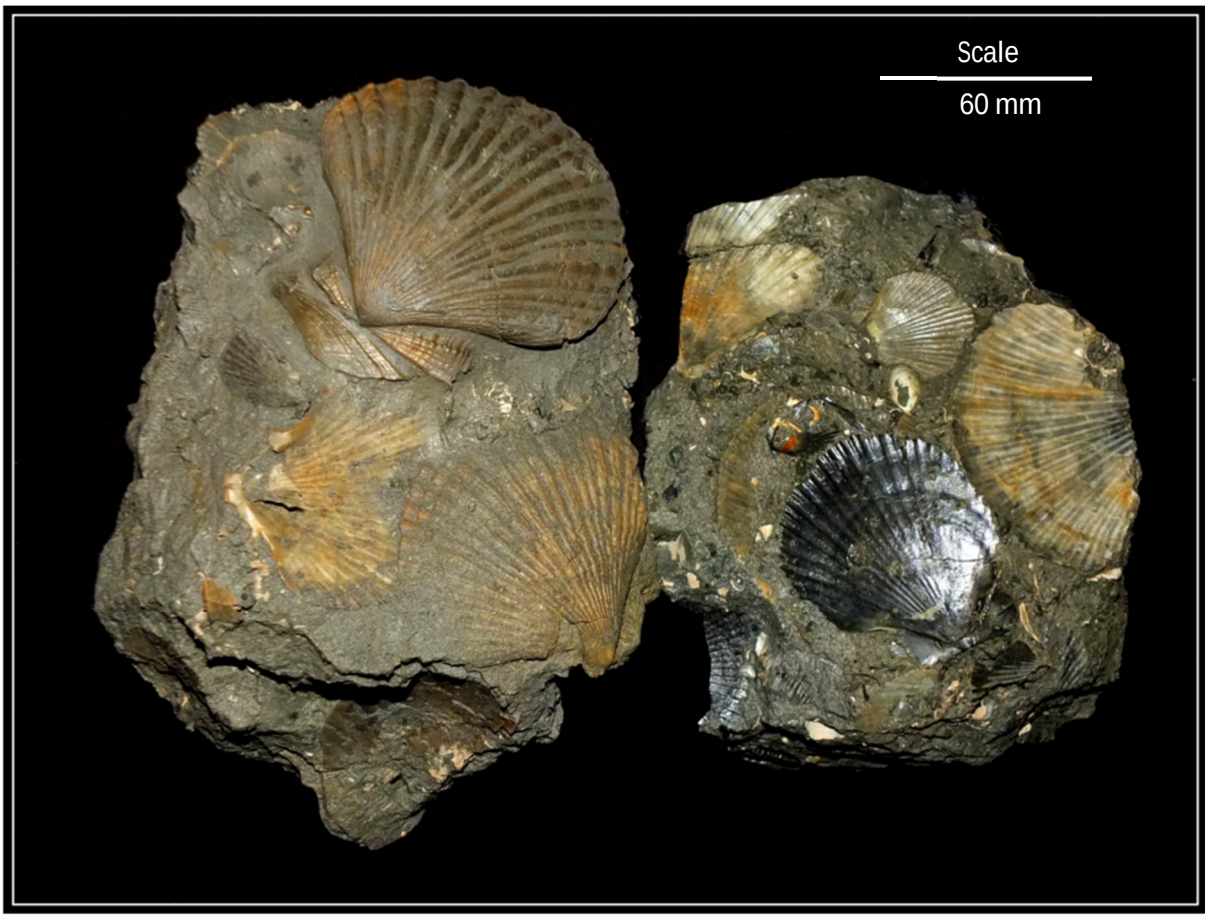


*Interpretation:*
Facies Sh is interpreted as an inner most shelf deposit. The sand fraction of the sediment has been transported out onto the shelf via traction currents while fine material has been deposited from suspension during slacker water periods.

The large concretions are interpreted to be secondary sedimentary structures formed post-depositionally. Often the concretions contain fossils characteristic of shallow water environments e.g. *Perna canaliculus* (Fig 5.6, number 4). It is likely that the carbonate which forms the concretions is not precipitated directly from the sea but represents detrital carbonate which has undergone recrystalisation (Pantin, 1958).

Facies MFS: Fine to coarse sands with common mud rip-up clasts
The MFS facies is characterised by fine to coarse sands displaying bedding structures ranging from ripples to planar laminae. Rip-up clasts of mud are common within this facies; these

range in size from 5-300 mm in diameter. The beds are 0.5-5 m thick. Thin (<5 mm) parallel laminae are the most common bed form observed.

*Interpretation:*
The MFS facies is interpreted as a shallow nearshore marine deposit formed during a TST. The start of the TST is marked by an unconformity (erosional surface). Rising sea level allows wave action to erode into the muddy beds of the LST, incorporating mud rip-up clasts within the fine grained laminated sand of a nearshore environment. The mud rip-up clasts are interpreted to have been derived from an estuarine system which has formed on the continental shelf during a sea level lowstand. During sea level rise, wave action has eroded into the estuarine muds forming rip-up clasts. The flooding surfaces are formed within a nearshore beach environment, displaying dominantly high flow regime laminated bedding structures. Each flooding surface is marked by a new erosional surface represented by the inclusion of rip-up mud clasts.

Facies Ss; Laminated sandstone facies
This facies is composed of fine to coarse grained, rippled to parallel laminated sandstone. Beds are commonly 1-3 m thick. Streaks of secondary iron oxide are present within laminations. Facies Ss contains granular to coarse sand layers alternating with medium grained sands. The granular to medium grained sands display thin generally <5 mm thick laminae.

*Interpretation:*
Facies Ss is interpreted as a lower shoreface deposit, formed in a shallow marine environment. Alternating rippled to parallel laminated sands are attributed to storm dominated deposition. Rippled sands are deposited during intervening quiescent periods. These beds are then eroded back and replaced by planar laminated sands during high flow regime periods associated with storm activity, and a lowering of the mean wave base.

Facies Sh; Fine grained laminated sandstone
Facies Sh is represented by fine grained sandstone with planar laminae. Beds are approximately 7 m thick. Laminations are thin ranging in from 2- 5 mm in thickness. Sediments are dominated by quartzofeldspathic minerals.

*Interpretation:*
The Facies Sh is interpreted as an offshore transitional zone deposit. Storm activity within this zone results in high flow regime laminated bedding. Sands are deposited by traction currents along the sea floor.

Facies Gcn: Normally graded, clast supported conglomerate

Facies Gcn is characterised by poorly sorted, clast supported conglomerate beds that are graded; often in a series of normally graded sets 300 mm thick. Beds are commonly 2 m thick. The matrix is composed of shell grit. Lower contacts range from sharp to gradational.

Interpretation:
The Gcn facies is interpreted as the bottom sets of a fan delta system. Deposition of the bottom sets is interpreted as being via subaqueous pseudoplastic debris flows. The non-erosive base of facies Gcn is characteristic of laminar flow, where movement occurs dominantly in the direction of the flow. Normal grading of the beds, however, indicates periods of turbulent flow, where mixing within the flow has resulted in settling and grading of the clasts. These debris flows have originated from the pro-delta foresets, as unstable areas cause avalanching of material down the pro-delta slope onto the sea floor (Galloway & Hobday, 1996). The constant reworking of clasts within the marine environment via wave action has led to the conglomerate being well sorted and along with the flow dynamics has resulted in normal grading.

Table 5.5: Lithofacies of Fss Member, Komako Formation, (Stratigraphic log of Fss Member, Fig 5.8); facies codes are modified from Horton & Schmitt (1996). Miall (1977), Limarino *et al*, (2002).

| Facies code | Description | Depositional processes | Environment |
|---|---|---|---|
| Sh | Laminated fine to medium sand with mud lenses | Traction current, suspension fall out | Siliciclastic inner most shelf |
| MFS | Fine to coarse sands with common mud rip up clasts | Marine flooding surface formed during transgression, erosional scour, wave action | Near shore- shore face transitional zone |
| Ss | Fine laminated medium to very coarse sands | tidal deposition, storm influenced wave action, | Siliciclastic lower shoreface |
| Gcn | Poorly sorted granule-boulder conglomerate, clast supported normal grading | Hyperconcentrated flows; high density turbidity currents | Transitional delta/shallow marine |

Fig 5.8: Stratigraphic log of Fss Member, Komako Formation, Stallion Stream, Broadlands Station, Pohangina (WGS84 40°16'24.14"S, 175°47'52.03"E, elev 110 m)

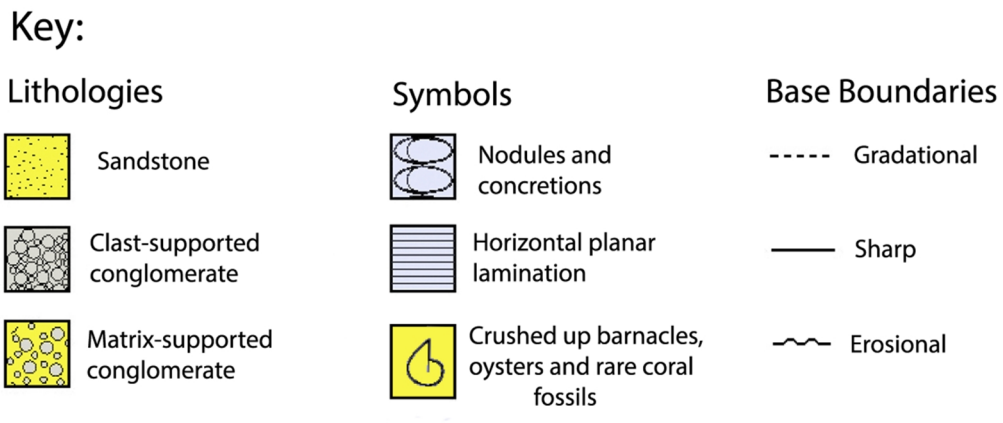


## Interpretation

The upper half of Fss Member is correlated with cycles 1-5 of the Whanganui cyclothem record (Fold-out Sheet II). This falls within the marine oxygen isotope stages 91–98. Marine oxygen isotope stages 99-103 are also represented within the lower half of this member. Basal time constraint is provided by the last occurrence of *Phialopecten thomsoni* and *Polinices waipipiensis.* The last occurrence of *Crassostrea ingens* and *Phialopecten triphooki* in the middle of Fss Member marks cycle 1 in the Whanganui Basin cyclostratigraphy. The erosional upper contact of Fss Member, Komako Formation and Cg Member, Konewa Formation is correlated with cycle 6, MIS 90 via the last occurrence of *Alcithoe brevis.*

Unconformities are interpreted to be present throughout Fss Member. The preserved deposits within this member are correlated to eustatic sea level highstands.

## 5.3.2 Regional correlations

The presence of Opoitian - Waipipian strata on the far eastern side of the Manawatu Gorge (near Woodville) has been noted by Beu (1995), Beanland (1995), and McIntyre (2002). The Opoitian – Waipipian strata are correlated to the Mangatoro Formation of Lillie (1953). The outcrop of Mangatoro Formation contains *Phialopecten marwicki, Crassostrea ingens, Maoricardium spatiosum, Austrofusus pagoda, Fissidentalium zelandicum*, (McIntyre, 2002) and a species of *Marama* ancestral to *Marama murdochi* (Beu pers. comm., 2014).

These Opoitian to Waipipian beds only occur on the far eastern side of the Manawatu Saddle, immediately west of the Mohaka Fault. The occurrence of Mangatoro Formation under Komako Formation on the far eastern side of the Manawatu Saddle (Beanland, 1995) represents the earliest sedimentation within the Manawatu Strait. During this time a depocentre was situated on the far eastern side of the Manawatu Strait. This depocentre migrated westwards as local uplift centred along the Ruahine, Mohaka and Wellington

Faults propagated east to west. Westwards migration of the depocentre occurred simultaneously with emergence of Waipipian to Earliest Nukumaruan sediments above Torlesse greywacke to the east. Emergence to the east resulted in a constriction of the waters of the Manawatu Strait, resulting in increased tidal currents (seen in Late Nukumaruan cross bedded sands, Rss Member and coquina limestone, Cq Member) and a general shallowing upwards trend.

Immediately to the south of Woodville the Mangatoro Formation is unconformably overlain by Nukumaruan Kumeroa Formation (Beu pers. comm., 2014). This implys a long lived Mangapanian unconformity within the sediments of the northern Pahiatua Basin.

On the top and western side of the Manawatu Saddle (this study's mapping area) Mid Mangapanian to Earliest Nukumaruan Komako Formation directly overlies Jurassic to Early Cretaceous Torlesse greywacke. No strata older than Mid Mangapanian have been found on the top or western side of the Manawatu Saddle, suggesting Opoitian to Waipipian deposition may have been restricted to the far eastern side of the Manawatu Strait and Pahiatua Basin. While Mid Mangapanian deposition was restricted to the Manawatu Strait area. Non-deposition or erosion prevailed within the Pahiatua Basin during the Mangapanian Stage.

## Micropalentological analysis

Relatively few age diagnostic species of microfauna are present within the sediments of the Komako Formation (Finlayson, 1980). *Hyalinea cf. balthica*, occurs near the base of the Komako Formation. This species is only found within New Zealand strata of Waipipian age (3.6 –3 Ma). However Finlayson (1980) identified only one specimen during micropalentological analysis and it is possible this speciemen could have been reworked from older deposits, and is therefore not considered diagnostic. *Notorotalia inornata* is common within Komako sediments and *Notorotalia zelandica mangaoaria* also occurs, although in lower numbers. Both these species are indicative of a Mangapanian age (3 -2.4 Ma). Microfaunal species characteristic of the Mid Pleistocene are completely absent from the samples and therefore a Castlecliffian age is dismissed. Based on the micropalentological evidence provided by Finlayson (1980) the Komako Formation ranges in age from Mangapanian to Early Nukumaruan in age.

Fig 5.9: The depth range of *Notorotalia zealandica* on the New Zealand shelf (after Hayward, 1986)

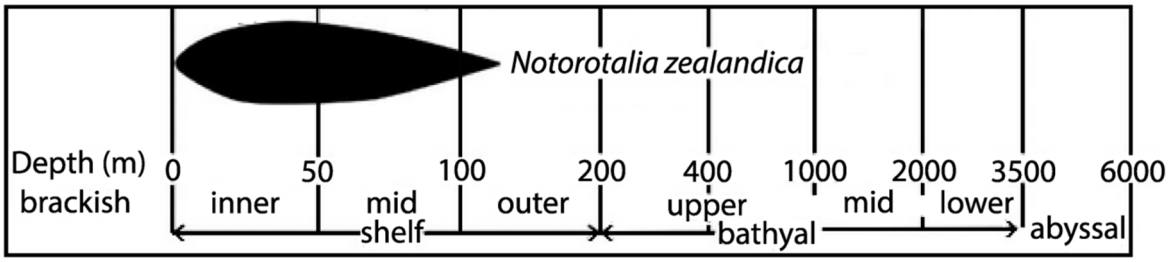


The occurrence of *Notorotalia zealandica* indicates a water depth of approximately 50 m (Fig 5.9). Komako Formation is interpreted as a shallow marine formation deposited within the inner-most shelf to shoreface environments of southeastern Whanganui-Wairarapa shelf. Therefore the paleo-water depth of approximately 50 m is interpreted as a maximum water depth.

# Chapter 6
# Konewa Formation

The Konewa Formation was defined by Carter (1972) as dominantly fine grained marine sediments including coquina limestone, sands and muds. The name is derived from Konewa Stream in Komako District. The base of the Konewa Formation as defined by Carter (1972) is the lowest coquina limestone unit in the type section. In this study the base of the Konewa Formation is interpreted to lie at the contact between Fss Member of the Komako Formation and Cg Member of the Konewa Formation. Correlation to Carters (1972) stratigraphy is tentative within the Manawatu Saddle as widespread, thick, Early to Mid Nukumaruan Conglomerate occurs, which rapidly thins northwards. This conglomerate (Cg Member) is interpreted as a localised member which does not occur within the Komako District.

The top of the Konewa Formation was defined by Carter as the top of the Mafic Sand Member (a readily recognisable sequence of brown sands with interbedded mafic bands and pumice). In this study the top of the Konewa Formation is marked by Cq Member, a 10 m coquina limestone. This coquina limestone marks a change from the dominantly shallow marine sands, muds, conglomerate and coquina of the Konewa Formation to the sandy mudstone with interbedded lignite and tephra of the Bms Member, Takapari Formation. The base of the Konewa Formation has been set at Cg Member which marks a substantial change in depositional style, from the inner-most shelf muddy sands of the Komako Formation to the shallow marine conglomerate, sands, muds and coquina of the Konewa Formation.

Carter correlated the Konewa Formation via biostratigraphy to the *Chlamys delicatula* zone (Lower Nukumaruan) progressing through to possible Upper Nukumaruan within the upper part of the formation. The Konewa Formation has been split into four members in this study from oldest to youngest; Cg (Conglomerate) Member, Kst (sandy mudstone) Member, Rss (Red cross bedded sandstone) Member, Kss (Marine laminated sandstone) Member and Cq (Coquina limestone) Member.

The Konewa Formation is characterised by shallow marine depositional environments. One notable change in depositional style occurs within the Cg Member which contains a thick sequence of conglomerate deposited within a prograding fan-delta to shallow marine environment.

# 6.1 Conglomerate Member

## Lithological description

**Code:** Cg

**Rock type:** Conglomerate

**Colour:** Grey (10YR 6/1) clasts in a fine yellow (10YR 8/6) sandy matrix.

**Hardness:** Hard, lime cemented (sparry calcite). With interbedded lenses of soft sands.

**Weathering:** Highly weathered.

**Grain size:** Boulder to pebble sized clasts, with a fine to coarse sandy matrix. The matrix changes up section to coarse/granule with crushed shell fragments.

**Texture:** Gritty, sandy texture

**Crystals/minerals:** Calcite, quartz, feldspar

**Thickness:** 79 m

**Type section:** Scrimmys Stream Broadlands Station, Pohangina (WGS84 40°16'55.62"S, 175°47'07.20"E, elev 137 m). Access via Saddle Rd with express permission of the land holders.

**Description:** Cg Member is a conglomerate sequence with a maximum thickness of 79 m. It is thickest within the Manawatu Saddle area, thinning rapidly to the north, persiting to the north boundary of mapping. Cg Member is conspicuous in the landscape forming large domed hills and talus slopes (Fig 6.14). A section of the Cg Member was logged (Fig 6.3) in a tributary of the Pohangina River. This tributary, informally named Scrimmys Stream drains the western side of the Ruahine Ranges and contains a very well exposed 66 m section of Konewa Formation. The strata dip between 5 and 20° in a northwest direction.

The stratigraphic log shows a range of lithologies which represent three main depositional environments; a wave dominated Gilbert-type fan delta environment, shore face environments and transitional to offshore shallow marine environments. The sedimentary sequence is interpreted as being largely shallow marine with a strong fluvial influence responsible for delivering large quantities of coarse material to the coast. Evidence for shallow marine deposition is seen in the abundance of fossils, condensed shell grit beds and matrix, calcite cemented beds, and evidence of wave sorting. The separate facies have been grouped into associations based on their occurrence within one of the three main depositional environments identified in this sequence.

## Fossils:

| Table 6.1: Fossil assemblages from Cg Member, Konewa Formation | | | |
|---|---|---|---|
| Family/species | Sample no | | |
| | FS10 | FS11 | FS12 |
| *Penion sulcata* (Lamarck, 1816). | x | | |
| *Purpurocardia purpurata* (Deshayes, 1854). | x | | |
| *Amalda mucronata* (Sowerby, 1830). | x | | |
| *Tucetona laticostata* (Quoy & Gaimard, 1834). | x | | |
| *Talochlamys gemmulata* (Reeve, 1853). | x | | |
| *Calloria inconspicua* (Sowerby, 1846). | x | | |
| *Tanea zelandica* (Quoy & Gaimard, 1834). | x | | |
| *Aeneator elegans* (Suter, 1917). | | x | |
| *Pelicaria convexa* (Beu & Maxwell, 1990). | | x | |
| *Alcithoe arabica* (Gmelin, 1791). | | x | |
| *Talabrica senecta* (Powell, 1931). | | x | |
| *Patro undatus* (Hutton, 1873). | | x | x |
| *Cominella (Eucominia) nassoides* (Reeve, 1853). | | | x |
| *Cookia sulcata* (Lightfoot, 1786). | | | x |
| *Paphies australis* (Gmelin, 1791). | | | x |
| *Barbatia novaezelandiae* (Smith, 1915). | | | x |

## Biostratigraphy

The presence of *Pelicaria convexa*, *Tanea zelandica*, and *Alcithoe arabica,* indicate that deposition can not have been older than Early Nukumaruan. While the presence of *Talabrica senecta* indicates deposition could not have been younger than Early Nukumaruan. *Pelicaria convexa* is a key index fossil for the Nukumaruan Stage. Beanland (1995) also notes the occurrence of the Nukumauran Stage restricted fossil *Pmacomitas protransenna* within Cg Member.

The last occurrence of *Cassostrea ingens* within the Plio-Pleistocene sediments of Pohangina Valley is right near the base of Cg Member Konewa Formation, where it occurs as a thick oyster reef within upper most Fss Member, Komako Formation. *Cassostrea ingens* becomes

fossil assemblage it is interpreted that Cg Member, Konewa Formation, was deposited during Early Nukumaruan time.

The extinction of *Crassostrea ingens* is interpreted to occur within the upper part of the Konewa Formation. This extinction provides further evidence of Early Nukumaruan deposition which is characterised by extreme changes in climate (a dramatic cooling episode) which lead to the extinction of warm water species and the first occurrence of cool water species e.g. *Zygochlamys delicatula* in Komako Formation, Komako District, 25 km north of the Manawatu Gorge (Carter, 1972). Carter notes the occurrence of *Patro undatus*, Zygo*chlamys delicatula* (Hutton, 1873), *Glycymeris shrimptoni* (Marwick, 1923), *Tawera subsulcata* (Suter, 1905), *Talabrica senecta*, and *Pelicaria sp.* (Marwick, 1923). This fossil assemblage is characteristic of the Nukumaruan Stage.

Cg Member is correlated to cycle 6 of the Whanganui Basin cyclothem record, falling within marine isotope stage (MIS) 91 (Fig 6.4). This correlation is based on the last occurrence of *Alcithoe brevis* directly below the contact between Komako and Konewa Formations. The last occurrence of *Crassostrea ingens* and *Phialopecten triphooki* within Fss Member, Komako Formation also provides age constraint. Stage 90 is a glacial period. In Pohangina it is represented by increased erosion and the choking of paleo-rivers with gravel and sediment. Stage 90 is correlated with the erosional unconfromtiy at the base of Cg Member. During the sea level highstand of 91 increased rainfall allowed the gravels eroded during the previous glacial (MIS 90) to be transported to the coast. Stacking patterns changed from retrogradation to progradation as sediments started to build out into the basin during the last part of the HST and into the RST.

The apparent lack of *Zygochlamys delicatula* within the Early Nukumaruan fossil assemblages collected is attributed to the paleoenvironment of the Manawatu Strait. *Zygochlamys delicatula* is characteristically found in deeper outer shelf environments open to the ocean, whereas Cg Member was deposited within a shallow water marginal marine environment with a strong fluvial influence. The Wairarapa shelf was open to the coast during Early Nukumaruan time (Beu, 1995). However within the narrow, confined seaway connecting the Whanganui and Wairarapa shelf, open mid to outer shelf conditions were not present. The 'Manawatu Strait' at this time was a series shallow marine environments enclosed by headlands to the north and south.

Beanland (1995) collected fossils from Cg Member noting the occurrence of *Fosterella tubulatus* and *Cominalla nassoides*. These two species indicate a cold water environment, which correlates to the occurrence of *Zygochlamys delicatula* within the Nukumaruan sediments of the Komako District (Carter, 1972).

The occurrence of *Tanea zelandica*, *Calloria inconspicua*, *Ostrea ingens*, *Paphies australis*, *Penion sulcata*, *and Purpurocardia purpurata* (Table 6.1) indicates a shallow water foreshore to beach environment. *Barbatia novaezelandiae* is characteristic of a shallow-water and high-energy facies (Beu & Raine, 2009).

The presence of the *Cookia sulcata* indicates that during the deposition of Cg Member, Konewa Formation the climate was relatively cool. This relatively cool climate is interpreted to be a function of a glacial period during which erosion rates were high, leading to river aggradation and coastal progradation. This interpretation fits with the identification of *Zygochlamys delicatula* within Konewa Formation sediments in the Komako District by Carter (1972). The occurrence of *Zygochlamys* signals the migration of cold water species into the eastern Whanganui Basin during Early Nukumaruan time.

*Cookia sulcata* is relatively rare in the fossil record. This large species of grazing snail lives under stones and ledges feeding on coralline and brown algae of the sublittoral fringe (Morton & Miller, 1968). The occurrence of this species suggests that the rocky shoreline in which Cg Member was accumulating supported fauna containing herbivourous gastropods, which browsed on algae in depths of up to 10 m.

The range of fossils within Cg Member also shows that several different ecological zones occurred within various habitats. The oyster *Patro undatus* began life attached to rocky substrate (fan delta facies of Cg Member), however, it appears to have been attached only while small, and to have been free-lying on the sea-bed upon reaching maturity (Beu & Raine, 2009). The high concentration of *Patro undatus* within concentrated shell beds of Cg Member indicates small oyster reef systems existed within the intertidal zone of a shallow marine environment. These oyster reef environments occurred adjacent to the delta facies of a nearby paleo-fluvial outlet which transported terrigenous, clastic sediment into the shallow Manawatu Strait area. The oyster reef provided a substrate suitable for the habitation of other organisms such as sea anemones.

Offshore from the rocky delta and adjacent oyster reef environments other species such as *Alcithoe arabica*, *Talabrica senecta*, *Amalda mucronata*, *Pelicaria convexa and Tanea zelandica* inhabited a soft ground area of the sea floor, more suited to their ecological traits. This area was composed of a medium to fine sandy sea floor suited to habitation of shallow marine dwelling mollusca.

The depth ranges of fossil species from Cg Member are shown in Fig 6.1. A minimum water depth of 25 m is estimated given the occurrence of the shallow water to mid shelf dwelling *Alicthoe Arabica* and *Penion sulcata.* A maximum water depth of 55 m is calculated by the overlap between the shallow water dwelling species with species found at up to 200 m depth e.g. *Barbatia novaezelandiae, Tanea zelandica* and *Amalda mucronata*. These water

dwelling organisms e.g. *Tanea zelandica* and *Purpurocardia purpurata.* Rocky substrate closer to shore provided suitable habitat for *Barbatia novaezelandia,* and *Talochlamys gemmulata.*

Fig 6.1: Depth ranges of selected mollusc taxa present within Cg Member (Powell, 1979; Morley, & Hayward, 1999; Beu & Maxwell, 1990; McIntyre, 2002; Morley & Hayward, 2007).

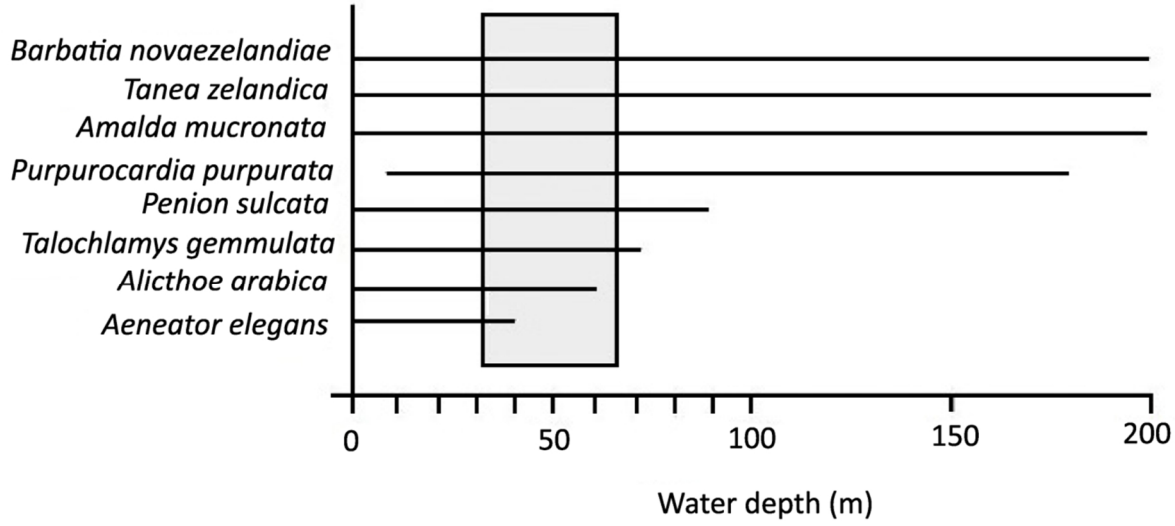


## Stratigraphy

The sedimentary sequence exposed at Scrimmys Stream is dominated by conglomerates interbedded with sandstones (Fig 6.3). The base of the sequence is characterised by matrix supported conglomerate. Concentration of clasts within the conglomerate units increases up section, with the upper half of the sequence characterised by clast supported conglomerate. The upper half of the sequence is also characterised by a change from terrigenous to bio-clastic matrix. The bio-clastic matrix is largely composed of crushed shell material and coarse sand. Fossils occur within the upper 40 m of the section. Barnacle fossils preserved whole and still attached to the top of clasts within bed number ten are presumed to be in growth position. Facies Gcn also occurs in Fss Member, Komako Formation (Fig 5.8) and is fully described there (see section 5.3.2). It is therefore not repeated in the facies descriptions below. Nine facies are recognised within Cg Member and are outlined in Table 6.2.

Table 6.2: Lithofacies of Cg Member, Konewa Formation. (Stratigraphic log of Cg Member, Fig 6.3) Facies codes are modified from Miall (1977), Postma (1990), Horton & Schmitt (1996).

| Facies code | Description | Interpretation |
|---|---|---|
| Fm | Massive or poorly laminated mudstone; no grading, mudcracks | Waning flood flows; suspension fallout |
| Gh | poorly sorted granule-cobble conglomerate; clast supported, no grading, horizontal stratification | Flood sheets - wave driven traction |
| Sp | Solitary or grouped planar crossbeds in sand | Linguoid, traverse bars, sand waves (lower flow regime) |
| Clm | Massive or laminated calcareous, coarse sand – pebble lenses | Concentration of shell material via wave action within near-shore environment |
| Gcn | Poorly sorted granule-boulder conglomerate; clast supported, normal grading | Hyperconcentrated flows; high density turbidity currents |
| Gcu | Poorly sorted granule-boulder conglomerate; clast supported, no grading or weak inverse grading | Plastic or pseudoplastic clast-rich debris flows; hyperconcentrated flows |
| Gmn | Poorly sorted granule-boulder conglomerate; matrix supported, normal grading | Pseudoplastic debris flows |
| Gmu | Poorly sorted granule-boulder conglomerate; matrix supported, no grading or weak inverse grading | Plastic debris flows |
| Gds | Well sorted, matrix supported conglomerate, with steeply dipping bedding planes. | Plastic or pseudoplastic debris flows; sheet floods – wave driven traction (Lower Delta Slope) |

### 6.1.1 Facies and Facies Associations

Facies Fm: Fine silt beds with lenses of sand

Facies Fm is characterised by fine silts and laminated sands. Beds range in thickness between 3 and 5 m. Laminations are thin, 2-5 mm thick. Ferromagnesian minerals compose approximately 5% of the sand grains, these weather to form orange iron oxide mottles on the outcrop. Silt beds are characteristically grey to blue grey in colour. Lower contact is sharp and erosional.

*Interpretation:*

Fine laminated sands in this facies are deposited during high energy storm dominated events within the mid flow regime. Whereas massive bedded silt lenses/beds are deposited during fair weather episodes within the lower flow regime. The fair weather episodes allowed silt sized sediment to be deposited instead of becoming reworked and transported into deeper water enviroments. The lower contact of this facies is sharp and unconformable. This facies is interpreted as being deposited offshore within inner to mid shelfal depths.

Facies Gh: Poorly sorted clast supported conglomerate

The Gh facies is composed of sorted, clast supported, conglomerates, often with bivalve, bryozoan and barnacle fossils. The clasts display weak horizontal stratification. The matrix, composing 10% of the entire facies, consists of 70% shell grit and 30% coarse grained sand. Clasts range in size from 64–256 mm. Beds are generally 3 to 4 m thick. There is no evidence of bioturbation; in keeping with the large grain size of the clasts and generally high rates of sedimentation and erosion associated with coarse grained coastal environments (Reading, 1996). Lower contacts range from sharp to erosional.

*Interpretation:*

Facies Gh is interpreted as a high energy shoreface deposit, where continued wave action has resulted in sorting of the conglomerate clasts, while winnowing out the finer material and transporting it into the basin. Wave action is interpreted to have generated the crushed shell material in the matrix. In unit 10 barnacles are present on many of the clasts, some in growth position. The high energy interpretation for this facies is preferred by robust thick shelled taxa, hence the preservation of fauna with low diversity, reflecting the limited number of benthic species adapted to the unstable substrate characteristic of this environment (Bourgeois & Leithold, 1984).

Fig 6.2: Part of the fossil assemblage collected from Cg Member, Konewa Formation. 1: *Aeneator elegans* (Suter, 1917), 2: *Amalda mucronata* (Sowerby, 1830), 3: *Barbatia novaezelandiae* (Smith, 1915) 4: *Penion sulcata* (Lamarck, 1816), 5: *Purpurocardia purpurata* (Deshayes, 1854), 6: *Ostrea ingens,* (Zittel, 1864), 7: *Paphies australis* (Gmelin, 1791), 8: *Tucetona laticostata* (Quoy & Gaimard, 1835), 9: *Tanea zelandica* (Quoy & Gaimard, 1832), 10: *Talochlamys gemmulata* (Reeve, 1853), 11: *Alcithoe arabica* (Gmelin, 1791).

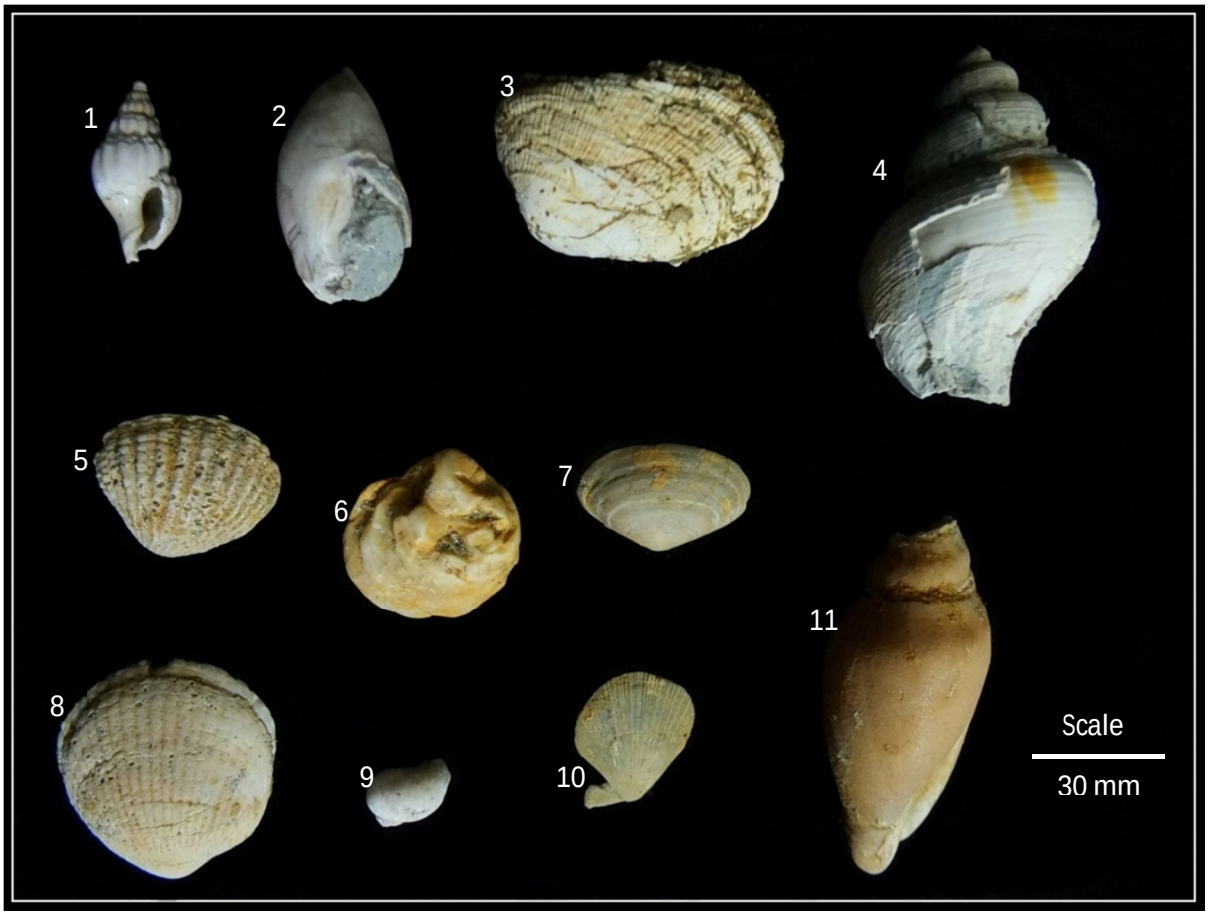

**Fig 6.3: Cg Member,** Konewa Formation, Scrimmys Stream (WGS84 40°16'56.47"S, 175°47'14.11"E), Broadlands Station, Pohangina, New Zealand

| Age | Formation | Bed number | Comments | Interpretation |
|---|---|---|---|---|
| Mid Nukumaruan | Kst Member, Konewa Formation | 19 | -Cross bedded, coarse sandstone , with some lenticular beds filled with fine grained mud towards the top of the bed, fossiliferous, common *Talochlamys gemmulata*, | -Lower shoreface, sand bar dunes becomming wiped out by storm dominated deposition of lamiated sand, mud settling out during fine weather periods into rippled sands |
| | | 18 | *Patro undatus*<br>- Blue grey mudstone , massive, *Amalda novaezelandiae* and *Alcithoe fusus* present | -Offshore transitional environment, where fine silt is settling out of suspension during fair weather |
| | | | -Obscured | -Fan delta bottom sets |
| Early Nukumaruan | Cg Member, Konewa Formation | 17 | -Well sorted coglomerate, normal grading , shell grit matrix | |
| | | 16 | -Shell grit | -Upper shoreface, wave sorting of gravels<br>-Condensed shell grit beds 14 and 16 occur on a sediment straved shoreface environment, terrigenous sedimentation has been cut off by local sea bed topography |
| | | 15 | - Well sorted conglomerate, clast supported, shell grit matrix | |
| | | 14 | -Shell grit | |
| | | 13 | -Alterating pebbles and sand layers | |
| | | 12 | -Clast supported conglomerate, shell grit matrix, iron oxide present, thick wave ripple laminations, sorted | -Slow sedimentation rate, shoreface<br>-Lower shoreface |
| | | 11 | -Well sorted laminated conglomerate, clast supported | |
| | | 10 | -Well sorted conglomerate, barnacles present some in growth position | -Shallow marine lower shoreface, terrigenous sedimentation rate slows allowing for barnacle colonisation |
| | | 9 | -Poorly sorted conglomerate, shell grit matrix clast supported<br>-Conglomerate, four sets of normal grading, clast supported | -Fan delta debris flow deposit<br>-Fan delta bottom sets |
| | | 8 | -Medium sand with six 7 mm thick shell grit layers spread throughout | -Lower shoreface, lower flow regime |
| | | | -Obscured | |
| | | 7 | -Laminated conglomerate showing normal grading with a coarse sand matrix | -Fan delta top sets |
| | | 6 | -Thick bedded conglomerate, cobbles to boulders clast supported, poorly sorted | -Proximal fan delta debris flow deposit |
| | | 5 | -Laminated matrix supported conglomerate, well sorted, paleoslope 20°@302 (NW) | - Wave dominated prograding fan delta foresets |
| | | 4 | -Laminated conglomerate with lenses of medium sand, some asymmetrical wave ripple laminations present | |
| | | | -Laminated coarse sand and pebbles | -Fan delta top sets |
| | | | -Obscured | |
| | | 3 | -2 sets of Iron oxide cemented reverse graded conglomerate, grading from coarse sand through to cobbles | |
| | | 2 | | -Proximal fan delta debris flow |
| Mangapanian | Komako Formation | 1 | -Fine laminated silt lenses in fine sand, orange mottles present, 5 mm clacite cemented sand layers present at 3 and 4 m | -Offshore transitional environment where finer silt is settling out during fair weather interbedded with storm generated laminated sands |

Scale (m): 65, 60, 55, 50, 45, 40, 35, 30, 25, 20, 15, 10, 5, 0

Lithology: Mud | Sand (clay, silt, vf, f, m, c, vc) | Gravel (gran, Pebb, cobb, boul)

Facies: Fm, Gh, Sp, Clm, Gcn, Gcu, Gmn, Gmu, Gds

## Lithologies

- Sandstone
- Matrix supported conglomerate
- Clast supported conglomerate
- Lime cemented shell grit

## Symbols

- Planar lamination
- Wave ripple cross lamination
- Herring-bone cross bedding

## Base boundaries

- ----- Gradational
- ~~~ Erosional
- —— Sharp

Fig 6.4: Correlation of Konewa Formation (Cg Member) to cycle 6 in the Wanganui Basin cyclothem record, marine isotope stages (MIS) 90 and 91 using isotope curve from Lisiecki & Raymo, (2005). The paleomagnetism is inferred from correlation of fossils to MIS.

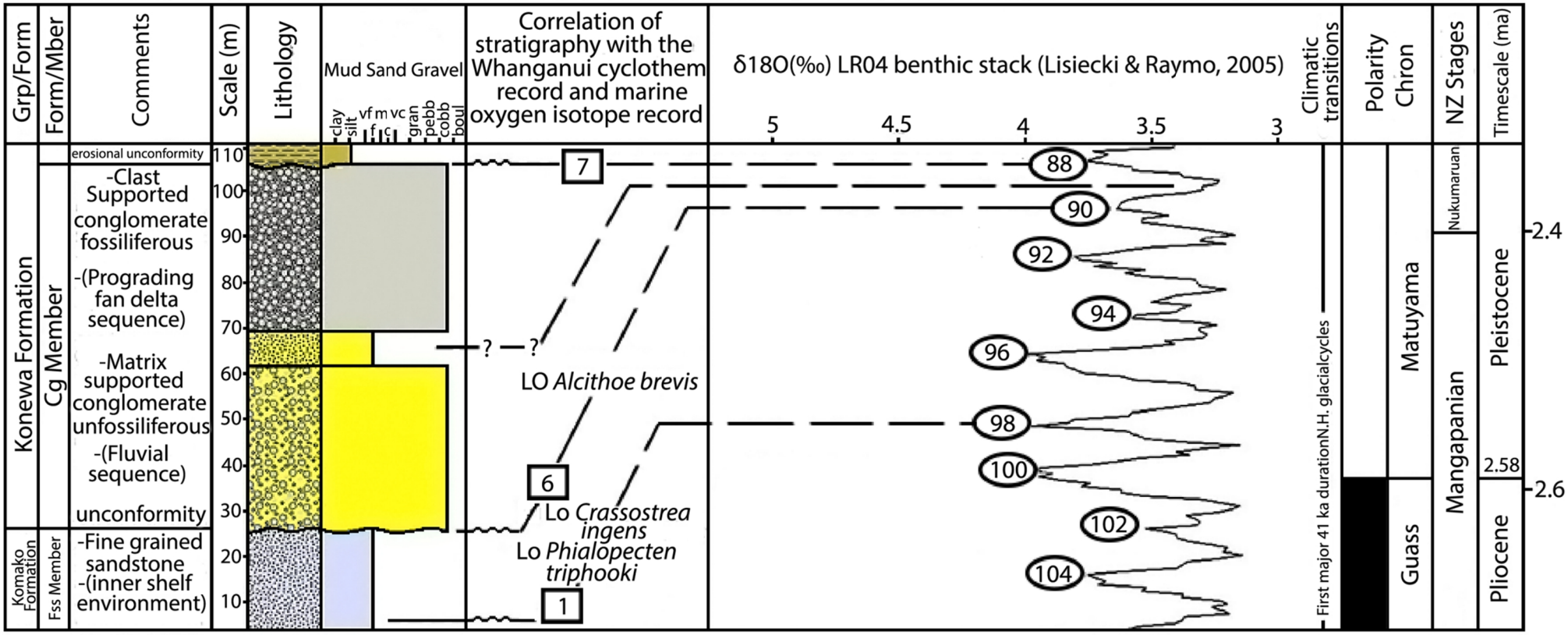

Facies Sp: rippled to laminated sandstone

The Sp Facies is represented by coarse to medium grained sands with parallel laminations, planar cross beds and ripples present. Beds are 3 – 3.5 m thick. The cross beds occur in sets 300 mm thick capped by a thinner parallel laminated interval 10-15 mm thick. The laminations are very thin from 1-5 mm thick. In the top of bed 19 (Fig 6.3) ripple sand layers occur with some lenses of mud infilling the ripples, some lenticular bedding and crushed shell material present. Six thin 7 mm thick shell grit layers are present within bed 8 (Fig 6.3). The lower contact is sharp and erosional.

*Interpretation:*

The presence of crushed shell material and laminated bedding suggests deposition on the lower shoreface. The ripples within this facies are attributed to ripple migration and deposition during quiescent periods between storm events (Reineck & Singh, 1980) (Fig 6.5). Some of the ripple troughs have been in-filled with finer sediments, forming lenticular bedding, and are interpreted to occur within the low flow regime. The planar cross bedding seen in bed 19 is interpreted as the depositional product of migrating dunes under lower-flow- regime conditions (Miall, 1977). The association of ripple and cross bedding is interpreted to be the result of shallow-water deposition. The 300 mm set thickness of cross bedded strata suggests that migrating bed- forms were subaqueous dunes or bars around 300mm in height. These dunes or bars were subsequently planed off during high energy periods replaced with thin parallel laminated sand. The thin laminated sand beds are interpreted as storm dominated deposits occurring in higher energy events. The Sp Facies is interpreted as a nearshore deposit.

Facies Clm: Condensed shell grit

The Clm facies contains 300 mm thick condensed shell grit beds. The shell grit is composed of crushed shell material that has been subsequently lithified by calcite cement. Some fossils are preserved whole including *Talabrica senecta* and *Patro undatus*. Beds are up to 300 mm thick. The lower contact is sharp and erosional.

*Interpretation:*

The Clm Facies is interpreted to represent a shoreface environment starved of terrigenous sediment. As longshore currents transport sediment down the coast, some areas are effectively cut off from terrigenous sediment supply. This allows for effective colonisation of the seafloor by marine organisms, and the concentration and precipitation of calcium carbonate material within the rock record. Within the high energy shoreface environment shell material becomes crushed by wave action and concentrated in a condensed bed. The Clm Facies is interpreted as a nearshore deposit.

Fig 6.5: Shoreline profile showing the different sub-environments, facies and processes (Reading, 1996).

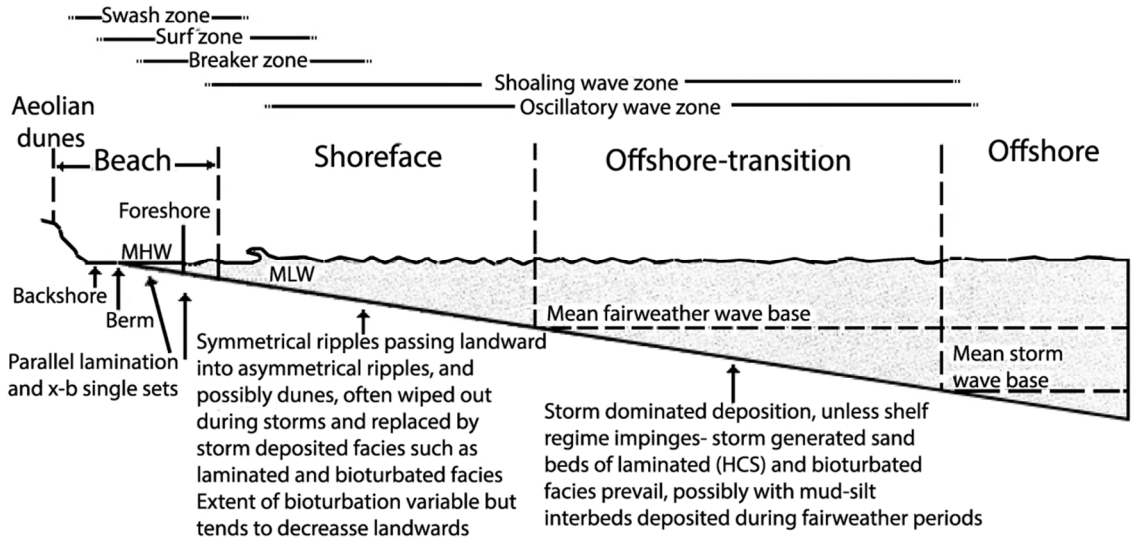


Facies Gcu: Poorly sorted, clast supported conglomerate

Facies Gcu is represented by a poorly sorted, chaotic conglomerate ranging in clast size from pebbles to boulders. Clasts 50-200 mm in diameter are abundant, while outsized clasts of > 500 mm occur in lower numbers. The conglomerate is clast supported. The matrix is up to 5% of the entire facies and is composed of 70% shell grit and 30% coarse grained sand. Beds are 2 m thick. The lower contact is gradational.

*Interpretation:*

The Gcu Facies is interpreted as a fan delta debris flow, caused by an avalanche of debris down the delta front. Evidence for a delta front is seen within facies Gds, where steep sedimentary dips occur. As the river delivers more gravel into the fan delta system, large quantities of gravel build up at the topsets of the fan delta. Such gravels move down onto the delta front in subaerial to subaqueous, plastic or pseudoplastic, clast-rich debris flows (Waresback & Turbeville, 1990). Debris flows originating from the delta front contain high clast concentration resulting in a clast supported conglomerate. Little mixing occurs within the flow as evidenced by the chaotic, poorly sorted nature of facies Gcu.

Facies Gmn: Normally graded matrix supported conglomerate

Facies Gmn consists of poorly sorted conglomerate in a matrix of medium sand. Lenses of medium grained sand occur within the conglomerate. This facies displays thick 300 mm laminations and normal grading. Beds range from 2 – 7 m thick. Clasts range from 32-256 mm in size. The lower contact is gradational. Clasts are sub-rounded to rounded.

*Interpretation:*
The Gmn facies is interpreted as the top sets of a Gilbert-type fan delta system. Facies Gmn is interpreted as deposits of sub-aerial or subaqueous pseudoplastic debris flows. The basal contact of facies Gmn is non-erosional which is interpreted to infer that mainly laminar flow occurred during deposition. However, the normal grading of the clasts also suggests that some turbulent flow occurred during transport, resulting in mixing within the flow and grading of the clasts.

The pseudoplastic debris flows which deposited the Gmn facies were more dilute and less viscous than the plastic debris flows of the Gmu or Gcu deposits. Evidence for this is that the Gmn deposits are generally of smaller clast size and have better grading. The pseudoplastic debris flows probably had low matrix strength and low dispersive pressure during transport (Shultz, 1984).

Facies Gmu: Matrix supported, poorly sorted conglomerate
The Gmu facies is represented by thickly bedded, very poorly sorted to poorly sorted conglomerate. The conglomerate is matrix supported. Clast size ranges from 64-300 mm with some isolated clasts being over 300mm in size. Bedding is massive and the matrix is medium sand. Beds are 2 m thick. The matrix content of the conglomerate generally increases up section. The lower contact is gradational.

*Interpretation:*
The lack of an erosive lower bedding contact and the lack of lamination suggest a low flow velocity and potentially laminar flow during transport. The high matrix content of facies Gmu is considered to be a result of a very viscous debris flow where both matrix strength and dispersive pressure acted as sediment support mechanisms. The general upward increase in matrix content is interpreted as being a product of water admixture and associated decrease in matrix strength during transport, a process suggestive of deposition in a subaqueous environment (Nemec & Steel, 1984).

Facies Gds: Steeply dipping, well sorted, conglomerate.

Facies Gds is characterised by a well sorted matrix supported conglomerate. The dip of bedding planes within this facies is up to 32 ° compared to the general structural dip of 5 ° for the facies both above and below. The matrix is composed of medium sand. Beds are 3m thick, with the bedding accentuated by the alignment of clasts. The bedding is trending in a SW direction. Lower contact is gradational.

*Interpretation:*
The steep sedimentary dip is interpreted to represent the steep face of fan delta foresets prograding out at the coast. The well sorted nature of this facies suggests some reworking

by wave action. This type of steeply inclined prograding profile is characteristic of a gilbert-type fan delta front (Galloway & Hobday, 1996). A fan delta (Fig 6.6) requires a high basin margin gradient and is therefore confined to coarse grained systems (Reading, 1996). The fan delta foresets form where bedload, dropped at the river mouth continues down the delta front as grain flows or frictional debris flows. The dip of this facies is interpreted to be a result of both the progradation of the fan delta out into the ocean and the constant reworking at the front of the foresets by both wave action and avalanching, resulting from the over-steepening of the slope by continuing bedload deposition in the upper fan delta.

Fig 6.6: Cross section of a Gilbert-type fan delta. MWL = Mean water level, (Reading, 1996)

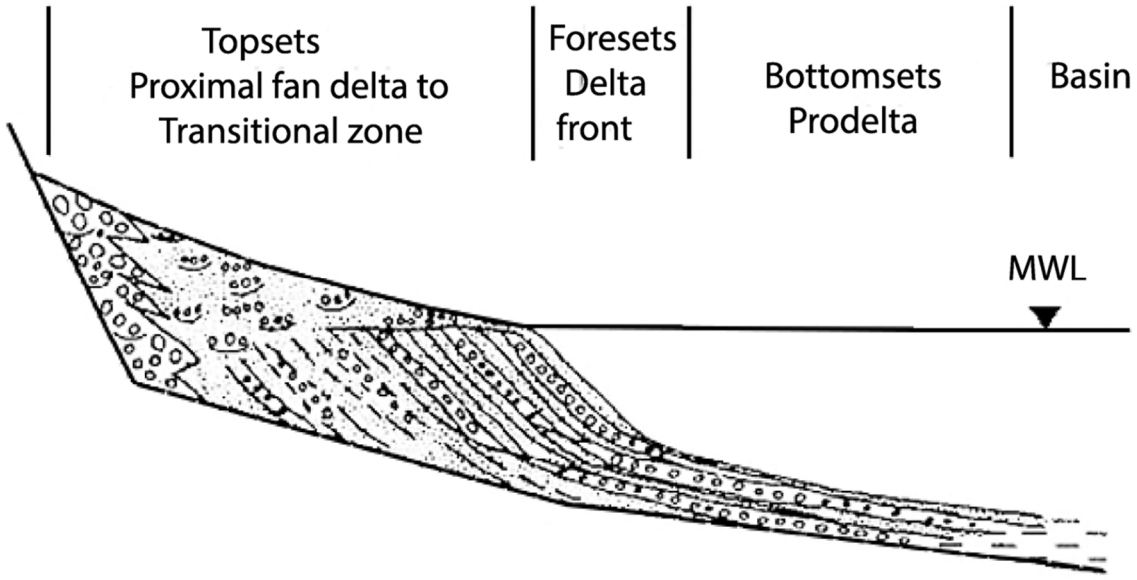


## 6.1.2 Fan delta clast analysis

The presence of well-rounded clasts is generally indicative of fluvial transport (Brackley, 1999). However, roundness is not a direct indicator of a fluvial environment. Disc or roller shaped clasts are rounded by wave action processes in a marine environment, whereas fluvial clasts tend to be spherical. The form of larger particles has an effect on their transportability, when they are moved by traction along the bed (Boggs, 1995). Equant and roller shaped clasts tend to be more readily transported than blades and discs of similar mass, and this may lead to preferential transportation of clasts downstream. Two variables that are important in determining the roundness of transported clasts are clast composition and size (Boggs, 1995).

Fig 6.7 is a Zingg diagram of the clast shapes from facies Gmu (bed 6) and Gds (bed 5) (Fig 6.3). Data was taken from 50 clasts from each facies to assess the differences in clast shape

between facies Gmu and facies Gds. Results show the Gmu Facies is characteristed by equant shaped clasts with a minor number of oblate (disc) shaped clasts. The Gds Facies contains a wider range of clast shapes with a majority of clasts ranging from bladed to oblate (disc) shapes. The dominantly equant clast shapes of Facies Gmu is interpreted as representing a fluvial signature. Facies Gds (prodelta foresets) has a wider range of clast shapes which are not diagnostic of a specific environment.

Large clasts are often more rounded than smaller clasts. This may explain why more of the clasts in unit Gmu are rounded, as the clasts sizes were larger. Facies Gmu has a larger range of clast size as this is unsorted to poorly sorted and more equant in shape. These are interpreted as a debris flow onto the proximal fan delta zone. The proximity to the fluvial source of the gravels is likely the reason the clasts have remained unsorted. Facies Gmu displays a more characteristic fluvial signature and less evidence of being reworked by wave action into a disc or blade shape.

Facies Gds clasts have been exposed to wave action at the front of the fan delta. Their position at the front of the delta leaves them exposed to constant wave action, causing slumping and reworking of clasts within the fan delta foresets. This has resulted in better sorting of the clasts and a large range of clast shapes with a broad signature, consistent with both fluvial and marine environments.

**Fig 6.7:** Zingg diagram showing clast shape from 50 clasts of facies Gds (bed 5) and facies Gmu (bed 6)

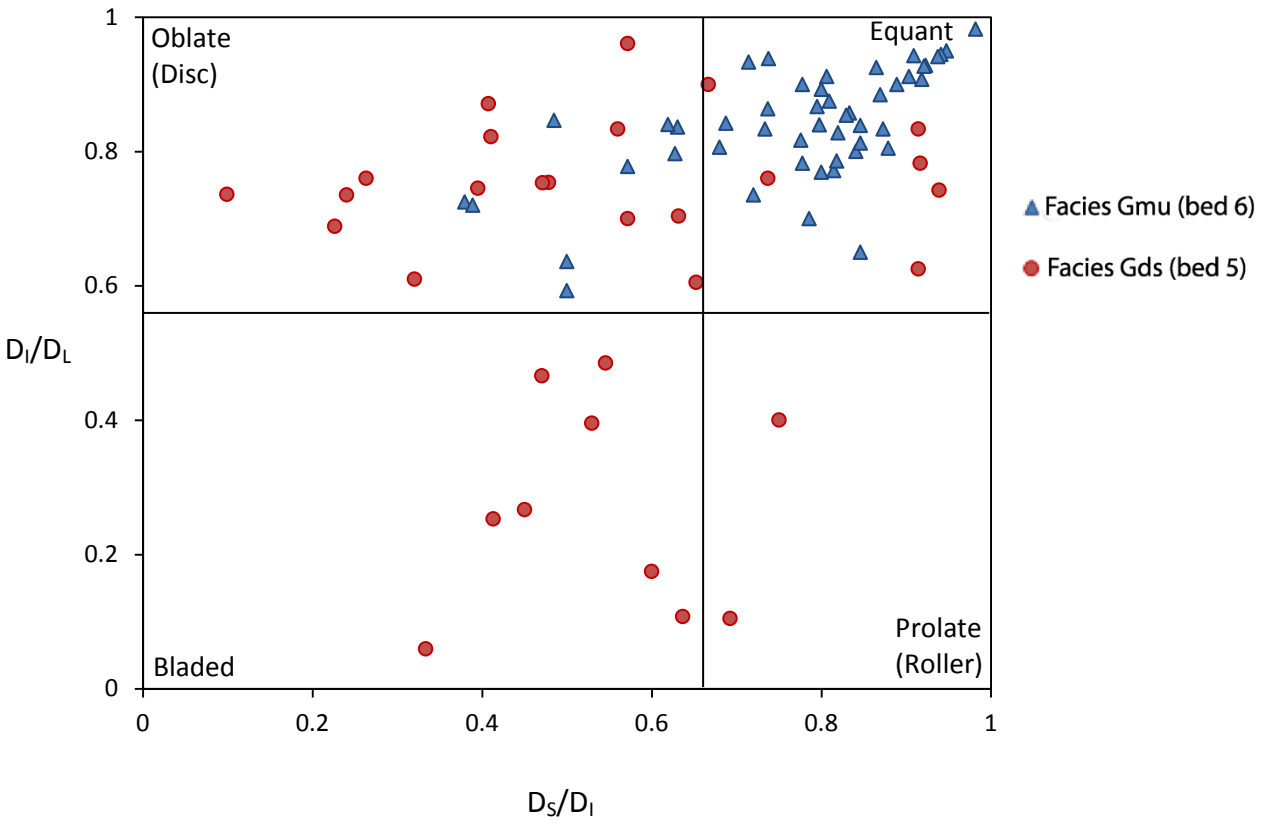

Samples of Cg Member were collected for clast size analysis at two separate locations (Appendix 3.2). The first location was Scrimmys Stream, where 50 clasts were measured from Facies Gds and Facies Gmu facies. From these 50 clasts measurements of the long, intermediate and short axis were made. 50 clasts were then measured from the same two facies at a second location in Stallion Stream, approximately 1.5 km NE from Scrimmys Stream. The conspicuous change in dip between facies Gds and Gmu made identification of the two facies at the two different localities possible.

The aim of this clast size analysis was to compare the results from Pohangina Valley with a model developed by Szabó *et al,* (2013) for the Williams River in Austrailia (Fig 6.8). Szabó *et al,* (2013) found a relationship between mean long axis length and distance travelled from source. From the clasts analysed the mean long axis data were calculated and plotted on a clast size vs distance from source model that was developed by Szabó *et al,* (2013). The Pohangina data plotted on the model show that the gravel within Cg Member has travelled approximately 40 – 70 km from source. The simulated trend of downstream fining within the model shows a decrease in gravel size with distance from source. These data along with data showing the mean of five maximum sized clasts (Appendix 3.2) can be used to estimate the approximate distance to source of Cg Member. This result is consistent with the relationship between the type of delta and the distance from source illustrated by MacPherson *et al*, (1987) (Fig 6.9).

There is a long standing debate on the relative importance of size selective transport versus abrasion in producing downstream fining in gravel bedded river (Brewer *et al*, 1992; Ferguson *et al*, 1996). Downstream fining is due to a combination of selective sorting, by which finer grains are preferentially transported downstream; and abrasion, by which individual particles are reduced in size (Parker, 1991).

Fig 6.8: Line graph showing decrease in clast size with distance from source. This model was developed by Szabó *et al,* (2013). Model results are shown by thick grey line, black triangles are field results from Williams River, Australia (Szabó *et al,* 2013). Coloured triangles represent the mean of 50 long axis measurements taken from clasts in Gds and Gmu facies, Cg Member, Konewa Formation. Adapted from Szabó *et al,* (2013).

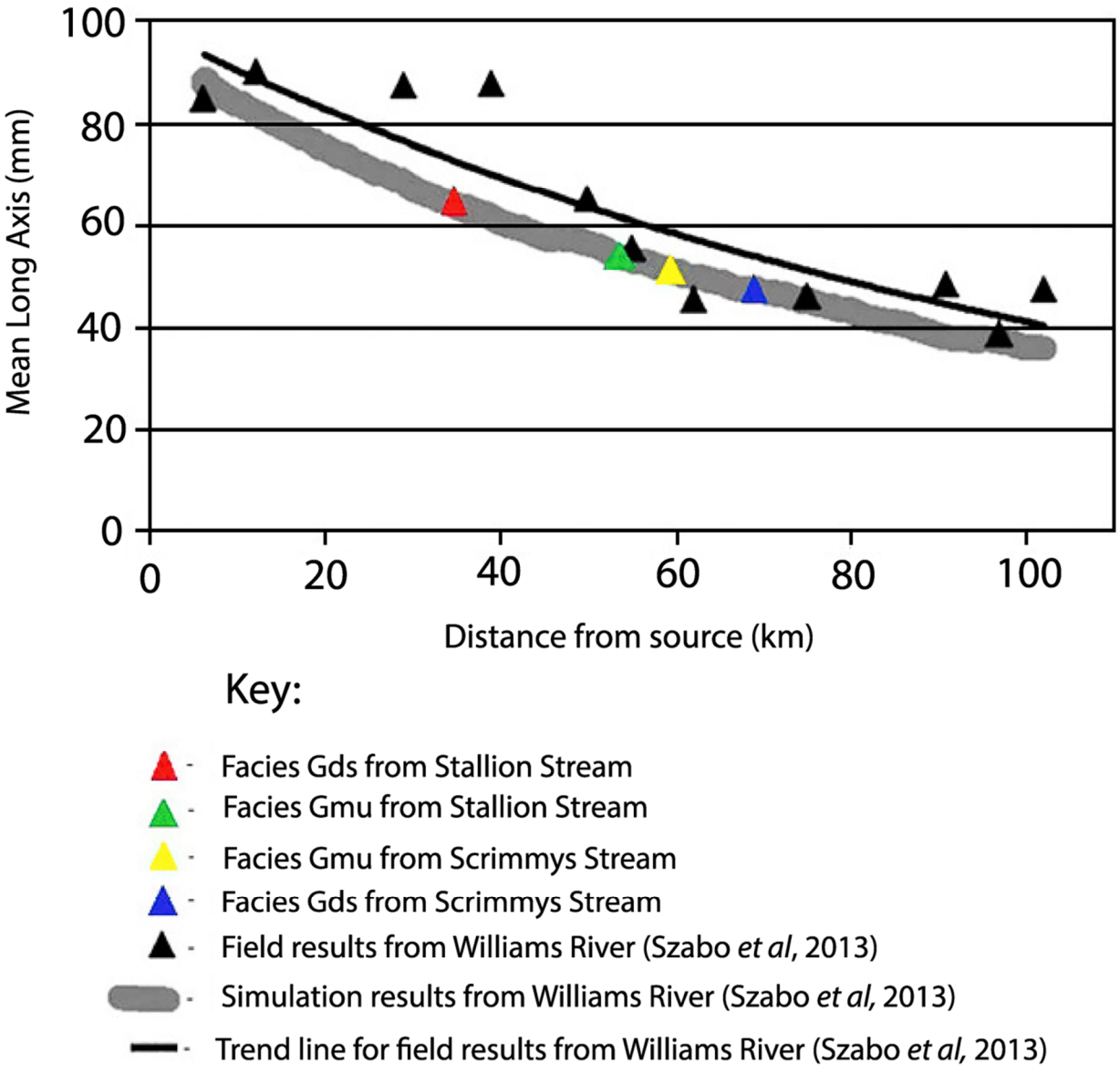

Szabo *et al*, (2013) use an abrasion model based on box equations to simulate downstream changes in grain shape and size. This study applies the model to basalt clasts along the Williams River in Hunter Valley, Australia. The application of this downstream fining model allows estimations on distance from source to be made based on clast size and shape. This model has been applied to Nukumaruan greywacke gravels within Cg Member. Although originally used to predict changes in basalt gravels within Williams River it is assumed the hardness of the two gravel types are relatively similar. Conclusions drawn from the use of this model are broad estimations, which nonetheless allow important paleogeographic interpretations to be made in relation to Cg Member, Konewa Formation.

Fig 6.9: A comparison of fan-deltas, braid deltas, and fine-grained deltas based on distributary-channel patterns, sediment load and size, stream gradient, flow velocity, steadiness of discharge and distance of shoreline from source (McPherson *et al,* 1987).

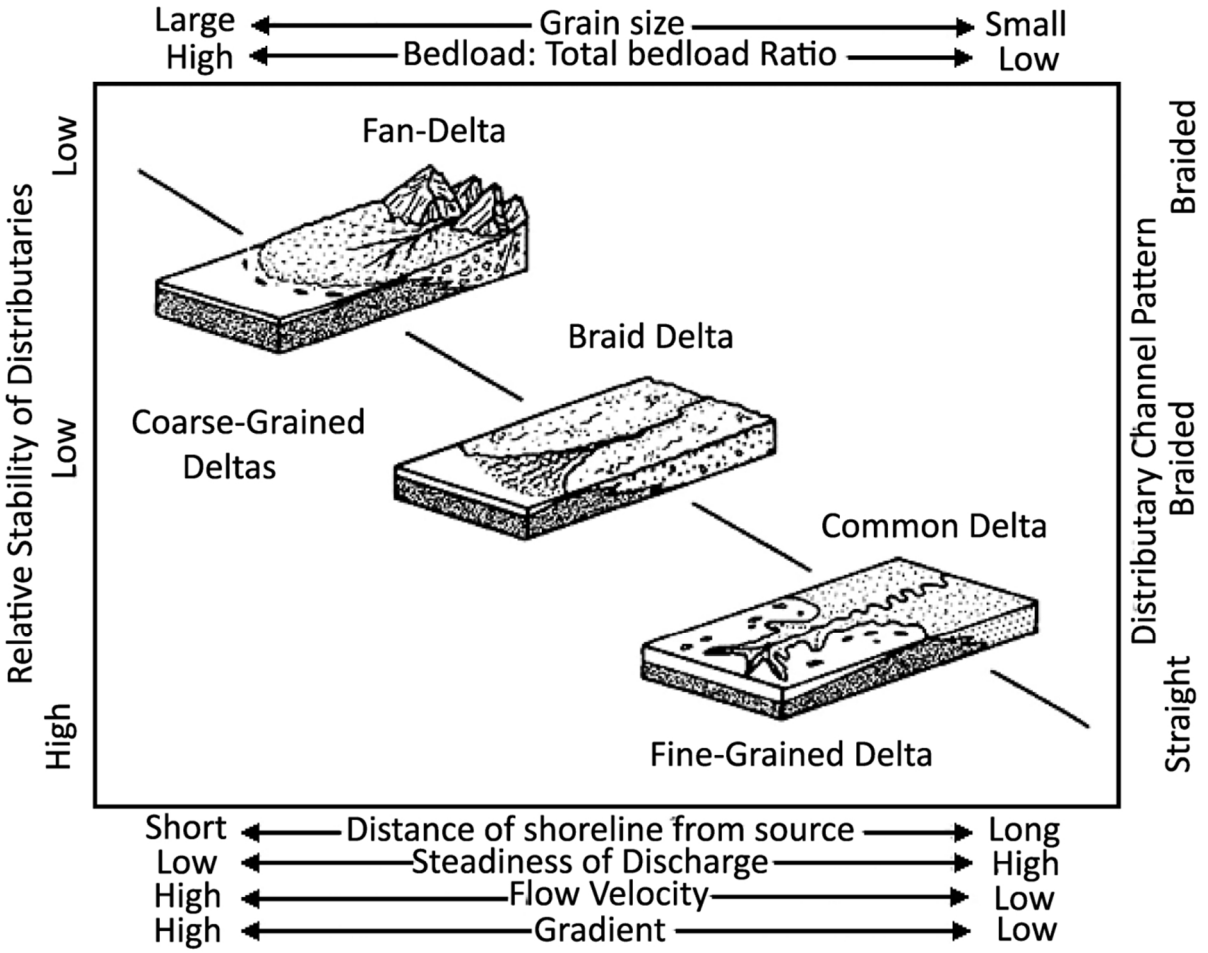

### 6.1.3 Fan delta foreset analyses

The declination and inclination of beds within the steeply dipping forsets (Fig 6.10) of facies Gds (bed 5) were taken from two locations (Appendix 3). Data from Scrimmys Stream (WGS84 40 °17'00.88"S, 175 °47'23.77"E, elev 183 m), show that the dominant foreset direction of the fan delta at this location were directed at 260° (WSW). The dominant foreset direction is interpreted to represent the paleo-river flow which is the driving force transporting clasts down slope on the prodelta foresets, orientating beds in a basinward direction. Therefore this foreset direction gives us the approximate direction at which the river entered the southeastern Whanganui Basin during Early Nukumaruan time.

**Fig 6.10:** Gilbert-type fan delta cross section (Reading, 1996).

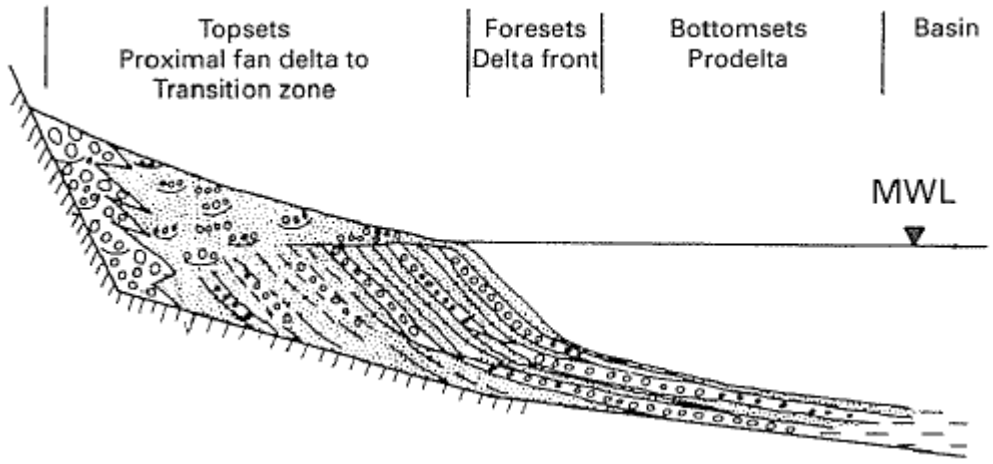


The second set of dip data are taken from Stallion Stream (WGS84 40 ° 16'24.86"S, 175 ° 47'56.16"E, elev 115 m) which is approximately 1.5 km NE of the first location at Scrimmys Stream (Fig 1.5). The data were collected from the same facies at both locations to determine if any there was any change in the dominant foreset direction. The second set of data show a dominant foreset direction of 330° (NW).

The change in dips is interpreted to represent the change in dip direction across the pro-delta forsets on the front of the delta (Fig 6.11). The delta front is inferred to be at least 1.5 km long as facies Gds can be traced across the landscape from both outcrops for this distance. The river at this time was actively prodgrading and contained an active braid plain. This braid plain which fed the Gilbert-type fan delta would have constantly changed course as it meandered over the elevated basement NE of Pohangina in Early Nukumaruan time.

The dip data demonstrate that the paleo-river entered the Whanganui Basin in a westwards direction. Clast analysis (Fig 6.8) also shows that the northern most outcrop in Stallion Stream has an overall larger mean clast size than the outcrop further to the south in

Scrimmys Stream. Therefore the outcrop in Stallion Stream, farther to the north was also closer to source, thus providing evidence of a gravel source to the north of Pohangina. From these two lines of evidence it is postulated that the paleo-river system had a northern source in the location of the present day northern Ruahine Range some 40-70 km NE of Pohangina, which at the time (approximately 2.4 Ma) was rising elevated basement. An eastern source for the gravels i.e. Puketoi Range is ruled out because during Early Nukumaruan time the Ruataniwha Strait occupied the area between Pohangina and the elevated basement to the east, thus making an eastern source improbable.

**Fig 6.11:** Schematic model illustrating the depositional setting of a fan-delta. Black arrows indicate the dip direction in which clasts of the prograding delta foresets are orientated. Note the rotation of dip around the delta front (adapted from McPherson *et al,* 1987).

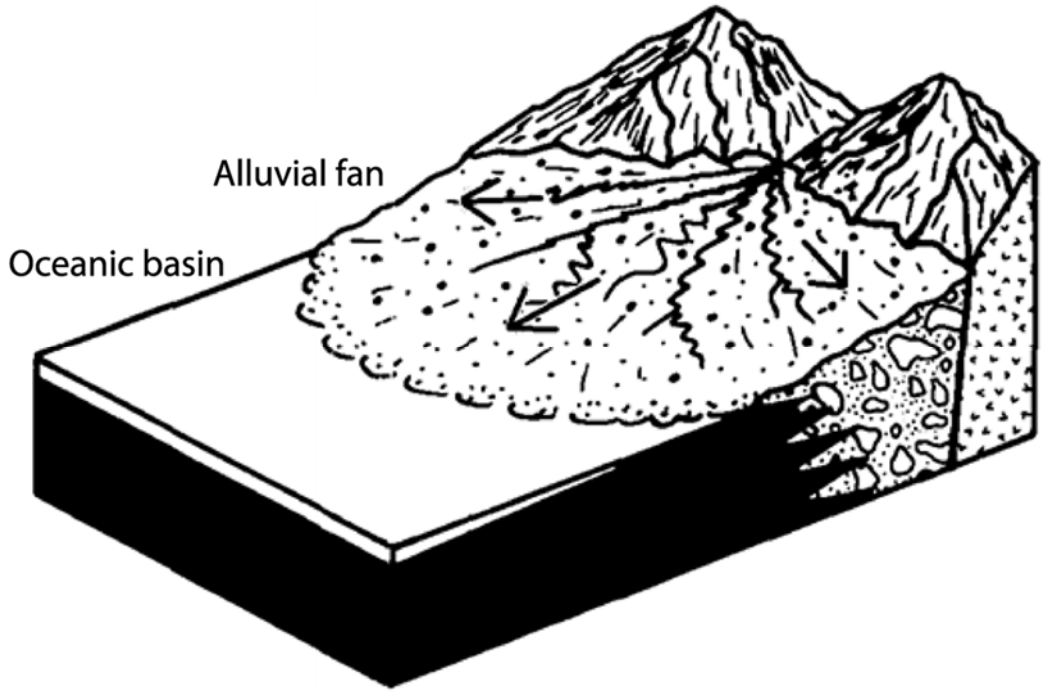

The paleo-river system meandered SW across this elevated landmass to where it formed a prograding fan delta directed westwards into the Whanganui Basin. The change in dip direction between the two successions of Cg Member are interpreted to represent opposing sides of the same fan delta which formed a long (at least 1.5 km) alluvial plain which built out a substantial fan delta (Fig 6.11).

The source of the Early Nukumaruan gravels which comprise Cg Member, Konewa Formation is interpreted to be the exposed greywacke basement in the vicinity of the modern day northern Ruahine Range (paleogeographic map; Fig 6.12). The interpretation based on the clast size analysis of the gravels which compose the Cg Member (maximum clast size >500 mm and mean long axis of 55.28 mm) is that these gravels have been transported between 40 and 70 km downstream from source. This means that the proto-Kaimanawa Range, located approximately 130 km NNE from Pohangina and which began to form around 2.4 Ma (Trewick & Bland, 2012), is an unlikely source for the Early Nukumaruan gravels.

The succession at Scrimmys Stream provides evidence for the influence of a large paleo-river system within the southeastern Whanganui Basin. Paleoslope and lineation measurements from the prograding delta foresets suggest the paleo-river system entered the Whanganui Basin from the NE delivering vast quantities of terrigenous sediments into a shallow marine environment. The sudden influx of gravel into the basin is attributed to the commencement of uplift in the paleo-river headwaters coinciding with a glacial period associated with a marine regession and a lowering of eustatic sea level. The cooling climate resulted in a lowering of the tree line and increased erosion within the source area of Torlesse greywacke. Increased erosion rates lead to river aggradation and an increased sedimentation rate. The sedimentation rate exceeded subsidence in the SE Whanganui Basin, rapidly filling accommodation space and causing coastal progradation. Associated with this cooling event in Early Nukumaruan time was the extinction of warm water taxa e.g. *Crassostrea ingens, Maoricardium spatiosum, Polinicies waipipiensis, and Phialopecten thomsoni;* and the northwards migration of *Zygochlamys delicatula.*

The arrival of the subantarctic mollusc *Zygochlamys delicatula* signals the incursion of the Australasian Subantarctic Watermass (ASW) to New Zealand's latitude of 41° south. This change in oceanic currents occurred in Early Nukumaruan time, possibly being connected with an increase in Northern Hemisphere glaciation (McIntyre, 2002). The occurrence of cold water taxa within the sediments of Konewa Formation (Carter, 1972) does not marks the arrival of subantarctic surface waters carrying cold water species to this latitude (McIntyre, 2002). A complete absence of *Zygochlamys delicatula* within the sediments of the lower Pohangina Valley and Manawatu Saddle is due to only eustatic sea level highstands being preserved i.e. during glacial periods when cold water migrants arrived; there was erosion or non-deposition in this area.

In the lower Pohangina Valley LST's are represented by unconformities, as sea level retreated exposing the continental shelf to erosion or non-deposition. Only the top of the TST, the HST, and the first part of the RST are preserved. Thus in the glacial period during MIS 90, the erosional unconformity at the base of Cg Member formed, and the gravel which was to later form Cg Member was eroded filling the paleo-river catchment. In the subsequent interglacial period during MIS 91 the climate ameliorated leading to an increase in rainfall and allowing the paleo-river to transport the gravels generated during the glacial period out toward the coast. The paleoriver system aggraded to meet rising sea level during this interglacial stage.

The fan delta described in the Lower Pohangina Valley, was directed westwards into the Whanganui Basin, and likely formed the border to the northwestern Manawatu Strait during Early Nukumaruan time. During this time the western side of the Manawatu Strait was characterised by clastic, fluvial to fan delta environments, while the eastern side was characterised by bioclastic accumulation in a shallow marine environment. In the centre of the Manawatu Strait connecting these two opposing depositional systems, fossiliferous, shallow marine sands were being deposited deposited. Based on Walthers Law (Middleton, 1973) Fss Member represents the shallow shelf sands deposited into the Manawatu Strait during Early Nukumaruan time. While in a laterally adjacent environment to the west, Cg Member (Konewa Formation) began accumulating within a fluvial to marginal marine environment.

An outcrop of Totaranui limestone occurs on the eastern side of the Manawatu Saddle (part of the 'aragontitic and calcitic shellbed facies' in Fig 6.12). This thick unit of cross-bedded, poorly fossiliferous Nukumaruan limestone containing rare *Zygochlamys delicatula*, was mapped originally as Kumeroa Formation (Lillie, 1953). Beu, (1995) correlated this outcrop to the Totaranui Limestone of Neef (1974, 1984). This particular outcrop was deposited on the western side of the Ruataniwha Strait, within shoal areas bordering the proto-Rauahine Range (Beu, 1995). The Totaranui limestone outcrop at the Manawatu Gorge was moved into position via dextral movement along the North Island Dextral Fault Belt (Beu, 1995).

This Totaranui Limestone outcrop is interpreted as a shell bed where wave action re-worked and concentrated the shells in a shallow marine setting, winnowing out fine material which was then transported farther out into the basin. This type of deposit is characteristic of a moderate to low siliciclastic sedimentation rate, where the bioclastic material is relatively undiluted by terrigenous sediments. A lower terrigenous sedimentation rate will also facilitate a greater biological production rate within the shallow marine environment generating greater quantities of bioclastic material for accumulation forming a coquina limestone. This setting contrasts markedly with the fan delta environment on the SE margin of the Whanganui Basin at this time, where terrigenous sedimentation rates were

substantially higher allowing both delta formation, fluvial aggradation and coastal progradation.

Fig 6.12: Paleogeographic map showing the lower North Island during Nukumaruan time, Early Pliocene time (2.4 Ma) Map depicts a interglacial period ;adapted from Trewick & Bland, 2012; McIntyre, 2002: Beu, 1995).

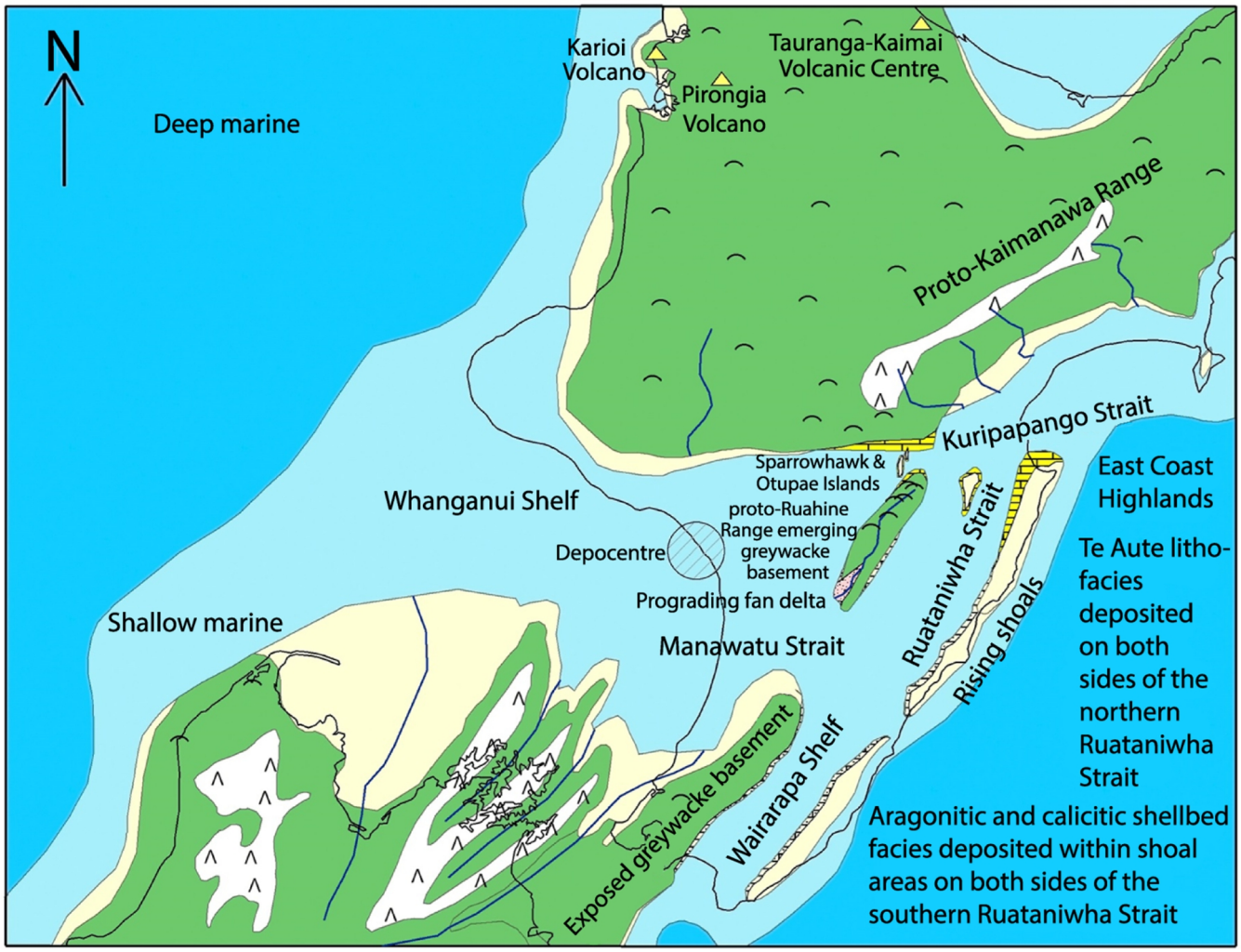


Legend

- Mountains
- Hills
- Volcanoes
- Outline of modern New Zealand
- Rivers
- Terrestrial
- Mountainous areas
- Coast
- Shallow marine
- Deep marine
- Prograding fan delta
- Te Aute lithofacies
- Aragonitic and calcitic shellbed facies

Scale

100 km

Fig 6.13: Cg Member forming a ridge, high angle dip planes formed by movement on the Whareroa Fault located in the far right of this image, Konewa Formation, Maungatukurangi Stream, Broadlands Station, Pohangina.


Fig 6.14 Classic dome shaped hills formed by Cg Member, Konewa Formation, Broadlands Station, Pohangina.

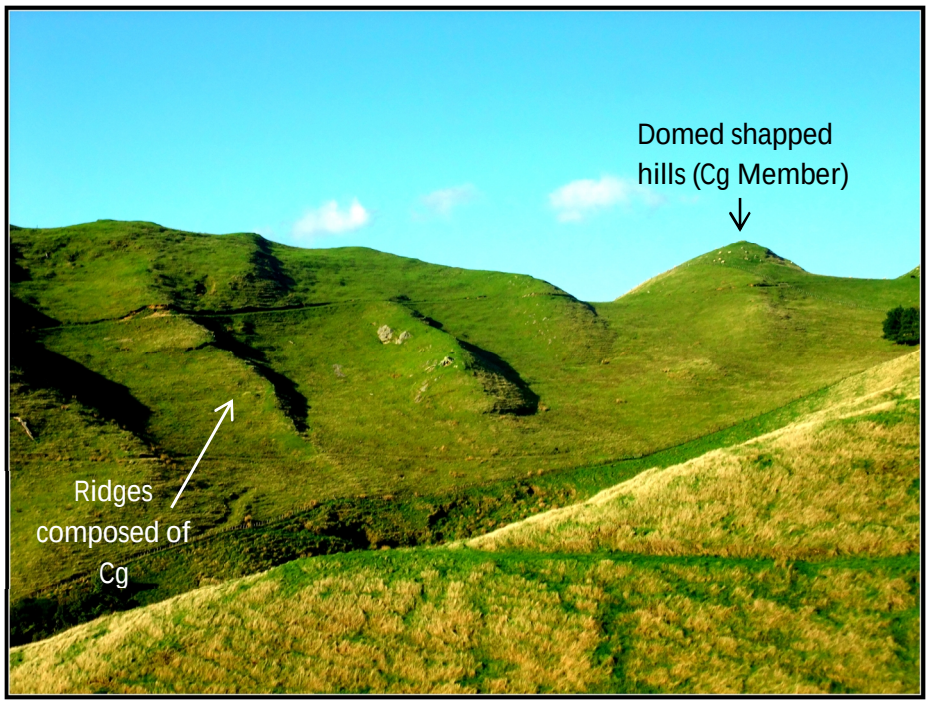

## 6.2 Sandy Blue Grey Mudstone Member

### Lithological Description

Code: Kst

Rock type: Sandy mudstone

Colour: Light grey (7.5YR N6/0) in colour

Hardness: Soft, moderately consolidated

Weathering: Moderately weathered

Grain size: Silt, clay and fine sand

Texture: Smooth silty texture

Crystals/minerals: Calcite, quartz, feldspar

Thickness: 28 m

Type section: Scrimmys Stream, Broadlands Station, Pohangina (WGS84 40°16'55.62"S, 175°47'07.20"E, elev 137 m). Access via Saddle Rd with express permission of the land holders.

Fossils:

Table 6.3: Fossil assemblage from Kst Member, Konewa Formation

| Family/species | Sample no |
|---|---|
| | FS9 |
| *Amalda novaezelandiae* (Sowerby, 1859). | x |
| *Alcithoe fusus* (Quoy & Gaimard, 1833). | x |

### Biostratigraphy

The presence of *Alcithoe fusus* indicates that deposition cannot have taken place earlier than Nukumaruan time. However, all the fossils found within Kst Member range into Recent times and therefore do not provide a constraint on the minimum age range for the timing of deposition.

Both *Amalda novaezelandiae* and *Alcithoe fusus* are characteristic of deposition within a marine shelf environment. They are commonly deposited within soft bottom facies such as massive silt and mudstones, below wave base.

## Magnetostratigraphy

Beanland (1995) conducted a series of paleomagnetic analyses on the Plio-Pleistocene sediments preserved along the Saddle Road on the Manawatu Saddle. This was a pilot study to test whether the Manawatu Saddle sediments had sufficient magnetization to warrant a more comprehensive paleomagnetic study. The objective of the study was to determine paleomagnetic age.

It was found the only unit to contain viable levels of magentization was Kst Member, Konewa Formation; located on the western Manawatu Saddle. Two sites were used; the first was located where Kst Member outcrops on the Saddle Road and the second within an outcrop in Scrimmys Stream. Paleomagnetic samples were spaced regularly at 2-3 m intervals throughout Kst Member in order to average out secular variation. 14 samples were analysed from the Saddle Road outcrop, and 52 samples from the Scrimmys Stream section (Appendix 5).

All the samples analysed from Kst Member show a reversed polarity. The reversed polarity demonstrates that the observed magnetization is primary, not a modern overprint which if present would show normal polarity. The reversed polarity of Kst Member is interpreted by Beanland (1995) to suggest that the sediments fall within the lower part of the Matuyama reversed polarity chron. This polarity chron is just above the Gauss/lMatuyama boundary; therefore Kst Member must be younger than 2.5 Ma.

The data shows a mean primary magnetization declination of 186±2° (Beanland, 1995). This is equivalent to a tectonic rotation of 4±2°. The rate of rotation obtained from Kst Member, Konewa Formation is approximately 2°/myr. This is a minimum value as it is possible that rotation did not commence immediately after deposition.

## 6.2.1 Grain Size Analysis

The grain size data from the Kst sample (Appendix 2.6) shows a bimodal distribution with two distinct grain size populations. A poorly sorted distribution with a fine tail would usually be indicative of a fluvial environment, however, no sedimentary features within this member point to fluvial deposition. The presence of *Amalda novaezelandiae* and *Alcithoe fusus* fossils, however, do provide evidence of shallow marine deposition

.

The bimodal distribution is interpreted to be a result of deposition on a heterolithic muddy shelf environment. The first population ranges from 0-3 Phi representing sand grains which have travelled mainy by rolling and sliding. The second finer population, ranges from 4 -10 Phi and has been transported by saltation and suspension within the water column.

The cumulative frequency graph on a probability scale (Appendix 2.6) allows separation of the grain size distributon into 4 distinct grain size populations. The pattern displayed on the cumulative curve is a function of the processes that formed the sediment and the avaliablity of the different grain sizes within the parent material (Friedman & Sanders 1978). A break occurs around 2.5 Phi between the rolling and sliding population and the saltation population. The steep gradient of the rolling and sliding population indicates good sorting of the grain size fraction between 0 and 3 phi. This sorting is initiated via traction currents moving the bedload along the sea floor within a shallow marine environment. The two suspension populations occur between 6-10.5 Phi. These populations are responsible for the fine skewed, poorly sorted nature of the unit.

Kst Member is interpreted as being deposited within an innermost shelf environment below storm wave base, where a river system delivered large amounts of fine suspended sediment. High suspended sediment load within the water column has resulted in large tracts of heterolithic facies developing. Heterolithic facies are characterised by a bi-modal grain size distribution containing two separate grain size populations.

## Interpretation

Kst Member unconformably overlies Cg Member, demonstrating a change from coarse deltaic deposition to fine grained shallow marine deposition. This change is marked by an erosional unconformity, representing a low stand glacial period. Kst Member is interpreted to have been deposited during the interglacial HST of MIS 87 (Fold out sheet II). Kst member unconformably underlies the Rss Member. Kst Member is massive and sparsely fossiliferous. The lack of bedding within Kst Member is interpreted to be the result of the homogenous nature of deposition. Most fossils are preserved whole and *in situ*; disseminated throughout the member in mainly oblique orientations. The sparseness of the fossils is interpreted to be due to a combination of high sedimentation rate, and relatively inhospitable (muddy) substrate for shelled macrofauna. Concentrations of shells in HST are usually a result of lower sedimentation rates and more hospitable (sandier) substrates for shelled macrofauna (Abbott, 2000).

### 6.2.2 Modern analogue

A modern analogue to the depositonal pattern observed within Kst Member is the modern Whanganui Basin where the Manawatu and Rangitikei Rivers enter the Taranaki Bight (Fig 6.15). Here extensive deposits of shelf muds occur at the mid-shelf mud depocentre offshore from Foxton. It is likely that during sea level high stands during the Quaternary, similar conditions to the modern day Whanganui Basin existed. During Late Nukumaruan and Castlecliffian highstands the palaeogeography and oceanographic setting of the northern and northeastern Whanganui Basin were similar to the modern Taranaki Bight today (Lewis *et al*, 1994).

Paleo-river systems running from central North Island southwards entered the Whanganui Basin during Late Nukumaruan time, bringing with them large quantites of suspended sediments. This enabled the deposition of heterolithic shelf sands and muds forming Kst Member. The oceanographic setting of the Whanganui Basin during Late Nukumaruan time was likely to have been storm dominanted like it is today. The deposition of heterolithic mud and sand facies was likely influenced by a gyre caused by the steering of storm controlled currents by the sea bed topography along the embayed margin of the Whanganui Basin (Abbott, 2000).

Both the Plio-Pleistocene and modern highstand system tract deposits have formed at peaks in the glacioeustatic regime which has existed since 2.6 Ma (Pillans *et al*, 1998). Kst Member is interpreted as a HST deposit closely resembling the Castlecliff HST, which is dominated by 1- 20 m thick blue-grey siltstone (Abbott & Carter, 1994). The difference in thickness between the Castlecliff HST and Kst Member (28 m) is attributed to a greater sedimentation rate and amount of accomadation space during Mid to Late Nukumaruan time, along the southeastern margin of the Whanganui Basin. The higher sedimentation rate was due to uplift within the Kaimanawa Ranges and proto-Ruahine Ranges, which actively supplied the southeastern coast of the Whanganui Basin via paleo-river systems draining south from the central North Island.

Fig 6.15: The genereralised distribution of sediments within the modern Whanganui Basin and Cook Strait area with contours of percent sand in the non-gravel fraction. Solid arrows indicate present sediment transport paths and broken arrows indicate transport during the last glacial (adapted from Lewis *et al*, 1994).

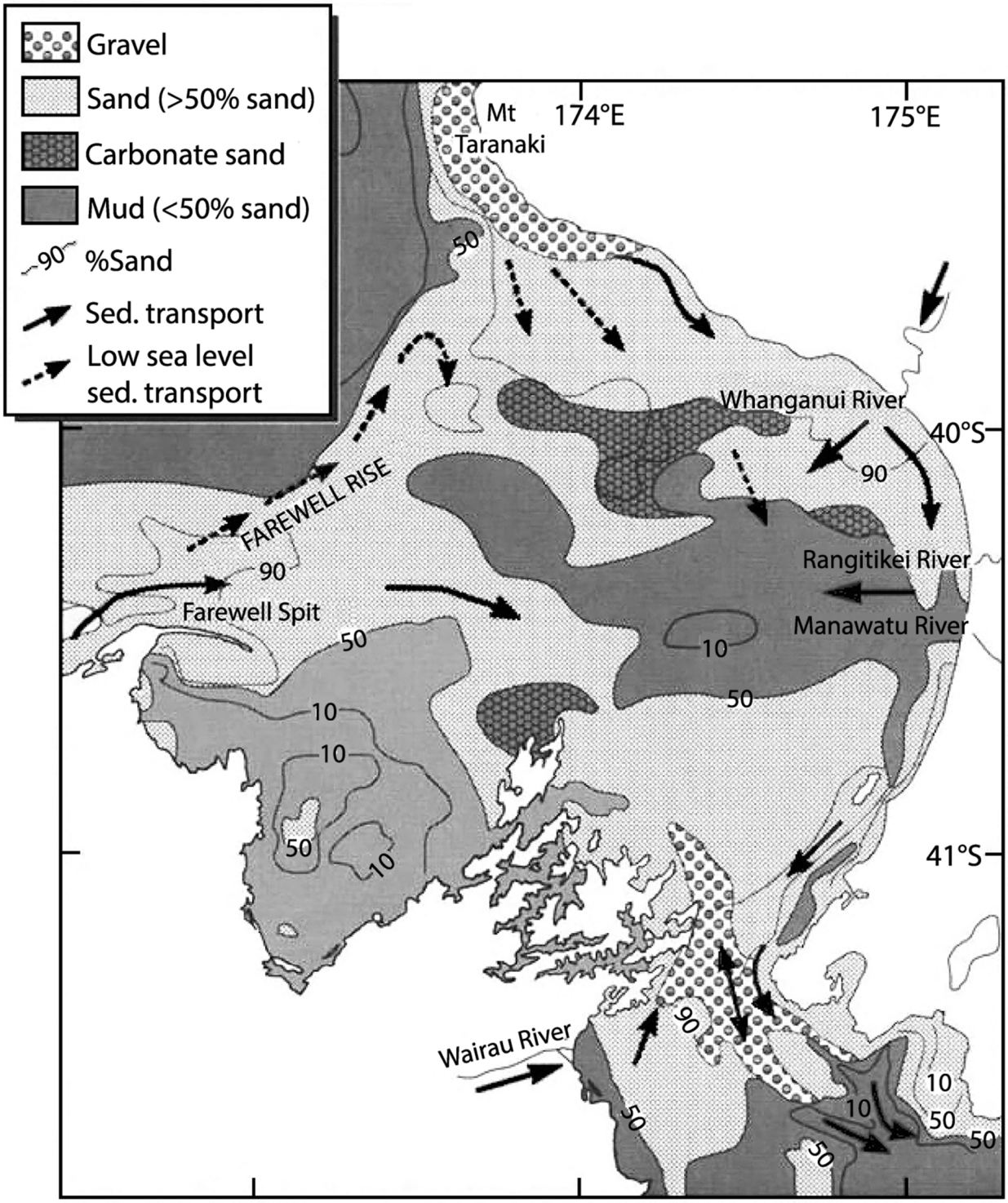

## 6.3 Red, Cross Bedded Sandstone Member

### Lithological Description

Code: Rss

Rock type: Sandstone

Colour: Light reddish brown (5YR 6/4) to pale olive (5Y 6/3), with many light red (2.5YR 6/8) iron oxide mottles present

Hardness: Soft to medium hard (largely due to cementation by iron oxides and calcite), well consolidated

Weathering: Moderately weathered, large amounts of iron oxide rich areas, highly fractured

Grain size: Fine to very coarse sand

Texture: Gritty sandy texture

Crystals/minerals: Calcite, quartz, biotite, titanomagnetite, feldspar, hornblende

Thickness: 47.8 m

Type section: Scrimmys Stream, Broadlands Station, Pohangina (WGS84 40°16'55.62"S, 175°47'07.20"E, elev 137 m). Access via Saddle Rd with express permission of the land holders.

Fossils:

Table 6.4: Fossil assemblages from Rss Member, Konewa Formation

| Family/species | Sample no | |
|---|---|---|
| | FS7 | FS8 |
| *Patro undatus* (Hutton, 1873). | | x |
| *Perna canaliculus* (Gmelin, 1791). | | x |
| *Ostrea chilensis (*Philippi, 1844). | | x |
| *Maoricrypta costata* (Sowerby, 1830). | | x |
| *Talochlamys gemmulata* (Reeve, 1853). | x | |
| *Purpurocardia purpurata* (Deshayes, 1854). | x | |
| *Calloria inconspicua* (Sowerby, 1846). | x | |
| *Struthiolaria papulosa* (Martyn, 1784). | x | |

| | | |
|---|---|---|
| *Tegulorhynchia doederltini* (Davidson, 1886). | x | |

## Biostratigraphy

The occurrence of *Patro undatus* indicates that deposition of Rss Member is not younger than Nukumaruan. While the presence of *Struthiolaria papulosa* (Fig 6.17) indicates that deposition could not have been earlier than the Nukumaruan Stage (Beu & Raine, 2009). Thus deposition of Rss Member, Konewa Formation is constrained to the Nukumaruan Stage.

The appearance of *Talochlamys gemmulata*, *Patro undatus*, *Perna canaliculus*, *Ostrea chilensis*, *Purpurocardia purpurata*, and *Struthiolaria papulosa* are indicative of shallow marine depositional environments. In particular *Ostrea chilensis and Purpurocardia purpurata* are characteristic of high energy shallow water environments such as tidal channels (Beu & Raine, 2009). This interpretation fits with the widespread occurrence of crossbedding and shell hash within Rss Member, indicating wave action within a shallow water environment which has broken up many of the more fragile shells and re-deposited a concentrated shell bed.

The occurrence of small <1 mm in diameter clasts of greywacke and a high concentration of *Talochlamys gemmulata* indicates a source of bedrock was delievering sediment to the coast. *Talochlamys gemmulata* is a common fossil within the biostratigraphic record, which attaches to hard substrates (canyon walls, worm tubes, boulders, other shells) from not far below low tide to the upper bathyal zone (Beu & Raine, 2009). The presence of terrigenous clasts within the shallow marine environment allowed colonisation within areas of the sea floor by *Patro undatus*, *Perna canaliculus*, *Ostrea chilensis*, and *Talochlamys gemmulata*.

Shells of rock colonising species were subsequently washed up and incoroporated with sand dwelling fauna shells such as *Purpurocardia purpurata*, and *Struthiolaria papulosa* within a nearshore environment. Thus several faunal zones have been incorporated into the one condensed shell bed deposit.

*Maoricrypta costata* is a warm water migrant from the northeastern North Island (Beu, *et al*, 2004). Its presence within Rss Member is suggestive of a warming climate. This is interpreted to provide further evidence for Rss Member being deposited during a transgressive systems tract. Within the stratigraphy of Rss Member (Fig 6.19) a general depositional trend is recognised, in which a gradual increase in water depth is identified up section. This trend which is characteristic of a transgressive tract is seen through changes in lithology and sedimentary structures.

It is possible that warm water migrant fauna such as *Maoricrypta costata* were transported into the southern Whanganui Basin via the Ruataniwha and Manawatu Straits in Nukumaruan time. Larvae of these species may have been transported from northern North Island areas south down the Ruataniwha Strait and subsequently through the Manawatu Strait and onto the Whanganui shelf. During warm interglacials (HST) the climate would have been suitable for these larvae to survive.

Fig 6.16 : Depth ranges of selected mollusc taxa present within Rss Member (Powell, 1979; Morley, & Hayward, 1999; Beu & Maxwell, 1990; McIntyre, 2002; Morley & Hayward, 2007).

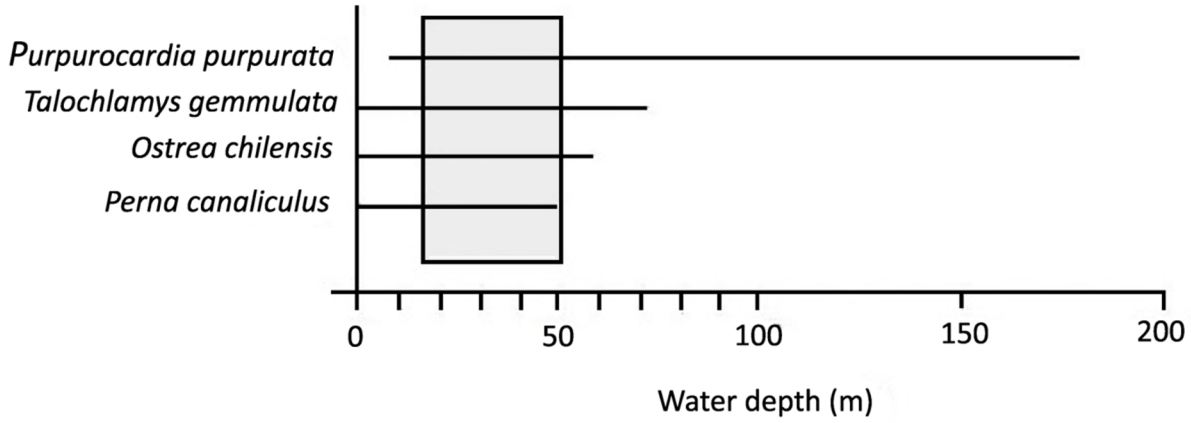


Fig 6.17: *Struthiolaria papulosa* from Rss Member, Konewa Formation, Stallion Stream, Broadlands Station, Pohangina Valley (WGS84 40°16'28.16"S, 175°48'04.51"E, elev 121 m).

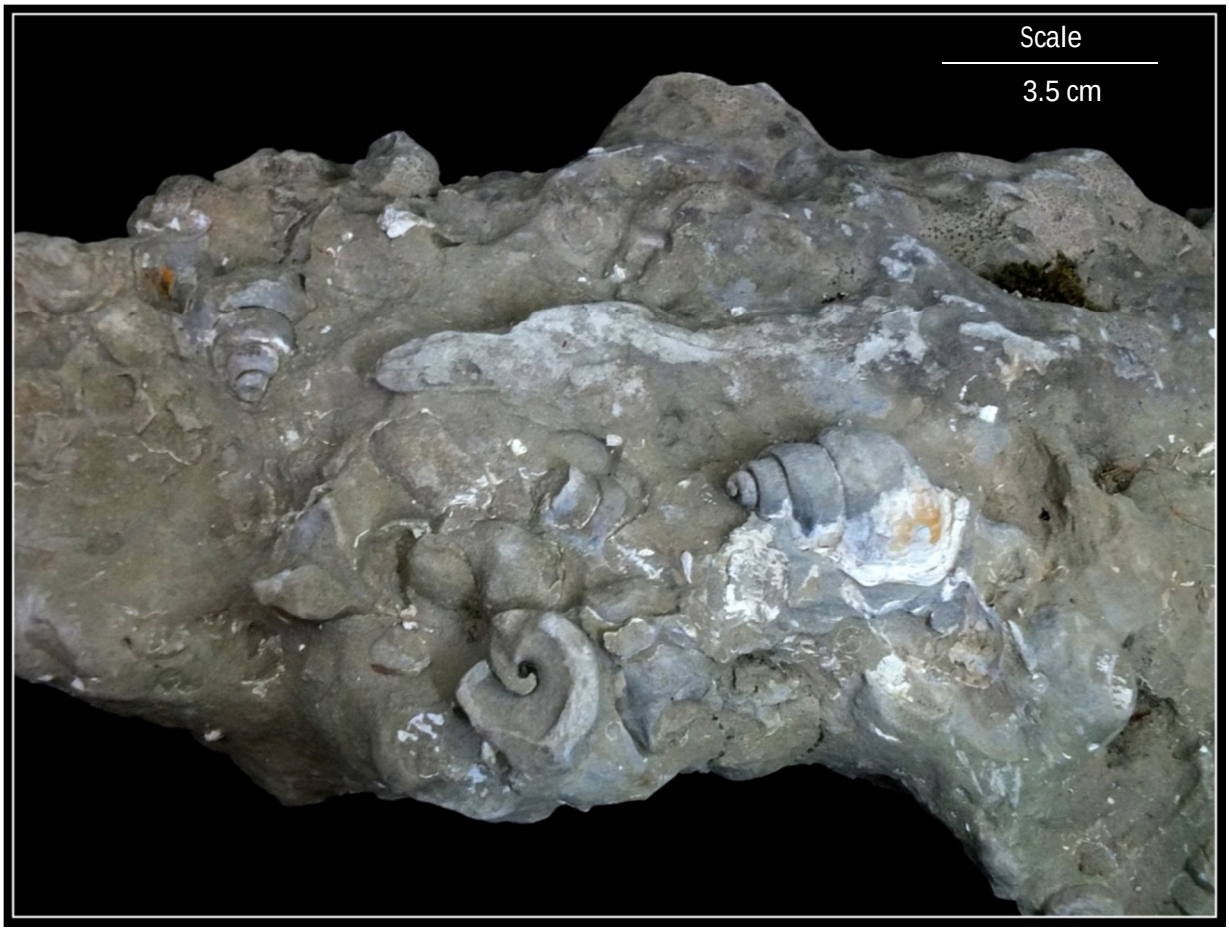

The water depth range obtained from a selection of mollusca in Rss Member shows an approximate depth of 15 – 50 m (Fig 6.16). A minimum water depth of 1 m is inferred from the occurrence of the very shallow water dwelling species *Perna canaliculus and Ostrea chilensis.* A maximum water depth of 50 m is estimated based on the overlap of *Perna canaliculus* with deep water dwelling species *Purpurocardia purpurata and talochlamys gemmulata.* Shallow water dwelling species such as *Ostrea chilensis* and *Perna canaliculus* have likely been transported from a nearby rocky habbitat and re-deposited within a nearshore marine environment. This shell bed contains fauna which represent several ecological zones.

FS7 was collected from a thin shellbed near the contact between Rss Member and Kss Member. This fossil sample contains reworked fossils and displays rip up clasts of mud from the underlying member. The faunal assemblage is indicative of a shelf environment e.g. *Talochlamys gemmulata* and *Purpurocardia purpurata*, which is interpreted to be a result of reworking of the underlying member.

FS8 is collected from the upper part of Rss Member, where cross beds of lime cemented sand occur. The fossil assemblage is characteristic of a high energy, near-shore environment. Rocky outcrops are likely to have been present within this near-shore environment providing suitable substrate for *Patro undatus, Perna canaliculus* and *Ostrea chilensis* to colonise.

### 6.3.1 Facies analysis of Rss Member, Konewa Formation, Stratigraphic log 6.2.

A 26 m exposure located at the type section of Rss Member in Scrimmys Stream was selected for detailed facies analysis. The sequence examined is characterised by fine grained lenticular bedded sand within mud, with minor beds of cross bedded coarse grained fossiliferous sandstone. Facies Sh also occurs in Fss Member, Komako Formation (Fig 5.10) where it is fully described within section 5.3.1, and is therefore not repeated in the facies descriptions below.

Facies Es; laminated mud and sandstone facies

This facies is characterised by fine grained mud with occasional beds of fossiliferous, coarse sand. Beds range in thickness from 2 – 8 m. Rip up clasts of both mud and sand are common throughout. Lenticular beds of alternating sand and mud occur, with the sand

Fig 6.18: Rss Member above Kst Member, Konewa Formation, Scrimmys Stream, Broadlands Station, Pohangina Valley (WGS84 40 °16'48.32"S, 175 °47'15.10"E, elev 137 m).


becoming both less dominant and finer up section. The lower contact is erosional, characterised by rip up clasts of coarse sand.

*Interpretation:*

Facies Es is interpreted as being deposited within a wave dominated estuary. Alternating lenticular beds of mud and sand are characteristic of intervening periods of strong current activity and relative quiescence. During periods of strong current activity (ingoing and outgoing tides) transportation and deposition of coarse sand with occasional shell fragments occurs, while during relatively quiescent periods fine grained muds are deposited. The presence of rip up clasts is interpreted to represent wave action on the soft bottom of the estuary, where wind generated waves erode clasts from the underlying sediment.

Fig 6.19: Stratigraphic log of Rss Member, Konewa Formation, Scrimmys Stream, Broadlands Station, Pohangina Valley, (WGS84 40 °16'50.47"S, 175 °46'46.25"E, elev 98 m).

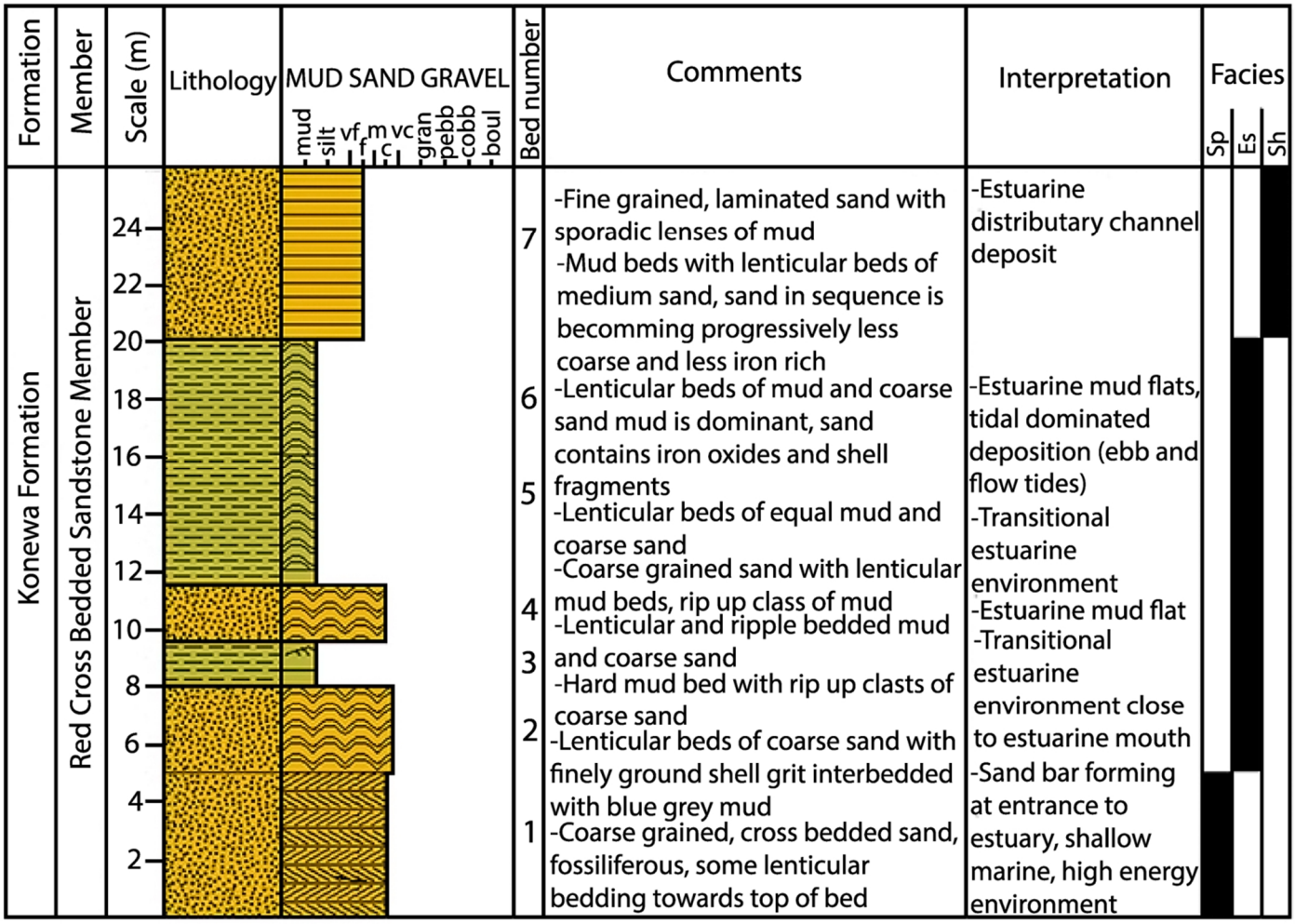


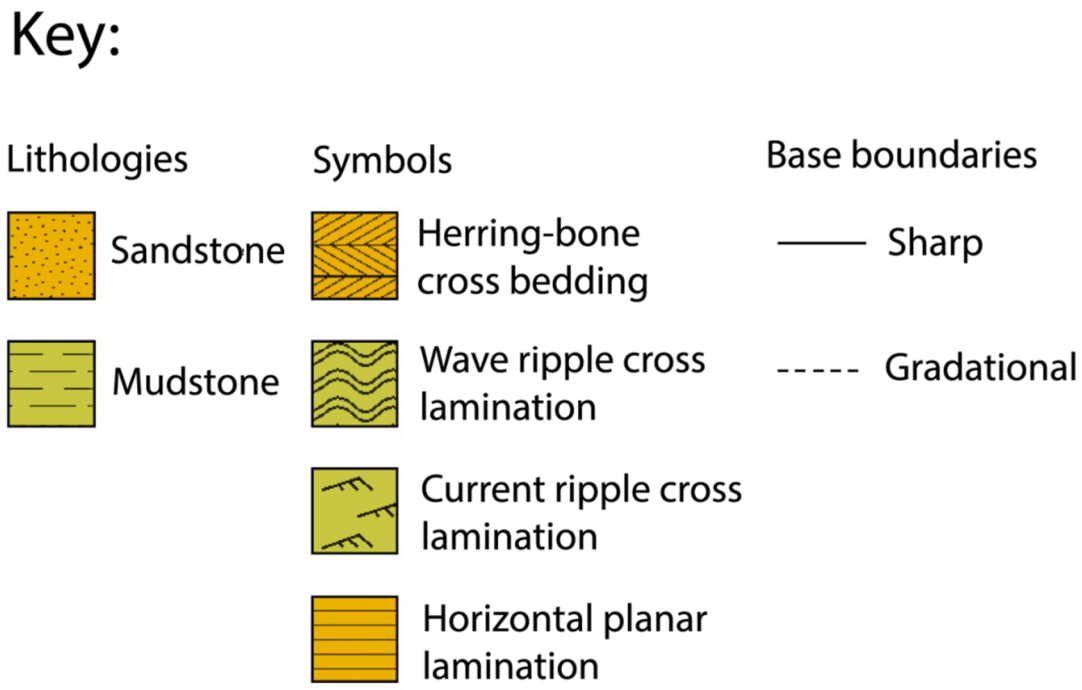

Facies Sp; cross bedded pumiceous sandstone facies

This facies is composed of coarse grained cross-bedded sandstone with minor lenticular beds of alternating sand and mud. Herringbone crossbed sets are typically 500 mm thick while lenticular beds are 45 mm thick. The lower contact is sharp and discontinuous.

*Interpretation:*

Facies Sp represents a migrating estuarine channel sand bar. The sand bar was likely located near the seaward end of the estuary, where suspended sediment concentrations are low. Herringbone cross bedding is interpreted to represent two opposing current directions most likely incoming and outgoing tides. Shell fragments and coarse sands become concentrated by both wave action and tidal flow.

Table 6.5: Lithofacies of Rss Member, Konewa Formation; (Stratgraphic log of Rss Member Fig 6.19). Facies codes are modified from Horton & Schmitt (1996). Miall (1977), Limarino *et al*, (2002).

| Facies code | Description | Depositional processes | Environment |
|---|---|---|---|
| Sp | Very fine- to coarse-grained sandstone:<br>no grading, cross bedding | Wave action, traction current, tidal deposition | Migrating bar at estuarine mouth |
| Es | Alternating mud and sands, laminated to lenticular bedding | Tidal deposition, ebb and flow tide, wave action | Wave dominated estuarine mud flat |
| Sh | Fine grained laminated sands intercalated with mud lenses | Planar bed flow, tidal dominated deposition | estuarine distributary channel |

## Interpretation

Rss Member unconformably overlies Kst Member and unconformably underlies Kss Member. The lower contact with Kst Member (Fig 6.18) is sharp and erosional with rip up clasts of silt found in the first 2 m of Rss Member. In Scrimmys Stream the base of Rss Member contains greywacke pebbles (up to 10 mm in diameter) and disarticulated bivalves lying concave down. Rss Member is interpreted as a shallow marine to estuarine sandstone rich in shell fragments. Calcite cemented layers are present throughout the unit up to 150

mm thick. These calcite cemented layers form trough cross bedding sets 300 mm to 500 mm thick. Fossils are common although they are generally highly fragmented.

Significant lateral variation is observed within this member. To the south near Saddle Road, Rss Member becomes more calcareous and contains a higher abundance of fossils. Within this area Rss Member approximates a limestone due to the concentration of lime cement. However, this lateral variation represents a small proportion of the member. Therefore it has been decided to catergorise Rss Member as sandstone.

When looking at the distribution of Rss Member, it is observed that this member has a close relationship with the Manawatu Saddle area. It is interpreted that Rss Member was formed in a shallow, high energy, marine to transitional environments on the western end of the Manawatu Strait. The depositional environments were confined to the Manawatu Strait so that only localised areas of Rss Member were deposited and preserved. To the north rapid thinning of the member occurs, a pattern observed in a majority of Mangapanian - Nukmaruan sediments of the Pohangina Valley.

Rss Member has formed under wave action and strong tidal current, which have resulted in the concentration of coarse sand and shell fragments in a near shore environment. The calcite cemented layers are interpreted to have formed post-deposition as a function of secondary mineralisation during diagenesis. Post depositional calcite rich fluids percolated through the rock and subsequently precipitated concentrating calcite into thin localised areas.

The initial phase of deposition within Rss Member is characterised by a transitional to estuarine sequence with lenticular bedded muds and fine grained sands. This phase of deposition grades into shallow marine deposition of coarse sand and shell fragments, forming highly calcite cemented, fossiliferous, cross beds of coarse sandstone.

Overall Rss Member represents a marine regression and coastal progradation during the last part of a HST and into the following RST. Parts of Rss Member are calcareous cemented almost becoming a limestone in areas; however, the cementation is too localised to classify Rss Member as a limestone.

## 6.4 Marine Sandstone Member

### Lithological description

Code: Kss
Rock type: Sandstone

Colour: Light yellowish brown (10YR 6/4), with many light red (2.5YR 6/8) mottles of iron oxide present.

Hardness: Soft, moderately consolidated (largely due to cementation by iron oxides).

Weathering: Moderately weathered, large amounts of iron oxide rich areas

Grain size: Fine to very coarse sand

Texture: Gritty sandy texture

Crystals/minerals: Calcite, quartz, biotite, titanomagnetite, feldspar, hornblende

Thickness: 97 m

Type section: Scrimmys Stream, Broadlands Station, Pohangina (WGS84 40°16'46.06"S, 175°46'35.37"E, elev 89 m). Access via Awahou South Rd with express permission of the land holders

Fossils:

Table 6.6: Fossil assemblages from Kss Member, Konewa Formation

| Family/species | Sample no | |
|---|---|---|
| | FS5 | FS6 |
| *Perna canaliculus* (Gmelin, 1791). | x | |
| *Patro undatus* (Hutton, 1873). | x | |
| *Talochlamys gemmulata* (Reeve, 1853). | x | x |
| *Alcithoe fusus* (Quoy & Gaimard, 1833). | | x |
| *Amalda novaezelandiae* (Sowerby, 1859). | | x |
| *Calloria inconspicua* (Sowerby, 1846). | | x |
| *Purpurocardia purpurata* (Deshayes, 1854). | | x |

## Biostratigraphy

The occurrence of *Patro undatus* indicates that the deposition of Kss Member was not younger than the Nukumaruan Stage. *Alcithoe fusus* first appears within the biostratigraphic record around Nukumaruan time, therefore indicating that deposition can not have taken place before Nukumaruan time.

The fossil assemblage within Kss Member is dominated by fauna characteristic of nearshore shallow marine environments e.g. *Talochlamys gemmulata*, *Patro undatus*, *Perna canaliculus*, and *Purpurocardia purpurata*. The occurrence of *Alcithoe fusus*, *Amalda novaezelandiae* represents a different ecological zone within the shallow marine depositional setting. *Alcithoe fusus* and *Amalda novaezelandiae* are characteristic of a soft bottom shelf setting. Their presence within the fossil assemblage is attributed to the transportation of their shells into shallow water, nearshore environments during storm events in which the mean wave base is lowered and strong currents allowed reworking of the sea floor. These species, post mortum, are also common washed up on beaches.

Fig 6.20: Depth ranges of selected mollusc taxa present within Kss Member (Powell, 1979; Morley, & Hayward, 1999; Beu & Maxwell, 1990; McIntyre, 2002; Morley & Hayward, 2007).

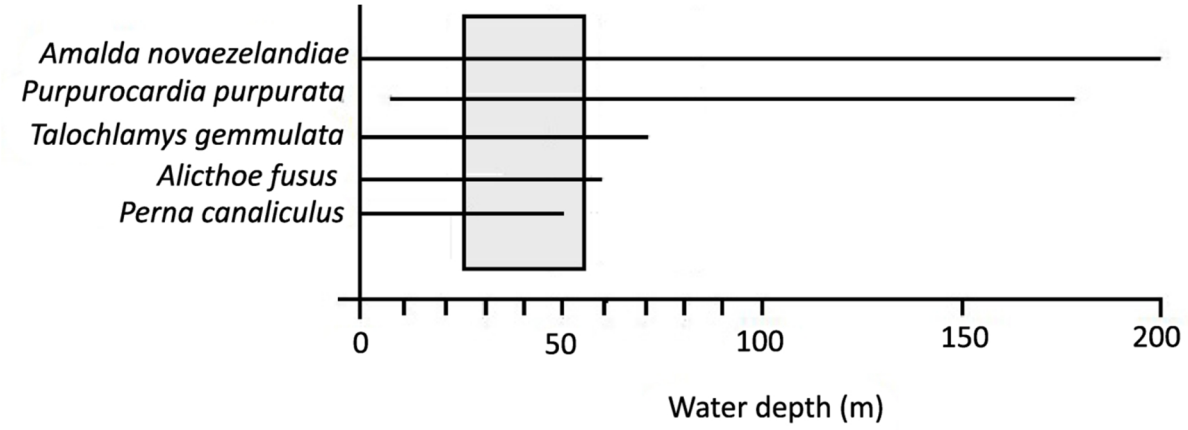


The water depth range obtained from fossils present within Kss Member is approximately 25 – 55 m (Fig 6.20). A minimum water depth of 1 m is estimated, given the occurrence of the shallow water dwelling *Perna canaliculus*. A maximum water depth of 55 m is estimated by using the overlap of shallow water species *Perna canaliculus* with the shelf dwelling *Amalda novaezelandia* and *Alicthoe fusus* (Beu & Maxwell, 1990).

This fits with the dominance of species within the fossil assemblage which dwell on sandy soft substrates e.g. *Alcithoe fusus*, *Amalda novaezelandiae*, *Calloria inconspicua*, and *Purpurocardia purpurata*. A few species within Kss are associated with a more rocky shallow water environment e.g. *Perna canaliculus*. It is likely that these species have been

transported from a rocky shallow water outcrop into the sandy shoreface to offshore transitional zone post-mortem.

### 6.4.1 Ichnofossils

Many large *Ophiomorpha* burrows up to 150 mm long and 50 mm wide are present within the Kss Member (Fig 6.21 A). Smaller tracks and burrows (up to a maximum size of 50 mm long and 10 mm wide) are also present.

In siliciclastic settings, the orientation and overall configuration of *Ophiomorpha* burrows can be used as an indicator of depositional environments (Frey & Mayou, 1971). *Ophiomorpha* burrows which display predominantly vertical elements suggest high energy environments i.e. near-shore environments. *Ophiomorpha* with oblique to horizontal burrows are characteristic of lower energy environments i.e. deep water shelf to abyssal plain environments (Fig 21 B).

Fig 6.21: Bioturbation; A: large oblique *Ophiomorpha* burrow with many smaller burrows. B: White pockmarks are burrows cut face on by the outcrop, oblique burrows are filled with lighter coloured fine, calcareous, silts and mud which contrast with the speckled appearance of the coarse sand, Kss Member, Konewa Formation, Scrimmys Stream, Broadlands Station, Pohangina Valley. (WGS84 40 °16'50.47"S, 175 °46'46.25"E, elev 98 m


## 6.4.2 Facies analysis of Kss Member, Konewa Formation

Kss Member unconformably overlies Rss Member and unconformably underlies Cq Member. Both the lower and upper boundaries of the Kss Member are sharp erosional contacts. A 28 m exposure located at the type section of Kss Member in Scrimmys Stream was selected for detailed facies analysis. The sequence examined is characterised by coarse grained, laminated to cross laminated sandstone with common bioturbation. One of the four facies analysed within the stratigraphic log of Kss Member (Facies Clm, Fig 22) also appears in the stratigraphic log of Cg Member (Fig 6.3). Facies Clm is described in detail in section 6.1.1 and is therefore not included in the facies descriptions below.

Facies Sr; Coarse grained Sandstone, cross laminated, bioturbated
Facies Sr is characterised by coarse grained sandstone displaying laminated to cross laminated sedimentary structures. This facies is intensely bioturbated in places with *Ophiomorpha* burrows of up to 150 mm long. The burrows and tracks from marine organisms are filled with finer silts and clays cemented together by calcite. Burrows are mainly sub-vertical commonly on an angle of up to 45°. Beds are 1.5 – 9 m thick with the amount of bioturbation increasing up section. Occasional 300 mm lenses of calcite cemented sand occur within the upper part of Facies Sr.

*Interpretation:*

Facies Sr is interpreted as softground within the offshore transitional zone. High energy wave environment results in the coarse grained sandstone while finer silts and clays are winnowed out and transported into deeper marine environments. Organisms have colonised the sea floor, burrowing into the soft sandy sediment using faecal pellets to stabilise tunnel and burrow walls. This results in micrite contributing to the filling of the tunnel and burrows, creating a contrast to the coarse sand. Most sedimentary structures (e.g. laminae) have been destroyed by intense bioturbation. Some cross laminae are present, deomonstrating that upper flow regime conditions occured in the environment.

Fig 6.22: Stratigraphic log of Kss Member, Konewa Formation, Scrimmys Stream, Broadlands Station, Pohangina Valley (WGS84 40 °16'50.47"S, 175 °46'46.25"E, elev 98 m).

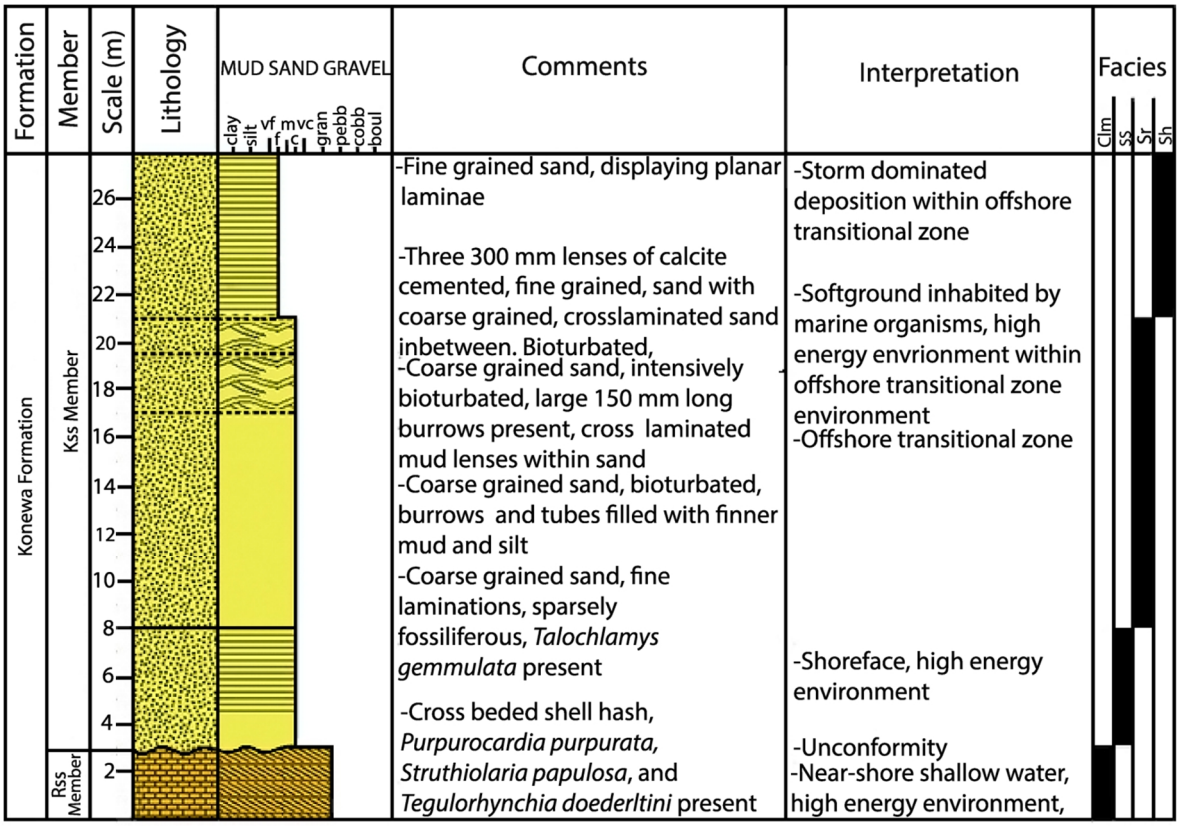


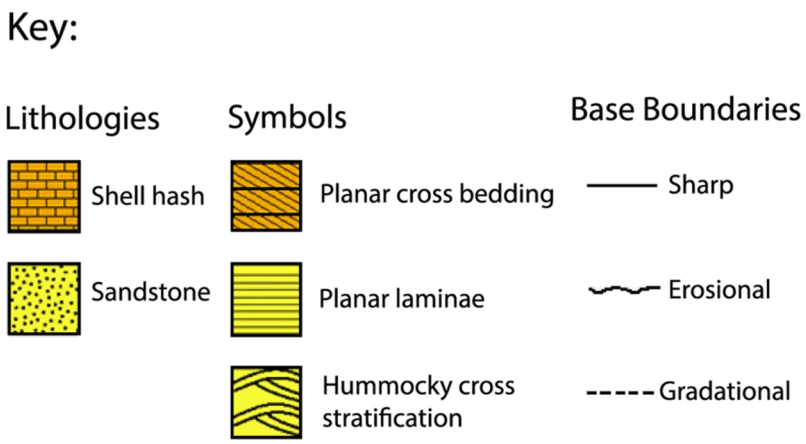

Table 6.7: Lithofacies of Kss Member, Konewa Formation; (Stratigraphic log of Kss Member, Fig 6.22). Facies codes are modified from Horton & Schmitt (1996). Miall (1977), Limarino *et al*, (2002).

| Facies code | Description | Depositional processes | Environment |
|---|---|---|---|
| Clm | Massive or laminated carbonate; stromatolitic hemispheroid laminations, secondary ooids and pisoids, coarse sand – pebble lenses | Carbonate precipitation and binding of calcareous sediment by algal mats | Sediment starved shoreface |
| Ss | Fine grained sandstone, laminated/ rippled | tidal deposition, wave action | Siliciclastic lower shoreface environment, |
| Sr | Coarse grained sandstone, cross laminated, bioturbated | Tidal deposition, wave action, bioturbation | Softground within offshore transitional zone |
| Sh | Fine grained laminated sandstone | Storm activity, traction current | Offshore transitional zone |

## 6.5 Coquina Limestone Member

### Lithological description

Code: Cq

Rock type: Coquina limestone

Colour: Brownish yellow (10YR 6/8)

Hardness: Moderately hard

Weathering: Highly weathered, however more resistant to erosion than other sandy mudstone/ sandstone lithologies due to the concentration of shell material and calcite cementation. This member often forms a conspicuous ridge line in the landscape.

Grain size: Coarse sand with sporadic pebble clasts, many crushed shells with some preserved whole.

Texture: Coarse, gritty texture

Crystals/ minerals: Calcite, Mica, Feldspar, Quartz

Thickness: 10 m

Type section: Scrimmys Stream, Broadlands Station, Pohangina (WGS84 40 °16'50.47"S, 175 °46'46.25"E, elev 98). Access via Awahou South Rd with express permission of the land holders.

Fossils:

| Table 6.8: Fossil assemblage from Cq Member, Konewa Formation | |
|---|---|
| Family/species | Sample no |
| | FS4 |
| *Ostrea chilensis* (Philippi, 1844). | x |
| *Talochlamys gemmulata* (Reeve, 1853). | x |
| *Patro undatus* (Hutton, 1873). | x |
| *Calloria inconspicua* (Sowerby, 1846). | x |
| *Purpurocardia purpurata* (Deshayes, 1854). | x |
| *Talabrica senecta* (Powell, 1931). | x |

## Biostratigraphy

The occurrence of both *Patro undatus* and *Talabrica senecta* indicate that the deposition of Cq Member cannot have been later than Nukumaruan. Other fossils preserved within Cq Member do not provide a precise maximum age, as they all occur in pre- Nukumaruan stages. Given its stratigraphic position and minimum age of Nukumaruan, Cq Member is interpreted as a Mid to Late Nukumaruan deposit.

All the fossils within the assemblage are characteristic of shallow marine envionments. The occurrence of species which grow on rocky substrates (*Ostrea chilensis*, *Talochlamys gemmulata*, *Patro undatus)* and species which prefer soft bottom, nearshore environments such as *Calloria inconspicua*, *Purpurocardia purpurata and Talabrica senecta* demonstrate two distinct ecological zones existed within the depositional setting.

The concentration of shells and other bioclastic material from these two ecological zones into a nearshore environment via wave action has resulted in the formation of a coquina limestone composed of mainly of shell fragments cemented together in a calcite matrix. This coquina limestone has many similarities to both the Piripiri Limestone of Carter (1972) and the Nukumaruan Limestone described by Fleming (1953) from the Whanganui Subdivision. Both authors note that shells from several sub-environments have become concentrated by

tidal scour in channels and wave action into condensed shell beds to form coquina limestone. The high percentage of broken shell hash which composes the matrix of the limestone is representative of strong current and wave sorting of the shellbeds prior to burial.

## Interpretation

Overall Cq Member is characterised by concentrated, clast-supported shellbeds. Shells are preserved both whole and broken, with a matrix composed of 30% shell grit and 70% coarse sand. Approximately 60% of the shells are broken into fragments while 40% are preserved whole. It is interpreted that the Cq Member was subjected to high energy wave action where winnowing out of the finer material resulted in a concentration of crushed shells and coarse sand within the matrix. Wave action also resulted in the abrasion and fragmentation of shells in a nearshore environment as the sediments were constantly reworked during deposition.

Tidal indicators include 300 mm to 1 m thick tabular cross bed sets, which show opposing current directions. Shells within this member are in part abraded and dominanted by molluscan taxa characteristic of nearshore shallow marine environments e.g. *Ostrea chilensis, Talochlamys gemmulata, Patro undatus, Purpurocardia purpurata, Talabrica senecta.*

The sharp base of the Cq Member suggests this deposit was formed via hydraulic concentration in a shallow marine environment. Shells display an inclined orientation which changes in attitude between cross beds. This suggests deposition under a unidirectional current (Kidwell & Bosence, 1991). Some shells are unbroken and well preserved, suggesting relatively rapid deposition (high sedimentation rate) with only moderate lateral transportation and reworking of the shells.

Cq Member is interpreted to have formed within shallow, current swept, shoal areas of the western Manawatu Strait, at water depths of 5 to 30 m (Fig 6.24). The shell concentration was likely built up over many individual events that deposited, winnowed and reworked the bio-clastic sediment. The coarse sand matrix is characteristic of a near shore environment where wave energy has concentrated the bio-clastic material and coarse sands while winnowing away finer sediments, transporting them into deeper water environments.

The coquina limestone was likely formed under the influence of storm events, in which the shells became reoriented, and concentrated while the finer matrix was progressively

removed. This concentration of bio-clastic and coarse sand material likely preserved the more robust fauna within the near-shore environment, while fauna with more delicate shells were crushed and incorporated into the matrix.

Fig 6.23: A: Cq Member in Scrimmys Stream. B: close up of the Cq Member showing the fossils *Talochlamys gemmulata* and *Ostrea chilensis*. Broadlands Station, Pohangina Valley (WGS84 40 °16'50.47"S, 175 °46'46.25"E, elev 98 m).


Fig 6.24: Environments of deposition within the northwestern Manawatu Strait during Late Nukumauan time. Note the formation of coquina limestone on shoal areas where siliciclastic by-pass allows accumulation and concentration of biogenic sediment. Uplift manifested along the North Island Dextral Fault Belt has propagated North to South regionally, and east to west in the vicinity of the Manawatu Strait. This pattern of regional and localised uplift has forced the depocentre of the Manawatu Strait westwards as the older Waipipian – Earliest Nukumaruan sediments begin to be uplifted to the east and eroded providing a source of siliciclastic sediment to the shallowing Manawatu Strait (after Caron *et al*, 2004).

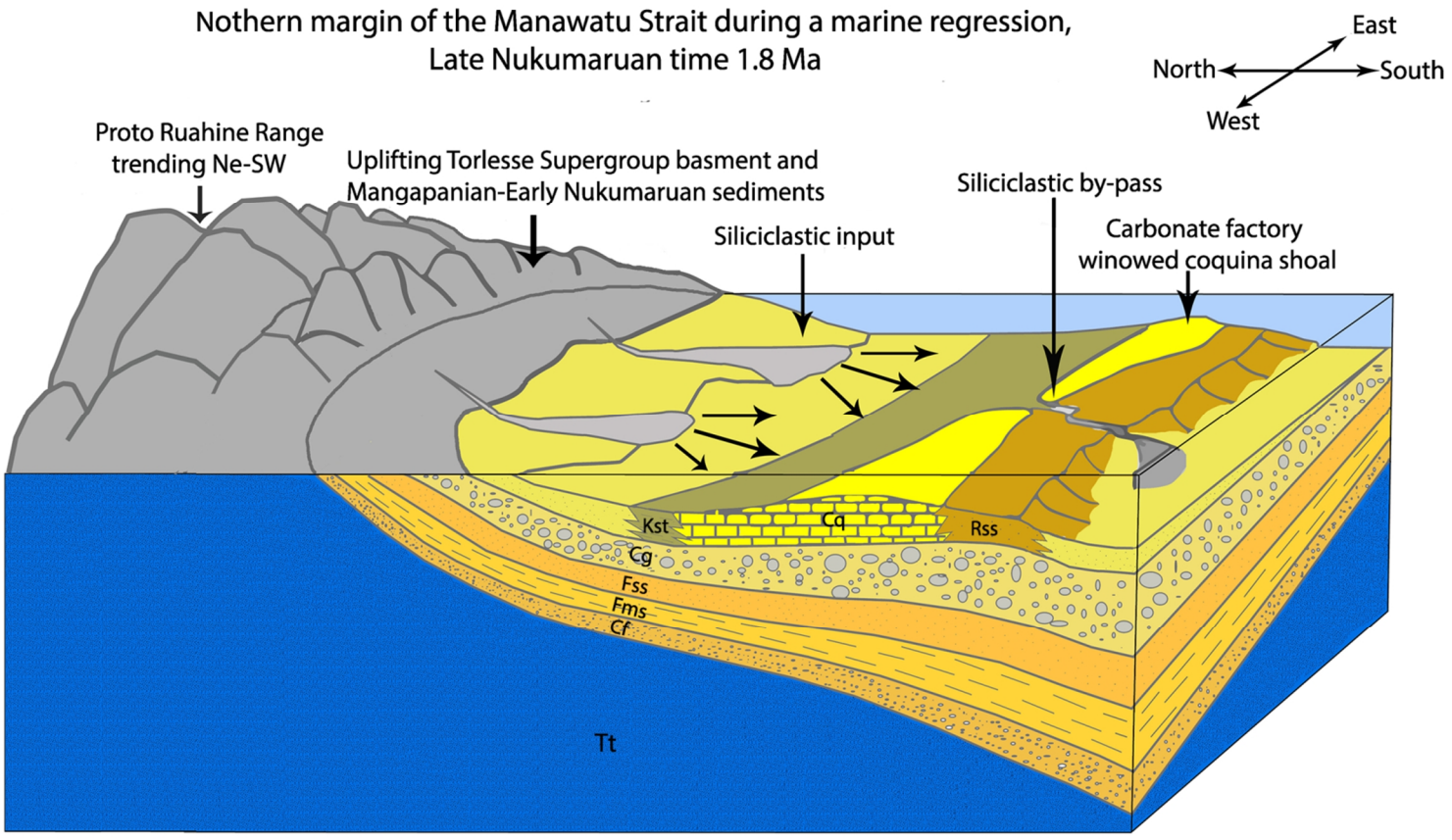

# Chapter 7
# Takapari Formation

The Takapari Formation was defined by Carter (1972) as dominantly non-marine pumiceous sands and coarse greywacke conglomerate, unconformably overlying Konewa Formation. This formation is considered to be a correlative of the Mangatarata Formation mapped in the Hawkes Bay Region (Lillie, 1953; Fleming, 1953). Other lithologies present within the formation are lignite, carbonaceous mudstone, and blue grey siltstone. The name is derived from Takapari Road, five miles north of Komako where Carter (1972) based his field work.

A Mid-Late Pleistocene age (Castlecliffian Stage) was assigned to the Mangatarata Formation (Lillie 1953) and to equivalent strata in central Hawke's Bay (Kingma, 1971) mainly on the basis of stratigraphic position and the first significant appearance of pumice in the sediments, which is considered to be indicative of the Castlecliffian. Carter (1972) and Neef (1984) considered the lower parts of the Takapari and Mangahao formations, respectively, could be, at least partly, Late Nukumaruan. Carter correlated the age of the formation to be of Late Nukumaruan, through to Castlecliffian in age.

The Takapari Formation has been correlated to the Late Nukumaruan and Early Castlecliffian sediments mapped during this study in the Lower Pohangina Valley. The formation has been split into two end members based on changes in lithology, sedimentary structures and biostratigraphy. These members include in order from oldest to youngest: Bms Member (blue grey sandy mudstone with lignite and tephra) and Css Member (cross bedded sandstone with lignite, tephra and tuff).

Carter (1972) set the base of the formation at a thick bed of massive medium-grained light-brown sand in Makawakawa Stream (Komako District, Pohangina) and left the top of the formation undefined. The base of the Takapari Formation within this study has been set at the contact between Cq Member (Konewa Formation) and base of Bms Member (Takapari Formation). The base of the Takapari Formation set in this study is tentatively correlated with Carter's (1972) stratigraphy, where the first thick mudstone sequence with common lignite begins following the more dominantly sandy Konewa Formation with common conquina limestone.

The new definition for the top of the Takapari Formation proposed in this study is set at the first occurrence of Potaka Pumice (1 Ma). It is also proposed that above the Potaka Pumice, Whanganui Basin stratigraphic nomenclature should be used based on the wide spread, and distinctive pumice, which allows basin wide correlation. Takapari Formation is able to be correlated across the eastern part of the Whanganui Basin via the Pakihikura and Mangapipi tephras, however beyond the Pahikura Tephra (1.58 Ma) correlation is limited to relative

dating provided by biostratigraphy. For this reason the biostratigraphic and lithostratigraphic work set out by Carter (1972) in his definitions of the regional formations of the Pohangina area will be used for all Plio-Pleistocene strata older than 1 Ma.

The Takapari Formation is characterised by mainly terrestrial deposition. Fluvial/estuarine depositional environments dominate within this formation with only a minor component of shallow marine deposition present within Bms Member. There is a marked angular unconformity between the Takapari and Recent formations. Many sections of Takapari Formation are unconformably overlain by late Pleistocene-Recent alluvial terrace conglomerate e.g. Ohakean Gravels (15-30 ka).

## 7.1 Blue Grey Sandy Mudstone Member

### Lithological description

Code: Bms

Rock type: Sandy mudstone

Colour: Grey (7.5YR N6/0), with some fine black (10YR 2/1) grains

Hardness: Soft, Moderately consolidated

Weathering: Moderately weathered, reduced conditions have contributed to blue grey colour, highly fractured prone to exfoliation in dry areas.

Grain size: Fine sand, silt and clay. Rare shell grit layers present.

Texture: Silty texture.

Crystals/ minerals: Titanomagnetite, feldspar, mica, quartz, calcite

Thickness: 73 m

Type section: Scrimmys Stream, Broadlands Station, Pohangina (WGS84 40°16’46.17”, 175°46’35.25”E, elev 89 m). Access via Awahou South Rd with express permission of the land holders.

Fossils:

| Table 7.1: Fossil assemblages from Bms Member, Takapari Formation | | |
|---|---|---|
| Family/species | Sample no | |
| | FS2 | FS3 |
| *Amalda mucronata* (Sowerby, 1830). | x | |
| *Talochlamys gemmulata* (Reeve, 1853). | x | |
| *Stiracolpus symmetricus* (Hutton, 1873). | x | |
| *Ostrea chilensis (*Philippi, 1844). | x | |
| *Austrovenus stutchburyi* (Wood, 1828). | | x |

## Biostratigraphy

The fossil assemblages within Bms Member are not indicative of a specific age range. The precence of *Stiracolpus symmetricus* indicates that Bms Member cannot be older than Nukumaruan. Many of the species including *Austrovenus stutchburyi*, *Talochlamys gemmulata*, *Stiracolpus symmetricus*, *Ostrea chilensis* and *Amalda mucronata*, are found in Recent deposits in New Zealand and therefore do not provide a minimum age of deposition.

The basal part of Bms Member contains common (<300 mm thick) shells beds which contain a varritey of marine fossil fauna. Fossil fauna within the basal shell beds include *Amalda mucronata*, *Talochlamys gemmulata*, *Stiracolpus symmetricus*, *and Ostrea chilensis*. *Amalda mucronata* is characteristic of an inner to mid shelf environment while *Talochlamys gemmulata*, *Stiracolpus symmetricus*, *and Ostrea chilensis* are more indicative of shallow marine environments. *Ostrea chilensis* in particular is characteristic of a high energy nearshore environment. It is possible that *Amalda mucronata* has been moved closer to shore via wave and tidal currents and hence is found within an assemblage of fossils more characteristic of nearshore environments.

Fossil depth indicators (Fig 7.1) display an estimated depth range of 25 – 55 m. This depth range is based on the overlap between shallow water dwelling species *Ostrea chilensis* and the inner to mid shelf dwelling *Amalda mucronata* (Beu & Maxwell, 1990).

The middle part of Bms Member is characterised by a change to estuarine deposition. Shell beds become much less common and display much less faunal diversity. The middle part of Bms Member is marked by the occurrence of Mangapipi Tephra (1.51 Ma) and Pakihikura Tephra (1.58 Ma). It is dominated by shellbeds containing the intertidal mollusc *Austrovenus*

*stutchburyi*. This species is found in high concentrations, and along with the occurrence of lignite is indicative of estuarine deposition.

**Fig 7.1:** Depth ranges of selected mollusc taxa present within Bms Member (Powell, 1979; Morley, & Hayward, 1999; Beu & Maxwell, 1990; McIntyre, 2002; Morley & Hayward, 2007).

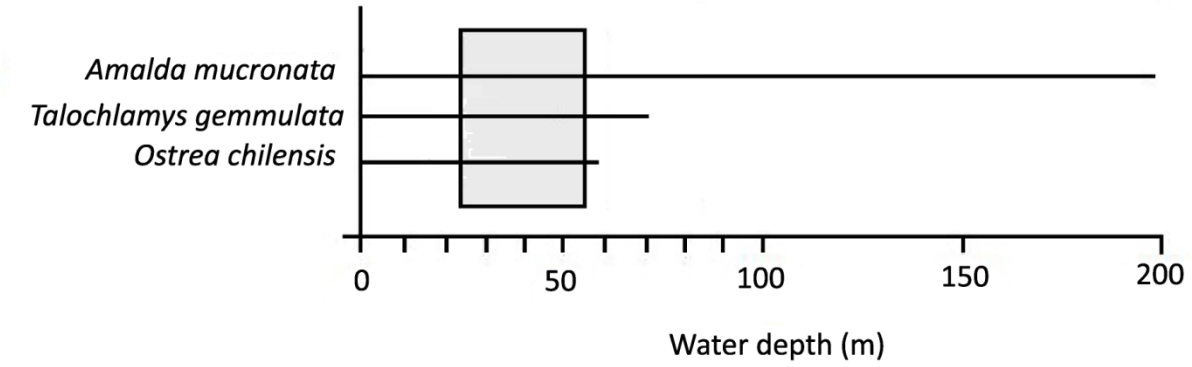


**Fig 7.2:** Part of the fossil assemblage from Bms Member, Takapari Formation; 1: *Austrovenus stutchburyi* (Wood, 1828), 2: *Talochlamys gemmulata* (Reeve, 1853) and *Stiracolpus symmetricus* (Hutton, 1873), 3: *Amalda (Baryspira) mucronata* (Sowerby, 1830).

### 7.1.1 Grain size analysis

The grain size distribution of the Bms (Appendix 2.4) is bimodal. The first population ranges from 0-3 Phi and the second from 4-10 Phi. The first population represents sand grains which have travelled mainly by rolling and saltation. The second finer population from 4-10 Phi has been transported by suspension within the water column. The fine skewed, poorly sorted grain size distribution represents a strong fluvial influence within the depositional environment. This member is interpreted as being deposited within shallow marine to marginal marine (estuarine) environments. The estuarine component of Bms deposition shows that the area had a strong fluvial influence. A paleo-river system delivered high amounts of suspended sediments into the shallow/marginal marine environments.

Within a marine environment fine sediment is winnowed out from coarse sediment and carried in suspension out into greater water depth, before finally settling out of suspension. However in river dominated shelf environments, where a river system is delivering vast quantities of fine suspended sediment out into the marine environment large deposits of shelf mud blankets or coast parallel mud belts may occur (McCave, 1985).

Modern analouges of such fluvial dispersal systems occur within the Amazon, Mississippi and Chang Jiang river systems. Within these sedimentary systems the high concentration of fine grained sediment forms shelf wide mud deposits. Large areas of the modern New Zealand shelf are covered by such deposits (Carter, 1975) (Fig 6.15). Abbott (2000) demonstrates how the modern analogue for the Castlecliff HST is the mid shelf mud depocentre in Taranaki Bight offshore from Whanganui. It is proposed a similar shelf setting occurred in the southeastern Whanganui Basin during the deposition of the Bms Member. Where a large fluvial system entered the Whanganui Basin bringing with it vast quantities of suspended sediment, generating a large mud blanket over the shelf environment. This is responsible for the bimodal fine skewed grain size distribution of the Bms Member. Terrigenous sources of sediment deposited into the Whanganui Basin at this time were from central North Island, elevated basement in the Kaimanawa and Kaweka Ranges, and northern South Island.

## Interpretation

Bms Member unconformably overlies Cq Member, Konewa Formation. Basal Bms Member is typically fine grained, with thin shell beds consisting of a variety of marine fauna. This initial phase is interpreted as inner-most shelf deposition. Shell beds are dominated by *Talochlamys gemmulata* with minor *Ostrea chilensis, Amalda mucronata* and *Stiracolpus symmetricus*. These shell beds are interpreted to represent mid cycle condensed shell beds

during a transgressive system tract, during which crushed shells and nearshore fauna have accumulated within a nearshore environment.

Within the middle of this member a rapid change to estuarine deposition is identified. This change in deposition is characterised by carbonaceous muds, lignite layers, and tephra beds. The occurrence of the Pakihikura (1.58 Ma) gives a lower age constraint to the timing of estuarine deposition while the Mangapipi Tephra (1.51 Ma) provides the upper age constraint. Shell beds occur thoughout this mudstone sequence and are dominated by *Austrovenus stutchburyi*.

Upper Bms Member is characterised by sandy muds with common shell hash beds (>300mm). Shell beds within the upper part of Bms Member are composed of a range of marine dwelling fauna characteristic of an inner-most shelf environment.

Bms Member represents a change in sedimentary environment from inner shelf to estuarine. It is interpreted to be a result of a change from retrogradational to progradation stacking during the last part of the HST, and the following marine regression as sea level begins to fall. The timing of this marine regression is unkown; however, semi-terrestrial conditions are known to have been in place by 1.58 Ma due to the occurrence of the Pakihikura Tephra within carbonaceous muds. Regression of the shoreline farther basinward during this time has allowed an estuarine environment to develop on the lower coastal plain, bordering the SE Whanganui Basin in the Pohangina area. This phase of estuarine deposition was then followed by an erosional surface marking the LST of the cyclothem. Overlying this erosion surface is another marine sequence representing a HST and a return to fully marine conditions.

# 7.2 Cross Bedded Sandstone Member

## Lithological description

**Code:** Css

**Rock type:** Fine to coarse sandstone with intercalated mudstone beds, cross bedded to fine laminations. Large pumice clasts (400+mm) are common.

**Colour:** Yellow (10YR 7/6) to light reddish brown (5YR 6/4) clay, with many light red (2.5YR 6/8) mottles of iron oxide present.

**Hardness:** Weakly consolidated soft sandstone to moderately consolidated mudstone.

**Weathering:** Moderately weathered and fractured, secondary iron oxides, reduced conditions present in mudstone beds.

Grain size: Fine to coarse sand with occasional beds containing larger clasts of pumice and rip up structures of silt present up to 400mm in size. Fine mudstone beds also present.

Texture: Silty mud to gritty sand texture.

Crystals/minerals: Quartz, feldspar, calcite, biotite, hornblende, titanomagnetite.

Thickness: Approximately 77 m

Type section: Maungatukurangi Stream, Broadlands Station, Pohangina (WGS84 40 °14'54.09"S, 175 °47'01.35"E, elev 92 m). Access via Awahou South Rd with express permission of the land holders.

Fossils: *Austrovenus stutchburyi* (Wood, 1828). (From sample no. FS1, see appendix 4)

### 7.2.1 Grain size comparison

The grain size distribution of Css Member has a fine tail (fine skewed) representing deposition within a water column with a high suspended sediment load. It is also poorly sorted. Overall sediment is classed as very fine sand with the highest peak in grain size at 3 Phi. However, the grain size distribution curve continues down to 10 Phi demonstrating a presence of a long tail. The grain size distribution of Css Member is interpreted as displaying a distinctly fluvial signature (Fig 7.3, Appendix 2.3). The fluvial environment was characterised by high suspended sediment loads, resulting in a fine tail and poorly sorted grain size distribution.

Fig 7.3: Grain size distributions of Takapari Formation and Kaimatira Pumice Sand Formation. Note the fine tail and poor sorting on the fluvially deposited Takapari

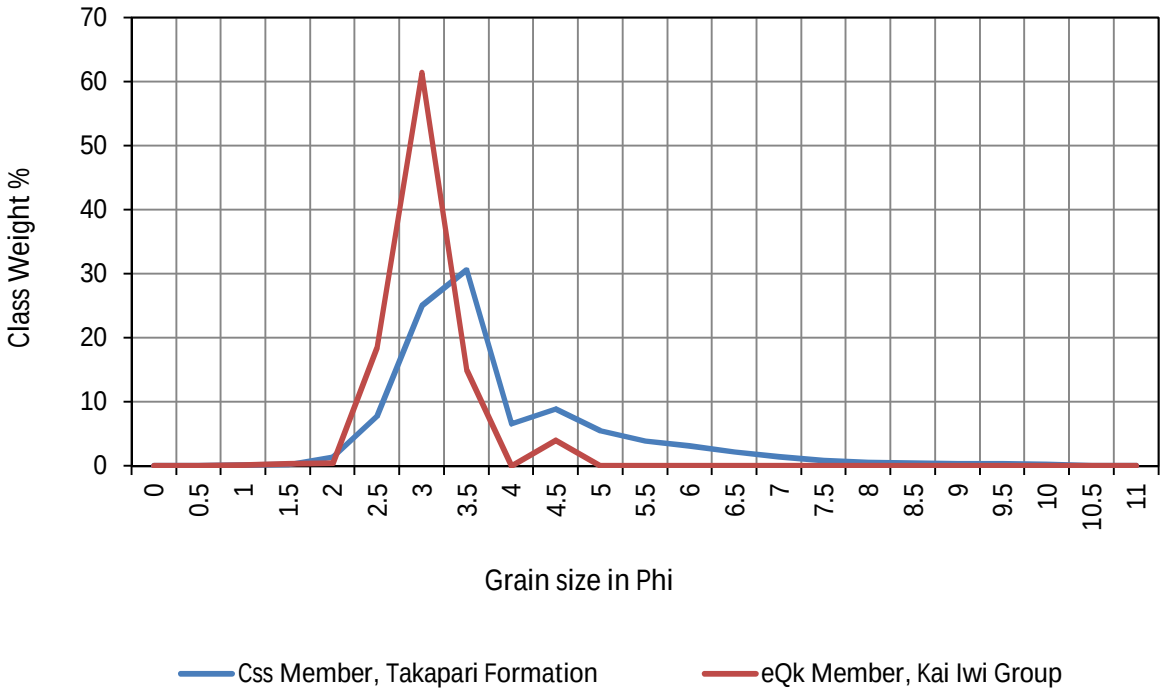

The grain size distribution of eQk Member is very well sorted. Overall the mean grain size is fine sand (2.6 Phi) with leptokurtic kurtosis. The grain size distribution (Fig 7.3) is symmetrical, which is a function of the very well sorted nature of the sediment.

The grain size distribution statistics for the eQk Member of the Kai Iwi Group (see Chapter 9) show a distinct marine signature (Fig 7.3, Appendix 2.2). The grain size distribution is very well sorted, which is characteristic of sorting via wave action, within a shallow marine environment. This is opposed to sorting within a fluvial environment where the main flow is unidirectional and the resulting facies are often less well sorted with isolated large clasts.
In fluvial environments there are usually high amounts of suspended sediment in the water column, resulting in a characteristic 'fine tail' or finely skewed distribution curve in fluvial facies. However, in a marine environment fine material is winnowed out from the sands and carried further out onto the shelf where in slacker water the clays and silts eventually fall from suspension.

### 7.2.2 Stratigraphy

The sequence (Fig 7.4) is dominated by vitric, volcaniclastic sands and carbonaceous muds. The lower 20 m is composed of mudstone and cross bedded to laminated heterolithic sediments. Fossils appear in abundance within bed 26; a shell bed containing well preserved *Austrovenus stutchburyi.* This bed also displays water escape structures. Muds are generally characterised by planar laminae while sands often show a variety of sedimentary structures including common cross bedding. Preservation of organic material is associated with the carbonaceous muds, including a 20 mm thick lignite layer which occurs at the top of bed 23. Pumice first appears in the sequence at bed 13, after which it comprises the dominant component of the sand fraction within the upper part of the stratigraphic column. The other component is quartzo-feldspathic.

### Facies analysis of Css Member, Takapari Formation

Facies Mm; Mudstone, massive bedding
The Mm Facies is characterised by blue grey, massive mudstone. Iron oxide streaks are present as laminations throughout. Beds range from 1-4 m in thickness. Thinner iron oxide rich mudstone beds of 200-300 mm thickness occur intermittently within this facies.

*Interpretation:*
Facies Mm is interpreted to have been deposited within an offshore marine environment on the inner most shelf. Sedimentation processes are dominated by finer material falling out of suspension. The alternating mafic rich and quartzofeldspathic rich laminae represents small scale grading, i.e. the heavier titanomagnetite minerals fall out of suspension first followed by lighter quartzo-feldspathic minerals, a cycle which is repeated over and over.

Table 7.2 Lithofacies of Css Member and Bms Member, Takapari Formation and Kaimatira Pumice Sand Formation; facies codes are modified from Smith (1987); Horton & Schmitt (1996); Miall (1977); and Waresback & Turbeville (1990).

| Facies code | Description | Interpretation |
|---|---|---|
| Mm | Massive sandy mudstone, iron oxide laminations | Marine inner most shelf environment, suspension fall out and traction deposition |
| He | Coarse to fine sand with mud drapes, some lenticular beds of mud | Storm dominated deposits on a muddy innermost shelf environment |
| Es | Alternating laminated mud and silts | Tidal dominated deposition within an estuarine mud flat |
| C | Lignite and carbonaceous muds | Vegetated estuarine back swamp environment, anaerobic conditions |
| Sp | Cross bedded pumiceous sands intercalated with massive silts | Linguoid, transverse bars, sand waves (lower flow regime), within a estuarine distributary system environment |
| Sh | Fine grained laminated sands intercalated with massive to rippled silts | Planar bed flow, tidal dominated deposition within estuarine distributary channel |
| Fl | Fine to coarse rippled pumiceous sand, normal grading | Overbank flow deposits out onto the alluvial floodplain, waning flood deposits |

Facies He; sand dominated heterolithic facies

Facies He is composed of coarse to fine sandstone with mud draped, trough, cross bed foresets. Some lenticular bedding is also present. The small scale cross beds are 300-400 mm in thickness and are commonly bounded by reactivation surfaces. Towards the base of the small-scale cross-bedded sets, mud drapes converge resulting in lenticular bedding. The overall bed thickness ranges from 1-3 m. Iron oxide stains are present.

*Interpretation:*

This facies is interpreted as being deposited onto a storm dominated muddy inner most shelf environment. Although heterolithic facies are often associated with tidal flat and other estuarine settings, the majority of heterolithic facies in the Whanganui Basin are interpreted as having been deposited in fully marine innermost shelf environments (Abbott *et al*, 2005).

This is due to the presence of shelf wide mud blankets on the modern Whanganui Shelf which may be used as a modern analogue for Whanganui Basin sediments (Fig 6.15).

Mud draped cross bedding sets are a sedimentary structure more commonly associated with tide dominated environments which have times of alternating strong (cross bedded sand deposition) and slack (finer sediment falling out of suspension draping cross beds) currents (Abbott, 1998). However, on a muddy inner-shelf marine environment a similar heterolithic facies could also develop as a result of fluctuating energy conditions such as; storm dominated (Swift & Rice, 1984), or tide dominated marine environments (Reineck & Singh, 1980). Under the influence of a strong predominant current, either flood or ebb, and a weak subordinate current a succession of sandy cross bedded sand separated by thin mud drapes from slack tide conditions may occur.

Evidence for Facies He being deposited on a muddy inner shelf environment include; no evidence of sub-tidal or intertidal channel facies and no evidence of peat, plant material or other fluvial/ supra-tidal flat facies which have a high preservation potential. Thirdly there are no fossils present which are characteristic of a tidal dominated environment. The origin of the cross-bedded sets with mud drapes is also suggested to be due to both a lowering of the wave base caused by spring-neap tidal cyclicity (Homewood & Allen, 1981) and strong storm activity (McCave , 1970).

During strong storms sediments are mobilised creating a rippled and cross bedded sea floor, which is then draped by mud during quiet periods. An interpretation of Facies He originating from storm activity seems probable when taking into account the modern analogue of a storm dominated inner-shelf setting off the coast of Manawatu today (Abbott, 2000). These storm dominated oceanographic conditions were likely similar during the Pleistocene when the Takapari Formation was being deposited.

Facies Es; laminated mud and siltstone facies

The Es Facies is characterised by thick (up to 7 m) beds of mud and siltstone. Beds are often fossiliferous and contain layers of concentrated organic material. Dominant sedimentary structures include planar laminations and flame structures. Rare tephra is also preserved. Laminations are generally 5-10 mm thick. Some wave ripples with uni-directional cross-stratification are also present.

*Interpretation:*

Facies Es is interpreted as being deposited on a tidal mud flat within an estuary. The fine rhythmic bedding characteristics of Facies Es are indicative of alternating periods of current

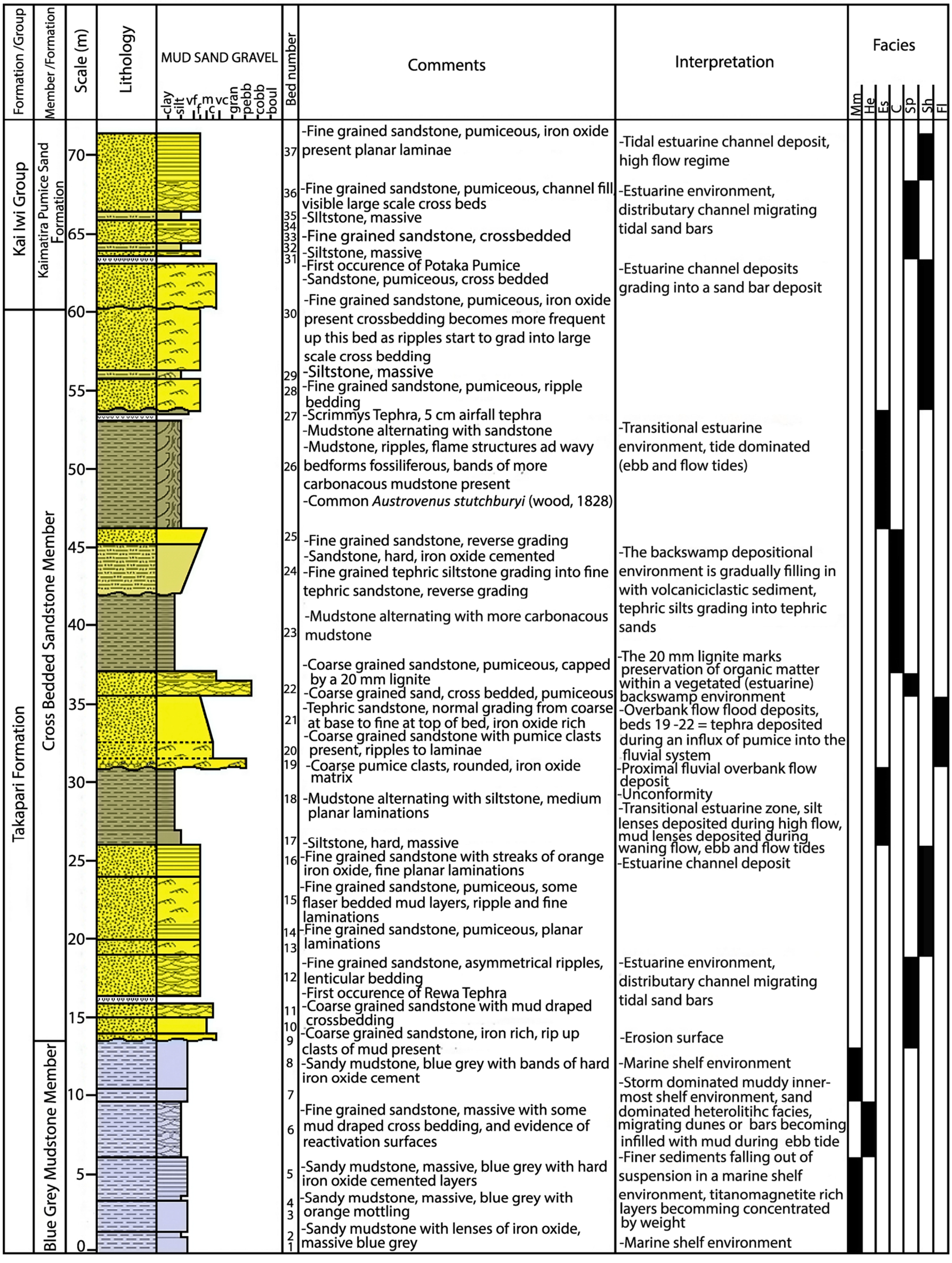


Key:

Lithologies
- Mudstone
- Sandstone
- Siltstone
- Granular pumice clasts
- Tephra
- Lignite

Symbols
- Trough cross bedding
- Current ripple lamination
- Planar laminae
- Water escape structures

Base boundaries
- Sharp
- Gradational
- Erosional

Fig 7.4: Stratigraphic log of Css Member, Takapari Formation and Kaimatira Pumice Sand Formation, Scrimmys Stream, Broadlands Station, Pohangina Valley (WGS84 40 °16'47.64"S, 175 °46 '29.48"E elev 79 m).

activity and of relative quiescence. These types of conditions prevail on intertidal mud flats within estuary systems (Klein, 1977, Reineck & Wunderlich, 1968). Flame structures are likely formed due to sediment loading under saturated conditions. These water escape structures are indicative of a relatively high sedimentation rate, where on-going deposition eventually generates enough pressure to cause liquefaction of the underlying sediment.

Facies C; lignite and carbonaceous mudstone facies

Facies C is composed of a 20 mm thick lignite bed at its base, which grades into laminated carbonaceous mudstone. The mudstone then grades up into silts then sands. Overall this facies is 9 m thick with the basal 5 m of sediment very carbonaceous.

*Interpretation:*

This facies is interpreted to have been deposited in an estuarine back-swamp (Fig 7.5). The initial preservation of organic material leading to the formation of a 20 mm lignite layer represents the vegetated area of an estuarine back-swamp in which organic matter was able to accumulate and become preserved under anaerobic conditions. Further accumulation of carbonaceous muds is interpreted as a continuation of anaerobic conditions, with some sediment deposition occurring. The increasing influx of siliciclastic material is derived from both colluvium eroding off the surrounding landscape and alluvial sedimentation into the estuarine system. The sediments then show reverse grading which is interpreted as the continued increase in siliciclastic deposition during high flow periods into the estuary.

Facies Sp; cross bedded pumiceous sandstone facies

The Sp Facies is composed of fine grained, trough cross-bedded sandstone and massive siltstone beds. Siltstone beds are massive and up to 500 mm thick. The cross bedded sands are 500 mm to 2 m thick becoming thicker up section. Cross bed sets are typically 500 mm thick.

*Interpretation:*

Facies Sp is interpreted as a migrating estuarine channel sand bar/point bar. The gradual change from fine rippled sands in bed 30 (Facies Sh) into the crossbedded sands of bed 31 (Facies Sp) is interpreted as the change from a channel into a sand bar/point bar landform. The increased thickness of the cross bedded sands up section into bed 36 represents a change from the bar slope (intercalated massive silt and thin cross bedded sands) to the bar crest (where cross bedded sands are thicker).

Bars which are deposited in areas with low suspended-sediment concentrations (e.g. the seaward end of estuaries or in areas near the inland limit of tidal influence) are less likely to display heterolithic sedimentation because of lower suspended-sediment concentrations. Instead facies within these areas consist of stacked dune cross beds with gently inclined set

boundaries (Dalrymple & Rhodes, 1995).The fine grain size and intercalation of sand and silt beds in facies Sp is interpreted as showing that this facies was deposited in an intermediate zone of the estuary between the far seaward zone and inland limit of tidal influence; where moderate suspended sediment concentrations prevailed.

Facies Sh; fine grained laminated sands with rippled silt lenses

Facies Sh consists of fine grained, laminated sands with silt lenses. Sedimentary structures include fine laminations and ripple bed forms. Iron oxide is present in the beds, often accentuating laminations. Sandstone beds are 2-7 m thick while intercalated silts are 500 mm.

*Interpretation:*

Facies Sh is interpreted as an estuarine distributary channel facies within the estuary funnel. Laminated sands are deposited during high flow periods in the upper flow regime. Intercalated silt deposits represent periods of slack water, where finer sediments are able to fall out of suspension.

Facies Fl: fine to coarse pumiceous sands with occasional large pumice clasts

The Fl Facies is characterised by an erosional base followed by a 500 mm thick bed of sand with large (up to 50 mm) rounded pumice clasts. Above the erosional base this facies contains pumiceous sands which show normal grading. Sedimentary structures include ripples and cross bedding. Overall facies Fl is 6 m thick with individual beds ranging from 500 mm to 3 m.

*Interpretation:*

Facies Fl is interpreted as overbank deposits derived from a paleo-river system which meandered its way across the coastal plain to the coast. The initial erosional base with large pumice clasts is suggested to represent a 'flood' event probably caused by the sudden influx of pumiceous sediments into the paleo-river following the emplacement of an ignimbrite sheet in the hinterland. Subsequent build up and release of the river as it began to erode into the ignimbrite sheet resulted in vast quantities of pumice entering the paleo-river system and becoming deposited onto the flood plain.

The normal grading of the overlying sands (bed 20) is characteristic of flood plain deposits, where heavier, coarse material is deposited relatively close to the river and the finer sediments are carried farther out over the flood plain with the flood water. Although floodplain deposits are generally characterised by fine grained sands, coarse pumiceous sands may be deposited in overbank settings because of its low density and high vesicularity.

## Interpretation

Css Member is characterised by terrestrial depositional environments and has a strong fluvial/estuarine influence. Underlying Css Member is Bms Member a shallow marine to estuarine sandy mudstone. The contact between these two members is sharp and erosive represented by the first incoming of thick vitric tuff deposits, identified as belonging to the Rewa Pumice (1.2 Ma). Several tuff units are evident within the Css Member displaying characteristic features such as large scale cross bedding, and channel cut and fill structures. Shells of the intertidal cockle *Austovenus* form 400 – 1000 mm thick shell beds throughout the unit, providing evidence for nearshore to estuarine deposition, punctuated by periodic influxes of coarse volcaniclastic sediment.

Depositional environments identified within Css Member include estuarine, alluvial plain, and back swamp environments. The beds have clearly been deposited into a terrestrial environment via fluvial processes. Evidence for this is seen in the presence of lignite beds; cross bedding, channel scour and fill structures, and poorly sorted grain sizes with a fine tail, characteristic of fluvial deposition.

The sedimentary sequence logged at Scrimmys Stream is interpreted as having two main phases of deposition; marine and terrestrial. The marine phase is characterised by shelf depositional environments. The estuarine phase is represented by wave dominated estuarine to fluvial depositional environments. The contact between the marine and terrestrial phases occurs between beds 8 and 9, (contact between Bms Member and Css Member) where a change from the fine grained mudstone of the marine shelf environment (facies Mm) to the medium grained sandstone deposits within a fluvial environment (facies Sp) occurs. This contact is erosional representing an unconformity between the two members of the Takapari Formation and a major change in depositional environments.

The estuary system formed in a transitional coastal plain setting within the southeastern Whanganui Basin. This would have been an exposed coastline similar to the Tarankai Bight today with no exposed basement to act as headlands. A sand spit was likely built out across the exposed estuarine channel, driven by longshore currents moving sediments along the coast from north to south, similar to Foxton estuary today. Based on its location on an exposed coast it is likely the paleo-estuary was wave dominated.

The sequence displays an increasingly fluvial influence up section. Beginning with marine deposition the sequence then moves into dominantly estuarine deposition with occasional influxes of fluvially deposited volcaniclastic sediments. These influxes of volcaniclastic sediments increase in thickness up section to become the dominant lithology within the upper 20 m. The transition from a marine to estuarine/fluvial setting is characterised by a

major change in sediment provenance, an increased sedimentation rate and fluctuations in eustatic sea level. Influxes of volcaniclastic sediments have contributed to the infilling of the estuarine system.

The grain size data for Css Member (Appendix 2.3) display a bimodal grain size distribution. The first population ranges from 1.5-4 Phi and the second from 4-8 Phi. The grain size distribution is fine skewed, which is characteristic of a fluvial environment with high suspended sediment concentrations in the water column.

### 7.2.3 Estuary depositional environments

An estuary can be defined as the seaward portion of a drowned valley system which receives sediment from both fluvial and marine sources, and which contains facies influenced by tide, wave and fluvial processes. An estuary extends from the land-ward limit of tidal facies to the sea-ward limit of coastal facies at its mouth (Dalrymple *et al,* 1992). Estuaries which occupy drowned valleys are commonly found on modern day transgressive coastlines. Using the occurrence of these estuaries as a modern analogue it is likely they were just as common during past transgressions through the Quaternary. In modern estuaries sediment supply has not kept pace with the sea-level rise, and the estuary acts as a sink for sediment of both terrestrial and marine origin (Guilcher 1967; Roy *el al,* 1980; Dalrymple *et al*, 1990).

Estuaries act as sediment traps and their resulting deposits have high preservation potential due to their location within paleo-valleys (Dalrymple *et al*, 1992).Therefore estuary systems should be widely represented in the geological record. However ancient estuarine deposits have not been widely recognised (Clifton, 1982; Zaitlin & Shultz, 1990). This is in part due to the complexity of estuarine systems and the lack of standardised terminology or facies models which can be applied to them.

Estuary depositional environments have been classified on the basis of the dominant marine processes in operation these include; wave and tide dominated estuaries (Dalrymple *et al*, 1992). Tidal dominance occurs if tidal currents are responsible for more sediment transport than river currents or waves and thus determine the larger geomorphology of the estuary (Galloway, 1975; Swift, 1976). The tidal dominance is reflected in the type of landforms which are created such as a predominance of coast normal elongate tidal bars and tidal-channel networks. There is also often an absence or limited occurrence of wave-generated, coast-parallel barriers and/or beaches (Dalrymple & Choi, 2007).

Wave dominated estuaries have tidal inlets that are constricted by wave deposited beach sand in the form of sand spits or sand barriers. Their flood-tidal deltas are commonly smaller than those in tide-dominated estuaries (Roy, *et al,* 1980). Tidal ranges within an estuary

basin are usually far less than in the ocean and tidal currents are negligible. Local wind waves and wind-induced water movements are the dominant sediment transporting mechanisms. Wave dominated estuaries are more strongly influenced by river discharge compared with tidal dominated estuaries.

The fluvial to transitional marine/fluvial zone is one of the most complicated depositional environments to interpret as there are many different terrestrial and marine processes interacting with each other. An understanding of how sedimentary facies change through this transitional zone is important for the correct interpretation of past environment of deposition and the application of sedimentary systems tracts.

One of the most important changes in the main depositional processes across this zone is the seaward decrease in the power of river flow and the seaward increase in both the intensity of tidal currents and wave action. Together these two trends create dominance

Fig 7.5: Diagram showing location of facies within a wave dominated estuary system (adapted from Hou *et al*, 2003).

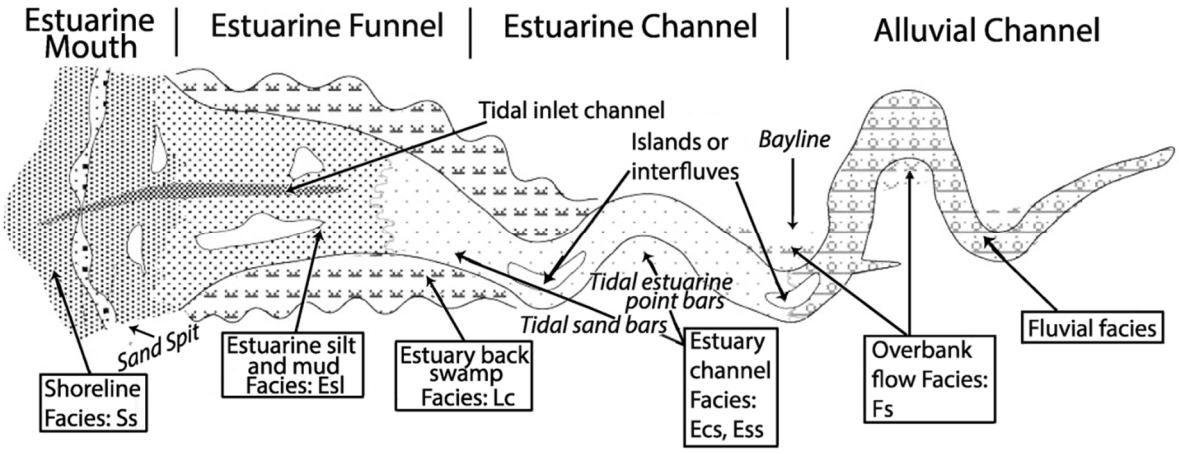


of river currents and a net seaward transport of sediment within the inner part of the transitional zone (landward zone). Tidal currents begin to dominate in the seaward part of the transitional zone creating a net landward transport of sediment (Dalrymple & Choi, 2007). The sediment transport pattern of these two converging depositional processes creates a bedload convergence within the middle part of the estuary system. The result of this convergence is the build-up of sand bars and the creation of multiple channels in the fluvial system.

The paths of sediment transport tend to create grain size trends within the sand fraction of estuarine sediments. Usually there is a seaward decrease in sand size through the river dominated part of the estuary and a landward decrease in sand size within the outer marine dominated portion of the estuary system. A turbidity maximum (a zone of greatly elevated suspended-sediment concentrations) is developed within estuaries as a result of flocculation

and density-driven water-circulation patterns (Dalrymple & Choi, 2007). This creates an area within the middle of the estuary where the concentration and thickness of mud drapes/ lenticular and flaser bedding is at its greatest.

Controversy surrounds the formation of lenticular and flaser bedding. It has been suggested that these alternations of mud and sand layers may reflect daily tidal cycles (Reineck & Wunderlich, 1968). Others however have suggested that this bedding likely reflects longer periods of time such as the accumulation of sediment through several slack water events representing several tidal cycles (Trewindt & Breusers, 1972). These arguments for longer periods of deposition suggest that the formation of the bedding is associated with neap-spring cycles or are perhaps influenced by seasonal cycles.

### 7.2.4 Cyclostratigraphy

The Whanganui Basin contains 47 cyclothems which correlate to MIS 1–100 over the last 2.4 Ma. Each cyclothem within the Pohangina Valley stratigraphy correlates with the transgressive and highstand part only of each glacial-interglacial isotope stage couplet i.e. odd numbered isotope stages. Even numbered glacial stages are represented by unconformities which separate individual cyclothems.

Cycles 30 to 34 are recognised within Css Member (Fig 7.6). The correlation of Css Member to Whanganui Basin cyclostratigaphy is based on tephrochronology. Each cycle contains two distinctive units. A basal unit consisting of coarse pumiceous sands with common cross bedding interpreted as the TST, and an overlying fine grained carbonaceous mudstone unit interpreted as the HST. The LST is represented by the bounding, erosional unconformity which separates each cyclothem.

Increased erosion during glacial periods (LST) led to river aggradation. Volcaniclastic sediments are rapidly eroded from the distal area of the ignimbrite sheet and transported to the coast which was located approximately 100 km farther out onto the continental self from the present day coastline. No sedimentary preservation occurs during the lowstand part of the cycle. This part of the cycle is characterised by high erosion rates.

Erosional unconformities within Css Member are clearly visible as stark contrasts in lithology, sedimentary structures and biostratigraphy. Rip up clasts of silt and pumice often overlie the erosional unconformity. These unconformities generally follow the local dip and dip direction, although they can display wavy and irregular surfaces. Erosional unconformities provide an important means of correlating the sequence to the marine oxygen isotope record (Fig 7.6).

Fig 7.6: Correlation of Takapari and Kaimatira Pumice Sand formations to the MIS and Whanganui cyclothem record.

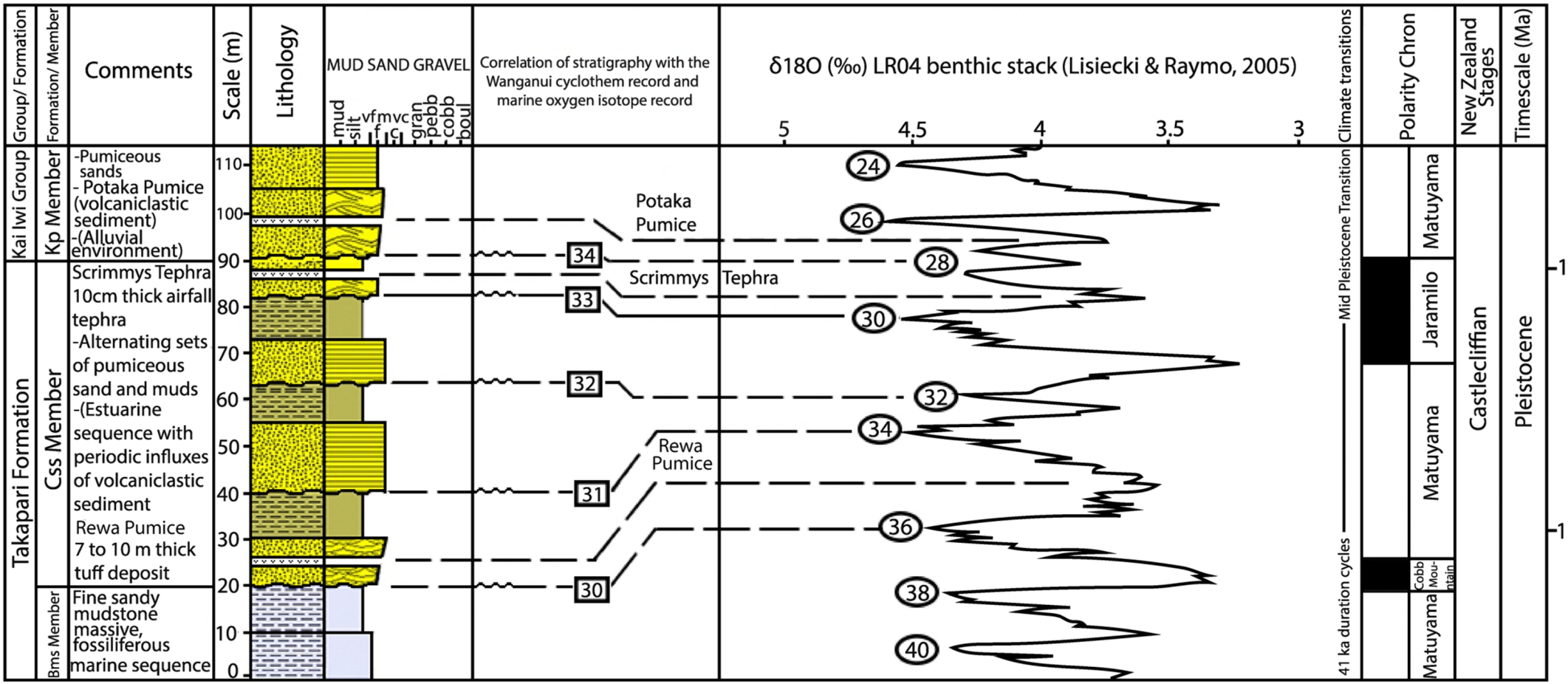

Influxes of volcaniclastic sediments into the sequence at Scrimmys Stream are related to increased rates of fluvial transportation. A warmer, wetter climate prevailed as the sedimentary cycle entered into the TST. This allowed rivers to transport the large amounts of the sediment generated in the previous LST out towards the coast. Rivers begin to cut down as the coastline moved farther inland. During the TST re-worked, volcaniclastic deposits formed within fluvial and marginal marine environments on the coastal plain of the southeastern Whanganui Basin.

During the HST the coastline reached its maximum landward extent and a return to marginal marine/estuarine deposition ensued in the area of present day Pohangina Valley. Only during the transgressive phase and high stand of eustatic sea level rise does the coastline travel far enough inland to reach Pohangina Valley.

Four stacks of these alternating cycles are recognised within Css Member, Takapari Formation. Although these cycles are coincident with the emplacement of ignimbrite sheets within the upper catchment area of a paleo-river system, they are a function of fluctuations in climate, sea level and accommodation space.

In Mid Castlecliffian time, during the deposition of Css Member, fully marine conditions were never attained; this can be partly attributed to the cycles of Css Member being dominated by 41 ka climatic fluctuations. The Quaternary is characterised by a transition from 41 ka to 100 ka climatic fluctuations termed the Mid Pleistocene Transition (MPT) which occurs around 800 ka (Berger *et al,* 1993). Fully marine conditions return during the deposition of Kai Iwi Group sediments. This is likely the result of higher amplitude, 100 ka fluctuations which result in the coastline transgressing farther inland. A transition to 100 ka cycles occured between MIS 25 and 22 (around 0.8Ma) (Berger, *et al*, 1993). Kai Iwi Group sediments in Pohangina Valley can be linked chronostratigraphically, via Potaka Pumice (1 Ma) and Kaukatea Tephra (800 ka).

### 7.2.5 Volcaniclastic facies

Volcaniclastic sediments occur within the non-marine facies Fl, Sh and Sp. The volcaniclastic sediments are composed of nearly pure vitric tuffs ranging in thickness from 4 – 17 m. Grain sizes are mainly coarse ash (< 3 mm), but some tuffs contain lapilli pumice up to 150 mm (Fig 7.6). The thickness of these volcaniclastic deposits and the grain sizes present, suggest that they are formed as a result of the reworking of volcanic deposits rather than as distal, primary air fall products.

Facies Fl is an overbank flow deposit associated with an erosional base and a 20 mm lignite bed. This association indicates that the tuff emplacement event followed a significant hiatus in the sedimentary record, which is marked by the establishment of vegetation and a

reduction in the siliciclastic sedimentation rate. This suggests that there was a significant volcaniclastic influx into the paleo-fluvial system, which caused sudden aggradation.

Fig 7.7: Tuff unit (Potaka Pumice) within Kaimatira Pumice Sand Formaton. Pumice clast 150 mm is diameter seen near spade handle, Broadlands Station Pohangina (WGS84 40 °15'21.85"S, 175 °47'00.87"E, elev 143 m).

The large inputs of volcaniclastic material into the paleo-river system following ignimbrite emplacement, caused rapid aggradation to occur. This was followed by a period of relative quiescence represented by a lower siliciclastic sedimentation rate and a higher rate of organic matter preservation. Rapidly aggraded river flood plains within the paleo-river valley were left higher than maximum flood level and due to the relatively high water tables within this low area of the landscape, anerobic conditions suitable for organic matter preservation prevailed in parts of the flood plain.

The volcaniclastic facies of the Takapari Formation display primary sedimentary structures indicative of a subaqueous deposition within a fluvial environment e.g. channel fill, cross bedding, and scoured erosional contacts (Fig 7.7). Often tuff units show normal grading and are capped by a thin (<20 mm) lignite bed or carbonaceous mud layer. These primary structures and the relatively thick nature of the volcaniclastic facies are interpreted to be a result of an increased sedimentation rate following volcanic events.

Fig 7.8: Water escape structures caused by sediment loading within tuff unit (Potaka Pumice), Kaimatira Pumice Sand Formation, entrance to Antler Stream, Broadlands Station, Pohangina (WGS84 40 °15’28.52”S, 175 °46’53.64”E,elev 77 m).

Fig 7.9: A+B : Css Member showing dewatering structures, Maungatukurangi Stream, Broadlands Station, Pohangina Valley (WGS84 40 °14'40.54"S, 175 ° 47'37.75"E, elev 137 m).


The increased sedimentation rate led to rapid channel migration and deposition in overbank settings. Sedimentary structures such as channel scour and fill (Fig 7.7) represent highly erosive paleo-currents and increased discharge within the paleo-river system. This is interpreted to represent catastrophic flood episodes caused by blocking/chocking of the paleo-river systems headwaters by volcaniclastic material following a large rhyolitic eruption. Increased sedimentation rates within the paleo-river system led to channel migration evidenced by channel scour and fill structures and overbank flow deposits (Manville *et al*, 2009). The presence of rip up stuctures and erosive contacts represent strong, viscous paleocurrents with high discharge rates (Fig 7.8).

Cross stratification within the tuff units ranges from millimetre scale ripples to 2 m scale trough cross bedding. In some cases the entire range of cross stratification occurs in a single tuff unit suggesting a rapid change in the strength of the paleocurrent. Generally sedimentary structures indicate very variable flow strength up section, with many changes from low flow (ripples) to higher flow (cross beds, laminae) indicators. Paleocurrent data taken from crossbed forsets indicate a NW sediment source (Brackley, 1999).

Many of the tuff units contain synsedimentary deformation in the form of water escape structures and convolute bedding (Figs 7.8, 7.9). These structures are interpreted to have formed during rapid deposition of saturated, subaqueous volcaniclastic material. The pressure of the overlying sediment results in liquefaction of the saturated sediment resulting in upward movement of water in response to overburden pressure.

## 7.3 Tephrochronology

### 7.3.1 New Zealand rhyolitic volcanism during the Quaternary

During the Quaternary Central North Island volcanic activity was characterised by large rhyolitic eruptions. Since 1.6 Ma eight major calderas have erupted at least 34 ignimbrite sheets during explosive rhyolitic volcanism (Wilson *et al,* 1984; Houghton *et al*, 1995). To the south of the Taupo Volcanic Zone (TVZ) there are peripheral sedimentary basins and southward flowing river systems which fed into the Whanganui Basin. In Pohangina Valley the Kaimatira Pumice Sand Formation was deposited in fluvial/marginal marine environments of the southeastern Whanganui Basin. The pumice in the Kaimatira Pumice Sand Formation has been identified as Potaka Pumice (see section 8.2.2).

The Potaka Pumice has been correlated to the Kiddnappers and Rocky Hill Ignimbrites erupted from the Mangakino Caldera (Wilson *et al*, 1995) depositing thick sheets of ignimbrite across the landscape. Following these eruptions paleo fluvial systems carried

pumice and tephra eroded from these ignimbrite sheets into the Whanganui and East Coast Basins (Shane, 1991).

The tephra deposits erupted during these rhyolitic eruptions are valuable stratigraphic marker horizons. Their widespread distribution and unique compositions allow regional correlations to be made within a basin (Shane *et al,* 1996). Early to Middle Pleistocene rhyolitic tephras have been found as far as 600 km from their source in onland exposures and as far as 1000 km away in deep sea cores (Froggatt, 1983; Nelson *et al*, 1985; Shane, 1994). Volcaniclastic sediments which have been fluvially deposited into the East Coast Basin, Hawkes Bay are currently separated from the volcanic source region by the North Island axial ranges (Shane, 1991). The ages and distribution of these tephras have important implications for the rates of uplift within the axial ranges and the paleogeography/paleodrainage of the lower North Island during the Quaternary.

### 7.3.2 Geochemistry

In this study an effort was made to locate and sample tephra beds, for electron microprobe analysis (EMA). Two tephra plugs were made containing sixteen tephra samples collected from around Broadlands Station, Pohangina Valley (see Appendix 1 for sample locations). The preparation of tephra plugs ready for EMA is outlined in the flow chart in Appendix 1.2.

Table 7.3: Tuffs and tephras identified in the Lower Pohangina Valley via EMA (Ages sourced from Pillans *et al*, 2005; * estimated based on stratigraphic position, see section 7.3.3).

| Tephra | Sample Numbers | Stratigraphic Member/ Formation | Age |
|---|---|---|---|
| Kawakawa Tephra | T3 | Ohakean Loess on Ratan Terrace. | 25.358 ± 0.162 ka |
| Kaukatea Tephra | T2 | Rc Member, Kai Iwi Group | 0.86 ± 0.08 Ma |
| Potaka Pumice (tuff) | T1, T10, T16 | Kaimatira Pumice Sand Formation. | 1.05 ± 0.05 Ma |
| Scrimmys Tephra | T7, T8 | Css Member, Takapari Formation. | 1.12 ± 0.1 Ma* |
| Rewa Pumice (tuff) | T12, T13, T14 | Css Member, Takapari Formation | 1.20 ±0.14 Ma |
| Mangapipi Tephra | T5, T6 | Bms Member, Takapari Formation. | 1.51 ± 0.16 Ma |
| Ridge Tephra | T9, T11 | Bms Member, Takapari Formation. | 1.56 Ma |
| Pakihikura Tephra | T4 | Bms Member, Takapari Formation. | 1.58 ±0.08 Ma |

Compositions of glass shards from each of the tephra beds were determined by EMA at Victoria University using a JEOL 733 electron microprobe. The individual shard analyses allow the homogeneity of the glass to be assessed as well as chemically fingerprinted. Such analyses are important in distal and fluvial environments where glass shards from different eruptive events can be mixed together into a single bed (Shane, *et al*, 1996). Ternary diagrams based on work by Pillans (1994) were plotted using FeO: 1/3 $K_2O$: CaO Wt % data. These diagrams, in conjunction with bivariate plots of FeO Vs CaO Wt % allow tephra identification. Tephras and tuffs in the Takapari Formation are discussed below. Younger tephras and tuffs are discussed in following chapters.

### 7.3.3 Scrimmys Tephra (New Tephra)

Scrimmys Tephra was first recognised in this study in Scrimmys Stream on Awahou South Rd, Broadlands Station, Pohangina (WGS84 40°16'48.07"S 175° 46'26.04"E, elev 82 m) here it occurs 40 m above Rewa Pumice and 10 m below Potaka Pumice (Fig 7.4). It occurs as a 5 cm layer of fine tephra within an estuarine sequence with periodic influxes of silicic volcaniclastic material. The type section has been chosen as the 70+ m section of pumiceous sediments exposed on Awahou South Road, Broadlands Station (Fig 7.6). This type section was chosen due to its accessibility and the presence of over 70 m of section which includes both the Rewa Pumice and Potaka Pumice.

Scrimmys Tephra can be traced 1.75 km SSW to an outcrop on the true left side of Saddle Stream. Outcrops were both sampled for geochemical analysis. The tephra occurs as both airfall tephra and volcaniclastic sediment (tuff unit) due to lateral variation across the landscape. The tephra is interpreted as being deposited aerially at Scrimmys Stream, due to its fine grain size and occurrence as a sharp 5 cm layer within esutarine backswamp facies. At Saddle Stream the tephra occurrs as a 1 m thick bed displaying high energy sedimentary structures such as cross beds and channel cut and fill structures. This unit is interpreted as a fluvial point bar/channel facies. This change in the style of transportation, deposition and preservation across the landscape is associated with the varying depositional conditions of laterally adajacent environments present within the paleo-estuarine system.

Scrimmys Tephra is correlated with Cycle 33 of the Whanganui cyclostratigraphy and falls within MIS 29. This provides an estimated age of 1.12 ± 0.1 Ma. Correlation with the oxygen isotope record is based on the the occurrence of Potaka Tephra which overlies Scrimmys Tephra.

## Geochemistry

Scrimmys Tephra is characterised by high calcium content averaging 1.4 Wt %. It also has a high iron content of 1.4 Wt % greater than Potaka Pumice with an average of 1 FeO Wt %. Fig 7.10 shows that Scrimmys Tephra has a greater Wt% of CaO than the other Pliestocene tephras from the TVZ. Scrimmys Tephra has a average of 2.619 Wt% $K^2O$ (Table 7.4) which is low compared with Potaka Pumice (3.66 Wt%) and Rewa Pumice (3.46 Wt%)(Appendix 1).

Table 7.4: Scrimmys Tephra Normalised data (Wt%)

| Reading | $SiO_2$ | $Al_2O_3$ | $TiO_2$ | FeO | MgO | CaO | $Na_2O$ | $K_2O$ | Cl |
|---|---|---|---|---|---|---|---|---|---|
| 1 | 76.51 | 13.6 | 0.15 | 1.48 | 0.3 | 1.42 | 3.78 | 2.59 | 0.18 |
| 2 | 76.35 | 13.85 | 0.12 | 1.28 | 0.32 | 1.52 | 3.88 | 2.46 | 0.22 |
| 3 | 76.13 | 13.77 | 0.14 | 1.52 | 0.3 | 1.48 | 3.64 | 2.75 | 0.27 |
| 4 | 76.46 | 13.63 | 0.15 | 1.31 | 0.31 | 1.45 | 3.82 | 2.73 | 0.15 |
| 5 | 76.43 | 13.72 | 0.13 | 1.43 | 0.3 | 1.49 | 3.72 | 2.58 | 0.2 |
| 6 | 77.6 | 14.25 | 0.15 | 1.39 | 0.28 | 1.48 | 2 | 2.64 | 0.21 |
| 7 | 76.31 | 13.84 | 0.13 | 1.5 | 0.27 | 1.4 | 3.8 | 2.56 | 0.19 |
| 8 | 76.42 | 13.7 | 0.15 | 1.39 | 0.25 | 1.49 | 3.77 | 2.65 | 0.19 |
| 9 | 76.11 | 13.8 | 0.18 | 1.59 | 0.31 | 1.42 | 3.77 | 2.6 | 0.22 |
| 10 | 76.6 | 13.68 | 0.11 | 1.28 | 0.27 | 1.42 | 3.77 | 2.63 | 0.22 |
| Average | 76.492 | 13.784 | 0.141 | 1.417 | 0.291 | 1.457 | 3.595 | 2.619 | 0.205 |
| Std | 0.42 | 0.18 | 0.02 | 0.11 | 0.02 | 0.04 | 0.56 | 0.08 | 0.03 |

Fig 7.10: CaO versus FeO (wt %) composition of volcanic glass shards from Kaukatea Tephra, Potaka Pumice, Scrimmys, Rewa, and Pakihikura Tephras sampled in various locations around Broadlands Station, Pohangina Valley (see appendix 1 for sample locations and remaining probe data).

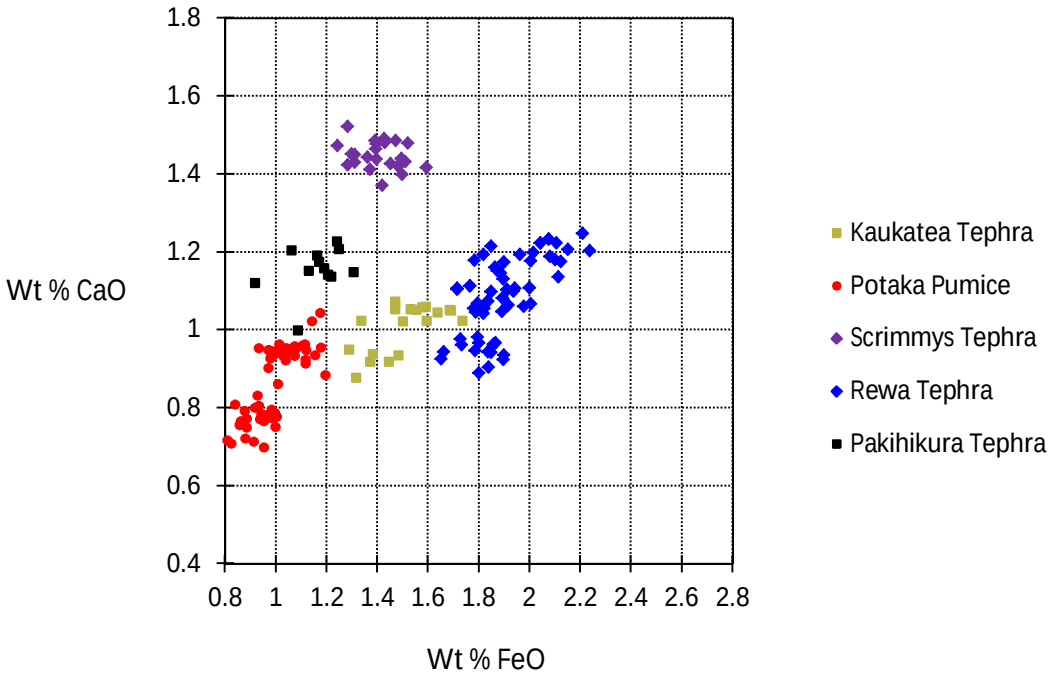

Fig 7.11: Location of the Scrimmys Tephra type locality on hair-pin corner of Awahou South Rd, entrance to Scrimmys Stream, Broadlands Station, Pohangina Valley (WGS84 40°16'47.40"S, 175°46'25.31"E, elev 92 m)(GoogleEarth, 2014).


## 7.3.4 Rewa Pumice

Seward (1976) designated a reference locality for Rewa Pumice on the road 400 m south of Rewa village, where a 1.5 m thick unit of poorly sorted pumice lapilli and ash, interbedded with cross bedded volcaniclastic sands crop out just above road level. Within the Whanganui Basin, Rewa Pumice mostly occurs within reworked conglomeratic shoreline facies similar to the Kamatira Pumice Sand (Potaka Pumice) (Pillans *et al*, 2005).

These types of facies are common in transgressive deposits in Early and Middle Pleistocene Whanganui sequences. In Pohangina the Rewa Pumice occurs as a series of 7-10 m thick tuff units deposited in fluvial overbank and estuarine facies of the Takapari Formation (Css Member). The tuff units are commonly capped by carbonaceous mud or thin (<50 mm thick) lignite beds. Tuff units display characteristic fluvial signatures such as large scale cross bedding and channel cut and fill.

Seward (1974a, 1974b, 1976) reported a glass fission track (FT) age of 0.74 ± 0.09 Ma at the reference locality near Rewa village. That age was revised (Seward & Kohn, 1997) to a mean zircon FT age of 1.00 ± 0.06 Ma. Following Sewards work in the 1970s it has been found FT

ages were erroneously young due to the effects of partial track annealing. The position of the tephra immediately above the Cobb Mountain Subchron (1.19 Ma) which is correlated with MIS 35 in deep sea cores provides an astronomically calibrated age estimate of 1.19 Ma (Cycle 30) (Shackleton *et al*, 1990). Pillans *et al*, (2005) report an ITPFT age of 1.20 ±0.14 Ma.

The Rewa Pumice is commonly found as reworked tephra within stratigraphically younger cycles of the Whanganui Basin. In places this has created problems for both correct identification of tuff units and correlation between outcrops.

In the Lower Pohangina Valley, the Rewa Pumice has an erosive base, and crossbedding grading into planar laminae. The best exposure of Rewa Pumice can be found on Awhaou South Rd, Broadlands Station, Pohangina (WGS84 40°16'48.07"S 175° 46'26.04"E, elev 82 m). The term Rewa Pumice is used in this study as the Rewa Pumice does not contain an airfall tephra in the lower Pohangina Valley.

### 7.3.5 Mangapipi Tephra

Seward (1976) named the Mangapipi Tephra at Mangapipi Stream in the Rangitikei Valley, describing an 18 m thick tephra-rich sequence. The Mangapipi Tephra is composed of an Upper Mangapipi Tephra (0.5 m thick) and a Lower Mangapipi Tephra (0.3 m thick) which occurs 8 m below the former.

The Mangapipi Tephra occurs enclosed by lignite beds at Rewa Hill in Rangitikei. Both Mangapipi tephras contain a high proportion of biotite in their ferromagnesian mineral assemblage. The Mangapipi Tephras commonly occur within carbonaceous mud and lignite beds; interpreted as a regressive coastal plain facies succession at the top of Cycle 23 (Pillans *et al,* 2005).

In Pohangina the Mangapipi Tephra occurs as an airfall tephra enclosed by two thin (100 mm thick) lignite layers (Fig 7.12) within a carbonaceous mud sequence which is part of the Bms Member, Takapari Formation. This part of the Bms Member is interpreted as an estuarine depositional environment where lignite and carbonaceous mud are being preserved within a back swamp area. Sections in the Turakina and Rangitikei Valley containing the Mangapipi Tephra also contain the intertidal mollusc *Austrovenus stuchburyi* representing an intertidal marine influence. Mangapipi Tephra is interpreted to have been deposited during MIS 53. Farther to the west of Turakina the Mangapipi Tephras are absent due to a 450 ka unconformity which occurs below the Butlers Shell Conglomerate (Cycle 31) (Pillans, *et al,* 2005).

Fig 7.12: Mangapipi Tephra enclosed by lignite beds within Takapari Formation, Antler Stream, Broadlands Station, Pohangina (WGS84 40°15'34.43"S, 175°47'08.24"E, elev 96 m).

Seward (1976) determined a glass FT age of 0.88 ± 0.13 Ma. In a revised age (Seward & Kohn, 1997) two separate and distinct zircon populations within the Mangapipi Tephra gave two ages; the first of over 2.5 Ma and a second giving a mean of 1.26 ± 0.08 Ma. It was interpreted that the younger age represents the true eruption age. Pillans *et al*, (2005) present an ITPFT age of 1.51 ± 0.16 Ma which corresponds to an astronomically calibrated age of 1.54 Ma (Pillans *et al*, 2005).

## 7.3.6 Ridge Tephra

Seward (1976) described Ridge Tephra as a light grey tephra sequence 4–5 m thick occurring some 27 m above the Pakihikura Tephra in the Rangitikei Valley. A type section in the Rangitikei Valley was nominated (New Zealand grid reference T22/357353). Pillans *et al*, (2005) re-sampled the Ridge tephra from the type section for glass chemistry following work by Seward (1976). At Pakihikura Bluff, Ridge Tephra lies 50 m above the Pakihikura Tephra

immediately above a thin *Austrovenus* shellbed, within marginal-marine transgressive deposits at the base of Cycle 23 (Pillans *et al,* 2005).

In Pohangina Valley Ridge Tephra occurs within Bms Member, Takapari Formation. This tephra is found in an estuarine sequence containing abundant *Austrovenus* shells and thin lignite beds. The sequence is interpreted to have been deposited during the HST of MIS 53. Ridge Tephra lies approximately 15 m above Pakihikura Tephra.

Seward (1974a, 1974b, 1976) reported a minimum glass FT age of 1.04 ± 0.15 Ma. No ITPFT dates are available for the Ridge Tephra. In this study the estimated astronomically calibrated age of 1.56 Ma presented by Pillans *et al*, (2005) is used. This estimated age is based on the occurrence of Ridge Tephra in the base of Cycle 23, correlating to MIS 53 (Pillans *et al*, 2005).

### 7.3.7 Pakihikura Tephra

Te Punga (1952) described a 25 m section of tephra rich beds at Pakihikura Bluff on the eastern side of the Rangitikei River naming it the Pakihikura Pumice. Boellstorff & Te Punga (1977) defined the type locality of the Pakihikura Tephra as a road cutting 200 m south of Pakihikura Stream. Seward (1976) described the tephra as a white vitric ash 0.5 m thick interbedded within tuffaceous sands. The name Pakihikura Tephra was formalised by Pillans *et al*, (2005). Within sections in the Turakina and Rangitikei River valleys the Pakihikura Tephra occurs within a 100 to 150 m thick sequence of marginal marine to non marine carbonaceous muds and tuffaceous sands (Cycle 22 within the Whanganui cyclostratigraphy) (Pillans *et al*, 2005). The Birdgrove Tephra also occurs within this sequence along with serveral other unnamed tephras.

Fig 7.13: Ternary diagram displaying FeO: 1/3 $K_2O$: CaO Wt % data for tephras collected from Takapari Formation, Kai Iwi Group, and Kaimatira Pumice Sand Formation.

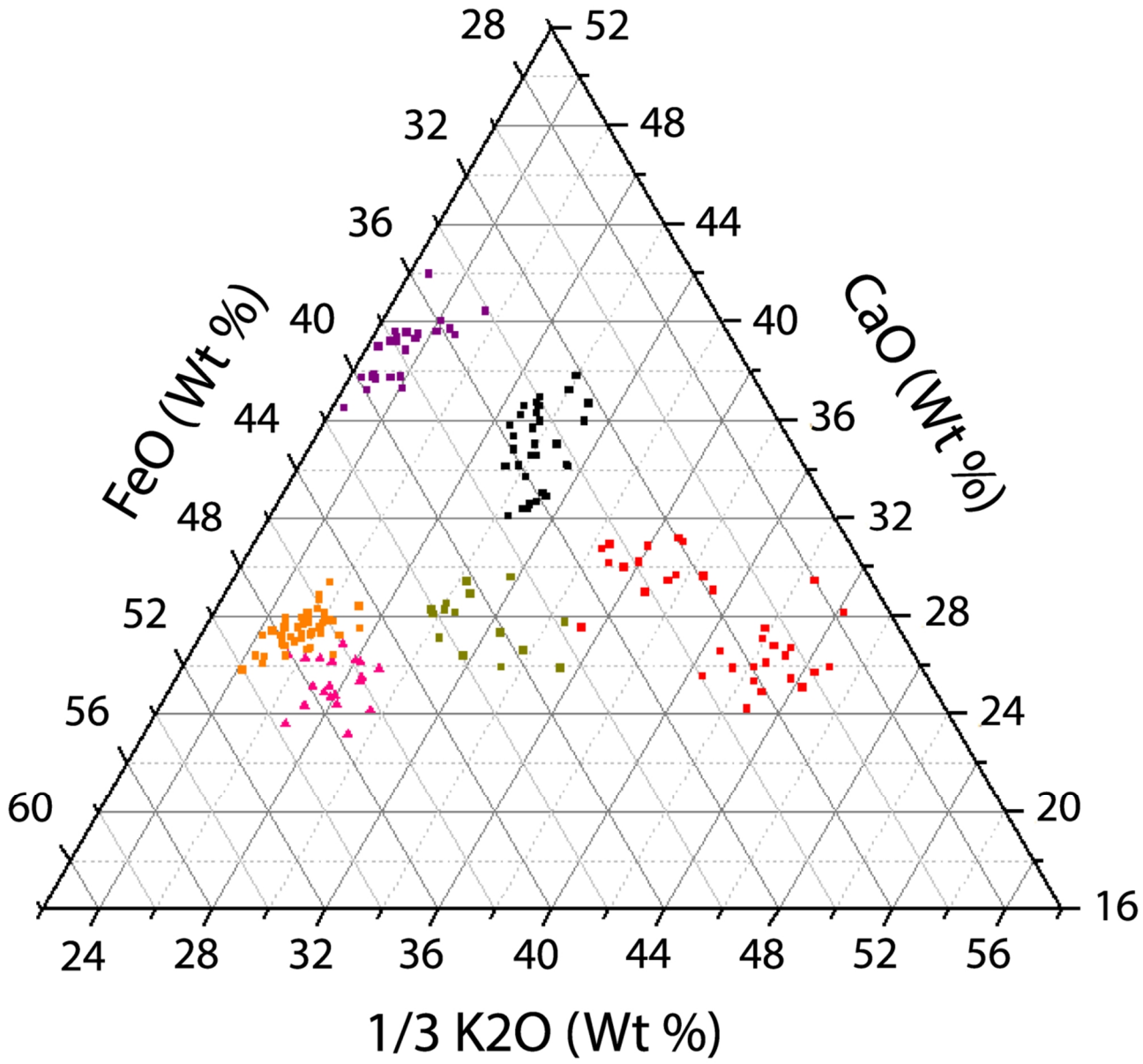


| Key | No of points | Tephra | Formation | Age (Pillans *et al*, 2005) |
|---|---|---|---|---|
| ▪ | 15 | Kaukatea Tephra | Kai Iwi Group | 0.86 ± 0.08 Ma |
| ▪ | 33 | Potaka Pumice | Kaimatira Pumice Sand Formation | 1.05 ± 0.05 Ma |
| ▪ | 24 | Scrimmys Tephra | Takapari Formation | 1.12 ± 0.1 Ma* |
| ▪ | 40 | Mangapipi Tephra | Takapari Formation | 1.51 ± 0.16 Ma |
| ▲ | 21 | Ridge Tephra | Takapari Formation | 1.56 Ma |
| ▪ | 12 | Pakihikura Tephra | Takapari Formation | 1.58 ±0.08 Ma |

* estimated based on stratigraphic position, see section 7.3.3.

In Pohangina the Pakihikura Tephra occurs within the Bms Member, Takapari Formation. The FeO: 1/3 $K_2O$: CaO Wt % data are displayed in Fig 7.13. Pakihikura Tephra is found within a thick tuffaceous sand sequence as a 0.5 m white vitric tephra bed, interpreted as being deposited within a marginal estuarine environment.

The source of the Pakihikura Tephra is unknown, however, two ignimbrites erupted from the Mangakino caldera have $^{40}Ar/^{39}Ar$ ages consistent with the zircon and glass FT ages of the Pakihikura Tephra (Wilson, 1986; Brigggs *et al,* 1993). Difficulties matching the Pakihikura Tephra with its correlative ignimbrite are: limited exposure, partial welding and extensive vapour phase alteration of the ignimbrite sheets (Pillans *et al*, 2005). The Pakihikura Tephra occurs within the upper regessive part of Cycle 22 which is correlated with late MIS 55 and early MIS 54 (Pillans *et al*, 2005). Pillans *et al*, (2005) provide an ITPFT age of 1.58 ±0.08 Ma and an astronomically calibrated age of 1.60 Ma.

## 7.3.8 Tephra grain size analysis

Grain size analysis was conducted on 3 tephra samples and 1 tuff sample from the Lower Pohangina Valley: Kawakawa, Pakihikura, and Mangapipi Tephras and Potaka Pumice. As expected there is a contrast in grain size between the fluvially deposited Potaka Pumice and the aerially deposited Kawakawa, Mangapipi and Pakihikura Tephras (Fig 7.15). The mean grain size is 270 µm which is substantially coarser than the mean grain sizes of 32 – 44 µm for the other aerially deposited tephras. The Potaka Pumice also has a fine skewed distribution which is characteristic of a fluvial environment where high quantites of suspended sediments are entrained. The sedimentary structures including cross bedding and channel cut and fill structures in the Potaka Tephra are consistent with a high energy sedimentary environment.

The Mangapipi and Pakihikura Tephras were deposited as airfall products within a backswamp/estuarine environment 1.51 Ma and 1.58 Ma respectively. They occur within the carbonaceous sandy mudstone sequence of Bms Member, Takapari Formation. These two tephras share a grain size distribution very similar to the Kawakawa Tephra. Both tephras have internal stratification, and are preserved within fine grained laminated sediments charactristic of a low energy mudflat/back swamp environment. Based on the sedimentological and grain size characteristics, both Pakihikura and Mangapipi Tephras are interpreted to have been preserved in Pohangina as primary airfall products. In some other places both these tephras are tuffaceous with signs of reworking by fluvial processes within Bms and Css members, Takapari Formation.

Fig 7.14: Grain size distribution curve of the fluvially deposited Potaka Pumice compared with grain size distributions of aerially deposited Tephras.

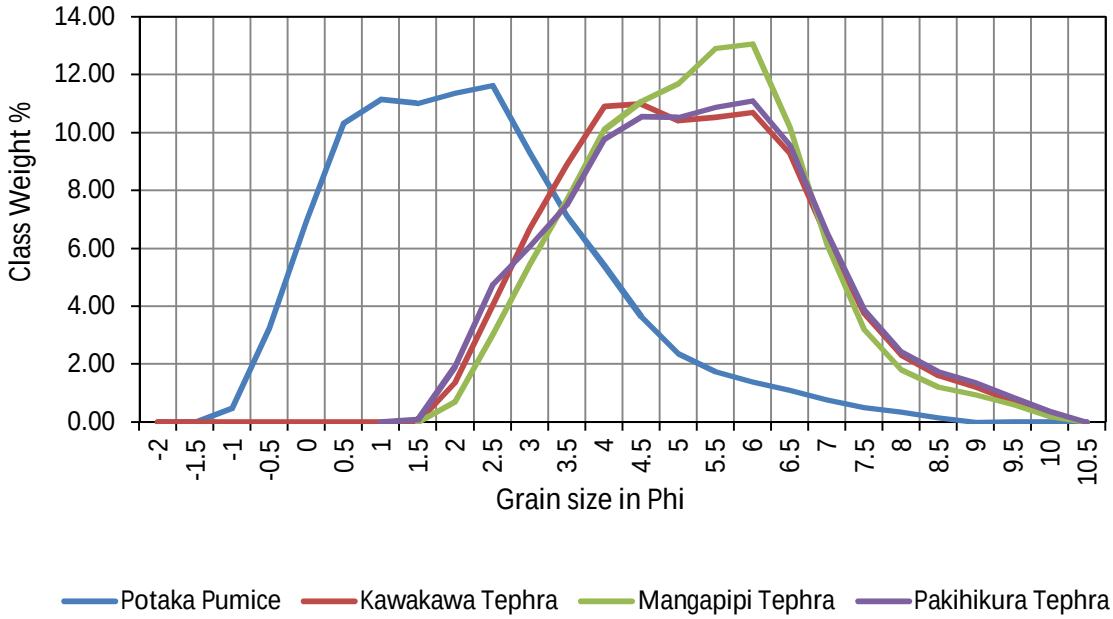


Table 7.5: Grain size distribution statistics for Kawakawa Tephra, Potaka Pumice, Mangapipi Tephra and Pakihikura Tephra:

| Tephra | Grain size statistic | Geometric μm | Logarithmic ϕ | Description |
|---|---|---|---|---|
| Kawakawa Tephra (T3) | Mean | 44.23 | 4.499 | Fine grained tephra |
| | Sorting | 3.754 | 1.909 | Poorly Sorted |
| | Skewness | -0.049 | 0.049 | Symmetrical |
| | Kurtosis | 0.901 | 0.901 | Mesokurtic |
| Potaka Pumice (T1) | Mean | 270.0 | 1889 | Coarse grained tephra |
| | Sorting | 3.252 | 1.702 | Poorly Sorted |
| | Skewness | -0.154 | 0.154 | Fine Skewed |
| | Kurtosis | 1.014 | 1.014 | Mesokurtic |
| Mangapipi Tephra (T5) | Mean | 32.45 | 4.946 | Fine Grained Tephra |
| | Sorting | 2.797 | 1.484 | Poorly Sorted |
| | Skewness | 0.028 | -0.028 | Symmetrical |
| | Kurtosis | 0.957 | 0.957 | Mesokurtic |
| Pakihikura Tephra (T4) | Mean | 33.22 | 4.912 | Fine Grained Tephra |
| | Sorting | 3.232 | 1.692 | Poorly Sorted |
| | Skewness | -0.015 | 0.012 | Symmetrical |
| | Kurtosis | 0.961 | 0.961 | Mesokurtic |

Kawakawa Tephra (25.5 ka) is a known airfall product preserved within the Ohakean loess sequence on the Ratan Terrace of Pohangina Valley. It has a symmetrical, mesokurtic grain size distribution with a mean grain size of 44.23 µm.

### 7.3.9 Paleoenvironmental reconstruction

Rhyolitic volcanism began within the TVZ at 1.6 Ma at the site of the Mangakino caldera (Houghton *et al*, 1995). This volcanism is recorded within the Whanganui Basin approximately 200 km south of the TVZ, and within the Mangatarata and Mangahao Formations on the eastern side of the Ruahine Range (Shane, 1991). At this time (Early Castlecliffian) a series of four cyclothems are recorded within Takapari Formation, driven by changes in eustatic sea level, sediment provenance, sedimentation rate, and accommodation space. A change from shallow marine/transitional into terrestrial/transitional depositional environments occurs between Bms Member and Css Member. This basinward regression of the maximum flooding surface is likely to have been caused by a combination of tectonic uplift (of the Mt Bruce block) and increased volcaniclastic sedimentation from TVZ.

There is a marked similarity between the volcaniclastic facies of the Takapari, Mangatarata and Mangahao Formations, which are present on both sides of the present day Ruahine Range. Regional uplift of the Mt Bruce in the Wairarapa at 1.5 Ma (Beu, 1995), blocked off the southern end of the Ruataniwha Strait leading to its closure, as regional uplift also commenced in the Hawkes Bay and Ruahine Ranges. This regional uplift lead to an east-west drainage across the current day Manawatu Gorge, and a marine regression marking the closure of the Manawatu Strait.

By the time the Rewa Pumice (1.2 Ma) was deposited into sedimentary basins on both sides of the main axial ranges, no marine connection existed near the former Manawatu Strait. Volcaniclastic facies are restricted to terrestrial and marginal marine depositional environments. The marked similarity of Mid Castlecliffian volcaniclastic facies on both sides of the main axial ranges must therefore be a combination of: a) widespread ignimbrite sheets which were deposited across the entire span of the North Island, i.e. from east to west, b) similar erosion and fluvial transportation from the distal areas of the unwelded ignimbrite sheets into the sedimentary basins, c) available accommodation space within sedimentary basins on both sides of the main axial ranges, d) an equal overall effect of glacioeustatic sea level fluctuations causing cycles of marine regression and transgressions through this period, which is reflected in alternating sequences of changing depositional environments.

# Chapter 8

# Kaimatira Pumice Sand Formation

The Kaimatira Pumice Sand Formation (Fleming 1953) is the basal formation of the Kai Iwi Group. This formation marks the first influx of Potaka Pumice into the Whanganui Basin. The Potaka Pumice is used as the base for the Kai Iwi Group due to its widespread and voluminous nature, allowing basin wide correlation to be made. The Kaimatira Pumice Sand Formation is dominated by shallow marine deposition, including large thicknesses of laminated pumiceous sands and intercalated mud beds. Cross bedded tephric sand units also make up a minor component of this formation (Seward, 1976).

On the western side of the Whanganui Basin the Superior Oil Company (Feldmeyer *et al*, 1943) mapped the Coutts Creek Horizon which was later correlated by Fleming (1953) with the Kaimatira Pumice Sand Formation. On the east side of the Whanganui Basin the Superior Oil Company (Feldmeyer *et al*, 1943) mapped a horizon they called the Kimbolton Ash, this horizon was later shown by Te Punga (1952) to be the Potaka Pumice. Te Punga (1952) was the first to introduce the name 'Potaka Pumice' and traced its extent in the eastern Whanganui Basin. The first influx of Potaka Pumice into the Whanganui Basin has now been shown by Seward (1976) and Pillans *et al* (2005) to be part of the Kaimatira Pumice Sand Formation. This correlation is based on stratigraphic position, field character and glass chemistry.

## 8.1 Cross Bedded Sandstone Member

### Lithological description

Code: Kp

Rock type: Sandstone with carbonaceous mudstone and lignite layers.

Colour: Grey (5Y 6/1) to yellow (5Y 7/6) sands, grey (5Y 5/1) muds and black (5YR 2.5/1) lignite.

Hardness: Weakly consolidated, soft sands.

Weathering: Moderately weathered, secondary iron oxides present.

Grain size: Fine sandy mud to granule sand.

Texture: silty mud to gritty sand texture.

Crystals/minerals: Quartz, feldspar, iron oxide.

Thickness: Approximately 10 to 17 m

Type section: Bridge across Whareroa Stream on Awahou South Rd, Broadlands Station, Pohangina (WGS84 40 °16'46.90"S, 175°46'25.98"E, elev 80 m). Access via Awahou South Rd with express permission of the land holders.

# 8.2 Tephrochronology

## 8.2.1 Potaka Pumice

The reference section for the Potaka Pumice is located at Rewa Hill (WGS84 39°59'23.84"S, 175°37'49.54"E, elev 177 m) (Seward, 1976). Seward (1976) correlated the Potaka Pumice with the Kaimatira Pumice Sand Formation mapped by Fleming (1953). The Potaka Pumice has previously been referred to as the Kaimatira Pumice Sand (Fleming, 1953), Kidnappers Tuff (Kingma, 1971), and more recently Potaka Tephra (Pillans *et al,* 2005). In this study the term Potaka Pumice is used as the Potaka Pumice does not contain an airfall tephra in the lower Pohangina Valley.

The Potaka Pumice is an important marker horizon in many Pleistocene sequences, which would otherwise lack numerical age control. It has been dated using the ITPFT method at 1.05 ± 0.05 Ma (Pillans *et al*, 2005). It has been used to correlate between stratigraphic sections at Oroua River and Rewa Hill in Manawatu-Rangitikei, Mangatewaiiti Stream, Mangatewainui Stream, Cape Kidnappers coastal section, Makaroro Stream and Leader River in the Hawkes Bay; allowing inter-basin and intra-basin correlations to be made between sections.

The Potaka Pumice is a secondary erosion product of ignimbrite sheets produced during large eruptions from the TVZ. The source vent is uncertain although ingnimbrites of a similar age are known to have been erupted from the Mangakino caldera, making this a likely source for the Potaka Pumice (Wilson *et al*, 1995; Pringle *et al*, 1992). The Potaka Pumice has been shown to be a composite deposit correlated to both the Rocky Hill and Kidnappers ignimbrites (Wilson *et al*, 1995).

Fig 8.1: Map of the North Island, New Zealand, showing the minimum inferred original extent (black outline) of the Kidnappers ignimbrite. The east and northeast limit of the Kidnappers ignimbrite is uncertain owing to uplift and erosion. Filled circles are sites visited by Wilson, *et al*, (1995) where Kidnappers ignimbrite was present. Black hollow circles are sites where Potaka Pumice has been documented, red filled circle is the locality of Potaka Pumice in this study. The orange filled circle shows the location of the Mangakino Caldera within the Taupo Volcanic Zone. Adapted from Wilson *et al*, (1995).

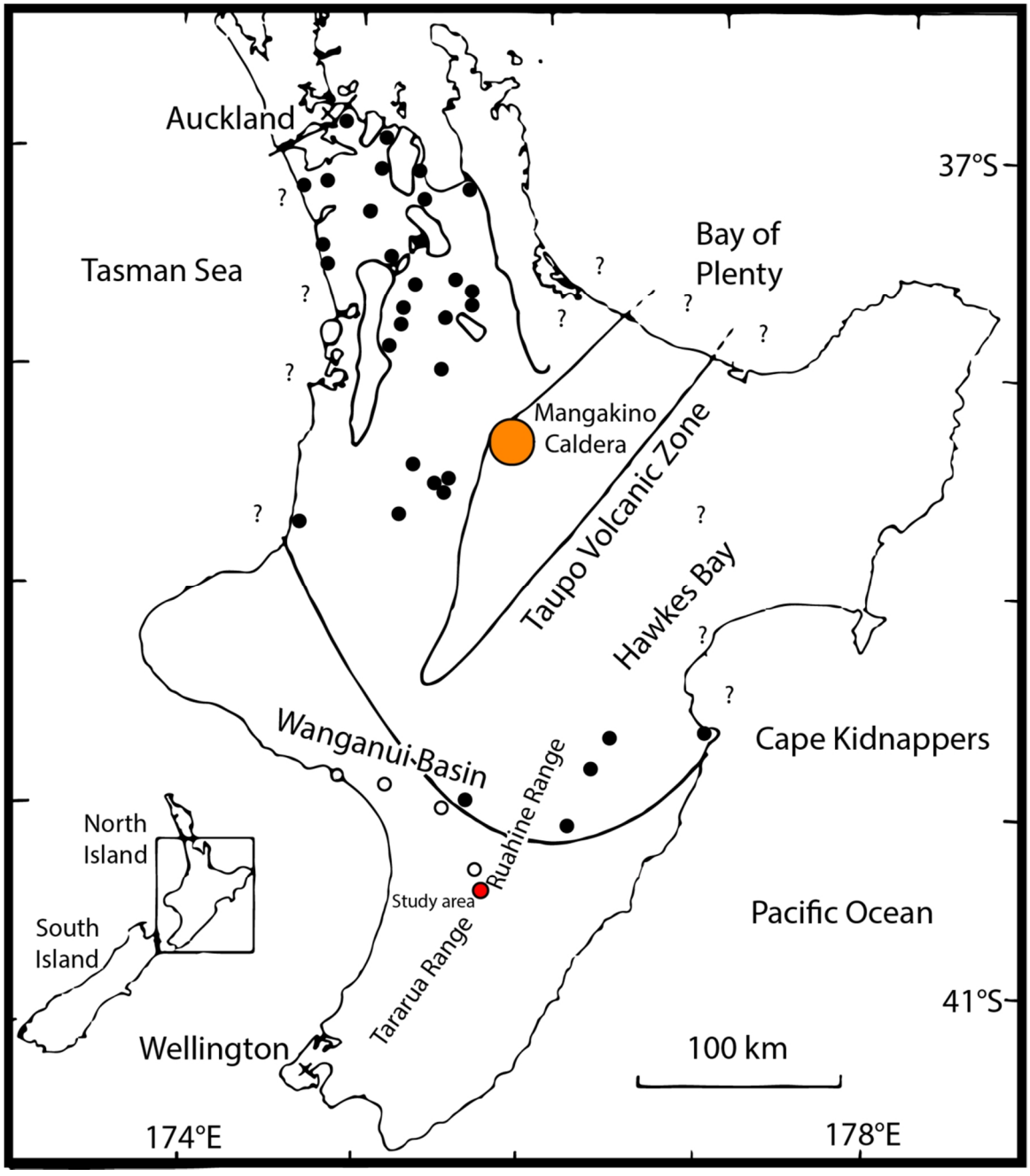

Reworked tephra and pumice with Potaka chemistry occurs as large scale trough cross bedded, tidally influenced pebbly shell conglomerate in the basal transgressive deposits of MIS 27 (Cycle 34) at the Castlecliff section (Pillans, *et al,* 2005). Potaka Pumice contains a chemical signature which allows it to be recognised and correlated in major stratigraphic sections across the Whanganui Basin. High rates of sediment supply to the coast from reworking of volcanic sediment during the MIS 27 transgression resulted in sediment supply keeping pace with the rise in sea level. As a result one of thickest transgressive deposits in the Whanganui Basin cyclothem record was preserved (Pillans *et al*, 2005).

A key characteristic of Potaka Pumice is the occurrence of compositional variation within its geochemistry, reflecting variation in the eruptive phase (Shane, 1994). A segragation of compositions indicates the initial eruptive phase was more FeO and CaO rich (Appendix 1.5).

### 8.2.2 Paleoenvironmental reconstruction

Shane (1991) reports Potaka Pumice clasts up to 150 mm in size at Mangatewaiiti and Mangatewainui Streams (approximately 250 km from TVZ source) in Hawkes Bay on the east side of the Ruahine Ranges. The relatively large size of these clasts suggests the pumice is derived from the unwelded, distal portion of the ignimbrite sheet, which is easily erodible compared with the proximal welded ignimbrite sheet found closer to the TVZ. The Kidnappers and Rocky Hill ignimbrite sheets are thought to be the source of the Potaka Pumice (Wilson *et al,* 1995). The Kidnappers ignimbrite sheet is found over an area of 385 $km^2$ surrounding the source vent (Fig 8.1) (Wilson *et al,* 1995). The distal portion of this exceptionally wide spread ignimbrite sheet would have easily reached the headwaters of paleo-river systems feeding into the southeastern Whanganui Basin.

The transport of pumice from the distal ignimbrite sheet into the present day Pohangina Valley requires a paleo-river system flowing southeast from the area now occupied by the northern Ruahine Ranges. The Kidnappers and Rocky Hill ignimbrite sheets erupted from the Mangakino Caldera around 1 Ma must have reached (at the very least), the headwaters of the paleo-river system feeding into the south eastern Whanganui Basin.

The Potaka Pumice was deposited into shallow marine and estuarine settings along the paleo-coastline of the Whanganui Basin. The tephra is found up to 40 km inland from the current coastline, showing a major marine regression and subsequent change in the position of the coast over the last million years. This has been caused by regional uplift in the Whanganui - Manawatu region. This suggests that the relief of the Whanganui - Manawatu

area was more of a subdued coastal plain with a gentle gradient into the Whanganui Basin, compared with the steeper topography found in the area today.

## Summary

The Kaimatira Pumice Sand Formation is interpreted as a transgressive shallow marine to fluvial flood deposit formed following the emplacement of a large ignimbrite sheet from the TVZ (Wilson *et al*, 1995). The identification of this formation is based on the presence of fluvially transported Potaka Pumice. The volcaniclastic sediments which comprise this formation have been transported south into the Whanganui Basin by a paleo-river system with its headwaters located somewhere within the distal area of the ignimbrite sheets. This has resulted in a period of rapid vertical accretion, as the paleo-river system has deposited vast quantities of volcaniclastic sediments in a series of overbank flow events. Commonly a thin lignite layer (<100 mm) caps the Kaimatira Pumice Sand Formation representing infilling of accomodaion space and the establishment of non-marine conditions in places.

# Chapter 9
# Kai iwi Group

The Kai Iwi Group is composed of thirteen separate units (Table 9.1), with reference sections near Kai Iwi Stream, Castlecliff, and Whanganui City (Abbott & Carter, 1994). Hutton (1886) and Park (1887) were among the first to describe the sediments of the Kai Iwi Group. They focused their work on the units containing well preserved mollusc fossils within the Castlecliff section near Whanganui. Later Fleming (1953) produced a detailed record of the Kai Iwi Group sediments in Geological Survey Bulletin 52 on the Whanganui and Waverley subdivisions. This piece of work was the first detailed subdivision of the Castlecliff section and still forms the basis of the classification system used today.

Abbott and Carter (1994) further subdivided Fleming's (1953) classification of the Kai Iwi Group and interpreted the sequences in terms of sequence stratigraphy. The base of the Kai Iwi Group, set at the base of the Kaimatira Pumice Sand Formation (Chapter 8), is interpreted as a thick transgressive systems tract marking the influx of volcaniclastic sediment (Potaka Pumice) into the Whanganui Basin. The Kai Iwi Group is composed of Kai Iwi, Omapu, Westmere and Kaikokopu units. The Kupe Tephra occurs within the upper part of the Group and is overlain by the Upper Kai Iwi Shellbed and Upper Kai Iwi Siltstone.

In this study a change in stratigraphic nomenclature occurs at the top of the Takapari Formation. This is based mainly on the occurrence of the Kaimatira Pumice Sand Formation (1 Ma) which allows the stratigraphy of the Pohangina Valley to be correlated to Whanganui Basin stratigraphic nomenclature.

The difference in sedimentary preservation from western to eastern Whanganui Basin is justification for maintaining a local classification system for all formations older than 1 Ma in Pohangina Valley. The sedimentary record preserved in Pohangina is sufficiently distinct and lack of absolute ages within the Konewa and Komako Formations, are the reasons for maintaining Carter's (1972) stratigraphic nomenclature for all formations older than 1 Ma. However, it is proposed that the base of the Kaimatira Pumice Sand Formation (Kai Iwi Group) mark the upper contact of the Takapari Formation. This provides a readily identifiable upper contact to Carter's (1972) Takapari Formation, which up until this point has remained undefined. It is proposed to use Whanganui Basin stratigraphic nomenclature to describe all formations and members younger than 1 Ma. This correlation will allow the Mid Castlecliffian strata of Pohangina Valley to be tied into the cyclothemic record of the western Whanganui Basin, and thereby linked to the marine isotope stages (Fig 7.2).

Table 9.1: Formations of the Kai Iwi Group (Proust *et al,* 2005).

| Group | Formation |
|---|---|
| Kai Iwi | Upper Kai-Iwi Siltstone |
| | Upper Kai-Iwi Shellbed |
| | Kupe Formation |
| | Upper Westmere Siltstone |
| | Upper Westmere Shellbed |
| | Kaikokopu Shell grit |
| | Lower Westmere Siltstone |
| | Lower Westmere Shellbed |
| | Ophiomorpha Sand |
| | Omapu Shellbed |
| | Lower Kai-Iwi Siltstone |
| | Lower Kai-Iwi Shellbed |
| | Kaimatira Pumice Sand |

The Whanganui Basin straigraphic nomenclature used is adopted from work by Fleming (1953); Abbott and Carter (1994); Pillans *et al*, (2005); and Naish *et al,* (2005). A table of the stratigraphic nomenclature used in this study is provided in Chapter 4 (Table 4.1).

## 9.1 Red Conglomerate Member

### Lithological description

Code: Rc

Rock type: Conglomerate with rounded, pebble sized clasts. Displays rip up mud clasts near base. Contains lateral facies change to cross bedded, coarse sands with pebble clasts.

Colour: Grey (5Y 5/1) to reddish yellow (5YR 6/8) coloured clasts in a light red (2.5YR 6/6) iron oxide matrix.

Hardness: Very hard, iron oxide cemented, resistant to erosion.

Weathering: Moderately weathered, secondary iron oxides present.

Grain size: Clasts range in size from 1-50 mm, fine grained mud rip up clasts present, occasional coarse sand layers occur within the lateral variations.

Texture: Gritty sandy texture.

Crystals/minerals: Quartz, feldspar, iron oxide.

Thickness: Approximately 8 to 14 m

Type section: Whareroa Stream, Telfords Farm, Pohangina (WGS84 40 °14'08.24"S, 175 °47'04.17"E, elev 97 m). Access via Awahou South Rd with express permission of the land holders.

Rc Member has been kept as a separate Member of Kai Iwi Group, due to its distinctive character in the landscape, forming bluffs and ridge tops. It is more resistant to erosion compared to the overlying eQk Member or the underlying Kp Member, because of its iron oxide cemented matrix. The iron oxide matrix also gives this member a distinctive red colouring.

## Facies Analysis

Rc Member is dominated by conglomerate deposits, which show significant lateral facies variation across the mapping area. Due to the variable nature of this member two main sections will be used in facies analysis.

In the first analysis river channel and bar environments are identified through facies analysis. The facies are dominanted by clast supported conglomerate deposits (Fig 9.1). This first facies association represents the most common facies within Rc Member. They are associated with erosional contacts and rip up structures.

Fig 9.1: Rc Member, Kai Iwi Group, Broadlands Station, Pohangina (WGS84 40°17'43.32"S, 175°46'15.20"E, elev 122 m).

## 9.1.1: Rc Member, Kai-iwi Group, Fig 9.3, Muangatukurangi Stream, Broadlands Station, Pohangina.

Facies Al: Fine sand, laminated to massive bedding

The Facie Al is composed of fine, laminated to massive bedded sands. The individual beds range in thickness from 500-1500 mm. Laminations are generally thick ranging in size from 10- 15 mm. The sediment is well sorted and dominated by quartzofeldspathic minerals.

*Interpretation:*

Facies Al is interpreted as an alluvial over bank deposit located near a river source. The absence of gravels within this flood deposit is due to the nature of sediment transport in the river, which mainly confines gravels to the river channel and bars whereas finer sands and silts are deposited on the surrounding flood plain during high flow, with coarse sands to gravel near the river and finer silts and muds farther away.

Table 9.2: Lithofacies of Rc Member, Kai Iwi Group stratigraphic log 9.2. Facies codes are modified from Smith (1987); Horton & Schmitt (1996); Miall (1977); and Waresback & Turbeville (1990).

| Facies code | Description | Interpretation |
|---|---|---|
| Al | Fine sand and silt, laminated to rippled bedding | Alluvial floodplain deposit, suspension fall out |
| Fsf | Matrix supported conglomerate with rip up structures of silt | Fluvial scour and fill channel, from changing course of a meandering paleo-river system |
| Fc | Unsorted clast supported conglomerate | Fluvial channel deposit |
| Gs | Matrix supported, sandy, cross laminated conglomerate | Point bar deposit, lateral accretion |

Facies Fsf: Matrix supported conglomerate with rip up structures of silt

Facies Fsf is composed of a very poorly sorted, matrix supported conglomerate. Isolated large rip up clasts of silt (long axis up to 400 mm) are present. Facies Fsf is 500 mm thick.

The matrix is composed of fine sand. Clasts range in size from cobbles to pebbles. The lower contact of the bed is erosional.

*Interpretation*

Facies Fsf is interpreted as a fluvial scour and fill channel. The erosional base of the facies is a result of channel migration in a meandering river system. The river has eroded into the silts and sands of the adjacent alluvial plain and incorporated “chunks” as rip-up clasts. While some of the eroded material has been incorporated as rip-up clasts, much of the fine matrial would have been carried farther downstream.

Facies Fc: Unsorted clast supported conglomerate

Facies Fc is composed of conglomerate with few bedding structures apart from normal grading. The conglomerate is composed of rounded, pebble size clasts and predominatly equant in shape (Fig 9.4). Inividual beds range from 1 to 3 m in thickness. The conglomerate is clast supported.

Fig 9.2: Base of Rc Member, showing Facies Fsf deposited by fluvial scour and fill processes, Telfords Farm, Pohangina (WGS84 40° 14’07.23”S, 175°47’04.24”E, elev 101 m).

,

Facies Fc is interpreted as a fluvial deposit. The equant shape of clasts supports this fluvial deposition interpretation. Fines from the bedload are entrained by the current enabling the formation of a clast supported conglomerate with very little matrix; characteristic of a channel deposit. During deposition clasts have been moved along the bed via rolling. Fine silts, clays and sands have been moved further downstream via suspension

Facies Gs: Matrix supported, cross laminated conglomerate

The Facies Gs is characterised by beds of matrix supported conglomerate. The conglomerates display normal grading; many of the beds grade into sand with sporadic pebbles spread throughout. Large scale cross lamination and trough crossbedding are present. The size of clasts ranges from cobbles through to pebbles. The matrix is composed of coarse to fine sand. Lenses of fine sand occur within these beds and follow the same pattern of cross lamination as the gravels.

*Interpretation*

This facies is interpreted as point bar deposits, formed within a meandering paleo-river system. Helical flow transports sediment, eroded from the cut bank, along the bottom of the river and then deposits it via lateral accretion in the point bar. The resulting point bar facies have characteristic normal grading and cross lamination to cross beds. The erosional nature of some of the bedding contacts is due to the meandering nature of the paleo-river system which creates channel cut and fill structures and erosional contacts as the river channels migrate and change course over time.

This type of river changes course frequently and eroding into previously deposited alluvium and re-depositing the sediment in point bars. The paleo-river system had a gravel bed resulting in the dominance of gravels within the point bars. The greater concentration of finer sands and muds in the over bank flow alluvial deposits is a result of sediment transport mechanisms. Gravels are transported along the bed of the river by rolling, while fine sands and mud are held in suspension and therefore are the dominant grain size in alluvial deposits farther from the river bed, during floods events.

Fig 9.3: Stratigraphic log of Rc Member 1st facies analysis, Kai Iwi Group, entrance to Whareroa Stream, Telfords Farm, Pohangina Valley (WGS84 40° 14'07.23"S, 175°47'04.24"E, elev 101 m).

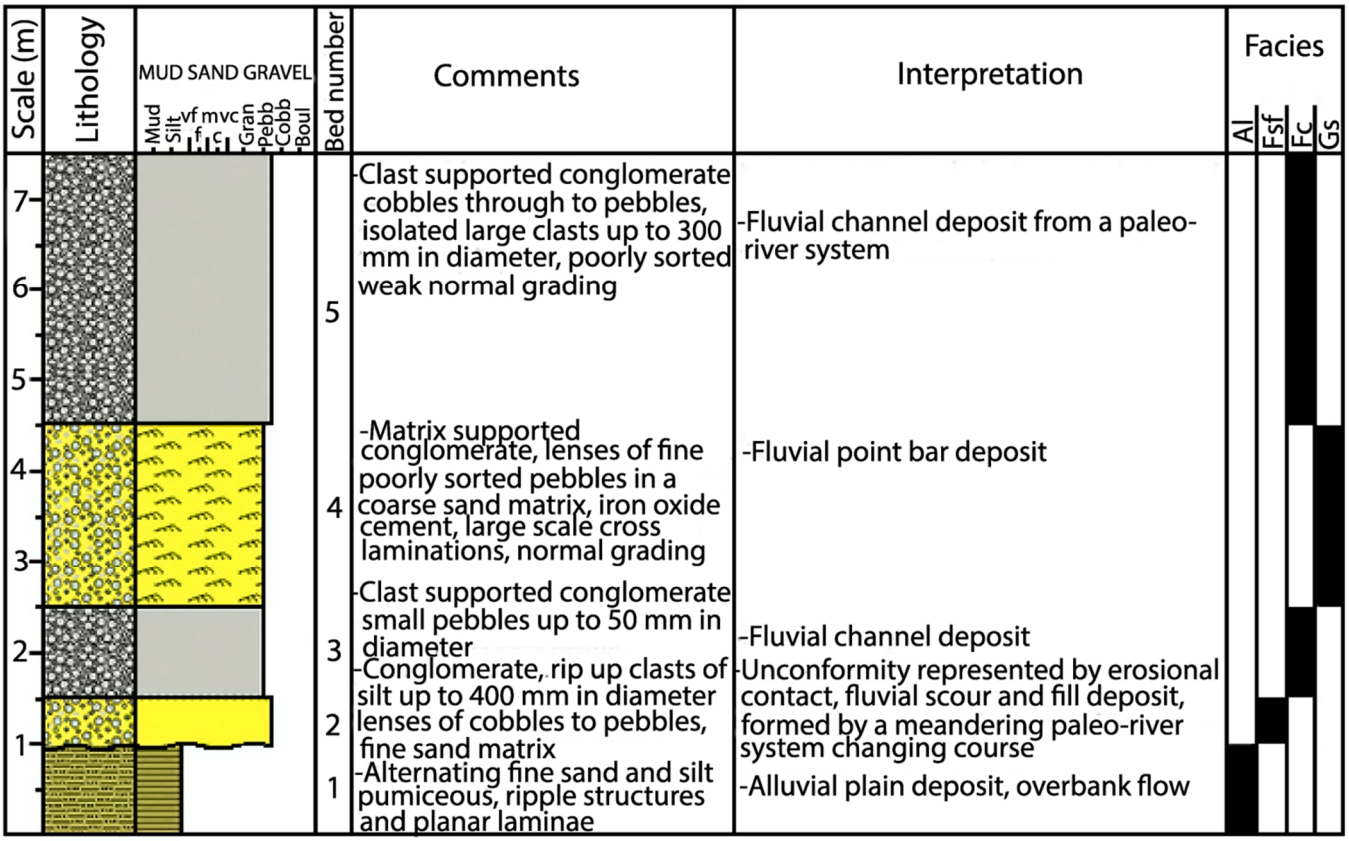


## Key:

### Lithologies

- Siltstone
- Matrix-supported conglomerate
- Clast-supported conglomerate

### Symbols

- Horizontal planar lamination
- Current ripple cross lamination

### Base Boundaries

- Sharp
- Erosion
- Gradational

Fig 9.4: Zingg diagram of facies Fc from the Rc Member, Telfords Farm, Pohangina (WGS84 40°14'07.23"S, 175°47'04.24"E, elev 101 m).

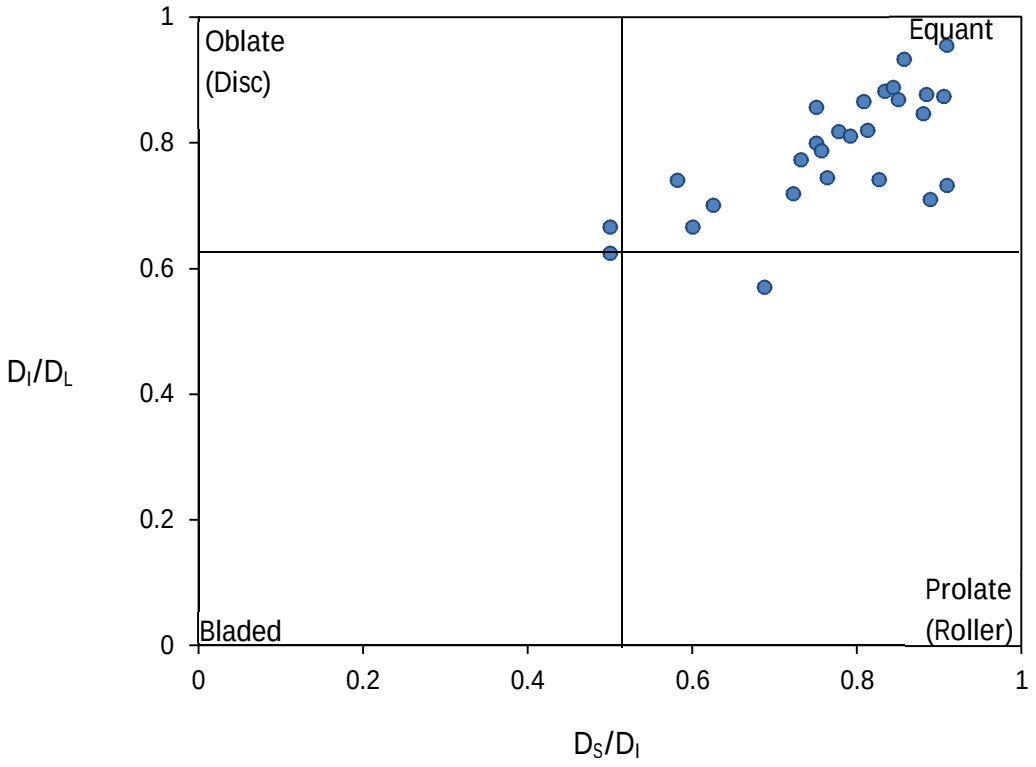


Fig 9.5: Rc Member unconformably overlying Kaimatira Pumice Sand Formation, forming a ridge at Broadlands Station, Pohangina Valley (WGS84 40°15'04.45"S, 175°47'41.10"E, elev 167 m).

## 9.1.2: Rc Member, Takapari Formation, Fig 9.6, Whareroa Stream, Telfords Farm, Pohangina

The second sequence of Rc Member described (Fig 9.6) is dominated by cross laminated to cross bedded, gravelly sands and laminated, clast supported conglomerate. Lenses of silt and fine sand are present along with rare tephra beds. Rc Member undergoes lateral facies change as it is followed north from the mouth of Stallion Stream; it can be traced to a second outcrop in Maungatukurangi Stream (Fig 1.5). Two of the four facies analysed within Fig 9.6; Facies Al and Gs also appear in Fig 9.3 where they are fully described in section 9.1.1; they will therefore not be repeated in the facies descriptions below.

Table 9.3: Lithofacies of Rc Member, Kai Iwi Group, from Fig 9.6. Facies codes are modified from Smith (1987); Horton & Schmitt (1996); Miall (1977); and Waresback & Turbeville (1990).

| Facies code | Description | Interpretation |
|---|---|---|
| Ms | Fine sand and mud with flame structures | Alluvial plain deposit undergone loading during subsequent sedimentation |
| Gs | Matrix supported, cross laminated conglomerate | Point bar deposit, lateral accretion |
| Al | Fine sand, laminated to massive bedding | Alluvial floodplain deposit, suspension fall out |
| Tp | Fine volcanic ash | Airfall tephra from the Taupo Volcanic Zone |

Facies Ms: Fine sand and mud with flame structures

Facies Ms is composed of fine, muddy sand with flame structures. The overall bed thickness is 2 m. Flame structures are present ranging in size from 10-30 mm thick. No primary sedimentary structures are observed. The fine sand is well sorted with an even grain size throughout the beds. The sands are dominated by quartzofeldspathic minerals.

*Interpretation:*

Facies Ms is interpreted as an overbank flow deposit on an alluvial floodplain. The flame structures are interpreted to have been caused by sediment loading of water-saturated mud layers by the deposition of heavier layers of sands above. This type of deposition could occur on an alluvial plain near a paleo-river channel. Fine muds are deposited over the bank of the river during a flood event. Subsequently in a larger flood event, denser sands are

deposited overtop of the muds causing the water to be squeezed upwards, carrying mud with it as the sediments are compressed downward.

The orientation of over turned crests within the flame structures suggests that loading may have been accompanied by some horizontal frictional drag movement between the mud and sand beds during deposition. The presence of flame structures and other water escape structures are often associated with a high sedimentation rate, where rapid vertical accumulation of sediments causes liquefaction and subsequent formation of secondary, sedimentary structures (Boggs, 2011).

Facies Tp: fine grained volcanic ash

The Tp Facies is characterised by a 300 mm thick bed of fine grained volcanic ash. This tephric bed tends to pinch and swell laterally ranging from 200 – 300 mm in thickness. The tephra has a characteristic white colour and very fine, smooth texture. Bedding is massive with no visible stratification.

*Interpretation:*

Facies Tp is interpreted to have been deposited by air-fall. No sedimentary structures, or bedding are visible, and the tephra is of a fine grain size. It is unlikely that this tephra is a fluvially re-deposited volcaniclastic unit as it is not associated with any tuff deposits either directly above or below it. The tephra was likely preserved within an adjacent fluvial environment such as the river flood plain, capable of preserving a thin tephra without erosion or reworking occurring.

Fig 9.6: Stratigraphic log of Rc Member 2nd facies analysis, Kai Iwi Group, Maungatukurangi Stream , Broadlands Station, Pohangina (WGS84 40°15'03.87"S, 175°47'54.67"E, elev 147 m).

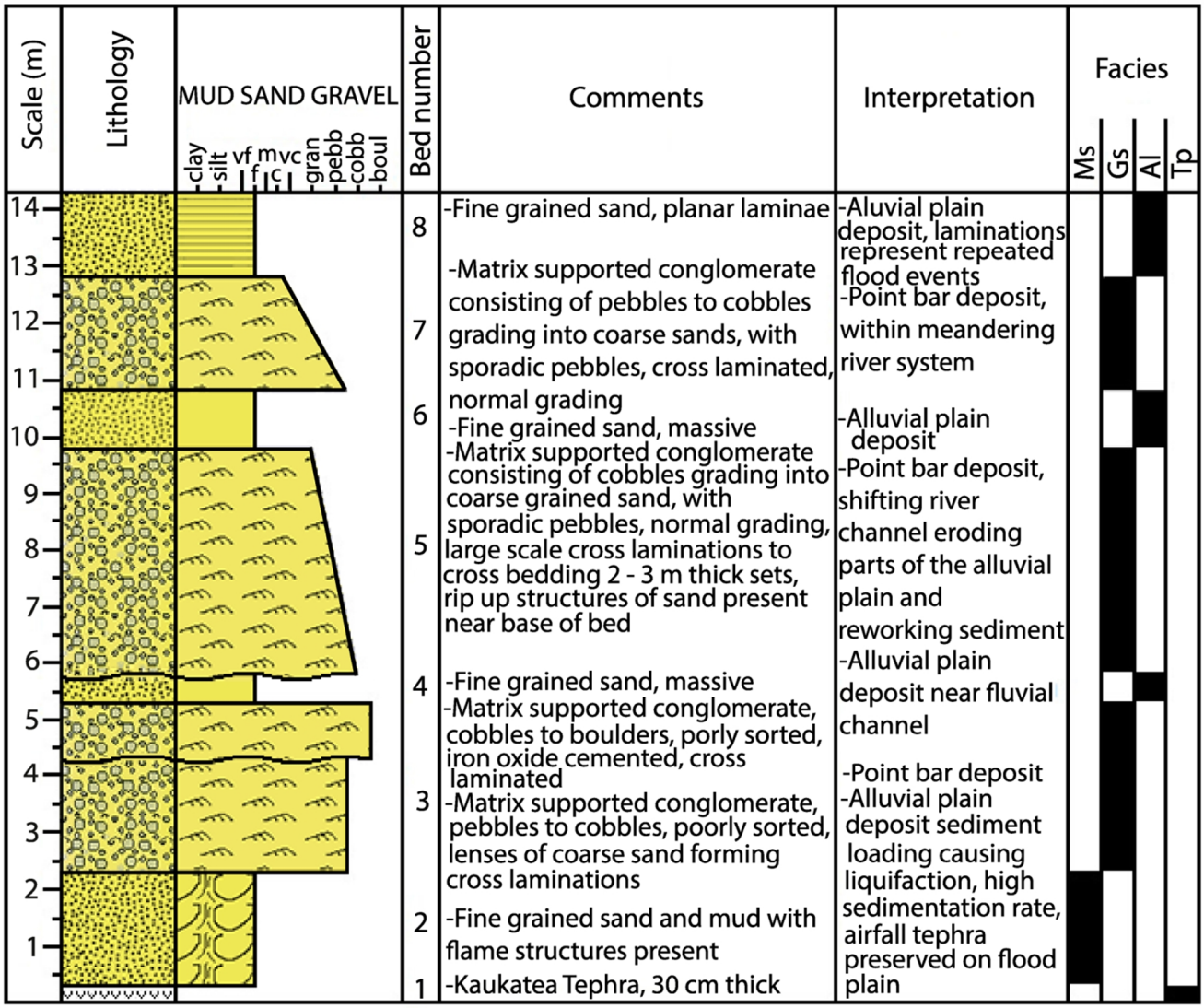


# Key:

Lithologies

- Tephra
- Sandstone
- Matrix-suppported conglomerate

Symbols

- Water structures
- Current ripple cross-lamination
- Horizontal planar lamination

Base boundaries

- Sharp
- Erosional

Fig 9.7: Rc Member, Kai Iwi Group, Maungatukurangi Stream, Broadlands Station, Pohangina (WGS84 40 °14’57.36”S, 175 °47’35.89”E, elev 116 m).

## Interpretation:

In the northern half of the map Rc Member is seen to outcrop twice. Firstly at steep dip angles near the axis of the Pohangina Faulted Monocline, and then again at shallow dip farther to the west. This repetition of outcrop is due to the folding of the strata by thrust faulting, and subsequent exposure caused by high erosion rates in the Pohangina Valley. This same pattern is observed with the Kaimatira Pumice Sand Formation which unconformably underlies Rc Member.

The change in sediment provenance from fluvially deposited Potaka pumice (Kaimatira Pumice Sand Formation) to clast supported greywacke conglomerate (Rc Member) is marked by an erosional unconformity. The soft pumiceous sands of the Kaimatira Pumice Sand Formation have been eroded back by fluvial scour and then gravels (<50 mm in diametre) have become the dominant lithology.

Small clast sizes within Rc Member (<50 mm) suggest that the source of the gravel was relatively distant (> 100 km), based on the effects of downstream fining within modern analouges (Szabó *et al,* 2013). The source of the gravel within Rc Member was likely the Proto-Kaimanawa Ranges which began rising 2.4 Ma (Trewick & Bland, 2012). Erosion of greywacke basement from north of Kuripapango, beginning at 2.4 Ma is evidenced by large alluvial fans and braided river systems found in western Hawkes Bay. This provides direct evidence of actively rising and eroding greywacke basement in the Kaimanawa Ranges during the early Quaternary. A large paleo-river system existed during the deposition of Rc Member, with the ability to transport large quantities of gravel from the central North Island south to the Pohangina area, and into the south eastern Whanganui Basin.

The section of Rc Member in Fig 9.3 is much more condensed than its laterally equivalent counterpart in Fig 9.6. It contains thick beds of clast supported conglomerate, with lesser amounts of silt and sand interbedded between clasts. The clasts are rounded to sub-rounded with the majority of clasts being of an equant shape (Fig 9.4). Clasts measured from Rc Member are consistent with deposition in a fluvial environment, clustering around the equant portion of the zingg diagram (Friedman & Johnson, 1982).

The clast supported conglomerate beds are strongly cemented making them relatively hard and resistant to erosion. Rc Member is approximately 10 m thick; however, laterally it pinches and swells. The change in thickess is interpreted to be both a function of changing preservation potential within the various laterally adjacent, fluvial, depositional environments observed within Rc Member; and fluvial channel migration.

The Kaukatea Tephra is preserved approximately 1 m below the first gravel lenses observed in the Maungatukurangi Stream section of Rc Member (Fig 9.6). This sequence is interpreted as overbank flow deposits in an alluvial plain setting where there is high preservation potential. This contrasts markedly with the erosional, clast supported conglomeratic deposits often found within Rc Member (Fig 9.3) which are characteristic of meandering, fluvial channel deposits.

### 9.1.3 Kaukatea Tephra

Seward (1976) first described the Kaukatea Tephra in Kaukatea Valley near Whanganui City, where it occurs as a 4 m thick tephra with a sharp basal contact over a 14 m thick massive siltstone which in turn overlays Kaimatira Pumice Sand Formation. In Turakina Valley Kaukatea tephra glass shards and pumice occur within the tough cross-bedded Makahou Shell Conglomerate (Van der Neut, 1996). This shell conglomerate is part of the early TST at the base of Cycle 35 (Pillans *et al*, 2005). In the Castlecliff section Kaukatea Tephra occurs within the Lower Kai Iwi Shellbed, above the Kaimatira Pumice Sand Formation (Pillans *et al*, 2005).

Seward (1974, 1976) determined a glass FT age of 0.57 ± 0.08 Ma at the reference locality in Kaukatea Valley. Pillans *et al*, (2005) revised that age using ITPFT to 0.86 ± 0.08 Ma. Based on its stratigraphic position Kaukatea Tephra has an astronomically tuned age of 0.90 Ma and is correlated with MIS 25.

In Maungatukurangi Stream, Pohangina Valley, Kaukatea Tephra occurs as a 30 cm thick airfall tephra preserved within over bank debris flow deposits. It occurs approximately 15 m above Kaimatira Pumice Sand Formation. 15 m of fine, laminated, pumiceous sand separates the Kaimatira Pumice Sand from Kaukatea Tephra. Approximately 1 m above the Kaukatea Tephra lies gravel lenses of Rc Member, Kai Iwi Group.

In Pohangina Valley, the preservation of Kaukatea Tephra is associated with a major lateral facies change of Rc Member. Kaukatea Tephra is only found where Rc Member contains point bar, and overbank flow deposits. In other areas where Rc Member is characterised by clast supported conglomerate, interpreted as fluvial channel deposits, Kaukatea Tephra is absent. This relationship demonstrates the potential for a river flood plain to preserve a tephra layer, by subsequent burial during alluvial sedimentation. While closer to the actively shifting channels of the river, the preservation potential of an aerially deposited tephra layer becomes significantly lower.

## 9.2 Sandstone Member

### Lithological description

Code: eQk

Rock type: Sandstone

Colour: Pale olive (5Y 6/4) to yellow (5Y 7/6) with light red (2.5YR 6/8) iron oxide present.

Hardness: weakly consolidated.

Weathering: Moderately weathered, secondary iron oxides present.

Grain size: Fine to coarse grained sand with intercalated fine grained muds.

Texture: Fine sand.

Crystals/minerals: Quartz, feldspar, hornblende, mica, titanomagnetite.

Thickness: Approximately 80 m

Type section: Maungatukurangi Stream, Broadlands Station, Pohangina (WGS84 40°14’08.24”S, 175°47’04.17”E, elev 97 m). Access via Awahou South Rd with express permission of the land holders.

## 9.2.1 Facies Analysis of eQk Member, Kai Iwi Group, (Fig 9.9)

eQk Member is composed of dominantly fine sand. This member displays fine laminae to fine lenticular bedding. Grain size ranges from mud through to granular sand. Grain size data taken from this unit demonstrate a well sorted, symmetrical distribution curve (Appendix 2.2). A 40 metre section of eQk Member (Fig 9.9) located in Maungatukurangi Stream (WGS84 40°14'55.31"S, 175°47'26.73"E elev 111 m) was chosen for detailed facies anaylsis. Two of the facies which occur in eQk Member, Facies Ss and Facies MFS both occur in Fss Member, Komako Formation and are fully described within section 5.3.1. The remaining three facies (Ssh, Cs and Fs) are described below:

Table 9.4: Lithofacies of eQk Member from Fig 9.9, Kai Iwi Group, Pohangina. Facies codes are modified from Smith (1987); Horton & Schmitt (1996); Miall (1977); and Waresback & Turbeville (1990).

| Facies code | Description | Interpretation |
|---|---|---|
| MFS | Fine to coarse sands with common mud rip up clasts | Marine flooding surface formed during transgression, erosional scour, wave action |
| Ssh | Laminated fine to medium sand with mud lenses | Siliciclastic inner most shelf environment, suspension fall out |
| Ss | Fine laminated medium to very coarse sands | Siliciclastic lower shoreface environment, tidal deposition, wave action |
| Cs | Cross bedded medium to very coarse sands | Migrating sand bar and dunes in a shallow marine shoreface environment, tidal deposition & wave action |
| Fs | Fine laminated sand | Foreshore environment, wave action |

Facies Ssh: Laminated fine to medium sand with mud lenses

Facies Ssh is characterised by fine to medium grained, laminated sand with mud lenses (Fig 9.8). Beds range in thickness from 5–7 m. Laminations are thin at between 2–5 mm. Alternating mud and sand laminae are present with sand being the dominant grain size. The grain size follows a general trend of coarsening up-section, starting with fine grained sand and grading into medium grained sands.

Interpretation

Facies Ssh is interpreted as being deposited during the HST. The environment of deposition is interpreted as a siliciclastic inner most shelf. Mud lenses are deposited during fairweather

low energy periods when finer silt and clay falls from suspension. Laminated fine and medium grained sand is deposited by a combination of wave sorting within a nearshore environment and then further transportation via saltation and rolling out into a shelf environment. Seaward transportation of the sand sized fraction of the sediment is initated by rip and tidal currents, moving offshore.

Fig 9.8: eQk Member, Kai Iwi group, planar laminations and lenticular bedding, Maungatukurangi Stream, Broadlands Station, Pohangina (WGS84 40 °14'57.36"S, 175 °47'35.89"E, elev 116 m) scale is 5 cm.

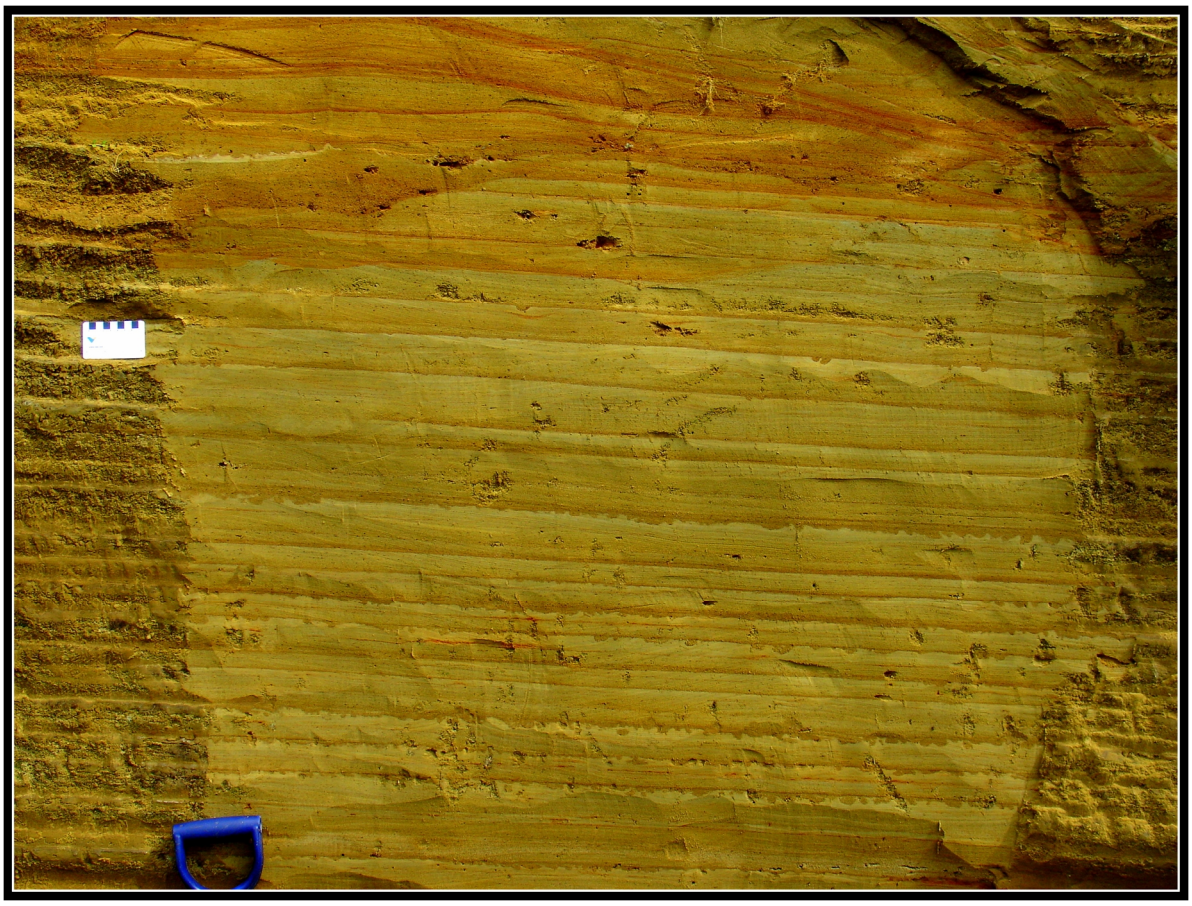

Facies Cs: Cross bedded medium to very coarse sands

Facies Cs is represented by cross bedded medium to very coarse sands. Sands are commonly pumiceous with some isolated large grits up to 3-5 mm in diameter. Trough cross bedding is more common in bed 10. While herringbone cross beds separated by planar laminae are seen in beds 3 and 7. Bed thickness ranges from 0.5–5 m. Reverse grading from medium grained sands to very coarse and granule sized pumiceous sands is present within bed 10.

*Interpretation:*

This facies is interpreted to have been formed in a shallow marine, shoreface setting. Large trough cross beds are interpreted as elongated migrating bars built up by tidal flow within the near shore environment. Thinner alternating herringbone and planar laminae sedimentary structures are considered to represent smaller dune forms on the sea bed, forming in the same zone as the sand bars just back from the foreshore. Tidal currents and wave action both play a critical role in the formation of these geomorphic features.

Facies Fs: Fine laminated sand

Facies Fs is composed of laminated fine sand. Sedimentary structures are dominated by parallel laminations which are characteristically thin, ranging from 1- 5 mm. Bed thickness is 3 m. The fine grained sands are well sorted and dominated by quartzofeldspathic minerals.

*Interpretation:*

Facies Fs is interpreted as a foreshore deposit in a high energy shallow marine environment. Very well sorted sand is a result of wave action constantly reworking the beach environment. The high flow regime planar laminations are characteristic of a near-shore beach environment. Fine silt and clay sized particles are winnowed out and carried farther seaward creating a well sorted fine grain size.

Fig 9.9: Stratigraphic log of eQk Member, Kai Iwi Group Maungatukurangi Stream, Broadlands Station, Pohangina Valley (WGS84 40°14'55.31"S, 175°47'26.73"E elev 111 m).

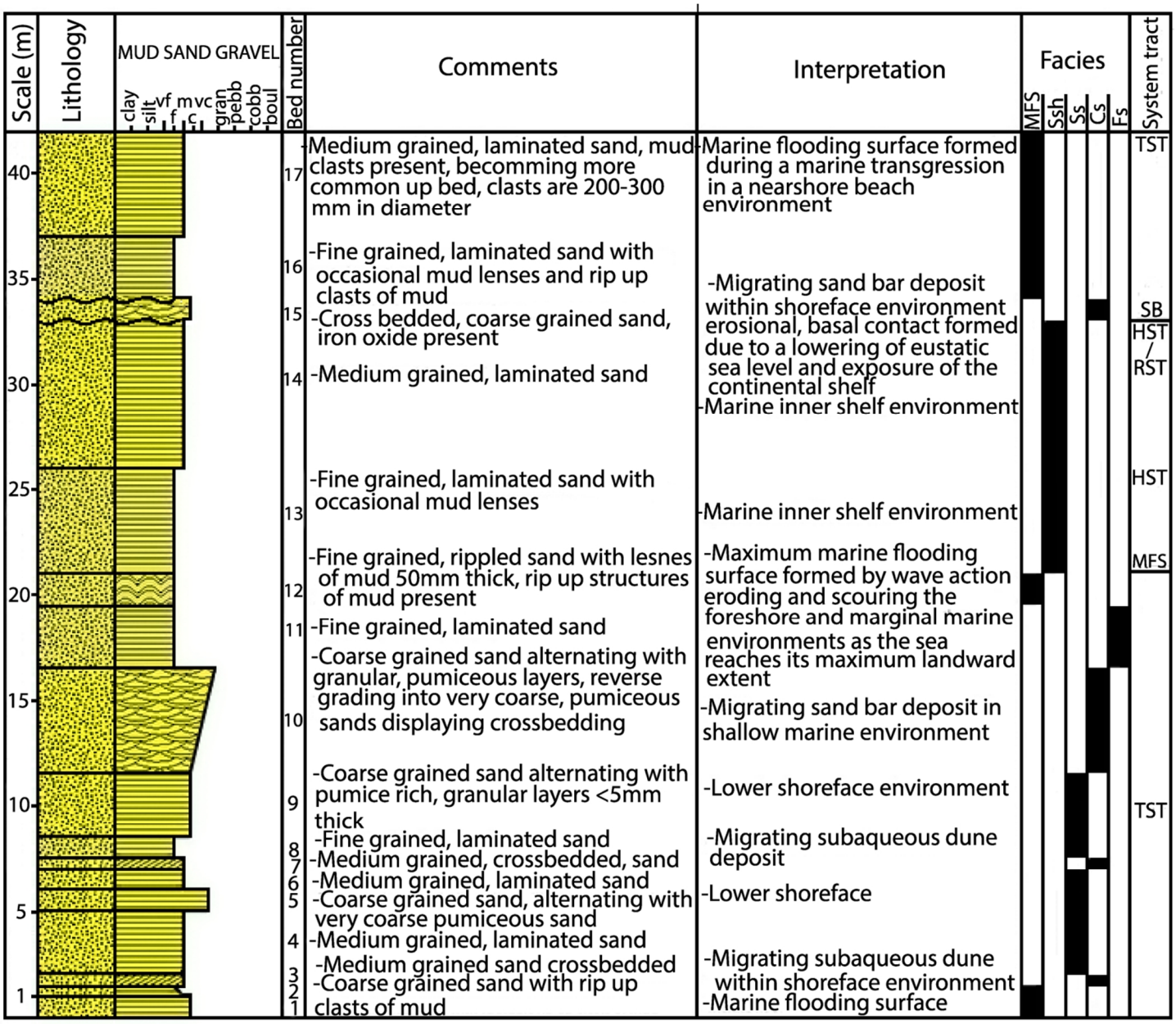


Key:

Lithologies

Sandstone

Symbols

Horizontal planar lamination

Herring-bone crossbedding

Trough crossbedding

Wave ripple cross-lamination

Base boundaries

Sharp

Gradational

Erosional

## Interpretation

The lithofacies within eQk Member are all shallow marine facies with the only fluvial influence being the inclusion of mud clasts eroded out of a transitional environment during marine transgression i.e. marine flooding surface (MFS). eQk Member represents one 100 ka cycle of sea level fluctuation during Mid Castlecliffian time. Transgressive systems tracts are represented by marine flooding surfaces and progressively increasing grain size. High stand systems tracts are recognised by finer grain sizes and settling of sediments from suspension within lower energy environments. Low stand systems tracts are represented by an erosional unconformity.

eQk Member is composed of dominantly planar laminated fine sand characteristic of shallow marine deposition. This member displays fine laminated and fine lenticular bedding. Grain size ranges from mud through to granular sand. Grain size data (Appendix 2.2) taken from this unit demonstrates a well sorted, symmetrical distribution curve, characteristic of a marine environment. Grain size analysis along with facies analysis provides evidence for shallow marine deposition. Pumice grains within this Member are considered to be reworked pumice from older deposits transported via a paleo-river system to the coast.

Kai Iwi Group sediments are characterised by glacioeustatic fluctuations dominated by high amplitude, low frequency 100 ka cycles, driven by the eccentricity of the earths orbit. The change from 41 ka to 100 ka cycles occurs at 800 ka (Berger *et al*, 1993). This Mid Pleistocene transition occurs between MIS 25 and 22 which correlates to cycles 35 and 36 in the Whanganui Basin cyclostratigraphy. Based on the correlation of Pohangina stratigraphy to the MIS and Whanganui cyclothem record the Mid Pleistocene transition occurs at Rc Member, Kai Iwi Group. Therefore eQk Member, Kai Iwi Group is the first member associated with 100 ka climatic cycles in Pohangina Valley.

Above eQk Member are younger sediments of Kai Iwi Group. These sediments do not occur on the eastern side of the Pohangina River. To the west younger Kai Iwi Group sediments have been described by MacPherson (1985), Manning (1988), Townsend (1993), and Brackley (1999).

# Chapter 10
# Geological History

This study isfocused on Plio-Pleistocene sediments the geology of the Pohangina which unconformably overlie Triassic to Early Cretaceous Torlesse greywacke. The geological history of the Waipipian to Castlecliffian units are presented in the following sections.

## Opoitian Stage 5.3 - 3.6 Ma

The paleogeography of the lower North Island during Opoitian time (4 Ma) (Fig 10.1). The map depicts an interglacial period, during a eustatic sea level high. The Pohangina area at this time was land, exposed to erosional processes. Whanganui Basin formed during the Pliocene, a period of rapid subsidence named the 'Tangahoe Pulldown' approximately 4.8 Ma (Kamp *et al,* 2004). The downwarping of the crust was caused by frictional shear between the westward dipping subducting Pacific Plate and the overriding Australian Plate (Stern *et al*, 1993).

During the Late Pliocene and Early Pleistocene the depocentre of the Whanganui Basin shifted from offshore southern Taranaki, southeastwards. Contemporaneous with the shift of the depocentre to the SE, offlap and emergence occurred in the north of the basin. By the early Pleistocene the basin was located in its present position. Major NNE-trending faults (e.g. Wellington-Mohaka, and Ruahine Faults) were active along the eastern margin of the basin, and basement block movements controlled the pattern of sedimentation (Anderton, 1981).

Rocks of upper Opoitian age (e.g. Beu, 1995; Bland *et al,* 2007) record the deposition of the first "Te Aute" limestone facies along the margins of a developing interior seaway named the "Ruataniwha Strait", which linked the Hawkes Bay and Wairarapa areas between exposed basement to the west and island shoals to the east (Fig 10.1) (Beu, 1995). The eastern margin of this seaway probably comprised a series of shoaling, shelf platforms, perhaps with a number of small islands (islets) during periods of low sea level. The western shelf of the basin was narrow, probably no more than several kilometres wide. The strait was bounded to the west by Torlesse basement with a rocky coastline, and uplifted shoal areas to the east. The presence of land in the west and shoals to the east resulted in the constriction of tidal currents through the seaway.

Fig 10.1 Paleogeographic map showing the lower North Island during Opoitian time, Early Pliocene time (4 Ma) Map depicts an interglacial stage; Data derived from Trewick & Bland, 2012; McIntyre, 2002: Beu, 1995).

# Opoitian: 4 Ma

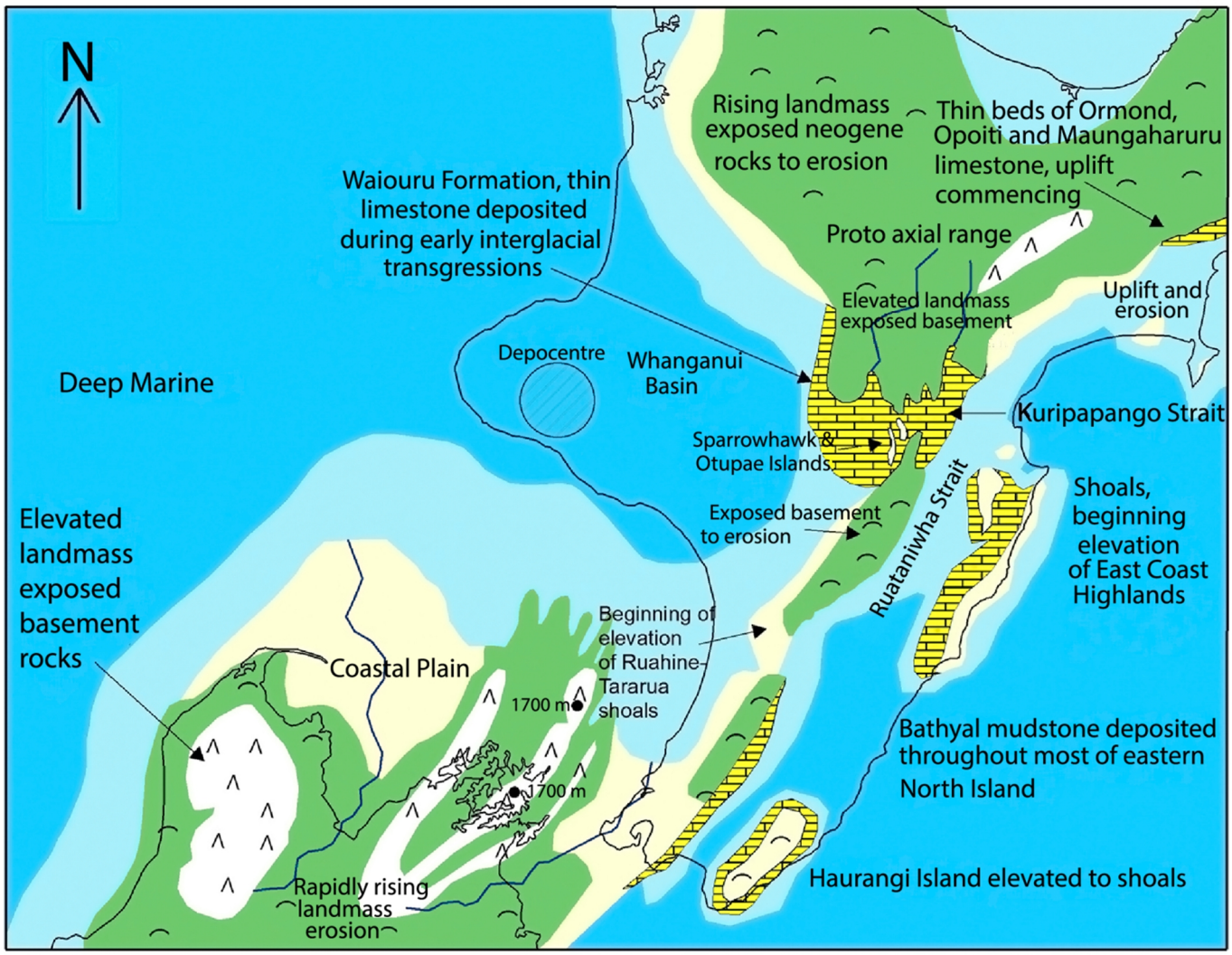

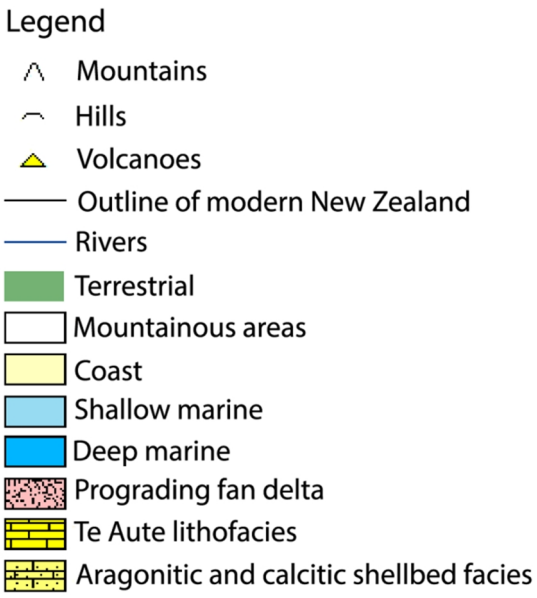


## Waipipian Stage 3.6 - 3.0 Ma

The Waipipian stage was characterised by the opening of the Manawatu Strait (previously closed), which linked the Whanganui Basin in the west to the Pahiatua Basin, Dannevirke Basin and Ruataniwha Strait in the east (Fig 10.2). The Manawatu and Kuripapango Straits were open simultaneously at this time (Browne, 2004). Shallow water limestone was deposited in shoal areas of the Ruataniwha Strait.

Rocks of Waipipian age (Beanland, 1995) are the oldest sediments preserved within the Manawatu Strait sequence. Suggesting the eastern side of the present day Manawatu Saddle area was undergoing a period of localised subsidence during the Waipipian Stage. On the north western side of the Manawatu Strait and in the Kuripapango area (Browne, 2004), elevated basement was still exposed to erosion and Waipipian aged sediments are absent.

Evidence for a period of regional uplift and erosion in the north is provided by the presense of terrestrial and marginal marine greywacke conglomerates. These Waipipian aged conglomerates outcrop west of the Ruahine Range, near Taihape, supporting the presence of elevated basement in the northern Ruahine Range (Trewick & Bland, 2012).

Fig 10.2 Paleogeographic map showing the lower North Island during Waipipian time, Early Pliocene time (3.35 Ma) Map depicts an interglacial stage ;Data derived from Trewick & Bland, 2012; McIntyre, 2002: Beu, 1995).

# Waipipian: 3.5 Ma

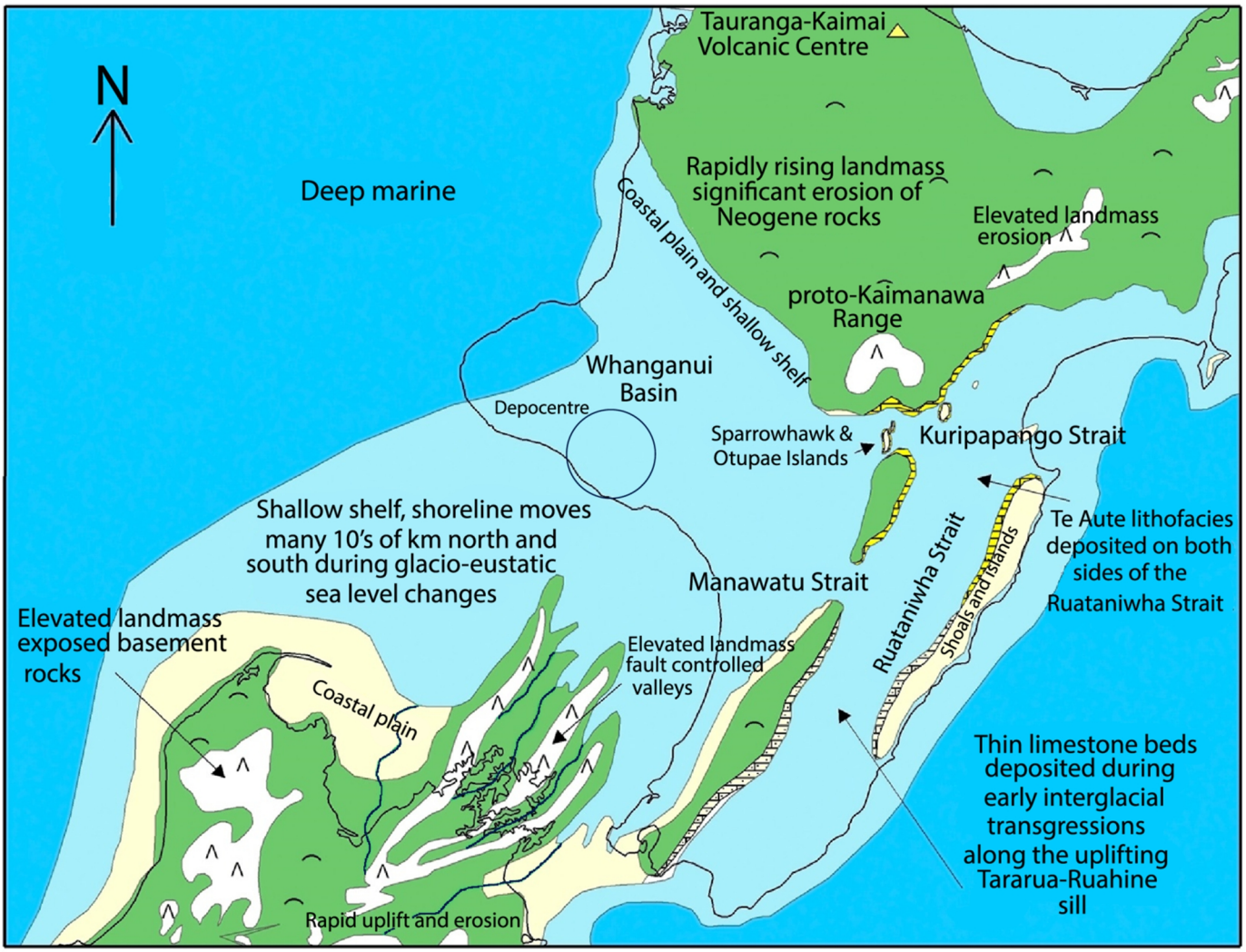


Legend

- Mountains
- Hills
- Volcanoes
- Outline of modern New Zealand
- Rivers
- Terrestrial
- Mountainous areas
- Coast
- Shallow marine
- Deep marine
- Prograding fan delta
- Te Aute lithofacies
- Aragonitic and calcitic shellbed facies

Scale

100 km

## Mangapanian Stage 3 - 2.4 Ma

Manawatu Strait was well established by Mangapanian to Early Nukumaruan time (Fig 10.3). This period of time correlates with the preservation of Komako Formation within the Pohangina Valley. Basal members of Komako Formation are dated using the occurrence of *Phialopecten thomsoni, Janthina typica*, *Lamprodomina neozelanica*, *Glycymeris (Glycymeris) shrimptoni*, and *Arca cottoni* to the Mangapanian Stage (Carter, 1972).

Fig 10.3 Paleogeographic map showing the lower North Island during Mangapanian time, Early Pliocene time (2.7 Ma) Map depicts a interglacial period ;Data derived from *Trewick & Bland, 2012; McIntyre, 2002: Beu, 1995).*

# Mangapanian: 2.7 Ma

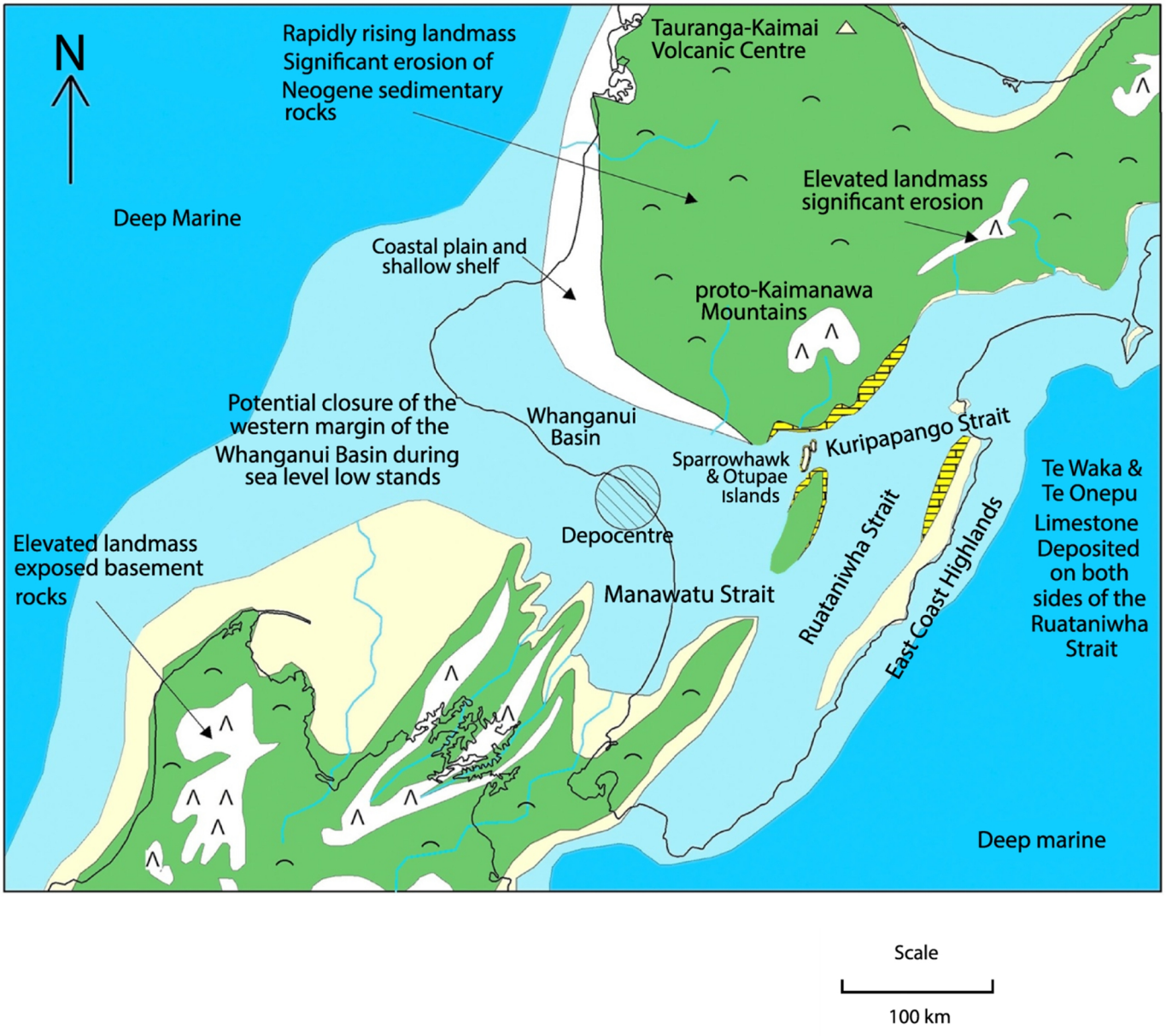

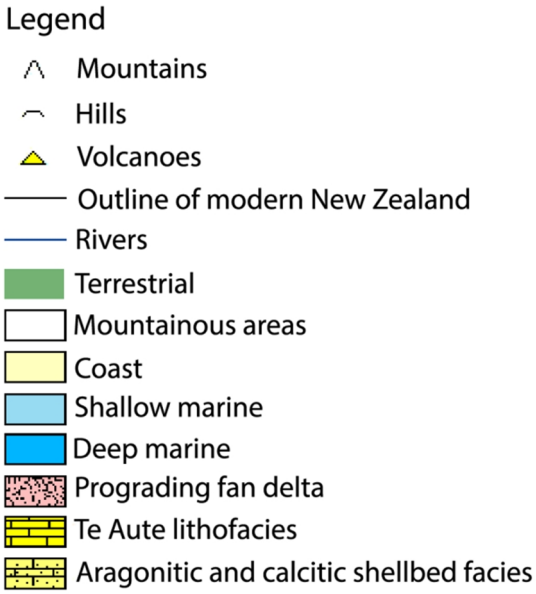


In the Pohangina region Mangapanian sediments (Komako Formation) rest unconformably on Torlesse greywacke (Fig 10.4). Subsequent shallow marine deposition and intermittent sedimentary preservation of Waipipian to Nukumaruan sediments suggests continued subsidence in the Manawatu Strait area. The oldest beds in the Pohangina area are Mangapanian grits and blue grey sandy mudstones laid on a gently dipping (up to 5°) eroded greywacke surface (Fig 10.5). Based on the biostratigraphic evidence from Komako Formation, the Manwatu Strait contained shallow, current swept waters with a maximum water depth of 50 m. The first major 41 ka glacio-eustatic cycles began during the Pliocene (5.3-2.58 Ma), during which time the first evidence of extensive ice rafting is found in the North Atlantic and North Pacific oceans (Haug, *et al*, 2005). These changes in sea level periodically exposed parts of the Whanganui-Wairarapa shelf through the Mangapanian resulting in widespread unconformities.

From Waipipian, Mangapanian and into Early Nukumaruan time, the depocentre of the Manawatu Strait has migrated westwards. Evidence for this migration includes uplift along the eastern flank of the Ruahine Range (Marden, 1984). This uplift is greatest in the east and is characterised by a steeply dipping eastern limb. The western limb dips more gently. This geometry is the result of uplift along the North Island Dextral Fault Belt (Lillie, 1953; Kingma, 1957b; Marden, 1984). The Manawatu Saddle contains a sedimentary sequence which is oldest in the east and youngs westward. The author suggests the eastern side of the Manawatu Strait was uplifted and became land before the western side. Waipipian aged strata on the flanks of the eastern Manawatu Strait in the vicinity of Woodville are unconformably overlain by Nukumaruan strata (Beu pers. coms. 2014). The absence of Mangapanian strata in the east suggests emergence of this area at 3 Ma. The unconformity becomes progressively younger to the west. The uplifted eroded beds from the eastern side of the Manawatu Strait are presumed to have been re-deposited to the west where shallow marine conditions persisted (Note diagram in Chapter 6: Fig 6.24).

Fig 10.4: Composite stratigraphic log showing stratigraphy of the Lower Pohangina Valley

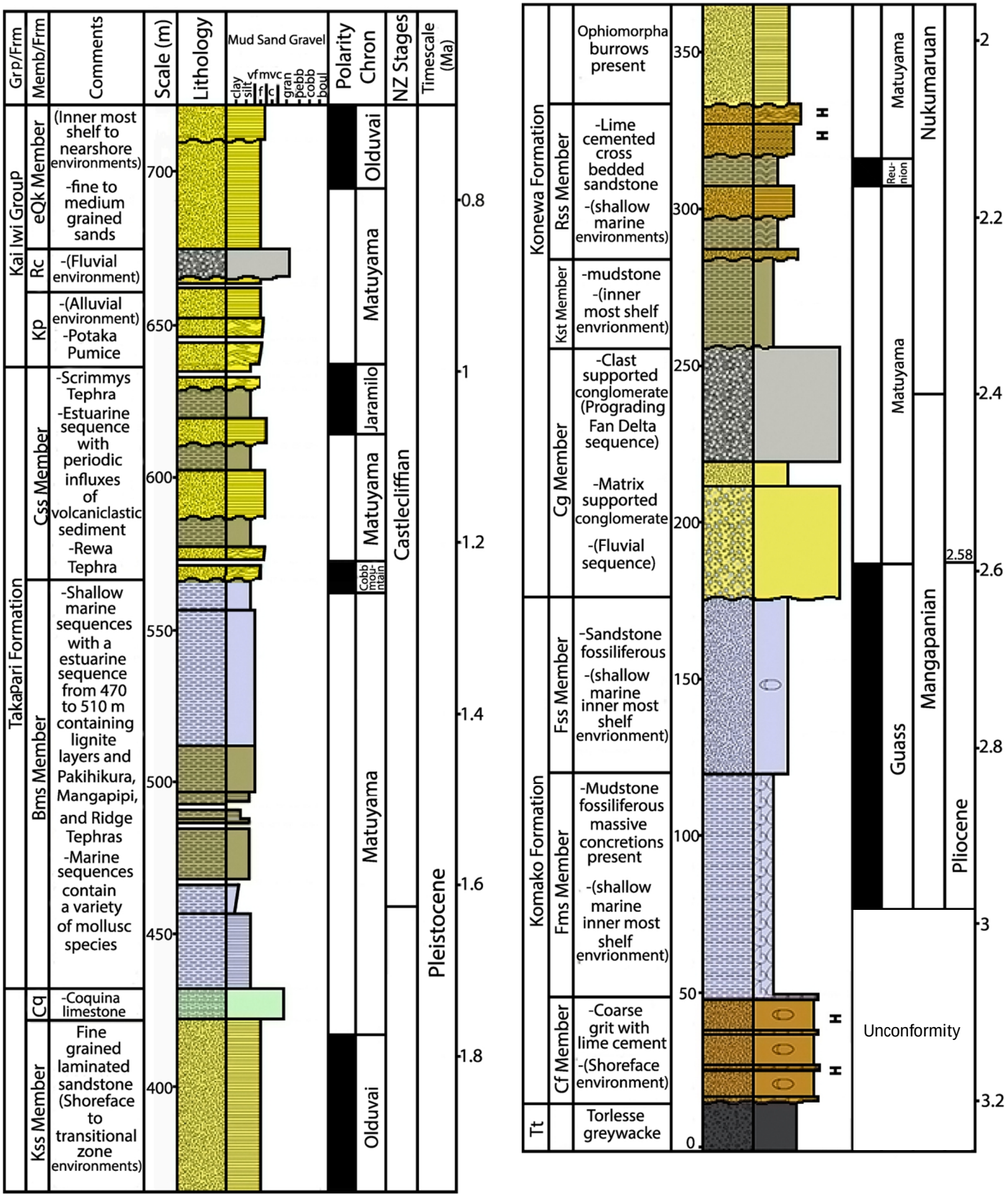

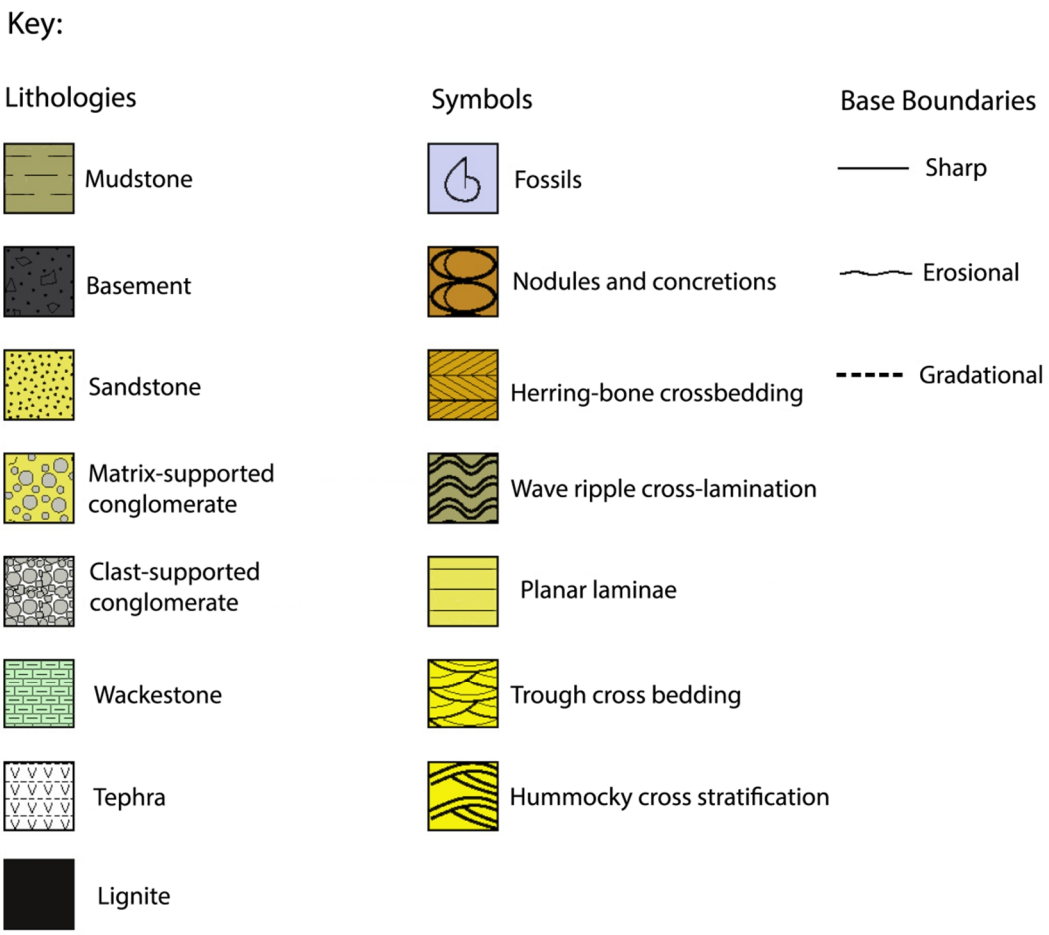


## Nukumaruan Stage 2.4-1.63 Ma

The presence of Torlesse greywacke gravels in Cg Member, Konewa Formation and within the Totaranui Limestone suggest a source area of greywacke gravels existed within an accessible distance of the Manawatu Saddle during Early Nukumaruan time. Clast size and shape, and paleocurrent analysis of these gravels indicates that the source was likely to be 40-70 km to the north of Pohangina.

The proto-Kaimanawa Range area was emergent by 4 Ma, and both basement and Cenozoic cover rocks were eroding from the range and being deposited in nearby sedimentary basins (Trewick & Bland, 2012). However, the proto-Kaimanawa Range is an unlikely source for the Nukumaruan gravels preserved at the Manawatu Saddle given its distance of over 120 km. Furthermore, the Kuripapango Strait was still open inhibiting fluvial transportation across this area (Browne, 2004) (Fig 10.6). A greywacke source located in the position of the current northern Ruahine Range is suggested as the provenance of the substantial conglomerate deposits found on the Manawatu Saddle (Fig 10.5).

**Fig 10.5:** Box diagrams displaying depositional environments on the northwestern side of the Manawatu Strait from Early Mangapanian - Early Castlecliffian time.

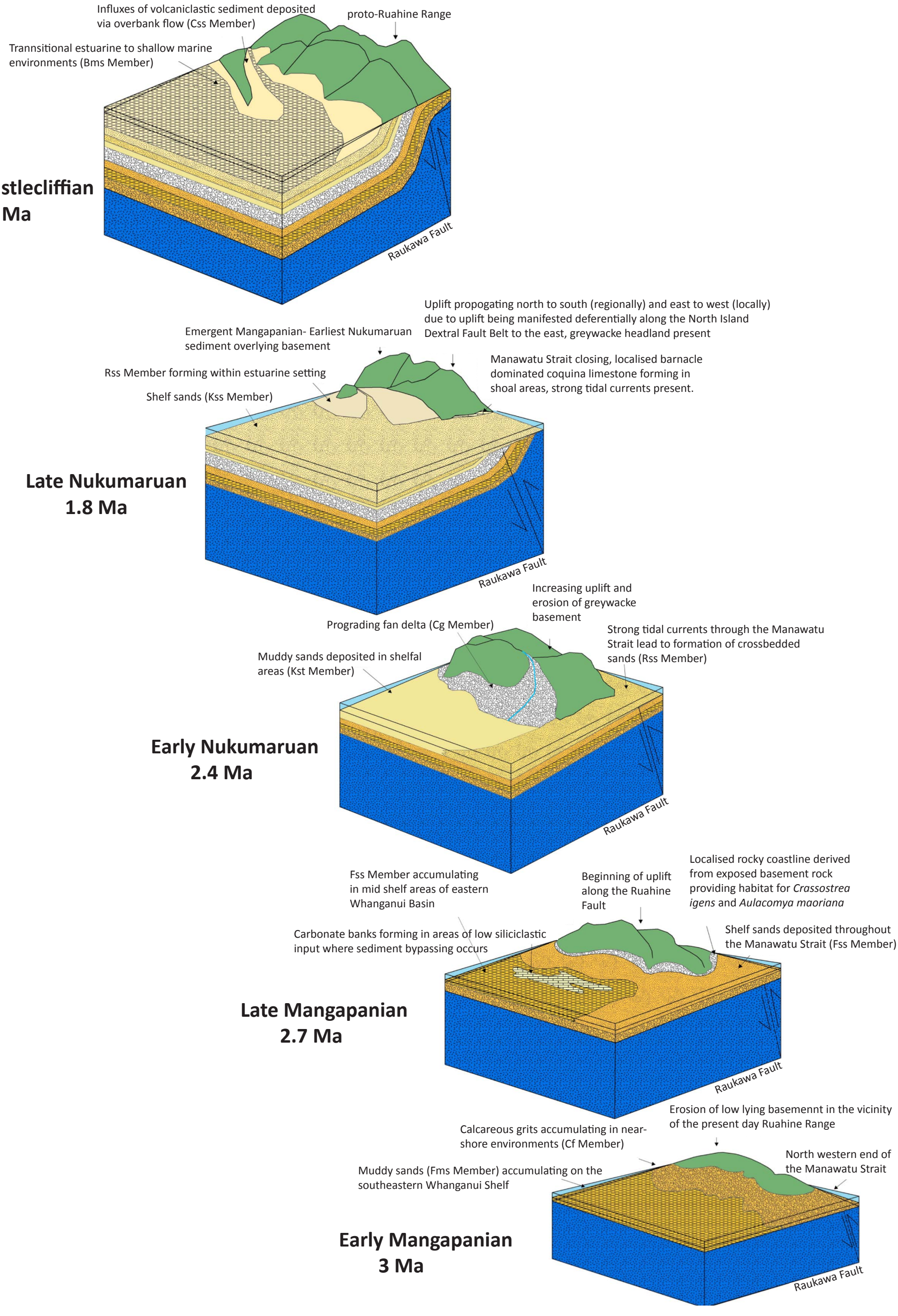

Fig 10.6 Paleogeographic map showing the lower North Island during Nukumaruan time, Early Pliocene time (2.4 Ma) Map depicts a interglacial period ;Data derived from *Trewick & Bland, 2012; McIntyre, 2002: Beu, 1995).*

# Nukumaruan: 2.4 Ma

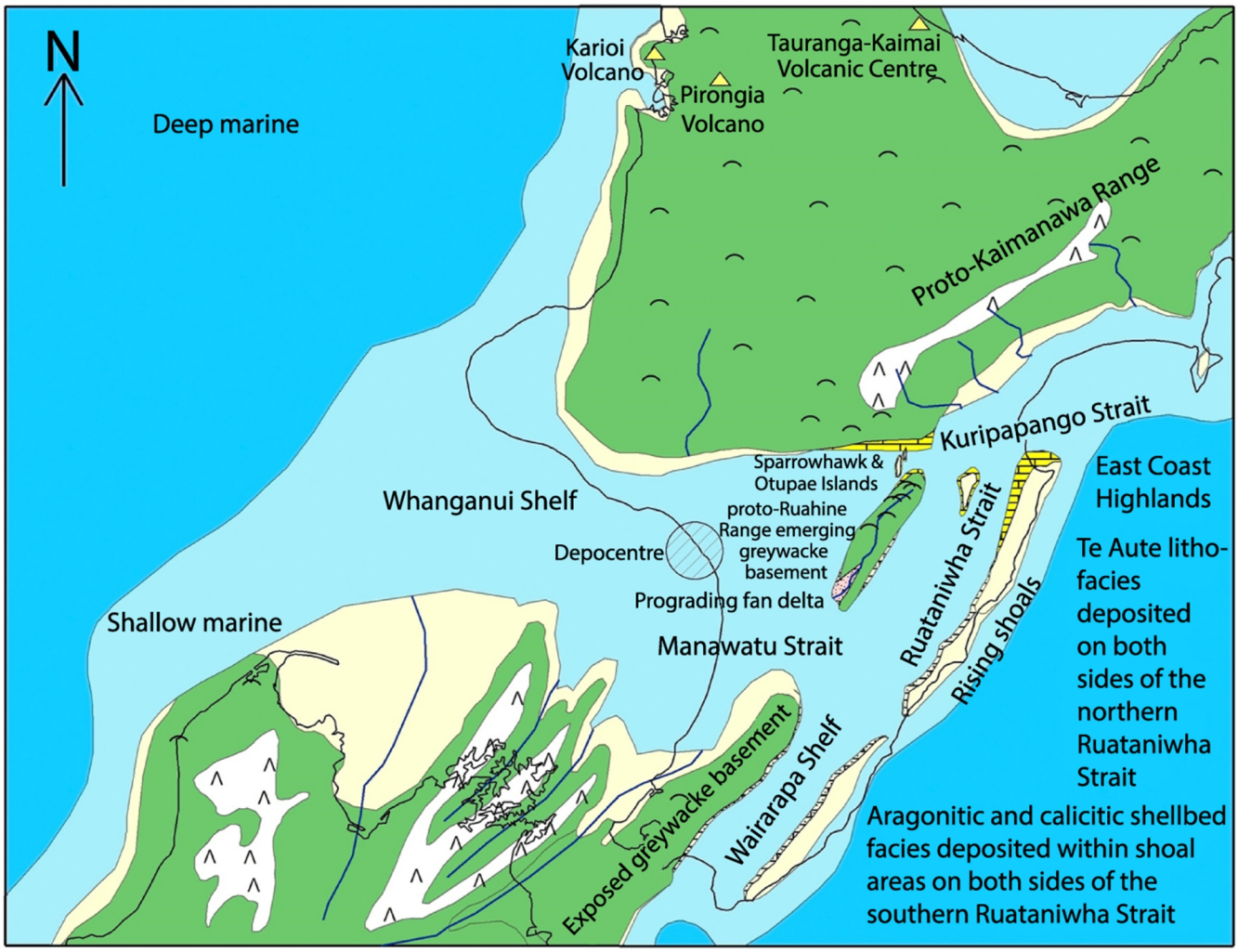


Legend

- Mountains
- Hills
- Volcanoes
- Outline of modern New Zealand
- Rivers
- Terrestrial
- Mountainous areas
- Coast
- Shallow marine
- Deep marine
- Prograding fan delta
- Te Aute lithofacies
- Aragonitic and calcitic shellbed facies

Scale

100 km

It is postulated that in Early Nukumaruan time an elevated landmass composed of greywacke extended down from the area now occupied by the northern Ruahine Range to the Manawatu Strait. A paleo-river system became established and transport gravels from the position of the current northern Ruahine Range, south to an outlet (paleo-coastline) in the SE Whanganui Basin (Fig 10.6). This paleo-river system carried large amounts of gravel and built a fan delta 1.5 km wide.

The influx of greywacke clasts into the sedimentary record preserved at the Manawatu Saddle is interpreted to be related to a phase of uplift within the axial range which began in Mangapanian time and continues to this day (Browne, 2004). An increase in the rate of tectonic uplift within the northern Ruahine Range is identified via influxes of greywacke clasts into the Komako Formation, Pohangina Valley (Carter, 1972; McIntyre, 2002) and NW East Coast Basin (Bland *et al*, 2008). This Late Mangapanian–Early Nukumaruan uplift can be linked with subsidence to the northeast (Ohara Depression, Fig 10.7), associated with displacement along the Ruahine, Glenross, Mohaka and possibly Wakarara Faults (Bland *et al*, 2008).

At the beginning of the Nukumaruan Stage (-2.4 Ma) the Manawatu Strait was at shallow shelf depths as indicated by coquina limestone on the eastern flank of the Ruahine Ranges near the Manawatu Gorge (Totaranui Limestone), and southern Kaweka Ranges (Beu *et al*, 1981; Beu, 1995; Browne, 2004a). Cg Member, Konewa Formation is considered in this study to be a correlative of the Totaranui Limestone (Neef, 1974, 1982; Beu, 1995) which was deposited into the Wairarapa Basin (Beu, 1995) south of the Ruataniwha Strait (fig 9.2).

Contemporaneous with the deposition of the Totaranui Limestone, a large prograding fan delta was building out into the eastern Whanganui Basin bordering the northwestern end of the Manawatu Strait. The source of the gravels which composed this fan delta are likely from the same hinterland which feed the shallow water depositional environments along the western margin of the Ruataniwha Strait and north western Wairarapa Basin. The proto-northern Ruahine Range at this time was likely an island of eroding basement rock supplying the gravels to both the conglomeratic limestones of the East Coast and Cg Member, Konewa Formation (Beu *et al,* 1980) (Fig 10.6).

Fig 10.7: The Ruahine Range showing faults and location of the Ohara Depression (GoogleEarth, 2014).


By Late Nukumaruan time (around 1.6 Ma) regional uplift of the Mount Bruce block (Fig 10.8) in the Wairarapa had closed off the southern end of the Ruataniwha Strait (Beu, 1995, Trewick & Bland, 2012). Marine deposition continued to occur in parts of Wairarapa and Hawke's Bay through the late Quaternary (Field *et al*, 1997). The uplift at Mount Bruce was in response to a change in the displacement along faults in central Wairarapa (Fig 10.8). This uplift also created a drainage divide east of the proto-axial ranges that restricted the Manawatu River system to the north of the divide and the Ruamahanga River system to the south (Trewick & Bland, 2012). Tectonic uplift of the Mt Bruce block forced a marine regression within the current Manawatu Gorge area, marking the closure of the Manawatu Strait at approximately Late Nukumaruan time (Vella, 1962).

Fig 10.8: Southern North Island showing Wairarapa region, Manawatu Saddle and location of the Pahiatua Basin, Mt Bruce, the Wellington Fault, West Wairarapa Fault, and Palliser-Kaiwhata Fault. (adapted from McFadgen, 2003).

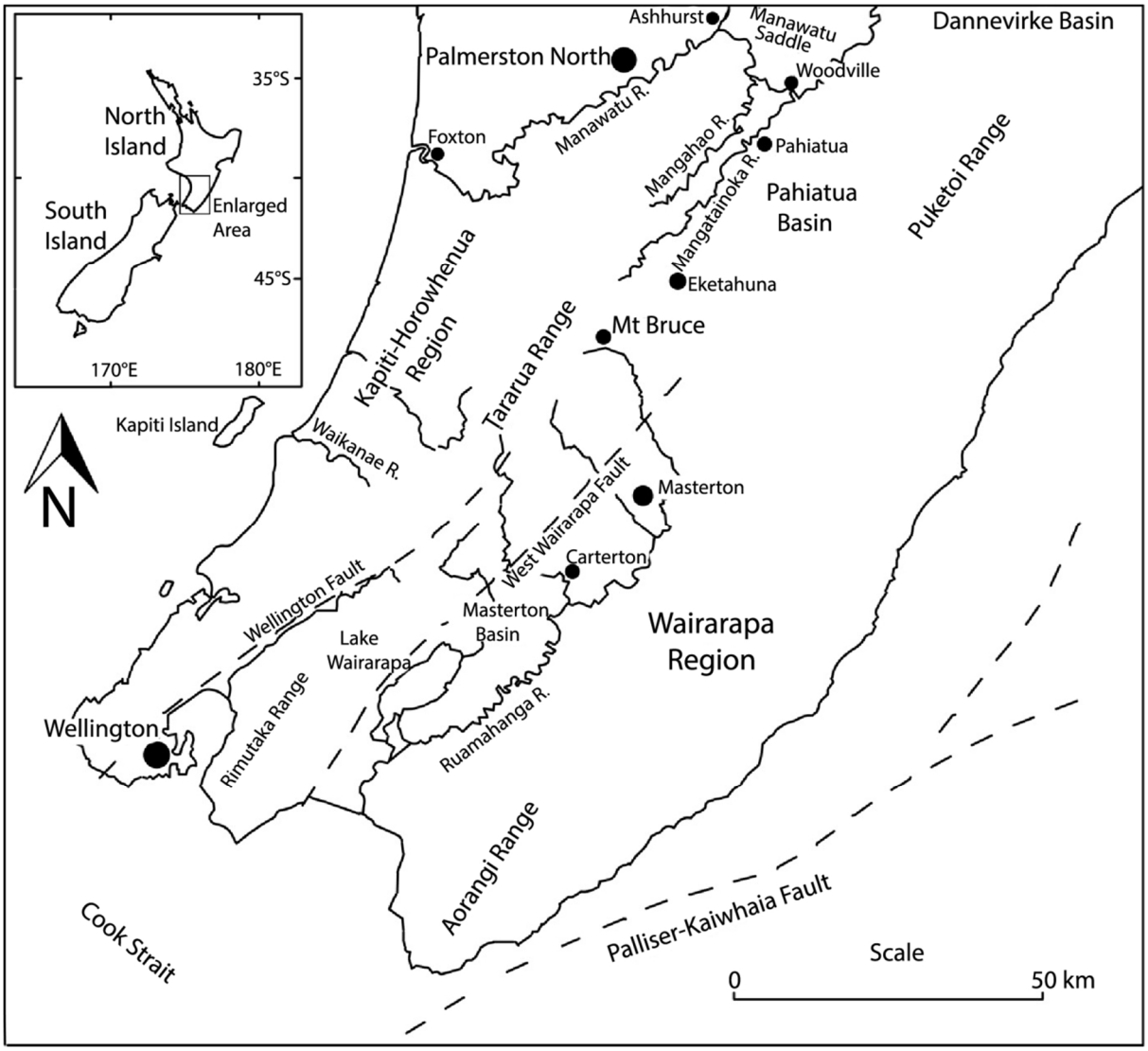


## Castlecliffian Stage 1.63–0.34 Ma

The majority of the uplift of the Ruahine and Tararua Ranges has occurred in the last 1 Ma. Uplift of the main axial ranges has been concentrated along transpressional fault lines with both dextral transcurrent and vertical slip components (e.g. Wellington- Mohaka Fault and Ruahine Fault). Uplift along these fault lines has not been evenly spread, either along the length of the fault trace or through time (Marden, 1984). The greatest uplift has occurred along the Wellington Fault on the eastern side of the ranges while in contrast the least amount of vertical fault displacement has occurred in the Manawatu Saddle area (Beanland, 1995). This difference in the amount of vertical displacement has resulted in the current contrast in altitude between the Manawatu Saddle and adjacent ranges.

Uplift along the western side of the Wellington Fault in the vicinity of the current Manawatu Saddle caused ponding and the formation of a lacustrine environment in the Woodville area at around 1 Ma (Shane 1991; Lee & Begg 2002) (Fig 10.9). Evidence for this lacustrine environment is provided by the occurrence of pinkish mudstone containing freshwater diatoms and the freshwater mussel *Hydridella* (Morrell, 1991; Shane, 1991). This lacustrine mudstone is part of the Mangatarata Formation found in the Woodville area (Lillie, 1953; Shane, 1991).

Fig 10.9 Paleogeographic map showing the lower North Island during Castlecliffian time, Early Pliocene time (1 Ma) Map depicts a interglacial period ;Data derived from *Trewick & Bland, 2012; McIntyre, 2002: Beu, 1995).*

# Castlecliffian: 1 Ma

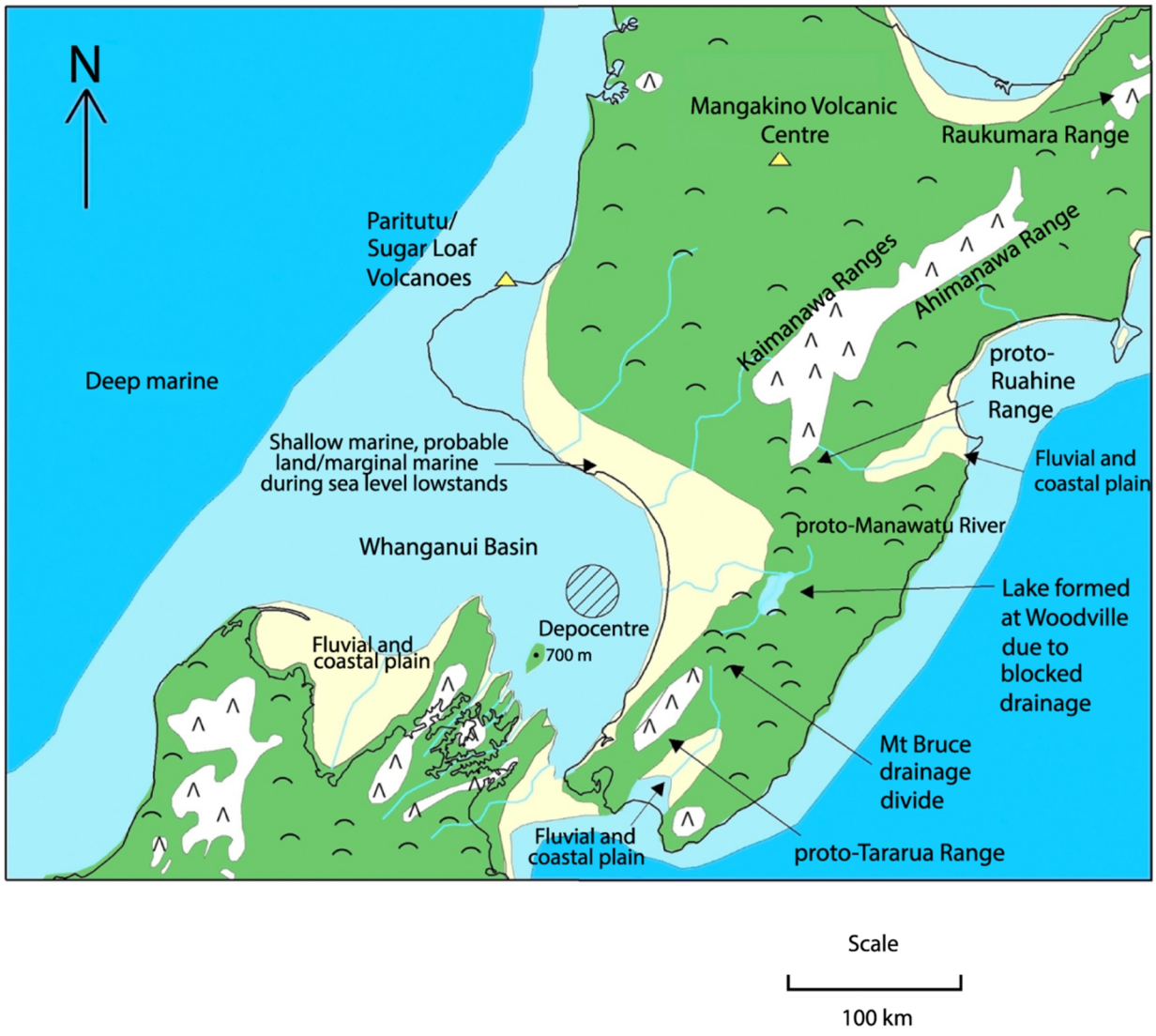

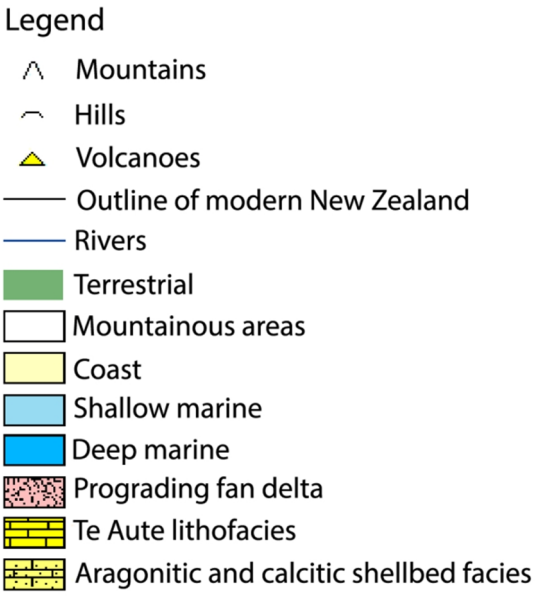


Uplift of the Mt Bruce block to the south restricted a southwards path for the Manawatu River, forcing the river that drained the lake to travel east to west (Fig 10.9). The Manawatu River maintained its east-west course through the Late Quaternary, downcutting at the present day Manawatu Gorge as the greywacke ranges were uplifting to the north and south. It has intrigued geologists for decades why the Manawatu River cuts across the main axial range at the southern end of the Manawatu Saddle and not 3 km to the north where the axis of a structural low occurs. At this axis the contact between Torlesse bedrock and Plio-Pleistocene sediments is only 200 m asl, providing the seemingly most obvious place for the Manawatu River to cut through the range (Marden, 1984).

The formation and location of the Manawatu Gorge has been variously explained by many geologists. The gorge is cut across the southern end of the Manawatu Saddle at the northern tip of the Tararua Range, and southern tip of the Ruahine Range. Its geological history, including the reason for its seemingly peculiar location has provided much controversy within the geological world. Ongley, (1935) gives a summary and critique of the main geological theories in his paper ‘Manawatu Gorge’.

During regional uplift of southern Hawkes Bay and northern Wairarapa a system of drainage was created, which flowed into the area of the Manawatu Strait. This drainage was therefore guided by and ‘consequent’ upon the Manawatu Strait (Cotton, 1922). Downcutting of the proto-Manawatu River through the overlying Tertiary strata and into the underlying Torlesse bedrock gave the river a superposed course at the location of the present day Manawatu gorge (Marden, 1984). This course was antecendent to the localised tectonic uplift of the southern Ruahine Range (Adkin, 1930). Cotton (1922) and Ongley (1935) describe the course of the Manawatu River as being consequent on the earlier and

antecedent to the later stages of a single series of deforming movements along the North Island dextral fault system. Therefore the course of the Manawatu River is termed a superposed anteconsequent gorge (Beu *et al,* 1980).

Other possible reasons for the location of the Manawatu Gorge have also been discussed by Ower (1943) and Beanland (1995). Firstly the Manawatu River has been forced eastward and southward by extensive piedmont gravel fans deposited by the streams draining the eastern front of the southern Ruahine Range (Ower, 1943). These fans were more extensive than the fans derived from the much lower and less striking northern Tararua Range.

The second line of evidence is the sinistral side step splinter fault of the Ruahine Fault postulated by Beanland (1995) along the Manawatu Gorge. Such fault movement would leave the Torlesse greywacke highly shattered and sheared making them very vunerable to fluvial erosion. Water will always find the weakest point to exploit, and therefore it is likely the course of the Manawatu River could have become influenced by a zone of fault gouge created by movement along the Ruahine Fault.

A block of Totaranui limestone on the north eastern end of the Manawatu Saddle has been shifted into position from south to north via dextral transcurrent movement along the Wellington-Mohaka Fault (Beu, 1995). This limestone acts as a headland to the Manawatu River on the far eastern side of the Manawatu Gorge. The position of this limestone may have had some influence on the position in which the Manawatu River has cut through the main axial range.

The first phase of rhyolitic volcanism in the TVZ had commenced by 1.6 Ma with large ignimbrite eruptions generated from the Mangakino Volcanic Centre (Carter *et al*, 2003; Briggs *et al*, 2005). Tuff derived from the ignimbrite eruptions was transported south from the central North Island via paleo-river systems to the Whanganui and Paihiatua Basins on both sides of the present day axial range (Fig 10.10).

It is postulated that during this time of volcanic activity, regional uplift and formation of new drainage patterns, a proto-Rangitikei River emerged. With headwaters in the northwestern Kaimanawa Range, the proto-Rangitikei flowed south, entering the eastern Whanganui Basin near the Pohangina area. The river carried vast quantities of pumiceous debris from the distal parts of large ignimbrite sheets. This fluvially transported sediment began infilling accommodation space centered on a localised depocentre slightly to the west of the Manawatu Saddle where a large estuarine system was developing (Fig 10.10).

Fig 10.10: Box diagram displaying depositional environments on the northwestern side of the Manawatu Saddle during Mid Castlecliffian time.

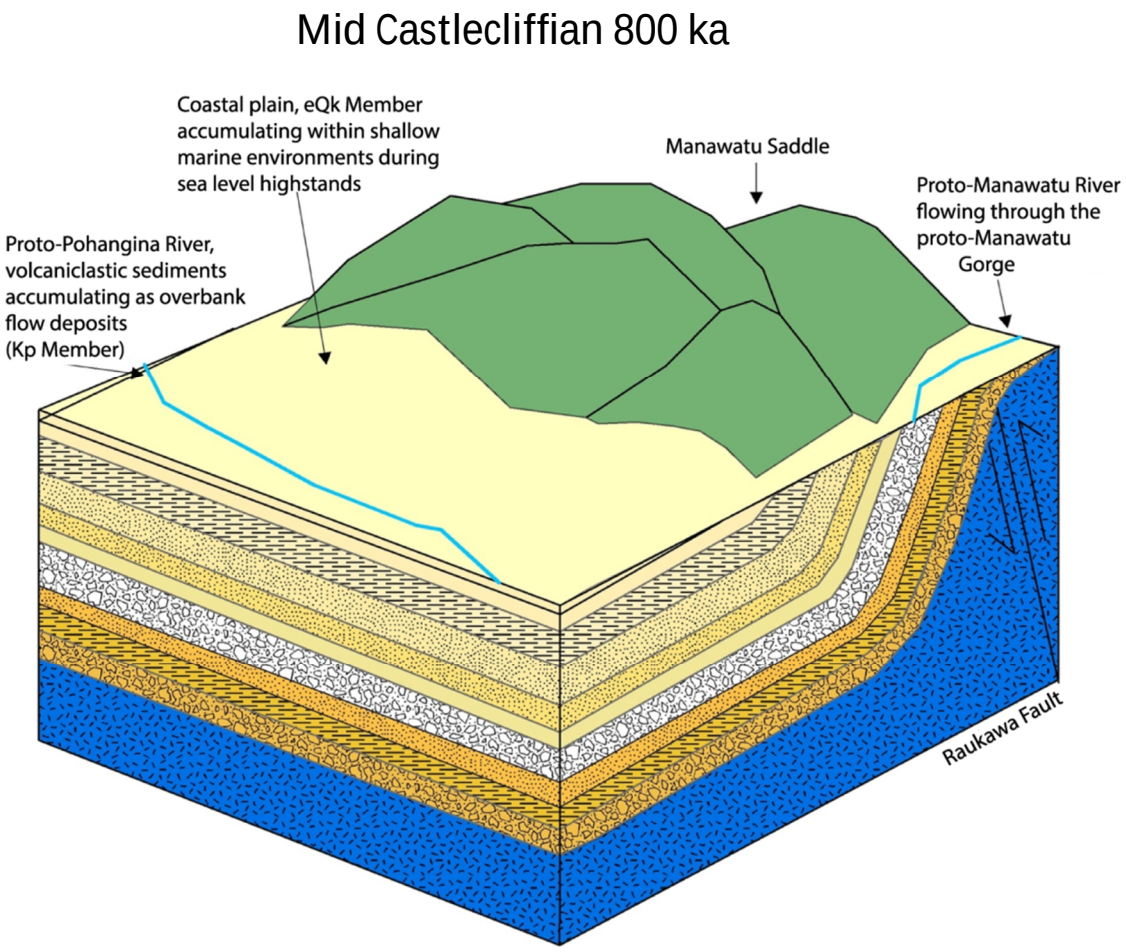


Increased uplift rates led to growth of the Ruahine Anticline, along with several smaller anticlines across the Manawatu Plains which become progressively younger to the west (Pohangina, Marton-Halcombe and Feilding Anticlines). The formation of these anticlines across a landscape which had up to this point been a relatively subdued, flat lying coastal plain led to the constriction of the drainage pathways which flowed out across the Manawatu Plains to the Tasman Sea. It is suggested that between 1.6 and 0.8 Ma the proto-Rangitikei River was slowly diverted by the growth of the Pohangina Anticline, forcing it to drain farther to the west; contemporaneous with this shift was growth of the southern Ruahine Range and the creation of the Pohangina and Oroua Rivers whose headwaters drain the western flank of the southern Ruahine Range. The Pohangina and Oroua Rivers were then constricted by the Oroua, Pohangina, and Ruahine Anticlines.

By 1 Ma the Kaimanawa and Kaweka Ranges were established and rapid uplift along the proto-Ruahine and proto-Tararua Ranges ensued (Beu *et al*, 1981; Erdman & Kelsey 1992). Most of the elevation of the Ruahine Range has occured since Early Castlecliffian time (Beu *et al*, 1981). Evidence for this is seen in the occurrence of Nukumaruan limestone on the northern Ruahine Range, the Castlecliffian strata, and the occurrence of Mesozoic greywacke thrust next to Castlecliffian strata on the eastern Ruahine Range (Beu, *et al,* 1981).

The increased rate of uplift in the Ruahine Range at this time coincides with the time when the Big Hill Fault (Fig 10.5) began to accommodate strike-slip displacement (Erdman & Kelsey, 1992). Various segments of the Mohaka Fault appear to have been active during the Neogene (Beanland, 1995). In the Ohara Depression, the Ruahine Fault is presently moving on average 1.0 - 2.0 mm/yr and the Mohaka Fault is moving at 3.0 -4.0 mm/yr (Erdman & Kelsey, 1992).

The Pohangina area during the Castlecliffian Stage comprised shallow to marginal marine environments, as evidenced by the sediments within the Castlecliffian strata of this region. The Whanganui Basin depocentre had moved south during the Pleistocene and by 1 Ma the depocentre lay off the coast of Foxton. The Pohangina region was characterised by a embayed coastal plain, bordered to the east by rapidly uplifting greywacke basement and Mangapanian to Nukumaruan sediments.

By 1 Ma subsidence had ceased in the Whanganui area and regional uplift began. This change from subsidence to uplift is marked by the formation of a well developed set of marine terraces that are preserved between Harewa and Kai Iwi in South Taranaki/ Whanganui (Pillans, 1994). Subsidence in the Manawatu District may have persisted into early Haweran time. The preservation of the Last Interglaical marine terrace (Tokomaru Marine Terrace, c. 128-115 ka), suggests subsidence pior to the Last Interglaical marine incusrsion (Clement *et al*, 2010).

## Haweran Stage 0.34 Ma- present day

During the Haweran Stage the greywacke of the Ruahine and Tararua ranges continued to become uplifted in a broad SW-NE trending anticlinal flexture. Uplift was manifested along the North Island Dextral Fault Belt, so that the highest rate of uplift occurred in the east of the ranges. The Ruahine and Tararua Ranges are characterised by differential fault movement. The least amount of uplift occurred within the vicinity of the Manawatu Saddle, resulting in the structural low seen in the landscape today. The overlying Plio-Pleistocene strata were stripped from the the higher parts of the Ruahine Range leaving the exposed Torlesse greywacke peaks seen today (Wellman, 1948). In the Manawatu Saddle area, erosion of the weakly consolidated Plio-Pleistocene sediments formed steep, deeply incised

gorges and valleys. While more resistant, iron oxide cemented, conglomerate and coquina limestone is left, forming the ridge tops and high, domed shaped hills.

Crustal shortening resulted in a series of anticlines trending NE-SW across the Manawatu, Rangitikei, Marton, and Whanganui Distircts. The formation of the Pohangina and Oroua Antclines forced the Rangitikei River westwards, while constricting and directing new drainage pathways south. The newly emerged Pohangina River was constricted by the Pohangina Antlicline in the west and the Ruahine Anticline and to the east. The Pohangina River was forced to drain southward running toward present day Ashhurst, where the river met the Manwatu River at the Manawatu Gorge. River aggradation and downcutting have formed a series of river terraces within the Whanganui Basin. Only the last two phases of river aggradation have been preserved within the Pohangina Valley, due to the greater rate of uplift and erosion in this area in comparison with the Rangitikei River Valley.

The marine terrace formed by the last retreat of the sea in the Last Interglacial period has been uplifted and dissected, to the south of the Manawatu Gorge. The Last Interglacial sea level did not reach as far as the Pohangina Valley. The Pohangina Valley has thus been characterised by fluvial erosion and deposition, over the last 120 ka.

## Conclusions:

The Lower Pohangina Valley contains a 720 m thick, discontinuous, sedimentary sequence. This sequence is dated using biostratigraphy and tephrochronology as Mangapanian (3 Ma) through to Mid Castlecliffian (800 ka) age. The Komako, Konewa and Takapari formations (Carter, 1972) are maintained in this study and are further subdivided into separate members. The upper boundary of the Takapari Formation is placed at the basal contact of the Kaimatira Pumice Sand Formation.

The Manawatu Strait opened in Waipipian time (3.6 Ma) linking the Whanganui Basin in the west to the Pahiatua Basin, Dannevirke Basin and Ruataniwha Strait in the east. During this period the oldest sediments of the Manawatu Saddle were deposited (Beanland, 1995). From Waipipian through Mangapanian and into Early Nukumaruan time, the depocentre of the Manawatu Strait migrated westwards. This migration is related to regional uplift which propagated along the North Island Dextral Fault Belt (Lillie, 1953; Kingma, 1957b; Marden, 1984; Beanland, 1995; Bland et al, 2007).

Komako Formation is characterised by blue, grey sandy mudstone and fossiliferous, grits. These Mangapanian sediments were deposited within the shallow and current swept waters of the central and western Manawatu Strait.

During Early Nukumaruan time a prograding fan delta was formed in the NW Manwatu Strait. This delta was approximately 1.5 km wide. The source of the Early Nukumaruan gravels was located within the northern Ruahine Range, approximately 40 and 70 km NE.

By Late Nukumaruan time (around 1.6 Ma) regional uplift of the Mount Bruce block in the Wairarapa had closed off the southern end of the Ruataniwha Strait. This uplift forced a marine regression within the Manawatu Saddle area, marking the closure of the Manawatu Strait. Drainage was blocked to the south, and a lacustrine environment formed near present day Woodville. The proto-Manawatu River was formed draining east-west into the Tasman Sea (Trewick & Bland, 2012).

The TVZ became active around 1.6 Ma (Wilson *et al,* 1984; Houghton *et al*, 1995). Six tephras/tuffs are recognised within the Takapari Formation and correlated to well known Pleistocene TVZ eruptions. Scrimmys Tephra is a new tephra recognised between the Rewa Pumice and Potaka Pumice. Airfall tephras have been preserved within estuarine and alluvial sedimentary environments. Volcaniclastic sediments (tuffs) are preserved within fluvial depositional environments, representing rapid aggradational episodes following ignimbrite emplacement.

By 1 Ma rapid uplift along the proto-Ruahine and proto-Tararua Ranges ensued (Beu *et al*, 1981). The Manawatu River maintained its E-W path through the Manawau Saddle area, downcutting, and forming the Manawatu Gorge.

# References


Abbott, S. T., and Carter, R. M. (1994). The sequence architecture of mid-Pleistocene (c. 1.1–0.4 Ma) cyclothems from New Zealand: facies development during a period of orbital control on sea-level cyclicity. *Orbital forcing and cyclic sequences*, 367-394.

Abbott, S.T. (1998). Transgressive systems tracts and onlap shellbeds from mid–Pleistocene sequences, Wanganui Basin, New Zealand. *Journal of Sedimentary Research* 68: 253–268

Abbott, S. T. (2000). Detached mud prism origin of highstand systems tracts from mid-Pleistocene sequences, Wanganui Basin, New Zealand. *Sedimentology*, *47*(1), 15-29.

Abbott, S. T., Naish, T. R., Carter, R. M., and Pillans, B. J. (2005). Sequence stratigraphy of the Nukumaruan Stratotype (Pliocene-Pleistocene, c. 2.08–1.63 Ma), Wanganui Basin, New Zealand. *Journal of the Royal Society of New Zealand*, 35(1-2), 123-150.

Adams, C. J., Mortimer, N., Campbell, H. J., and Griffin, W. L. (2009). Age and isotopic characterisation of metasedimentary rocks from the Torlesse Supergroup and Waipapa Group in the central North Island, New Zealand. *New Zealand Journal of Geology and Geophysics*, 52(2), 149-170.

Adkin, G.L. (1930). The origin of the Manawatu Gorge. *New Zealand Journal of Science and Technology* 11, 353–6.

Alloway, B. V., Pillans, B. J., Sandhu, A. S., and Westgate, J. A. (1993). Revision of the marine chronology in the Wanganui Basin, New Zealand, based on the isothermal plateau fission-track dating of tephra horizons. *Sedimentary geology*, 82(1), 299-310.

Anderton, P. W. (1981). Structure and evolution of the south Wanganui Basin, New Zealand. *New Zealand journal of geology and geophysics*, 24(1), 39-63.

Batt, G.E., Baldwin, S.L., Cottam, M.A., Fitzgerald, P.G., Brandon, M.T., and Spell, T.L. (2004). Cenozoic plate boundary evolution in the South Island of New Zealand: New thromochronological constraints. *Tectonics*, *23*(4).

Beanland, S. (1995). The North Island dextral fault belt. PhD. (Geology) thesis, Victoria University of Wellington.

Begg, J.G., and Johnston, M.R. (2000). Geology of the Wellington Area. 1:250 000 Geological Map 10. Institute of Geological and Nuclear Sciences, Lower Hutt, New Zealand.

Begg, J.G., Palmer, A., and Gyopari, M. (2005). Geological synopsis of the Manawatu-Horowhenua area for a review of the regions hydrogeology (IGNS Client Report 2005/172). Institue of Geological & Nuclear Sciences, Lower Hutt.

Berger, W.H., Bickert, T., Schmidt, H., and Wefer, G. (1993). Quaternary oxygen isotope record of pelagic foraminifers: Site 806, Ontong Java Plateau, In: Berger, W.H., Kroenke, L.W., Mayer, L.A., *et al*., *Proceedings of the Ocean Drilling Program, Scientific results, Volume 130*: College Station, Texas, Ocean Drilling Program, 381–395.

Berggren, W.A., Kent, D.V., Flynn, J.J., and Van Couvering, J.A. (1985). Cenozoic geochronology, *Gelogical Society of America Bulletin 96*: 1407-1418

Beu, A. G., Grant-Taylor, T. L., and Hornibrook, N. D. B. (1980). The Te Aute Limestone Facies: Poverty Bay to Northern Wairarapa, 1: 250 000 New Zealand Geological Survey miscellaneous series map 13 (2 sheets) and map notes (36), Department of Scientific and Industrial Research.

Beu, A.G., Browne, G.H., and Grant-Taylor T.L. (1981). New Chlamys delicatula localities in the central North Island and uplift of the Ruahine Range. *New Zealand Journal of Geology and Geophysics* 24: 127-132.

Beu A.G. (1995). Pliocene limestones and their scallops. Lithostratigraphy, pectinid biostratigraphy and palaeogeography of eastern North Island Late Neogene limestone. *Institute of Geological and Nuclear Sciences Monograph 10*. Lower Hutt, Institute of Geological and Nuclear Sciences. 243-244.

Beu, A. G., and Maxwell, P. A. (1990). *Cenozoic Mollusca of New Zealand,* New Zealand Geological Survey. 518-519.

Beu, A. G., Alloway, B. V., Pillans, B. J., Naish, T. R., & Westgate, J. A. (2004). Marine Mollusca of oxygen isotope stages of the last 2 million years in New Zealand. Part 1: Revised generic positions and recognition of warm-water and cool-water migrants. *Journal of the Royal Society of New Zealand*, *34*(2): 111-265.

Beu, A.G., and Raine, J.I. (2009). Revised descriptions of New Zealand Cenozoic Mollusca from Beu and Maxwell (1990). GNS Science miscellaneous series no. 27.

Bland, K.J., Kamp, P.J.J., and Nelson, C.S. (2007). Systematic lithostratigraphy of the Neogene succession exposed in central parts of Hawke's Bay Basin, eastern North Island, New Zealand. Ministry of Economic Development New Zealand Unpublished Petroleum Report PR3742. 0-259. + 2 enclosures

Bland, K.J., Kamp, P.J.J., and Nelson, C.S. (2008). Late Miocene- Early Pleistocene palaeogeography of the onshore central Hawke's Bay sector of the forearc basin, eastern North Island, New Zealand, and some implications for hydrocarbon prospectivity. In: 2008 New Zealand Petroleum Conference proceedings: Beyond 08. Ministry of Economic Development, Wellington, 22-23.

Boellstorff, J. D., and Te Punga, M. T. (1977). Fission-track ages and correlation of middle and lower Pleistocene sequences from Nebraska and New Zealand. *New Zealand journal of geology and geophysics*, *20*(1), 47-58.

Boggs, S. (1995). Principles of sedimentology and stratigraphy (Vol. 23117923), *Prentice Hall,* New Jersey, USA.

Boggs, S. (2011). Principals of Sedimentology and Stratigraphy, Fifth Edition, *Perason Education Inc*, New Jersey, USA.

Bourgeois, J., and Leithold, E. L. (1984). Wave-worked conglomerates—depositional processes and criteria for recognition. Sedimentology of Gravels and Conglomerates, *American Association of Petroleum Geologists Memoir 10*: 331-343.

Brackley, H.L. (1999). The stratigraphy and environments of deposition of Early-Mid Pleistocene sediments of the Pohangina Region, eastern Whanganui Basin, New Zealand, Unpublished Msc (Masters) thesis, Massey University, Palmerston North.

Brewer, P. A., Leeks, G. J. L., and Lewin, J. (1992). Direct measurement of in-channel abrasion processes. In *Erosion and sediment transport monitoring programmes in river basins (Proceedings of the Oslo Symposium, August 1992),* 21-29.

Briggs, R.M., Gifford. M.G., Moyle, A.R., Taylor, S.R., Norman, M.D.. Houghton, B.E., and Wilson, C.J.N. (1993). Geochemical zoning and eruptive mixing in ignimbrites from Mangakino volcano, Taupo Volcanic Zone, New Zealand. *Journal of Volcanology and Geothermal Research*, 56, 175-203.

Briggs, R. M., Houghton, B. F., McWilliams, M., and Wilson, C. J. N. (2005). 40Ar/39Ar ages of silicic volcanic rocks in the Tauranga-Kaimai area, New Zealand: Dating the transition between volcanism in the Coromandel Arc and the Taupo Volcanic Zone. *New Zealand Journal of Geology and Geophysics*, *48*(3), 459-469.

Browne, G.H. (2004). Late Neogene sedimentation adjacent to the tectonically evolving North Island axial ranges: Insights from Kuripapango, western Hawke's Bay. New Zealand *Journal of Geology and Geophysics* 47: 663-674

Buchanan, J. (1870). On the Whanganui beds (upper Tertiary). In *Transactions of the New Zealand Institute*, Vol. 2: 163-166.

Bui, E.N., Mazullo, J., and Wilding, L.P. (1990). Using quartz grain size and shape analysis to distinguish between aeolian and fluvial deposits in the Dallol Bosso of Niger (West Africa). *Earth Surface Processes and Landforms* 14: 157–166.

Bussell, M.R. (1984). Geology and palaeobotany of the Rangitawa Stream area, southeast Wanganui Basin. Unpublished B.Sc. (Hons) thesis, Victoria University of Wellington

Bye, J.A.T. and Heath, R.A. (1975). The New Zealand semi-diurnal tide. *Journal of Marine Research 33:* 423-442

Campbell, H., Malahoff, A., Browne, G., Graham, I., and Sutherland, R. (2012). New Zealand geology. *Episodes* 35, 57-71.

Caron, V., Nelson, C. S., and Kamp, P. J. (2004). Contrasting carbonate depositional systems for Pliocene cool-water limestones cropping out in central Hawke's Bay, New Zealand. *New Zealand journal of geology and geophysics*,*47*(4), 697-717.

Carter, R. M. (1972). Wanganui strata of Komako District, Pohangina Valley, Ruahine Range, Manawatu. *Journal of the Royal Society of New Zealand*, *2*(3), 293-324.

Carter, L. (1975). Sedimentation on the continental terrace around New Zealand: a review. *Marine geology*, *19*(4), 209-237.

Carter, L., Wright, I.C., Collins, N., Mitchell, J.S., and Win, G. (1991). Seafloor stability along the Cook Strait power cable corridor. *Proceedings of the Australasian Conference of Coastal and Ocean Engineering, I0:* 565-570.

Carter, R.M., Abbott, S.T., Naish, T., and Saul, G. (1997). High resolution Plio-Pleistocene (2.5-0 Ma) chronocyclostratigraphy and section correlations, Wanganui Basin, New Zealand, Poster 2, School of Earth Sciences, James Cook University, Townsville.

Carter, R. M., and Naish, T. R. (1998). A review of Wanganui Basin, New Zealand: global reference section for shallow marine, Plio–Pleistocene (2.5–0 Ma) cyclostratigraphy. *Sedimentary geology*, *122*(1), 37-52.

Carter, L., Shane, P., Alloway, B., Hall, I. R., Harris, S. E., and Westgate, J. A. (2003). Demise of one volcanic zone and birth of another—A 12 my marine record of major rhyolitic eruptions from New Zealand. *Geology*, *31*(6), 493-496.

Christoffel, D.A. (1971). Motion of the New Zealand Alpine Fault deduced from the pattern of seafloor spreading. In: B.W. Collins and R. Fraser (Editors), Recent Crustal Movements. *Geological Society of New Zealand Bulletin 9*: 25-30.

Clement, A. J., Sloss, C. R., and Fuller, I. C. (2010). Late quaternary geomorphology of the Manawatu coastal plain, North Island, New Zealand.*Quaternary International*, 221(1), 36-45.

Clement, A.J.H. (2011). Holocene sea-level change in the New Zealand Archipelago and the geomorphic evolution of a Holocene coastal plain incised-valley system: the lower Manawatu valley, North Island, New Zealand. Unpublished PhD. thesis, Massey University, Palmerston North.

Clifton, H.E. (1982). Estuarine Deposits: in Scholle, P.A., & Spearing, D.S., (Editors), Sandstone Depositional Environments: *American Association of Petroleum Geologists, Memoir no. 31*, p. 179-189.

Cole, J. W., and Lewis, K. B. (1981). Evolution of the Taupo-Hikurangi subduction system: *Tectonophysics*, v. 72, p. 1–21.

Cotton, C. A. (1922). The geomorphology of New Zealand. Part I-systematic: an introduction to the study ofland-forms. *New Zealand Board of Science and Art, Manual No.3*. Dominion Museum, Wellington

Cowie, J.D. (1964a). Aokautere Ash in the Manawatu district, New Zealand. *New Zealand Journal of Geology and Geophysics*, 7: 66-77.

Cowie, J.D. (1964b). Loess in the Manawatu district, New Zealand. *New Zealand Journal of Geology and Geophysics*, 7: 389-396.

Cowie, J. D., Milne, J. D. G. (1973). Maps and sections showing the distribution and stratigraphy of North Island loess and associated deposits, New Zealand. *New Zealand Soil Survey report 6.*

Dalrymple, R. W., Knight, R., Zaitlin, B. A., and Middleton, G. V. (1990). Dynamics and facies model of a macrotidal sand-bar complex, Cobequid Bay—Salmon River Estuary (Bay of Fundy). *Sedimentology*, *37*(4), 577-612.

Dalrymple, R.W., Zaitlin, B.A., and Boyd, R.A. (1992). A conceptual model of estuarine sedimentation. *Journal of Sedimentary Petrology*. 62, 1130- 1146.

Dalrymple, R. W., and Rhodes, R. N. (1995). Estuarine dunes and bars.*Geomorphology and sedimentology of estuaries*, *53*, 359-422.

Dalrymple, R. W., and Choi, K. (2007). Morphologic and facies trends through the fluvial–marine transition in tide-dominated depositional systems: a schematic framework for environmental and sequence-stratigraphic interpretation. *Earth-Science Reviews*, *81*(3), 135-174.

Embry, A. (2009). Practical Sequence Stratigraphy, The Units of Sequence Stratigraphy, Part 2: Time-based Depositional Sequences. Practical Sequence Stratigraphy, *Canadian Society of Petroleum Geologists*, 81.

Erdman, C. F., and Kelsey, H. M. (1992). Pliocene and Pleistocene stratigraphy and tectonics, Ohara Depression and Wakarara Range, North Island, New Zealand. *New Zealand journal of geology and geophysics*, *35*(2), 177-192.

Fair, E. E. (1968). Structural, tectonic and climatic control of the fluvial geomorphology of the Manawatu River west of the Gorge. Unpublished M.Sc (Masters) thesis, Massey University, Palmerston North, New Zealand.

Feldmeyer, A.E., Jones, B.C., Firth, C.W., and Knight, J. (1943). The geology of the Palmerston-Wanganui Basin, "West side", North Island, New Zealand. (Unpublished report). Typescript and maps held by N.Z. Geological Survey, Lower Hutt.

Ferguson, R. I., T. Hoey, S. Wathen, and Werritty, A. (1996). Field evidence for rapid downstream fining of river gravels through selective transport, *Geology,* 24(2), 179–182.

Field, B.D., and Uruski, C.I. (1997). Cretaceous-Cenozoic geology and petroleum systems of the East Coast Region, New Zealand. *Monograph 19. Institute of Geological and Nuclear Sciences Limited*, Lower Hutt, New Zealand. 276-301.

Finlayson, L.J. (1980). The geology of the northern Pohangina Valley, Unpublished B.Sc. (Hons.) thesis, Victoria University of Wellington

Finlay, H.J., and Marwick, J. (1940). The divisions of the Upper Cretaceous and Tertiary of New Zealand. *Transactions of the Royal Society of New Zealand*. 70, 77–135.

Finlay, H.J., and Marwick, J. (1947). New divisions of the Upper Cretaceous and Tertiary in New Zealand. *New Zealand Journal of Science and Technology*. B28, 228–236

Fleming, C. A. (1953). The geology of Wanganui subdivision, Waverley and Wanganui sheet districts (N137-138). *New Zealand Geological.Survey Bulletin.*, *52*, 1-362.

Fleming, C.A. (1957). The genus Pecten in New Zealand. *New Zealand Geological Survey Palentology Bulletin*, 26:69

Folk, R. L. (1954). The distinction between grain size and mineral composition in sedimentary-rock nomenclature. *The Journal of Geology*, 344-359

Folk R.L., and Ward W.C. (1957). Brazos River bar: a study in the significance of grain size parameters. *Journal of Sedimentary Petrology,* 27:3–26

Frey, R.W., and Mayou, T.V. (1971). Decapod burrows in Holocene barrier island beaches and washover fans: *Senckenbergiana Maritima*, v. 4, 53-77.

Friedman, G.M., and Sanders J.E. (1978). Principles of Sedimentology. *Wiley:* New York, 23-234.

Friedman, G.M. (1979). Differences in size distributions of populations of particles among sands of various origins. *Sedimentology,* 26:3–32.

Friedman, G.M., and Johnson K.G. (1982). Exercises in Sedimentology. *Wiley:* New York.

Froggatt, P.C. (1983). Toward a comprehensive upper Quaternary tephra and ignimbrite stratigraphy In New Zealand using Electron Microprobe analysis of glass shards*. Quaternary Research* 19, 188-200.

Galloway, W. E. (1975). Process framework for describing the morphologic and stratigraphic evolution of deltaic depositional systems. In: Broussard, M.L., (Editor), Deltas-Models for Exploration. *Houston Geolological Society*, Houston, Texas, 87-98.

Galloway, W.E., and Hobday, D.K. (1996). Terrigenous clastic depositional systems, *Springer*, Berlin, Germany, 489.

Gillespie, J. L., Nelson, C. S., and Nodder, S. D. (1998). Post-glacial sea-level control and sequence stratigraphy of carbonate–terrigenous sediments, Wanganui shelf, New Zealand. *Sedimentary geology*, *122*(1), 245-266.

GoogleEarth (2014). Digital Globe Imagery, Imagery date: 1/09/2013, Date last accessed: 17/07/2014

Greenall, A.F., Hamilton, D., Glass, A., Sutherland, N., and Osborne, B. (1951). Soil Conservation Survey of the Pohangina District, North-East Manawatu. *Report to the Soil Conservation and Rivers Control Council,* Wellington, New Zealand.

Guilcher, A. (1967). Origin of sediments in estuaries, in Lauff, G.H., (editor), Estuaries: *American Association for the Advancement of Science Publication 83*: 149-157.

Hanson, J. A. (1998). The neotectonics of the Wellington and Ruahine faults between the Manawatu Gorge and Puketitiri, North Island, New Zealand. PhD thesis, Massey University, New Zealand.

Harris, T.F.W. (1990). Greater Cook Strait — Form and Flow. *DSIR Marine and Freshwater*, Wellington, 212.

Haug, H.H., Ganopolski, A., Sigman, D.M., Rosell-Mele, A., Swann, G.E.A., Tiedemann, R., Jaccard, S.L., Bollman, J., Maslin, M.A., Leng, M.J., and Eglinton, G. (2005). North Pacific seasonality and the glaciation of North America 2.7 million years ago. *Nature*, 433, 821–825.

Hayward, B., W. (1986). A guide to paleoenvironmental assessment using New Zealand Cenozoic foraminiferal faunas. *New Zealand Geological Survey report*, *109*, 73.

Hayward, B. W., Black, P. M., Smith, I. E., Ballance, P. F., Itaya, T., Doi, M., and Robertson, D. J. (2001). K-Ar ages of early Miocene arc-type volcanoes in northern New Zealand. *New Zealand Journal of Geology and Geophysics*, *44*(2), 285-311.

Hochstetter, F. Von. (1864). Geology of New Zealand. Contributions to the geology of the provinces of Auckland and Nelson. Translated from the German and edited by C A. Fleming. (1959) Wellington, Government Printer. XXI + 310 p

Holland, S. (2013) UGA Stratigraphy lab; An Online Guide to Sequence Stratigraphy, URL: http://strata.uga.edu/, Date last accessed: 29/01/2015

Homewood, P., and Allen, P. (1981). Wave-, tide-, and current-controlled sand bodies of Miocene Molasse, Western Switzerland: *American Association of Petroleum Geologists Bul letin 65*: 2534–2545

Horton , B.K., and Schmitt, J.G. (1996). Sedimentology of a lacustrine fan-delta system, Miocene Horse Camp Formation, Nevada, USA: *Sedimentology 43*: 133-155

Hou, B., Alley, N. F., Frakes, L. A., Gammon, P. R., and Clarke, J. D. (2003). Facies and sequence stratigraphy of Eocene palaeovalley fills in the eastern Eucla Basin, South Australia, *Sedimentary Geology*, *163*(1), 111-130.

Houghton, B. F., Wilson, C. J. N., McWilliams, M. D., Lanphere, M. A., Weaver, S. D., Briggs, R. M., and Pringle, M. S. (1995). Chronology and dynamics of a large silicic magmatic system: Central Taupo volcanic zone, *New Zealand Geology 23*: 13–16.

Hutton, F. W. (1873). Report on the geology of the north-east portion of the South Island, from Cook Straits to the Rakaia. *Reports of the Geological Explorations during*, *4*, 27-58.

Hutton, F.W. (1886). The Wanganui System. *Transactions of New Zealand Institute* 18: 336-367.

Jackli, R. (1957). Review of the Superior Oil Company report on the Rangitikei area. Shell, D'Arcy and Todd Oil Services geological report 7. Unpublished, held as open-file petroleum report 410 by New Zealand Geological Survey, Lower Hutt.

Jackson, J., van Dissen, R., and Berryman, K. (1998). Tilting of active folds and faults in the Manawatu region, New Zealand: evidence from surface drainage patterns. *New Zealand Journal of Geology and Geophysics*, *41*(4), 377-385.

Kamp, P.J.J., Vonk, A.J., Bland, K.J., Hansen, R.J., Hendy, A.J.W., McIntyre, A.P., Ngatai, M., Cartwright, S.J., Hayton, S., and Nelson, C.S. (2004). Neogene stratigraphic architecture and tectonic evolution of Wanganui, King Country, and eastern Taranaki basins, New Zealand. *New Zealand Journal of Geology and Geophysics 47*: 625-644.

Kidwell, S.M., and Bosence, D.W.J. (1991). Taphonomy and time-averaging of marine shelly faunas, *in*: Allison, P.A., & Briggs, D.E.G., (editors) Taphonomy, releasing the data locked in the fossil record: New York, *Plenum Press*, 115-209.

Kingma, J.T. (1957a). The North Island Geanticline in the Hawke's Bay Sector. *New Zealand Journal of Science and Technology B38*: 496-99.

Kingma, J.T. (1957b). The Tectonic Setting of the Ruahine-Rimutaka Range. *New Zealand Journal of Science and Technology B38:* 858-61.

Kingma, J.T. (1958). The Tongaporutuan Sedimentation in Central Hawke's Bay. *New Zealand Journal of Geology and Geophysics 1* : 1-30

Kingma, J.T. (1959). The tectonic history of New Zealand. *New Zealand journal of geology and geophysics*, *2*(1), 1-55.

Kingma, J.T. (1962). Sheet ll-Dannevirke. Geological map of New Zealand 1:250000. Wellington, Department of Scientific and Industrial Research.

Kingma, J.T. (1967). Wellington, 1st Edition. Geological Map of New Zealand 1: 250,000, Sheet 12. New Zealand Department of Scientific and Industrial Research, Wellington.

Kingma, J.T. (1971). Geology of Te Aute subdivision. *New Zealand Geological Survey bulletin 70: 173*

Klein, G., De, V. (1977). Tidal circulation model for deposition of clastic sediment on epeiric and mioclinal shelf seas, *Sedimentary Geology 18*: 1-12.

Kohn, B. P., Pillans, B., and McGlone, M.S. (1992). Zircon fission track age for middle Pleistocene Rangitawa Tephra, New Zealand: stratigraphic and paleoclimatic significance. *Palaeogeography, palaeoclimatology, palaeoecology*, *95*(1), 73-94.

Lee, J. M., and Begg, J. G. (2002). Geology of the Wairarapa area, Institute of Geological & Nuclear Sciences 1: 250 000 Geological Map 11. *Lower Hutt, New Zealand. Institute of Geological and Nuclear Sciences Limited*, 1-10.

Lensen, G.J. (1977). Late Quaternary tectonic map of New Zealand 1:2 000 000. New Zealand Geological Survey miscellaneous series map 12. Wellington, *Department of Scientific and Industrial Research*

Lewis, K.B. (1979). A storm dominated inner-shelf, western Cook Strait, New Zealand: *Marine Geology* 31: 31–43

Lewis, K. B., Carter, L., Davey, F. J. (1994). The opening of Cook Strait: interglacial tidal scour and aligning basins at a subduction to transform plate edge. *Marine geology*, *116*(3), 293-312.

Lisiecki, L. E., & Raymo, M. E. (2005). A Pliocene-Pleistocene stack of 57 globally distributed benthic δ18O records. *Paleoceanography*, *20*(1).

Lillie, A. R. (1953). The geology of the Dannevirke Subdivision. *New Zealand Geological Survey Bulletin 46*: 156.

Limarino, C. O., Césari, S. N., Net, L. I., Marenssi, S. A., Gutierrez, R. P., and Tripaldi, A. (2002). The Upper Carboniferous postglacial transgression in the Paganzo and Rio Blanco basins (northwestern Argentina): facies and stratigraphic significance. *Journal of South American Earth Sciences*, *15*(4), 445-460.

LINZ, (2015) Land Information New Zealand, URL: http://www.topomap.co.nz/NZTopoMap/nz47645/Pohangina/Manawatu-Whanganui, Date last accessed: 27/01/2015

Lowe, D. J., Blaauw, M., Hogg, A. G., and Newnham, R. M. (2013). Ages of 24 widespread tephras erupted since 30,000 years ago in New Zealand, with re-evaluation of the timing and palaeoclimatic implications of the Lateglacial cool episode recorded at Kaipo bog. *Quaternary Science Reviews*, *74*, 170-194.

MacPherson, A.T. (1985). Stratigraphy and tephra correlations of Pleistocene sediments from the Finnis Road area, Pohangina, Manawatu. Unpublished BSc. (Hons.) thesis, Victoria University.

McPherson, J.G., Shanmugan, G., and Moiola, R.J. (1987). Fan deltas and braid deltas: Varieties of coarse-grained deltas: *Geological Society of America Bulletin* 99: 331-340

Manning, D.A. (1988). Stratigraphy and paleoenvironment of deposition of mid-Quaternary sedimeents in Culling's Gullies, Pohangina Valley, Manawatu, New Zealand. Un-published BSc. (Hons.) thesis, Massey University.

Manville, V., Németh, K., and Kano, K. (2009). Source to sink: a review of three decades of progress in the understanding of volcaniclastic processes, deposits, and hazards. *Sedimentary Geology*, *220*(3), 136-161.

Marden, M. (1984). Geology and its relationship to erosion in the southern Ruahine Range, North Island, New Zealand. Unpublished PhD. thesis, lodged in the Library, Massey University, Palmerston North.

McCave, I.N. (1970). Deposition of fine-grained suspended sediment from tidal currents. *Journal of Geophysical Research*, 4151-4159.

McCave, I. N. (1985). Recent shelf clastic sediments. *Geological Society, London, Special Publications*, *18*(1), 49-65.

McFadgen, B. (2003). Archaeology of the Wellington Conservancy: Wairarapa. *A study in tectonic archaeology. Department of Conservation, Wellington*. 1- 10.

McIntyre, A.P. (2002). Geology of Mangapanian (late Pliocene) strata, Wanganui Basin: lithostratigraphy, palaeontology and sequence stratigraphy. Unpublished PhD thesis, lodged in the Library, University of Waikato, Hamilton, New Zealand. 1-431 +2 maps.

McPherson, J. G., Shanmugam, G., and Moiola, R. J. (1987). Fan-deltas and braid deltas: varieties of coarse-grained deltas. *Geological Society of America Bulletin*, 99(3), 331-340.

Melhuish, A., Van Dissen, R., Berryman, K. (1996). The Mount Stewart-Halcombe Anticline: a look inside a growing fold in the Manawatu region, New Zealand. *New Zealand journal of geology and geophysics* 39: 123-133.

Miall, A. D. (1977). Lithofacies types and vertical profile models in braided river deposits: a summary. In: Fluvial Sedimentology (Edited by Miall, A.D.), *Memoirs* of *the Canadian Association of Petroleum Geologists* 5. 597-604.

Middleton, G. V. (1973). Johannes Walther's law of the correlation of facies.*Geological Society of America Bulletin*, *84*(3), 979-988.

Mildenhall, D. C. (1975). Palynology of the Acacia-bearing beds in the Komako District, Pohangina Valley, North Island, New Zealand. *New Zealand journal of geology and geophysics*, *18*(2), 209-228.

Milne, J. D. G. (1973a). Upper Quaternary geology of the Rangitikei drainage basin, North Island, New Zealand. Unpublished Ph.D. thesis, lodged in the Library, Victoria University of Wellington.

Milne, J.D.G. (1973b). Maps and sections of river terraces in the Rangitikei basin, North Island, New Zealand. New Zealand Soil Survey Report, 4.

Morley, J.J., and Shackleton, N.J. (1978). Extension of the radiolarian *Stvlatrartus univerus* as a biostratigraphic datum to the Atlantic Ocean. *Geology* 6: 309-311.

Morley, M. S., and Hayward, B. W. (1999). Inner shelf mollusca of the Bay of Islands, New Zealand, and their depth distribution. *Records of the Auckland Museum*, 119-140.

Morley, M. S., and Hayward, B. W. (2007). Intertidal and shallow-water Ostracoda of the Waitemata Harbour, New Zealand. *Records of the Auckland Museum*, 17-32

Morrell, .W.J. (1991). The geology of a Holocene to Modern flood plain of the Manawatu River upstream of the Manawatu Gorge near Woodville. Unpublished Hon. Thesis, Massey University, Palmerston North.

Mortimer, N. (2004). New Zealand's geological foundations. *Gondwana Research*, *7*(1), 261-272.

Morton, J., and Miller, M. (1968). The New Zealand sea shore, London, *Collins*, 1-638.

Munsell, A. H., (1988) Munsell Soil Color Chart, Munsell Publishing Company.

Naish, T., and Kamp, P. J. (1995). Pliocene-Pleistocene marine cyclothems, Wanganui Basin, New Zealand: A lithostratigraphic framework. *New Zealand journal of geology and geophysics 38*(2): 223-243.

Naish, T., Kamp, P. J., Alloway, B. V., Pillans, B., Wilson, G. S., and Westgate, J. A. (1996). Integrated tephrochronology and magnetostratigraphy for cyclothemic marine strata, Wanganui Basin: implications for the Pliocene-Pleistocene boundary in New Zealand. *Quaternary international 34*: 29-48.

Naish, T.R., and Kamp, P.J.J. (1997a). High resolution sequence stratigraphy of 6$^{th}$ order (40ka) Plio-Pleistocene cyclothems, Wanganui Basin, New Zealand: A case for the regressive systems tract. *Geological society of America Bulletin* 109: 978-999

Naish, T. R., Abbott, S. T., Alloway, V., Beu, A. G., Carter, R. M., Edwards, A. R., and Woolfe, K. J. (1998). Astronomical calibration of a southern hemisphere Plio-Pleistocene reference section, Wanganui Basin, New Zealand.*Quaternary Science Reviews*, *17*(8), 695-710.

Naish, T., Alloway, B., Beu, A., and Palmer, A. (2004). New Zealand Friends Of The Quaternary, *Institute of Geological and Nuclear Sciences Information Series 66. 7-16.*

Naish, T. R., Field, B. D., Zhu, H., Melhuish, A., Carter, R. M., Abbott, S. T., and Maslen, G. (2005). Integrated outcrop, drill core, borehole and seismic stratigraphic architecture of a cyclothemic, shallow-marine depositional system, Wanganui Basin, New Zealand. *Journal of the royal society of new zealand*,*35*(1-2), 91-122.

Neef, G. (1974). Sheet N 153, Eketahuna (1$^{st}$ ed), In: Geological map of New Zealand: *New Zealand Department of Science and Industrial Research*, scale 1:63,360.

Neef, G. (1984). Late Cenozoic and early Quaternary stratigraphy of the Eketahuna District (N153). *New Zealand Geological Survey bulletin* 96: 101.

Nelson, C. S., Froggatt, P. C., and Gosson, G. J. (1985). Nature, chemistry and origin of late Cenozoic megascopic tephras in Leg 90 cores from the southwest Pacific,inKennett, J. P., and others, *Initial reports of the Deep Sea Drilling Project, Volume 90*: Washington, D.C., U.S. Government Printing Office, 1161–1173

Nemec, W., and Steel, R.J. (1984). Alluvial and coastal conglomerates; their significant features and some comments on gravelly mass-flow deposits. In: Koster, E.H., and Steel, R.J, (Editors) Sedimentology of Gravels and Conglomerates. *Canadian Society of Petroleum Geologists Memoir* 10: 1-31

Nittrouer, C. A., & Wright, L. D., (1994). Transport of particles across continental shelves. *Reviews of Geophysics 32*(1): 85-113.

NZ TopoMap 250 (2014). URL: http://www.topomap.co.nz/ Map last updated May 21st, 2014. Date last accessed: 2/06/2014.

Ongley, M. (1935). Eketahuna Subdivision. *New Zealand Geological Survey 29th Annual Report* 1934-1935: 1-6

Ower, J. (1943). The Geology of the Manawatu Saddle and the Adjacent Fronts of the Ruahine Range, North Island, New Zealand. (Unpublished Report of the Superior Oil Co. of N,Z. Ltd., deposited in the N.Z. Geological Survey library).

Pantin, H. M. (1958). Rate of formation of a diagenetic calcareous concretion. *Journal of Sedimentary Research 28*(3).

Park, J. (1887). On the geology of the western part of Wellington Provincial District and part of Taranaki. *Reports of the geological explorations of the New Zealand Geological Survey* (1886-87) 18: 24-73.

Parker, G. (1991). Selective sorting and abrasion of river gravel. I, II: Theory and Applications. *Journal of Hydraulic Engineering 117*(2): 131-171.

Pickrill, R.A., and Mitchell, J.S. (1979). Ocean wave characteristics around New Zealand. *New Zealand Journal of Marine and Freshwater Resources 13*: 501–520.

Pillans, B., Chappell, J., and Naish, T.R. (1998). A review of the Milankovitch climate beat: template for Plio-Pleistocene sea-level changes and sequence stratigraphy. *Sedimentary Geology 122:* 5-21

Pillans, B. (1994). Direct marine-terrestrial correlations, Wanganui Basin, New Zealand: the last 1 million years. *Quaternary science reviews 13*(3): 189-200.

Pillans, B., Alloway, B., Naish, T., Westgate, J., Abbott, S., and Palmer, A. (2005). Silicic tephras in Pleistocene shallow-marine sediments of Wanganui Basin, New Zealand. *Journal of the Royal Society of New Zealand 35*(1-2): 43-90.

Postma G. (1990). Depositional architecture and facies of river and fan deltas: a synthesis. In: Colella, A., & Prior, D.B., (Editors), Coarse Grained Deltas. *Special Publication International Association of Sedimentology* 10: 13-27.

Powell, A. W. B. (1979). New Zealand Mollusca: Marine, land and freshwater shells. Auckland. *Collins*. 1-500.

Pringle, M. S., McWilliams, M., Houghton, B. F., Lanphere. M. A., and Wilson, C. J. N. (1992). 40Ar/39Ar dating of Quaternary feldspar: examples from the Taupo Volcanic Zone, *New Zealand. Geology* 20: 531-534.

Proctor, R., and Carter, L. (1989). Tidal and sedimentary response to the late Quaternary closure and opening of Cook Strait, New Zealand: results from numerical modelling *Paleoceanography* 4: 167–180

Proust, J. N., Lamarche, G., Nodder, S., and Kamp, P. J. (2005). Sedimentary architecture of a Plio-Pleistocene proto-back-arc basin: Wanganui Basin, New Zealand. *Sedimentary Geology 181*(3): 107-145.

Reading, H.G. (1996). Sedimentary Environments; Processes, Facies, and Stratigraphy, Third Edition: Oxford, U.K., *Blackwell Science*, 688.

Reineck, H. E., and Wunderlich, F. (1968). Classification and origin of flaser and lenticular bedding. *Sedimentology 11*(1-2): 99-104.

Reineck, H.E., and Singh, I.B. (1980). Depositional Sedimentary Environments, 2nd Edition: Berlin, *Springer-Verlag*, 551.

Reyners, M. (1980). A microearthquake study of the plate boundary, North Island, New Zealand. *Geophysical Journal International 63*(1): 1-22.

Rich, C. C. (1959). Late Cenozoic geology of the lower Manawatu valley, New Zealand. Unpublished PhD. thesis, Harvard University; copy lodged in the Library, Victoria University of Wellington, New Zealand.

Roy, P. S., Thom, B. G., and Wright, L. D. (1980). Holocene sequences on an embayed high-energy coast: an evolutionary model. *Sedimentary Geology 26*(1): 1-19.

Saul, G., Naish, T. R., Abbott, S. T., and Carter, R. M. (1999). Sedimentary cyclicity in the marine Pliocene-Pleistocene of the Wanganui basin (New Zealand): Sequence stratigraphic

motifs characteristic of the past 2.5 my. *Geological Society of America Bulletin 111*(4): 524-537.

Schellart, W. P. (2007). North-eastward subduction followed by slab detachment to explain ophiolite obduction and Early Miocene volcanism in Northland, New Zealand. *Terra Nova 19*(3): 211-218.

Seward, D. (1974a). Some aspects of sedimentology of the Wangnaui Basin, North Island New Zealand, Unpublished Phd thesis, Victoria University of Wellington, Wellington, New Zealand

Seward, D. (1974b). Age of New Zealand Pleistocene substages by fission- track dating of glass shards from tephra horizons. *Earth and Planetary Science Letters 24*: 242-248.

Seward, D. (1976). Tephrostratigraphy of the marine sediments in the Wanganui Basin, New Zealand. *New Zealand journal of geology and geophysics 19*(1): 9-20.

Seward, D. (1979). Comparison of zircon and glass fission-track ages from tephra horizons. *Geology 7*: 479-482.

Seward, D., and Kohn, B.P. (1997). New zircon fission-track ages from New Zealand Quaternary tephra: an interlabratory experiment and recommendations for the determination of young ages. *Chemical Geology 141*: 127-140.

Seymour, R. J. (1990). Autosuspending turbidity flows, *The Sea 9*: 919 – 940.

Shackleton, N. J., Berger, A., and Peltier, W. R. (1990). An alternative astronomical calibration of the lower Pleistocene timescale based on ODP Site 677. *Transactions of the Royal Society of Edinburgh: Earth Sciences 81*(04): 251-261.

Shane, P. A. R. (1991). Remobilised silicic tuffs in middle Pleistocene fluvial sediments, southern North Island, New Zealand. *New Zealand journal of geology and geophysics 34*(4): 489-499.

Shane, P. A. (1994). A widespread, early Pleistocene tephra (Potaka tephra, 1 Ma) in New Zealand: Character, distribution, and implications. *New Zealand Journal of Geology and Geophysics 37*(1): 25-35.

Shane, P. A., Black, T. M., Alloway, B. V., and Westgate, J. A. (1996). Early to middle Pleistocene tephrochronology of North Island, New Zealand: implications for volcanism, tectonism, and paleoenvironments. *Geological Society of America Bulletin 108*(8): 915-925.

Shultz, A. W. (1984). Subaerial debris-flow deposition in the upper Paleozoic Cutler Formation, western Colorado. *Journal of Sedimentary Research 54*(3).

Smith, G. A. (1987). The influence of explosive volcanism on fluvial sedimentation: the Deschutes Formation (Neogene) in central Oregon. *Journal of Sedimentary Research 57*(4).

Sporli, K.B. (1980). New Zealand and oblique-slip margins: tectonic development up to and during Cenozoic. In: Balance, P.F., and Reading, H.G., (Editors), Sedimentation on Oblique-Slip Mobile Zones. *Special Publication of the International Assocociation of Sedimentologists 4*: 147-170.

Stratford, W. R., and Stern, T.A. (2004). Strong seismic reflections and melts in the mantle of a continental back-arc basin, *Geophysical Research Letters 31*, L06622, doi:10.1029/2003GL019232

Stern, T.A., Quinlan, G.M., and Holt, W.E. (1993). Crustal dynamics associated with the formation of Whanganui Basin, New Zealand. In: Balance, P.F., (Editor) South Pacific sedimentary basins. Sedimentary Basins of the world 2. *Elsevier Science Publications*, 413.

Stern, T. A., Stratford, W. R., and Salmon, M. L. (2006). Subduction evolution and mantle dynamics at a continental margin: Central North Island, New Zealand. *Reviews of Geophysics 44*(4).

Suggate, R.P. (1978). The Kaikoura Orogeny. In: Suggate, R.P., Stevens, G.R., & Te Punga, M.T., (Editors), *The Geology of New Zealand. Government Printer*, Wellington, 672-701.

Swift, D.J.P. (1976). Continental shelf sedimentation. In: Stanley, D.J., & Swift, D.J.P., (Editors), Marine Sediment Transport and Environmental Management. *Wiley,* New York, 311-350.

Swift, D.J.P., and Rice, D.D. (1984). Sand bodies on muddy shelves: a model for sedimentation in the western interior Cretaceous seaway, North America, In: Tillman, R.W., & Seimers, C.T., (Editors), Siliciclastic Shelf Sediments: *SEPM, Special Publication 34*: 43–62.

Thorne, J. A., and Swift, D. J. P. (1991). Sedimentation on continental margins, VI: a regime model for depositional sequences, their component systems tracts, and bounding surfaces. *Shelf Sand and Sandstone Bodies: Geometry, Facies and Sequence Stratigraphy*, 189-255.

Szabo, T., Fityus, S., and Domokos, G. (2013). Abrasion model of downstream changes in grain shape and size along the Williams River, Australia. *Journal of Geophysical Research: Earth Surface 118*(4): 2059-2071.

Te Punga, M. (1952). The geology of the Rangitikei Valley. *New Zealand Geological Survey Memoir 8:* 46.

Te Punga, M.T. (1957). Live anticlines in western Wellington. *New Zealand Journal of Science and Technology* B38: 433-46.

Terwindt, J. H. J., and Breusers, H. N. C. (1972). Experiments on the origin of flaser, lenticular and sand-clay alternating bedding. *Sedimentology 19*(1-2): 85-98.

Thomson, J.A. (1917). Diastrophism and other considerations in classification and correlation, and the existence of minor diastrophic districts in the Notocene. *New Zealand Institue Transactions* 49: 397–413.

Townsend, T.D. (1993). Beehive Creek, Pohangina Valley, Manawatu, New Zealand – Stratigraphy and paleoenvironment of deposition of mid-Quaternary sediments. Unpublished BSc (Hons) thesis, Massey University, Palmerston North.

Trewick, S. A., and Bland, K. J. (2012). Fire and slice: palaeogeography for biogeography at New Zealand's North Island/South Island juncture. *Journal of the Royal Society of New Zealand 42*(3): 153-183.

Turner, G. M., and Kamp, P. J. (1990). Palaeomagnetic location of the Jaramillo Subchron and the Matuyama-Brunhes transition in the Castlecliffian stratotype section, Whanganui Basin, New Zealand. *Earth and planetary science letters 100*(1): 42-50.

Vandergoes, M. J., Hogg, A. G., Lowe, D. J., Newnham, R. M., Denton, G. H., Southon, J., and Blaauw, M. (2013). A revised age for the Kawakawa/Oruanui tephra, a key marker for the Last Glacial Maximum in New Zealand. *Quaternary Science Reviews 74*: 195-201.

Van der Neut, M. (1996). Sequence stratigraphy of Plio-Pleistocene sediments in lower Turakina Valley, Whanganui Basin, New Zealand. Unpublished MSc thesis, Massey University, Palmerston North.

Veevers, J.J. (2000). Billion-year Earth history of Australia and neighbours in Gondwanaland: Sydney, *GEMOC Press*, 400.

Vella, P. (1962). Biostratigraphy and paleoecology of Mauriceville District, New Zealand. *Transactions of the Royal Society of New Zealand., Geology, 1*(12): 1893-99.

Walcott, R. I. (1978). Preset tectonics and late Cenozoic evolution of New Zealand. *Geophysical Journal of the Royal Astronomical Society* 52: 137 -164.

Walcott, R.I. (1978a). Geodetic strains and large earthquakes in the axial tectonic belt of North Island, *New Zealand Journal of Geophysical Research* 83: 4419-4429.

Waresback, D.B. and Turbeville, B.N. (1990). Evolution of a Plio-Pleistocene volcanogenic-alluvial fan: the Puye Formation, Jemez Mountains, New Mexico. *Geolological Society of America Bulletin 102*: 298-314.

Wellman, H.W. (1948), Tararua Range summit height accordance, *New Zealand Journal of Science and Technology* B30: 123-127.

Wellman, H. W. (1953). Data for the study of Recent and late Pleistocene faulting in the South Island of New Zealand: *New Zealand Journal of Science and Technology* B34: 270-288.

Westgate, J.A. (1988). Isothermal plateau fission-track age of the late Pleistocene Old Crow tephra. *Geophysical Research Letters* 15: 376-379.

Westgate, J.A. (1989). Isothermal plateau fission-track ages of hydrated glass shards from silicic tephra beds. *Earth and Planetary Science Letters 95*: 226-234.

Wilgus, C. K., Hastings, B.S., Kendall, C. G. St. C., Posamentier, H. W., Ross, C. A. and Van Wagoner, J. C. (1988). Sea-level changes: an integrated approach. *Society of Economic Paleontologists and Mineralogists, Special Publication, 42*: 47-70.

Wilson, C. J. N., Rogan, A. M., Smith, I. E., Northey, D. J., Nairn, I. A., and Houghton, B. F. (1984). Caldera volcanoes of the Taupo volcanic zone, New Zealand: *Journal of Geophysical Research* 89: 8463–8484.

Wilson, C. J. N. (1986). Reconnaissance stratigraphy and volcanology of ignimbrites from Mangakino volcano. *Late Cenozoic volcanism in New Zealand. Royal Society of New Zealand Bulletin 23*: 179-193.

Wilson, C. J. N., Houghton, B. F., Kamp, P. J. J., and McWilliams, M. O. (1995). An exceptionally widespread ignimbrite with implications for pyroclastic flow emplacement. *Nature*, *378*(6557), 605-607.

Wilson, C. J. N., Houghton, B. F., McWilliams, M. O., Lanphere, M. A., Weaver, S. D., and Briggs, R. M. (1995). Volcanic and structural evolution of Taupo Volcanic Zone, New Zealand: a review. *Journal of volcanology and geothermal research 68*(1): 1-28.

Whitehouse, I.E., and Pearce, A.J. (1992). Shaping the Mountains of New Zealand, In: Soons, J.M., Selby, M.J. (Editors), Landforms of New Zealand, 2nd edition. *Longman*, Auckland, 144–160.

# Appendices

## Appendix 1: Tephra geochemical and grain size data

1.1 Sample locations:

| Sample Number | Tephra | Stratigraphic Member/ Formation | Location & Coordinates |
|---|---|---|---|
| T1 | Potaka Pumice | Kaimatira Pumice Sand Formation. | 40°15'28.02"S 175°46'52.15"E, elev 74 m. Entrance to Antler Stream. |
| T2 | Kaukatea Tephra | Rc Member, Kai Iwi Group | 40°14'58.17"S 175°47'42.42"E, elev 118 m. Maungatukurangi Stream. |
| T3 | Kawakawa Tephra | Ohakean Loess on Ratan Terrace. | 40°14'33.92"S 175°47'05.43"E, elev 121m. Ratan Terrace, 600 m north of entrance to Maugatukurangi Stream |
| T4 | Pakihikura Tephra | Bms Member, Takapari Formation. | 40°13'29.61"S 175°48'45.35"E, elev 226m. No 4 line, 200 m east of Ohakean Terrace |
| T5 | Mangapipi Tephra | Bms Member, Takapari Formation. | 40°16'37.40"S 175°46'28.35"E, elev 69 m. True left bank of Pohangina River. |
| T6 | Mangapipi Tephra | Bms Tephra, Takapari Formation. | 40°15'43.72"S 175°47'15.50"E, elev 120 m. 650 m up Antler Stream. |
| T7 | Scrimmys Tephra | Css Member, Takapari Formation. | 40°17'43.16"S 175°46'08.88"E, elev 88 m. True left side of entrance to Saddle Creek |
| T8 | Scrimmys Tephra | Css Member, Takapari Formation. | 40°16'47.11"S 175°46'26.04"E, elev 82 m. True left side of entance to Scrimmys Stream |
| T9 | Ridge Tephra | Bms Member, Takapari Formation. | 40°14'41.76"S 175°48'21.69"E, elev 179 m. True left fork of Whareroa Stream |

| | | | |
|---|---|---|---|
| T10 | Potaka Pumice | Kaimatira Pumice Sand Formation. | 40°18'02.44"S 175° 45'32.32"E, elev 59 m. True right bank of Pohangina River, 500 m south of Ashhurst train bridge. |
| T11 | Ridge Tephra | Bms Member, Takapari Formation | 40°14'36.58"S 175°48'13.31"E, elev 160 m. True left fork of Whareroa Stream. |
| T12 | Rewa Pumice | Css Member, Takapari Formation | 40°16'48.07"S 175°46'28.47"E, elev 86 m. Beds 18 - 20 from stratigraphic log 6.1. Entrance to Scrimmys Stream. |
| T13 | Rewa Pumice | Css Member, Takapari Formation | 40°16'48.05"S 175°46'27.53"E, elev 88 m. Beds 24 - 25 from stratigraphic log 6.1. Entrance to Scrimmys Stream. |
| T14 | Rewa Pumice | Css Member, Takapari Formation | 40°16'47.53"S 175°46'26.56"E, elev 83 m. Beds 29 – 30 from straitgraphic log 6.1. Entrance to Scrimmys Stream. |
| T15 | Unkown | Kamatira Pumice Sand Formation | 40°14'55.45"S 175°40'52.26"E, elev 83 m. Entrance to Maungatukurangi Stream (stream bank) |
| T16 | Potaka Pumice | Kaimatira Pumice Sand Formation | 40°14'54.82"S 175°46'55.06"E, elev 90 m. Entrance to Maungatukurangi Stream, true right side of stream, road cutting. |

Note: Points which contained totals lower than 90% were removed from the data sets. Isolated outliers were also removed. Included below are the normalised data sets for each tephra sample. Included in the data sets below are the Wt % of water, 1/3 $K_2O$, sum (FeO+ 1/3 $K_2O$+ CaO), and % of FeO, 1/3 $K_2O$, and CaO in relation to the sum. The percentages of FeO, 1/3 $K_2O$, and CaO in relation to the sum were used to construct ternary diagrams, while the normalised data was used to construct CaO vs FeO diagrams. Raw data sets were omitted from the appendices given the shear size of the data sets. To obtain raw data sets please feel free to contact the author at callumjrees @gmail.com.

1.2 Flow chart of procedures taken during sample preparation for EMP analysis:

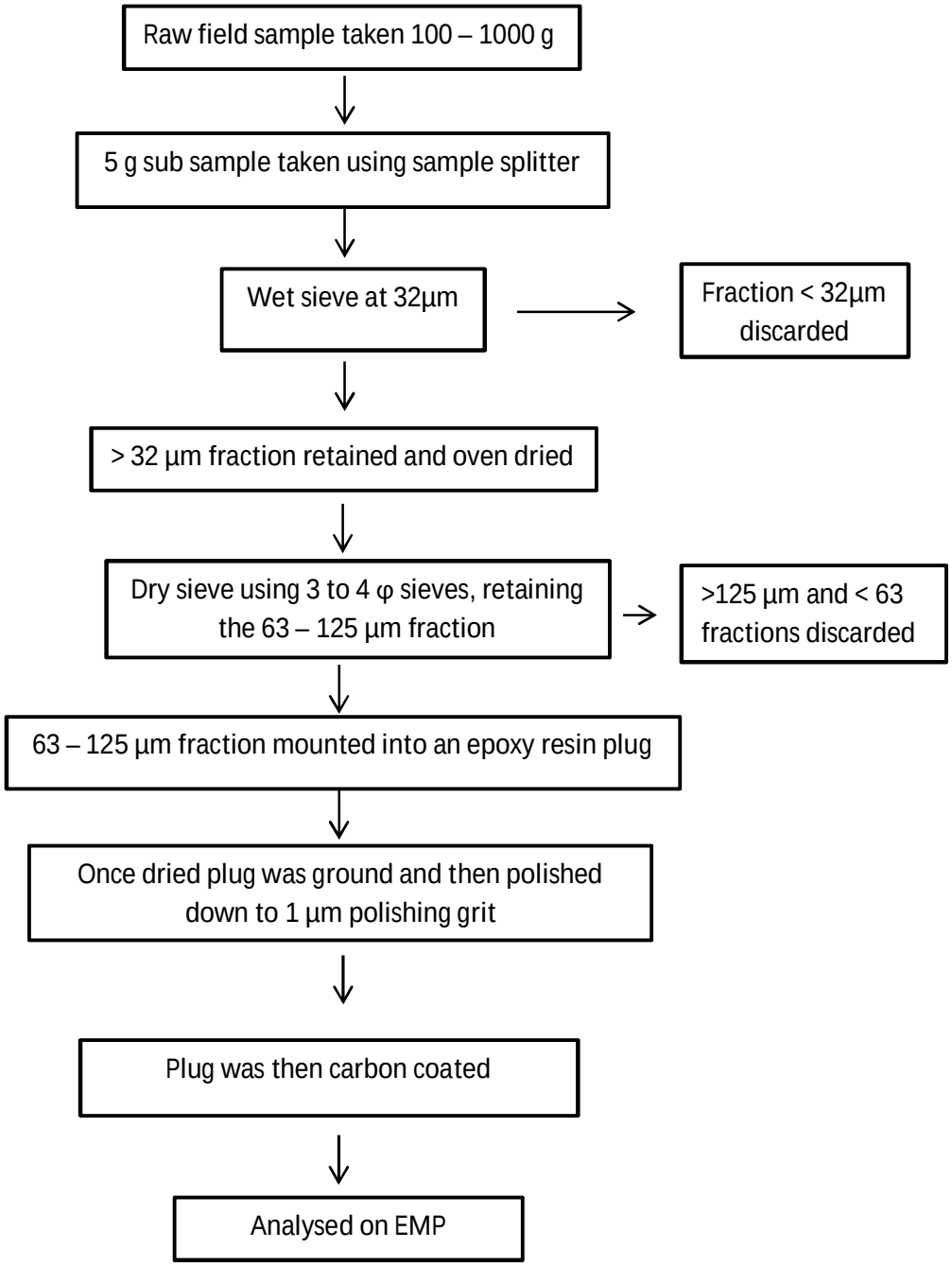

1.3 Kawakawa Tephra – sample T3:

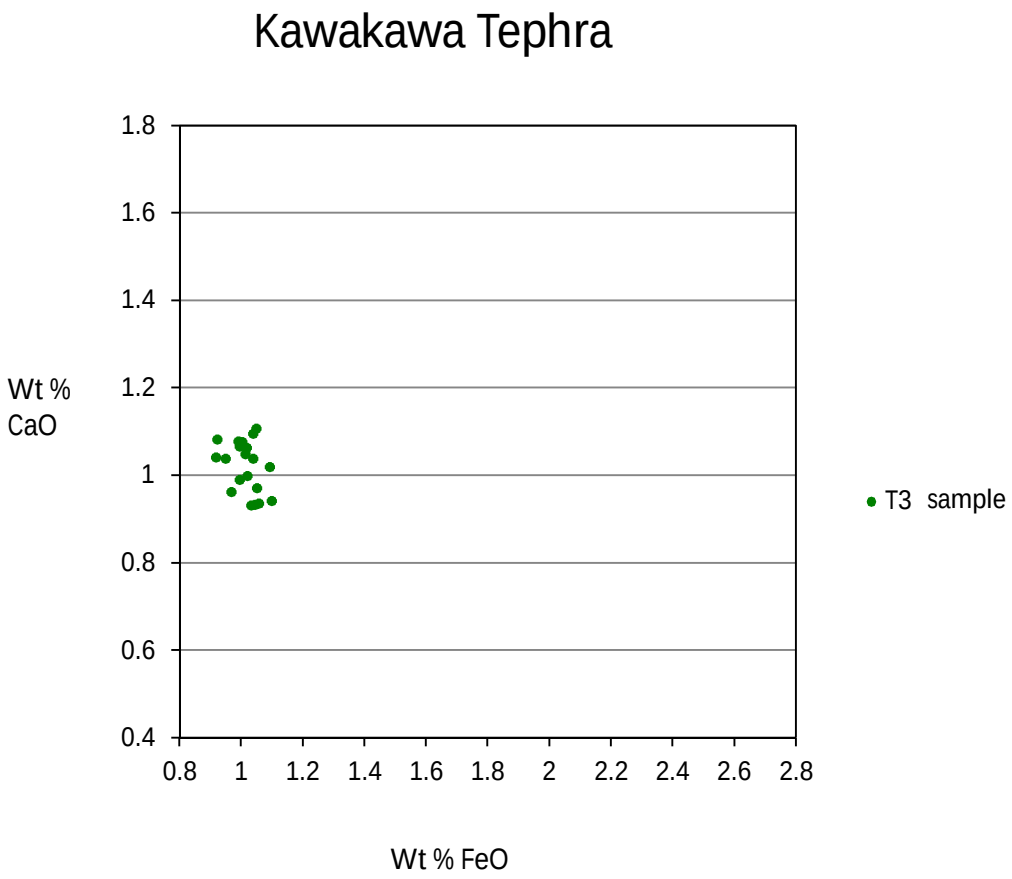


| T3 Normalised data (Wt %) | | | | | | | | | |
|---|---|---|---|---|---|---|---|---|---|
| Readings | SiO2 | Al2O3 | TiO2 | FeO | MgO | CaO | Na2O | K2O | Cl |
| 1 | 79.17 | 11.92 | 0.13 | 1.04 | 0.14 | 1.10 | 3.63 | 2.65 | 0.23 |
| 2 | 79.12 | 11.76 | 0.13 | 0.99 | 0.10 | 0.99 | 3.93 | 2.72 | 0.26 |
| 3 | 79.11 | 12.01 | 0.15 | 0.95 | 0.11 | 1.04 | 3.70 | 2.70 | 0.23 |
| 4 | 79.46 | 11.77 | 0.13 | 1.06 | 0.11 | 0.94 | 3.63 | 2.67 | 0.23 |
| 5 | 79.41 | 11.76 | 0.12 | 0.97 | 0.09 | 0.96 | 3.78 | 2.66 | 0.25 |
| 6 | 79.54 | 11.86 | 0.13 | 0.92 | 0.08 | 1.04 | 3.57 | 2.63 | 0.24 |
| 7 | 79.13 | 11.78 | 0.13 | 1.09 | 0.07 | 1.02 | 3.91 | 2.62 | 0.24 |
| 8 | 79.28 | 11.82 | 0.13 | 1.04 | 0.13 | 1.04 | 3.65 | 2.65 | 0.25 |
| 9 | 78.99 | 12.03 | 0.14 | 0.99 | 0.12 | 1.07 | 3.87 | 2.55 | 0.25 |
| 10 | 79.06 | 11.92 | 0.09 | 1.02 | 0.11 | 1.06 | 3.87 | 2.61 | 0.26 |
| 11 | 79.58 | 11.77 | 0.09 | 1.03 | 0.10 | 0.93 | 3.61 | 2.65 | 0.23 |
| 12 | 79.56 | 11.80 | 0.14 | 1.01 | 0.07 | 1.05 | 3.65 | 2.49 | 0.22 |
| 14 | 79.09 | 11.82 | 0.14 | 1.05 | 0.11 | 1.11 | 3.84 | 2.60 | 0.25 |
| 15 | 79.53 | 11.71 | 0.12 | 1.04 | 0.11 | 0.93 | 3.63 | 2.65 | 0.27 |
| 16 | 79.33 | 11.80 | 0.12 | 0.92 | 0.09 | 1.08 | 3.83 | 2.57 | 0.26 |

| | | | | | | | | | |
|---|---|---|---|---|---|---|---|---|---|
| 17 | 79.58 | 11.54 | 0.15 | 1.10 | 0.13 | 0.94 | 3.66 | 2.66 | 0.23 |
| 18 | 80.54 | 11.86 | 0.15 | 0.99 | 0.11 | 1.08 | 2.49 | 2.54 | 0.24 |
| 19 | 79.43 | 11.75 | 0.13 | 1.02 | 0.07 | 1.00 | 3.72 | 2.61 | 0.26 |
| 20 | 79.42 | 11.66 | 0.15 | 1.05 | 0.09 | 0.97 | 3.67 | 2.74 | 0.24 |
| 21 | 79.19 | 11.78 | 0.13 | 1.00 | 0.12 | 1.08 | 3.91 | 2.55 | 0.23 |
| Average | 79.38 | 11.81 | 0.13 | 1.01 | 0.10 | 1.02 | 3.68 | 2.63 | 0.24 |
| Std | 0.34 | 0.11 | 0.02 | 0.05 | 0.02 | 0.06 | 0.30 | 0.06 | 0.01 |

| Readings | Water | 1/3 K | Sum | %Fe/sum | %Ca/ sum | %1/3K/ sum |
|---|---|---|---|---|---|---|
| 1 | 8.440679 | 0.882124 | 3.017352 | 0.344233 | 0.363417 | 0.292350386 |
| 2 | 4.642781 | 0.905368 | 2.888437 | 0.343822 | 0.342733 | 0.31344548 |
| 3 | 8.390866 | 0.898382 | 2.886175 | 0.328669 | 0.360061 | 0.311270802 |
| 4 | 7.072753 | 0.89102 | 2.883977 | 0.366418 | 0.324627 | 0.308955224 |
| 5 | 7.601169 | 0.886736 | 2.816414 | 0.343538 | 0.341616 | 0.314845651 |
| 6 | 5.685795 | 0.876149 | 2.836618 | 0.323698 | 0.367431 | 0.308871169 |
| 7 | 5.802564 | 0.874051 | 2.986635 | 0.365758 | 0.341588 | 0.292654028 |
| 8 | 5.71113 | 0.882748 | 2.959345 | 0.350854 | 0.350854 | 0.298291721 |
| 9 | 6.718396 | 0.850471 | 2.911971 | 0.341637 | 0.366303 | 0.292060376 |
| 10 | 8.580214 | 0.871438 | 2.950856 | 0.344372 | 0.360311 | 0.295316941 |
| 11 | 5.814085 | 0.884775 | 2.848975 | 0.362236 | 0.327205 | 0.310559006 |
| 12 | 4.291425 | 0.830647 | 2.892113 | 0.350072 | 0.362717 | 0.287210983 |
| 14 | 5.539248 | 0.86738 | 3.023831 | 0.346948 | 0.366204 | 0.28684794 |
| 15 | 8.325794 | 0.882836 | 2.860492 | 0.364942 | 0.326427 | 0.30863099 |
| 16 | 7.087014 | 0.855998 | 2.8611 | 0.322382 | 0.378433 | 0.299184953 |
| 17 | 7.795546 | 0.888243 | 2.92936 | 0.375046 | 0.321733 | 0.303221029 |
| 18 | 6.773337 | 0.847397 | 2.915475 | 0.339588 | 0.369757 | 0.290654893 |
| 19 | 8.208954 | 0.870455 | 2.889171 | 0.352564 | 0.346154 | 0.301282051 |
| 20 | 4.476259 | 0.913211 | 2.935745 | 0.358017 | 0.330916 | 0.311066207 |
| 21 | 6.158758 | 0.851083 | 2.931192 | 0.342099 | 0.367547 | 0.290353854 |
| Average | 6.655838 | 0.875526 | 2.911262 | 0.3469 | 0.348345 | 0.350801627 |
| Std | 1.392225 | 0.020671 | 0.056718 | 0.014527 | 0.014215 | 0.017721482 |

Ternary diagram displaying FeO: 1/3 K2O: CaO Wt % of sum, Kawakawa Tephra (T3).

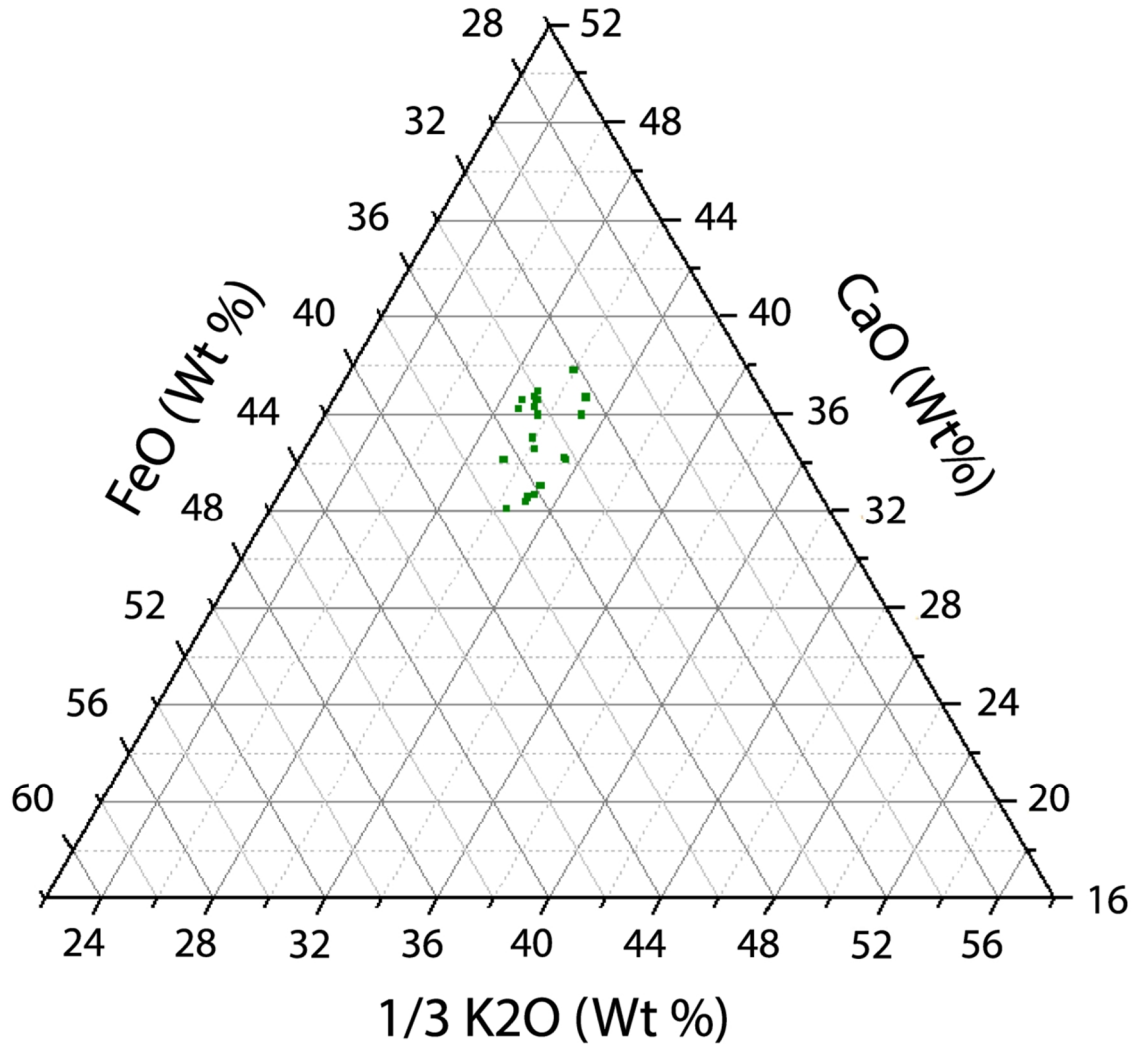


- Kawakawa Tephra

Grain size distribution frequency (%) graph showing grain size distribution of Kawakawa Tephra (T3) Ohakean Loess preserved on the Ratan Terrace.

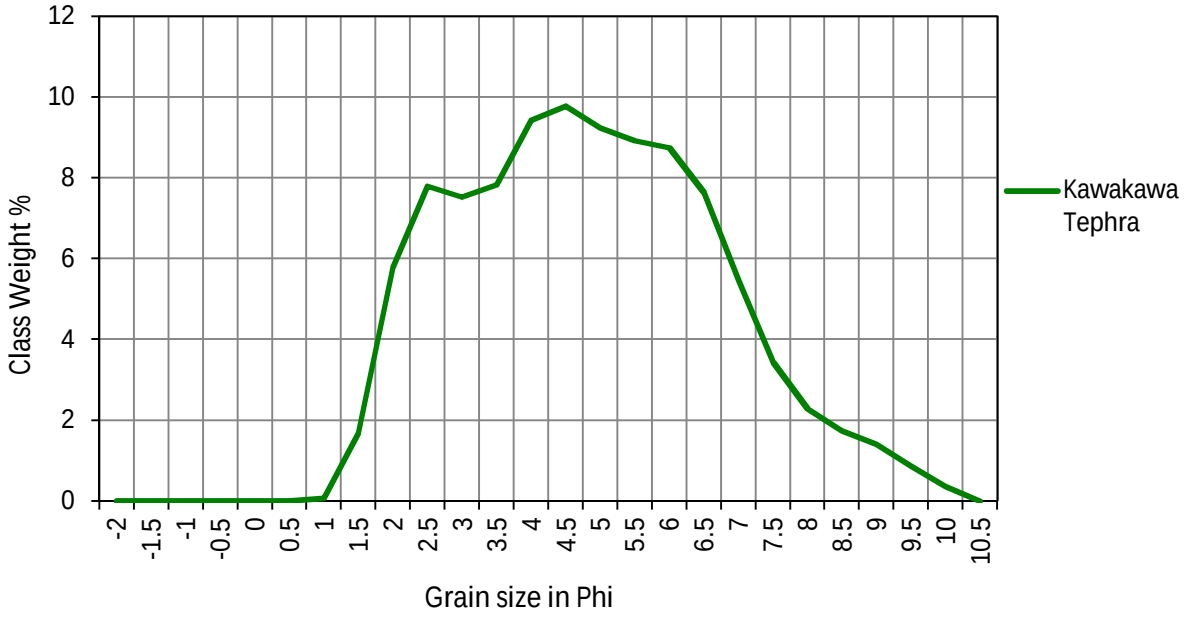


Grain size data from Kawakawa Tephra – T3

| Grain size in microns | Grain size in Phi | Class weight % |
|---|---|---|
| 707.107 | 0.5 | 0.00 |
| 500 | 1.0 | 0.06 |
| 353.553 | 1.5 | 1.67 |
| 250 | 2.0 | 5.79 |
| 176.777 | 2.5 | 7.80 |
| 125 | 3.0 | 7.53 |
| 88.388 | 3.5 | 7.83 |
| 62.5 | 4.0 | 9.44 |
| 44.194 | 4.5 | 9.77 |
| 31.25 | 5.0 | 9.25 |
| 22.097 | 5.5 | 8.93 |
| 15.625 | 6.0 | 8.75 |
| 11.049 | 6.5 | 7.64 |
| 7.813 | 7.0 | 5.46 |
| 5.524 | 7.5 | 3.43 |
| 3.906 | 8.0 | 2.28 |
| 2.762 | 8.5 | 1.73 |
| 1.953 | 9.0 | 1.40 |
| 1.381 | 9.5 | 0.86 |
| 0.977 | 10.0 | 0.36 |

Histogram displaying the grain size distribution of Kawakawa Tephra (T3)

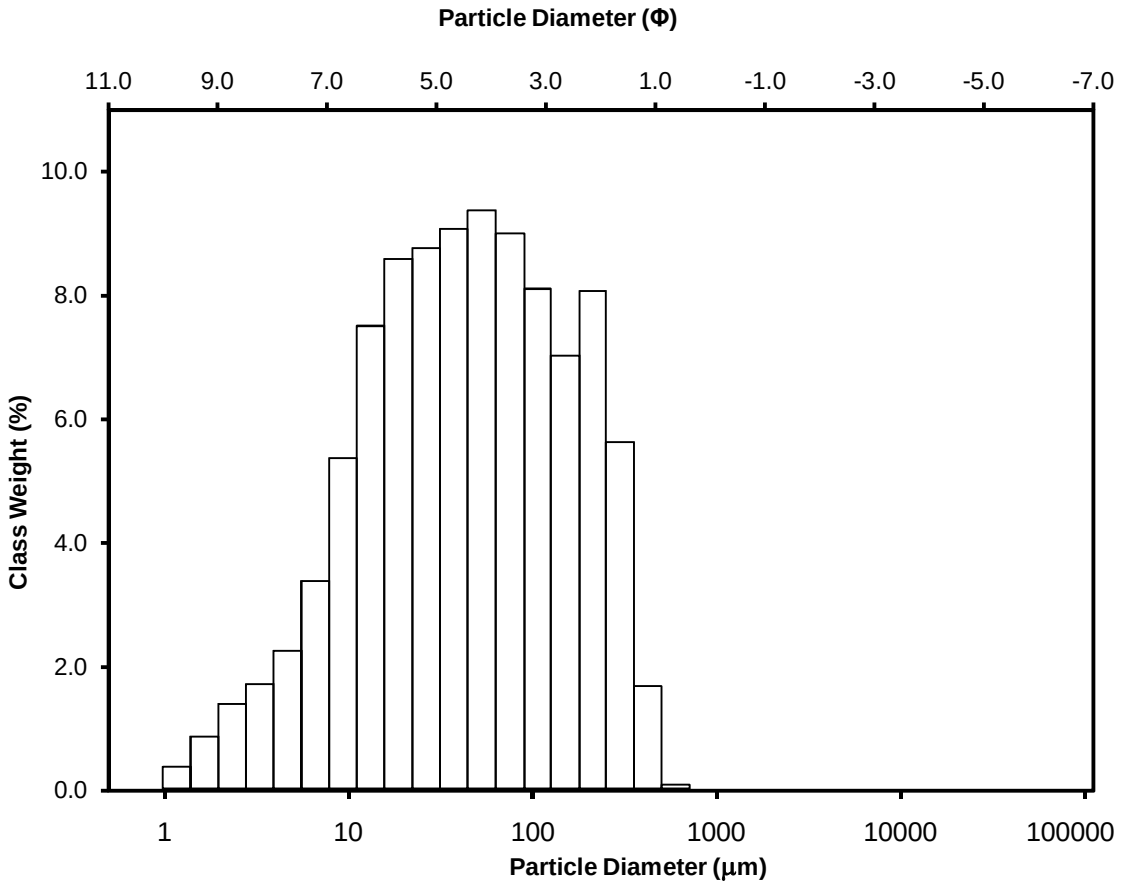


| Kawakawa Tephra T3 sample statistics: | | | |
|---|---|---|---|
| | Geometric µm | Logarithmic ϕ | Description |
| Mean | 44.23 | 4.499 | Fine grained tephra |
| Sorting | 3.754 | 1.909 | Poorly Sorted |
| Skewness | -0.049 | 0.049 | Symmetrical |
| Kurtosis | 0.901 | 0.901 | Mesokurtic |

1.4 Kaukatea Tephra – Sample T2:

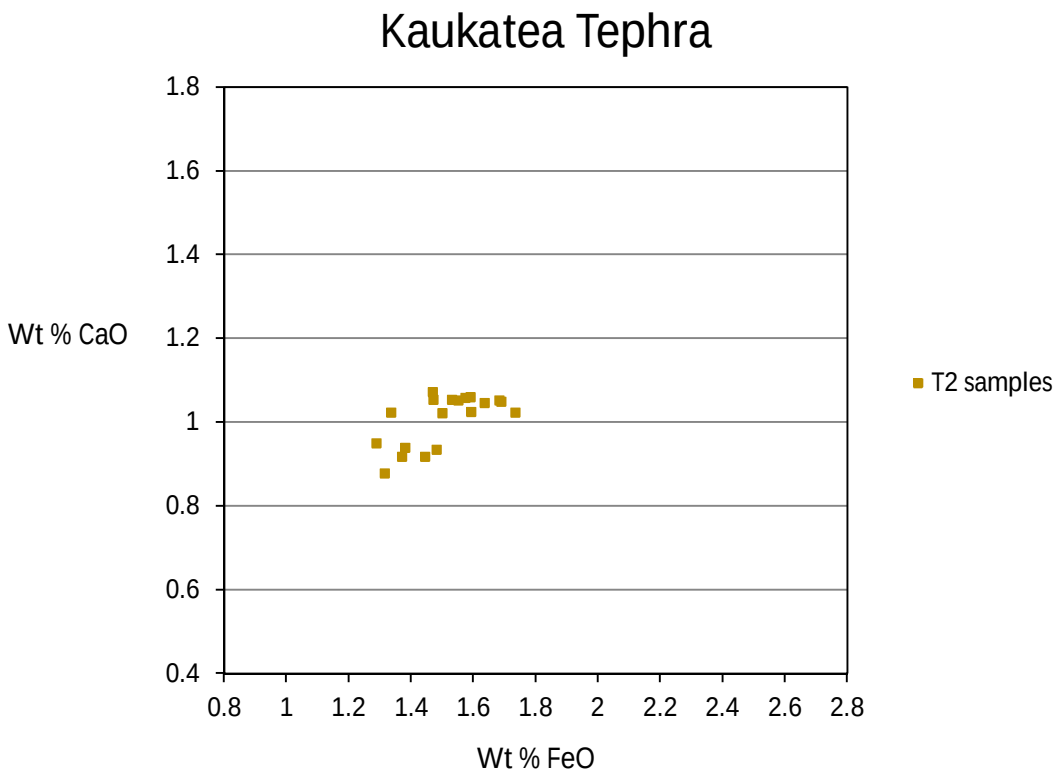


| T2 Normalised data (Wt %) | | | | | | | | | |
|---|---|---|---|---|---|---|---|---|---|
| Readings | SiO2 | Al2O3 | TiO2 | FeO | MgO | CaO | Na2O | K2O | Cl |
| 1 | 77.06 | 12.77 | 0.14 | 1.73 | 0.07 | 1.02 | 3.74 | 3.22 | 0.24 |
| 2 | 76.91 | 12.90 | 0.15 | 1.59 | 0.07 | 1.03 | 3.80 | 3.30 | 0.26 |
| 3 | 76.62 | 12.82 | 0.15 | 1.68 | 0.08 | 1.05 | 3.84 | 3.52 | 0.24 |
| 4 | 77.22 | 12.60 | 0.13 | 1.44 | 0.04 | 0.92 | 3.86 | 3.52 | 0.26 |
| 5 | 77.23 | 12.63 | 0.11 | 1.38 | 0.07 | 0.94 | 4.05 | 3.35 | 0.25 |
| 6 | 77.43 | 12.66 | 0.10 | 1.29 | 0.03 | 0.95 | 3.74 | 3.54 | 0.26 |
| 7 | 76.99 | 12.83 | 0.12 | 1.53 | 0.07 | 1.05 | 3.82 | 3.32 | 0.27 |
| 8 | 76.82 | 12.85 | 0.11 | 1.59 | 0.07 | 1.06 | 3.88 | 3.36 | 0.26 |
| 9 | 76.96 | 12.88 | 0.12 | 1.50 | 0.05 | 1.02 | 3.90 | 3.32 | 0.24 |
| 10 | 76.65 | 12.75 | 0.13 | 1.63 | 0.07 | 1.05 | 3.94 | 3.52 | 0.26 |
| 11 | 77.53 | 12.60 | 0.12 | 1.31 | 0.05 | 0.88 | 3.70 | 3.59 | 0.22 |
| 12 | 77.47 | 12.65 | 0.11 | 1.37 | 0.07 | 0.92 | 3.64 | 3.48 | 0.29 |
| 13 | 77.25 | 12.81 | 0.11 | 1.34 | 0.07 | 1.02 | 3.84 | 3.28 | 0.26 |
| 14 | 77.10 | 12.80 | 0.14 | 1.47 | 0.07 | 1.07 | 3.80 | 3.30 | 0.24 |
| 15 | 76.72 | 12.78 | 0.16 | 1.69 | 0.07 | 1.05 | 3.94 | 3.33 | 0.25 |
| 16 | 76.77 | 12.84 | 0.13 | 1.57 | 0.09 | 1.06 | 3.97 | 3.31 | 0.25 |
| 17 | 77.42 | 12.49 | 0.09 | 1.48 | 0.03 | 0.93 | 3.93 | 3.35 | 0.28 |

| | | | | | | | | | |
|---|---|---|---|---|---|---|---|---|---|
| 18 | 76.96 | 12.71 | 0.14 | 1.55 | 0.07 | 1.05 | 3.91 | 3.36 | 0.25 |
| 19 | 77.13 | 12.72 | 0.13 | 1.47 | 0.03 | 1.05 | 3.89 | 3.34 | 0.23 |
| Average | 77.07 | 12.74 | 0.13 | 1.51 | 0.06 | 1.01 | 3.85 | 3.39 | 0.25 |
| Std | 0.28 | 0.11 | 0.02 | 0.13 | 0.02 | 0.06 | 0.10 | 0.11 | 0.02 |

| Readings | Water | 1/3 K | Sum | %Fe/sum | %Ca/ sum | %1/3K/ sum |
|---|---|---|---|---|---|---|
| 1 | 7.03 | 1.07 | 3.83 | 0.45 | 0.27 | 0.28 |
| 2 | 5.17 | 1.10 | 3.72 | 0.43 | 0.28 | 0.30 |
| 3 | 4.29 | 1.17 | 3.91 | 0.43 | 0.27 | 0.30 |
| 4 | 3.84 | 1.17 | 3.54 | 0.41 | 0.26 | 0.33 |
| 5 | 3.88 | 1.12 | 3.43 | 0.40 | 0.27 | 0.32 |
| 6 | 4.53 | 1.18 | 3.42 | 0.38 | 0.28 | 0.35 |
| 7 | 5.11 | 1.11 | 3.69 | 0.41 | 0.29 | 0.30 |
| 8 | 5.23 | 1.12 | 3.77 | 0.42 | 0.28 | 0.30 |
| 9 | 4.35 | 1.11 | 3.63 | 0.41 | 0.28 | 0.30 |
| 10 | 4.04 | 1.17 | 3.85 | 0.42 | 0.27 | 0.30 |
| 11 | 4.74 | 1.20 | 3.39 | 0.39 | 0.26 | 0.35 |
| 12 | 5.18 | 1.16 | 3.45 | 0.40 | 0.27 | 0.34 |
| 13 | 4.71 | 1.09 | 3.45 | 0.39 | 0.30 | 0.32 |
| 14 | 6.43 | 1.10 | 3.64 | 0.40 | 0.29 | 0.30 |
| 15 | 5.18 | 1.11 | 3.85 | 0.44 | 0.27 | 0.29 |
| 16 | 5.23 | 1.10 | 3.74 | 0.42 | 0.28 | 0.30 |
| 17 | 5.86 | 1.12 | 3.53 | 0.42 | 0.26 | 0.32 |
| 18 | 5.03 | 1.12 | 3.72 | 0.42 | 0.28 | 0.30 |
| 19 | 5.11 | 1.11 | 3.64 | 0.40 | 0.29 | 0.31 |
| Average | 5.00 | 1.13 | 3.64 | 0.41 | 0.28 | 0.31 |
| Std | 0.81 | 0.04 | 0.23 | 0.02 | 0.01 | 0.02 |

Ternary diagram displaying FeO: 1/3 K2O: CaO Wt % of sum, Kaukatea Tephra (T2).

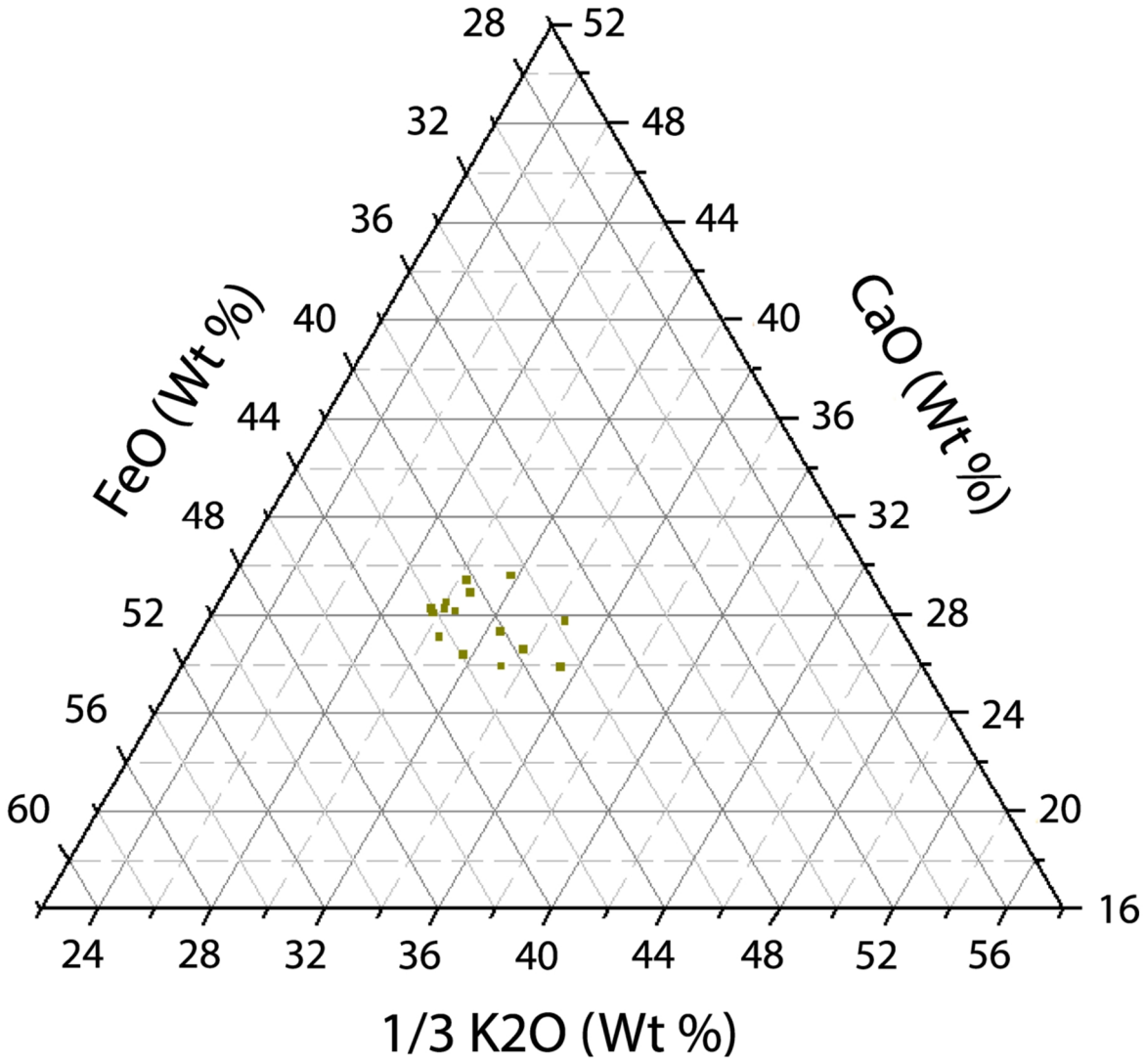


- Kaukatea Tephra

1.5 Potaka Pumice – Samples T1, T10, T16:

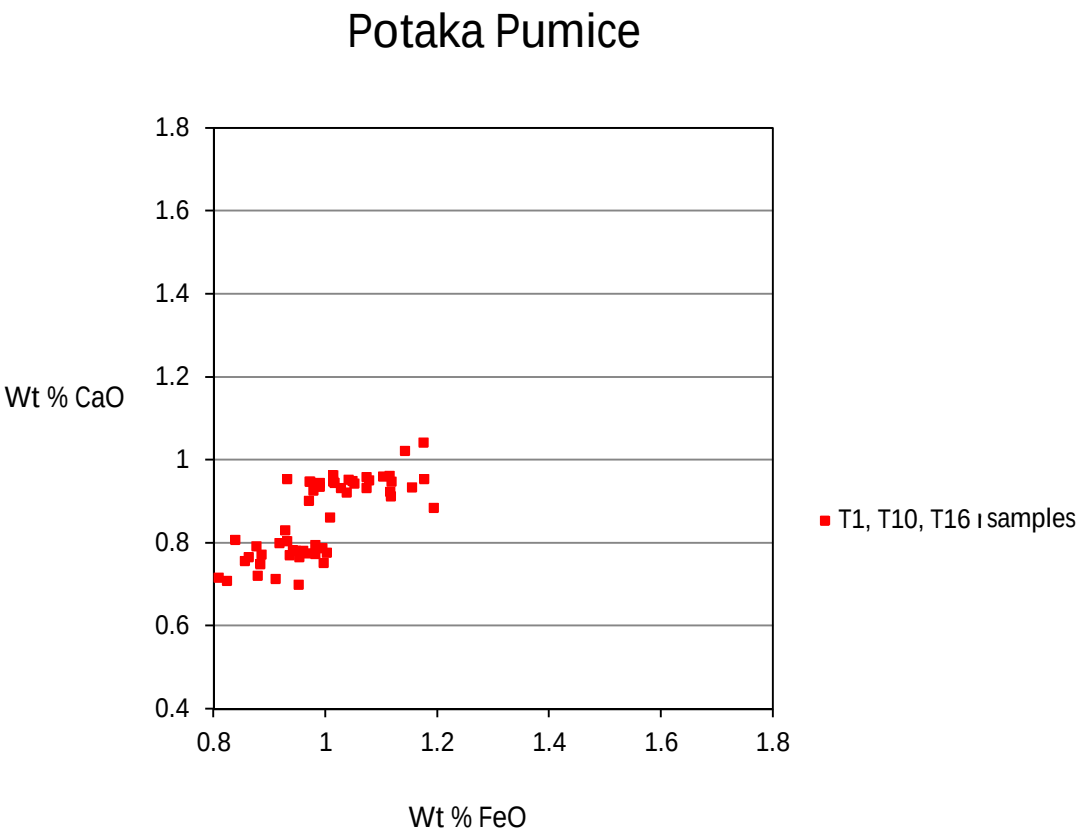


| T1 Normalised data (Wt %) | | | | | | | | | |
|---|---|---|---|---|---|---|---|---|---|
| | Element | | | | | | | | |
| Reading | SiO2 | Al2O3 | TiO2 | FeO | MgO | CaO | Na2O | K2O | Cl |
| 1 | 74.73 | 11.80 | 0.14 | 1.06 | 0.10 | 0.92 | 3.34 | 3.19 | 0.27 |
| 2 | 73.62 | 11.39 | 0.12 | 0.95 | 0.06 | 0.89 | 3.29 | 3.09 | 0.25 |
| 3 | 76.16 | 12.03 | 0.14 | 1.02 | 0.09 | 0.93 | 3.25 | 3.50 | 0.26 |
| 4 | 75.93 | 12.04 | 0.11 | 0.90 | 0.05 | 0.81 | 3.27 | 3.67 | 0.29 |
| 5 | 75.26 | 11.91 | 0.10 | 0.96 | 0.07 | 0.76 | 3.34 | 3.64 | 0.26 |
| 6 | 75.66 | 11.93 | 0.14 | 1.08 | 0.11 | 0.92 | 3.21 | 3.49 | 0.27 |
| 7 | 75.20 | 11.84 | 0.11 | 0.94 | 0.07 | 0.75 | 3.35 | 3.73 | 0.28 |
| 8 | 73.75 | 11.47 | 0.15 | 1.01 | 0.08 | 0.90 | 3.42 | 2.99 | 0.29 |
| 9 | 74.91 | 11.92 | 0.08 | 0.92 | 0.05 | 0.75 | 3.40 | 3.65 | 0.30 |
| 10 | 76.03 | 11.86 | 0.10 | 0.91 | 0.07 | 0.76 | 3.22 | 3.70 | 0.30 |
| 11 | 75.87 | 12.15 | 0.12 | 0.91 | 0.05 | 0.78 | 3.28 | 3.82 | 0.29 |
| 12 | 75.75 | 12.02 | 0.08 | 0.97 | 0.08 | 0.75 | 3.15 | 3.89 | 0.29 |

| | | | | | | | | | |
|---|---|---|---|---|---|---|---|---|---|
| 13 | 76.24 | 11.93 | 0.09 | 0.89 | 0.03 | 0.78 | 3.38 | 3.69 | 0.29 |
| 14 | 75.67 | 11.93 | 0.12 | 1.01 | 0.13 | 0.93 | 3.37 | 3.74 | 0.28 |
| 15 | 75.60 | 11.97 | 0.10 | 0.92 | 0.05 | 0.76 | 3.33 | 3.89 | 0.30 |
| 16 | 73.68 | 11.54 | 0.14 | 1.04 | 0.06 | 0.91 | 3.38 | 3.21 | 0.27 |
| Average | 75.25 | 11.86 | 0.11 | 0.97 | 0.07 | 0.83 | 3.31 | 3.56 | 0.28 |
| Std | 0.88 | 0.21 | 0.02 | 0.06 | 0.02 | 0.08 | 0.08 | 0.29 | 0.01 |

| Readings | Water | 1/3 K | Sum | Fe/sum | Ca/sum | 1/3K /sum |
|---|---|---|---|---|---|---|
| 1 | 4.45098 | 1.1122 | 3.1886 | 0.34923 | 0.30197 | 0.3487965 |
| 2 | 6.35432 | 1.0995 | 3.0612 | 0.33174 | 0.30907 | 0.35918605 |
| 3 | 2.63685 | 1.1989 | 3.1966 | 0.32773 | 0.2972 | 0.37506694 |
| 4 | 2.93967 | 1.2594 | 3.0181 | 0.30724 | 0.27549 | 0.41727355 |
| 5 | 3.7067 | 1.2583 | 3.0404 | 0.32688 | 0.25925 | 0.4138677 |
| 6 | 3.20196 | 1.2008 | 3.2669 | 0.34215 | 0.29029 | 0.3675556 |
| 7 | 3.74044 | 1.2923 | 3.047 | 0.32185 | 0.25401 | 0.42413911 |
| 8 | 5.95125 | 1.0601 | 3.0888 | 0.34871 | 0.30809 | 0.34320138 |
| 9 | 4.01992 | 1.2676 | 3.0086 | 0.31894 | 0.25973 | 0.4213321 |
| 10 | 3.04882 | 1.2735 | 2.9981 | 0.31376 | 0.26147 | 0.42477064 |
| 11 | 2.74916 | 1.3104 | 3.0461 | 0.3055 | 0.26432 | 0.43017891 |
| 12 | 3.01516 | 1.3359 | 3.1146 | 0.32145 | 0.24961 | 0.42893401 |
| 14 | 2.67571 | 1.2638 | 2.9808 | 0.30748 | 0.26853 | 0.42399173 |
| 15 | 2.84908 | 1.2815 | 3.2753 | 0.31772 | 0.29101 | 0.39126336 |
| 16 | 3.09071 | 1.3387 | 3.0671 | 0.30851 | 0.25502 | 0.43646966 |
| Average | 3.76317 | 1.2306 | 3.0998 | 0.3246 | 0.27783 | 0.39756928 |
| Std | 1.23671 | 0.0866 | 0.0957 | 0.01505 | 0.02126 | 0.03364823 |

| T10 Normalised data (Wt %) | | | | | | | | | |
|---|---|---|---|---|---|---|---|---|---|
| Reading | SiO2 | Al2O3 | TiO2 | FeO | MgO | CaO | Na2O | K2O | Cl |
| 1 | 72.69 | 11.33 | 0.06 | 0.75 | 0.05 | 0.67 | 3.60 | 3.45 | 0.28 |
| 3 | 73.95 | 11.19 | 0.12 | 1.09 | 0.10 | 0.88 | 3.57 | 2.89 | 0.25 |
| 4 | 73.47 | 11.31 | 0.06 | 0.89 | 0.03 | 0.65 | 3.21 | 3.44 | 0.28 |
| 5 | 74.81 | 11.58 | 0.09 | 0.34 | 0.03 | 0.66 | 3.54 | 3.56 | 0.17 |
| 6 | 73.33 | 11.33 | 0.06 | 0.77 | 0.05 | 0.66 | 3.49 | 3.43 | 0.30 |
| 7 | 74.72 | 11.28 | 0.12 | 1.03 | 0.11 | 0.92 | 3.78 | 3.26 | 0.30 |
| 8 | 73.24 | 11.43 | 0.07 | 0.82 | 0.03 | 0.68 | 3.47 | 3.56 | 0.28 |
| 9 | 72.84 | 11.25 | 0.14 | 0.90 | 0.06 | 0.88 | 3.43 | 3.15 | 0.28 |
| 10 | 74.99 | 11.53 | 0.08 | 0.84 | 0.08 | 0.74 | 3.49 | 3.42 | 0.27 |
| 11 | 75.80 | 11.56 | 0.09 | 0.96 | 0.06 | 0.73 | 3.46 | 3.44 | 0.29 |
| 12 | 74.57 | 11.27 | 0.15 | 0.99 | 0.11 | 0.88 | 3.38 | 3.32 | 0.28 |
| 13 | 74.56 | 11.51 | 0.08 | 0.93 | 0.08 | 0.76 | 3.24 | 3.46 | 0.29 |

| | | | | | | | | | |
|---|---|---|---|---|---|---|---|---|---|
| 14 | 72.35 | 11.03 | 0.12 | 1.05 | 0.10 | 0.94 | 3.43 | 2.71 | 0.26 |
| 15 | 72.75 | 11.04 | 0.12 | 0.97 | 0.11 | 0.87 | 3.13 | 2.91 | 0.29 |
| 16 | 73.38 | 11.29 | 0.14 | 0.91 | 0.08 | 0.89 | 3.37 | 3.14 | 0.28 |
| 17 | 73.56 | 11.24 | 0.10 | 0.70 | 0.09 | 0.72 | 3.33 | 3.38 | 0.25 |
| 18 | 73.28 | 11.29 | 0.12 | 1.12 | 0.06 | 0.83 | 3.38 | 3.17 | 0.33 |
| 19 | 75.11 | 11.48 | 0.12 | 0.82 | 0.09 | 0.72 | 3.31 | 3.49 | 0.29 |
| 20 | 73.11 | 11.29 | 0.09 | 0.73 | 0.08 | 0.77 | 3.36 | 3.34 | 0.29 |
| 21 | 74.33 | 11.35 | 0.12 | 0.92 | 0.06 | 0.85 | 3.26 | 3.32 | 0.28 |
| Average | 73.84 | 11.33 | 0.10 | 0.88 | 0.07 | 0.78 | 3.41 | 3.29 | 0.28 |
| Std | 0.96 | 0.15 | 0.03 | 0.17 | 0.03 | 0.10 | 0.15 | 0.23 | 0.03 |

| Reading | Water | 1/3 K | Sum | %Fe/sum | %Ca/ sum | %1/3K/ sum |
|---|---|---|---|---|---|---|
| 1 | 7.12 | 1.24 | 2.76 | 0.29 | 0.26 | 0.45 |
| 3 | 5.96 | 1.02 | 3.11 | 0.37 | 0.30 | 0.33 |
| 4 | 6.66 | 1.23 | 2.88 | 0.33 | 0.24 | 0.43 |
| 5 | 5.22 | 1.25 | 2.31 | 0.16 | 0.30 | 0.54 |
| 6 | 6.59 | 1.22 | 2.75 | 0.30 | 0.26 | 0.44 |
| 7 | 4.48 | 1.14 | 3.17 | 0.34 | 0.30 | 0.36 |
| 8 | 6.42 | 1.27 | 2.87 | 0.31 | 0.25 | 0.44 |
| 9 | 7.05 | 1.13 | 3.05 | 0.32 | 0.31 | 0.37 |
| 10 | 4.56 | 1.19 | 2.85 | 0.31 | 0.27 | 0.42 |
| 11 | 3.61 | 1.19 | 2.94 | 0.34 | 0.26 | 0.40 |
| 12 | 5.06 | 1.17 | 3.13 | 0.33 | 0.29 | 0.37 |
| 13 | 5.09 | 1.21 | 2.99 | 0.33 | 0.27 | 0.41 |
| 14 | 8.00 | 0.98 | 3.15 | 0.36 | 0.33 | 0.31 |
| 15 | 7.83 | 1.05 | 3.05 | 0.35 | 0.31 | 0.35 |
| 16 | 6.53 | 1.12 | 3.04 | 0.32 | 0.31 | 0.37 |
| 17 | 6.62 | 1.21 | 2.73 | 0.28 | 0.28 | 0.44 |
| 18 | 6.43 | 1.13 | 3.21 | 0.37 | 0.28 | 0.35 |
| 19 | 4.58 | 1.22 | 2.83 | 0.30 | 0.27 | 0.43 |
| 20 | 6.95 | 1.20 | 2.81 | 0.28 | 0.30 | 0.43 |
| 21 | 5.51 | 1.17 | 3.04 | 0.32 | 0.30 | 0.38 |
| Average | 6.02 | 1.17 | 2.93 | 0.31 | 0.28 | 0.40 |
| Std | 1.19 | 0.08 | 0.21 | 0.05 | 0.02 | 0.05 |

| T16 Normalised data (Wt %) | | | | | | | | | |
|---|---|---|---|---|---|---|---|---|---|
| Reading | SiO2 | Al2O3 | TiO2 | FeO | MgO | CaO | Na2O | K2O | Cl |
| 1 | 78.41 | 12.16 | 0.12 | 0.99 | 0.07 | 0.95 | 3.36 | 3.64 | 0.31 |

| | | | | | | | | | |
|---|---|---|---|---|---|---|---|---|---|
| 2 | 78.66 | 12.04 | 0.14 | 0.93 | 0.06 | 0.95 | 3.24 | 3.69 | 0.29 |
| 3 | 78.77 | 12.07 | 0.14 | 0.94 | 0.05 | 0.77 | 3.24 | 3.70 | 0.31 |
| 4 | 78.49 | 12.16 | 0.11 | 0.84 | 0.07 | 0.81 | 3.49 | 3.76 | 0.28 |
| 5 | 78.54 | 12.26 | 0.10 | 0.80 | 0.05 | 0.78 | 3.53 | 3.64 | 0.31 |
| 6 | 79.16 | 11.79 | 0.08 | 1.07 | 0.04 | 0.57 | 3.36 | 3.67 | 0.26 |
| 7 | 78.57 | 12.18 | 0.11 | 1.01 | 0.08 | 0.95 | 3.15 | 3.66 | 0.29 |
| 8 | 78.31 | 12.27 | 0.11 | 0.88 | 0.05 | 0.79 | 3.45 | 3.85 | 0.29 |
| 9 | 79.08 | 12.07 | 0.13 | 0.98 | 0.08 | 0.93 | 3.23 | 3.22 | 0.29 |
| 10 | 78.57 | 12.25 | 0.08 | 0.71 | 0.06 | 0.69 | 3.55 | 3.77 | 0.32 |
| 11 | 78.83 | 12.13 | 0.13 | 1.07 | 0.08 | 0.93 | 3.38 | 3.18 | 0.27 |
| 12 | 78.34 | 12.21 | 0.15 | 0.99 | 0.09 | 0.94 | 3.29 | 3.70 | 0.31 |
| 13 | 78.53 | 12.13 | 0.12 | 1.03 | 0.08 | 0.93 | 3.31 | 3.55 | 0.31 |
| 14 | 78.18 | 12.15 | 0.13 | 1.18 | 0.07 | 0.95 | 3.39 | 3.67 | 0.28 |
| 15 | 78.21 | 12.33 | 0.13 | 1.17 | 0.08 | 1.04 | 3.12 | 3.61 | 0.29 |
| 16 | 78.75 | 12.14 | 0.08 | 0.91 | 0.03 | 0.71 | 3.35 | 3.73 | 0.30 |
| 17 | 78.50 | 12.15 | 0.08 | 0.86 | 0.05 | 0.77 | 3.30 | 3.99 | 0.29 |
| 18 | 78.94 | 12.01 | 0.10 | 0.97 | 0.07 | 0.78 | 3.10 | 3.75 | 0.30 |
| 19 | 78.49 | 11.93 | 0.11 | 1.12 | 0.10 | 0.91 | 3.33 | 3.73 | 0.29 |
| 20 | 78.83 | 12.04 | 0.10 | 0.88 | 0.08 | 0.75 | 3.32 | 3.72 | 0.28 |
| 21 | 78.28 | 12.25 | 0.12 | 1.01 | 0.10 | 0.96 | 3.51 | 3.47 | 0.30 |
| 22 | 78.26 | 12.12 | 0.14 | 1.12 | 0.10 | 0.92 | 3.44 | 3.61 | 0.28 |
| 23 | 78.53 | 12.08 | 0.14 | 0.95 | 0.05 | 0.77 | 3.27 | 3.92 | 0.29 |
| Average | 78.58 | 12.13 | 0.11 | 0.97 | 0.07 | 0.85 | 3.34 | 3.66 | 0.29 |
| Std | 0.27 | 0.12 | 0.02 | 0.12 | 0.02 | 0.12 | 0.12 | 0.18 | 0.01 |

| Reading | Water | 1/3 K | Sum | %Fe/sum | %Ca/ sum | %1/3K/ sum |
|---|---|---|---|---|---|---|
| 1 | 4.14 | 1.21 | 3.15 | 0.31 | 0.39 | 0.30 |
| 2 | 4.53 | 1.23 | 3.11 | 0.30 | 0.39 | 0.31 |
| 3 | 6.49 | 1.23 | 2.94 | 0.32 | 0.42 | 0.26 |
| 4 | 4.15 | 1.25 | 2.90 | 0.29 | 0.43 | 0.28 |
| 5 | 5.62 | 1.21 | 2.79 | 0.29 | 0.43 | 0.28 |
| 6 | 3.86 | 1.22 | 2.86 | 0.37 | 0.43 | 0.20 |
| 7 | 3.60 | 1.22 | 3.18 | 0.32 | 0.38 | 0.30 |
| 8 | 5.72 | 1.28 | 2.95 | 0.30 | 0.43 | 0.27 |
| 9 | 7.36 | 1.07 | 2.98 | 0.33 | 0.36 | 0.31 |
| 10 | 4.45 | 1.26 | 2.66 | 0.27 | 0.47 | 0.26 |
| 11 | 8.15 | 1.06 | 3.07 | 0.35 | 0.35 | 0.30 |
| 12 | 4.50 | 1.23 | 3.16 | 0.31 | 0.39 | 0.30 |
| 13 | 4.41 | 1.18 | 3.14 | 0.33 | 0.38 | 0.30 |
| 14 | 4.38 | 1.22 | 3.35 | 0.35 | 0.36 | 0.28 |

| | | | | | | |
|---|---|---|---|---|---|---|
| 15 | 3.20 | 1.20 | 3.42 | 0.34 | 0.35 | 0.30 |
| 16 | 3.55 | 1.24 | 2.87 | 0.32 | 0.43 | 0.25 |
| 17 | 3.53 | 1.33 | 2.96 | 0.29 | 0.45 | 0.26 |
| 18 | 7.23 | 1.25 | 2.99 | 0.32 | 0.42 | 0.26 |
| 19 | 3.92 | 1.24 | 3.27 | 0.34 | 0.38 | 0.28 |
| 20 | 5.37 | 1.24 | 2.87 | 0.31 | 0.43 | 0.26 |
| 21 | 3.80 | 1.16 | 3.13 | 0.32 | 0.37 | 0.31 |
| 22 | 3.87 | 1.20 | 3.24 | 0.34 | 0.37 | 0.28 |
| 23 | 6.65 | 1.31 | 3.03 | 0.31 | 0.43 | 0.25 |
| Average | 4.89 | 1.22 | 3.04 | 0.32 | 0.40 | 0.28 |
| Std | 1.43 | 0.06 | 0.19 | 0.03 | 0.04 | 0.03 |

Ternary diagram displaying FeO: 1/3 K2O: CaO Wt % of sum, Potaka Pumice (T1, T10, T16).

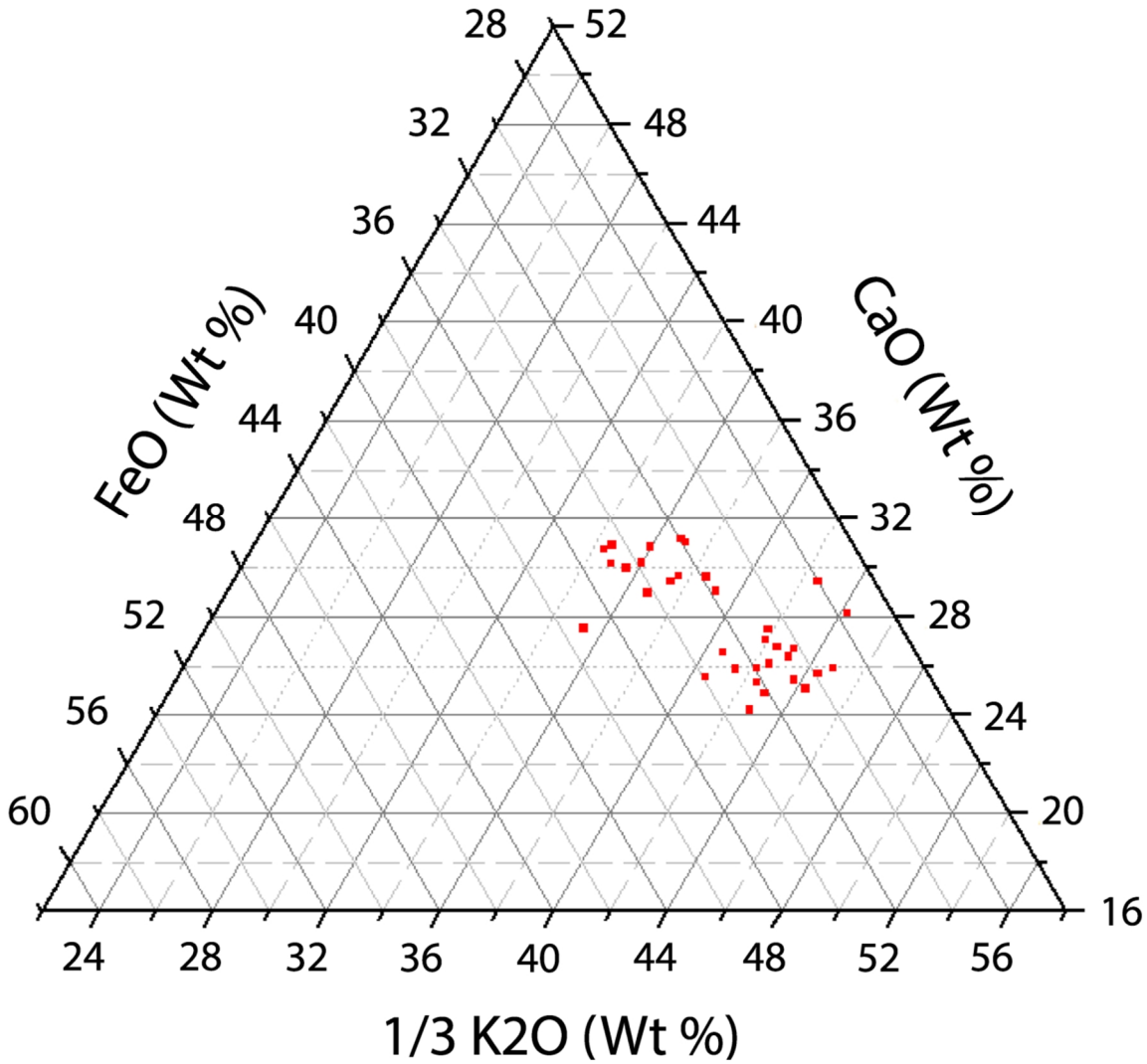

# Potaka Pumice

Grain size distribution frequency (%) graph showing grain size distribution of Potaka Tephra (T1) Kaimatira Pumice Sand Formation

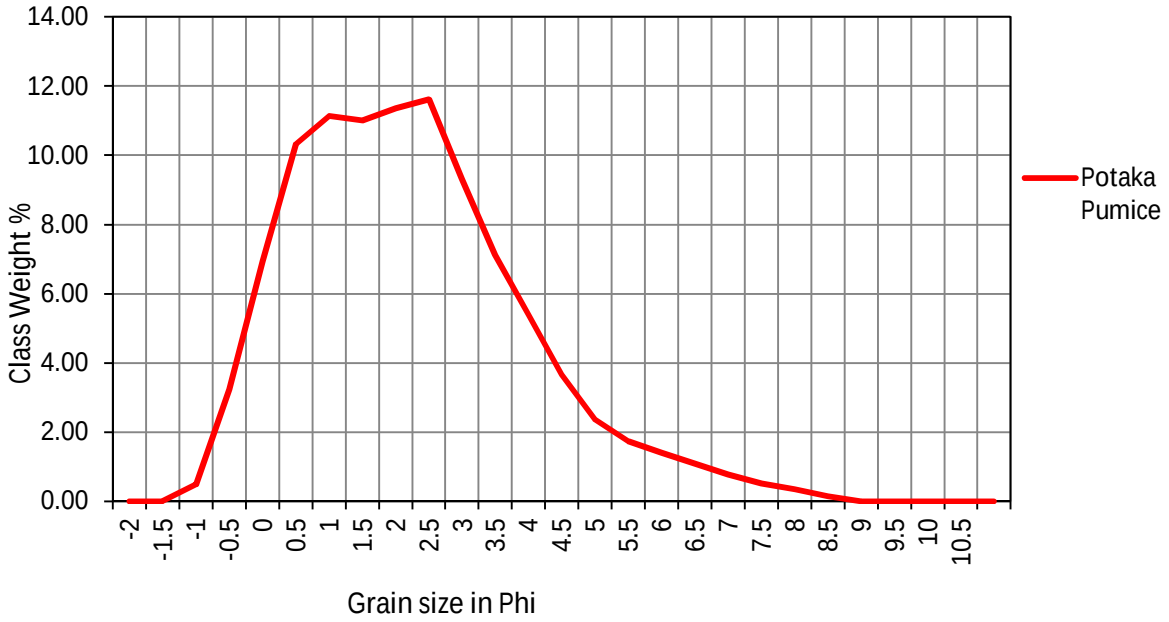


Grain size data from Potaka Pumice – T1

| Grain size in microns | Grain size in Phi | Class weight % |
|---|---|---|
| 2828.427 | -1.5 | 0 |
| 2000 | -1 | 0.49 |
| 1414.214 | -0.5 | 3.24 |
| 1000 | 0 | 6.94 |
| 707.107 | 0.5 | 10.33 |
| 500 | 1 | 11.13 |
| 353.553 | 1.5 | 11.01 |
| 250 | 2 | 11.36 |
| 176.777 | 2.5 | 11.62 |

| | | |
|---|---|---|
| 125 | 3 | 9.32 |
| 88.388 | 3.5 | 7.12 |
| 62.5 | 4 | 5.41 |
| 44.194 | 4.5 | 3.66 |
| 31.25 | 5 | 2.36 |
| 22.097 | 5.5 | 1.74 |
| 15.625 | 6 | 1.40 |
| 11.049 | 6.5 | 1.10 |
| 7.813 | 7 | 0.78 |
| 5.524 | 7.5 | 0.51 |
| 3.906 | 8 | 0.35 |
| 2.762 | 8.5 | 0.15 |

Histogram displaying the grain size distribution of Potaka Pumice (T1)

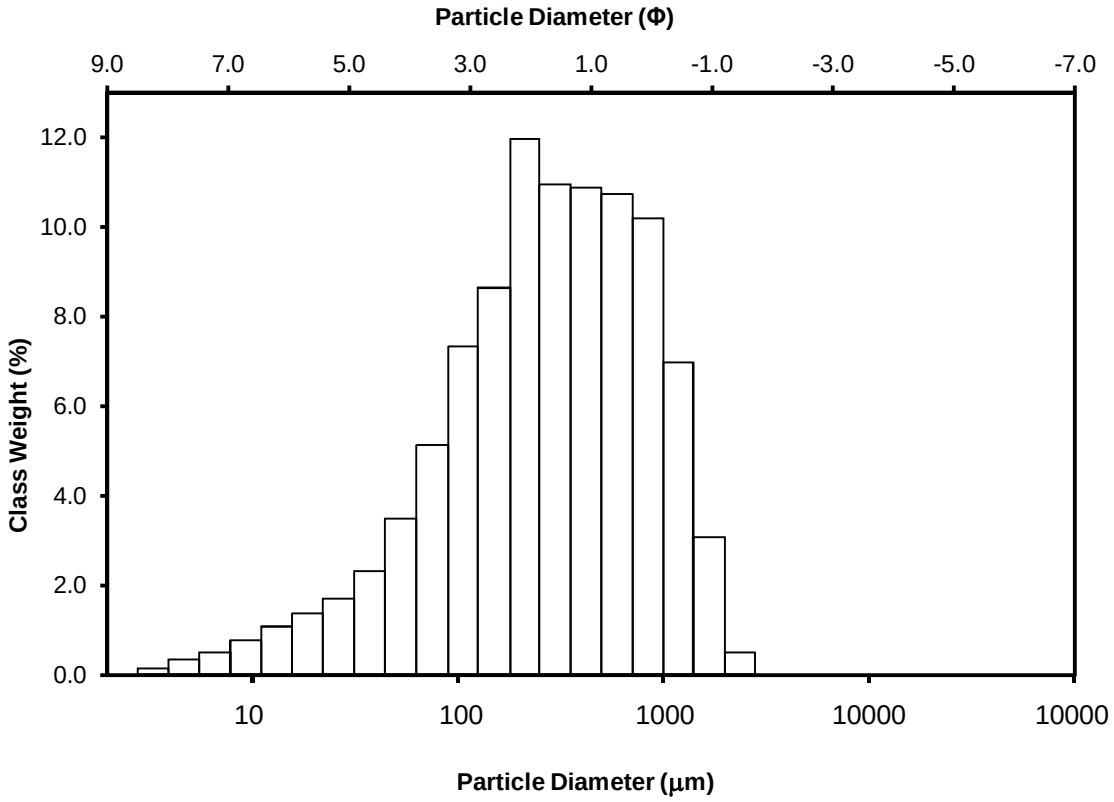


| Potaka Pumice T1 sample statistics: | | | |
|---|---|---|---|
| | Geometric μm | Logarithmic ϕ | Description |
| Mean | 270.0 | 1889 | Coarse grained tephra |
| Sorting | 3.252 | 1.702 | Poorly Sorted |
| Skewness | -0.154 | 0.154 | Fine Skewed |
| Kurtosis | 1.014 | 1.014 | Mesokurtic |

CaO versus FeO (wt %) composition of volcanic glass shards from Kaukatea Tephra, Potaka Pumice and Rewa Pumice sampled in various localities within Kai Iwi Group, Kaimatira Pumice Sand Formation, and Takapari Formation respectively, Broadlands Station, Pohangina Valley (see appendix 1 for sample locations).

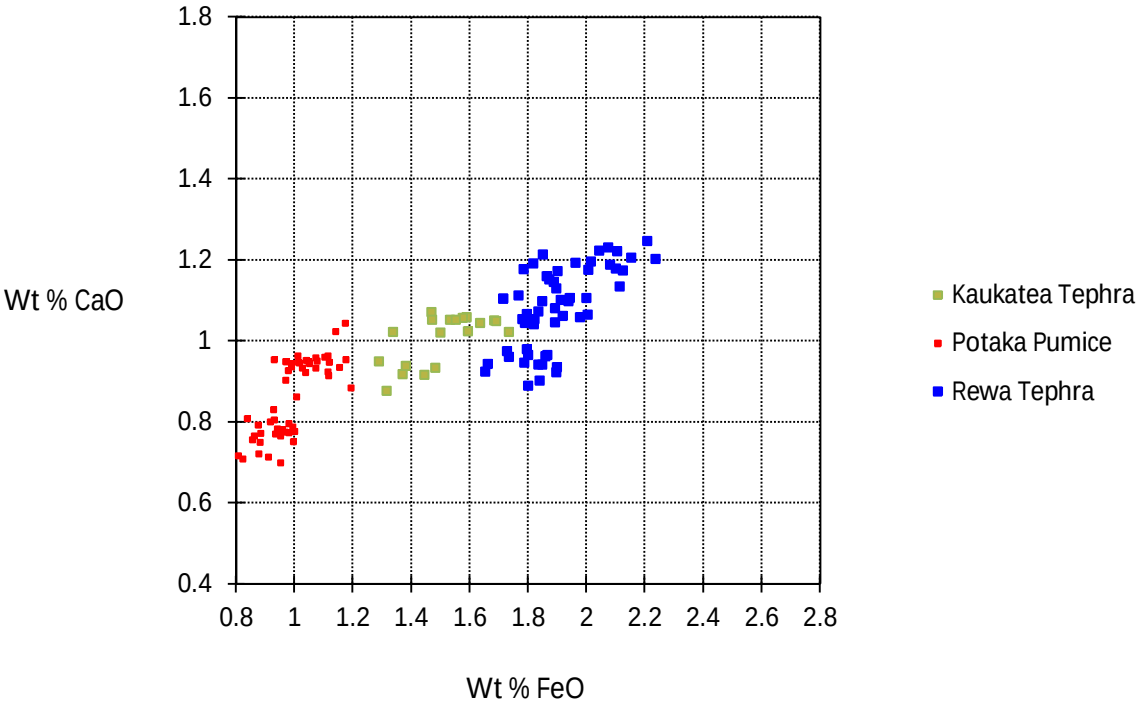

Ternary diagram displaying FeO: 1/3 $K_2O$: CaO Wt % data for tephras collected from Takapari Formation, Kaimatira Pumice Sand Formation, Kai iwi Group and Ohakean loess sequence.

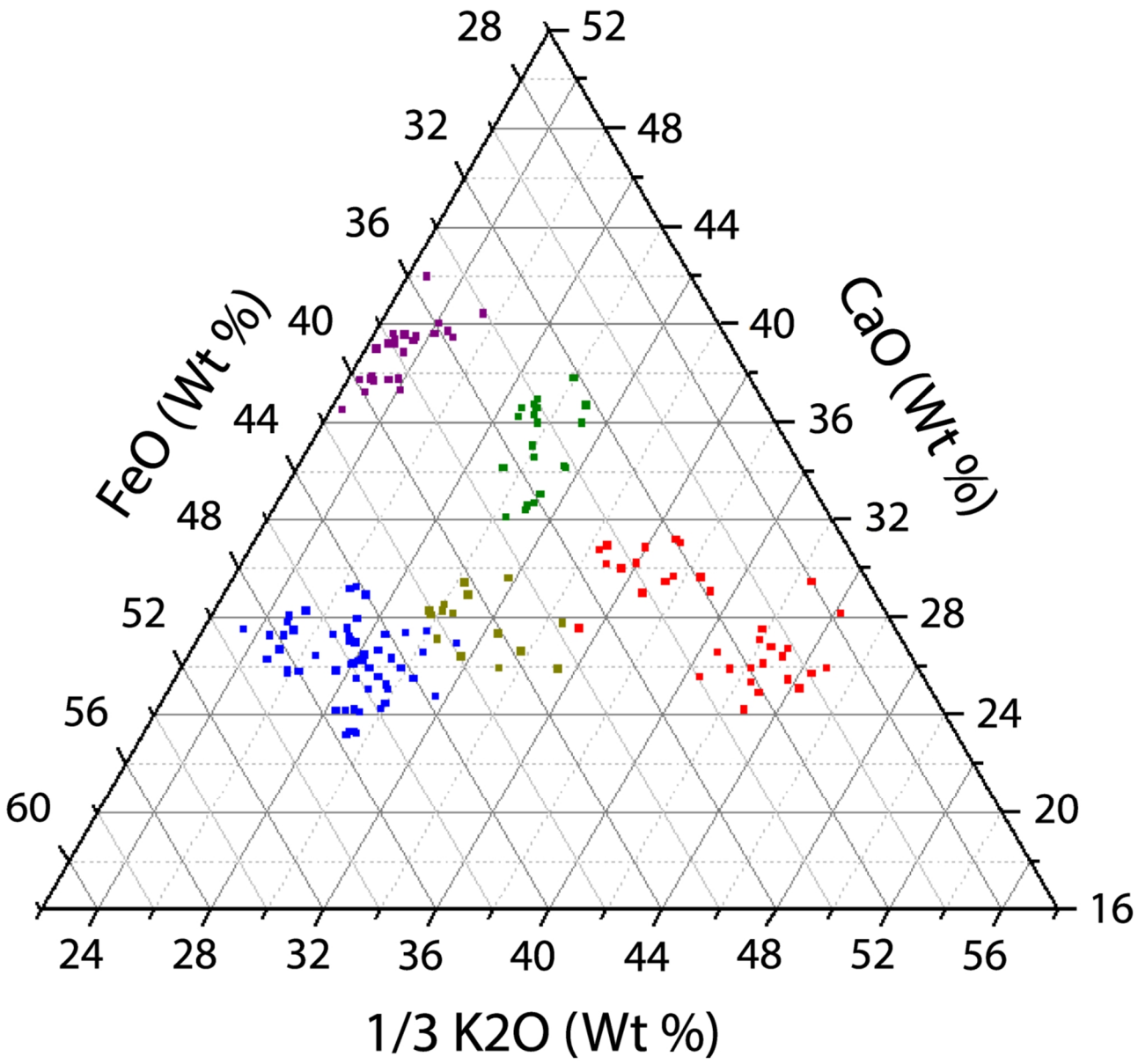


| Key | No of points | Tephra | Formation | Age (Pillans, *et al*, 2005) |
|---|---|---|---|---|
| ■ | 20 | Kawakawa Tephra | Ohakean loess sequence | 25.358 ± 0.162 ka |
| ■ | 15 | Kaukatea Tephra | Kai Iwi Group | 0.86 ± 0.08 Ma |
| ■ | 33 | Potaka Pumice | Kaimatira Pumice Sand Formation | 1.05 ± 0.05 Ma |
| ■ | 24 | Scrimmys Tephra | Takapari Formation | 1.12 ± 0.1 Ma* |
| ■ | 55 | Rewa Pumice | Takapari Formation | 1.20 ±0.14 Ma |

*estimated age based on stratigraphic position

1.6 Scrimmys Tephra - Samples T7, T8:

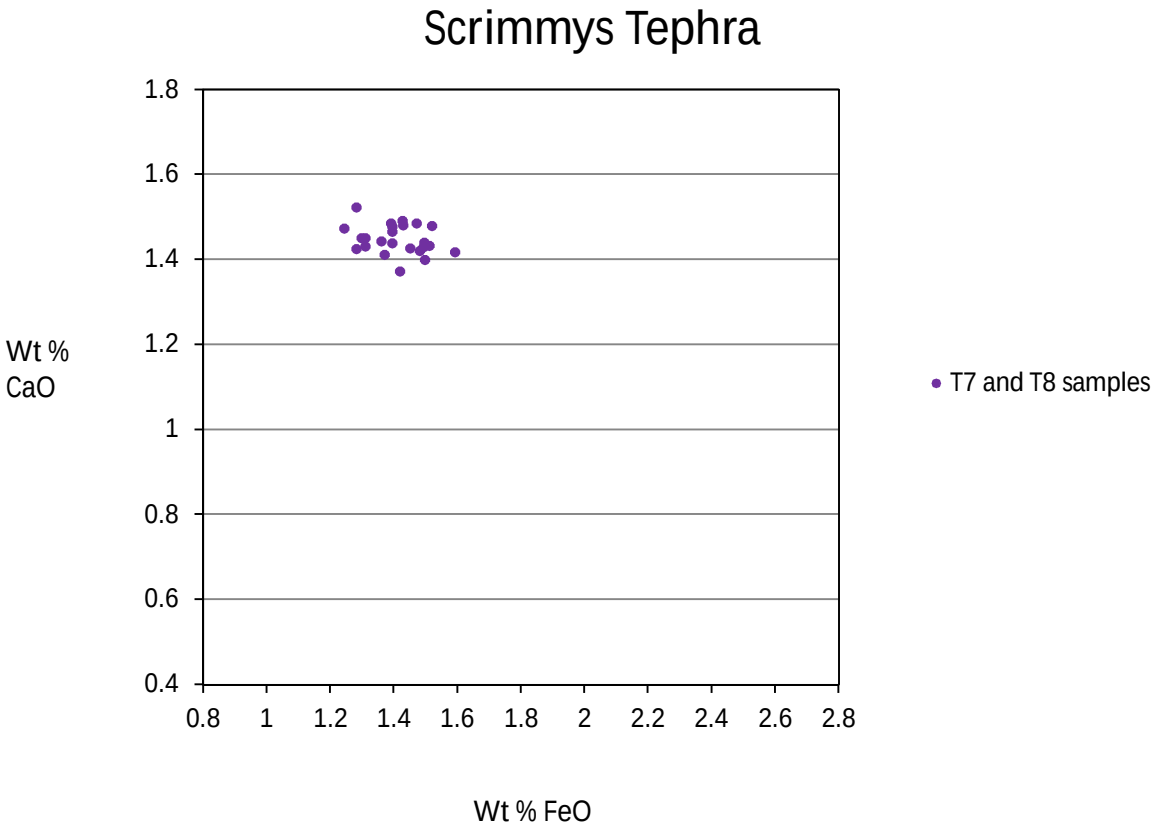


| T7 Normalised data (Wt %) | | | | | | | | | |
|---|---|---|---|---|---|---|---|---|---|
| Reading | SiO2 | Al2O3 | TiO2 | FeO | MgO | CaO | Na2O | K2O | Cl |
| 1 | 76.51 | 13.60 | 0.15 | 1.48 | 0.30 | 1.42 | 3.78 | 2.59 | 0.18 |
| 2 | 76.35 | 13.85 | 0.12 | 1.28 | 0.32 | 1.52 | 3.88 | 2.46 | 0.22 |
| 3 | 76.13 | 13.77 | 0.14 | 1.52 | 0.30 | 1.48 | 3.64 | 2.75 | 0.27 |
| 4 | 76.46 | 13.63 | 0.15 | 1.31 | 0.31 | 1.45 | 3.82 | 2.73 | 0.15 |
| 5 | 76.43 | 13.72 | 0.13 | 1.43 | 0.30 | 1.49 | 3.72 | 2.58 | 0.20 |
| 6 | 77.60 | 14.25 | 0.15 | 1.39 | 0.28 | 1.48 | 2.00 | 2.64 | 0.21 |
| 7 | 76.31 | 13.84 | 0.13 | 1.50 | 0.27 | 1.40 | 3.80 | 2.56 | 0.19 |
| 8 | 76.42 | 13.70 | 0.15 | 1.39 | 0.25 | 1.49 | 3.77 | 2.65 | 0.19 |
| 9 | 76.11 | 13.80 | 0.18 | 1.59 | 0.31 | 1.42 | 3.77 | 2.60 | 0.22 |
| 10 | 76.60 | 13.68 | 0.11 | 1.28 | 0.27 | 1.42 | 3.77 | 2.63 | 0.22 |
| Average | 76.492 | 13.784 | 0.141 | 1.417 | 0.291 | 1.457 | 3.595 | 2.619 | 0.205 |
| Std | 0.42 | 0.18 | 0.02 | 0.11 | 0.02 | 0.04 | 0.56 | 0.08 | 0.03 |

| Reading | Water | 1/3 K | Sum | %Fe/sum | %Ca/ sum | %1/3K/ sum |
|---|---|---|---|---|---|---|
| 1 | 2.18 | 0.09 | 8.68 | 0.02 | 0.97 | 0.01 |
| 2 | 1.64 | 0.10 | 8.07 | 0.02 | 0.97 | 0.01 |
| 3 | 6.80 | 0.86 | 3.76 | 0.39 | 0.38 | 0.23 |
| 4 | 8.38 | 0.82 | 3.63 | 0.35 | 0.42 | 0.23 |
| 5 | 9.25 | 0.92 | 3.91 | 0.39 | 0.38 | 0.23 |
| 6 | 4.97 | 0.91 | 3.67 | 0.36 | 0.40 | 0.25 |
| 7 | 6.29 | 0.86 | 3.78 | 0.38 | 0.39 | 0.23 |
| 8 | 8.81 | 0.88 | 3.75 | 0.37 | 0.39 | 0.23 |
| 9 | 8.67 | 0.85 | 3.75 | 0.40 | 0.37 | 0.23 |
| 10 | 9.02 | 0.88 | 3.76 | 0.37 | 0.40 | 0.23 |
| 11 | 7.25 | 0.87 | 3.88 | 0.41 | 0.37 | 0.22 |
| 12 | 7.81 | 0.88 | 3.58 | 0.36 | 0.40 | 0.24 |
| Average | 6.76 | 0.74 | 4.52 | 0.32 | 0.49 | 0.20 |
| Std | 2.59 | 0.30 | 1.81 | 0.14 | 0.23 | 0.09 |

| T8 Normalised data (Wt %) | | | | | | | | | |
|---|---|---|---|---|---|---|---|---|---|
| Reading | SiO2 | Al2O3 | TiO2 | FeO | MgO | CaO | Na2O | K2O | Cl |
| 1 | 76.28 | 13.80 | 0.13 | 1.24 | 0.30 | 1.47 | 3.85 | 2.77 | 0.16 |
| 2 | 76.31 | 13.64 | 0.14 | 1.47 | 0.29 | 1.49 | 3.92 | 2.55 | 0.21 |
| 3 | 76.84 | 13.58 | 0.12 | 1.36 | 0.25 | 1.44 | 3.71 | 2.52 | 0.18 |
| 4 | 76.55 | 13.73 | 0.15 | 1.45 | 0.29 | 1.43 | 3.50 | 2.68 | 0.22 |
| 5 | 76.20 | 13.84 | 0.14 | 1.51 | 0.30 | 1.43 | 3.90 | 2.54 | 0.14 |
| 6 | 76.32 | 13.69 | 0.13 | 1.49 | 0.29 | 1.43 | 3.89 | 2.58 | 0.18 |
| 7 | 76.55 | 13.60 | 0.15 | 1.49 | 0.32 | 1.44 | 3.72 | 2.59 | 0.14 |
| 8 | 76.77 | 13.64 | 0.14 | 1.40 | 0.23 | 1.44 | 3.68 | 2.49 | 0.20 |
| 9 | 76.25 | 13.78 | 0.15 | 1.43 | 0.31 | 1.48 | 3.80 | 2.59 | 0.20 |
| 10 | 76.77 | 13.61 | 0.14 | 1.39 | 0.28 | 1.47 | 3.62 | 2.51 | 0.21 |
| 11 | 76.58 | 13.77 | 0.15 | 1.37 | 0.26 | 1.41 | 3.72 | 2.55 | 0.20 |
| 12 | 76.60 | 13.62 | 0.15 | 1.30 | 0.27 | 1.45 | 3.83 | 2.61 | 0.18 |
| 13 | 76.74 | 13.84 | 0.13 | 1.31 | 0.28 | 1.43 | 3.52 | 2.61 | 0.15 |
| 14 | 76.64 | 13.66 | 0.12 | 1.42 | 0.27 | 1.37 | 3.67 | 2.65 | 0.21 |
| Avergage | 76.53 | 13.70 | 0.14 | 1.40 | 0.28 | 1.44 | 3.74 | 2.59 | 0.18 |
| Std | 0.22 | 0.09 | 0.01 | 0.08 | 0.02 | 0.03 | 0.13 | 0.07 | 0.03 |

| Reading | Water | 1/3 K | Sum | %Fe/sum | %Ca/ sum | %1/3K/ sum |
|---|---|---|---|---|---|---|
| 1 | 6.96 | 0.92 | 3.64 | 0.34 | 0.40 | 0.25 |
| 2 | 8.45 | 0.85 | 3.81 | 0.39 | 0.39 | 0.22 |
| 3 | 6.97 | 0.84 | 3.64 | 0.37 | 0.40 | 0.23 |

| | | | | | | |
|---|---|---|---|---|---|---|
| 4 | 6.95 | 0.89 | 3.77 | 0.38 | 0.38 | 0.24 |
| 5 | 4.07 | 0.85 | 3.79 | 0.40 | 0.38 | 0.22 |
| 6 | 7.71 | 0.86 | 3.78 | 0.39 | 0.38 | 0.23 |
| 7 | 7.60 | 0.86 | 3.80 | 0.39 | 0.38 | 0.23 |
| 8 | 6.39 | 0.83 | 3.67 | 0.38 | 0.39 | 0.23 |
| 9 | 8.22 | 0.86 | 3.78 | 0.38 | 0.39 | 0.23 |
| 10 | 6.77 | 0.84 | 3.70 | 0.38 | 0.40 | 0.23 |
| 11 | 6.74 | 0.85 | 3.63 | 0.38 | 0.39 | 0.23 |
| 12 | 6.88 | 0.87 | 3.62 | 0.36 | 0.40 | 0.24 |
| 13 | 6.67 | 0.87 | 3.61 | 0.36 | 0.40 | 0.24 |
| 14 | 5.96 | 0.88 | 3.67 | 0.39 | 0.37 | 0.24 |
| Avergage | 6.88 | 0.86 | 3.71 | 0.38 | 0.39 | 0.23 |
| Std | 1.06 | 0.02 | 0.08 | 0.02 | 0.01 | 0.01 |

Ternary diagram displaying FeO: 1/3 K2O: CaO Wt % of sum, Scrimmys Tephra (T7, T8).

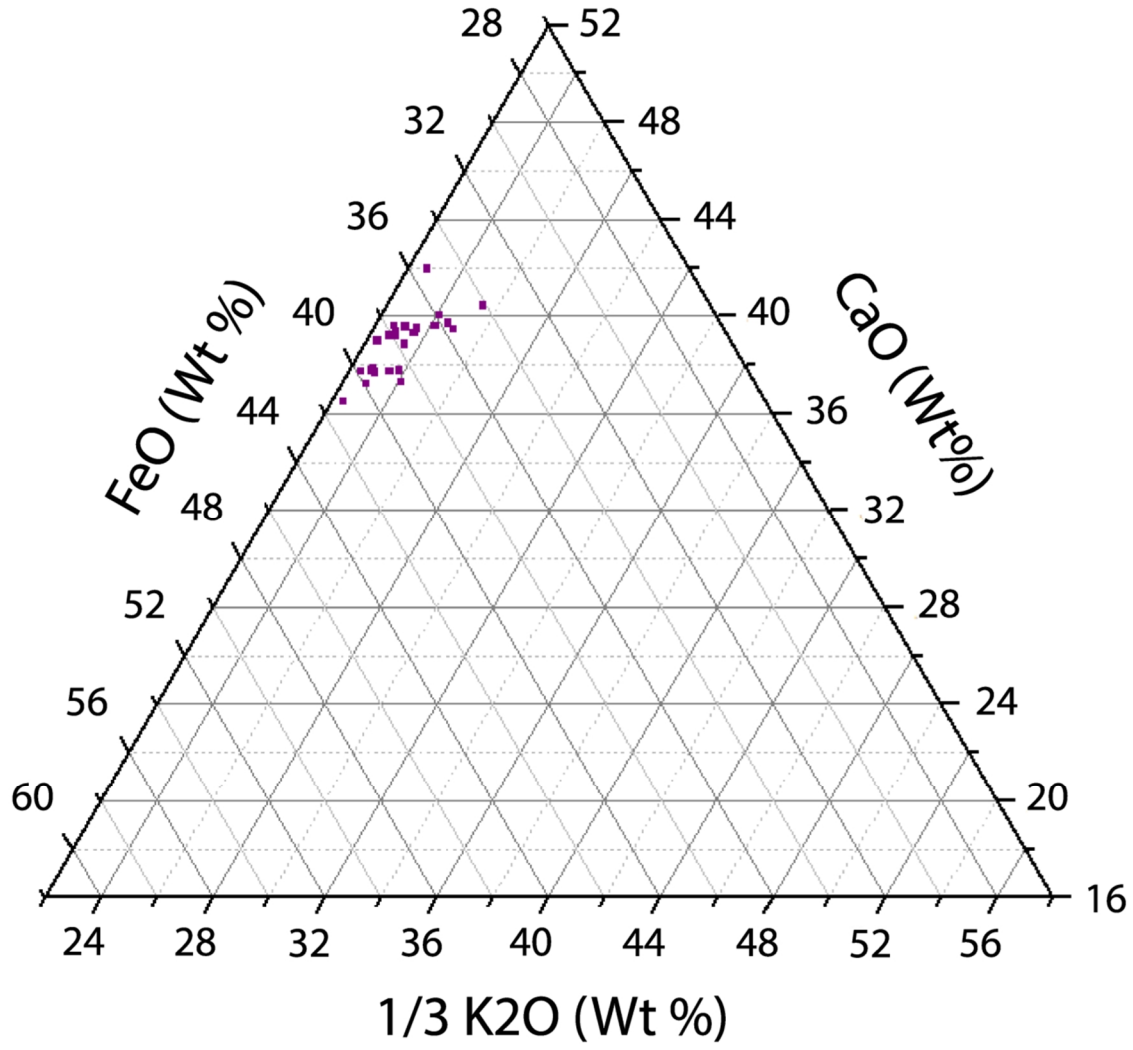


- Scrimmys Tephra

1.7 Rewa Pumice – Samples T12, T13, T14:

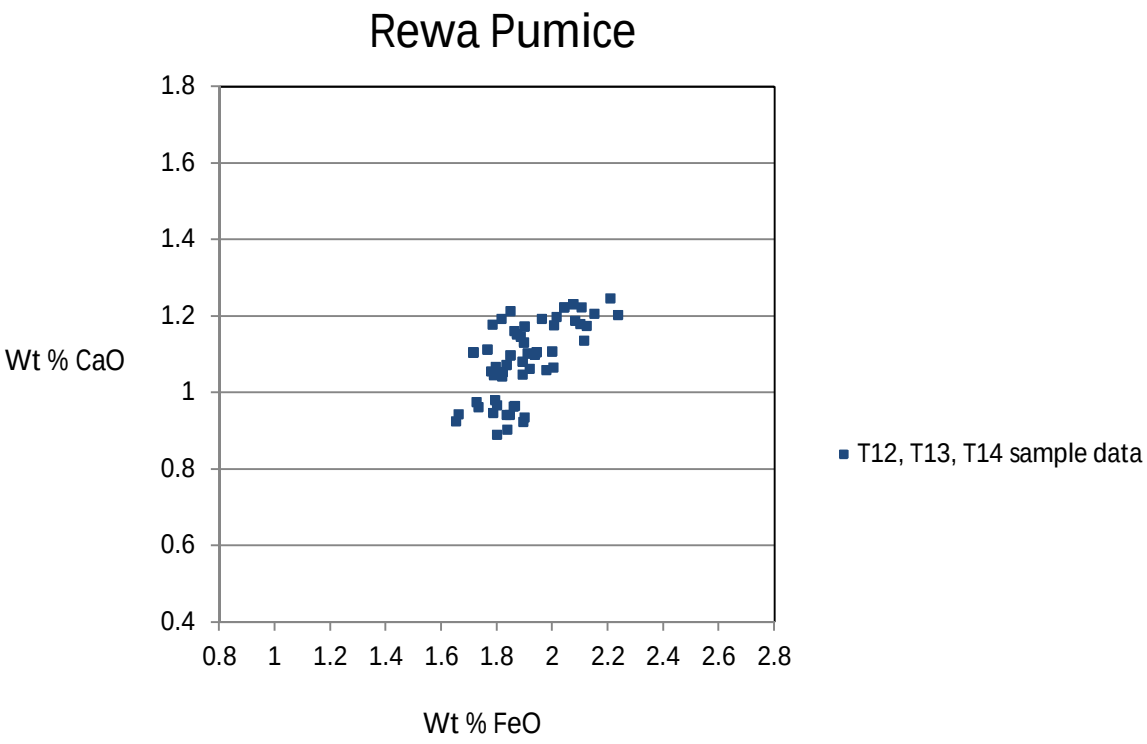


| T12 Normalised data (Wt %) | | | | | | | | | |
|---|---|---|---|---|---|---|---|---|---|
| Reading | SiO2 | Al2O3 | TiO2 | FeO | MgO | CaO | Na2O | K2O | Cl |
| 1 | 75.75 | 13.41 | 0.16 | 1.90 | 0.09 | 1.17 | 3.62 | 3.68 | 0.22 |
| 2 | 76.16 | 13.15 | 0.18 | 1.76 | 0.13 | 1.11 | 3.73 | 3.55 | 0.23 |
| 3 | 76.33 | 13.11 | 0.17 | 1.71 | 0.09 | 1.11 | 3.66 | 3.61 | 0.21 |
| 4 | 76.06 | 13.12 | 0.17 | 1.94 | 0.06 | 1.11 | 3.78 | 3.55 | 0.21 |
| 5 | 75.84 | 13.23 | 0.20 | 2.00 | 0.07 | 1.11 | 3.64 | 3.69 | 0.23 |
| 6 | 76.35 | 12.94 | 0.17 | 1.94 | 0.06 | 1.10 | 3.69 | 3.52 | 0.23 |
| 7 | 55.79 | 25.87 | 0.39 | 2.35 | 0.44 | 11.77 | 2.68 | 0.53 | 0.16 |
| 8 | 75.42 | 13.44 | 0.15 | 2.04 | 0.09 | 1.22 | 3.74 | 3.67 | 0.22 |
| 9 | 75.55 | 13.32 | 0.18 | 2.07 | 0.08 | 1.23 | 3.74 | 3.60 | 0.22 |
| 10 | 75.98 | 13.21 | 0.18 | 1.90 | 0.08 | 1.13 | 3.67 | 3.63 | 0.23 |
| 11 | 75.97 | 13.19 | 0.14 | 1.91 | 0.08 | 1.10 | 3.83 | 3.55 | 0.22 |
| 12 | 76.16 | 13.10 | 0.18 | 1.71 | 0.09 | 1.11 | 3.58 | 3.84 | 0.25 |
| 13 | 76.65 | 13.28 | 0.20 | 1.87 | 0.07 | 1.15 | 2.59 | 3.92 | 0.26 |
| 14 | 76.01 | 13.34 | 0.20 | 1.85 | 0.12 | 1.10 | 3.78 | 3.37 | 0.24 |
| 15 | 76.18 | 12.99 | 0.15 | 1.82 | 0.06 | 1.06 | 3.74 | 3.77 | 0.24 |
| 16 | 76.14 | 13.15 | 0.16 | 1.89 | 0.07 | 1.08 | 3.71 | 3.57 | 0.23 |

| | | | | | | | | | |
|---|---|---|---|---|---|---|---|---|---|
| 17 | 77.55 | 13.18 | 0.18 | 1.83 | 0.07 | 1.07 | 2.20 | 3.69 | 0.22 |
| Average | 74.93 | 13.94 | 0.19 | 1.91 | 0.10 | 1.75 | 3.49 | 3.46 | 0.22 |
| Std | 4.95 | 3.08 | 0.06 | 0.15 | 0.09 | 2.58 | 0.49 | 0.76 | 0.02 |

| Reading | Water | 1/3 K | Sum | %Fe/sum | %Ca/ sum | %1/3K/ sum |
|---|---|---|---|---|---|---|
| 1 | 7.36 | 1.23 | 4.30 | 0.44 | 0.27 | 0.29 |
| 2 | 6.17 | 1.18 | 4.06 | 0.43 | 0.27 | 0.29 |
| 3 | 6.53 | 1.20 | 4.02 | 0.43 | 0.27 | 0.30 |
| 4 | 5.66 | 1.18 | 4.23 | 0.46 | 0.26 | 0.28 |
| 5 | 6.93 | 1.23 | 4.34 | 0.46 | 0.26 | 0.28 |
| 6 | 6.53 | 1.17 | 4.21 | 0.46 | 0.26 | 0.28 |
| 7 | 4.78 | 0.18 | 14.30 | 0.16 | 0.82 | 0.01 |
| 8 | 5.79 | 1.22 | 4.49 | 0.45 | 0.27 | 0.27 |
| 9 | 6.35 | 1.20 | 4.51 | 0.46 | 0.27 | 0.27 |
| 10 | 6.31 | 1.21 | 4.24 | 0.45 | 0.27 | 0.29 |
| 11 | 5.65 | 1.18 | 4.20 | 0.46 | 0.26 | 0.28 |
| 12 | 8.16 | 1.28 | 4.10 | 0.42 | 0.27 | 0.31 |
| 13 | 8.50 | 1.31 | 4.33 | 0.43 | 0.27 | 0.30 |
| 14 | 5.44 | 1.12 | 4.07 | 0.45 | 0.27 | 0.28 |
| 15 | 7.35 | 1.26 | 4.13 | 0.44 | 0.26 | 0.30 |
| 16 | 5.86 | 1.19 | 4.16 | 0.45 | 0.26 | 0.29 |
| 17 | 8.16 | 1.23 | 4.14 | 0.44 | 0.26 | 0.30 |
| Average | 6.56 | 1.15 | 4.81 | 0.43 | 0.30 | 0.27 |
| Std | 1.05 | 0.25 | 2.45 | 0.07 | 0.14 | 0.07 |

| T13 Normalised data (Wt %) | | | | | | | | | |
|---|---|---|---|---|---|---|---|---|---|
| Reading | SiO2 | Al2O3 | TiO2 | FeO | MgO | CaO | Na2O | K2O | Cl |
| 1 | 76.74 | 12.94 | 0.16 | 1.90 | 0.05 | 0.94 | 3.47 | 3.55 | 0.25 |
| 2 | 77.17 | 12.89 | 0.19 | 1.65 | 0.04 | 0.93 | 3.63 | 3.24 | 0.27 |
| 3 | 77.00 | 12.74 | 0.13 | 1.84 | 0.06 | 0.90 | 3.67 | 3.39 | 0.25 |
| 4 | 76.09 | 13.18 | 0.16 | 1.79 | 0.08 | 1.05 | 4.06 | 3.33 | 0.27 |
| 5 | 76.89 | 12.85 | 0.18 | 1.85 | 0.04 | 0.94 | 3.71 | 3.30 | 0.25 |
| 6 | 76.56 | 12.93 | 0.15 | 1.78 | 0.05 | 0.95 | 3.84 | 3.49 | 0.25 |
| 7 | 76.48 | 12.80 | 0.18 | 1.89 | 0.05 | 0.92 | 3.92 | 3.48 | 0.26 |
| 8 | 76.60 | 12.79 | 0.12 | 1.86 | 0.06 | 0.96 | 3.91 | 3.44 | 0.25 |
| 9 | 76.72 | 12.93 | 0.18 | 1.73 | 0.07 | 0.96 | 3.72 | 3.41 | 0.27 |
| 10 | 76.56 | 12.98 | 0.18 | 1.66 | 0.06 | 0.94 | 3.74 | 3.60 | 0.28 |
| 11 | 76.87 | 12.84 | 0.18 | 1.80 | 0.06 | 0.89 | 3.74 | 3.35 | 0.26 |
| 12 | 76.13 | 13.10 | 0.15 | 1.92 | 0.09 | 1.06 | 3.90 | 3.39 | 0.27 |
| 13 | 76.22 | 13.18 | 0.17 | 1.82 | 0.08 | 1.04 | 3.87 | 3.35 | 0.27 |

| | | | | | | | | | |
|---|---|---|---|---|---|---|---|---|---|
| 14 | 76.18 | 13.12 | 0.17 | 1.89 | 0.04 | 1.05 | 3.94 | 3.34 | 0.27 |
| 15 | 76.07 | 13.26 | 0.14 | 1.98 | 0.05 | 1.06 | 4.01 | 3.16 | 0.27 |
| 16 | 76.36 | 12.78 | 0.15 | 1.80 | 0.03 | 0.97 | 4.07 | 3.54 | 0.30 |
| 17 | 76.44 | 13.20 | 0.21 | 1.79 | 0.06 | 1.07 | 3.72 | 3.24 | 0.26 |
| 18 | 76.50 | 12.88 | 0.16 | 1.86 | 0.06 | 0.97 | 3.80 | 3.49 | 0.27 |
| 19 | 76.76 | 12.90 | 0.17 | 1.79 | 0.07 | 0.98 | 3.70 | 3.40 | 0.23 |
| 20 | 76.60 | 12.79 | 0.15 | 1.83 | 0.07 | 0.94 | 4.02 | 3.34 | 0.26 |
| 21 | 76.43 | 12.98 | 0.16 | 2.00 | 0.04 | 1.07 | 3.86 | 3.20 | 0.25 |
| Average | 76.54 | 12.95 | 0.16 | 1.83 | 0.06 | 0.98 | 3.82 | 3.38 | 0.26 |
| Std | 0.30 | 0.16 | 0.02 | 0.09 | 0.02 | 0.06 | 0.15 | 0.12 | 0.01 |

| Reading | Water | 1/3 K | Sum | %Fe/sum | %Ca/ sum | %1/3K/ sum |
|---|---|---|---|---|---|---|
| 1 | 7.82 | 1.18 | 4.02 | 0.47 | 0.23 | 0.29 |
| 2 | 8.23 | 1.08 | 3.66 | 0.45 | 0.25 | 0.30 |
| 3 | 7.31 | 1.13 | 3.87 | 0.47 | 0.23 | 0.29 |
| 4 | 6.86 | 1.11 | 3.94 | 0.45 | 0.27 | 0.28 |
| 5 | 7.28 | 1.10 | 3.89 | 0.47 | 0.24 | 0.28 |
| 6 | 6.60 | 1.16 | 3.89 | 0.46 | 0.24 | 0.30 |
| 7 | 6.67 | 1.16 | 3.98 | 0.48 | 0.23 | 0.29 |
| 8 | 6.43 | 1.15 | 3.97 | 0.47 | 0.24 | 0.29 |
| 9 | 7.07 | 1.14 | 3.83 | 0.45 | 0.25 | 0.30 |
| 10 | 5.92 | 1.20 | 3.80 | 0.44 | 0.25 | 0.32 |
| 11 | 7.44 | 1.12 | 3.81 | 0.47 | 0.23 | 0.29 |
| 12 | 7.01 | 1.13 | 4.11 | 0.47 | 0.26 | 0.27 |
| 13 | 6.91 | 1.12 | 3.98 | 0.46 | 0.26 | 0.28 |
| 14 | 7.15 | 1.11 | 4.05 | 0.47 | 0.26 | 0.27 |
| 15 | 6.42 | 1.05 | 4.09 | 0.48 | 0.26 | 0.26 |
| 16 | 5.90 | 1.18 | 3.95 | 0.46 | 0.25 | 0.30 |
| 17 | 7.57 | 1.08 | 3.94 | 0.46 | 0.27 | 0.27 |
| 18 | 6.97 | 1.16 | 4.00 | 0.47 | 0.24 | 0.29 |
| 19 | 7.49 | 1.13 | 3.91 | 0.46 | 0.25 | 0.29 |
| 20 | 6.81 | 1.11 | 3.89 | 0.47 | 0.24 | 0.29 |
| 21 | 7.19 | 1.07 | 4.14 | 0.48 | 0.26 | 0.26 |
| Average | 7.00 | 1.13 | 3.94 | 0.46 | 0.25 | 0.29 |
| Std | 0.57 | 0.04 | 0.11 | 0.01 | 0.01 | 0.01 |

| T14 Normalised data (Wt %) | | | | | | | | | |
|---|---|---|---|---|---|---|---|---|---|
| Reading | SiO2 | Al2O3 | TiO2 | FeO | MgO | CaO | Na2O | K2O | Cl |

| | | | | | | | | | |
|---|---|---|---|---|---|---|---|---|---|
| 1 | 76.78 | 12.84 | 0.15 | 1.73 | 0.05 | 0.98 | 3.89 | 3.33 | 0.27 |
| 2 | 75.68 | 13.32 | 0.19 | 1.86 | 0.13 | 1.16 | 4.03 | 3.38 | 0.24 |
| 3 | 75.60 | 13.47 | 0.18 | 1.85 | 0.07 | 1.21 | 4.09 | 3.28 | 0.25 |
| 4 | 75.82 | 13.40 | 0.20 | 1.96 | 0.07 | 1.19 | 3.94 | 3.19 | 0.23 |
| 5 | 75.66 | 13.33 | 0.20 | 2.11 | 0.08 | 1.14 | 3.79 | 3.46 | 0.22 |
| 6 | 75.49 | 13.29 | 0.20 | 2.23 | 0.07 | 1.20 | 3.87 | 3.40 | 0.24 |
| 7 | 75.36 | 13.38 | 0.20 | 2.10 | 0.09 | 1.18 | 3.91 | 3.54 | 0.23 |
| 8 | 75.87 | 13.19 | 0.18 | 2.01 | 0.11 | 1.20 | 4.04 | 3.16 | 0.25 |
| 9 | 75.26 | 13.41 | 0.17 | 2.21 | 0.10 | 1.25 | 4.04 | 3.35 | 0.22 |
| 10 | 75.79 | 13.26 | 0.18 | 2.08 | 0.10 | 1.19 | 3.90 | 3.25 | 0.26 |
| 11 | 75.99 | 13.35 | 0.19 | 2.15 | 0.07 | 1.21 | 3.71 | 3.07 | 0.25 |
| 12 | 75.88 | 13.17 | 0.18 | 1.82 | 0.07 | 1.19 | 4.12 | 3.34 | 0.24 |
| 13 | 75.70 | 13.30 | 0.18 | 2.00 | 0.09 | 1.18 | 4.18 | 3.15 | 0.22 |
| 14 | 75.91 | 13.36 | 0.17 | 1.89 | 0.10 | 1.15 | 3.80 | 3.37 | 0.27 |
| 15 | 76.09 | 13.09 | 0.18 | 1.78 | 0.07 | 1.06 | 3.95 | 3.50 | 0.28 |
| 16 | 76.06 | 13.31 | 0.20 | 1.78 | 0.09 | 1.18 | 3.95 | 3.20 | 0.23 |
| 17 | 75.63 | 13.22 | 0.21 | 2.10 | 0.12 | 1.22 | 3.90 | 3.35 | 0.24 |
| 18 | 75.72 | 13.34 | 0.17 | 2.12 | 0.09 | 1.18 | 3.83 | 3.31 | 0.24 |
| Average | 75.80 | 13.28 | 0.19 | 1.99 | 0.09 | 1.17 | 3.94 | 3.31 | 0.24 |
| Std | 0.33 | 0.14 | 0.02 | 0.16 | 0.02 | 0.06 | 0.12 | 0.13 | 0.02 |

| Reading | Water | 1/3 K2O | Sum | %Fe/sum | %Ca/ sum | %1/3K/ sum |
|---|---|---|---|---|---|---|
| 1 | 6.26 | 1.11 | 3.81 | 0.45 | 0.26 | 0.29 |
| 2 | 7.01 | 1.13 | 4.15 | 0.45 | 0.28 | 0.27 |
| 3 | 6.88 | 1.09 | 4.16 | 0.44 | 0.29 | 0.26 |
| 4 | 5.95 | 1.06 | 4.22 | 0.46 | 0.28 | 0.25 |
| 5 | 5.73 | 1.15 | 4.40 | 0.48 | 0.26 | 0.26 |
| 6 | 5.99 | 1.13 | 4.57 | 0.49 | 0.26 | 0.25 |
| 7 | 4.98 | 1.18 | 4.46 | 0.47 | 0.26 | 0.26 |
| 8 | 6.52 | 1.05 | 4.26 | 0.47 | 0.28 | 0.25 |
| 9 | 5.69 | 1.12 | 4.57 | 0.48 | 0.27 | 0.24 |
| 10 | 6.99 | 1.08 | 4.35 | 0.48 | 0.27 | 0.25 |
| 11 | 7.67 | 1.02 | 4.38 | 0.49 | 0.28 | 0.23 |
| 12 | 6.08 | 1.11 | 4.12 | 0.44 | 0.29 | 0.27 |
| 13 | 5.14 | 1.05 | 4.23 | 0.47 | 0.28 | 0.25 |
| 14 | 6.04 | 1.12 | 4.15 | 0.45 | 0.28 | 0.27 |
| 15 | 5.19 | 1.17 | 4.00 | 0.44 | 0.26 | 0.29 |
| 16 | 6.02 | 1.07 | 4.03 | 0.44 | 0.29 | 0.26 |
| 17 | 5.34 | 1.12 | 4.45 | 0.47 | 0.28 | 0.25 |
| 18 | 5.10 | 1.10 | 4.40 | 0.48 | 0.27 | 0.25 |

| | | | | | | |
|---|---|---|---|---|---|---|
| Average | 6.03 | 1.10 | 4.26 | 0.47 | 0.27 | 0.26 |
| Std | 0.76 | 0.04 | 0.20 | 0.02 | 0.01 | 0.02 |

Ternary diagram displaying FeO: 1/3 K2O: CaO Wt % of sum, Rewa Pumice (T12, T13, T14).

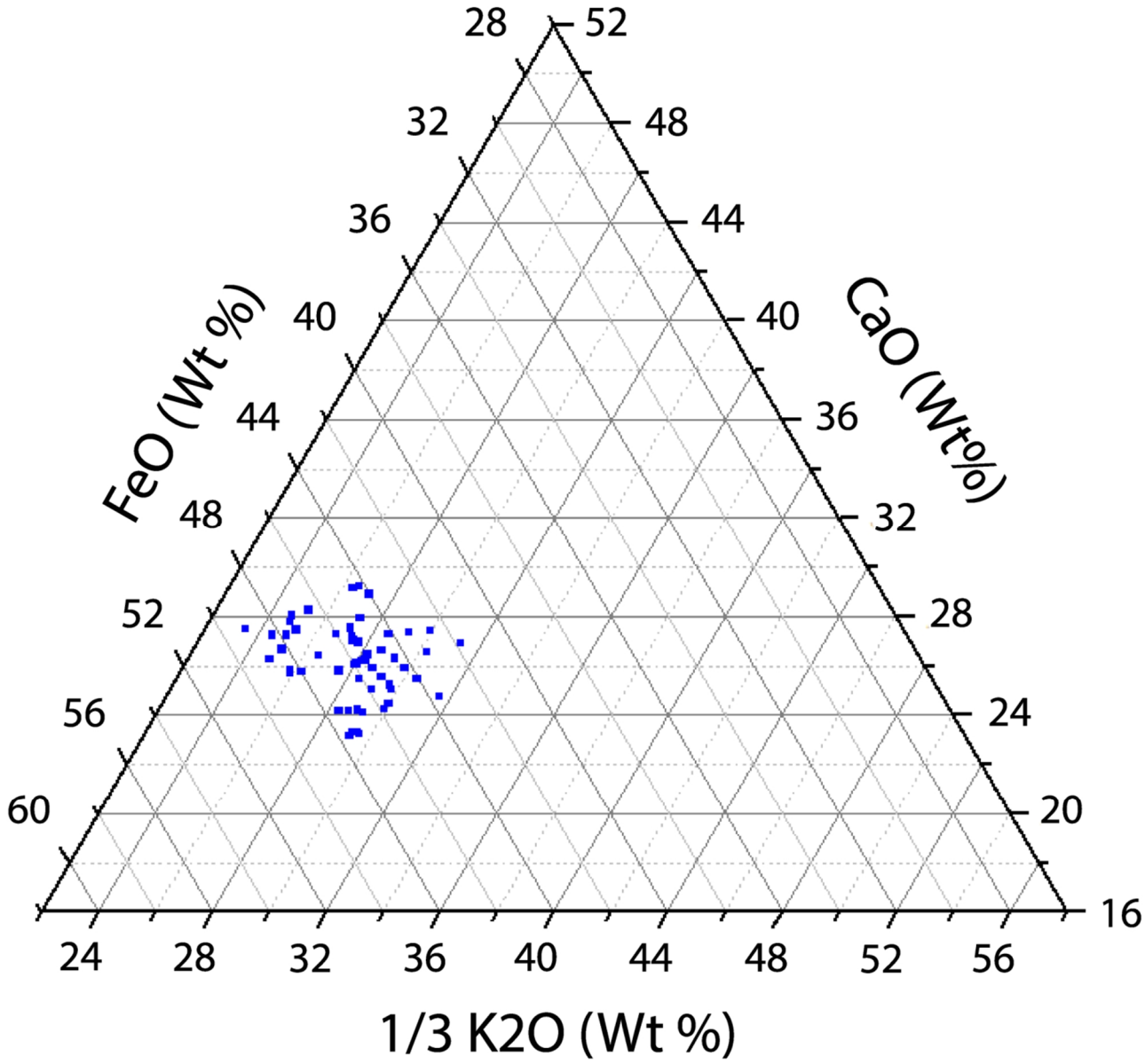

1.8 Mangapipi Tephra – Samples T5, T6:

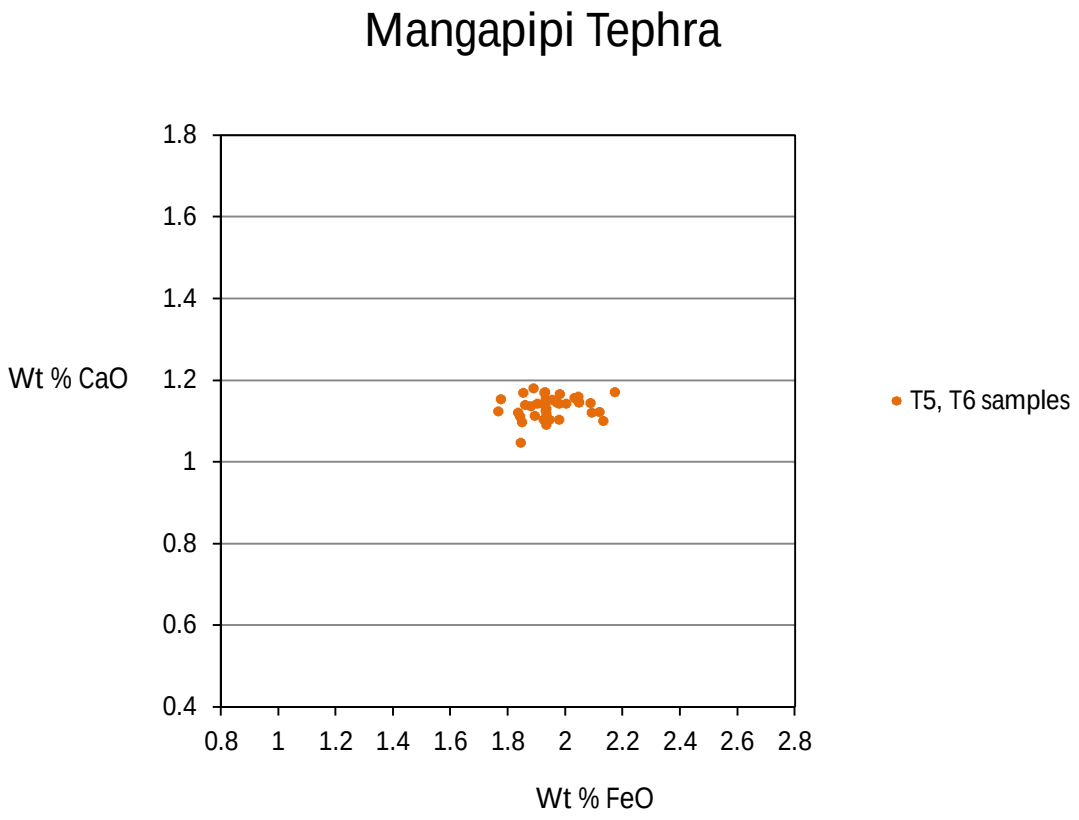


| T5 Normalised data Wt% | | | | | | | | | |
|---|---|---|---|---|---|---|---|---|---|
| Reading | SiO2 | Al2O3 | TiO2 | FeO | MgO | CaO | Na2O | K2O | Cl |
| 1 | 75.18 | 13.38 | 0.20 | 1.93 | 0.13 | 1.17 | 4.43 | 3.32 | 0.26 |
| 2 | 75.47 | 13.46 | 0.18 | 1.77 | 0.11 | 1.15 | 4.59 | 2.99 | 0.27 |
| 3 | 75.48 | 13.34 | 0.20 | 1.95 | 0.06 | 1.15 | 4.39 | 3.16 | 0.26 |
| 4 | 75.47 | 13.37 | 0.18 | 2.05 | 0.11 | 1.15 | 4.26 | 3.19 | 0.23 |
| 5 | 75.49 | 13.31 | 0.20 | 2.09 | 0.10 | 1.15 | 4.13 | 3.29 | 0.24 |
| 6 | 75.22 | 13.37 | 0.23 | 1.93 | 0.09 | 1.17 | 4.45 | 3.29 | 0.26 |
| 7 | 75.78 | 13.25 | 0.22 | 1.88 | 0.11 | 1.14 | 4.29 | 3.06 | 0.28 |
| 8 | 75.52 | 13.21 | 0.20 | 2.00 | 0.10 | 1.14 | 4.40 | 3.17 | 0.25 |
| 9 | 75.25 | 13.33 | 0.20 | 2.04 | 0.10 | 1.15 | 4.30 | 3.38 | 0.25 |
| 10 | 75.64 | 13.20 | 0.21 | 1.92 | 0.10 | 1.14 | 4.36 | 3.14 | 0.27 |
| 11 | 75.39 | 13.29 | 0.18 | 2.09 | 0.12 | 1.12 | 4.46 | 3.09 | 0.26 |

| | | | | | | | | | |
|---|---|---|---|---|---|---|---|---|---|
| 12 | 75.35 | 13.30 | 0.21 | 1.93 | 0.14 | 1.15 | 4.42 | 3.24 | 0.26 |
| 13 | 75.68 | 13.18 | 0.20 | 1.85 | 0.10 | 1.17 | 4.49 | 3.07 | 0.26 |
| 14 | 75.66 | 13.34 | 0.20 | 1.93 | 0.09 | 1.12 | 4.37 | 3.01 | 0.27 |
| 15 | 75.46 | 13.29 | 0.21 | 1.98 | 0.11 | 1.17 | 4.44 | 3.08 | 0.25 |
| 16 | 75.42 | 13.06 | 0.19 | 2.17 | 0.11 | 1.17 | 4.33 | 3.27 | 0.26 |
| 17 | 75.46 | 13.28 | 0.18 | 2.12 | 0.10 | 1.12 | 4.27 | 3.19 | 0.28 |
| 18 | 75.67 | 13.16 | 0.21 | 2.13 | 0.11 | 1.10 | 4.30 | 3.08 | 0.24 |
| 19 | 76.07 | 13.11 | 0.20 | 1.84 | 0.08 | 1.05 | 4.19 | 3.21 | 0.25 |
| 20 | 75.72 | 13.22 | 0.17 | 1.93 | 0.09 | 1.09 | 4.31 | 3.19 | 0.28 |
| Average | 75.52 | 13.27 | 0.20 | 1.98 | 0.10 | 1.14 | 4.36 | 3.17 | 0.26 |
| Std | 0.21 | 0.10 | 0.01 | 0.11 | 0.02 | 0.03 | 0.11 | 0.11 | 0.01 |

| Reading | Water | 1/3 K | Sum | %Fe/sum | %Ca/ sum | %1/3K/ sum |
|---|---|---|---|---|---|---|
| 1 | 6.70 | 1.11 | 4.21 | 0.46 | 0.28 | 0.26 |
| 2 | 7.26 | 1.00 | 3.93 | 0.45 | 0.29 | 0.25 |
| 3 | 5.77 | 1.05 | 4.16 | 0.47 | 0.28 | 0.25 |
| 4 | 6.90 | 1.06 | 4.26 | 0.48 | 0.27 | 0.25 |
| 5 | 5.59 | 1.10 | 4.33 | 0.48 | 0.26 | 0.25 |
| 6 | 5.08 | 1.10 | 4.19 | 0.46 | 0.28 | 0.26 |
| 7 | 5.51 | 1.02 | 4.04 | 0.47 | 0.28 | 0.25 |
| 8 | 6.30 | 1.06 | 4.20 | 0.48 | 0.27 | 0.25 |
| 9 | 6.99 | 1.13 | 4.32 | 0.47 | 0.27 | 0.26 |
| 10 | 5.71 | 1.05 | 4.11 | 0.47 | 0.28 | 0.25 |
| 11 | 8.10 | 1.03 | 4.24 | 0.49 | 0.26 | 0.24 |
| 12 | 7.26 | 1.08 | 4.16 | 0.46 | 0.28 | 0.26 |
| 13 | 7.15 | 1.02 | 4.05 | 0.46 | 0.29 | 0.25 |
| 14 | 6.52 | 1.00 | 4.06 | 0.48 | 0.28 | 0.25 |
| 15 | 6.84 | 1.03 | 4.17 | 0.47 | 0.28 | 0.25 |
| 16 | 5.31 | 1.09 | 4.43 | 0.49 | 0.26 | 0.25 |
| 17 | 6.76 | 1.06 | 4.31 | 0.49 | 0.26 | 0.25 |
| 18 | 5.70 | 1.03 | 4.26 | 0.50 | 0.26 | 0.24 |
| 19 | 5.48 | 1.07 | 3.96 | 0.47 | 0.26 | 0.27 |
| 20 | 6.35 | 1.06 | 4.09 | 0.47 | 0.27 | 0.26 |
| Average | 6.36 | 1.06 | 4.17 | 0.47 | 0.27 | 0.25 |
| Std | 0.81 | 0.04 | 0.13 | 0.01 | 0.01 | 0.01 |

| T6 Normalised data (Wt %) | | | | | | | | | |
|---|---|---|---|---|---|---|---|---|---|
| Reading | SiO2 | Al2O3 | TiO2 | FeO | MgO | CaO | Na2O | K2O | Cl |
| 1 | 75.68 | 13.22 | 0.19 | 1.86 | 0.13 | 1.14 | 4.43 | 3.08 | 0.27 |
| 2 | 75.78 | 13.09 | 0.22 | 1.76 | 0.13 | 1.13 | 4.43 | 3.20 | 0.27 |

| | | | | | | | | | |
|---|---|---|---|---|---|---|---|---|---|
| 3 | 75.46 | 13.34 | 0.25 | 1.85 | 0.13 | 1.10 | 4.39 | 3.24 | 0.26 |
| 4 | 75.44 | 13.21 | 0.19 | 2.05 | 0.09 | 1.15 | 4.57 | 3.05 | 0.26 |
| 5 | 75.55 | 13.33 | 0.22 | 1.98 | 0.08 | 1.10 | 4.35 | 3.10 | 0.28 |
| 6 | 75.82 | 13.05 | 0.23 | 2.03 | 0.06 | 1.16 | 4.30 | 3.08 | 0.26 |
| 7 | 75.98 | 13.10 | 0.17 | 1.83 | 0.10 | 1.12 | 4.10 | 3.35 | 0.24 |
| 8 | 75.52 | 13.36 | 0.23 | 1.90 | 0.11 | 1.14 | 4.27 | 3.21 | 0.26 |
| 9 | 75.85 | 13.01 | 0.22 | 1.98 | 0.11 | 1.14 | 4.24 | 3.20 | 0.26 |
| 10 | 75.97 | 13.23 | 0.19 | 1.93 | 0.11 | 1.15 | 4.07 | 3.11 | 0.24 |
| 11 | 75.75 | 13.11 | 0.22 | 1.92 | 0.12 | 1.10 | 4.42 | 3.12 | 0.24 |
| 12 | 75.34 | 13.26 | 0.21 | 2.04 | 0.10 | 1.16 | 4.45 | 3.17 | 0.26 |
| 13 | 76.14 | 13.07 | 0.22 | 1.93 | 0.09 | 1.13 | 4.08 | 3.09 | 0.27 |
| 14 | 75.55 | 13.08 | 0.23 | 1.89 | 0.13 | 1.18 | 4.57 | 3.14 | 0.24 |
| 15 | 75.59 | 13.24 | 0.23 | 1.89 | 0.09 | 1.11 | 4.42 | 3.19 | 0.24 |
| 16 | 75.51 | 13.03 | 0.21 | 1.97 | 0.12 | 1.15 | 4.50 | 3.25 | 0.26 |
| 17 | 75.79 | 13.15 | 0.21 | 1.93 | 0.11 | 1.13 | 4.23 | 3.20 | 0.25 |
| 18 | 75.78 | 13.13 | 0.20 | 1.84 | 0.11 | 1.11 | 4.46 | 3.12 | 0.26 |
| 19 | 75.72 | 13.04 | 0.21 | 1.94 | 0.12 | 1.10 | 4.51 | 3.11 | 0.24 |
| 20 | 75.76 | 13.23 | 0.19 | 1.87 | 0.10 | 1.15 | 4.28 | 3.16 | 0.25 |
| Average | 75.70 | 13.16 | 0.21 | 1.92 | 0.11 | 1.13 | 4.35 | 3.16 | 0.25 |
| Std | 0.20 | 0.11 | 0.02 | 0.07 | 0.02 | 0.02 | 0.15 | 0.07 | 0.01 |

| Reading | Water | 1/3 K | Sum | %Fe/sum | %Ca/ sum | %1/3K/ sum |
|---|---|---|---|---|---|---|
| 1 | 7.26 | 1.03 | 4.03 | 0.46 | 0.28 | 0.26 |
| 2 | 7.67 | 1.07 | 3.95 | 0.45 | 0.28 | 0.27 |
| 3 | 7.60 | 1.08 | 4.03 | 0.46 | 0.27 | 0.27 |
| 4 | 7.11 | 1.02 | 4.21 | 0.49 | 0.27 | 0.24 |
| 5 | 7.49 | 1.03 | 4.12 | 0.48 | 0.27 | 0.25 |
| 6 | 7.01 | 1.03 | 4.22 | 0.48 | 0.27 | 0.24 |
| 7 | 6.37 | 1.12 | 4.07 | 0.45 | 0.28 | 0.27 |
| 8 | 8.32 | 1.07 | 4.12 | 0.46 | 0.28 | 0.26 |
| 9 | 7.18 | 1.07 | 4.19 | 0.47 | 0.27 | 0.25 |
| 10 | 7.26 | 1.04 | 4.12 | 0.47 | 0.28 | 0.25 |
| 11 | 4.96 | 1.04 | 4.07 | 0.47 | 0.27 | 0.26 |
| 12 | 7.46 | 1.06 | 4.26 | 0.48 | 0.27 | 0.25 |
| 13 | 6.28 | 1.03 | 4.09 | 0.47 | 0.28 | 0.25 |
| 14 | 5.86 | 1.05 | 4.11 | 0.46 | 0.29 | 0.25 |
| 15 | 5.96 | 1.06 | 4.07 | 0.46 | 0.27 | 0.26 |
| 16 | 6.93 | 1.08 | 4.20 | 0.47 | 0.27 | 0.26 |
| 17 | 7.45 | 1.07 | 4.13 | 0.47 | 0.27 | 0.26 |
| 18 | 4.17 | 1.04 | 3.99 | 0.46 | 0.28 | 0.26 |

| | | | | | | |
|---|---|---|---|---|---|---|
| 19 | 5.32 | 1.04 | 4.09 | 0.48 | 0.27 | 0.25 |
| 20 | 8.15 | 1.05 | 4.08 | 0.46 | 0.28 | 0.26 |
| Average | 6.79 | 1.05 | 4.11 | 0.47 | 0.28 | 0.26 |
| Std | 1.08 | 0.02 | 0.08 | 0.01 | 0.01 | 0.01 |

Ternary diagram displaying FeO: 1/3 K2O: CaO Wt % of sum, Mangapipi Tephra (T5, T6).

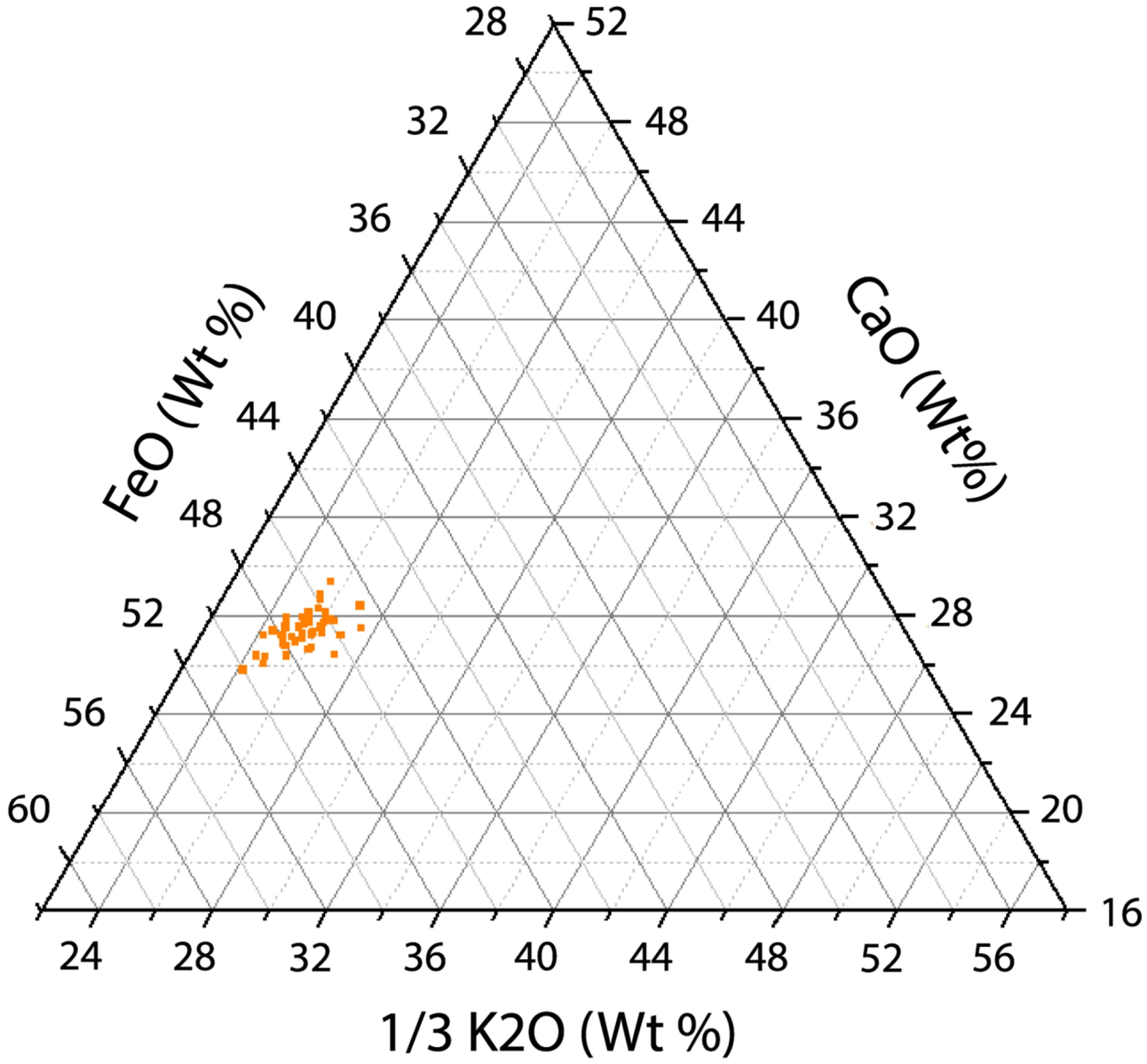

# Mangapipi Tephra

Grain size distribution frequency (%) graph showing grain size distribution of Mangapipi Tephra (T5) Bms Member, Takapari Formation.

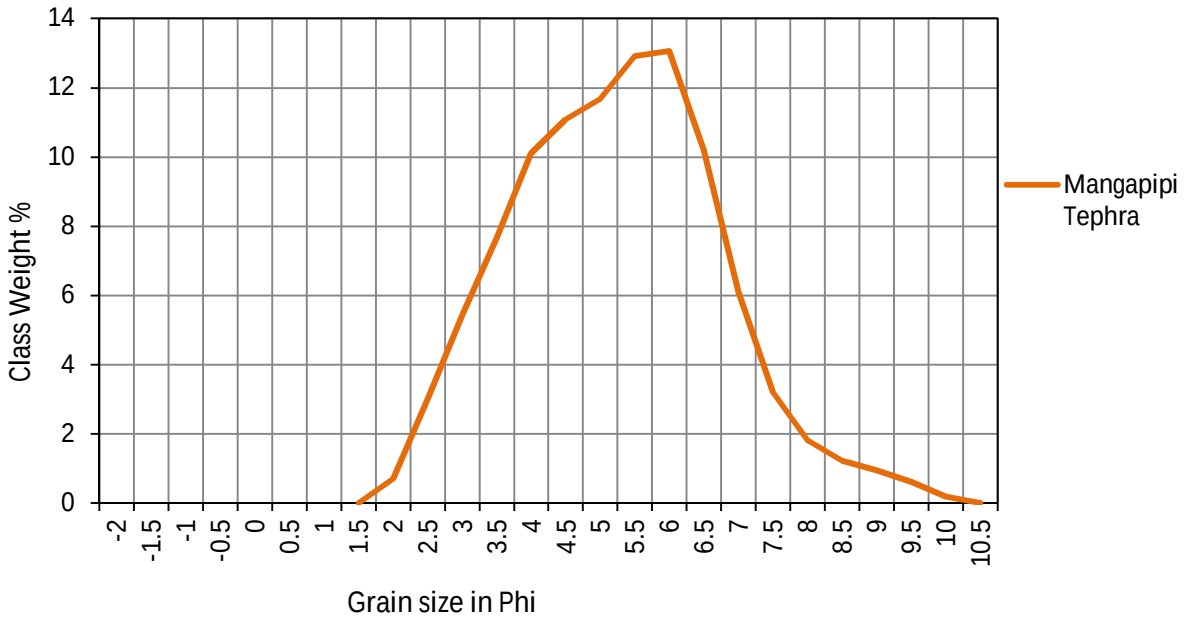


Grain size data from Mangapipi Tephra – T5

| Grain size in microns | Grain size in Phi | Class weight % |
|---|---|---|
| 250 | 2.0 | 0.00 |
| 176.777 | 2.5 | 0.71 |
| 125 | 3.0 | 3.02 |
| 88.388 | 3.5 | 5.45 |
| 62.5 | 4.0 | 7.69 |
| 44.194 | 4.5 | 10.11 |
| 31.25 | 5.0 | 11.08 |
| 22.097 | 5.5 | 11.69 |
| 15.625 | 6.0 | 12.92 |
| 11.049 | 6.5 | 13.06 |
| 7.813 | 7.0 | 10.19 |

| | | |
|---|---|---|
| 5.524 | 7.5 | 6.11 |
| 3.906 | 8.0 | 3.20 |
| 2.762 | 8.5 | 1.81 |
| 1.953 | 9.0 | 1.22 |
| 1.381 | 9.5 | 0.95 |
| 0.977 | 10.0 | 0.61 |
| 0.691 | 10.5 | 0.193666667 |

Histogram displaying the grain size distribution of Mangapipi Tephra (T5)

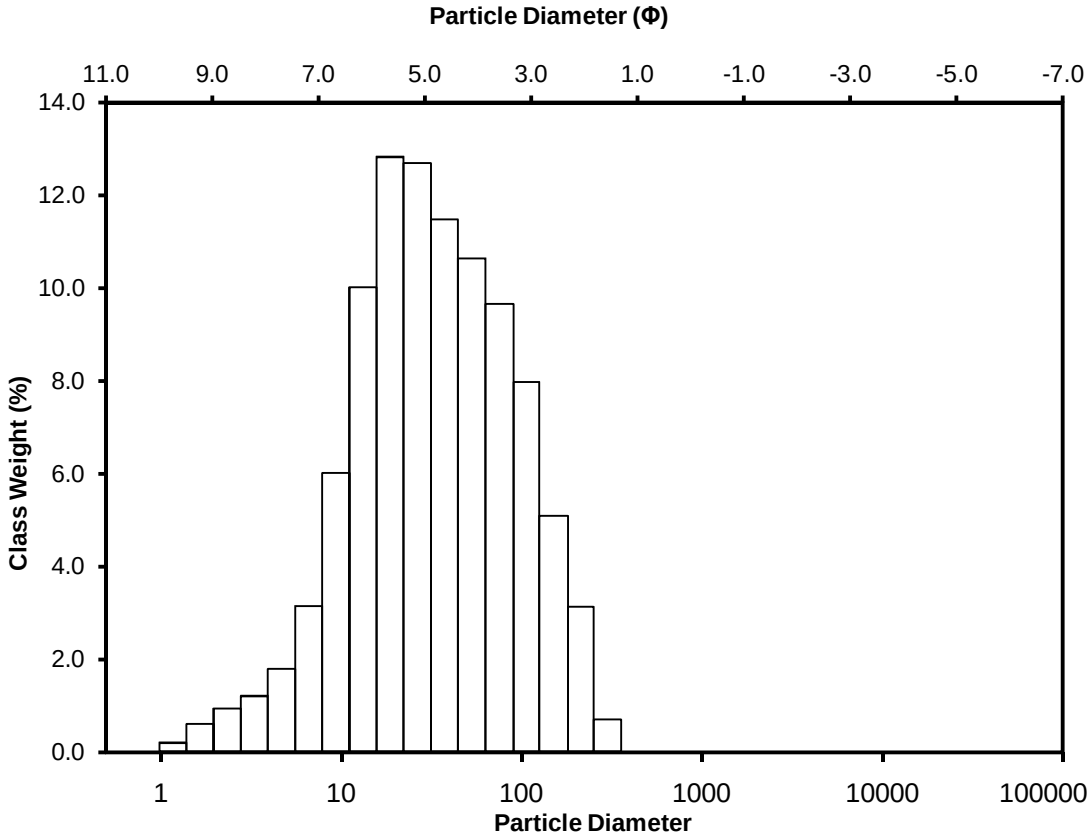


| Mangapipi Tephra T5 sample statistics: | | | |
|---|---|---|---|
| | Geometric μm | Logarithmic ϕ | Description |
| Mean | 32.45 | 4.946 | Fine Grained Tephra |
| Sorting | 2.797 | 1.484 | Poorly Sorted |
| Skewness | 0.028 | -0.028 | Symmetrical |
| Kurtosis | 0.957 | 0.957 | Mesokurtic |

1.9 Ridge Tephra – Samples T9, T11:

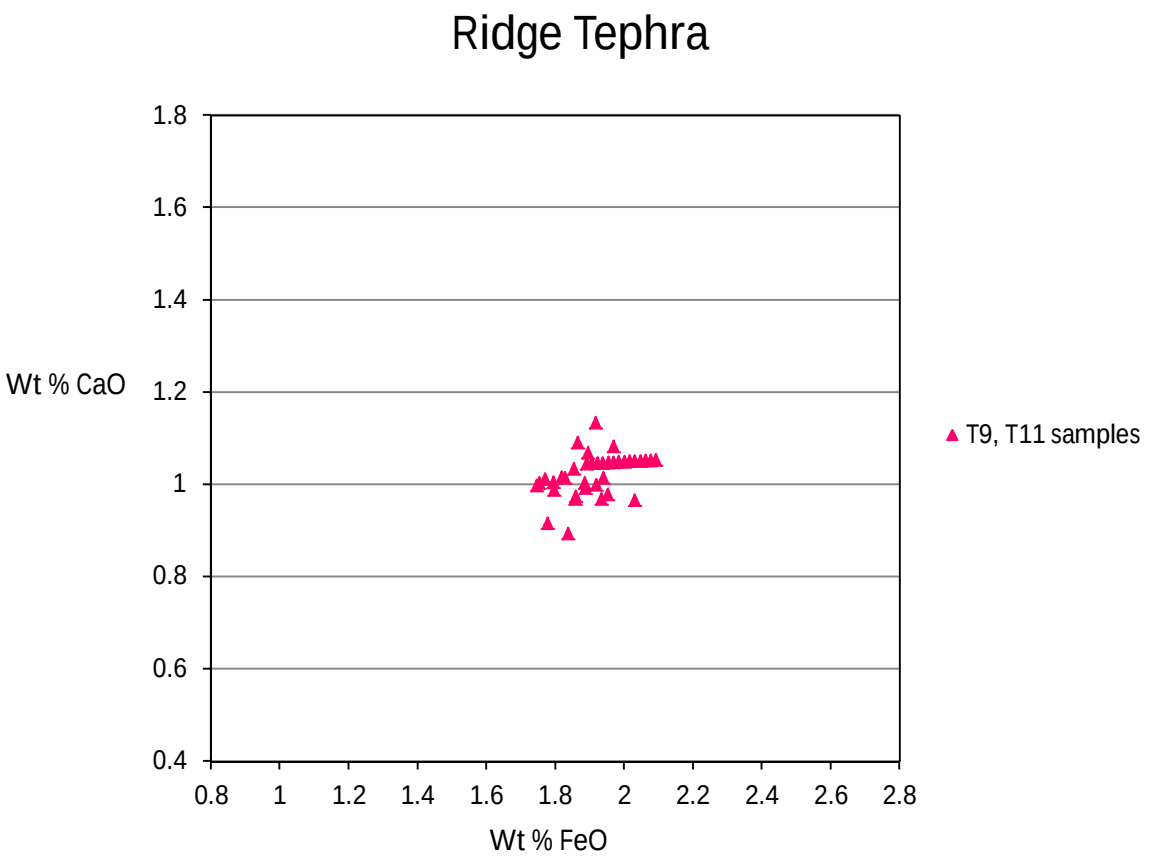


| T9 Normalised data (Wt %) | | | | | | | | | |
|---|---|---|---|---|---|---|---|---|---|
| Reading | SiO2 | Al2O3 | TiO2 | FeO | MgO | CaO | Na2O | K2O | Cl |
| 1 | 77.05 | 12.48 | 0.17 | 1.95 | 0.05 | 0.98 | 3.76 | 3.27 | 0.29 |
| 2 | 76.96 | 12.56 | 0.19 | 1.93 | 0.05 | 0.97 | 3.85 | 3.23 | 0.26 |
| 3 | 77.18 | 12.39 | 0.13 | 1.89 | 0.04 | 1.00 | 3.79 | 3.30 | 0.28 |
| 4 | 77.10 | 12.32 | 0.15 | 1.80 | 0.07 | 0.99 | 3.96 | 3.34 | 0.28 |
| 5 | 76.90 | 12.47 | 0.21 | 1.75 | 0.11 | 1.00 | 3.92 | 3.38 | 0.26 |
| 7 | 77.01 | 12.43 | 0.18 | 1.83 | 0.07 | 1.01 | 3.79 | 3.40 | 0.29 |
| 8 | 76.66 | 12.48 | 0.16 | 1.86 | 0.07 | 0.97 | 4.19 | 3.30 | 0.30 |
| 9 | 76.90 | 12.56 | 0.13 | 1.77 | 0.05 | 1.01 | 4.00 | 3.28 | 0.30 |
| 10 | 76.64 | 12.60 | 0.18 | 1.84 | 0.05 | 0.89 | 4.13 | 3.38 | 0.28 |
| 11 | 76.18 | 13.02 | 0.18 | 1.82 | 0.10 | 1.02 | 4.33 | 3.09 | 0.27 |
| 12 | 76.60 | 12.52 | 0.17 | 1.89 | 0.09 | 0.99 | 4.24 | 3.19 | 0.30 |
| 13 | 77.19 | 12.46 | 0.18 | 1.75 | 0.09 | 1.00 | 3.86 | 3.20 | 0.28 |
| 14 | 76.63 | 12.52 | 0.19 | 1.94 | 0.07 | 1.01 | 4.03 | 3.36 | 0.25 |
| 15 | 76.54 | 12.75 | 0.17 | 1.85 | 0.05 | 1.03 | 4.36 | 2.99 | 0.26 |

| | | | | | | | | | |
|---|---|---|---|---|---|---|---|---|---|
| 16 | 76.02 | 13.09 | 0.16 | 1.79 | 0.07 | 1.00 | 4.46 | 3.13 | 0.27 |
| 17 | 76.78 | 12.52 | 0.16 | 1.92 | 0.06 | 1.00 | 3.90 | 3.38 | 0.29 |
| 18 | 76.65 | 12.51 | 0.20 | 2.03 | 0.08 | 0.97 | 3.99 | 3.29 | 0.28 |
| 19 | 76.45 | 12.52 | 0.20 | 1.86 | 0.08 | 0.97 | 4.08 | 3.55 | 0.29 |
| Average | 76.75 | 12.57 | 0.17 | 1.86 | 0.07 | 0.99 | 4.04 | 3.28 | 0.28 |
| Std | 0.33 | 0.20 | 0.02 | 0.08 | 0.02 | 0.03 | 0.21 | 0.13 | 0.02 |

| Reading | Water | 1/3 K | Sum | %Fe/sum | %Ca/ sum | %1/3K/ sum |
|---|---|---|---|---|---|---|
| 1 | 7.21 | 1.09 | 4.02 | 0.49 | 0.24 | 0.27 |
| 2 | 6.15 | 1.08 | 3.98 | 0.49 | 0.24 | 0.27 |
| 3 | 6.93 | 1.10 | 3.99 | 0.47 | 0.25 | 0.28 |
| 4 | 4.73 | 1.11 | 3.90 | 0.46 | 0.25 | 0.29 |
| 5 | 6.56 | 1.13 | 3.88 | 0.45 | 0.26 | 0.29 |
| 7 | 6.01 | 1.13 | 3.97 | 0.46 | 0.26 | 0.29 |
| 8 | 6.30 | 1.10 | 3.93 | 0.47 | 0.25 | 0.28 |
| 9 | 6.18 | 1.09 | 3.87 | 0.46 | 0.26 | 0.28 |
| 10 | 7.84 | 1.13 | 3.86 | 0.48 | 0.23 | 0.29 |
| 11 | 7.41 | 1.03 | 3.86 | 0.47 | 0.26 | 0.27 |
| 12 | 6.20 | 1.06 | 3.94 | 0.48 | 0.25 | 0.27 |
| 13 | 6.13 | 1.07 | 3.81 | 0.46 | 0.26 | 0.28 |
| 14 | 7.15 | 1.12 | 4.08 | 0.48 | 0.25 | 0.28 |
| 15 | 6.20 | 1.00 | 3.88 | 0.48 | 0.27 | 0.26 |
| 16 | 9.72 | 1.04 | 3.84 | 0.47 | 0.26 | 0.27 |
| 17 | 6.56 | 1.13 | 4.04 | 0.47 | 0.25 | 0.28 |
| 18 | 7.27 | 1.10 | 4.09 | 0.50 | 0.24 | 0.27 |
| 19 | 5.32 | 1.18 | 4.01 | 0.46 | 0.24 | 0.30 |
| Average | 6.66 | 1.09 | 3.94 | 0.47 | 0.25 | 0.28 |
| Std | 1.07 | 0.04 | 0.08 | 0.01 | 0.01 | 0.01 |

| T11 Normalised data (Wt %) | | | | | | | | | |
|---|---|---|---|---|---|---|---|---|---|
| Reading | SiO2 | Al2O3 | TiO2 | FeO | MgO | CaO | Na2O | K2O | Cl |
| 1 | 76.08 | 13.00 | 0.20 | 1.92 | 0.10 | 1.13 | 4.37 | 2.96 | 0.25 |
| 2 | 76.72 | 12.66 | 0.17 | 1.78 | 0.09 | 0.92 | 4.24 | 3.17 | 0.27 |
| 3 | 76.03 | 12.99 | 0.19 | 1.97 | 0.11 | 1.08 | 4.42 | 2.92 | 0.28 |
| 4 | 75.95 | 13.06 | 0.19 | 1.89 | 0.10 | 1.07 | 4.53 | 2.93 | 0.27 |
| 5 | 76.11 | 13.24 | 0.21 | 1.86 | 0.08 | 1.09 | 3.85 | 3.31 | 0.24 |
| 6 | 76.11 | 13.10 | 0.19 | 1.89 | 0.09 | 1.04 | 4.19 | 3.12 | 0.26 |
| 8 | 76.07 | 13.13 | 0.19 | 1.91 | 0.09 | 1.05 | 4.27 | 3.03 | 0.25 |
| 9 | 76.04 | 13.16 | 0.19 | 1.92 | 0.09 | 1.05 | 4.36 | 2.94 | 0.25 |
| 10 | 76.00 | 13.19 | 0.19 | 1.94 | 0.09 | 1.05 | 4.44 | 2.85 | 0.25 |
| 11 | 75.96 | 13.22 | 0.19 | 1.95 | 0.09 | 1.05 | 4.53 | 2.77 | 0.25 |
| 12 | 75.92 | 13.25 | 0.19 | 1.97 | 0.09 | 1.05 | 4.61 | 2.68 | 0.24 |

| | | | | | | | | | |
|---|---|---|---|---|---|---|---|---|---|
| 13 | 75.88 | 13.28 | 0.19 | 1.98 | 0.08 | 1.05 | 4.70 | 2.59 | 0.24 |
| 14 | 75.84 | 13.31 | 0.19 | 2.00 | 0.08 | 1.05 | 4.78 | 2.50 | 0.24 |
| 15 | 75.80 | 13.34 | 0.19 | 2.02 | 0.08 | 1.05 | 4.87 | 2.42 | 0.24 |
| 16 | 75.76 | 13.37 | 0.19 | 2.03 | 0.08 | 1.05 | 4.95 | 2.33 | 0.23 |
| 17 | 75.72 | 13.40 | 0.19 | 2.05 | 0.08 | 1.05 | 5.04 | 2.24 | 0.23 |
| 18 | 75.68 | 13.43 | 0.19 | 2.06 | 0.08 | 1.05 | 5.12 | 2.15 | 0.23 |
| 19 | 75.64 | 13.46 | 0.19 | 2.08 | 0.08 | 1.05 | 5.20 | 2.07 | 0.23 |
| 20 | 75.61 | 13.49 | 0.19 | 2.09 | 0.08 | 1.05 | 5.29 | 1.98 | 0.22 |
| Average | 75.94 | 13.22 | 0.19 | 1.96 | 0.09 | 1.05 | 4.62 | 2.68 | 0.25 |
| Std | 0.25 | 0.20 | 0.01 | 0.08 | 0.01 | 0.04 | 0.39 | 0.40 | 0.02 |

| Reading | Water | 1/3 K | Sum | %Fe/sum | %Ca/ sum | %1/3K/ sum |
|---|---|---|---|---|---|---|
| 1 | 5.85 | 0.99 | 4.04 | 0.48 | 0.28 | 0.24 |
| 2 | 6.36 | 1.06 | 3.75 | 0.47 | 0.24 | 0.28 |
| 3 | 6.84 | 0.97 | 4.02 | 0.49 | 0.27 | 0.24 |
| 4 | 7.47 | 0.98 | 3.94 | 0.48 | 0.27 | 0.25 |
| 5 | 8.45 | 1.10 | 4.06 | 0.46 | 0.27 | 0.27 |
| 6 | 7.78 | 1.04 | 3.98 | 0.48 | 0.26 | 0.26 |
| 8 | 7.70 | 1.01 | 3.96 | 0.48 | 0.26 | 0.26 |
| 9 | 7.63 | 0.98 | 3.95 | 0.49 | 0.26 | 0.25 |
| 10 | 7.55 | 0.95 | 3.94 | 0.49 | 0.27 | 0.24 |
| 11 | 7.48 | 0.92 | 3.92 | 0.50 | 0.27 | 0.24 |
| 12 | 7.41 | 0.89 | 3.91 | 0.50 | 0.27 | 0.23 |
| 13 | 7.33 | 0.86 | 3.90 | 0.51 | 0.27 | 0.22 |
| 14 | 7.26 | 0.83 | 3.88 | 0.51 | 0.27 | 0.21 |
| 15 | 7.18 | 0.81 | 3.87 | 0.52 | 0.27 | 0.21 |
| 16 | 7.11 | 0.78 | 3.86 | 0.53 | 0.27 | 0.20 |
| 17 | 7.03 | 0.75 | 3.84 | 0.53 | 0.27 | 0.19 |
| 18 | 6.96 | 0.72 | 3.83 | 0.54 | 0.27 | 0.19 |
| 19 | 6.89 | 0.69 | 3.82 | 0.54 | 0.28 | 0.18 |
| 20 | 6.81 | 0.66 | 3.80 | 0.55 | 0.28 | 0.17 |
| Average | 7.21 | 0.89 | 3.91 | 0.50 | 0.27 | 0.23 |
| Std | 0.56 | 0.13 | 0.08 | 0.03 | 0.01 | 0.03 |

Ternary diagram displaying FeO: 1/3 K2O: CaO Wt % of sum, Ridge Tephra (T9, T11).

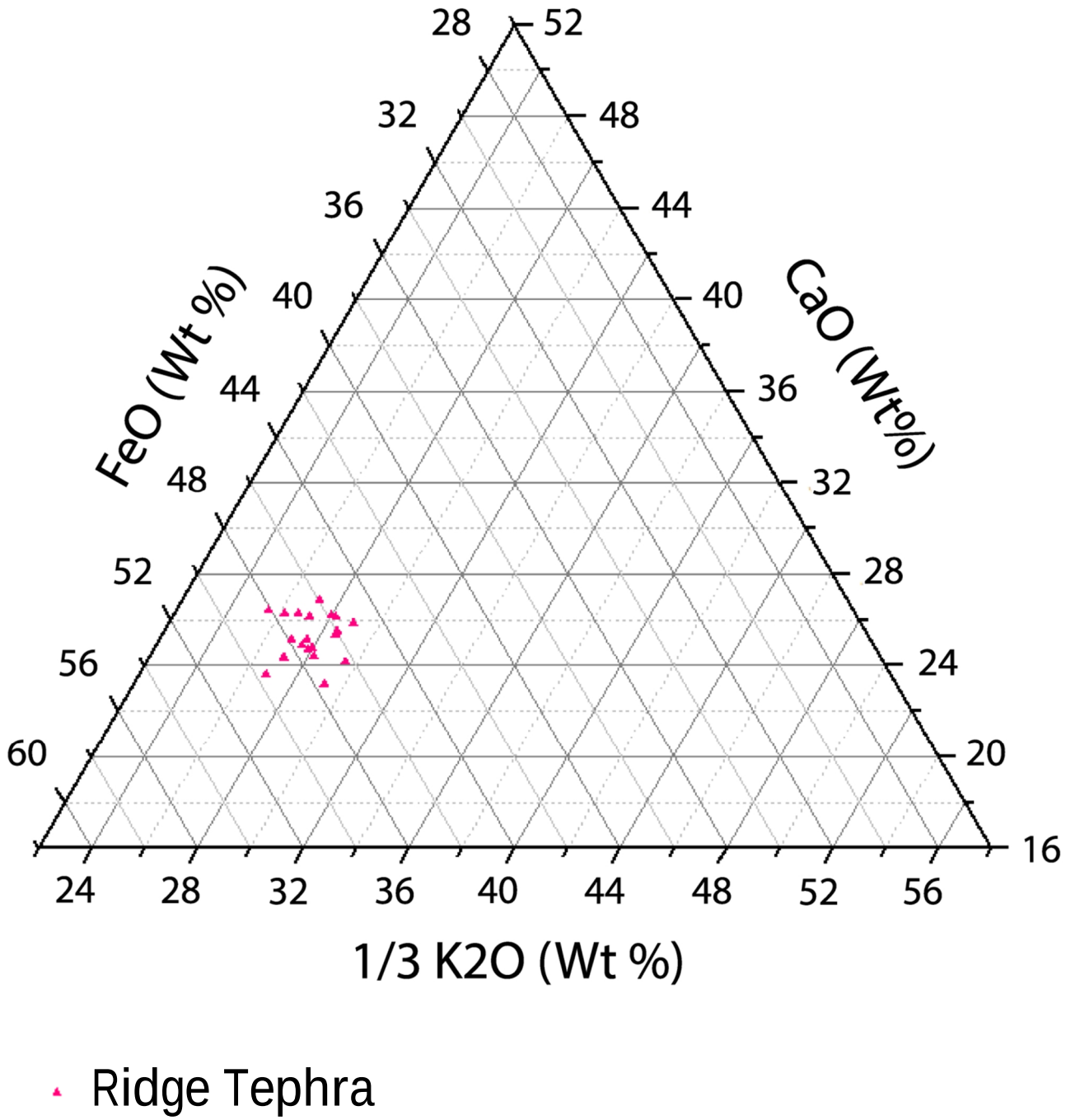

1.10 Pakihikura Tephra sample T4:

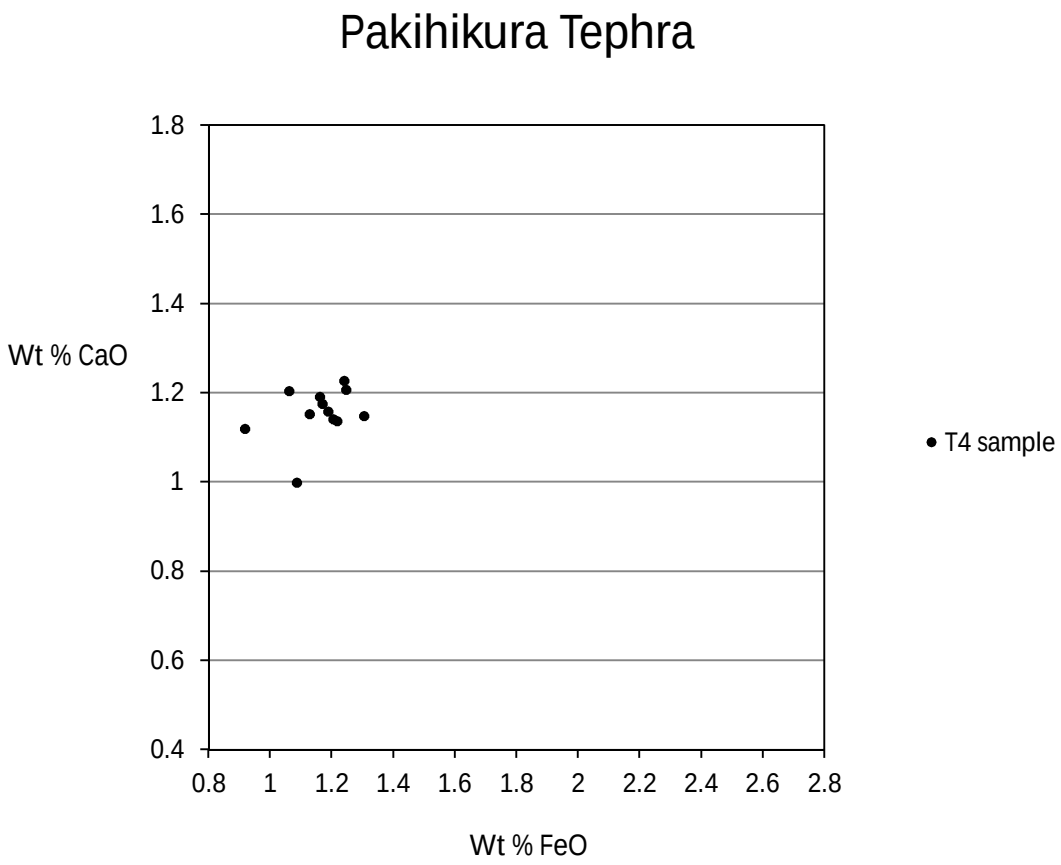


| T14 Normalised data (Wt %) | | | | | | | | | |
|---|---|---|---|---|---|---|---|---|---|
| Reading | SiO2 | Al2O3 | TiO2 | FeO | MgO | CaO | Na2O | K2O | Cl |
| 1 | 78.59 | 12.22 | 0.10 | 1.19 | 0.08 | 1.16 | 3.43 | 3.01 | 0.22 |
| 2 | 79.24 | 12.43 | 0.08 | 1.25 | 0.09 | 1.21 | 2.47 | 3.03 | 0.19 |
| 3 | 78.12 | 12.34 | 0.10 | 1.30 | 0.06 | 1.15 | 3.49 | 3.26 | 0.18 |
| 4 | 78.73 | 12.18 | 0.07 | 1.16 | 0.05 | 1.19 | 3.47 | 2.95 | 0.20 |
| 5 | 78.49 | 12.27 | 0.08 | 1.22 | 0.06 | 1.14 | 3.49 | 3.05 | 0.21 |
| 6 | 78.29 | 12.38 | 0.10 | 1.13 | 0.06 | 1.15 | 3.67 | 3.02 | 0.20 |
| 7 | 78.54 | 12.26 | 0.13 | 1.20 | 0.04 | 1.14 | 3.52 | 2.97 | 0.19 |
| 8 | 78.27 | 12.30 | 0.07 | 1.24 | 0.08 | 1.23 | 3.60 | 3.01 | 0.21 |
| 9 | 78.61 | 12.43 | 0.07 | 1.06 | 0.08 | 1.20 | 3.44 | 2.90 | 0.20 |
| 10 | 78.98 | 11.94 | 0.14 | 1.08 | 0.12 | 1.00 | 3.63 | 2.85 | 0.25 |
| 11 | 78.58 | 12.25 | 0.09 | 1.17 | 0.06 | 1.18 | 3.68 | 2.82 | 0.18 |
| 12 | 78.45 | 12.42 | 0.10 | 0.92 | 0.09 | 1.12 | 3.34 | 3.38 | 0.18 |
| Average | 78.57 | 12.29 | 0.09 | 1.16 | 0.07 | 1.16 | 3.44 | 3.02 | 0.20 |
| Std | 0.31 | 0.14 | 0.02 | 0.10 | 0.02 | 0.06 | 0.32 | 0.16 | 0.02 |

| Reading | Water | 1/3 K | Sum | %Fe/sum | %Ca/ sum | %1/3K/ sum |
|---|---|---|---|---|---|---|
| 1 | 5.09 | 1.00 | 3.35 | 0.35 | 0.35 | 0.30 |
| 2 | 6.88 | 1.01 | 3.46 | 0.36 | 0.35 | 0.29 |
| 3 | 3.82 | 1.09 | 3.54 | 0.37 | 0.32 | 0.31 |
| 4 | 5.78 | 0.98 | 3.34 | 0.35 | 0.36 | 0.29 |
| 5 | 5.94 | 1.02 | 3.37 | 0.36 | 0.34 | 0.30 |
| 6 | 6.06 | 1.01 | 3.29 | 0.34 | 0.35 | 0.31 |
| 7 | 5.27 | 0.99 | 3.34 | 0.36 | 0.34 | 0.30 |
| 9 | 6.62 | 1.00 | 3.47 | 0.36 | 0.35 | 0.29 |
| 10 | 7.18 | 0.97 | 3.23 | 0.33 | 0.37 | 0.30 |
| 11 | 7.26 | 0.95 | 3.03 | 0.36 | 0.33 | 0.31 |
| 12 | 5.03 | 0.94 | 3.28 | 0.36 | 0.36 | 0.29 |
| 13 | 4.96 | 1.13 | 3.16 | 0.29 | 0.35 | 0.36 |
| Average | 5.82 | 1.01 | 3.32 | 0.35 | 0.35 | 0.30 |
| Std | 1.04 | 0.05 | 0.14 | 0.02 | 0.01 | 0.02 |

Ternary diagram displaying FeO: 1/3 K2O: CaO Wt % of sum, Pakihikura Tephra (T4).

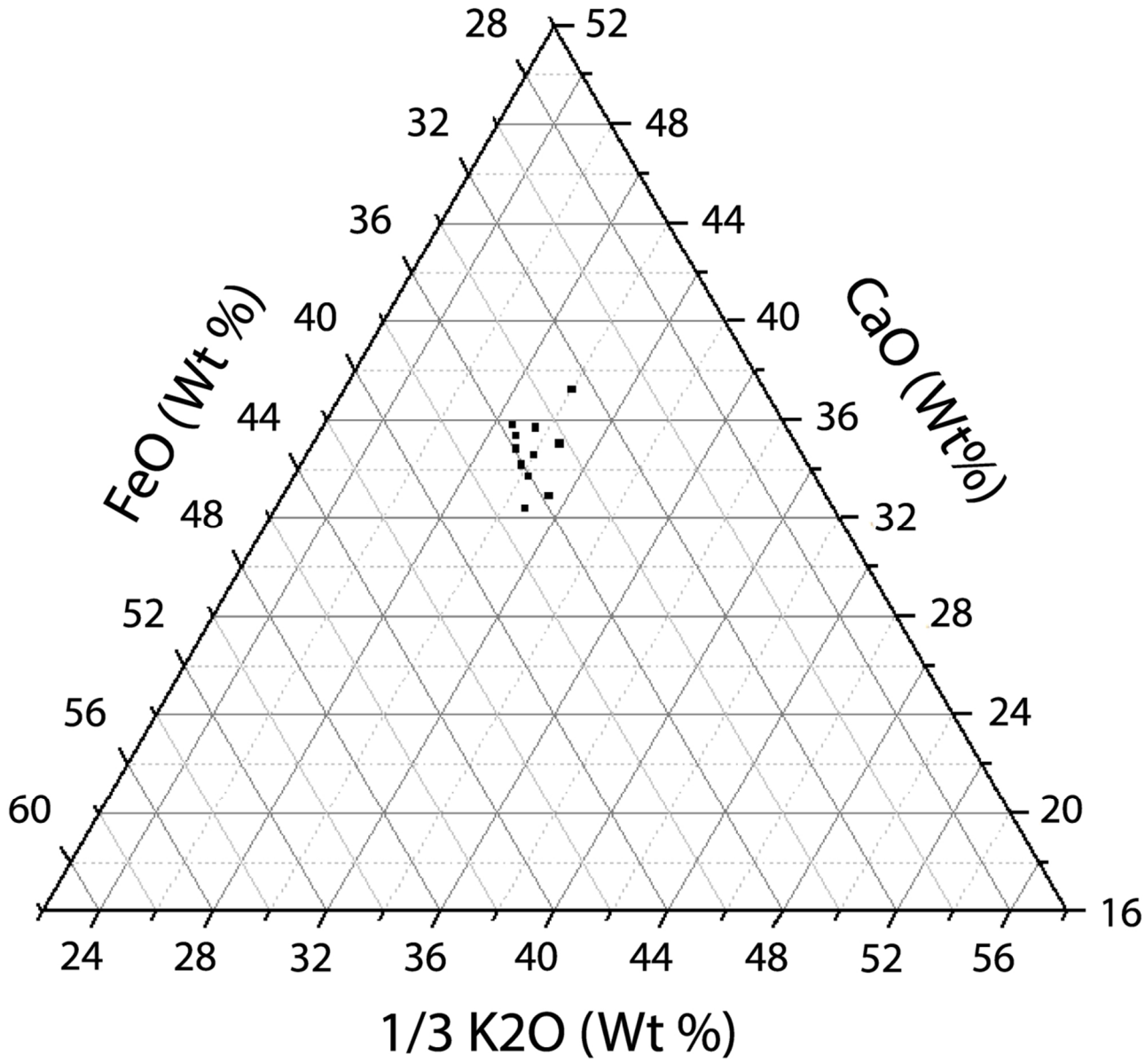


▪ Pakihikura Tephra

Grain size distribution frequency (%) graph showing grain size distribution of Pakihikura Tephra (T4) Bms Member, Takapari Formation.

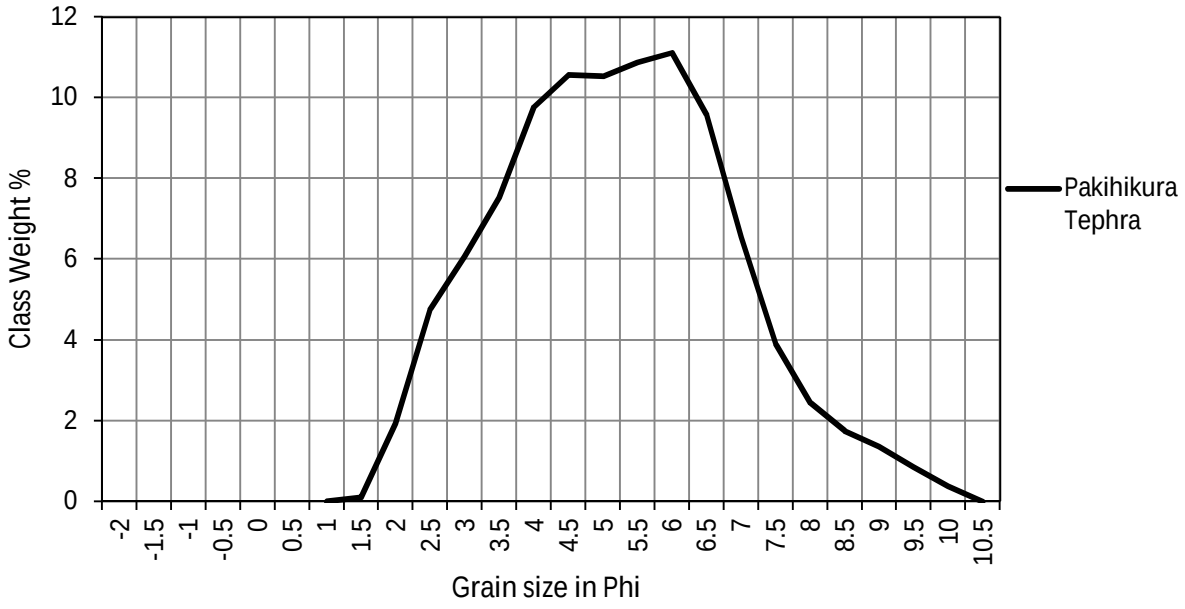


Grain size data from Pakihikura Tephra – T4

| Grain size in microns | Grain size in Phi | Class weight % |
|---|---|---|
| 500 | 1.0 | 0.00 |
| 353.553 | 1.5 | 0.09 |
| 250 | 2.0 | 1.93 |
| 176.777 | 2.5 | 4.75 |
| 125 | 3.0 | 6.07 |
| 88.388 | 3.5 | 7.52 |
| 62.5 | 4.0 | 9.77 |
| 44.194 | 4.5 | 10.55 |
| 31.25 | 5.0 | 10.53 |
| 22.097 | 5.5 | 10.88 |
| 15.625 | 6.0 | 11.11 |
| 11.049 | 6.5 | 9.58 |
| 7.813 | 7.0 | 6.55 |
| 5.524 | 7.5 | 3.89 |
| 3.906 | 8.0 | 2.44 |
| 2.762 | 8.5 | 1.75 |
| 1.953 | 9.0 | 1.37 |

| | | |
|---|---|---|
| 1.381 | 9.5 | 0.85 |
| 0.977 | 10.0 | 0.38 |

Histogram displaying the grain size distribution of Pakihikura Tephra (T4)

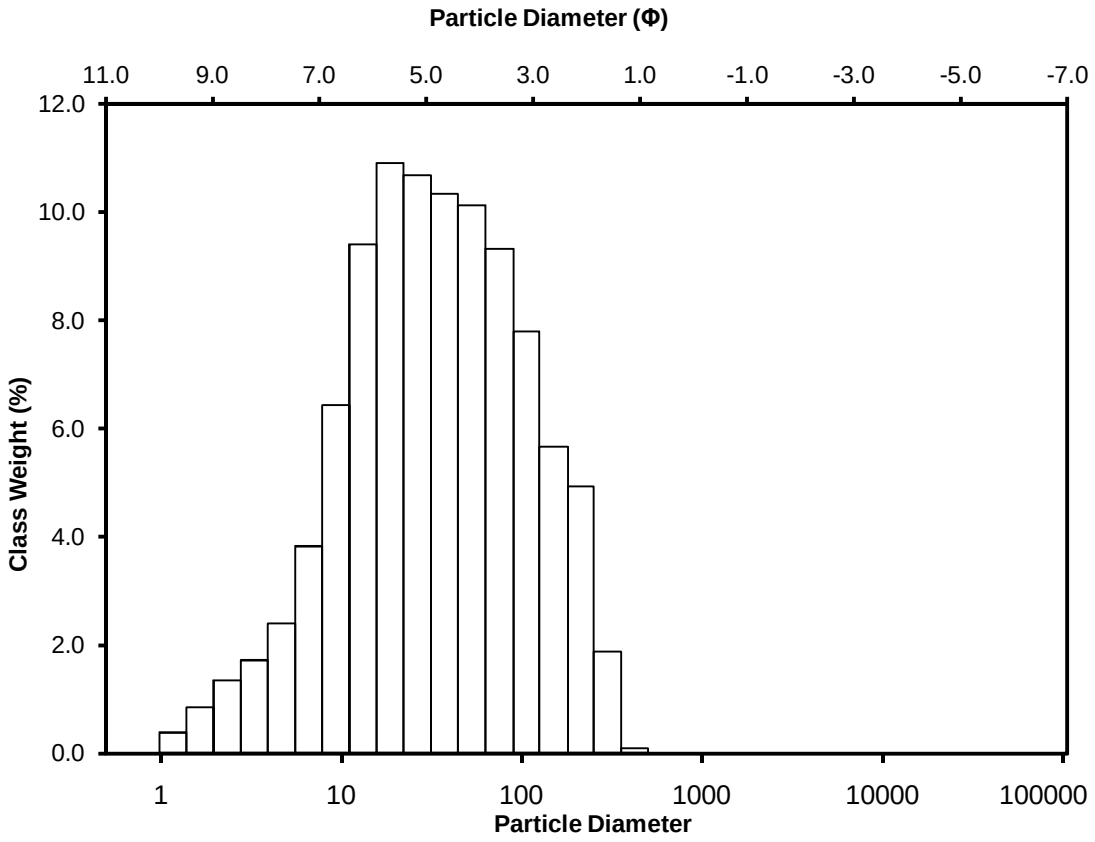


| Pakihikura Tephra T4 sample statistics: | | | |
|---|---|---|---|
| | Geometric μm | Logarithmic ϕ | Description |
| Mean | 33.22 | 4.912 | Fine Grained Tephra |
| Sorting | 3.232 | 1.692 | Poorly Sorted |
| Skewness | -0.015 | 0.012 | Symmetrical |
| Kurtosis | 0.961 | 0.961 | Mesokurtic |

# Appendix 2: Grain size data

## 2.1 Modern day Pohangina River sand grain size data:

| Grain size in Microns | Grain size in Phi | Class weight % |
|---|---|---|
| 707.107 | 0.5 | 0.03 |
| 500 | 1 | 0.09 |
| 353.553 | 1.5 | 0.49 |
| 250 | 2 | 4.49 |
| 176.777 | 2.5 | 51.83 |
| 125 | 3 | 31.69 |
| 88.388 | 3.5 | 7.19 |
| 62.5 | 4 | 0.04 |
| 44.194 | 4.5 | 3.73 |

Graph contrasting modern day Pohangina River sand with Css Member, Takapari Formation. Css Member is a fluvially deposited pumiceous sand of Castlecliffian age.

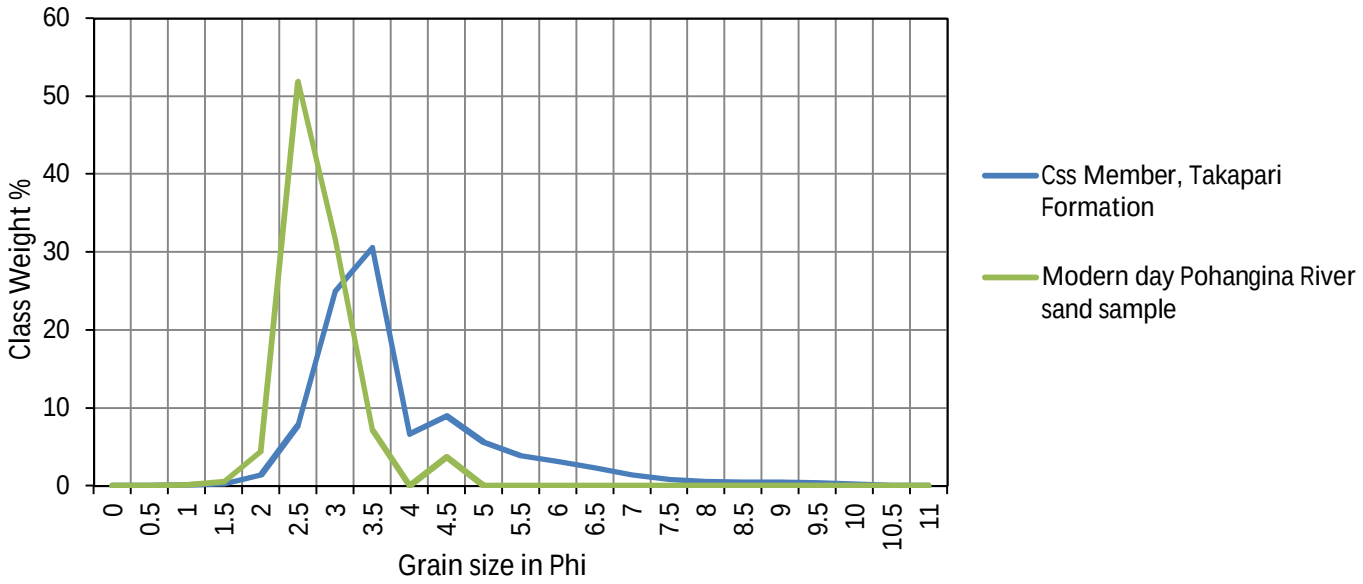

Since deforestation has occurred in the Pohangina Valley approximately 100 years ago, erosion and sedimentation rates have increased dramatically. Notice how the sand in the modern day river is of a coarser grain size than in Css Member. This is a function of the difference in provenance, with the modern day river deriving a majority of its sediment from the nearby Torlesse greywacke and Plio-Pleistocene sediments of the Ruahine Range. While the paleo-river system responsible for the deposition of Css Member was deriving sediment from volcanics in the Central North Island and uplifted basement in the Kaimanawa, Kaweka and proto-Ruahine Ranges.

Cumulative frequency (%) graph showing grain size distribution of modern day Pohangina River sand sample

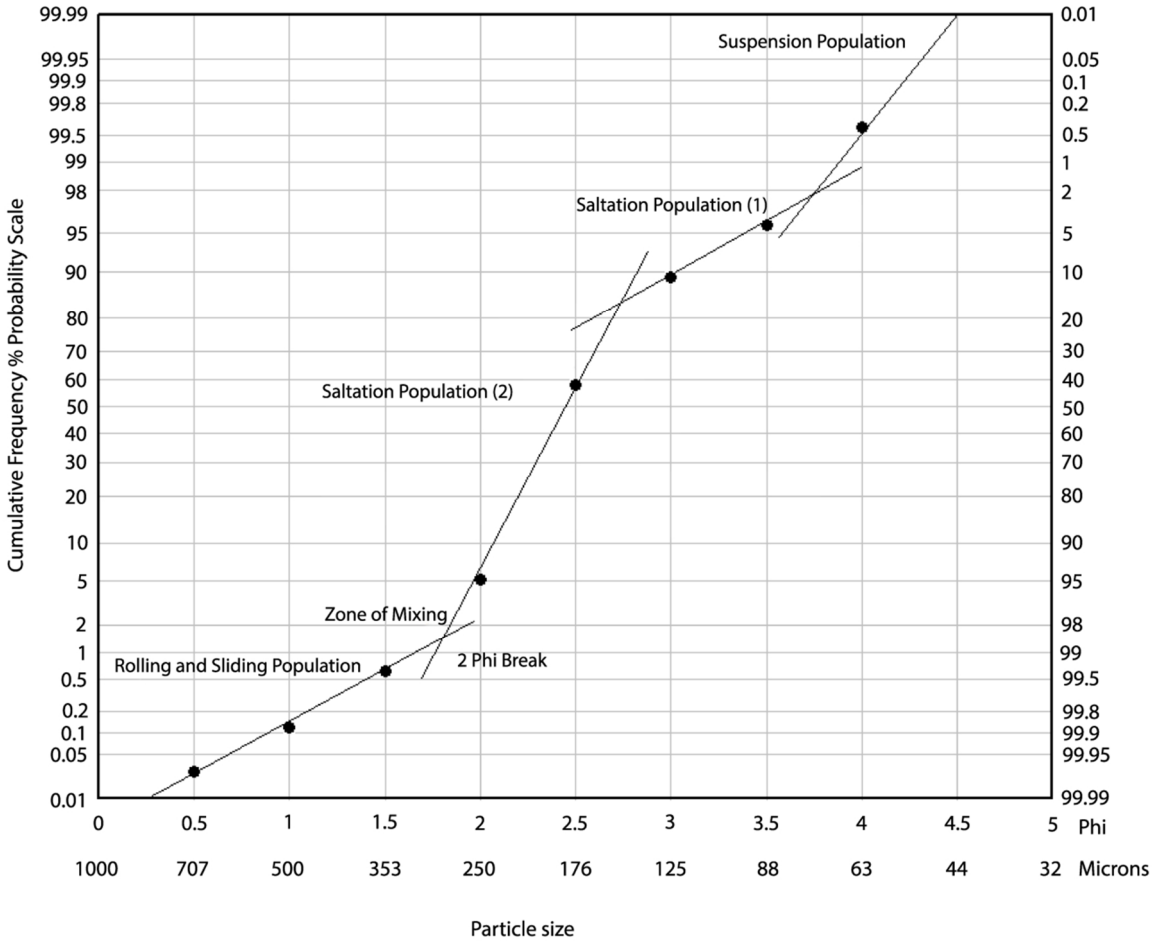

2.2: eQk Member, Kai Iwi Group, grain size data:

Grain size distribution frequency (%) graph showing grain size distribution of eQk Member, Kai Iwi Group

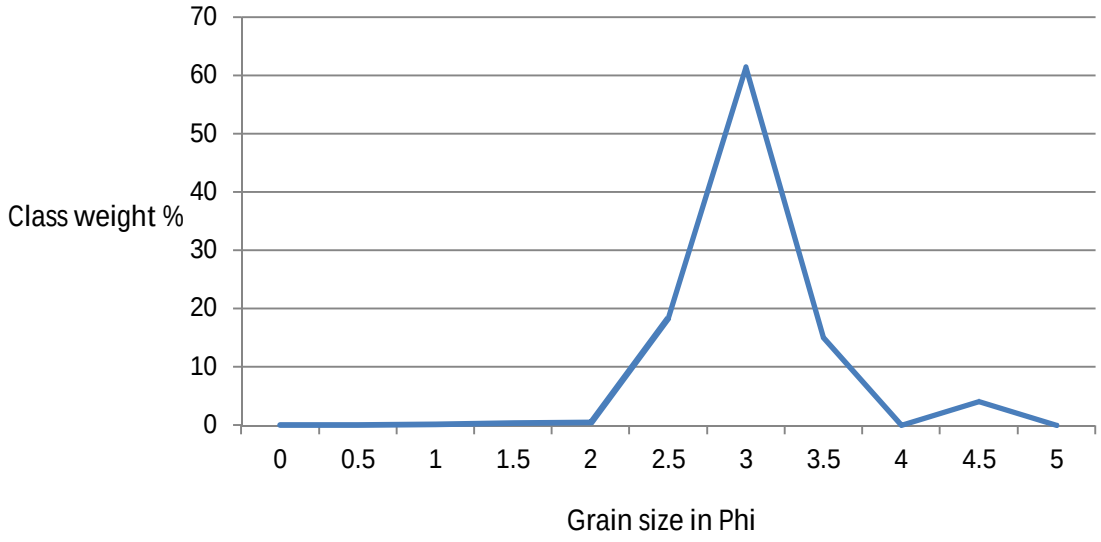


| Grain size in Microns | Grain size in Phi | Class weight % |
|---|---|---|
| 707.107 | 0.5 | 0.02 |
| 500 | 1 | 0.12 |
| 353.553 | 1.5 | 0.32 |
| 250 | 2 | 0.47 |
| 176.777 | 2.5 | 18.52 |
| 125 | 3 | 61.39 |
| 88.388 | 3.5 | 15.07 |
| 62.5 | 4 | 0.01 |
| 44.194 | 4.5 | 4.06 |

Cumulative frequency (%) graph showing grain size distribution of eQk Member, Kai Iwi Group

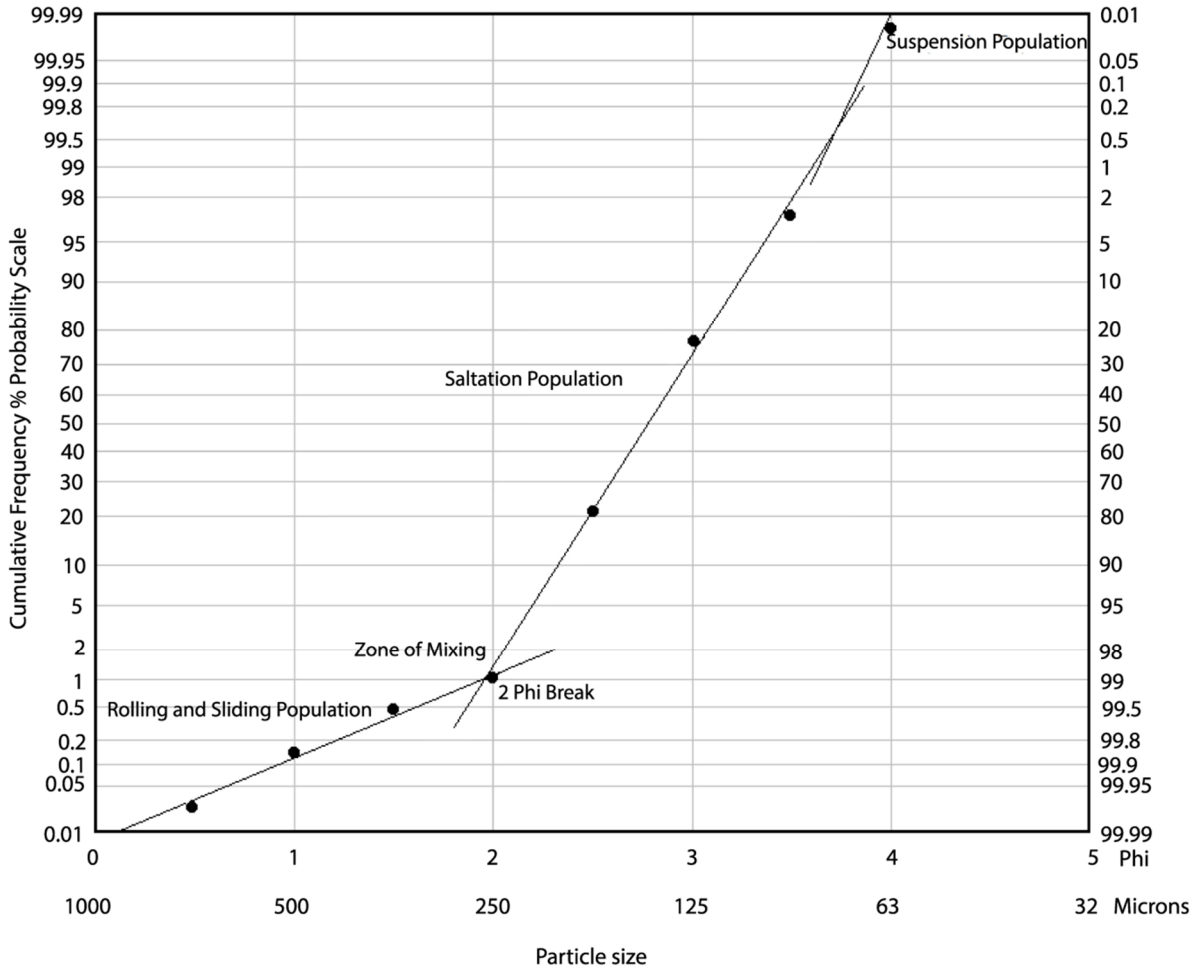


| eQk Member, Kai-iwi Group, grain size sample statistics: | | | |
|---|---|---|---|
| | Geometric µm | Logarithmic Φ | Description |
| Mean | 154.5 | 2.695 | Fine Sand |
| Sorting | 1.268 | 0.343 | Very Well Sorted |
| Skewness | 0.061 | -0.061 | Symmetrical |
| Kurtosis | 1.221 | 1.221 | Leptokurtic |

2.3 Css Member, Takapari Formation grain size data:

Grain size distribution frequency (%) graph showing grain size distribution of Css Member, Takapari Formation

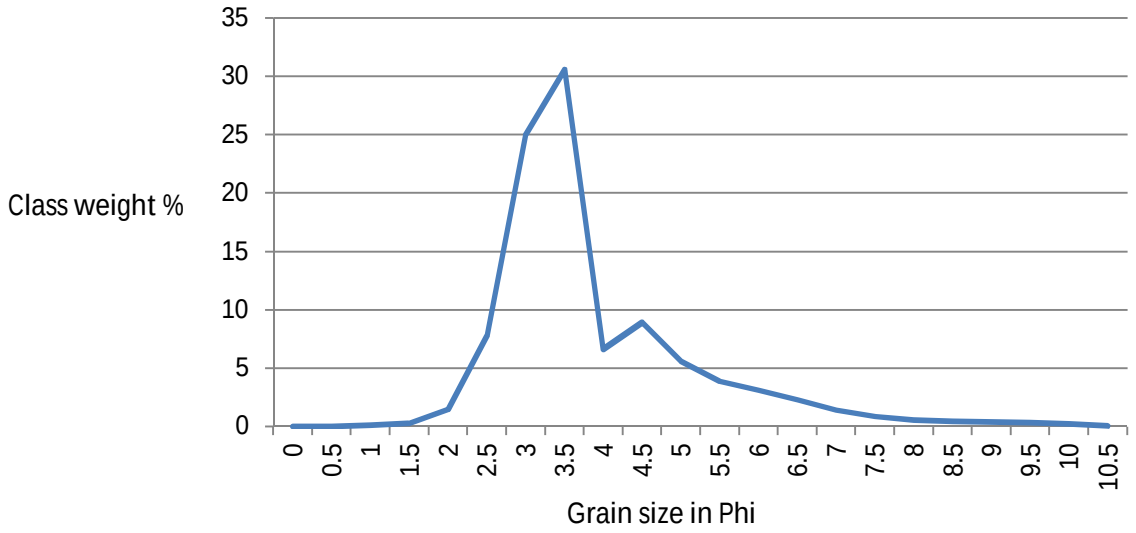


| Grain size in Microns | Grain size in Phi | Class weight % |
|---|---|---|
| 707.107 | 0.5 | 0.01 |
| 500 | 1 | 0.10 |
| 353.553 | 1.5 | 0.25 |
| 250 | 2 | 1.45 |
| 176.777 | 2.5 | 7.82 |
| 125 | 3 | 25.00 |
| 88.388 | 3.5 | 30.60 |
| 62.5 | 4 | 6.66 |
| 44.194 | 4.5 | 8.96 |
| 31.25 | 5 | 5.58 |
| 22.097 | 5.5 | 3.91 |
| 15.625 | 6 | 3.13 |
| 11.049 | 6.5 | 2.29 |
| 7.813 | 7 | 1.44 |
| 5.524 | 7.5 | 0.84 |
| 3.906 | 8 | 0.55 |
| 2.762 | 8.5 | 0.44 |

| | | |
|---|---|---|
| 1.953 | 9 | 0.39 |
| 1.381 | 9.5 | 0.32 |
| 0.977 | 10 | 0.22 |
| 0.691 | 10.5 | 0.04 |

| Css Member, Takapari Formation, grain size sample statistics: | | | |
|---|---|---|---|
| | Geometric µm | Logarithmic Φ | Description |
| Mean | 85.78 | 3.543 | Very Fine Sand |
| Sorting | 2.252 | 1.171 | Poorly Sorted |
| Skewness | -0.458 | 0.458 | Very Fine Skewed |
| Kurtosis | 1.240 | 1.240 | Leptokurtic |

Cumulative frequency (%) graph showing grain size distribution of Css Member, Takapari Formation

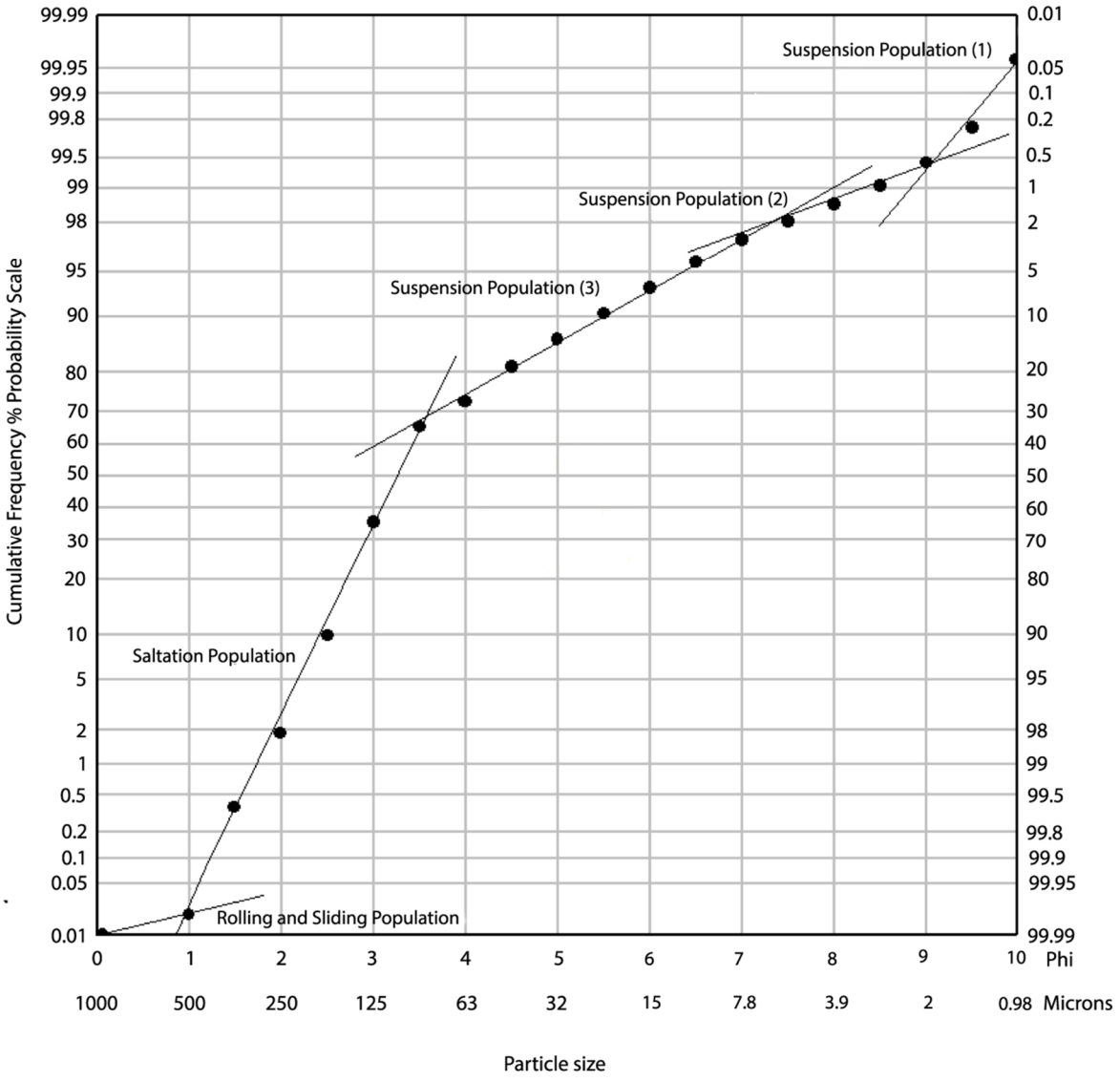

2.4 Bms Member, Takapari Formation grain size data:

Grain size distribution frequency (%) graph showing grain size distribution of Css Member, Takapari Formation

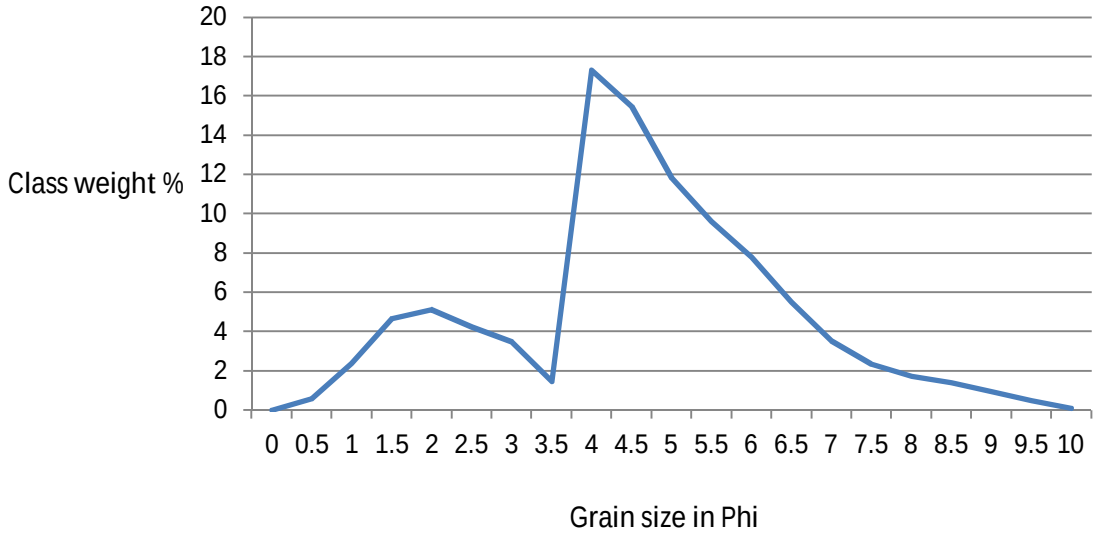


Histogram showing grain size distribution of the Bms Member

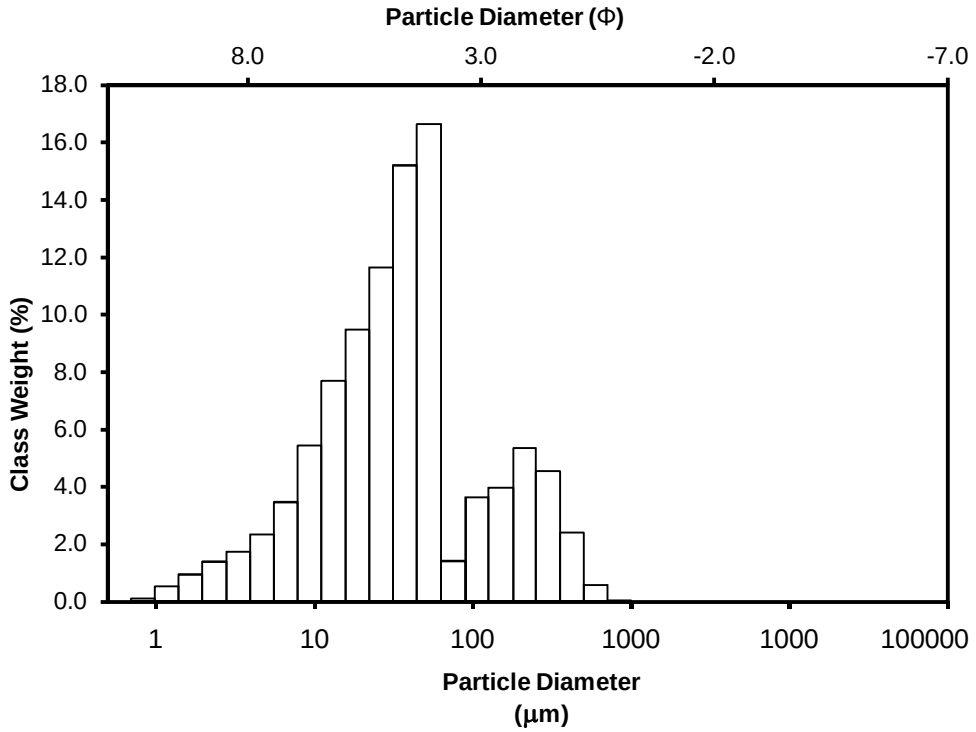

Cumulative frequency (%) graph showing grain size distribution of Bms Member, Takapari Formation

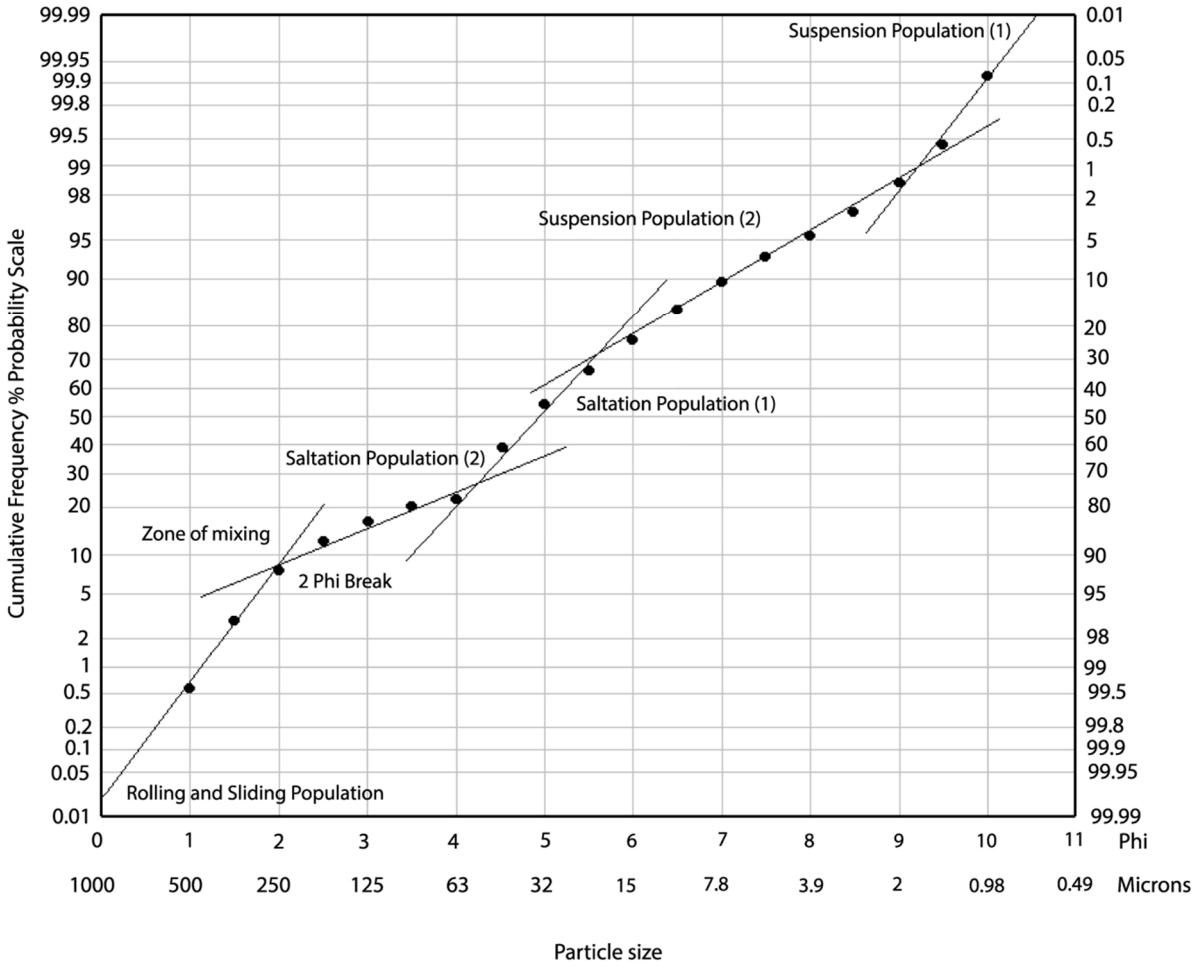


| Grain size in Microns | Grain size in Phi | Class weight % |
|---|---|---|
| 707.107 | 0.5 | 0.00 |
| 500 | 1 | 0.57 |
| 353.553 | 1.5 | 2.39 |
| 250 | 2 | 4.66 |
| 176.777 | 2.5 | 5.13 |
| 125 | 3 | 4.22 |
| 88.388 | 3.5 | 3.49 |
| 62.5 | 4 | 1.45 |
| 44.194 | 4.5 | 17.32 |
| 31.25 | 5 | 15.46 |
| 22.097 | 5.5 | 11.84 |
| 15.625 | 6 | 9.63 |
| 11.049 | 6.5 | 7.80 |
| 7.813 | 7 | 5.51 |

| | | |
|---|---|---|
| 5.524 | 7.5 | 3.51 |
| 3.906 | 8 | 2.35 |
| 2.762 | 8.5 | 1.74 |
| 1.953 | 9 | 1.39 |
| 1.381 | 9.5 | 0.93 |
| 0.977 | 10 | 0.50 |
| 0.691 | 10.5 | 0.08 |

| Bms Member sample statistics: | | | |
|---|---|---|---|
| | Geometric μm | Logarithmic ϕ | Description |
| Mean | 85.78 | 3.543 | Very Fine Sand |
| Sorting | 2.252 | 1.171 | Poorly Sorted |
| Skewness | -0.458 | 0.458 | Very Fine Skewed |
| Kurtosis | 1.240 | 1.240 | Leptokurtic |

2.5 Kss Member, Konewa Formation grain size data:

Grain size distribution frequency (%) graph showing grain size distribution of Kss Member, Konewa Formation

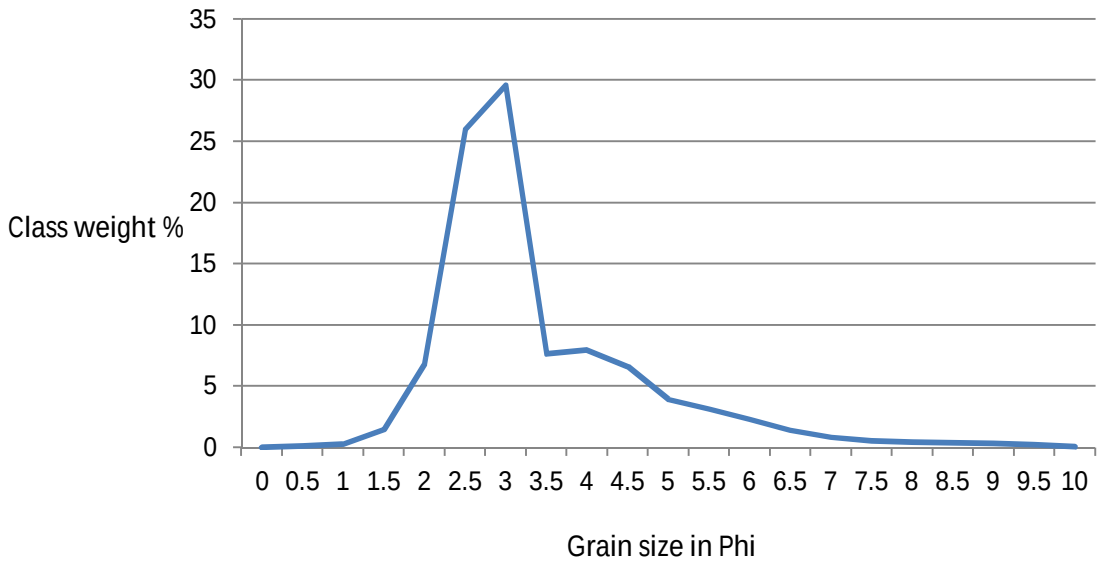


| Grain size in Microns | Grain size in Phi | Class weight % |
|---|---|---|
| 707.107 | 0.5 | 0.01 |
| 500 | 1 | 0.10 |
| 353.553 | 1.5 | 0.25 |
| 250 | 2 | 1.45 |
| 176.777 | 2.5 | 6.82 |
| 125 | 3 | 26.00 |
| 88.388 | 3.5 | 29.60 |
| 62.5 | 4 | 7.66 |
| 44.194 | 4.5 | 7.96 |
| 31.25 | 5 | 6.58 |
| 22.097 | 5.5 | 3.91 |
| 15.625 | 6 | 3.13 |
| 11.049 | 6.5 | 2.29 |
| 7.813 | 7 | 1.44 |
| 5.524 | 7.5 | 0.84 |
| 3.906 | 8 | 0.55 |
| 2.762 | 8.5 | 0.44 |
| 1.953 | 2709 | 0.39 |

| | | |
|---|---|---|
| 1.381 | 9.5 | 0.32 |
| 0.977 | 10 | 0.22 |
| 0.691 | 10.5 | 0.04 |

Cumulative frequency (%) graph showing grain size distribution of Kss Member, Konewa Formation

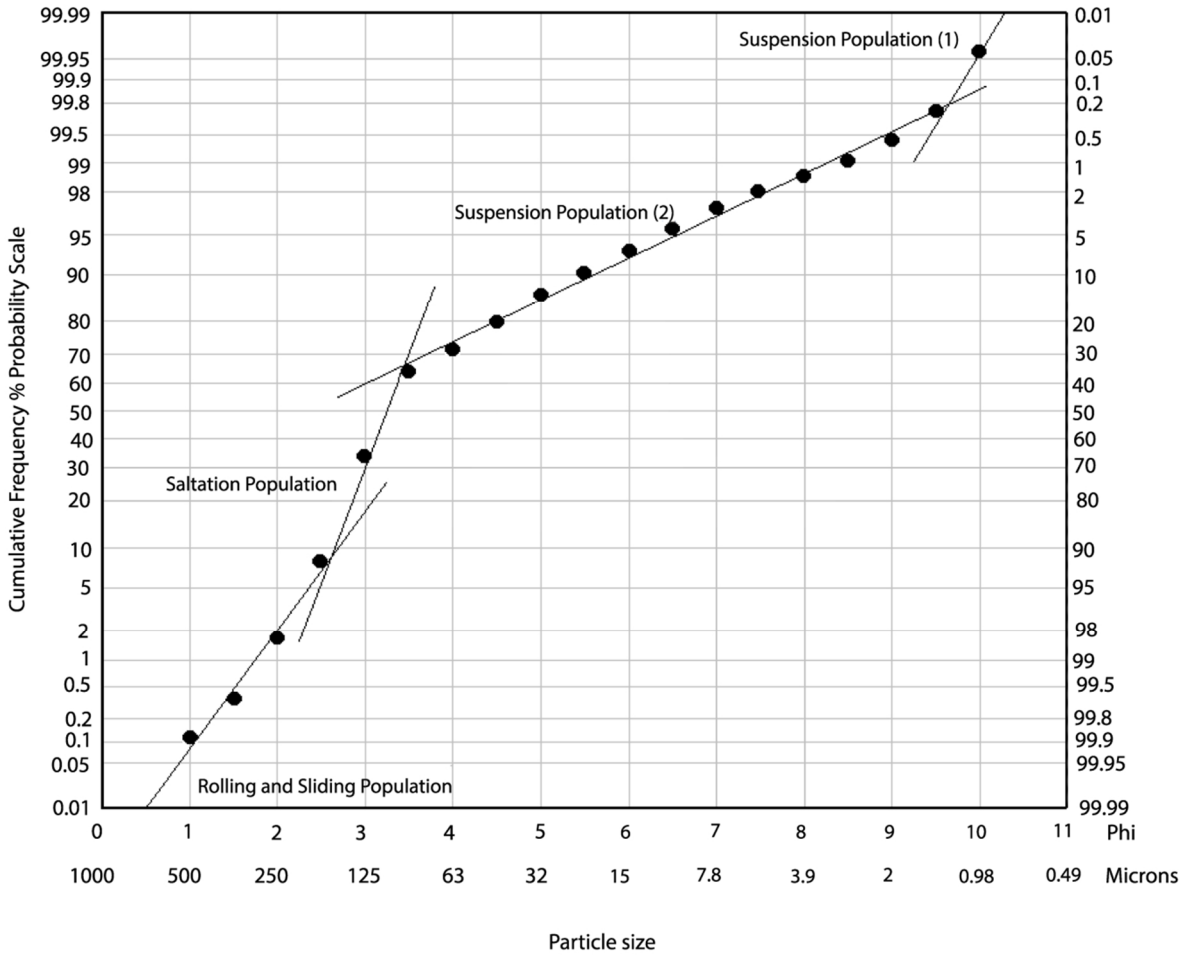

2.6 Kst Member, Konewa Formation grain size data:

Grain size distribution frequency (%) graph showing grain size distribution of Kst Member, Konewa Formation

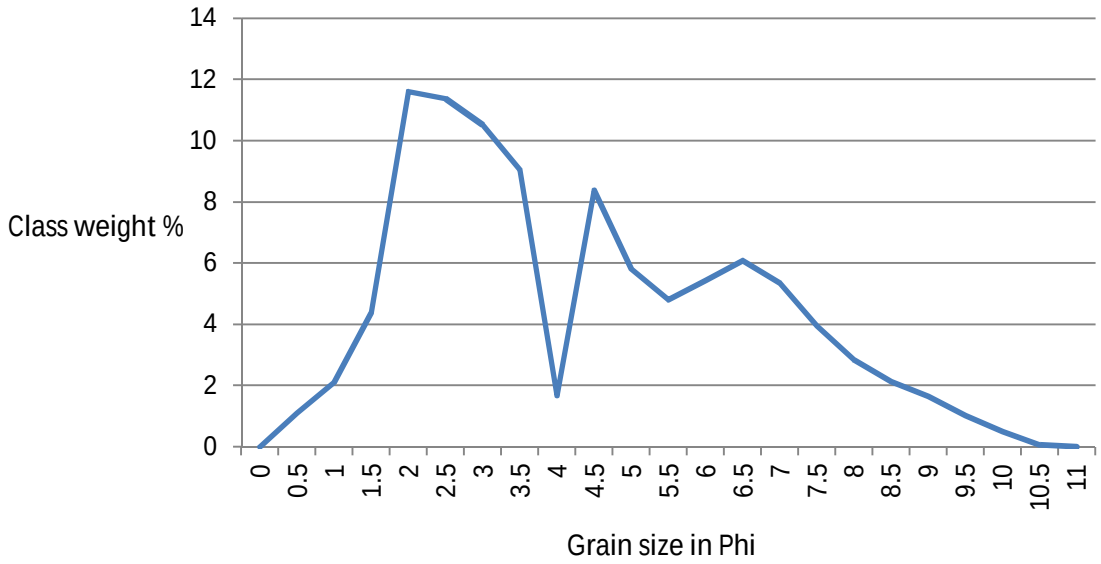


Histogram showing grain size distribution of Kst Member, Konewa Formation, Scrimmys Stream, Broadlands Station, Pohangina.

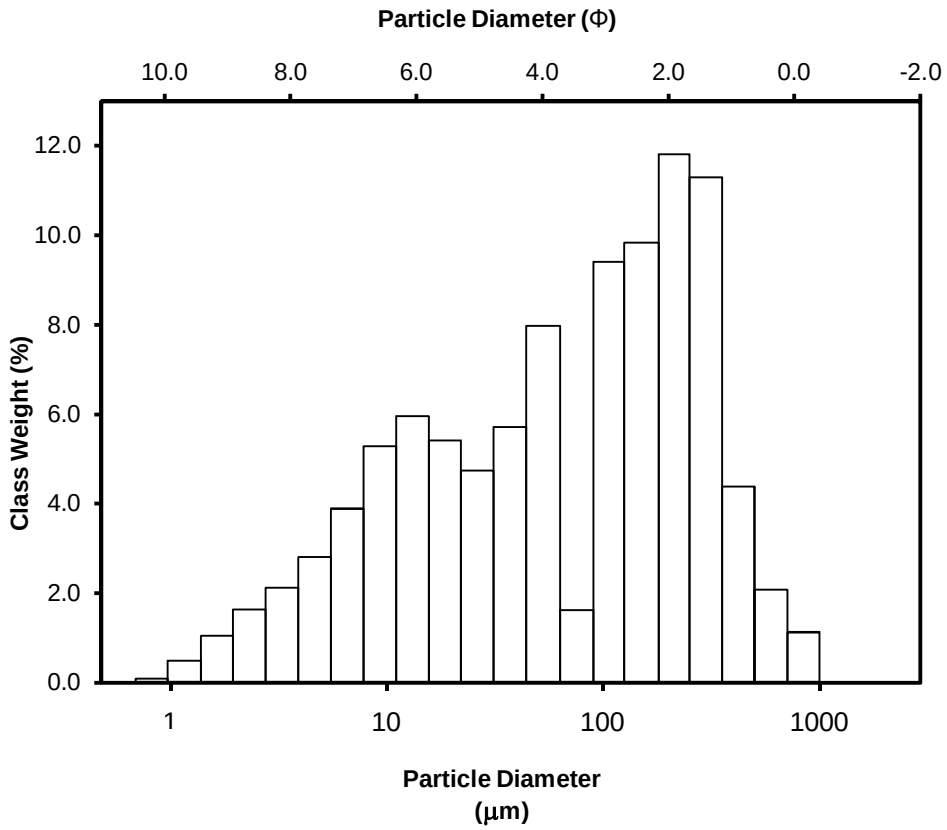

Cumulative frequency (%) graph showing grain size distribution of Kst Member, Konewa Formation

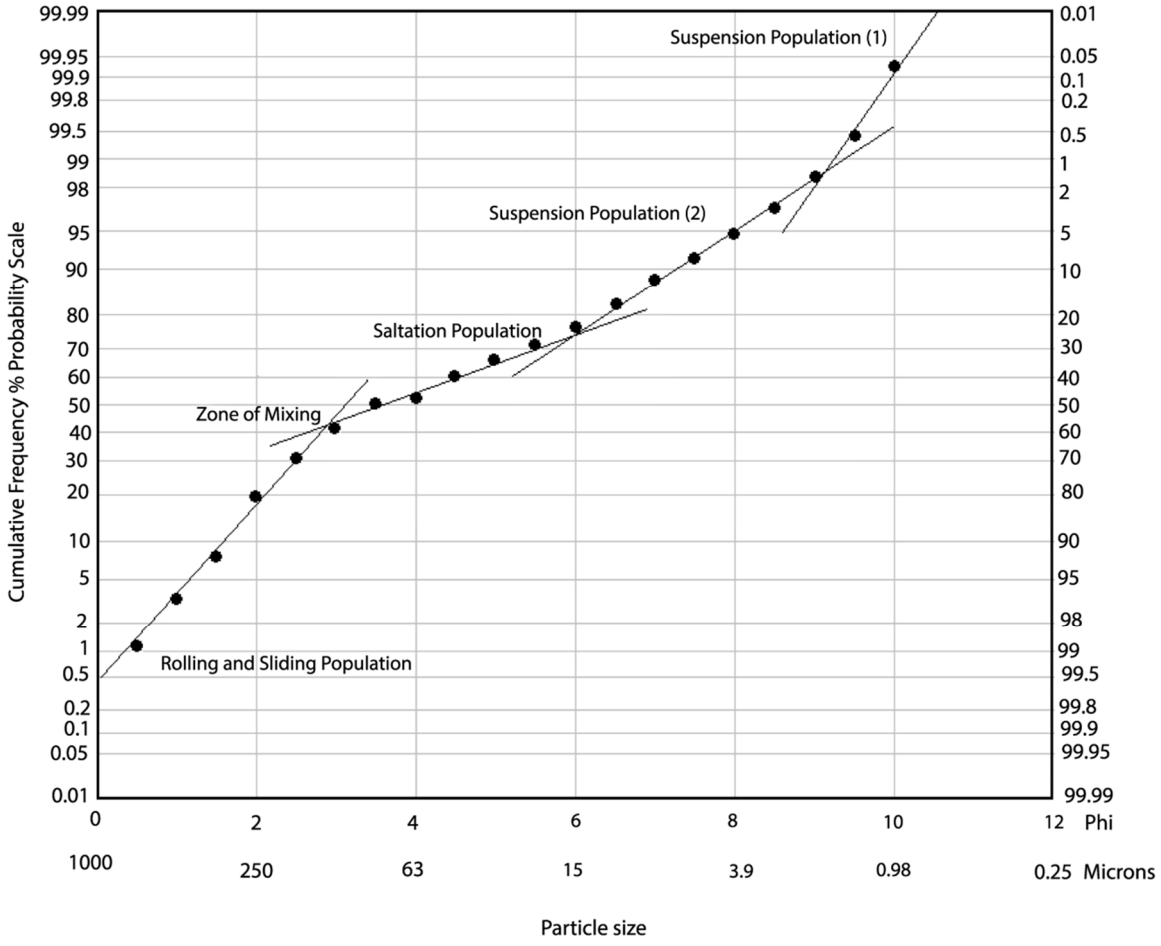


| Grain size in Microns | Grain size in Phi | Class weight % |
|---|---|---|
| 707.107 | 0.5 | 1.12 |
| 500 | 1 | 2.12 |
| 353.553 | 1.5 | 4.39 |
| 250 | 2 | 11.62 |
| 176.777 | 2.5 | 11.39 |
| 125 | 3 | 10.52 |
| 88.388 | 3.5 | 9.07 |
| 62.5 | 4 | 1.68 |
| 44.194 | 4.5 | 8.40 |

| | | |
|---|---|---|
| 31.25 | 5 | 5.81 |
| 22.097 | 5.5 | 4.80 |
| 15.625 | 6 | 5.45 |
| 11.049 | 6.5 | 6.10 |
| 7.813 | 7 | 5.36 |
| 5.524 | 7.5 | 3.95 |
| 3.906 | 8 | 2.84 |
| 2.762 | 8.5 | 2.14 |
| 1.953 | 9 | 1.66 |
| 1.381 | 9.5 | 1.03 |
| 0.977 | 10 | 0.49 |
| 0.691 | 10.5 | 0.07 |

Table 6.2: Kst Member, Konewa Formation, grain size statistics:

| | Geometric μm | Logarithmic ϕ | Description |
|---|---|---|---|
| Mean | 62.93 | 3.990 | Very Fine Sand |
| Sorting | 4.734 | 2.243 | Very Poorly Sorted |
| Skewness | -0.337 | 0.337 | Very Fine Skewed |
| Kurtosis | 0.777 | 0.777 | Platykurtic |

2.7 Fss Member, Komako Formation grain size data:

Grain size distribution frequency (%) graph showing grain size distribution of Fss Member, Komako Formation

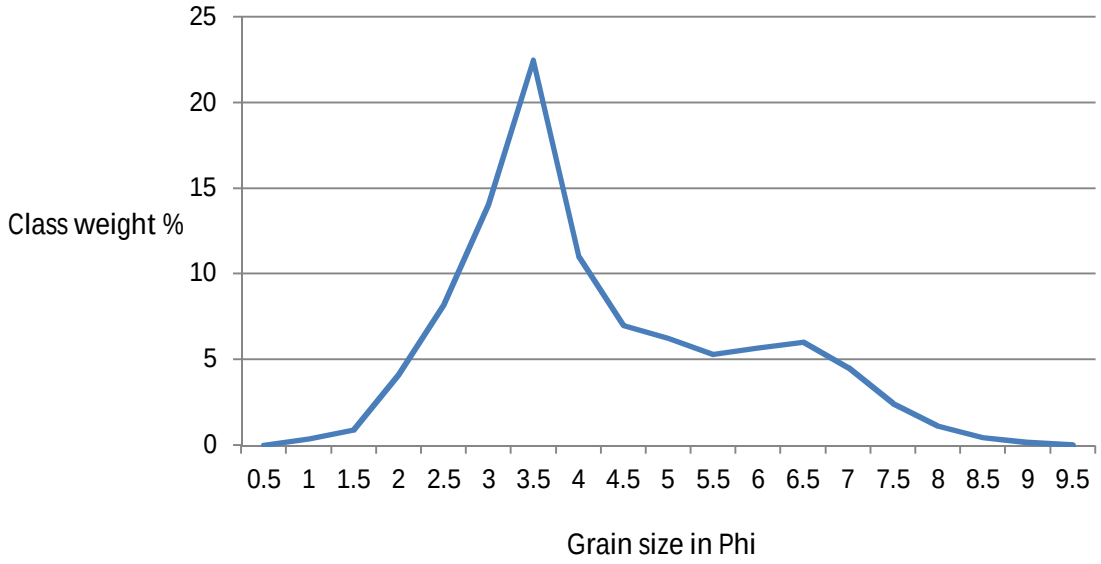


| Grain size in Microns | Grain size in Phi | Class weight % |
|---|---|---|
| 707.107 | 0.5 | 0 |
| 500 | 1 | 0.36 |
| 353.553 | 1.5 | 0.90 |
| 250 | 2 | 4.13 |
| 176.777 | 2.5 | 8.18 |
| 125 | 3 | 14.06 |
| 88.388 | 3.5 | 22.44 |
| 62.5 | 4 | 11.01 |
| 44.194 | 4.5 | 6.98 |
| 31.25 | 5 | 6.26 |
| 22.097 | 5.5 | 5.32 |
| 15.625 | 6 | 5.68 |
| 11.049 | 6.5 | 6.00 |
| 7.813 | 7 | 4.52 |

| | | | |
|---|---|---|---|
| 5.524 | | 7.5 | 2.44 |
| 3.906 | | 8 | 1.11 |
| 2.762 | | 8.5 | 0.46 |
| 1.953 | 9 | 0.14 | |

| Fss Member, Komako Formation, grain size statistics: | | | |
|---|---|---|---|
| | Geometric μm | Logarithmic ϕ | Description |
| Mean | 63.61 | 3.975 | Very Fine Sand |
| Sorting | 2.994 | 1.582 | Poorly Sorted |
| Skewness | -0.420 | 0.420 | Very Fine Skewed |
| Kurtosis | 0.937 | 0.937 | Mesokurtic |

Cumulative frequency (%) graph showing grain size distribution of Fss Member, Komako Formation

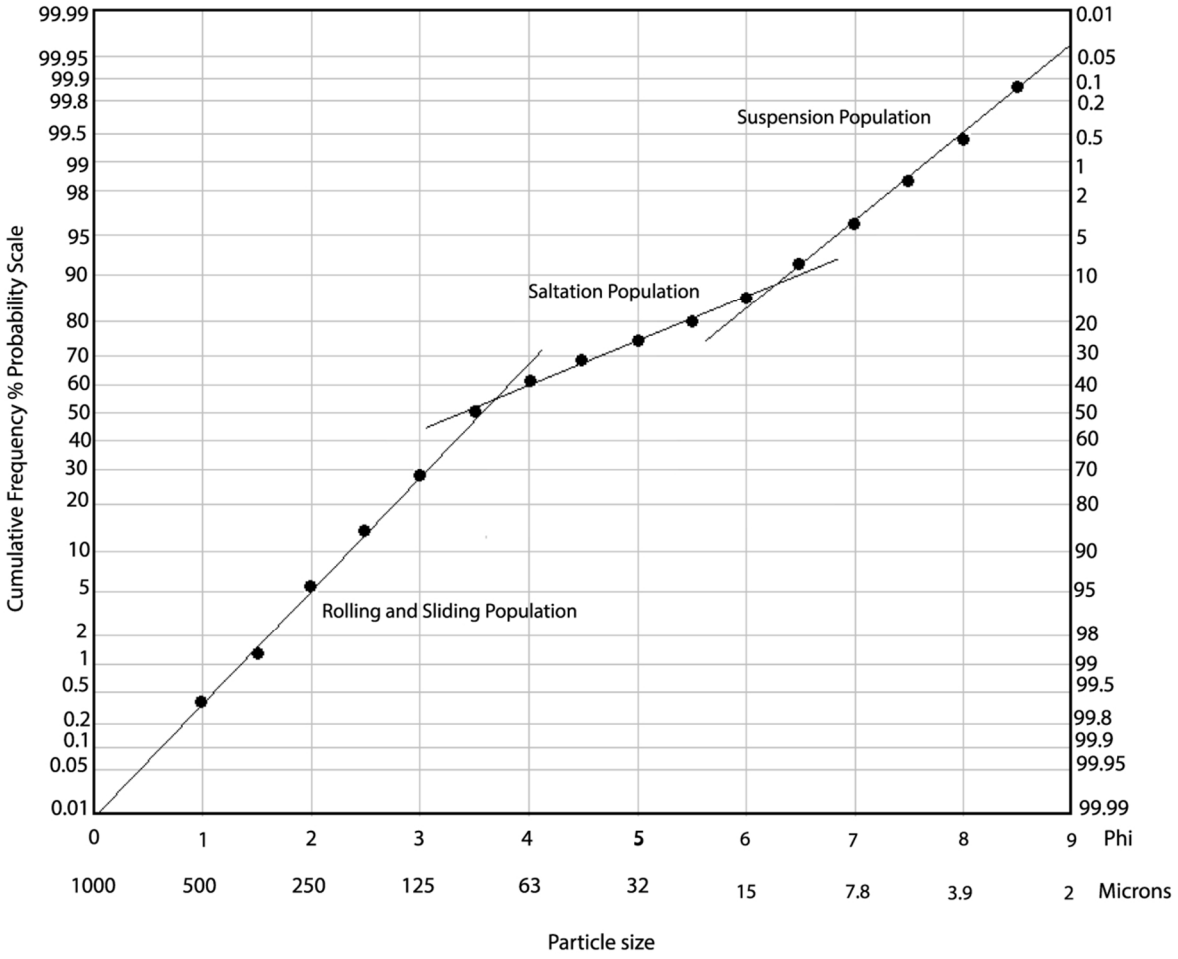

2.8 Fms Member, Komako Formation grain size data:

Grain size distribution frequency (%) graph showing grain size distribution of Fms Member, Komako Formation

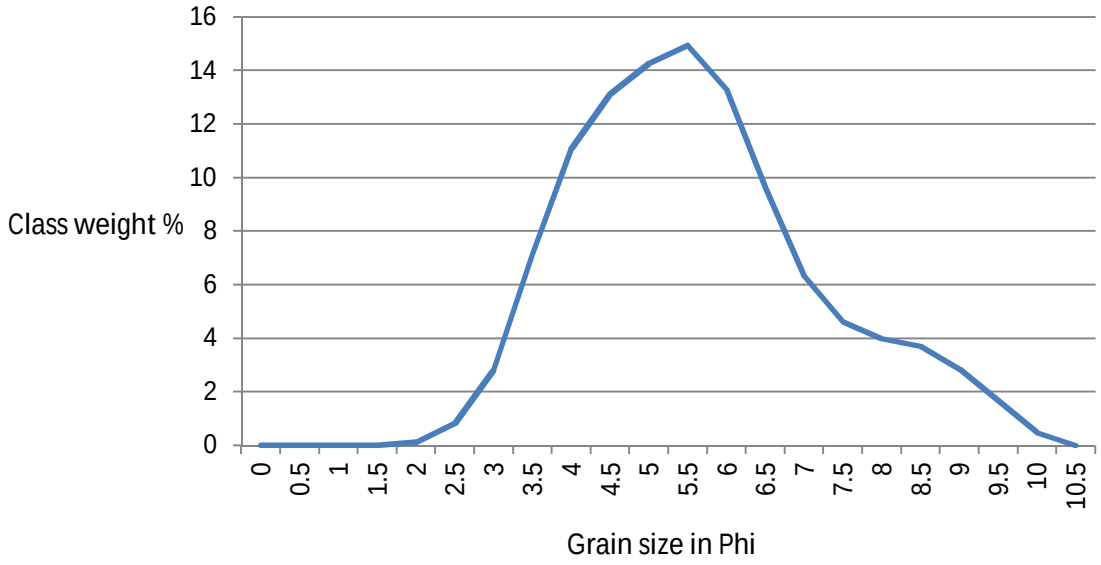


Graph 5.4: Fms Member, Komako Formation, histogram showing grain size distribution

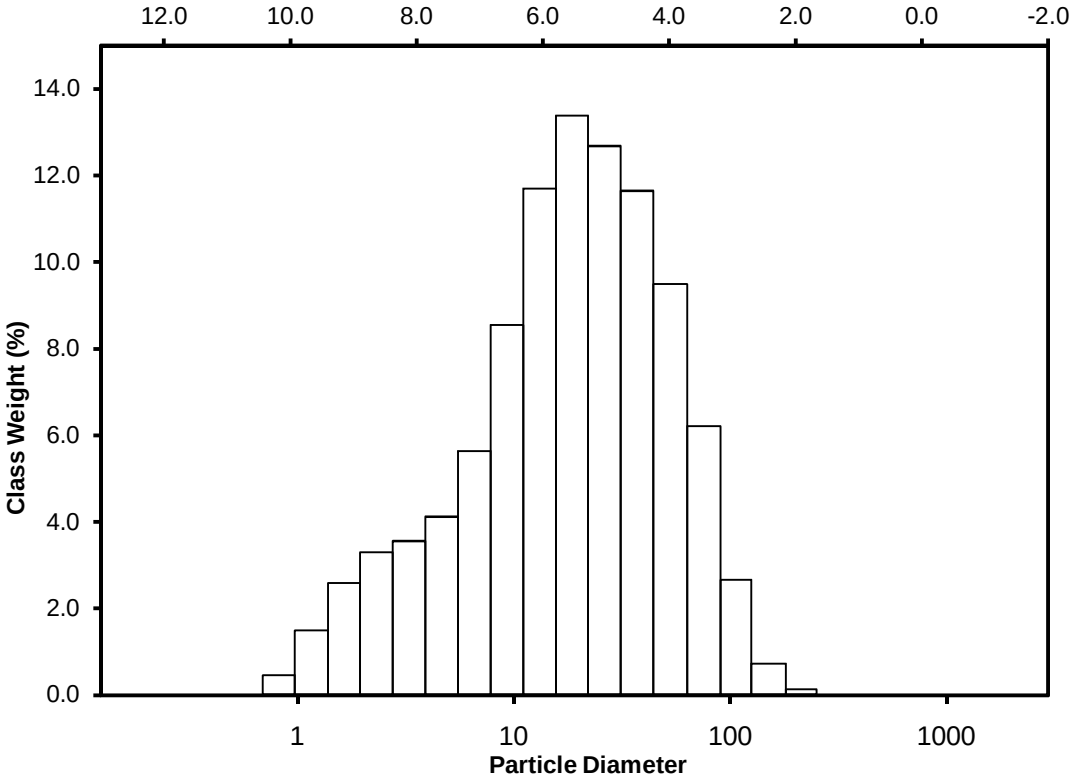

Cumulative frequency (%) graph showing grain size distribution of Fms Member, Komako Formation

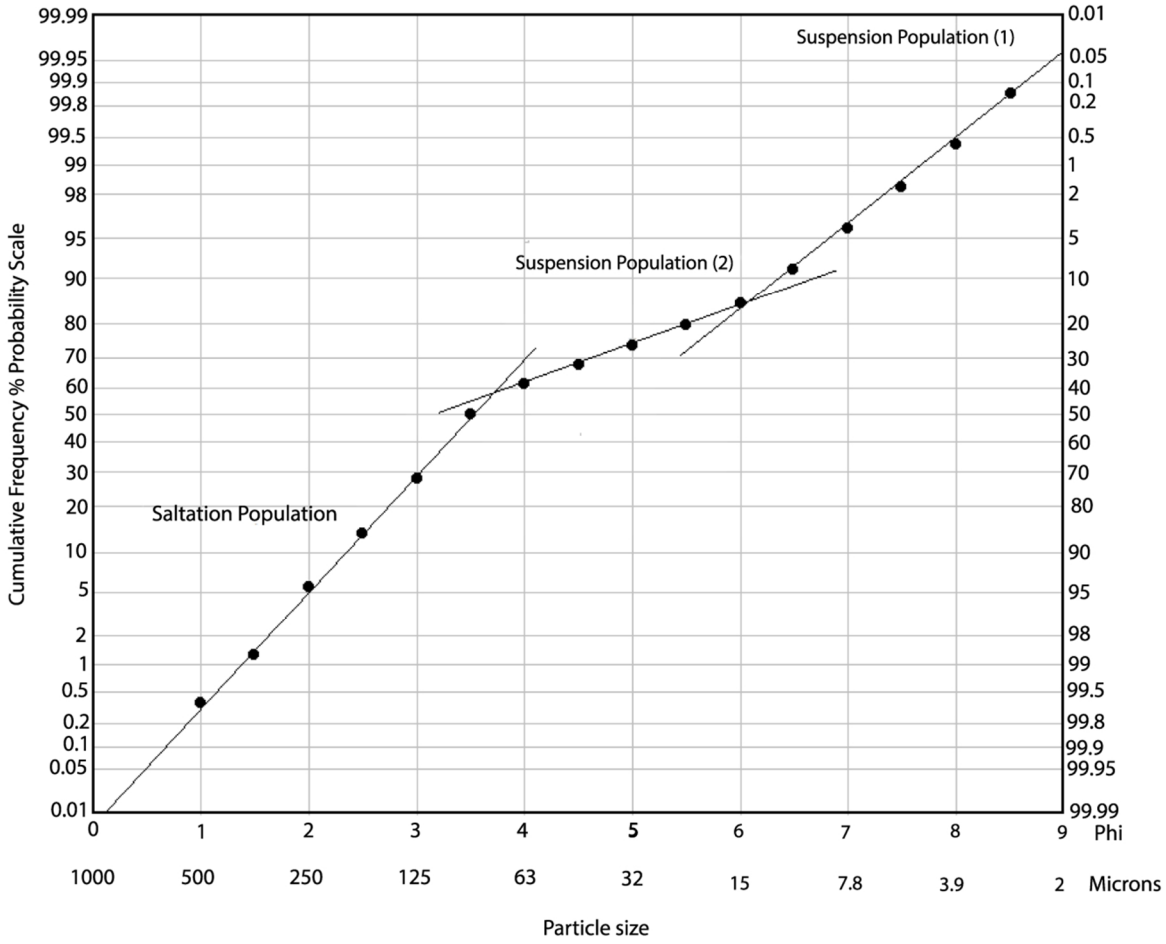


| Grain size in Microns | Grain size in Phi | Class weight % |
|---|---|---|
| 707.107 | 0.5 | 0.00 |
| 500 | 1 | 0.00 |
| 353.553 | 1.5 | 0.00 |
| 250 | 2 | 0.00 |
| 176.777 | 2.5 | 0.00 |
| 125 | 3 | 0.12 |
| 88.388 | 3.5 | 2.10 |
| 62.5 | 4 | 5.01 |
| 44.194 | 4.5 | 7.18 |
| 31.25 | 5 | 11.07 |
| 22.097 | 5.5 | 13.13 |
| 15.625 | 6 | 14.95 |

| | | |
|---|---|---|
| 11.049 | 6.5 | 13.29 |
| 7.813 | 7 | 9.61 |
| 5.524 | 7.5 | 6.34 |
| 3.906 | 8 | 4.62 |
| 2.762 | 8.5 | 3.99 |
| 1.953 | 9 | 3.72 |
| 1.381 | 9.5 | 2.84 |
| 0.977 | 10 | 1.54 |
| 0.691 | 10.5 | 0.48 |

| Fms Member, Komako Formation, grain size statistics: | | | |
|---|---|---|---|
| | Geometric μm | Logarithmic ϕ | Description |
| Mean | 17.59 | 5.829 | Very Coarse Silt |
| Sorting | 3.032 | 1.600 | Poorly Sorted |
| Skewness | -0.163 | 0.163 | Fine Skewed |
| Kurtosis | 1.056 | 1.056 | Mesokurtic |

2.9 Cf Member, Komako Formation grain size data:

Grain size distribution frequency (%) graph showing grain size distribution of Cf Member, Komako Formation

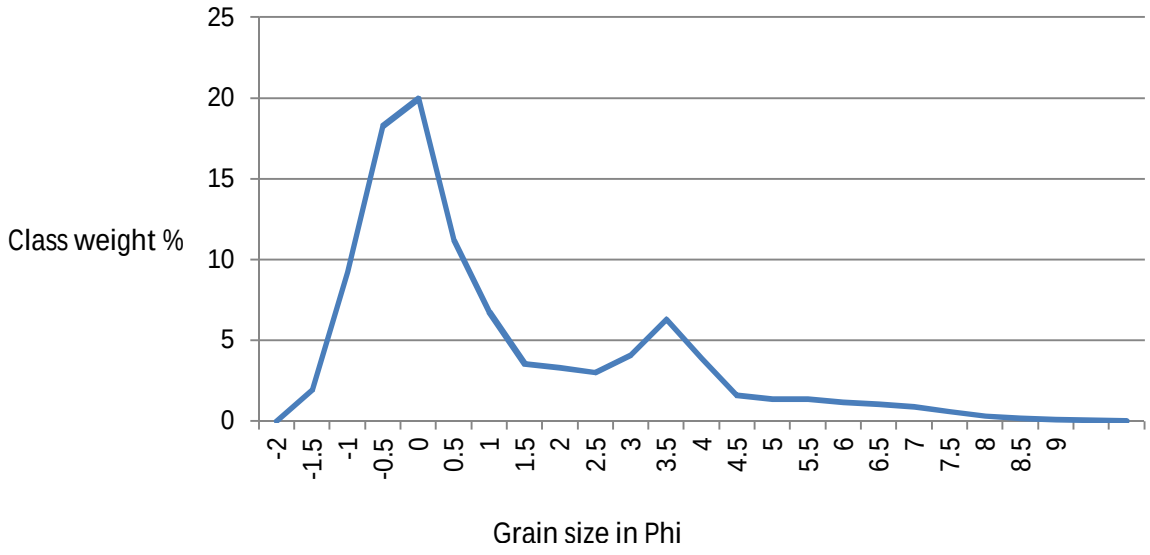


Histogram showing grain size distribution of Cf Member, Komako Formation.

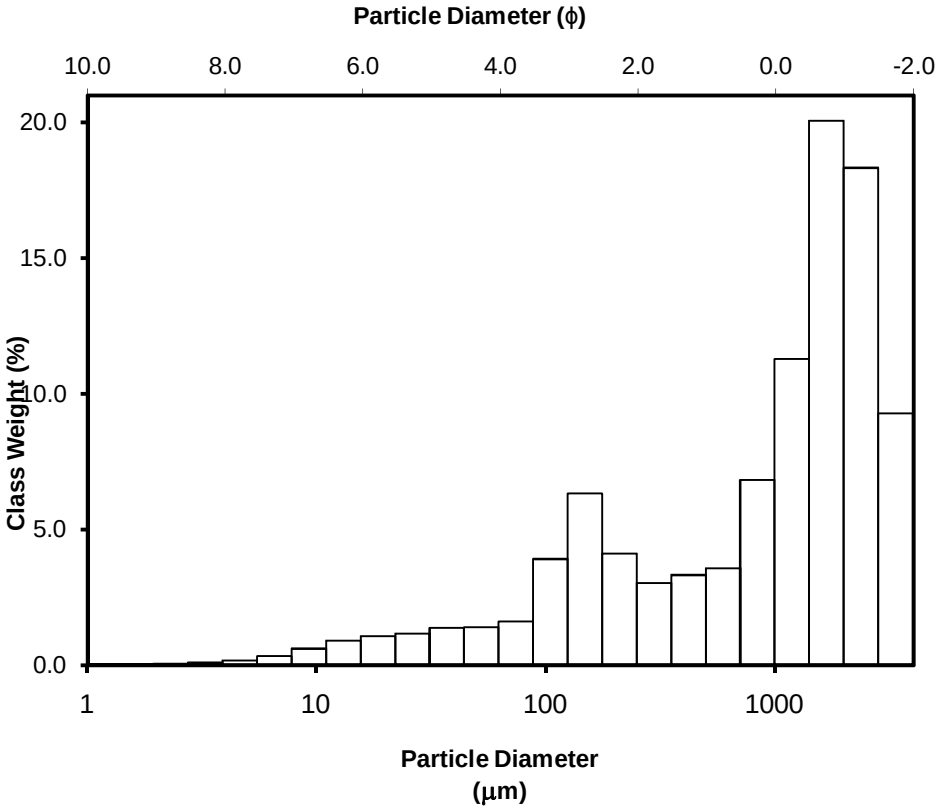

Cumulative frequency (%) graph showing grain size distribution of Cf Member, Komako Formation

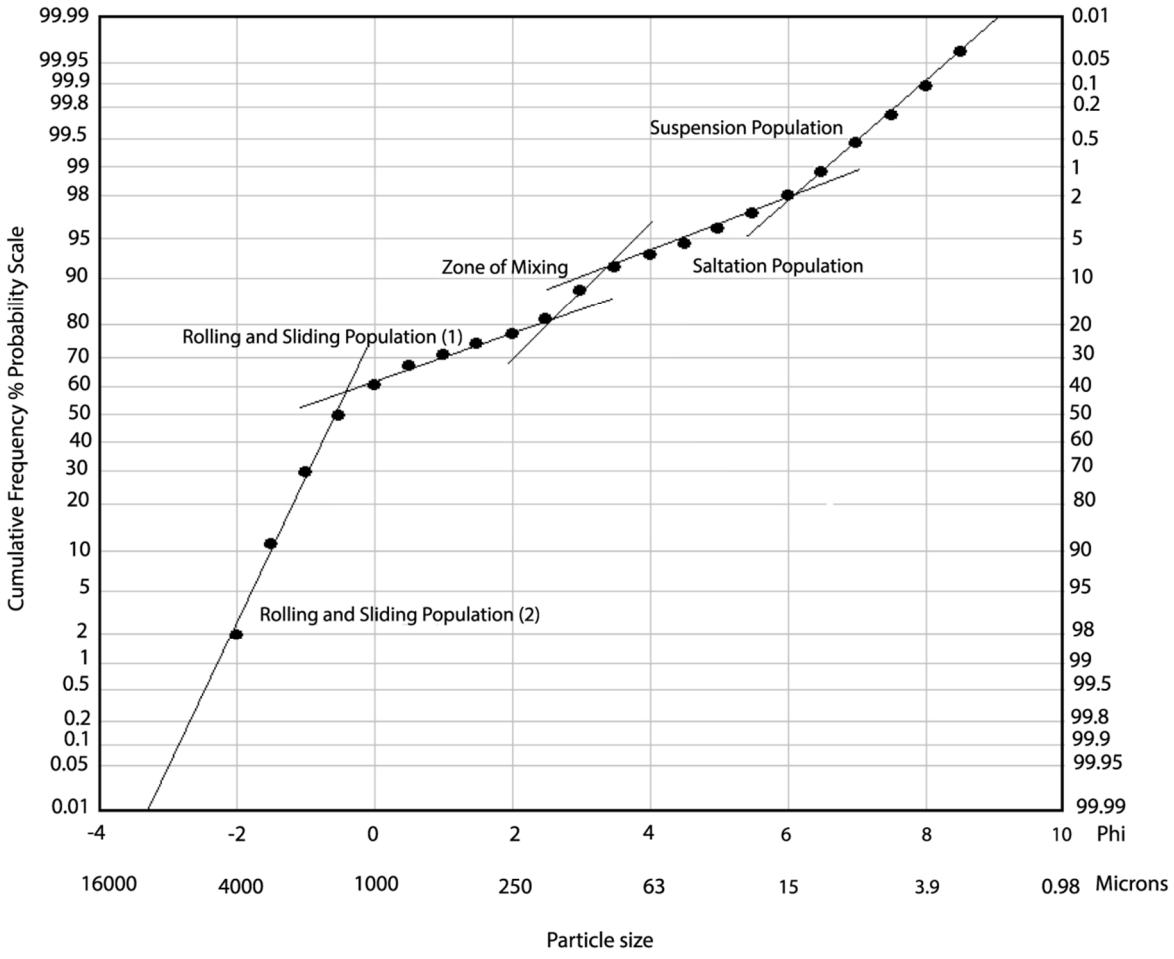


| Grain size in Microns | Grain size in Phi | Class weight % |
|---|---|---|
| 4000 | -2 | 1.93 |
| 2828.427 | -1.5 | 9.24 |
| 2000 | -1 | 18.27 |
| 1414.214 | -0.5 | 20.00 |
| 1000 | 0 | 11.23 |
| 707.107 | 0.5 | 6.79 |
| 500 | 1 | 3.54 |
| 353.553 | 1.5 | 3.29 |
| 250 | 2 | 3.00 |
| 176.777 | 2.5 | 4.08 |
| 125 | 3 | 6.28 |
| 88.388 | 3.5 | 3.88 |
| 62.5 | 4 | 1.58 |

| | | |
|---|---|---|
| 44.194 | 4.5 | 1.36 |
| 31.25 | 5 | 1.34 |
| 22.097 | 5.5 | 1.14 |
| 15.625 | 6 | 1.03 |
| 11.049 | 6.5 | 0.88 |
| 7.813 | 7 | 0.58 |
| 5.524 | 7.5 | 0.30 |
| 3.906 | 8 | 0.15 |
| 2.762 | 8.5 | 0.07 |
| 1.953 | 9 | 0.04 |

| Cf Member, Komako Formation, grain size statistics: | | | |
|---|---|---|---|
| | Geometric μm | Logarithmic ϕ | Description |
| Mean | 818.6 | 0.289 | Coarse Sand |
| Sorting | 4.025 | 2.009 | Very Poorly Sorted |
| Skewness | -0.573 | 0.573 | Very Fine Skewed |
| Kurtosis | 0.977 | 0.977 | Mesokurtic |

# Appendix 3: Clast analysis data

## 3.1 Rc Member, Kai Iwi Group, clast shape data

| Rc Member, Kai Iwi Group, Whareroa Stream section, measurements in mm | | | | | |
|---|---|---|---|---|---|
| | | Axis | | | |
| Clast № | L | I | S | S/I | I/L |
| 1 | 65 | 50 | 40 | 0.8 | 0.769230769 |
| 2 | 35 | 34 | 32 | 0.941176471 | 0.971428571 |
| 3 | 68 | 50 | 39 | 0.78 | 0.735294118 |
| 4 | 48 | 34 | 25 | 0.735294118 | 0.708333333 |
| 5 | 35 | 24 | 20 | 0.833333333 | 0.685714286 |
| 6 | 17 | 15 | 14 | 0.933333333 | 0.882352941 |
| 7 | 33 | 30 | 26 | 0.866666667 | 0.909090909 |
| 8 | 32 | 27 | 17 | 0.62962963 | 0.84375 |
| 9 | 18 | 16 | 15 | 0.9375 | 0.888888889 |
| 10 | 19 | 17 | 16 | 0.941176471 | 0.894736842 |
| 11 | 56 | 51 | 40 | 0.784313725 | 0.910714286 |
| 12 | 34 | 31 | 25 | 0.806451613 | 0.911764706 |
| 13 | 24 | 20 | 17 | 0.85 | 0.833333333 |
| 14 | 39 | 35 | 30 | 0.857142857 | 0.897435897 |
| 15 | 37 | 32 | 28 | 0.875 | 0.864864865 |
| 16 | 22 | 16 | 14 | 0.875 | 0.727272727 |
| 17 | 8 | 7 | 6 | 0.857142857 | 0.875 |
| 18 | 25 | 19 | 14 | 0.736842105 | 0.76 |
| 19 | 16 | 15 | 11 | 0.733333333 | 0.9375 |
| 20 | 47 | 34 | 20 | 0.588235294 | 0.723404255 |
| 21 | 23 | 20 | 16 | 0.8 | 0.869565217 |
| 22 | 37 | 31 | 26 | 0.838709677 | 0.837837838 |
| 23 | 7 | 6 | 5 | 0.833333333 | 0.857142857 |
| 24 | 32 | 20 | 10 | 0.5 | 0.625 |
| 25 | 38 | 27 | 24 | 0.888888889 | 0.710526316 |
| 26 | 39 | 32 | 26 | 0.8125 | 0.820512821 |
| 27 | 59 | 50 | 44 | 0.88 | 0.847457627 |
| 28 | 24 | 21 | 19 | 0.904761905 | 0.875 |
| 29 | 34 | 30 | 25 | 0.833333333 | 0.882352941 |
| 30 | 28 | 16 | 11 | 0.6875 | 0.571428571 |
| 31 | 49 | 43 | 38 | 0.88372093 | 0.87755102 |
| 32 | 36 | 32 | 27 | 0.84375 | 0.888888889 |
| 33 | 15 | 10 | 6 | 0.6 | 0.666666667 |
| 34 | 23 | 22 | 20 | 0.909090909 | 0.956521739 |

| | | | | | |
|---|---|---|---|---|---|
| 35 | 5 | 4 | 3 | 0.75 | 0.8 |
| 36 | 31 | 23 | 19 | 0.826086957 | 0.741935484 |
| 37 | 51 | 38 | 29 | 0.763157895 | 0.745098039 |
| 38 | 57 | 40 | 25 | 0.625 | 0.701754386 |
| 39 | 22 | 18 | 14 | 0.777777778 | 0.818181818 |
| 40 | 53 | 41 | 30 | 0.731707317 | 0.773584906 |
| 41 | 14 | 12 | 9 | 0.75 | 0.857142857 |
| 42 | 15 | 11 | 10 | 0.909090909 | 0.733333333 |
| 43 | 3 | 2 | 1 | 0.5 | 0.666666667 |
| 44 | 15 | 14 | 12 | 0.857142857 | 0.933333333 |
| 45 | 30 | 26 | 21 | 0.807692308 | 0.866666667 |
| 46 | 23 | 20 | 17 | 0.85 | 0.869565217 |
| 47 | 52 | 41 | 31 | 0.756097561 | 0.788461538 |
| 48 | 25 | 18 | 13 | 0.722222222 | 0.72 |
| 49 | 58 | 43 | 25 | 0.581395349 | 0.74137931 |
| 50 | 2 | 1 | 1 | 1 | 0.5 |
| Mean | 30.52 | 25.38 | 20.12 | 0.795690639 | 0.805473336 |

3.2 Cg Member, Konewa Formation, clast shape and bedding orientation (lineation)

| Facies Gmu from the Stallion Stream sequence of Cg Member, measurements in mm | | | | | |
|---|---|---|---|---|---|
| Clast | | Axis | | | |
| № | Long | Intermediate | Short | S/I | I/L |
| 1 | 130 | 122 | 90 | 0.737704918 | 0.938461538 |
| 2 | 110 | 70 | 35 | 0.5 | 0.636363636 |
| 3 | 35 | 27 | 22 | 0.814814815 | 0.771428571 |
| 4 | 40 | 29 | 11 | 0.379310345 | 0.725 |
| 5 | 31 | 25 | 17 | 0.68 | 0.806451613 |
| 6 | 21 | 18 | 15 | 0.833333333 | 0.857142857 |
| 7 | 22 | 19 | 14 | 0.736842105 | 0.863636364 |
| 8 | 19 | 16 | 11 | 0.6875 | 0.842105263 |
| 9 | 64 | 51 | 32 | 0.62745098 | 0.796875 |
| 10 | 56 | 55 | 54 | 0.981818182 | 0.982142857 |
| 11 | 68 | 62 | 56 | 0.903225806 | 0.911764706 |
| 12 | 71 | 58 | 45 | 0.775862069 | 0.816901408 |
| 13 | 26 | 23 | 20 | 0.869565217 | 0.884615385 |
| 14 | 23 | 18 | 14 | 0.777777778 | 0.782608696 |
| 15 | 40 | 37 | 32 | 0.864864865 | 0.925 |
| 16 | 41 | 33 | 29 | 0.878787879 | 0.804878049 |
| 17 | 36 | 30 | 22 | 0.733333333 | 0.833333333 |
| 18 | 34 | 31 | 25 | 0.806451613 | 0.911764706 |

| | | | | | |
|---|---|---|---|---|---|
| 19 | 31 | 26 | 22 | 0.846153846 | 0.838709677 |
| 20 | 20 | 13 | 11 | 0.846153846 | 0.65 |
| 21 | 26 | 20 | 16 | 0.8 | 0.769230769 |
| 22 | 28 | 26 | 24 | 0.923076923 | 0.928571429 |
| 23 | 20 | 18 | 16 | 0.888888889 | 0.9 |
| 24 | 55 | 46 | 29 | 0.630434783 | 0.836363636 |
| 25 | 20 | 19 | 18 | 0.947368421 | 0.95 |
| 26 | 24 | 21 | 17 | 0.80952381 | 0.875 |
| 27 | 54 | 49 | 45 | 0.918367347 | 0.907407407 |
| 28 | 28 | 22 | 18 | 0.818181818 | 0.785714286 |
| 29 | 20 | 12 | 14 | 1.166666667 | 0.6 |
| 30 | 66 | 55 | 48 | 0.872727273 | 0.833333333 |
| 31 | 87 | 72 | 59 | 0.819444444 | 0.827586207 |
| 32 | 100 | 84 | 52 | 0.619047619 | 0.84 |
| 33 | 55 | 44 | 37 | 0.840909091 | 0.8 |
| 34 | 60 | 42 | 33 | 0.785714286 | 0.7 |
| 35 | 82 | 76 | 70 | 0.921052632 | 0.926829268 |
| 36 | 34 | 25 | 18 | 0.72 | 0.735294118 |
| 37 | 36 | 28 | 16 | 0.571428571 | 0.777777778 |
| 38 | 15 | 14 | 10 | 0.714285714 | 0.933333333 |
| 39 | 106 | 89 | 71 | 0.797752809 | 0.839622642 |
| 40 | 48 | 41 | 34 | 0.829268293 | 0.854166667 |
| 41 | 18 | 17 | 16 | 0.941176471 | 0.944444444 |
| 42 | 35 | 33 | 30 | 0.909090909 | 0.942857143 |
| 43 | 45 | 39 | 31 | 0.794871795 | 0.866666667 |
| 44 | 40 | 36 | 28 | 0.777777778 | 0.9 |
| 45 | 39 | 33 | 16 | 0.484848485 | 0.846153846 |
| 46 | 28 | 25 | 20 | 0.8 | 0.892857143 |
| 47 | 16 | 13 | 11 | 0.846153846 | 0.8125 |
| 48 | 17 | 16 | 15 | 0.9375 | 0.941176471 |
| 49 | 54 | 32 | 16 | 0.5 | 0.592592593 |
| 50 | 25 | 18 | 7 | 0.388888889 | 0.72 |
| Mean | 57.5 | 36.56 | 28.24 | | |

| five largest clasts |
|---|
| 130 |
| 106 |
| 100 |
| 110 |
| 87 |
| Mean = 106.6 |

| Facies LDS from the Stallion Stream sequence of Cg Member, measurements in mm | | | | | | |
|---|---|---|---|---|---|---|
| | Axis | | | | | |
| Clast № | L ong | Intermediate | Short | S/I | I/L | lineation |
| 1 | 102 | 76 | 30 | 0.394736842 | 0.745098039 | 19@330 |
| 2 | 163 | 134 | 55 | 0.410447761 | 0.82208589 | 21@329 |
| 3 | 41 | 25 | 8 | 0.32 | 0.609756098 | 22@290 |
| 4 | 63 | 100 | 42 | 0.42 | 1.587301587 | 24@320 |
| 5 | 61 | 46 | 22 | 0.47826087 | 0.754098361 | 21@334 |
| 6 | 38 | 48 | 24 | 0.5 | 1.263157895 | 6@310 |
| 7 | 31 | 27 | 11 | 0.407407407 | 0.870967742 | 18@350 |
| 8 | 23 | 26 | 8 | 0.307692308 | 1.130434783 | 14@285 |
| 9 | 43 | 17 | 9 | 0.529411765 | 0.395348837 | 38@310 |
| 10 | 40 | 36 | 24 | 0.666666667 | 0.9 | 20@95 |
| 11 | 73 | 34 | 16 | 0.470588235 | 0.465753425 | 21@321 |
| 12 | 17 | 61 | 45 | 0.737704918 | 3.588235294 | 40@324 |
| 13 | 124 | 13 | 9 | 0.692307692 | 0.10483871 | 41@320 |
| 14 | 25 | 85 | 41 | 0.482352941 | 3.4 | 6@216 |
| 15 | 152 | 9 | 3 | 0.333333333 | 0.059210526 | 32@225 |
| 16 | 46 | 104 | 36 | 0.346153846 | 2.260869565 | 25@220 |
| 17 | 68 | 33 | 18 | 0.545454545 | 0.485294118 | 60@335 |
| 18 | 23 | 40 | 13 | 0.325 | 1.739130435 | 31@320 |
| 19 | 27 | 19 | 12 | 0.631578947 | 0.703703704 | 30@330 |
| 20 | 143 | 25 | 15 | 0.6 | 0.174825175 | 35@316 |
| 21 | 70 | 130 | 95 | 0.730769231 | 1.857142857 | 28@350 |
| 22 | 26 | 56 | 34 | 0.607142857 | 2.153846154 | 55@340 |
| 23 | 38 | 23 | 15 | 0.652173913 | 0.605263158 | 6@325 |
| 24 | 205 | 22 | 14 | 0.636363636 | 0.107317073 | 8@223 |
| 25 | 22 | 155 | 50 | 0.322580645 | 7.045454545 | 35@350 |
| 26 | 66 | 74 | 60 | 0.810810811 | 1.121212121 | 4@330 |
| 27 | 38 | 55 | 31 | 0.563636364 | 1.447368421 | 32@328 |
| 28 | 26 | 27 | 10 | 0.37037037 | 1.038461538 | 30@327 |
| 29 | 75 | 20 | 9 | 0.45 | 0.266666667 | 35@335 |
| 30 | 182 | 46 | 19 | 0.413043478 | 0.252747253 | 4@152 |
| 31 | 38 | 128 | 104 | 0.8125 | 3.368421053 | 35@355 |
| 32 | 46 | 36 | 33 | 0.916666667 | 0.782608696 | 26@322 |
| 33 | 51 | 49 | 28 | 0.571428571 | 0.960784314 | 5@319 |
| 34 | 52 | 40 | 42 | 1.05 | 0.769230769 | 36@003 |
| 35 | 122 | 84 | 19 | 0.226190476 | 0.68852459 | 9@328 |
| 36 | 66 | 49 | 46 | 0.93877551 | 0.742424242 | 14@330 |
| 37 | 56 | 35 | 32 | 0.914285714 | 0.625 | 5@360 |

| | | | | | | |
|---|---|---|---|---|---|---|
| 38 | 60 | 50 | 28 | 0.56 | 0.833333333 | 18@338 |
| 39 | 42 | 35 | 32 | 0.914285714 | 0.833333333 | 35@344 |
| 40 | 23 | 19 | 23 | 1.210526316 | 0.826086957 | 18@319 |
| 41 | 30 | 21 | 12 | 0.571428571 | 0.7 | 8@325 |
| 42 | 110 | 81 | 8 | 0.098765432 | 0.736363636 | 20@334 |
| 43 | 138 | 104 | 49 | 0.471153846 | 0.753623188 | 35@350 |
| 44 | 40 | 28 | 82 | 2.928571429 | 0.7 | 18@335 |
| 45 | 25 | 19 | 14 | 0.736842105 | 0.76 | 16@335 |
| 46 | 15 | 18 | 9 | 0.5 | 1.2 | 19@334 |
| 47 | 34 | 25 | 6 | 0.24 | 0.735294118 | 40@140 |
| 48 | 50 | 38 | 10 | 0.263157895 | 0.76 | 34@320 |
| 49 | 44 | 22 | 28 | 1.272727273 | 0.5 | 64@14 |
| 50 | 50 | 20 | 15 | 0.75 | 0.4 | 6@325 |
| Mean | 63.5 | 49.34 | 27.96 | | | |

| five largest clasts |
|---|
| 163 |
| 144 |
| 143 |
| 205 |
| 182 |
| Mean = 182 |

| Facies Gmu from the Scrimmys Stream sequence of Cg Member, measurements in mm | | | | | |
|---|---|---|---|---|---|
| | | Axis | | | |
| Clast № | Long | Intermediate | Short | S/I | I/L |
| 1 | 89 | 68 | 45 | 0.661764706 | 0.764044944 |
| 2 | 48 | 40 | 34 | 0.85 | 0.833333333 |
| 3 | 75 | 62 | 41 | 0.661290323 | 0.826666667 |
| 4 | 45 | 40 | 24 | 0.6 | 0.888888889 |
| 5 | 58 | 30 | 21 | 0.7 | 0.517241379 |
| 6 | 50 | 34 | 10 | 0.294117647 | 0.68 |
| 7 | 42 | 38 | 34 | 0.894736842 | 0.904761905 |
| 8 | 45 | 36 | 20 | 0.555555556 | 0.8 |
| 9 | 41 | 29 | 30 | 1.034482759 | 0.707317073 |
| 10 | 35 | 26 | 26 | 1 | 0.742857143 |
| 11 | 30 | 66 | 24 | 0.363636364 | 2.2 |
| 12 | 80 | 27 | 48 | 1.777777778 | 0.3375 |
| 13 | 35 | 15 | 23 | 1.533333333 | 0.428571429 |
| 14 | 19 | 27 | 11 | 0.407407407 | 1.421052632 |
| 15 | 30 | 71 | 24 | 0.338028169 | 2.366666667 |

| | | | | | |
|---|---|---|---|---|---|
| 16 | 85 | 56 | 60 | 1.071428571 | 0.658823529 |
| 17 | 79 | 28 | 45 | 1.607142857 | 0.35443038 |
| 18 | 30 | 6 | 23 | 3.833333333 | 0.2 |
| 19 | 80 | 45 | 51 | 1.133333333 | 0.5625 |
| 20 | 50 | 36 | 41 | 1.138888889 | 0.72 |
| 21 | 44 | 86 | 28 | 0.325581395 | 1.954545455 |
| 22 | 110 | 89 | 75 | 0.842696629 | 0.809090909 |
| 23 | 101 | 35 | 62 | 1.771428571 | 0.346534653 |
| 24 | 41 | 41 | 26 | 0.634146341 | 1 |
| 25 | 47 | 39 | 38 | 0.974358974 | 0.829787234 |
| 26 | 43 | 34 | 34 | 1 | 0.790697674 |
| 27 | 37 | 56 | 30 | 0.535714286 | 1.513513514 |
| 28 | 75 | 22 | 43 | 1.954545455 | 0.293333333 |
| 29 | 25 | 45 | 20 | 0.444444444 | 1.8 |
| 30 | 67 | 43 | 26 | 0.604651163 | 0.641791045 |
| 31 | 57 | 43 | 41 | 0.953488372 | 0.754385965 |
| 32 | 46 | 36 | 28 | 0.777777778 | 0.782608696 |
| 33 | 47 | 36 | 31 | 0.861111111 | 0.765957447 |
| 34 | 40 | 58 | 46 | 0.793103448 | 1.45 |
| 35 | 65 | 44 | 40 | 0.909090909 | 0.676923077 |
| 36 | 54 | 50 | 41 | 0.82 | 0.925925926 |
| 37 | 57 | 38 | 35 | 0.921052632 | 0.666666667 |
| 38 | 44 | 33 | 30 | 0.909090909 | 0.75 |
| 39 | 39 | 30 | 23 | 0.766666667 | 0.769230769 |
| 40 | 34 | 32 | 20 | 0.625 | 0.941176471 |
| 41 | 36 | 86 | 61 | 0.709302326 | 2.388888889 |
| 42 | 105 | 71 | 60 | 0.845070423 | 0.676190476 |
| 43 | 76 | 34 | 23 | 0.676470588 | 0.447368421 |
| 44 | 41 | 31 | 26 | 0.838709677 | 0.756097561 |
| 45 | 43 | 23 | 16 | 0.695652174 | 0.534883721 |
| 46 | 36 | 28 | 22 | 0.785714286 | 0.777777778 |
| 47 | 34 | 49 | 43 | 0.87755102 | 1.441176471 |
| 48 | 60 | 80 | 72 | 0.9 | 1.333333333 |
| 49 | 85 | 60 | 51 | 0.85 | 0.705882353 |
| 50 | 65 | 40 | 22 | 0.55 | 0.615384615 |
| Mean | 54 | 43.44 | 34.96 | | |

| five largest clasts |
|---|
| 110 |
| 101 |
| 105 |
| 89 |
| 98 |

| Mean = 100.6 |
|---|

| Facies LDS from the Scrimmmys Stream sequence of Cg Member, measurements in mm | | | | | | |
|---|---|---|---|---|---|---|
| Clast | Axis | | | | | |
| № | L ong | Intermediate | Short | S/I | I/L | lineation |
| 1 | 54 | 32 | 16 | 0.5 | 0.592592593 | 16@269 |
| 2 | 95 | 60 | 28 | 0.466666667 | 0.631578947 | 24@263 |
| 3 | 45 | 25 | 18 | 0.72 | 0.555555556 | 15@270 |
| 4 | 23 | 10 | 7 | 0.7 | 0.434782609 | 10@264 |
| 5 | 60 | 30 | 20 | 0.666666667 | 0.5 | 4@99 |
| 6 | 20 | 14 | 9 | 0.642857143 | 0.7 | 24@270 |
| 7 | 24 | 15 | 9 | 0.6 | 0.625 | 4@264 |
| 8 | 9 | 6 | 4 | 0.666666667 | 0.666666667 | 9@264 |
| 9 | 110 | 84 | 5 | 0.05952381 | 0.763636364 | 8@260 |
| 10 | 46 | 35 | 20 | 0.571428571 | 0.760869565 | 14@254 |
| 11 | 36 | 16 | 10 | 0.625 | 0.444444444 | 15@258 |
| 12 | 20 | 14 | 5 | 0.357142857 | 0.7 | 28@250 |
| 13 | 55 | 47 | 35 | 0.744680851 | 0.854545455 | 25@254 |
| 14 | 35 | 23 | 15 | 0.652173913 | 0.657142857 | 19@268 |
| 15 | 44 | 32 | 25 | 0.78125 | 0.727272727 | 1@255 |
| 16 | 14 | 9 | 5 | 0.555555556 | 0.642857143 | 14@290 |
| 17 | 50 | 35 | 20 | 0.571428571 | 0.7 | 25@246 |
| 18 | 30 | 19 | 11 | 0.578947368 | 0.633333333 | 30@280 |
| 19 | 70 | 50 | 19 | 0.38 | 0.714285714 | 16@284 |
| 20 | 58 | 42 | 36 | 0.857142857 | 0.724137931 | 4@275 |
| 21 | 81 | 62 | 38 | 0.612903226 | 0.765432099 | 50@251 |
| 22 | 34 | 30 | 16 | 0.533333333 | 0.882352941 | 23@250 |
| 23 | 26 | 15 | 9 | 0.6 | 0.576923077 | 4@261 |
| 24 | 24 | 18 | 11 | 0.611111111 | 0.75 | 35@248 |
| 25 | 23 | 16 | 12 | 0.75 | 0.695652174 | 3@260 |
| 26 | 35 | 30 | 22 | 0.733333333 | 0.857142857 | 28@99 |
| 27 | 11 | 8 | 6 | 0.75 | 0.727272727 | 17@268 |
| 28 | 16 | 10 | 6 | 0.6 | 0.625 | 19@249 |
| 29 | 52 | 38 | 23 | 0.605263158 | 0.730769231 | 20@251 |
| 30 | 26 | 20 | 15 | 0.75 | 0.769230769 | 19@260 |
| 31 | 90 | 55 | 34 | 0.618181818 | 0.611111111 | 16@255 |
| 32 | 60 | 40 | 15 | 0.375 | 0.666666667 | 36@275 |
| 33 | 72 | 53 | 39 | 0.735849057 | 0.736111111 | 30@90 |
| 34 | 66 | 51 | 34 | 0.666666667 | 0.772727273 | 31@264 |
| 35 | 68 | 35 | 20 | 0.571428571 | 0.514705882 | 11@270 |

| | | | | | | |
|---|---|---|---|---|---|---|
| 36 | 44 | 20 | 9 | 0.45 | 0.454545455 | 23@250 |
| 37 | 76 | 54 | 33 | 0.611111111 | 0.710526316 | 16@280 |
| 38 | 26 | 19 | 14 | 0.736842105 | 0.730769231 | 9@249 |
| 39 | 89 | 68 | 47 | 0.691176471 | 0.764044944 | 13@268 |
| 40 | 61 | 49 | 34 | 0.693877551 | 0.803278689 | 19@244 |
| 41 | 58 | 32 | 15 | 0.46875 | 0.551724138 | 5@269 |
| 42 | 31 | 19 | 9 | 0.473684211 | 0.612903226 | 29@270 |
| 43 | 53 | 46 | 28 | 0.608695652 | 0.867924528 | 20@240 |
| 44 | 38 | 25 | 19 | 0.76 | 0.657894737 | 25@85 |
| 45 | 34 | 21 | 15 | 0.714285714 | 0.617647059 | 16@250 |
| 46 | 70 | 10 | 4 | 0.4 | 0.142857143 | 1@256 |
| 47 | 46 | 31 | 9 | 0.290322581 | 0.673913043 | 5@252 |
| 48 | 63 | 45 | 17 | 0.377777778 | 0.714285714 | 16@269 |
| 49 | 25 | 20 | 11 | 0.55 | 0.8 | 24@263 |
| 50 | 11 | 8 | 6 | 0.75 | 0.727272727 | 15@265 |
| Mean | 46.14 | 30.92 | 17.74 | | | |

| five largest clasts |
|---|
| 110 |
| 89 |
| 95 |
| 90 |
| 93 |
| Mean = 95.4 |

# Appendix 4: Fossil data

4.1 Fossil sample localities:

| Sample Number | Stratigraphic Member/ Formation | Location & Coordinates |
|---|---|---|
| FS1 | Css Member, Takapari Formation. | 25 m up from contact between Css and Bms Members, hair pin corner section (stratigraphic log 6.1), Awahou South Rd, Broadlands Station (WGS84 40°16'47.36"S, 175°46'26.73"E elev 80 m). |
| FS2 | Bms Member, Takapari Formation. | 120 m up from contact between Cq Member, Konewa Formation and Bms Member, Takapari Formation. Near Scrimmys Stream's confluence with the Pohangina River, outcrop exposed in Scrimmys Stream bed (WGS84 40°16'45.80"S, 175°46'25.71"E, elev 74 m). |
| FS3 | Bms Member, Takapari Formation. | 70 m up from contact between Cq Member, Konewa Formation and Bms Member, Takapari Formation, outcrop exposed in true right fork of Whaeroa Stream (WGS84 40°14'08.55"S, 175°48'26.36"E, elev 170 m). |
| FS4 | Cq Member, Konewa Formation. | Outcrop exposed 420 m east of Awhaou South Rd, following Scrimmys Stream. 20 m climb up the bank of Scrimmys Stream to outcrop (WGS84 40° 16'51.15"S, 175°46'47.48"E, elev 107 m). |
| FS5 | Kss Member, Konewa Formation. | 25 m downstream of Rss Member, Konewa Formation following Scrimmys Stream (WGS84 40°16'43.04"S, 175°46'56.51"E elev 111 m). |
| FS6 | Kss Member, Konewa Formation. | 100 m upstream of Cq Member, Konewa Formation, following Scrimmys Stream (WGS84 40°16'46.86"S, 175°46'53.92"E, elev 121 m). |
| FS7 | Rss Member, Konewa Formation. | Scrimmys Stream 600 m north of Saddle Road. Near contact between Kst Member and Rss Member, Konewa Formation (WGS84 40°16'55.35"S, 175°47'05.80"E elev 140 m). |
| FS8 | Rss Member, Konewa Formation. | Interfluve between the true right and left forks of Scrimmys Stream, ridge formed by Rss Member (very calcite rich in this area). 100 m climb up from Scrimmys Stream at fist sign of Cg Member, Konewa Formation (WGS84 40°16'54.18"S, 175°47'19.48"E, elev 216 m). |
| FS9 | Kst Member, Konewa Formation. | Scrimmys Stream 600 m north of Saddle Road. Just above contact between Cg Member and Kst Member, Konewa Formation (WGS84 |

| | | |
|---|---|---|
| | | 40°16’55.35”S, 175°47’05.80”E elev 140 m). |
| FS10 | Cg Member, Konewa Formation. | 100 m downstream of contact between Fss Member, Komako Formation and Cg Member, Konewa Formation following Saddle Creek. Sandy unit inbetween two conglomerate units (WGS84 40°17’30.97”S, 175°46’49.72”E, elev 118 m). |
| FS11 | Cg Member Konewa Formation. | 200 m downstream of contact between Fss Member, Komako Formation and Cg Member, Konewa Formation following the true left fork of Scrimmys Stream. Conglomerate unit with shell hash matrix (WGS84 40°16’56.71”S, 175°47’11.15”E, elev 149 m). |
| FS12 | Cg Member, Konewa Formation | 100 m downstream of contact between Fss Member, Komako Formation and Cg Member, Konewa Formation following the true left fork of Scrimmys Stream. Sandy unit between two conglomerate units (WGS84 40°16’57.29”S, 175°47’16.62”E, elev 157 m). |
| FS13 | Fss Member, Komako Formation. | 300 m upstream from contact between Cg Member, Konewa Formation and Fss Member, Komako Formaiton following Stallion Stream (WGS84 40°16’22.90”S, 175°48’00.89”E, elev 180 m). |
| FS14 | Fss Member, Komako Formation. | 150 m upstream from contact between Cg Member, Konewa Formation and Fss Member, Komako Formaiton following Stallion Stream (WGS84 40°16’24.14”S, 175°47’52.03”E, elev 110 m) |
| FS15 | Fss Member, Komako Formation. | Thick oyster bed found 900 m up Saddle Creek. Near contact between Cg Member, Konewa Formation and Fss Member, Komako Formation (WGS84 40°17’31.48”S, 175°46’58.61”E, elev 152 m). |
| FS16 | Fms Member, Komako Formation. | Side tributary on the true left side of Stallion Stream 3 km upstream from Awahou South Rd (WGS84 40°16’40.49”S, 175°48’25.16”E, elev 195 m) |
| FS17 | Fms Member, Komako Formation. | 600 m downstream of contact between Cf Member and Fms Member, Komako Formation following Stallion Stream (WGS84 40°16’27.34”S, 175°48’14.70”E, elev 131 m). |
| FS18 | Cf Member, Komako Formation | 100m downstream of contact between Torlesse greywacke and Cf Member, Komako Formation following Stallion Stream (WGS84 40°16’36.95”S, 175°48’33.14”E, elev 155 m). |
| FS19 | Cf Member, Komako | Side tributary on true left side of Stallion Stream |

| | | |
|---|---|---|
| | Formation | 250 m downstream of contact between Cf Member Komako Formation and Torlesse greywacke (WGS84 40°16'37.65"S, 175°48'28.07"E, elev 187 m). |

4.2 Micropalentological data (Finlayson, 1980):

| Species name: | Sample Name | | | | | | | | | | | | |
|---|---|---|---|---|---|---|---|---|---|---|---|---|---|
| | P1 | P2 | P3 | P4 | P5 | D3 | H6 | K3 | T6 | T8 | K7 | H5 | T1 |
| *Textularia proxispira* (Vella) | X | | | | | | | | | | | | |
| *Quinqueloculina delicatula* (Vella) | | | | | | | X | | | | | | |
| *Quinqueloculina lamarkiana (d'Orbigny)* | X | X | X | | X | X | X | X | | X | | | |
| *Quinqueloculina miles (Vella)* | | | X | X | X | | | | | | | | |
| *Quinqueloculina sigmoilinoides (Vella)* | | | X | X | | | | | | | | | |
| *Quinqueloculina triangularis (d'Orbigny)* | | X | | | | | | | | | | | |
| *Pyrgo tasmanensis* (Vella) | | | | | | | | | X | X | X | | |
| *Biloculina cf. elongate* (d'Orbigny) | X | | | X | | | | | | | | | |
| *Siphonaperta macbeathi* (Vella) | X | | | | | | | | | | | | |
| *Quinqueloculina hornibrooki (Vella)* | | X | X | | | | | | | | | | |
| *Chrysalogonium verticale* (Stache) | | | | | | | | X | | | | | |
| *Dentalina albatrossi* (Cushman) | | X | | | | | | | | | | | |
| *Lagena distoma* (Parker and Jones) | | X | | | | | | | | | | | |
| *Lagena gracilis* (Williamson) | X | X | | X | | | | | | | | | |
| *Lagena hispida* (Reuss) | X | | | | | | | | | | | | |
| *Lagena striata* (d'Orbigny) | X | X | X | X | X | | | | | | | | |
| *Lagena sulcata* (Walker and Jacob) | X | X | | | X | X | | X | X | | | | |
| *Lagena sp.* | | | | X | | | | | | | | | |
| *Lenticulina sp.* | | | X | | | | | | | | | | |
| *Vaginulina vagina* (Stache) | X | | | | | | | | | | | | |
| *Glandulina symmetrica* (d'Orbigny) | | | | | | | | | | | X | | |
| *Oolina globosa* (Montagu) | | | | | | | | | X | | | | |
| *Oolina hexagona* (Williamson) | X | X | X | X | | X | | | X | | | | |
| *Oolina melo* (d'Orbigny) | X | X | X | X | X | X | X | | X | X | | X | X |
| *Fissurina deltoidea* (Seguenza) | X | | | | | | X | | | | | | |
| *Fissurina orbignyana* (Seguenza) | | | X | X | | | | | | | | | |
| *Fissurina submarginata* (Boomgart) | X | | X | X | X | | | X | X | | | | X |
| *Fissurina subulata* (d'Orbigny) | | | | | | | X | | | | | | |
| *Fissurina yokoyamae* (Millett) | | | | | X | | | | | | | | |
| *Fissurina sp.* | | X | | X | | | | | | | | | |
| *Shaeroidina bulloides* (d'Orbigny) | | | | | | | | | X | | | | |
| *Boliviniata pliozea* (Finlay) | | X | | | | | | | | | | | |
| *Boliviniata pohana* (Finlay) | X | | | | | | X | X | X | | | | |
| *Bolivina fyfei* (Hornibrook) | | | | | | | X | | | | | | |
| *Bolivina hornibrooki* (Collen) | | | | | X | | X | | | | | | |
| *Bolivina minuta* (Natland) | | | | | | | | | | | | | X |
| *Bolivina cf. petiae* (Gibson) | | | | | | | | | X | | | | |

| | | | | | | | | | | | | | |
|---|---|---|---|---|---|---|---|---|---|---|---|---|---|
| *Bolivina plicatella* (Cushman) | | | | | X | | | | | | | | |
| *Stilostomella sp.* | | X | | | | | | | | | | | |
| *Bulimina aculeate* (d'Orbigny) | X | X | | X | X | X | | | | | | | |
| *Bulimina sp.* | | | | | | X | | | | | | | |
| *Virgulopsis turris* (Heron-Allen, Earland) | | | | | X | | | | | | | | X |
| *Euuvigerina pliozea* (Vella) | | | | | | | X | | | X | X | | |
| *Euuvigerina rodleyi* (Vella) | | X | X | X | | X | X | | | X | X | X | |
| *Euuvigerina zeacuminate* (Vella) | | | | | X | | | | | | X | X | |
| *Euuvigerina sp.* | | | | | | | X | | | | | | |
| *Angulogerina bradyi* (Cushman) | | | | | | | X | | | | | | |
| *Neouvigerina vadescens* (Cushman) | | | | X | | | | | | | | | |
| *Elphidium argentum* (Parr) | | X | | | X | | | | | | | | |
| *Elphidium ns.* | X | X | | | | | | | | | | | |
| *Elphidium ns. Cf. incertum* (Williamson) | | | | | | | | | | X | | | |
| *Elphidiononion simplex* (Cushman) | X | X | X | X | X | | X | X | | X | | | X |
| *Cribroelphidum charlottensis* (Vella) | X | X | X | | X | | X | X | | X | | | |
| *Notorotalia depressi* (Vella) | X | X | X | | X | | | | | | | | |
| *Notorotalia cf. depressi* (Vella) | X | X | X | | X | | X | X | | X | | | |
| *Notorotalia finlayi* (Vella) | | X | X | | X | | X | | X | X | | | |
| *Notorotalia cf. finlayi* (Vella) | X | | | | | | | | | | | | |
| *Notorotalia inornata* (Vella) | | | X | | X | X | X | | X | X | X | | |
| *Notorotalia mammiligera* (Kenneta) | | | | | X | | | | | | | | |
| *Notorotalia zelandica mangaoparia* (Vella) | | | | | | | | | | | X | | |
| *Globigerina bulloides* (d'Orbigny) | | | | X | X | | X | X | | | | | |
| *Globigerina foliate* (Brady) | X | X | X | X | X | | X | | | | | | |
| *Globigerina woodi* (Takayanagi & Saito) | X | | | | X | | | | | | | | |
| *Neogloboquadrina dutetrei* (d'Orbigny) | X | | | | | | | | | | | | |
| *Neogloboquadrina achyderma* (Ehrenberg) | X | X | X | X | | | | | | | | | |
| *Globigerinita glutinata* (Egger) | X | | | | | | X | | | | | | |
| *Hyalinea cf. balthica* (Schroeter) | | | | | | | X | | | | | | |
| *Cibicides sp. Cf. ihungia* (Finaly) | | | | | | X | | | | | | | |
| *Cibcides sp.* | X | X | | | | X | | | | | | | |
| *Dyocibicides biserialis* (Cushman, Valentine) | | | | | | | X | | | | | | |
| *Cassidulina neocurinata* (Thalmann) | | X | X | | X | | X | | | | | | |
| *Cassidulina subglobosa* (Brady) | | X | X | X | X | | X | X | X | | X | X | |
| *Evolvocassidulina orientalis* (Cushman) | X | X | | X | X | X | X | X | X | | | | |
| *Astrononion parki* (Hornibrook) | X | | | | | | X | | | | | | |
| *Astrononion vadorum* (Vella) | | | | | | | X | | | | | | |
| *Zeaflorilus parri* (Cushman) | | | X | X | | | X | | | | | | |
| *Nonionellina flemingi* (Vella) | X | X | X | X | X | X | X | X | X | X | X | | X |
| *Pullenia quiqeloba* (Reuss) | | | | | X | | | | | | | | |
| *Gyroidinoides zelandica* (Finlay) | X | X | X | X | X | | | X | | X | | | |
| *Anomalinoides sphenia* (Finlay) | | | | | | | | | X | | X | | |

| Micropalentological sample number and grid references: Grid references refer to NZMS 260; 1:50,000 sheet T23; (Finlayson, 1980) | |
|---|---|
| Sample Number | Grid Reference |
| P1 | 608240 |
| P2 | 612240 |
| P3 | 616241 |
| P4 | 619240 |
| P5 | 606239 |
| D3 | 607226 |
| K3 | 598225 |
| T6 | 638250 |
| T8 | 637248 |
| K7 | 607222 |
| H6 | 625242 |
| H5 | 623242 |
| T1 | 640256 |

4.3 Carter (1972) fossil data from the Komako Formation a correlative of the Hautawa Shellbed, Komako Distirict, Pohangina.

| Fossil name: | Occurrence : |
|---|---|
| Arca cottoni (Waghorn, 1926). | X (t) |
| Glycymeris waipipiensis (Marwick, 1923). | X |
| Aulacomya maoriana (Iredale, 1915). | X (l) |
| Modilus areolatus (Gould, 1850). | X |
| Panis zelandicus (Hutton in Suter, 1917). | X |
| Talochlamys gemmulata (Reeve, 1853). | X |
| Zygrochlamys delicatula (Hutton, 1873). | X (u) |
| Mesopeplum convexum (Quoy & Gaimard, 1835). | X |
| Phialopecten thomsoni (Marwick, 1965). | X (l) |
| Phailopecten triphooki (Zittel, 1864). | X(u) |
| Anomia trignopsis (Hutton, 1877). | X |
| Limatula maoria (Finlay, 1926). | X |
| Crassostrea igens (Zittel, 1864). | X (l) |
| Divaricella huttoniana (Vanatta, 1901). | X |
| Mysells larochei (Powell, 1940). | X |
| Pleuromeris finlayi (Powell, 1938). | X |
| Purpurocardia purpurata (Deshayes, 1854). | X |
| Talabrica senecta (Powell, 1931). | X |
| Gari linoleata (Gray, 1835). | X |
| Gari (Gobraeus) stranger (Gray, 1843). | X |
| Bassina parva (Marwick, 1927). | X |
| Tawera subsulcata (Suter, 1905). | X(l) |

| | |
|---|---|
| Dosinia subrosea (Gray, 1835). | X |
| Notocallista multistriata (Sowerby, 1851). | X |
| Eumarcia benhami (Marwick, 1927). | X |
| Panopea zelandica (Quoy & Gaimard, 1835). | X |
| Offadesma angasi (Crosse & Fischer, 1864). | X |
| Myadora stephaniae (Carter, 1972). | X |
| Haliotis sp. | X |
| Aoteadrillia alpha (King, 1933). | X |
| Fissidentalium zelandicum (Sowerby, 1860). | X |

4.4: Fossil data from McIntyre (2002) Saddle Road locality, exact location or formation is unspecified.

| Fossil name | Sample locality | |
|---|---|---|
| | Saddle Rd Lwr Lst | Saddle Rd Uper Lst |
| *Phialopecten marwicki* (Beu, 1970). | t - r | t - c |
| *Crassostrea ingens* (Zittel, 1864). | - | l - r |
| *Maoricardium spatiosum* (Hutton, 1873). | - | l – r |
| *Austrofusus pagoda* (Finlay, 1924). | - | u - c |
| *Alcithoe haweraensis* (Marwick, 1926) | u - r | - |
| *Fissidentalium zelandicum* (Sowerby, 1860) | - | u – r |

# Appendix 5: Paleomagentic analysis data

5.1 Kst Member paleomagnetic results from Beanland (1995).

| Specimen | D | Q | Specimen | D | Q | Specimen | D | Q |
|---|---|---|---|---|---|---|---|---|
| 020.00 | A | A | 031.00 | A | B | 037.20 | T | B |
| 020.10 | T | A | 031.10 | T | A | 037.30 | T | A |
| 020.20 | T | B | 032.00 | A | B | 039.00 | A | A |
| 021.00 | A | A | 032.10 | T | C | 039.10 | T | C |
| 021.10 | T | A | 032.20 | T | B | 040.00 | A | A |
| 021.20 | T | B | 033.10 | T | B | 041.00 | T | B |
| 022.00 | A | A | 033.20 | A | A | 040.20 | T | A |
| 022.10 | T | B | 034.00 | A | A | 040.30 | T | C |
| 022.20 | T | A | 034.10 | T | C | 041.00 | A | A |
| 022.30 | T | A | 034.20 | T | C | 041.10 | T | C |
| 023.00 | A | A | 035.00 | A | B | 041.20 | T | A |
| 023.10 | T | B | 035.10 | T | C | 042.00 | A | A |
| 024.00 | A | A | 035.20 | T | C | 042.20 | T | A |
| 024.10 | T | A | 035.30 | T | A | 042.30 | T | B |
| 029.00 | A | B | 036.00 | A | C | 043.00 | A | A |
| 029.10 | T | B | 036.10 | T | C | 043.20 | T | C |
| 029.20 | T | C | 036.20 | T | C | 044.20 | T | A |
| 029.30 | T | B | 037.00 | A | B | 045.00 | A | A |
| 029.40 | A | A | 037.10 | T | C | 045.20 | T | B |
| 046.00 | A | A | 047.20 | T | C | 048.00 | A | B |
| 046.20 | T | C | 047.30 | T | C | 048.20 | T | C |
| 047.00 | A | B | 047.40 | T | C | 048.30 | T | C |

Notes:

D= Demagnetization technique Q= Result quality

A= Alternating field demagnetization T= Thermal demagnetization

Samples: 020-024 from Saddle Road site; Samples: 029-048 from Scrimmys Stream site.

Results are classified into types A (well constrained), B (medium constraint) and C (Low constraint). Due to the use of the data within a tectonic rotation study, the direction of primary magnetization is of paramount importance, hence only the most stable third of the specimens are utilised. Only well constrained demagnetization trends (Type A) are used by Beanland, (1995). Magnetic north in the Manawatu Strait area was 22.5° east of geographic

north during 1980, increasing at the rate of 0.5°/yr (Topographical map, I:50,000, NZMS 260 T24, edition I). Correction for the earth's current magnetic field during Beanlands study (1995) involved adding 24° to give declinations relative to geographic north.

| A 30 Specimens | Declination | Inclination | T 250 Specimens | Declination | Inclination |
|---|---|---|---|---|---|
| 020.00 | 190.4 | 61.2 | 020.10 | 202.4 | 68.3 |
| 021.00 | 180.7 | 66.7 | 021.10 | 189.1 | 64.7 |
| 022.00 | 185.9 | 62.6 | 022.20 | 185.3 | 64.6 |
| 023.00 | 182.2 | 65.7 | 022.30 | 196.0 | 63.4 |
| 024.00 | 183.0 | 59.7 | 024.10 | 186.0 | 57.9 |
| 033.20 | 201.0 | 70.8 | 031.10 | 187.1 | 69.7 |
| 034.00 | 172.0 | 59.6 | 037.30 | 168.5 | 64.9 |
| 06.00 | 172.7 | 63.8 | 040.20 | 202.9 | 76.4 |
| 039.00 | 170.5 | 64.4 | 041.20 | 193.5 | 68.4 |
| 040.00 | 205.9 | 74.6 | 042.20 | 185.1 | 66.5 |
| 041.00 | 188.2 | 68.8 | 044.20 | 195.2 | 71.3 |
| 042.00 | 183.3 | 65.6 | | | |
| 043.00 | 202.2 | 65.0 | | | |
| 045.00 | 162.2 | 73.5 | | | |
| 046.00 | 186.7 | 68.7 | | | |
| Average | 183.9 | 66.6 | | 189.2 | 67.2 |
| Alpha95 k-statistic | 2.83 | 162.6 | | 3.14 | 180.3 |
| Combined average | 186.12 | 66.9 | | | |
| Alpha95 k-statistic | 2.10 | 171.12 | | | |

Notes:

A 30 Specimens demagnetized to a 30 A/m that showed A quality results;

T 250 Speciemens demagnetized to 250°C that showed A quality results;

DEC Declination and INC inclination after sample orientation and bedding corrections;

Alpha 95 95% confindence limit in pole position